Ethylene tetramerization: structure and reactivity investigation of metal based catalyst precursors

by

Nicoline Cloete

THESIS

submitted in the fulfilment of the requirements for the degree

PHILOSOPHIAE DOCTOR

in

CHEMISTRY

in the

FACULTY OF NATURAL AND AGRICULTURAL SCIENCES

at the

UNIVERSITY OF THE FREE STATE

SUPERVISOR: PROFESSOR ANDREAS ROODT
CO-SUPERVISOR: HENDRIK G. VISSER

JANUARY 2010

Dankbetuigings

Hiermee wens ek om my opregte dank en waardering te betuig aan:

My hemelse Vader en God vir al die geleenthede en voorregte wat U my lewenspad mee gevul het tot dusver.

My studieleier, Prof Roodt. Dit was 'n absolute voorreg om van u te leer, u kennis, insig en algehele nederigheid is 'n inspirasie vir almal om u.

My medestudieleier en goeie vriend, Deon Visser, dankie dat jy nooit enige moeite ontsien het vir elkeen van jou studente nie, vanaf die eerstejaartjie tot jou "langste kort" PhD student. Jy stel die standaard vir studieleiers en dosente baie hoog.

William Gabrielli, my Sasol mentor, vir jou waadevolle bydrae en moeite, ek het dit werklik geniet om saam met jou te werk.

My ouers, Hennie en Elize Cloete, vir die onvoorwaardelike liefde en ondersteuning. Woorde kan nie beskyf hoe dankbaar ek is vir sulke wondelike ouers nie.

Shaun Cronjé, vir jou oneindige liefde en ondersteuning, jy is die rots in my lewe.

My twee broers, Henk en Deon, asook hul gesinne, vir jul belangstelling en aanmoediging.

My mede-studente in die anorganiese groep. Daar was nooit 'n vervelige oomblik in die lab of kantoor nie. Julle sal altyd 'n spesiale plek in my hart hê.

Aan al my vriende, julle humor en passie vir die lewe, maak die lewe 'n fees!

Al die personeel en studente by Departement Chemie vir julle wonderlike bydraes.

Sasol vir finansiele steun wat hierdie studie moontlik gemaak het.

"The journey of a thousand miles begins with a single step." (Lao Tzu)

Table of contents

Abbreviations and symbols

Label	Definitions
Å	Angstrom
δ	Chemical shift
ν	Stretching frequency on IR
°	Degrees
℃	Degrees Celsius
K	Kelvin
g	Gram
M	$Mol.dm^{-3}$
$\theta_{N\text{-}sub}$	Effective Tolman-based N-substituent steric effect
ΔE	Energy difference
$\Delta H^{\neq}$	Enthalpy of activation
$\Delta S^{\neq}$	Entropy of activation
T	Temperature
d	Doublet
m	Multiplet
$CDCl_3$	Deuterated chloroform
s	Singlet
k_B	Boltzman's constant
k_{obs}	Observed *pseudo* first-order constant
K	Equilibrium constant
HF	Hartree-Fock method
UV	Ultraviolet
PNP	Bis(diphenylphosphino)alkylamine
ppm	(Unit of chemical shift) Parts per million
DCE	Dichloroethane
DFT	Density functional theory
NMR	Nuclear magnetic resonance
Vis	Visible
λ	Wavelength
X···X	Non-bonded atomic interaction
Z	Number of asymmetric units per unit cell

Summary

Transition metal-catalyzed ethylene oligomerization typically produces a broad range of α-olefins. The selective tetramerisation of ethylene to 1-octene is possible with the use of diphosphinoamine ligands together with chromium(III) and an aluminoxane activator as catalyst system.

The aim of this study was therefore to synthesize and characterise a range of diphosphinoamine (PNP) ligands with varying catalytic activity and selectivity (see **Figure 1)**. The stereo-electronic properties of these ligands were evaluated by varying the alkyl group in a systematic way. The single crystal X-ray crystallographic study of the above-mentioned PNP ligands revealed a decreasing trend of the P-N-P bond angle to decrease as the steric bulk of the alkyl moiety increases.

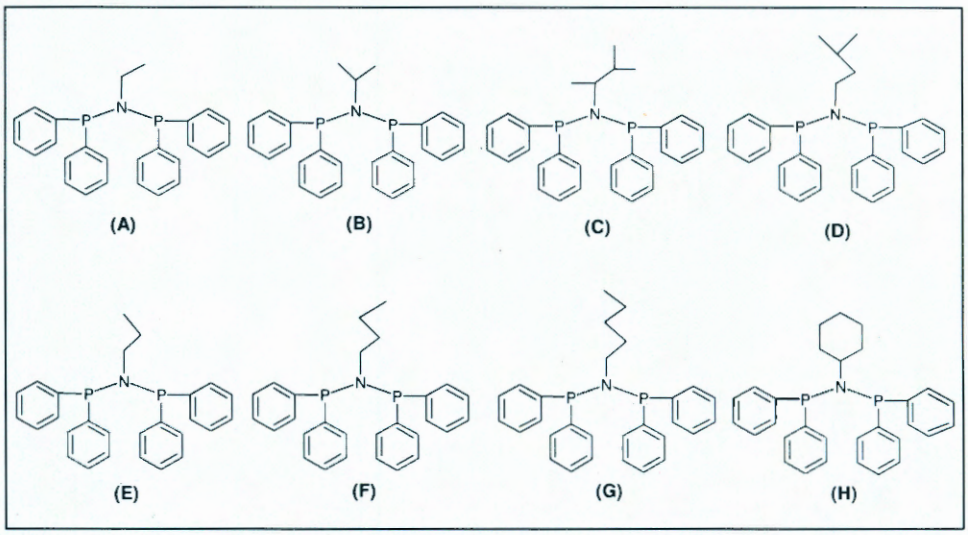

Figure 1: The diphosphinoamine ligands (PNP-ligands) synthesized, characterised and used in this study. (A) Bis(diphenylphosphino)ethylamine (PNP-Ethyl); (B) Bis(diphenylphosphino)-isopropylamine (PNP-*i*-Prop); (C) Bis(diphenylphosphino)-1,2-dimethylpropylamine (PNP-Dimprop); (D) Bis(diphenylphosphino)-isopentylamine (PNP-*i*-Pent); (E) Bis(diphenylphosphino)-*n*-propylamine (PNP-*n*-Prop); (F) Bis(diphenylphosphino)-*n*-butylamine (PNP-*n*-Butyl); (G) Bis(diphenylphosphino)-*n*-pentylamine (PNP-*n*-Pent); (H) Bis(diphenylphosphino)-cyclohexylamine (PNP-Cychex).

An important part of this investigation was concerned with the synthesis and evaluation of the solid state characteristics of the PNP ligands bonded to Cr(III). This was extended by

complexing other metal cations (eg. Pt(II) and Pd(II)) with the various PNP ligands in order to provide further information on the coordination mode of these ligands.

The study was also supplemented with theoretical chemistry. The comparison between the optimised structure and the crystal data revealed small differences, resulting in the possibility that predictions can be made in terms of ligand design. The calculated structure indicated that the phenyl ring arrangement is affected by the steric bulk of the nitrogen-coordinated alkyl moiety which could ultimately affect the catalytic selectivity.

A steric parameter was defined (Effective Tolman-based N-substituent steric effect ($\theta_{N\text{-}sub}$)) in which the steric bulk of the nitrogen-coordinated alkyl substituent was quantified. A comparison between $\theta_{N\text{-}sub}$ for various diphosphinoamine ligands (free and metal-coordinated) and the catalytic selectivity (for 1-C_6 and 1-C_8) revealed a relatively good correlation with the catalytic selectivity increasing as $\theta_{N\text{-}sub}$ for the varying ligands increased. It was also possible to compare the $\theta_{N\text{-}sub}$* (from theoretically calculated structures) with the catalytic selectivity and a similar trend was observed for the optimized structures than the solid state structures ($\theta_{N\text{-}sub}$).

The kinetics of the substitution of two chlorido ligands of the [$PtCl_2$(PNP-*i*-Pent)] complex with Br^- was investigated. Two consecutive reversible reactions were observed and analysed separately. Three platinum(II) species [($PtCl_2$(PNP-*i*-Pent)], [($PtBrCl$(PNP-*i*-Pent)] and [($PtBr_2$(PNP-*i*-Pent)], are present in equilibrium after the completion of the two reactions and was characterized with ^{31}P NMR. An associative mechanism was identified for both reactions, with large negative entropy and low positive enthalpy values.

Keyterms:

Ethylene tetramerisation

Diphosphinoamine ligands

Crystallographic study

Kinetic study

1-octene

Theoretical study

Steric parameter

Phenyl ring arrangement

Sterically bulky

Metal-PNP complexes

Opsomming

Oorgangsmetaal gekataliseerde etileen oligomerisering produseer tipies 'n wye verskeidenheid van α-olefiene. Die selektiewe tetramerisasie van etileen na 1-okteen word gedoen deur difenielfosfino-amien ligande, Cr(III) en 'n alumienoksaan as aktiveerder as katalissisteem te gebruik.

Die doel van hierdie studie was die sintese en karakterisering van 'n reeks difosfino-amien (PNP) ligande wat verskil in terme van katalitiese aktiwiteit en selektiwitieit (sien **Figuur 1**). Die stereo-elektroniese eienskappe van hierdie ligande is evalueer deur die alkielsubstituent sistematies te verander. Die enkelkristal X-straal kristallografiese studie van die ongebonde PNP ligande het aangedui dat die P-N-P hoek afneem soos wat die steriese bonkigheid van die alkielgroep toeneem.

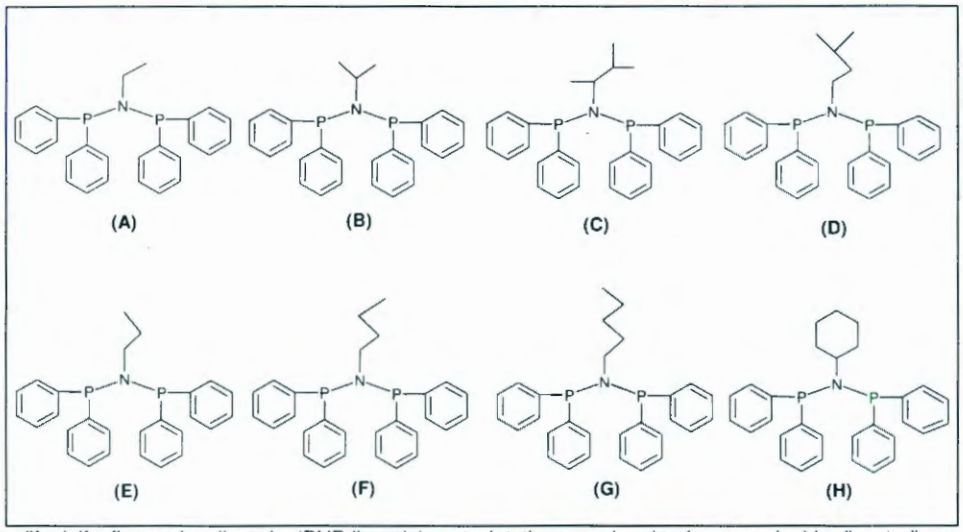

Figuur 1: Die difenielfosfino-amien ligande (PNP-ligande) wat sintetiseer, gekarakteriseer en in hierdie studie gebruik is. (A) Bis(difenielfosfino)etielamien (PNP-Ethyl); (B) Bis(difenielfosfino)isopropielamien (PNP-*i*-Prop); (C) Bis(difenielfosfino)-1,2-dimetielpropielamien (PNP-Dimprop); (D) Bis(difenielfosfino)isopentielamien (PNP-*i*-Pent); (E) Bis(difenielfosfino)-*n*-propielamien (PNP-*n*-Prop); (F) Bis(difenielfosfino)-*n*-butielamien (PNP-*n*-Butyll); (G) Bis(difenielfosfino)-*n*-pentielamien (PNP-*n*-Pent); (H) Bis(difenielfosfino)sikloheksielamien (PNP-Cychex).

'n Belangrike deel van hierdie ondersoek het die sintese en vaste toestand eienskappe van chroom(III)-PNP komplekse behels. Dit is verder gevoer deur ook ander metaalkatione (bv. Pt(II) en (Pd(II)) met die verskeidenheid PNP ligande te komplekseer om meer inligting omtrent die koordinatiewe eienskappe van hierdie ligande te ondersoek.

Hierdie studie is aangevul met berekeningschemie. Die vergelyking tussen die ge-optimiseerde (berekende) strukture en die kristaldata het klein verskille getoon, met die gevolg dat dit in die toekoms moontlik sal wees om voorspellings in terme van ligand ontwerp te bewerkstellig. Die berekende strukture het getoon dat die fenielring rangskikking meestal deur die steriese grootte van die stikstofgebonde alkielgroep geaffekteer word en dat dit 'n groot invloed op die katalitiese selektiwiteit uitoefen.

'n Steriese parameter is gedefinieer (Effektiewe Tolman-gebaseerde N-substituent steriese effek ($(\theta_{N\text{-}Sub})$ waarmee die steriese hindering van die stikstof-gekoordineerde alkielgroep gekwantifiseer word. 'n Vergelyking tussen die $\theta_{N\text{-}Sub}$ en die verskeie difenielfosfino-amien ligande (vry en gebonde) en die katalisselektiwiteit (vir 1-C_6 en 1-C_8) het 'n goeie korrelasie tussen stygende selektiwiteit getoon soos wat $\theta_{N\text{-}sub}$ groter word. Dit was ook moontlik om die as $\theta_{N\text{-}sub}^*$ (van berekende strukture) met die katalitiese selektiwiteit te vergelyk en 'n ooreenstemmende tendens kon tussen die berekenings chemie en die ware vaste toestand waarnemings getref word.

Die kinetika van die substitusiereaksies van die twee chloorligande deur bromied in [$PtCl_2$(PNP-*i*-Pent)] is ook ondersoek. Twee opeenvolgende, omkeerbare reaksies is waargeneem en kon onafhanklik van mekaar bestudeer word. Drie platinum(II) spesies [($PtCl_2$(PNP-*i*-Pent)], [(PtBrCl(PNP-*i*-Pent)] en [($PtBr_2$(PNP-*i*-Pent)], is in ewewig en is gekakateriseer met behulp van ^{31}P NMR. 'n Assosiatiewe meganisme is vir beide reaksies voorgestel en bevestig deur die hoë negatiewe entropie en lae positiewe entalpiewaardes.

1 Aim of the study

In this chapter...

The brief history of homogeneous catalysis and background information on platinum, palladium and chromium are presented. The aim of this study is also discussed in detail.

1.1 Introduction

1.1.1 Homogeneous catalysis

A catalyst is defined as a substance that increases the rate of a chemical reaction without itself undergoing any permanent chemical change. Catalysts that have the same phase as the reactants are known as homogeneous catalysts. Examples of this are enzymes in biochemical reactions or transition-metal complexes used in the liquid phase for catalyzing organic reactions in industry.[1] One of the first man-made catalytic processes, the "lead chamber process", was developed in the 1750's and involved the synthesis of sulphuric.[2] The process involves nitrogen oxides (NO/NO_2) that oxidize sulphur dioxide to the trioxide. The resultant NO is re-oxidised by air to NO_2, thereby completing the catalytic cycle.

The first industrially applied liquid phase catalyst and which employed organometallic intermediates is most likely the conversion of acetylene to acetaldehyde with mercury sulphate as catalyst in the 1920's. Many homogeneous catalysed processes have since been employed successfully in various industrial areas, including nickel hydrocyanation (Dupont), the cobalt catalysed carbonylation of methanol (BASF) and molybdenum catalysed epoxidation of propene (Halcon Corporation) to name a few.

---

[1] Leeuwen, P.W.N.M., Homogeneous catalysis understanding the art, Kluwer academic Publishers, **2004**, p1-8.
[2] Moulijn, J.A., van Leeuwen, P.W.N.M. and van Santen, R.A., *Catalysis, an integrated approach to homogeneous, heterogeneous and industrial catalysis*, Elsevier Amsterdam, **1993**,Volume 79, Chapter 1.

In recent years it has been shown that the ligand effects in homogeneous catalysis by metal complexes are extremely important, inspiring a lot of research in this area. A variety of products can be obtained from a single metal by merely changing the ligands around the metal centre. The ligand effects on catalytic processes will be discussed in more detail in the next chapter.

1.1.2 Background on metals

Selected platinum group metals

Impure, native platinum (Pt) seems to have been used unwittingly by ancient Egyptian craftsmen in place of silver, and was used to make small items of jewellery by the Indians of Ecuador before the Spanish conquest. In 1736 de Ulloa, a Spanish astronomer and naval officer, discovered an unworkable metal, *platina* (spanish for little silver) in the gold mines of what is now Colombia. Platinum occurs accompanied by small quantities of iridium, osmium, palladium, ruthenium and rhodium, all belonging to the same group of metals. The metal is extensively used in jewelery, electrical contacts, corrosion resistant apparatus and in dentistry. In the finely divided state, platinum is an excellent catalyst, having long been used in the process for producing sulphuric acid. It is also used as a catalyst in cracking petroleum products. The platinum compound, cisplatin ([*cis*-$(PtCl_2(NH_3)_2]$) was the first of a series of square planar platinum(II)-containing chemotherapy drugs. Platinum's most common oxidation states are +2 and +4 while the +1 and +3 oxidation states are less common.[3,4]

In 1803, in the course of his study of platinum, Wollaston isolated and identified palladium (Pd) from the mother liquor remaining after platinum had been precipitated as $[(NH_4)_2PtCl_6]$ from its solution in aqua regia. He named it after the newly discovered asteroid, Pallas, itself named after the Greek goddess of wisdom. Palladium is a soft

[3] Weast, R.C., *Handbook of Chemistry and Physics*, 60th Ed., CRC Press, **1979**, p. B16-17.
[4] Greenwood, N.N. and Earnshaw, A., *Chemistry of the Elements*, 2nd Ed., Pergamon Press, **1997**, p. 1144-1165.

silver-white metal that resembles platinum. It is the least dense and has the lowest melting point of the platinum group metals. An interesting fact is that at room temperature and atmospheric pressure, palladium can absorb up to 900 times its own volume of hydrogen in a reversible process. Palladium is used in the catalytic control of car exhaust emissions and when finely divided it forms a good catalyst and is used to speed up hydrogenation and dehydrogenation reactions, as well as petroleum cracking. The largest single use for palladium is in the manufacture of electronic components, but it is also used in dentistry and the jewellery trade. Common oxidation state of palladium are 0,+1, +2 and +4.[3,4]

Middle transition metals

Chromium (Cr) was first isolated in 1797 by French chemist, Vauquelin. He named it chromium, derived from the Greek word *chroma*, meaning colour, because of the wide variety of colours displayed by its compounds. It is of no wonder then that one of the first applications of chromium was in the dying industry. One of the most important applications of chromium, namely its use as an alloying element, was developed during the nineteenth century. Its first application was in 1874 with, the construction of the famous East Bridge across the Mississippi river. Today, the applications of chromium compounds are too numerous to mention, from uses in electronics, ceramics, catalysts, dyes and corrosion inhibitors to uses as fungicides in the agricultural industry. Known oxidation states are Cr^0, Cr^{1+}, Cr^{2+}, Cr^{3+}, Cr^{4+} and Cr^{6+}.[3,5,6]

1.2 Aim of this study

Transition metal-catalyzed ethylene oligomerization typically produces a broad range of α-olefins. The development of the technology for the selective production of alpha

[5] Westbrook, J.H., *Chromium and chromium alloys.* (In Grayson, M. ed. Kirk-Othmer Encyclopedia of Chemical Technology. New York: John Wiley & Sons., **1979,** p. 54-82 ...(and references therein).
[6] Hartford, WH., *(In Grayson, M. ed. Kirk-Othmer Encyclopedia of Chemical Technology.* New York: John Wiley & Sons., **1979**, p. 82-120.

olefins is an ongoing process[7] and recently the selective tetramerisation of ethylene to 1-octene was reported.[8] A large number of diphosphinoamine (PNP) ligands with various substituents on both the N and P atoms were evaluated (when combined with Cr(III) and an aluminoxane activator).[9,10,11,12,13] It was found that the predominant factor in the catalysis selectivity (in particular the α-selectivity) is the steric bulk on the central nitrogen atom compared to the basicity of the phosphine. The steric bulk of the varying alkyl moieties were however estimated.

Based on this information, a systematic synthetic, solid state and computational study was envisaged to ensure an overarching correlation of the general behaviour of these ligand systems. Thus, additional PNP ligands (see **Figure 1.1**) have been synthesised and single crystal X-ray crystallographic studies initiated to further evaluate any correlations. A comparison of the crystallographic data of a variety of PNP ligands with varying activity and selectivity (when complexed with chromium(III)) could provide valuable information for future ligand design and explaining current catalytic behaviour. Complexing other metal cations (eg. Pt(II) and Pd(II)) with the various PNP-ligands will provide further information on the coordination mode of these ligands. An additional part of this investigation involves the theoretical calculations of the crystal structures of the metal-PNP complexes and the non-coordinated ligands. These structures could provide a more in-depth understanding of the observed structures from the crystallographic data. The calculated structures obtained by optimisation *via*

---

[7] Dixon, J.T., Green, M.J., Hess, F.M. and Morgan, D.H., *J. Organomet. Chem.*, **2004**, *689*, 3641.

[8] Bollmann, A., Blann, K., Dixon, J.T., Hess, F. M., Killian, E., Maumela, H., McGuinness, D. S., Morgan, D. H., Neveling, A., Otto, S., Overett, M.J., Slawin, A.M.Z., Wasserscheid, P. and Kuhlmann, S., *J. Am. Chem. Soc.*, **2004**, *126*, 14712.

[9] Blann, K., Bollmann, A., de Bod, H., Dixon, J.T., Killian, E., Nongodlwana, P., Maumela, M.C., Maumela, H., McConnell, A.E., Morgan, D.H., Overett, M.J., Prétorius, M., Kuhlmann, S. and Wasserscheid, P., *.J. Catal.*, **2007**, *249*, 244.

[10] Overett, M.J., Blann, K., Bollmann, A., Dixon, J.T., Hess, F.M., Killian, E., Maumela, H., Morgan, D.H. Neveling, A. and Otto, S., *Chem. Commun.*, **2005**, 622.

[11] Blann, K., Bollmann, A., Dixon, J.T., Hess, F.M., Killian, E., Maumela, H., Morgan D.H., Neveling, A., Otto, S. and Overett, M., *Chem. Commun.*, **2005**, 620.

[12] Kuhlmann, S., Blann, K., Bollmann, A., Dixon, J.T., Killian, E., Maumela, M.C., Maumela, H., Morgan, D.H., Prétorius, M., Taccardi, N. and Wasserscheid, P., *J. Catal.*, **2007**, *245*, 277.

[13] Killian, E., Blann, K., Bollmann, A., Dixon, J.T., Kuhlmann, S.E., Maumela, M.C., Maumela, H., Morgan, D.H., Nongodlwana, P., Overett, M.J., Prétorius, M., Höfener, K. and Wasserscheid, P., *J. Mol. Catal. Chem.* **2007**, *270*, 214.

computational chemistry techniques of selected non-coordinated ligands are reported here and compared with the crystallographic data of the corresponding ligands.

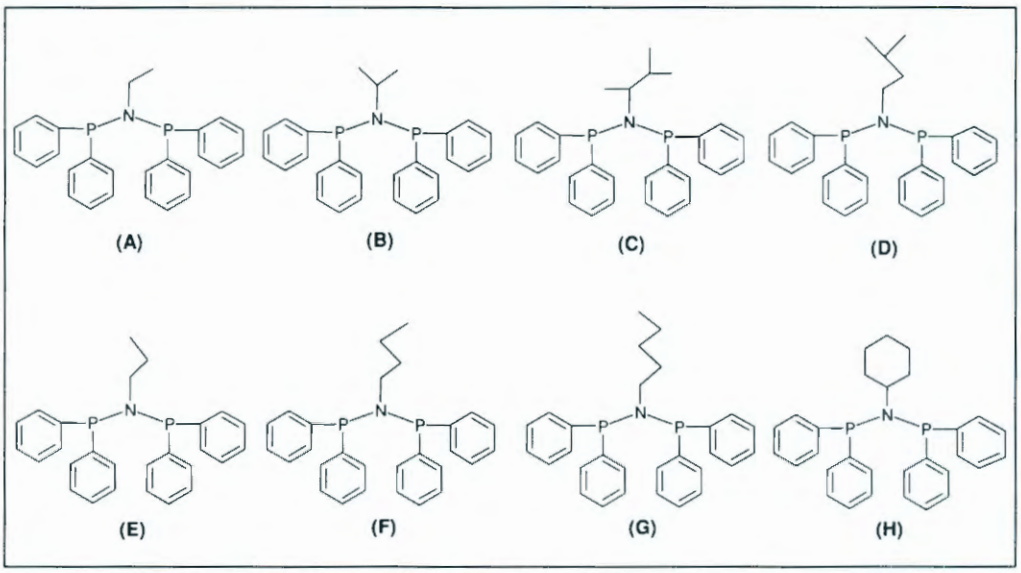

Figure 1.1: The diphosphinoamine ligands (PNP-ligands) synthesized, characterised and used in this study. (A) Bis(diphenylphosphino)ethylamine (PNP-Ethyl); (B) Bis(diphenylphosphino)-isopropylamine (PNP-*i*-Prop); (C) Bis(diphenylphosphino)-1,2-dimethylpropylamine (PNP-Dimprop); (D) Bis(diphenylphosphino)-isopentylamine (PNP-*i*-Pent); (E) Bis(diphenylphosphino)-*n*-propylamine (PNP-*n*-Prop); (F) Bis(diphenylphosphino)-*n*-butylamine (PNP-*n*-Butyl); (G) Bis(diphenylphosphino)-*n*-pentylamine (PNP-*n*-Pent); (H) Bis(diphenylphosphino)-cyclohexylamine (PNP-Cychex).

Proceeding from the previous paragraphs, the following stepwise goals were set for this study:

1) To synthesize a systematic range of diphosphinoamine ligands and collect single crystal X-ray crystallographic data of the non-coordinated PNP-ligands.
2) Synthesize metal-PNP compounds (metal = Cr(III), Pt(II) and Pd(II)) and collect single crystal X-ray crystallographic data.
3) Perform theoretical calculations of the various compounds of which crystallographical data was collected (free PNP-ligands and metal-PNP complexes). Compare the optimised structures with the corresponding crystal structures.

4) Compare the crystallographic data of the variety of PNP-ligands with the catalytic 1-hexene (1-C_6) and 1-octene (1-C_8) selectivity and evaluate any possible correlations.
5) Define a steric parameter for the nitrogen-coordinated alkyl substituent of the various PNP compounds (using crystallographic and theoretically optimised structures) and compare this with the catalytic 1-hexene (1-C6) and 1-octene (1-C8) selectivity of the PNP-ligands (when complexed with Cr(III) in the catalytic process).
6) Perform a solution behavioural kinetic study of a crystallgraphically characterised metal-PNP complex to evaluate the general kinetic behaviour of selected metal-PNP complexes.
7) Develop a systematic approach to evaluating catalysis by incorporating X-ray crystallographic data and theoretical calculations in order to improve future ligand design methods.

In the following chapter a brief literature review of the discovery and development of the ethylene tri- and tetramerisation catalytic processes is presented, followed by the systematic presentation and discussion of the experimental results.

2 Literature study

In this chapter...

The history of the discovery and development of the selective ethylene tri-and tetramerisation processes are briefly discussed. Background information on the steric and electronic parameters used in this study is included at the end of this chapter.

2.1 Introduction

Linear alpha olefins (LAO's) represent an important group of industrial chemical products which are useful intermediates for amongst others, the production of co-polymers, detergents, synthetic lubricants and plasticizer alcohols. Conventional ethylene oligomerisation typically produce a broad Schulz-Flory distribution of α-olefins which must then be separated to give specific carbon number products.[1,2,3] The various components of this distribution has varying commercial value. There is consequently an increasing interest in the development of catalyst systems which are able to produce greater selectivity towards more desirable olefins. Of particular interest is the tri- and tetramerisation of ethylene to 1-hexene and 1-octene respectively, due to the importance of these co-monomers in the polymer industry. Of the systems known to tri- and tetramerise ethylene, most are based on homogeneous chromium catalyst systems.

2.2 Ethylene trimerisation

2.2.1 The discovery of ethylene trimerisation

During 1967 three researchers, Manyik, Walker and Wilson, of Union Carbide Corporation filed a patent on the continuous processes for the production of

[1] Schulz, G.V.*Z., Phys. Chem. B.*, **1935**, *30*, 379.
[2] Flory, P.J., *J. Am. Chem. Soc.*, **1936**, *58*, 1877.
[3] Skupinska, J., *Chem. Rev.*, **1991**, *91*, 613.

polyethylene.[4] Observations were made that during the polymerization of ethylene using chromium(III)-2-ethylhexanoate (Cr(III)-2-EH) activated by partially hydrolysed tri-isobutylaluminium (PIBOA), a portion of the ethylene trimerised to form 1-hexene. It was stated that the difference in temperature and pressure dependence on the rates of formation of polyethylene and 1-hexene, indicated that the mechanism for the formation of 1-hexene differed from that of polyethylene. Ten years later Manyik *et al.* published the discovery of the formation of 1-hexene during the Cr(III)-2-EH/(PIBOA) catalysed polymerization of ethylene.[5] The chromatographic analysis of the supernatant of these polymerization reactions revealed that 1-butene, 1-hexene, 1-octene and 1-decene were produced, with 1-hexene being predominant. The 1-hexene content of the liquid sample was however only 1.1 %.

2.2.2 Homogeneous chromium-based trimerisation catalysts

(i) Chromium-based catalyst systems: Aromatic ligands.

Chromium-based cyclopentadienyl complexes are used extensively as catalysts in the ethylene polymerization industry.[6,7] This catalytic system inspired Reagan from the Phillips Petroleum Company to initiate the investigation of pyrrolide ligands, as these ligands are the closest heterocyclic analogues to the cyclopentadienide ligands with regards to electronic and steric properties.[8] Various chromium pyrrolide compounds were prepared by reacting $CrCl_2$ and $CrCl_3$ with various stoichiometric ratios of sodium pyrrolide.[8,9] Reagan managed to isolate and characterize a pentanuclear complex, $[Cr_5(C_4H_4N)_{10}(C_4H_4O)_4]$ from the reaction between $CrCl_2$ and two molar equivalents of pyrrolide in tetrahydrofuran (THF). This pentanuclear complex was the minor product, while the major product was an inorganic polymer. The reaction between $CrCl_2$ and an excess of sodium pyrrolide yielded two totally different compounds. The major product

[4] Manyik, R.M., Walker, W.E. and Wilson,T.P., US 3300458 (Union Carbide Corporation), January 24, **1967**.
[5] Manyik, R.M., Walker, W.E. and Wilson,T.P., *J. Catal.*, **1977**, *47*, 197.
[6] Theopold, K.H., *Eur., J. Inorg. Chem.*, **1998**, 15.
[7] Britovsek, G.J.P., Gibson, V.C. and Wass, D.F., *Angew. Chem. Int. Ed.*, **1999**, *38*, 428.
[8] Reagan, W.K., Symp. Prepr. Conv. Light Olefins, Div. Pet. Chem., *J. Am. Chem. Soc.* **1989**, *34* , 583.
[9] Reagan, W.K., EP 0417477 (Phillip etroleum Company), March 20, **1991**.

being a square planar complex, $Na_2[Cr(C_4H_4N)_4]\cdot 2OC_4H_4$, and the minor product the octahedral complex, $Na_2[Cr(C_4H_4N)_5(C_4H_4O)]\cdot 4C_4H_4O$. The presence of the Cr(III) octahedral product was accredited to the $CrCl_2$ reagent that contained 5-10 % by weight $CrCl_3$. The reaction between $CrCl_3$ and three molar equivalents of sodium pyrrolide in THF yielded only one product: an inorganic polymer which consisted of multiple $[Cr(C_4H_4N)_2Cl]$ units.[8]

All the above-mentioned Cr-pyrrolide complexes (except the octahedral Cr(III) complex, $Na_2[Cr(C_4H_4N)_5(C_4H_4O)]\cdot 4C_4H_4O$, which was not evaluated) proved to be catalytically active towards ethylene oligomerisation. These complexes were also found to be catalytically active when supported on SiO_2, Al_2O_3 and $AlPO_4$. The highest catalyst activity exceeding 10 500 g/g Cr per hour (activity is presented as ethylene consumed per gram of catalyst per hour throughout the chapter) was achieved by using the Al_2O_3-supported pentanuclear complex, $[Cr_5(C_4H_4N)_{10}(C_4H_4O)_4]$. This reaction however produced only 31 % liquid oligomers and 69 % polyethylene. Selectivity of more than 99 % towards liquid oligomers was achieved with the Cr(III) polymer consisting of $[Cr(C_4H_4N)_2Cl]$ units. The liquid oligomers contained up to 90.5 % hexenes of which was approximately 92 % 1-hexene and there was less than 2 % polyethylene produced. These Cr-pyrrolide compounds formed the basis of what is now known as the Phillips ethylene trimerisation catalyst systems.[9] The discovery of this catalyst system was a major contribution towards the progress of the selective ethylene trimerisation as it was the first example of a trimerisation catalyst that produced 1-hexene in a greater than 90 % overall selectivity.

Over the next few years the Phillips Petroleum Company improved significantly on their initial discovery. By 1999 their ethylene trimerisation catalyst performed to such an extent that a catalyst activity of 94700 g/g Cr in 36 minutes (155 245 g/g Cr per hour) was reported.[10] The reaction yielded 99.9 % liquid oligomers, with 93 % 1-hexene overall. The catalyst system was prepared by combining chromium(III)-2-ethylhexanoate, 2,5-dimethylpyrrole, diethylaluminium chloride and triethylaluminium at

[10] Freeman, J.W., Buster, J.L. and Knudsen, R.D., US 5856257 (Phillips Petroleum Company), January 5, **1999**.

room temperature, using a nitrogen purge to stir the reagents. The catalytic reaction was performed at 115°C, with a reaction pressure of 100 bar. The 2,5-dimethylpyrrole ligand seemed to be the preferred choice in their catalyst systems due to its excellent performance and the fact that it has a higher light, air and temperature stability than their other counterparts.

Shortly after the discovery of the Phillips trimerisation catalyst system, many other commercial companies filed patents which were based on this catalyst system. These companies included, Idemitsu Kosan Company[11], Chinese Petroleum Group[12], Sumitomo Chemical Company[13], Sasol Technology[14], BASF[15] and Beijing Yanshan Petrohemical Company.[16] It has to be noted that these patents included only slight variations of the Phillips catalyst system, where mostly one of the three key components were modified. The performances of these catalysts were however only moderate in comparison to the optimized results that the Phillips Petroleum Company has achieved. There was nonetheless one company, Mitsubishi Chemical Corporation, that actually improved upon the Phillips catalyst by preparing the catalyst with non-coordinating Lewis acids, such as $B(C_6F_5)_3$ in addition to Cr(III)-2-EH, pyrrole and TEA. This resulted in significantly higher activities.[17] Exceptional catalyst activities of 3 780 000 g/g Cr per hour were also obtained by developing a protocol in which the Phillips catalyst system (using chromium(III)-2-ethylhexanoate, 2,5-dimethylpyrrole, hexachloroethane and triethylaluminium) was prepared in situ during a continuous trimerisation reaction.[18]

Various chromium systems based on aromatic ligands, similar to the pyrrole ligands, were assessed for ethylene trimerisation. These included the maleimide ligands by the

[11] Sato, H. and Nakajima, H., JP 06329562 (Idemitsu Chemical Company) November 29, **1994**.
[12] Wang, G., Xie, M., Wang, S., Qu, J., Zhao, J., Zhang, B., Chen, Q., Yuan, Z., Han, X. and Li, L., CN 1294109 (Chinese Petroleum Group), May 9, **2001**.
[13] Tamura M., Uchida, K., Ito, Y. and Iwanga, K., EP 0614865 (Sumitomo Chemical Company), September 14, **1994**.
[14] Dixon, J.T., Grové, C. and Ranwell, A., WO 01/83447 (Sasol Tehnology (Pty) Ltd), November 8, **2001**.
[15] Maas, H., Mihan, S., Kohn, R., Seifert, G. and Tropsch, J., WO 2000058319 (BASF Aktiengesellshaft), October 5, **2000**.
[16] Sui, J., Du, X. and Li, T., *Hecheng Shuzhi Ji Suliao* 18 (2) **2001** 23.
[17] Tanaka, E., Urata, H., Oshiki, T., Aoshima, T., Kawashima, R., Iwade, S., Nakamura, H., Katsuki, S. and Okanu, T. EP 0611743 (Mitsubishi Chemical Corporation), August 24 **1994**.
[18] Araki, Y., Nakamura, H., Nanba, Y. and Okanu, T., US 5,856,612 (Mitsubishi Chemical Corporation), January 5, **1999**.

Tosoh Corporation in the late 1990's,[19] the boratabenzenyl ligand system by Mitsubishi Corporation[20] and the aryloxide ligands by the Institut Francais du Petrole.[21] The cyclopentadienyl ligands were also investigated, but showed to be merely good ethylene polymerization catalysts even though these systems are isoelectronically and sterically very similar to the pyrrolyl ligand systems. Sasol Technology however, showed it is possible to attain a highly active ethylene trimerisation catalyst by introducing bulky aromatic substituents onto the cyclopentadienyl ring.[22,23] An impressive overall 1-hexene selectivity of 77.2 % was achieved with 5-(4-*t*-butylphenyl)-1,2,3,4-tetraphenylcyclopentadienyl as ligand together with Cr(III)-2-EH and triethylaluminium (TEA) as activator (see **Scheme 2.1**).

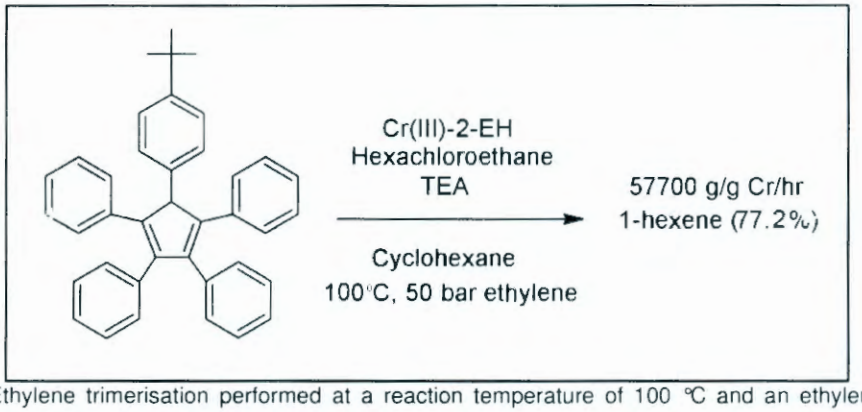

Scheme 2.1: Ethylene trimerisation performed at a reaction temperature of 100 °C and an ethylene pressure of 50 bar with 5-(4-*t*-butylphenyl)-1,2,3,4-tetraphenylcyclopentadienyl as ligand, using a catalyst prepared with Cr(III)-2-EH:ligand:hexachloroethane:TEA in molar ratios of 1:3:2.5:45.[24]

(ii) Chromium-based catalyst systems: Multidentate heteroatomic ligands.

The donor atoms of the multidentate heteroatomic ligands (which are usually bi- or tridentate) coordinate with chromium. The tridentate ligands can coordinate facially or meridionally.

[19] Aoyama, T., Mimura, H., Yamamoto, T., Oguri, M. and Koie, Y., JP 09176299 (Tosoh Corporation), July 8, **1997**.
[20] Aoshima, T. and Urata, T., JP 11181016 (Mitsubishi Chemical Industries) July 6, **1999**.
[21] Commereuc, D.C., Drochon, R.M. and Saussine, C., US 6031145 (Institut Francais du Petrole) June 17, **1998**.
[22] Mahomed, H., Bollmann, A., Dixon, J., Gokul, V., Griesel, L., Grove, C., Hess, F., Maumela, H. and Pepler, L., *Appl. Catal.* **2003**, *A 255*, 355.
[23] Grove, J.J.C., Mahomed, H.A. and Griesel, L., WO 03/004158 (Sasol Technology (Pty Ltd), June 27, **2002**.
[24] Dixon, J.T., Green, M., Hess, F.M. and Morgan, D.H., *J. Organomet. Chem.*, **2004**, *689*, 3641 ...(and reference therein).

Wu proposed that a sterically demanding ligand system such as 1,4,7-trimethyl-1,4,7-triazacyclononane, which coordinates facially to the chromium (see **Figure 2.1**), would prove to be a successful nitrogen based ligand system with regards to ethylene oligomerisation.[25] He postulated that these ligands would permit ethylene trimerisation and oligomerisation, while inhibiting polymerization, due to its steric bulk. In his study of chromium complexes of triazacyclononane ligand systems he found that these catalyst systems yielded a Schulz-Flory distribution of alpha olefins which were selectively enriched with 1-hexene. Formation of large amounts of polyethylene and vinylidine olefins was also inhibited. Further proof towards the necessity of steric bulk for increased oligomerisation compared to polymerization was provided by the fact that the triazacyclononane ligand without substituents on the nitrogen atoms only gave polymerization of ethylene.

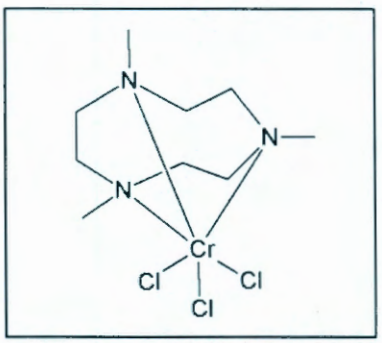

Figure 2.1: A schematic representation of the compound,[$CrCl_3$(1,4,7-trimethyl-1,4,7-triazacyclononane)], which is used together with n-hexylaluminoxane in toluene to catalyze the oligomerisation of ethylene.[25]

Chromium complexes of polydentate phosphines with the general formula, $R_2P(CH_2)_nP(R')(CH_2)_mPR_2$, were developed by Amoco Corporation.[26] These act as ethylene trimerisation catalysts when activated by an aluminoxane co-catalyst. Crystal studies of the chromium complexes revealed an octahedral geometry with a meridional arrangement of the phosphine ligand. This is in contrast to the facially coordinated chromium coordinated triazacycloalkane complexes discussed earlier.

[25] Wu, F.J., EP 0537609 (Albemarle Corporation) July 10, **1992**.
[26] Wu, F.J., US 5811618 (Amoco Corporation), August 25, **1995**.

The symmetrical ligand systems such as $CH_3P[(C_3H_6)PCH_2CH_2)]_2$ coordinate with chromium to form catalysts which deactivate over a short period of time (20 minutes). The best results were however achieved by using a chromium(III) complex of an unsymmetrical tridentate phosphine ligand, (2-dimethyl-phosphinoethyl)(3-dimethylphosphinopropyl)phenylphosphine (see **Scheme 2.2**). This complex, when activated by butylaluminoxane yielded 97.7 % hexene (96.5 % 1-hexene overall), 1 % octene and 0.3 % polyethylene, with a catalyst activity of 33 926 g/g Cr/hr. It was proposed that the 1-hexene could be used without further purification. This is surprising as many of the other trimerisation catalyst systems required fractionisation of the 1-hexene from the higher oligomeric products. Unfortunately the high cost of the synthesis of these phosphine ligands prohibits it from being used commercially.

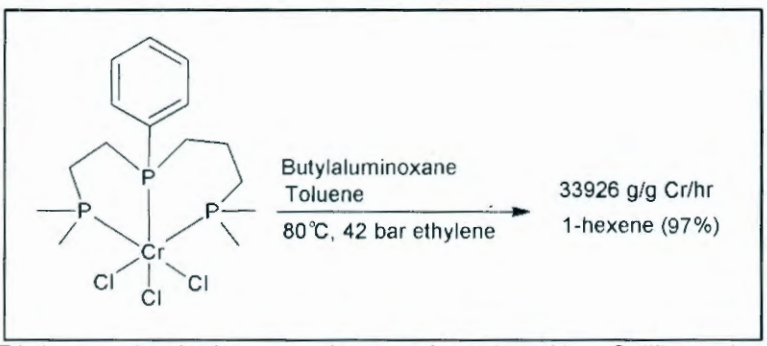

Scheme 2.2: Ethylene trimerisation reaction performed with Cr(III)-complex coordinated to (2-dimethyl-phosphinoethyl)(3-dimethylphosphinopropyl)phenylphosphine.[24, 26]

British Petroleum patented[27] and published[28] the first chromium-based trimerisation system with diphosphinoamine ligands of the type $Ar_2PN(Me)PAr_2$, where Ar is an *o*-methoxy substituted aryl group. This catalyst system proved to be extremely active and selective when acitivated by MAO. When using very low concentrations of the Cr and ligand, the best trimerisation results were obtained. A concentration as low as 0.005 millimolar $[CrCl_3(THF)_3]$ and (2-methoxy-phenyl)$_2$PN(methyl)P(2-methoxy-phenyl)$_2$ trimerised ethylene (when activated with MAO (methylaluminoxane)) and yielded 90 % hexene (99.9 % 1-hexene). An impressive catalyst activity of

[27] Wass, D.F., WO 02/04119 (BP Chemicals Ltd) January 17, **2002**.
[28] Carter, A., Cohen, S.A., Cooley, N.A., Murphy, A., Scutt, J. and Wass, D.F., *Chem. Commun.* **2002**, 858.

1 033 200 g/g Cr per hour was reported (see **Scheme 2.3**). In addition, the loss in catalyst activity was less than 10 % per hour, this is in contrast to most trimerisation catalyst systems which seem to lose most of their activity over a 30 minute period.

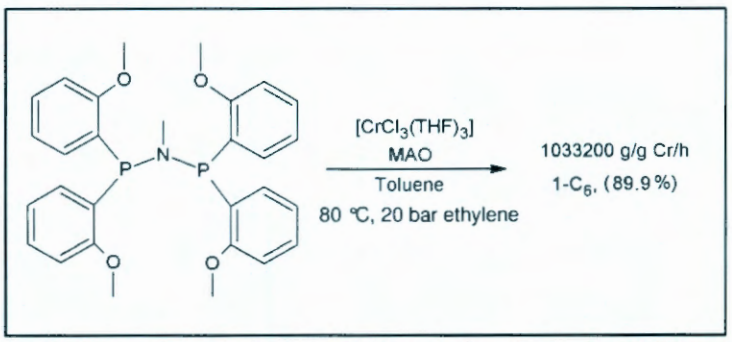

Scheme 2.3: Ethylene trimerisation performed with $CrCl_3(THF)_3$ and (2-methoxy-phenyl)$_2$PN(methyl)P(2-methoxy-phenyl)$_2$ as part of the precatalyst system. [24, 28]

The performance of the catalyst system was initially attributed to the steric bulk in the *ortho* position. It was however reported that an *o*-ethylphenyl PNP analogue gave no catalytic activity under similar reaction conditions, while the *p*-methoxy analogue was also inactive. It was then postulated that the *o*-methoxy groups could act as pendant donors and that this is a prerequisite for ethylene trimerisation catalyst activity.

Another interesting trimerisation catalyst system containing mixed phosphorous and nitrogen donor atoms, was patented[29] and published[30] by Sasol Technology and consists of Cr(III) complexes of tridentate bis-phosphinoamine ligands, $R_2PCH_2CH_2N(H)CH_2CH_2PR_2$. These complexes were prepared by reacting the bis-diphosphinoamine ligand with $[CrCl_3(THF)_3]$ at room temperature. When activated by MAO these systems perform as very selective and active trimerisation catalysts. Modifications of the R groups on the phosphorus atoms were made in an effort to improve the activity of the system. Highly basic and sterically demanding dicyclohexylphosphino moieties led to a decreased activity and increased polyethylene

[29] Dixon, J.T., Grove, J.J.C., Wasserscheid, P., McGuinness, D.S., Hess, F.M., Maumela, H., Morgan, D.H. and Bollmann, A., WO 03053891 (Sasol Technology (Pty) Ltd), December 20, **2001**.
[30] McGuinness, D.S., Wasserscheid, P., Keim, W., Dixon, J.T., Grove, J.J.C., Hu, C. and Englert, U., *Chem. Commun.*, **2003**, 334.

production. Increased activity and excellent 1-hexene selectivity was however observed for the basic and less sterically demanding diethylphosphino moieties. The best activity was achieved using [$CrCl_3$(bis(2-diethylphosphino(ethylamine)], which when activated with 850 equivalents of MAO yielded a reaction mixture containing 94 % hexene (93.2 % 1-hexene overall) and 2.1 % polyethylene (see **Scheme 2.4**).

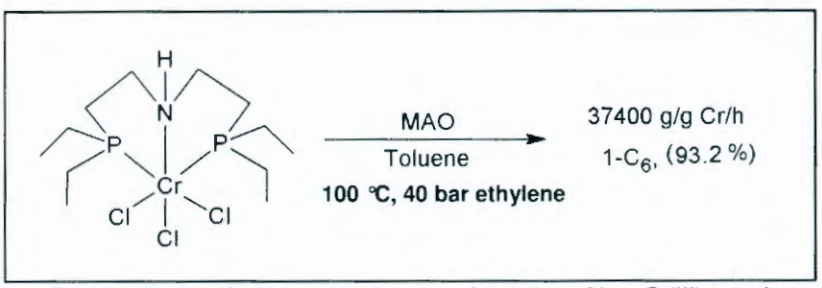

Scheme 2.4: Ethylene trimerisation reaction performed with Cr(III)-complex coordinated to bis(2-diethylphosphino-ethyl)amine.[24, 30]

2.2.3 Mechanism

The process of oligomerisation of ethylene to form linear alpha olefins usually produces a statistical series of products that follows the Schulz-Flory[1,2] distribution. The generally accepted mechanism for this process was proposed by Cossee and Arlman.[31,32] It was postulated that chain growth occurred through the coordination of an ethylene molecule and then the insertion into a transition metal alkyl bond. The chain termination then occurred *via* β-hydrogen transfer to the metal to form a metal-hydride species, upon which a linear alpha olefin is released (see **Scheme 2.5**).

[31] Cossee, P. *J., Catal.*, **1964**, *3*, 80.
[32] Arlman, E.J., Cossee, P., *J. Catal.*, **1964**, *3*, 99.

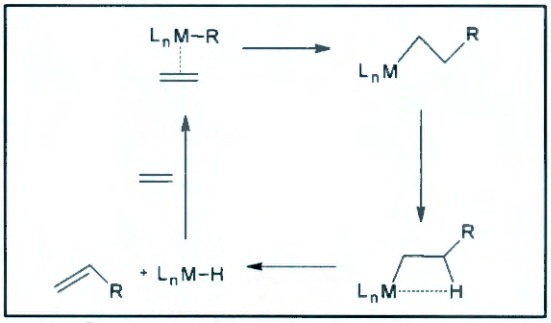

Scheme 2.5: Mechanism proposed by Cossee and Arlman for oligomerisation of ethylene to form linear alpha olefins from ethylene.[24,31,32]

When Manyik and co-workers published the discovery of ethylene trimerisation,[5] they also reported that changes in pressure and temperature had a noticeable effect on the rates of polymerization and 1-hexene formation. It appeared that the rate of 1-hexene formation was dependent on the square of the ethylene pressure, suggesting a second order reaction in ethylene. It was as a result concluded by the authors that the 1-hexene was not produced by way of linear chain growth, but rather a metallocycle mechanism. The postulated mechanism (see **Scheme 2.6**) involves the coordination of two ethylene molecules, followed by the formation of a chromacyclopentane species. A third ethylene molecule would coordinate to the metal centre, followed by a β-hydrogen transfer from the chromacyclopentane to the additionally coordinated ethylene molecule. 1-Hexene is then liberated by reductive elimination.

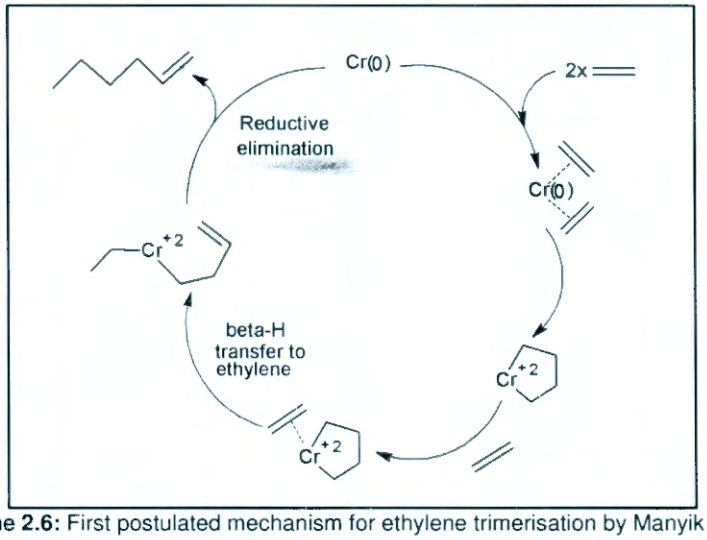

Scheme 2.6: First postulated mechanism for ethylene trimerisation by Manyik *et.al.*[24]

The existence of a metallocyclic intermediate in a catalytic cycle was proved to be viable with the synthesis of Pt(II) metallocycle complexes.[33,34] It was also shown that the thermal elimination of olefins from platinacycloheptanes is much more rapid than from smaller sized rings.

This information lead Briggs to postulate a mechanism which includes the formation of metallocyclopentane and metallocycloheptane intermediate species.[35] The insertion of an ethylene molecule into the metallocyclopentane would yield a metallocycloheptane. Ring opening then occurs with the formation of a chromium hexenyl hydride species, which undergoes reductive elimination to liberate 1-hexene (see **Scheme 2.7**). In order to selectively yield 1-hexene, the elimination of 1-hexene from the metallocycloheptane must be faster than further insertions of ethylene to produce larger rings.

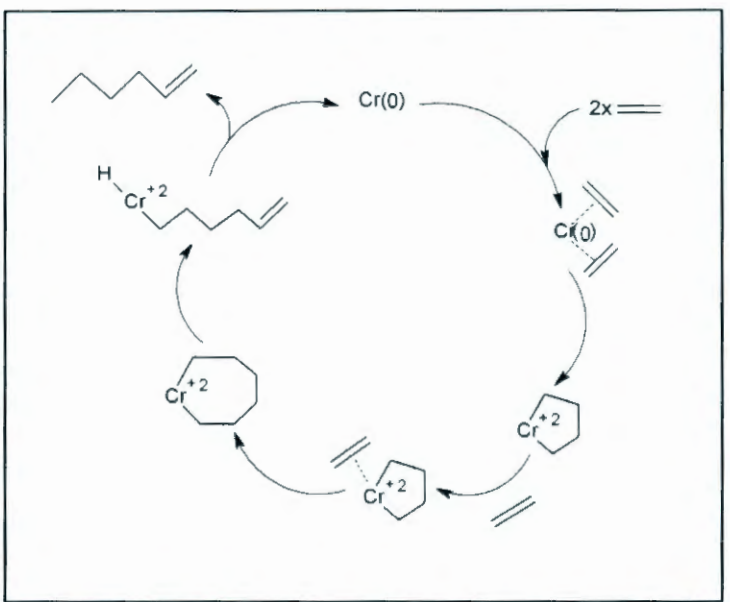

Scheme 2.7: Ethylene trimerisation mechanism proposed by Briggs.[24,35]

The legitimacy of this mechanism was ultimately confirmed by Emrich *et. al.* which reported the crystal structures of chromium metallocyclopentane and –cycloheptane

[33] McDermott, J.X., White, J.F, and Whitesides, G.M., *J. Am. Chem. Soc.*, **1973**, *95*, 4451.
[34] McDermott, J.X., White, J.F. and Whitesides, G.M., *J. Am. Chem. Soc.*, **1976**, *98*, 6521.
[35] Briggs, J.R., *Chem. Commun.*, **1989**, *11*, 674.

derivatives.[36] The seven-membered species was shown to decompose more readily, (yielding 1-hexene), than the five-membered species. Lending even further support to the above mechanism is the fact that even though stable alkyl hydride species of chromium are extremely rare, a crystal structure of a dinuclear chromium alkyl hydride was also reported.[37] Agapie and co-workers provided further evidence by performing a trimerisation reaction using a 1:1 mixture of C_2D_4 and C_2H_4.[38] It was reasoned that the Cossee-type mechanism would result in H/D scrambling, yielding isotopomers containing odd numbers of deuterons and that a metallocyclic mechanism would lead to no H/D scrambling. The experiment only yielded even-numbered isotopomers (C_6D_{12}, $C_6D_8H_4$, $C_6D_4H_8$ and C_6H_{12} in a 1:3:3:1 ratio).

The metallocycle mechanism that has been proposed necessitates that the formal oxidation state of chromium changes from M^0 to M^{2+} during the initial addition of two ethylene molecules, forming the metallocyclopentane species. The oxidation state then has to decrease during the reductive elimination step from M^{2+} to M^0. The actual oxidation states of the chromium atom during the trimerisation cycle is not yet known with surety, but Cr(I)/Cr(III),[5,39] Cr(II)/Cr(IV)[40,41] and Cr(III)/Cr(V)[42] pairs have been proposed.

Since the initial discovery of ethylene trimerisation in which merely 1 % 1-hexene was reported, the technology has developed significantly over the past three decades, with overall selectivities of 1-hexene of more than 99 % and huge improvements in catalyst activities. The progress has also included the extension of the trimerisation catalyst

[36] Emrich, R., Heinemann, O., Jolly, P.W., Krüger, C. and Verhovnik, G.P.J., *Organometallics*, **1997**, *16*, 1511.
[37] MacAdams, L.A., Buffone G.P., Incarvito, C.D., Golen, J.A., Rheingold, A.L. and Theopold, K.H., *Chem. Commun.*, **2003**,1164.
[38] Agapie, T., Schofer, S.J., Labinger, J.A. and Bercaw, J.E., *J. Am. Chem. Soc.*, **2004**, *126*, 1304.
[39] Köhn, R.D., Haufe, M., Mihan, S. and Lilge, D., *Chem. Commun.*, **2000**, 1927.
[40] Morgan, D.H., Schwikkard, S.W., Dixon, J.T., Nair, J.J. and Hunter, R., *Adv. Synth. Catal.*, **2003**, *345*, 939.
[41] van Rensburg, W.J., Grově, C., Steynberg, J.P., Stark, K.B., Huyser, J.J. and Steynberg, P.J., *Organometallics*, **2004**, *23*,1207.
[42] Meijboom, N., Schaverien, C.J. and Orpen, A.G., *Organometallics*, **1990**, *9*, 774.

system to other transition metals such as titanium,[43] vanadium,[43] and zirconium[43] even though these have yet to prove to be as successful as the chromium catalyst systems.

2.3 Ethylene tetramerisation

2.3.1 Homogeneous chromium-based tetramerisation catalysts

A selective route to 1-octene is highly desirable from an economic perspective as this α-olefin is one of the co-monomers in the synthesis of polymers. Ethylene tetramerisation was thought to be highly improbable. The reason for this was that if ethylene tetramerisation was to proceed according to the same mechanism as trimerisation (see **Scheme 2.7**), it would mean that another ethylene molecule would be inserted in the seven-membered ring to form a nine-membered metallocycle intermediate. This has been argued to be unlikely as the nine-membered ring is the least favoured medium-sized ring.[44,45] Against all odds an ethylene tetramerisation reaction that produced 1-octene in good selectivity was however reported by Sasol Technology in 2004.[46] A catalyst system consisting of an aluminoxane-activated chromium/$(Ph_2P)_2N$(isopropyl) system (see **Scheme 2.8**) produced 1-octene in selectivities up to 70 %. Various diphosphinoamine (PNP) ligands with substituents on both the N and P atoms were evaluated, and all these systems gave 1-octene in good selectivity with other major products consisting of 1-hexene, methylcyclopentane and methylenecyclopentane. It was found that the predominant factor in the catalytic selectivity (in particular the α-selectivity) is the steric bulk on the central nitrogen atom compared to the basicity of the phosphine. The fact that the highest α-selectivity for hexene was achieved with the isopropyl and cyclohexyl substituents bonded to the central nitrogen atom indicated that the α-branching is crucial.

[43] Reagan, W.K., Freeman, J.W., Conroy, B.K., Pettijohn, T.M. and Benham E.A., US 5451645 (Phillips Petroleum Company), September 19, 1995.
[44] Yu, Z.X. and Houk, K.N., *Angew. Chem., Int. Ed.*, **2003**, *42*, 808.
[45] Blok, A.N.J., Budzelaar, P.H.M. and Gal, A.W., *Organometallics*, **2003**, *22*, 2564.
[46] Bollmann, A., Blann, K., Dixon, J.T., Hess, F. M., Killian, E., Maumela, H.; McGuinness, D. S.; Morgan, D. H.; Neveling, A.; Otto, S.; Overett, M.J.; Slawin, A.M.Z.; Wasserscheid, P. and Kuhlmann, S., *J. Am. Chem. Soc.*, **2004**, *126*, 14712.

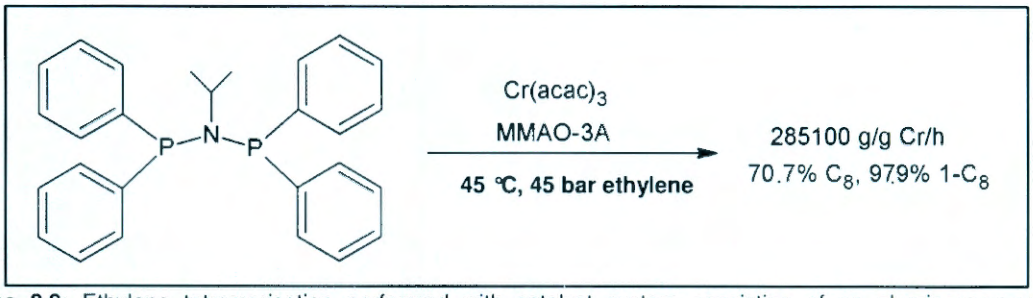

Scheme 2.8: Ethylene tetramerisation performed with catalyst system consisting of an aluminoxane-activated chromium/$(Ph_2P)_2N$(isopropyl) (MMAO-3A = modified methylaluminoxane).[46]

The catalyst evaluations were largely performed *in situ* (the ligand, Cr(III) precursor, PNP ligand and activator were each added separately to reactor), while some catalytic reactions were conducted successfully using pre-formed Cr(III)-PNP complexes. One such compound, $[Cr(Ph_2P)_2N(Ph)Cl_2(\mu\text{-}Cl)]_2$, was synthesized and a X-ray structure determination revealed a chloride-bridged dimer (see **Figure 2.2**).[46]

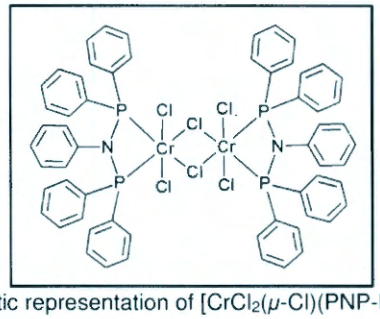

Figure 2.2: Schematic representation of $[CrCl_2(\mu\text{-}Cl)(PNP\text{-}Ph)]_2$ (Ph = phenyl).[46]

Sasol Technology continued the study of the selective tetramerisation of ethylene by investigating *ortho*-alkyl substituted diphosphinoamine ligand systems.[47] It was reported that the selectivity can shift from trimerisation to tetramerisation by merely reducing the number of *ortho*-alkyl substituents from four to zero (see **1** in **Figure 2.3**). This clearly indicated that the selectivity of these systems was significantly influenced by steric effects. The selectivity changed from trimerisation to predominantly

[47] Blann, K., Bollmann, A., Dixon, J.T., Hess, F.H., Killian, E., Maumela, H., Morgan, D.H., Neveling, A., Otto, S. and Overett, M.J., *Chem. Commun.*, **2005**, 620.

tetramerisation as the pattern of aryl substitution is changed progressively from *ortho*, to *meta*, to *para* (see **1**, **2**, **3** respectively in **Figure 2.3**).

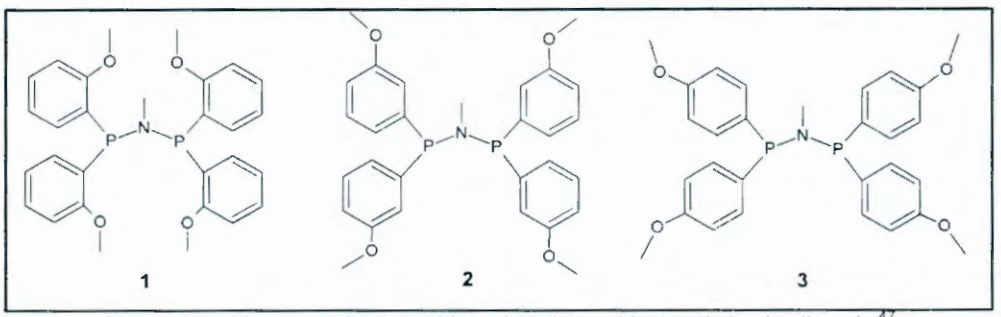

Figure 2.3: Methoxy substituted bis(diphenylphosphino)methylamine ligands.[47]

In order to fully comprehend the prerequisites of the selectivity of the diphosphinoamine oligomerisation systems, further investigations were performed wherein chromium catalysts containing polar-substituted diphosphinoamine ligands were analysed.[48] To establish whether the *ortho*-methoxy substituted diphosphinoamine systems' selectivity were due to steric effects (similar to the *ortho*-alkyl substituted diphosphinoamine ligands) or pendant coordination effects,[28] ligands with two and one *ortho*-methoxy groups were evaluated respectively. Only a small shift towards tetramerisation was observed upon the reduction of the number of methoxy groups. It was reasoned that only a single *ortho*-methoxy substituent is needed to coordinate with the metal centre and therefore a reduction in the *ortho*-methoxy groups did not have a large effect on the preference of the system for trimerisation. It was consequently postulated that it is perhaps both steric effects and a coordination effect of a pendant donor that possibly act as a hemilabile ligand that could determine whether a reaction is predominantly selective towards hexene or octene.

[48] Overett, M.J., Blann, K., Bollmann, A., Dixon, J.T., Hess, F., Killian, E., Maumela, H., Morgan, D.H., Neveling, A. and Otto, S., *Chem. Commun.*, **2005**, 622.

It was stated by Carter *et al.*[28] that for a catalyst system containing an *ortho*-methoxy substituted diphosphinoamine (see **1** in **Figure 2.3**) the *ortho*-methoxy groups act as pendant donors to the chromium centre and this is a prerequisite for ethylene trimerisation catalyst activity. This was claimed after diphosphinoamine ligand in which the *ortho*-methoxy substituents were replaced by ethyl groups and this ligand system was reported as being catalytically inactive. It was however shown during the study of bulky *ortho*-alkyl diphosphinoamine systems by Sasol Technology[47] that the chromium based *ortho*-ethyl diphosphinoamine catalyst system was surprisingly active and selective towards ethylene trimerisation. This clearly proved that pendant coordination is not a prerequisite for selective ethylene trimerisation and that it is largely the steric demand that plays a significant role in the hexene and octene seletivities. The less steric hindrance is experienced around the chromium centre the more selective towards octene these catalyst systems seem to be. These catalyst systems have been optimized in such a manner that it is possible to give various ratios of 1-hexene to 1-octene as required, by slight modifications to the diphosphinoamine ligand system.

The next step for Sasol Technology was to further investigate the structural effects of the nitrogen-bonded alkyl moiety of the bis(diphenylphosphino)amine (PNP) ligand system.[49] Various PNP ligands with nitrogen bonded alkyl and cycloalkyl substituents were evaluated together with chromium as part of the ethylene tetramerisation catalyst systems (see **Figure 2.4**). It was concluded that an increase in ring size from three to twelve carbon atoms of the cycloalkyl N-substituent lead to a significant increase in catalyst performance and combined 1-olefin selectivity. Substitution of alkyl groups at the 2-position of the cyclohexyl moiety resulted in further improvement of the combined 1-olefin selectivity. A decline in 1-octene selectivity to a 1:1 1-hexene/1-octene ratio was however observed when methyl substituents were placed in the 2- and 6-position of the nitrogen coordinated cyclohexyl group.

[49] Kuhlmann, S., Blann, K., Bollmann, A., Dixon, J.T., Killian, E., Maumela, M.C., Maumela, H., Morgan, D.H., Pretorius, M., Taccardi, N. and Wasserscheid, P., *J. Catal.*, **2007**, *245*, 277.

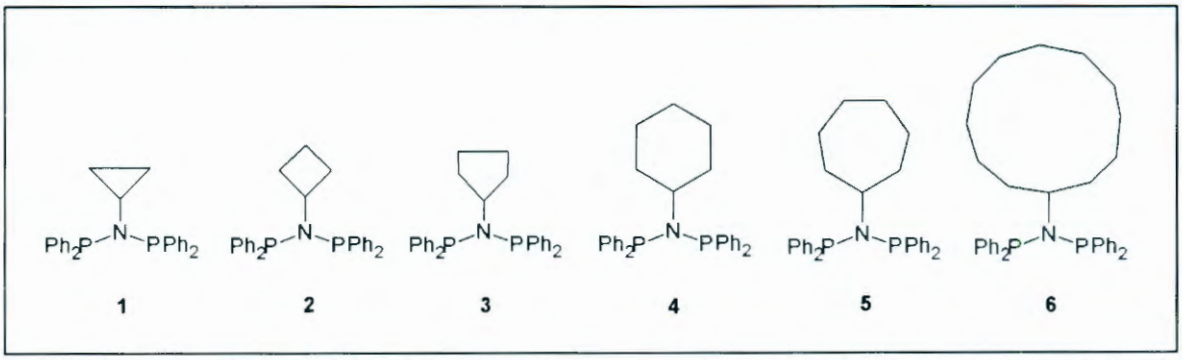

Figure 2.4: Various PNP ligands with nitrogen bonded cycloalkyl substituents, which were evaluated together with chromium as part of the ethylene tetramerisation catalyst systems.[49]

It was consequently concluded that the steric effect of substituents on the phosphorous-bonded phenyl rings and the nitrogen-bonded alkyl groups play a crucial role in determining the activity and 1-olefin selectivity of the chromium-based diphosphinoamine catalyst systems.

2.3.2 Mechanism

As discussed earlier, the ethylene trimerisation and tetramerisation reactions with Cr/diphosphinoamines/aluminoxane catalyst systems was shown to be closely related, as it is possible to shift between the selectivity of 1-hexene and 1-octene by subtle modifications of the ligands.[47,48] It was consequently reasoned that both reactions share a common seven-membered ring intermediate.[35, 36, 38, 42] This was supported by deuterium labeling studies by Sasol Technology[50] which were performed in a similar way to that of the trimerisation mechanism investigation.[38] This study, together with the analysis of the molar distributions of the 1-alkene products and the identification of the secondary co-oligomerisation reaction products proved that an extended metallocycle mechanism is in operation during the tetramerisation reaction. The mechanism proceeds by a further ethylene coordination and insertion into the seven-membered metallocyclic intermediate and is followed by the formation of a nine-membered

[50] Overett, M.J., Blann, K., Bollmann, A., Dixon, J.T., Haasbroek, D., Killian, E., Maumela, H., McGuinness, D.S. and Morgan, D.H., *J. Am. Chem. Soc.*, **2005**, *127*, 10723.

metallocyclic species from which 1-octene is then eliminated. The distinguishing factor between the tetramerisation and the trimerisation catalyst system is that the tetramerisation catalyst creates an enhanced stability of the seven-membered metallocyclic intermediate and as a result decreases 1-hexene elimination. This stability allows the competing insertion of another ethylene molecule, leading to the formation of a nine-membered metallocyclic intermediate, which is less stable than the metallocycloheptane species, thus eliminating 1-octene. It was hypothesized that these differences with respect to the ethylene trimerisation catalyst system is caused by subtle steric and electronic effects of the ligand.

The reaction kinetics of an ethylene catalyst system, comprising of $[Cr(acac)_3]$, a bis(diphenylphosphino)isopropylamine ligand and MAO as catalyst activator, was investigated.[51] It was reported that the reaction rate is dependent on temperature and ethylene concentration to the order of 1.57. An increase in the formation of 1-hexene and a decrease in 1-octene was observed with increased temperature and decreased pressure. The fact that an increase of pressure from 20 to 45 bar led to an increase in 1-octene formation indicated a strong ethylene concentration dependence for the formation of this 1-alkene. This discovery prompted Sasol Technology to investigate the influence of temperature and pressure on the chromium-based tetramerisation of ethylene.[52] The ethylene concentration was correlated at specific reaction conditions with the respective catalytic results. The ethylene concentrations in the binary ethylene-cyclohexane mixtures were determined by extending literature vapour-liquid equilibrium curves into the relevant temperature and pressure range. It was found that the data corresponded well with the proposed metallocycle mechanism. The ethylene insertion into the seven-membered metallocyclic intermediate was found to be dependent on the ethylene concentration, but to a lesser extent than expected. The 1-octene selectivity was however primarily temperature dependent. With an increase in temperature at a constant pressure the selectivity towards 1-hexene increased and that of 1-octene decreased.

[51] Walsh, R., Morgan, D.H., Bollmann, A. and Dixon, J.T., *Appl. Catal. A: General*, **2006**, *306*, 184.
[52] Kuhlmann, S., Dixon, J.T., Haumann, M., Morgan, D.H., Ofili, J., Spuhl, O., Taccardi, N. and Wasserscheid, P., *Adv. Synth. Catal.*, **2006**, *348*, 1200.

In an effort to elucidate the oxidation state of the chromium centre during the tetramerisation mechanism, Rucklidge *et al.* synthesized and characterized a variety of Cr(0) and Cr(I) carbonyl complexes of diphosphinoamine and related ligands.[53] The carbonyl complexes were evaluated for ethylene tetramerisation. This revealed that a Cr(I) cation along with a weakly coordinated anion, such as $[Al(CO(CF_3)_3)_4]^-$, is required to produce an active catalytic system which yields 1-octene in good selectivity. The compound $[Cr(CO)_4(PNP\text{-isopropyl})]^+$, of which crystallographic data was collected and published, together with the anion $[Al(CO(CF_3)_3)_4]^-$ and triethylaluminium constituted the first example of Cr(I) being used as catalyst precursor. The lack of activity displayed by any of the Cr(0) complexes lends further support to the evidence that the catalytic cycle could entail a Cr(I) → Cr(III) cationic mechanism (see **Scheme 2.9**).

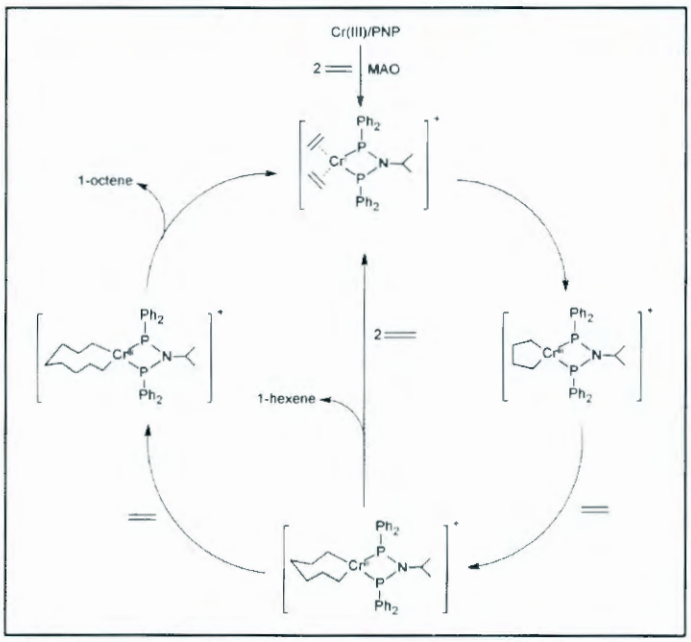

Scheme 2.9: Cationic metallocycle mechanism proposed for the Cr/PNP ethylene tetramerisation system.[53]

Numerous investigations on the effect of various changes to the key constituents of the ethylene tetramerisation catalyst system have been performed over the past years since

[53] Rucklidge, A.J., McGuinness, D.S., Tooze, R.P., Slawin, A.M.Z., Pelletier, J.D.A., Hanton, M.J. and Webb, P.B., Am. *Organomet.*, **2007**, *26*, 2782.

the initial discovery was published in 2004. It can only be expected that these studies should continue to produce more effective catalyst systems in future.

2.4 Ligand effects

The steric and electronic properties of phosphine ligands have a major influence on the properties induced on the metal to which the ligand is coordinated. These properties are however difficult to separate as they are closely related.

Various models have been developed to describe and quantify the steric demand of a ligand[54] and the Tolman cone angle[55] is still the most widely used. This is due to, amongst others, the easy calculation of this parameter from molecular models or crystallographic data. Tertiary phosphine ligands are commonly classified using the Tolman cone angle in which the steric bulk of a phosphine ligand is measured from CPK models.

A good example of the effect of the steric parameters of ligands in kinetic reaction systems is illustrated by the oxidative addition reaction of $[(\eta^5\text{-}C_5H_5)Co(CO)(L)]$ (L = PPh_3, $PMePh_2$ and PMe_2Ph with MeI (Me = methyl, Ph = phenyl).[56] The reaction rates were obtained by monitoring the disappearance of CO stretching bands of the starting reagent in the infrared spectrum. It was proposed that the rate determining step is the nucleophilic attack by the metal atom on the alpha-carbon of the alkyl iodide. The authors stated that the increase in reaction rates of oxidative addition from PPh_3 to PMe_2Ph may be attributed to mainly steric effects (with an increase in reaction rates as the steric bulk of the ligands increase). This was concluded as the electronic properties of the ligands proved to be similar, since the differences in the υ_{CO} values are negligible.

[54] Bunten, K.A., Chen, L., Fernandez, A.L. and Poë, A.J., *Coord. Chem. Rev.*, **2002**, *233*, 41.
[55] Tolman, C.A., *Chem. Rev.*, **1977**, *77*, 313.
[56] Hart-Davis, A.J. and Graham, W.A.G., *Inorg. Chem.*, **1970**, *9*, 2658.

The use of a steric parameter is further illustrated by a study in which bicyclic phosphines as ligands for cobalt catalysed hydroformylation were investigated.[57] Comparative runs were performed using PBu_3 (Bu = butyl) and a range of tertiary bicyclic phosphine ligands derived from *cis,cis*-1,5-cyclooctadiene (Phoban group). The Phoban derivatives showed significantly faster reaction rates of up to 2 h^{-1} in comparison with the slower rates of PBu_3 (0.6 h^{-1}). Interestingly the ligands are all electronically similar, it was however found that the most prominent difference between the two classes of ligands are the cone angles, which is 132 ° for PBu_3 and approximately 165 ° for the Phoban group. The conclusion was consequently made that the steric bulkiness of the Phoban ligands played a significant role in the faster reaction rate and this was established by determining the cone angle of the ligands.

A range of methods to rapidly evaluate ligands' electronic properties have also been developed, for example, measuring the coupling constants between ^{31}P and other NMR active nuclei[58,59,60] such as ^{11}B, ^{195}Pt or ^{77}Se. Allen *et al.* demonstrated that the $^{1}J_{P\text{-}Se}$ coupling constant was a good measure of the phosphine basicity, irrespective of the size of the phosphine ligand.[59] The rapid oxidative addition of $SeCN^-$ to tertiary phosphine ligands has proved to be an easy way of producing the phosphine selenides,[61] making it even easier and faster to evaluate the electronic properties of a specific phosphorous ligand.

The $^{1}J_{P\text{-}Se}$ coupling constants of phosphine selenides and the cone angle (which is slightly modified Tolman cone angle) was successfully used together to determine the steric and electronic parameters respectively for bicyclic phosphine ligands.[62] The evaluation of these parameters was used to study the catalytic behaviour of the hydroformylation catalyst systems of which these phosphine ligands formed part of. A

[57] Bungu, P.N. and Otto, S., *J. Chem. Soc. Dalton Trans.*, **2007**, 2876.
[58] Cowley, A.H. and Damasco, M.C., *J. Am. Chem. Soc.*, **1971**, *93*, 6815.
[59] Allen, D.W. and Taylor, B.F., *J. Chem. Soc. Dalton Trans.*, **1982**, 51.
[60] Allen, D.W., Nowel, I.W. and Taylor, B.F., *J. Chem. Soc. Dalton Trans.*, **1985**, 2505.
[61] Nicpon, P. and Meek, D.W., *Inorg. Chem.*, **1966**, *5*, 1297.
[62] Bungu, P.N. and Otto, S., *J. Organomet. Chem.*, **2007**, *692*, 3370.

similar study on the diphosphinoamine ligands used in the ethylene tetramerisation catalyst system has not been reported to date. Such an evaluation could prove to be important in determining what are the prerequisites to produce an active and selective ethylene tetramerisation catalyst system.

3 Synthesis and characterisation of metal coordinated and free PNP compounds

In this chapter...

The synthesis of a range of bis(diphenylphosphino)alkylamine ligands is described as well as the subsequent coordination of these ligands to various metal centres (Pt(II), Pd(II) and Cr(III)). The charaterisation of the isolated products with NMR and IR spectroscopy are also presented.

3.1 Introduction

A range of diphosphinoamine ligands (PNP-ligands) was synthesized in which only the alkyl moiety bonded to the nitrogen atom is systematically changed from one compound to the next. These ligands were then coordinated to metal cations such as platinum(II), palladium(II) and chromium(III), to investigate the structural effects of the alkyl moiety changes of the PNP-ligands for the various compounds.

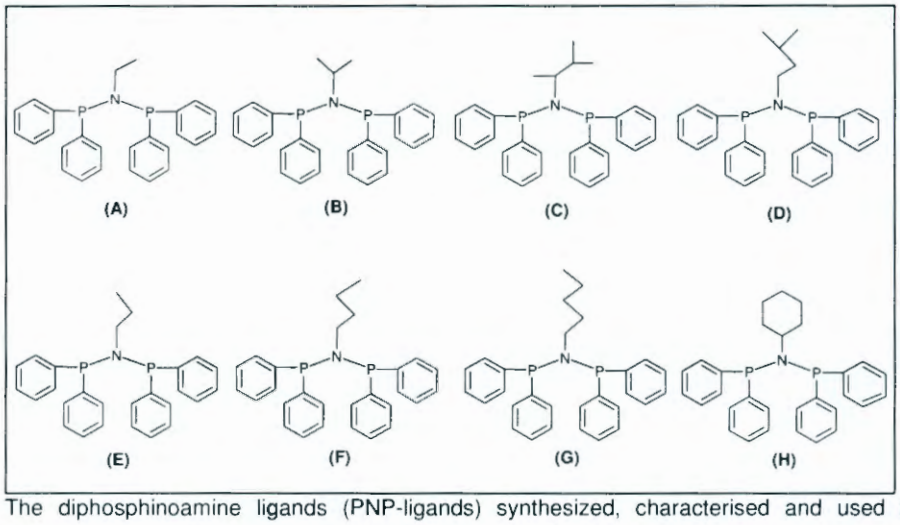

Figure 3.1: The diphosphinoamine ligands (PNP-ligands) synthesized, characterised and used in this study. (A) Bis(diphenylphosphino)ethylamine (PNP-Ethyl); (B) Bis(diphenylphosphino)-isopropylamine (PNP-*i*-Prop); (C) Bis(diphenylphosphino)-1,2-dimethylpropylamine (PNP-Dimprop); (D) Bis(diphenylphosphino)-isopentylamine (PNP-*i*-Pent); (E) Bis(diphenylphosphino)-*n*-propylamine (PNP-*n*-Prop); (F) Bis(diphenylphosphino)-*n*-butylamine (PNP-*n*-Butyl); (G) Bis(diphenylphosphino)-*n*-pentylamine (PNP-*n*-Pent); (H) Bis(diphenylphosphino)-cyclohexylamine (PNP-Cychex).

The synthesis of the starting materials will be discussed in detail in this chapter as well as the synthesis and characterization of each of the final products used for the single crystal X-ray crystallographic study (see Chapters 4, 5 and 6).

3.2 Synthesis and spectroscopic characterization

3.2.1 Chemicals and instrumentation

The following general experimental procedures apply to all complexes synthesized for this study and reported in Chapters 4 to 11. All chemicals used for the preparation of the complexes were reagent grade. General reagents 1,5-cyclo-octadiene, triethylamine, chlorodiphenylphosphine, alkylamines, tetraphenylphosphonium bromide, tetraphenylphosphoniumchloride and $[Cr(III)Cl_3(THF)_3]$ (THF = tetrahydrofuran) (Aldrich) were used as received. The metal complexes $[K_4PtCl_4]$ and $[PdCl_2]$ were obtained commercially from Next Chimica, South Africa. All solvents used, were of analytical grade and used as received, except where dry conditions were required. In these cases solvents were purified and dried according to literature procedures.[1] In the case of moisture and oxygen sensitive chemicals all reactions were performed under argon atmosphere using standard anaerobic conditions.

All infrared spectra were recorded as neat samples on a Digilab FTS 2000 Fourier transform spectrometer (ATR) utilizing a He-Ne laser at 632.6 nm, in the range of 3000 to 600 cm^{-1}. The complexes were identified by NMR techniques using magnetically active nuclei in the complexes (600 MHz Bruker spectrometer operating at 600 and 242.9 MHz respectively for ^{1}H and ^{31}P). The NMR spectra were recorded in $CDCl_3$ with ^{1}H calibrated relative to the residual $CHCl_3$ peak (7.24 ppm) and the ^{31}P NMR spectra calibrated reative to 85 % H_3PO_4 as external standard in a capillary (0 ppm). All chemical shifts are reported in ppm and coupling constants in Hz. The $[PtCl_2(PNP\text{-}alkyl)]$ and $[PdCl_2(PNP\text{-}alkyl)]$ complexes were quite insoluble in the

[1] Perrin, D.D.; Armarego, W.L.F. Purification of Laboratory Chemicals, 3rd Edition, Pergamon Press, **1988**.

deuterated solvents at hand and therefore the complexes were dissolved in dichloroethane. Approximately 0.1 ml of $CDCl_3$ was added to the sample solution to be used as a solvent to "lock" on when operating the 600 MHz NMR spectrometer. For this reason, no ^1H NMR data was collected for the platinum(II) and palladium(II) complexes. No NMR data could be collected for the chromium(III) complexes reported here due to the paramagnetic nature of the metal centre.

The UV/Vis spectra were collected on a Varian Carey 50 Conc. spectrometer, equipped with a Julabo F12-mV temperature cell regulator (accurate within 0.1 °C) in a 1 cm quartz cuvette cell. The reflection data was collected on a Bruker X8 ApexII 4K diffractometer[2] using graphite monochromated Mo K_α radiation with ω-and-φ-scans. All data collections were done at 100 K. COSMO[3] was utilized for optimum collection of more than a hemisphere of reciprocal space. After a completed collection, the first 50 frames were repeated to check for any decomposition, but all the crystals remained stable throughout the collection. The frames were integrated using a narrow-frame integration algorithm and reduced with the Bruker SAINT-Plus[4] and XPREP[4] software packages, respectively. Data was corrected for absorption effects using the multi-scan technique SADABS.[5] All structures were solved by the direct methods package SIR97[6] and refined using the software package WinGX,[7] incorporating SHELXL.[8] The molecular graphics were prepared with DIAMOND[9] and all structures are shown with thermal ellipsoid drawn at 50 % probability.

All non-hydrogen atoms were refined anisotropically. The aromatic, methine, methylene and methyl H atoms were placed in geometrical idealized positions (C-H = 0.97-0.98 Å) and constrained to ride on their parent atoms with $U_{iso}(H) = 1.2_{eq}(C)$ for aromatic,

[2] Bruker, APEX2 (Version 1.0-27), Bruker AXS Inc., Madison, Wisconsin, USSA, **2005**.
[3] Bruker, COSMO, (Version 1.48), Bruker AXS Inc., Madison, Wisconsin, USA, **2003**.
[4] Bruker, SAINT-Plus (Version 7.12) (including XPREP), Bruker AXS Inc., Madison, Wisconsin, USA, **2004**.
[5] Bruker. SADABS, Version 2004/1, Bruker AXS Inc. Madison, Wisconsin, USA, **1998**.
[6] Altomare, A.; Burla, M.C.; Camalli, M.; Cascarano, G.L.; Giacovazzo, C.; Guagliardi, A.; Moliterni, A.G.G.; Polidori, G.; Spagna, R. *J. Appl. Cryst.* **1999**, 32, 115.
[7] Farrugia, L.J., *J. Appl. Cryst.*, **1999**, *32*, 837.
[8] Sheldrick, G.M., SHELXL97, *Program for Solving Crystal Structures*, University of Gottingen, Germany, **1997**.
[9] Brandenburg, K.; Putz, H., DIAMOND, Release 3.0c, Crystal Impact GbR, Bonn, Germany, **2005**.

methine, methylene and $U_{iso}(H) = 1.5_{eq}(C)$ for methyl. Supplementary data containing complete lists of atomic coordinates, anisotropic displacement parameters, bond distances and angles as well as hydrogen coordinates are given in Appendix A-C respectively for each chapter.

3.2.2 Synthesis of reagents

3.2.2.1 *cis*-(η^4-Cycloocta-1,5-diene-dichloridoplatinum(II)) ([$PtCl_2$(1,5-cod)])

K_2PtCl_4 (2.4 mmol, 1g) was dissolved in a mixture of distilled water (16 ml) and n-propanol (11ml). 1,5-Cyclooctadiene (2.4 mmol, 2 ml) and $SnCl_2$ (2.4 mmol, 15 mg) was added. The reaction mixture was stirred at room temperature for 48 hours. The solvent was evaporated overnight. The product was extracted with boiling dichloromethane. The solution was allowed to evaporate slowly overnight forming light yellow crystals.

Yield: Solid: 0.865 g (96.0 %)
^{1}H NMR: δ (ppm) 2.20-2.30 (m, 4H, CH_2); 2.60-2.80 (m, 4H, CH_2); 5.59 (m, 4H, CH).

3.2.2.2 *cis*-(η^4-Cycloocta-1,5-diene-dichloridopalladium(II)) ([$PdCl_2$(1,5-cod)])

$PdCl_2$ (11.3 mmol, 2 g) was dissolved in hot concentrated HCl (10 M, 5 ml). The solution was cooled to room temperature and diluted with ethanol (150 ml) and filtered. 1,5-Cyclooctadiene (11.3 mmol, 3ml) was added to the filtrate with rapid stiring. The yellow product precipitated immediately and was stirred for a further 10 minutes. The solution was filtered and the precipitate was washed with diethyl ether (100 ml).

Yield: Solid: 2.93 g (91.0 %)
^{1}H NMR: δ (ppm) 2.6 (m, 4H, 2 x CH_2); 2.9 (m, 4H, 2 x CH_2); 5.3 (m, 4H, 4 x CH).

3.2.3 Synthesis of bis(diphenylphosphino)amine ligands

3.2.3.1 Bis(diphenylphosphino)-ethylamine

The title compound, PNP-Ethyl, was prepared by dissolving ethylamine (0.010 mol, 0.451 g) in dichloromethane (30 ml) after which the solution was placed on an ice bath. Triethylamine (0.03 mol, 4.22 ml) was added to the solution while it was being stirred. Chlorodiphenylphosphine (0.02 mol, 3.62 ml) was slowly added to the reaction mixture. The ice bath was removed after 30 minutes and the reaction mixture was allowed to stir at room temperature for a further 12 hours. The dichloromethane was removed under reduced pressure. A mixture of hexane (20 ml) and toluene (2 ml) was added to the remaining white powder and was passed through a column containing neutral activated alumina (35 g). The solvent of the eluent was removed under reduced pressure and the white precipitate was collected. The product was crystallised in methanol and single crystals suitable for X-ray crystallography was collected.

Yield: Solid: 3.33 g (74.0 %)
IR (ATR): ν (cm^{-1}) = 1434 to 1584 (C-C (Ar) (Ar = aromatic)); 1311 (N-P); 1068 (N-C)
^{1}H NMR: δ (ppm) = 1.0 (t, 3H, CH_3); 1.6 (m, 2H, CH_2); 7.3 to 8.0 (m, 20H, Ar).
^{31}P NMR: δ (ppm) = 50.5

3.2.3.2 Bis(diphenylphosphino)-isopropylamine

The title compound, PNP-*i*-Prop, was prepared in good yield in a similar fashion as PNP-Ethyl in §3.2.3.1 using isopropylamine (0.01mol, 0.591 g).

Yield: Solid: 3.67 g (79.1%)
IR (ATR): ν (cm^{-1}) = 1431 to 1585 (C-C (Ar)); 1307 (N-P); 1040 (N-C)
^{1}H NMR: δ (ppm) = 1.0 (d, 6H, 2 x CH_3); 3.8 (m, 1H, CH); 7.2 to 8.0 (m, 20H, Ar).
^{31}P NMR: δ (ppm) = 50.8

3.2.3.3 Bis(diphenylphosphino)-1,2-dimethylpropylamine

The title compound, PNP-Dimprop, was prepared in good yield in a similar fashion as PNP-Ethyl in §3.2.3.1 using 1,2-dimethylpropylamine (0.01mol, 0.872 g). The product was crystallised in methanol and single crystals suitable for X-ray crystallography was collected.

Yield: Solid: 3.52 g (77.4%)
IR (ATR): ν (cm^{-1}) = 1430 to 1584 (C-C (Ar)); 1312 (N-P); 1045 (N-C)
^{1}H NMR: δ (ppm) = 0.5 to 1.5 (d, 3H, 3 x CH_3); 1.8 and 3.6 (m, 1H, 2 x CH); 6.9 to 7.8 (m, 20H, Ar).
^{31}P NMR: δ (ppm) = 53.0

3.2.3.4 Bis(diphenylphosphino)-isopentylamine

The title compound, PNP-*i*-Pent, was prepared in good yield in a similar fashion as PNP-Ethyl in §3.2.3.1 using isopentylamine (0.01mol, 0.872 g). The product was crystallised in methanol and single crystals suitable for X-ray crystallography was collected.

Yield: Solid: 3.29 g (72.2 %)
IR (ATR): ν (cm^{-1}) = 1439 to 1587 (C-C (Ar)); 1311 (N-P); 1071 (N-C)
^{1}H NMR: δ (ppm) = 0.7 to 1.0 (d, 3H, 2 x CH_3); 1.5 (m, H, CH); 1.4 (m, 1H, CH); 1.7 (t, 2H, CH_2); 6.8 to 7.8 (m, 20H, Ar).
^{31}P NMR: δ (ppm) 62.7

3.2.3.5 Bis(diphenylphosphino)-*n*-propylamine

The title compound, PNP-*n*-Prop, was prepared in good yield in a similar fashion as PNP-Ethyl in §3.2.3.1 using propylamine (0.01mol, 0.591 g).

Yield: Solid: 3.08g (66.5%)
IR (ATR): ν (cm^{-1}) = 1432 to 1584 (C-C (Ar)); 1306 (N-P); 1023 (N-C)

^{1}H NMR: δ (ppm) = 1.0 (t, 3H, CH_3); 1.7 (m, 2H, CH_2); 3.0 (t, 2H, N-CH_2); 7.3 to 8.0 (m, 20H, Ar).

^{31}P NMR: δ (ppm) = 62.4

3.2.3.6 Bis(diphenylphosphino)-*n*-butylamine

The title compound, PNP-*n*-Butyl, was prepared in good yield in a similar fashion as PNP-Ethyl in §3.2.3.1 using butylamine (0.01mol, 0.731 g).

Yield: Solid: 2.64g (59.8%)

IR (ATR): ν (cm^{-1}) = 1432 to 1584 (C-C (Ar)); 1307 (N-P); 1024(N-C)

^{1}H NMR: δ (ppm) = 0.6 (t, 3H, CH_3); 1.3 to 1.7 (m, 4H, 2 x CH_2); 2.9 (m, 2H, N-CH_2); 7.3 to 8.0 (m, 20H, Ar).

^{31}P NMR: δ (ppm) = 63.0.

3.2.3.7 Bis(diphenylphosphino)-*n*-pentylamine

The title compound, PNP-*n*-Pent, was prepared in good yield in a similar fashion as PNP-Ethyl in §3.2.3.1 using pentylamine (0.01mol, 0.872 g). The product was crystallised in methanol and single crystals suitable for X-ray crystallography was collected.

Yield: Solid: 3.05g (67.3%)

IR (ATR): ν (cm^{-1}) = 1434 to 1585 (C-C (Ar)); 1308 (N-P); 1030 (N-C)

^{1}H NMR: δ (ppm) = 0.9 (t, 3H, CH_3); 1.3 to 1.9 (m, 6H, 3 x CH_2); 3.0 (t, 2H, N-CH_2); 7,3 to 8.0 (m, 20H, Ar).

^{31}P NMR: δ (ppm) = 62.1

3.2.3.8 Bis(diphenylphosphino)-cyclohexylamine

The title compound, PNP-Cychex, was prepared in good yield in a similar fashion as PNP-Ethyl in §3.2.3.1 using cyclohexylamine (0.01mol, 0.992 g). The product was

crystallised in methanol and single crystals suitable for X-ray crystallography was collected.

Yield: 3.13 (67 %)

IR (ATR): ν (cm^{-1}) = 1432 to 1584 (C-C (Ar)); 1311 (N-P); 1069 (N-C)

^{1}H NMR: δ (ppm) = 1.0 to 2.0 (m, 10H, 5 x CH_2); 3.1 (m, 1H, CH); 7.25 to 8.0 (m, 20H, Ar).

^{31}P NMR: δ (ppm) = 50.0.

3.2.4 Synthesis of Pt(II)-PNP and Pd(II)-PNP complexes

3.2.4.1 Dichlorido-bis(diphenylphosphino)-ethylamine-platinum(II)

The title compound, [$PtCl_2$(PNP-Ethyl)], was prepared by dissolving [$PtCl_2$(1,5-cod)] (0.13 mmol, 50 mg) in dichloromethane (15 ml). PNP-Ethyl (0.13 mmol, 54.0 mg) was also dissolved in dichloromethane (10 ml) and was added drop-wise to the [$PtCl_2$(1,5-cod)] solution. The solution was stirred for 2 hours at room temperature. The reaction mixture was layered with methanol (10 ml). Colourless single crystals suitable for X-ray crystallography were obtained after 1 day with slow evaporation of the solvent mixture.

Yield: Solid: 63 mg (71.2%)

IR (ATR): ν (cm^{-1}) = 1434 to 1584 (C-C (Ar)); 1307 (N-P); 1070 (N-C)

^{31}P NMR: δ (ppm) = 16.3 (t, $^1J_{Pt-P}$ = 3228.0 Hz)

3.2.4.2 Dichlorido-bis(diphenylphosphino)-1,2-dimethylpropylamine-platinum(II)

The title compound, [$PtCl_2$(PNP-Dimprop)] was prepared in good yield in a similar fashion as [$PtCl_2$(PNP-Ethyl)] in §3.2.4.1 using PNP-Dimprop (0.13 mmol, 59.2 mg). Colourless single crystals suitable for X-ray crystallography were obtained after 1 day of slow evaporation of the solvent mixture.

Yield: Solid: 71mg (78.5%)

IR (ATR): ν (cm^{-1}) = 1434 to 1583 (C-C (Ar)); 1307 (N-P); 1070 (N-C)
^{31}P NMR: δ (ppm) = 18.4 (t, $^{1}J_{Pt\text{-}P}$ = 3228.0 Hz)

3.2.4.3 Dichlorido-bis(diphenylphosphino)-isopentylamine-platinum(II)

The title compound, [$PtCl_2$(PNP-*i*-Pent)], was prepared in good yield in a similar fashion as [$PtCl_2$(PNP-Ethyl)] in §3.2.4.1 using PNP-*i*-Pent (0.13 mmol, 59.2 mg). Colourless single crystals suitable for X-ray crystallography were obtained after 1 day of slow evaporation of the solvent mixture.

Yield: Solid: 68mg (76.0 %)
IR (ATR): ν (cm^{-1}) = 1435 to 1585 (C-C (Ar)); 1311 (N-P); 1071 (N-C)
^{31}P NMR: δ (ppm) = 15.8 (t, $^{1}J_{Pt\text{-}P}$ = 3240.0 Hz)

3.2.4.4 Dichlorido-bis(diphenylphosphino)-*n*-propylamine-platinum(II)

The title compound, [$PtCl_2$(PNP-*n*-Prop)], was prepared in good yield in a similar fashion as [$PtCl_2$(PNP-Ethyl)] in §3.2.4.1 using PNP-*n*-Prop (0.13 mmol, 55.6mg). Colourless single crystals suitable for X-ray crystallography were obtained after 1 day of slow evaporation of the solvent mixture.

Yield: Solid: 66 mg (73.4 %)
IR (ATR): ν (cm^{-1}) = 1434 to 1583 (C-C (Ar)); 1311 (N-P); 1070 (N-C)
^{31}P NMR: δ (ppm) = 16.4 (t, $^{1}J_{Pt\text{-}P}$ = 3228 Hz)

3.2.4.5 Dichlorido-Bis(diphenylphosphino)-cyclohexylamine-platinum(II)

The title compound, [$PtCl_2$(PNP-Cychex], was prepared in good yield in a similar fashion as [$PtCl_2$(PNP-Ethyl)] in §3.2.4.1 using PNP-Cychex (0.13 mmol, 60.8 mg). Colourless single crystals suitable for X-ray crystallography were obtained after 1 day of slow evaporation of the solvent mixture.

Yield: Solid: 68 mg (71.2 %)

IR (ATR): ν (cm^{-1}) = 1435 to 1584 (C-C (Ar)); 1308 (N-P); 1068 (N-C)
^{31}P NMR: δ (ppm) = 14.4 (t, $^{1}J_{Pt\text{-}P}$ = 3231 Hz)

3.2.4.6 Dichlorido-bis(diphenylphosphino)-isopropylamine-palladium(II)

The title compound, [$PdCl_2$(PNP-*i*-Prop)], was prepared by dissolving [$PdCl_2$(1,5-cod)] (0.175 mmol, 50 mg) in dichloromethane (15 ml). PNP-*i*-Prop (0.175 mmol, 75 mg) was also dissolved in dichloromethane (10 ml) and was added drop wise to the [$PdCl_2$(1,5-cod)] solution. The solution was stirred for 1 hour at room temperature. The reaction mixture was layered with diethyl ether (10 ml). Yellow single crystals suitable for X-ray crystallography were obtained after a few hours with the slow evaporation of the solvent mixture.

Yield: Solid: 72 mg (69%)
IR (ATR): ν (cm^{-1}) = 1434 to 1585 (C-C (Ar)); 1306 (N-P); 1041 (N-C)
^{31}P NMR: δ (ppm) 29.4

3.2.4.7 Dichlorido-bis(diphenylphosphino)-1,2-dimethylpropylamine-palladium(II)

The title compound, [$PdCl_2$(PNP-Dimprop)], was prepared in good yield in a similar fashion as [$PdCl_2$(PNP-*i*-Prop)] in §3.2.4.6 using PNP-Dimprop (0.175 mmol, 79.7 mg). Yellow single crystals suitable for X-ray crystallography were obtained after 1 day of slow evaporation of the solvent mixture.

Yield: Solid: 61 mg (68.0 %)
IR (ATR): ν (cm^{-1}) = 1434 to 1584 (C-C (Ar)); 1311 (N-P); 1066 (N-C)
^{31}P NMR: δ (ppm) = 32.0

3.2.4.8 Dichlorido-bis(diphenylphosphino)-isopentylamine-palladium(II)

The title compound, [$PdCl_2$(PNP-*i*-Pent)], was prepared in good yield in a similar fashion as [$PdCl_2$(PNP-*i*-Prop)] in §3.2.4.6 using PNP-*i*-Pent (0.175 mmol, 79.7 mg).

Yellow single crystals suitable for X-ray crystallography were obtained after a few hours of slow evaporation of the solvent mixture.

Yield: Solid: 67 mg (78.0 %)
IR (ATR): ν (cm^{-1}) = 1434 to 1586 (C-C (Ar)); 1313 (N-P); 1060 (N-C)
^{31}P NMR: δ (ppm) = 32.1

3.2.4.9 Dichlorido-bis(diphenylphosphino)-*n*-propylamine-palladium(II)

The title compound, [$PdCl_2$(PNP-*n*-Prop)], was prepared in good yield in a similar fashion as [$PdCl_2$(PNP-*i*-Prop)] in §3.2.4.6 using PNP-*n*-Prop (0.175 mmol, 74.8 mg). Yellow single crystals suitable for X-ray crystallography were obtained with slow evaporation of the solvent mixture after 1 day.

Yield: Solid: 55 mg (79.0 %)
IR (ATR): ν (cm^{-1}) = 1433 to 1584 (C-C (Ar)); 1308 (N-P); 1068 (N-C)
^{31}P NMR: δ (ppm) = 30.3

3.2.4.10 Dichlorido-bis(diphenylphosphino)-*n*-butylamine-palladium(II)

The title compound, [$PdCl_2$(PNP-*n*-Butyl)], was prepared in good yield in a similar fashion as [$PtCl_2$(PNP-*i*-Prop)] in §3.2.4.7 using PNP-*n*-Butyl (0.175 mmol, 77 mg). Yellow single crystals suitable for X-ray crystallography were obtained after 1 day of slow evaporation of the solvent mixture.

Yield: Solid: 86 mg (78.1 %)
IR (ATR): ν (cm^{-1}) = 1436 to 1585 (C-C (Ar)); 1311 (N-P); 1065 (N-C)
^{31}P NMR: δ (ppm) = 30.1.

3.2.5 Synthesis of Cr(III)-PNP complexes

3.2.5.1 (Isopentylammonium)(tetrachlorido-bis(diphenylphosphino)-isopentylamine-chromate(III))ditoluene solvate

The title compound, [*i*-Pent-NH_3][$CrCl_4$(PNP-*i*-Pent)]·$2C_7H_8$, was prepared by dissolving [$CrCl_3(THF)_3$] (0.27 mmol, 0.1g) in toluene (20 ml). PNP-*i*-Pent (0.27 mmol, 74.9 mg) was added to the solution. The reaction mixture was stirred for 12 hours at 85℃. The solution was filtered. Hexane (5 ml) was layered upon the toluene filtrate in a sealed Shclenk tube and kept at -20℃. Dark purple single crystals suitable for X-ray crystallography were obtained after 9 days.

Yield: Solid: 0.20 g (40.1 %)
IR (ATR): ν (cm^{-1}) = 1430 to 1595 (C-C (Ar)); 1312 (N-P); 1068 (N-C)

3.2.5.2 (*n*-Butyl-ammonium)(tetrachlorido-bis(diphenylphosphino)-*n*-butylamine-chromate(III))-ditoluene solvate

The title compound, ([*n*-Butyl-NH_3][$CrCl_4$(PNP-*n*-Butyl)]·$2C_7H_8$), was prepared in relatively good yield in a similar fashion as [*i*-Pent-NH_3][$CrCl_4$(PNP-*i*-Pent)]·$2C_7H_8$ in §3.2.5.1 using PNP-*n*-Butyl (0.27 mmol, 0.118g). Dark purple single crystals suitable for X-ray crystallography were obtained after 15 days.

Yield: Solid: 0.30 g (31.1 %)
IR (ATR): ν (cm^{-1}) = 1433 to 1589 (C-C (Ar)); 1309 (N-P); 1068 (N-C)

3.2.5.3 (*n*-Pentylammonium)(tetrachlorido-bis(diphenylphosphino)-*n*-pentylamine-chromate(III))-ditoluene solvate

The title compound, [*n*-Pent-NH_3][$CrCl_4$(PNP-*n*-Pent)]·$2C_7H_8$, was prepared in relatively good yield in a similar fashion as [*i*-Pent-NH_3][$CrCl_4$(PNP-*i*-Pent)]·$2C_7H_8$ in §3.2.5.1 using PNP-*n*-Pent (0.27 mmol, 0.122 g). Dark purple single crystals suitable for X-ray crystallography were obtained after 10 days.

Yield: Solid: 0.20 g (38.4 %)
IR (ATR): ν (cm^{-1}) = 1435 to 1595 (C-C (Ar)); 1312 (N-P); 1070 (N-C)

3.3 Conclusion

A range of non-coordinated and metal-coordinated PNP compounds (metals = Pt(II), Pd(II), Cr(III)) were successfully synthesized and characterized. The following compounds are novel and were synthesized specifically for this study: PNP-*n*-Butyl, PNP-*n*-Pent, PNP-*n*-Prop, [$PtCl_2$(PNP-Ethyl)], [$PtCl_2$(PNP-*i*-Pent)], [$PtCl_2$(PNP-*n*-Prop)], [$PtCl_2$(PNP-Dimprop)], [$PtCl_2$(PNP-Cychex)], [$PdCl_2$(PNP-*i*-Prop)], [$PdCl_2$(PNP-Dimprop)], [$PdCl_2$(PNP-*i*-Pent)], [$PdCl_2$(PNP-*n*-Pent)], [*i*-Pent-NH_3][$CrCl_4$(PNP-*i*-Pent)]·$2C_7H_8$, [*n*-Butyl-NH_3][$CrCl_4$(PNP-*n*-Butyl)]·$2C_7H_8$ and [*n*-Pent-NH_3][$CrCl_4$(PNP-*n*-Pent)]·$2C_7H_8$. Six of the eight PNP ligands used in this study have previously been synthesized by a research team within Sasol Technology, PNP-Ethyl, PNP-*i*-Prop, PNP-Dimprop, PNP-*i*-Pent PNP-*n*-Pent and PNP-Cychex. The procedures to synthesize these ligands as described in this chapter were provided by Sasol Technology.

The ^{31}P NMR data for the free PNP- ligands yielded singlet peaks with chemical shifts which range between 50.0 and 63.0 ppm.

The [$PtCl_2$(PNP-alkyl)] complexes could easily be identified by ^{31}P NMR as the chemical shifts of the singlet for the platinum(II)-PNP compounds shifted significantly upfield with values that range from 14.4 to 18.4 ppm. A relatively large sample or a relatively long scan time was required to obtain the $J_{Pt\text{-}P}$, since the peaks of the doublet are only 34 % each (the natural abundance of the active ^{195}Pt is 66 %) compared to the intensity of the inactive platinum-phosphorous peak. The $J_{Pt\text{-}P}$ for the various platinum(II) complexes, determined from the doublet peaks for each platinum(II) complex, are every similar with values in a narrow range between 3228 and 3240 Hz. This is a clear indication that the electronic properties of the PNP ligands are similar as these complexes are similar with only the alkyl substituents that are different for each complex.

The chemical shifts of the singlet observed for the [$PdCl_2$(PNP-alkyl)] complexes range between 29.4 and 32.1 ppm, indicating a significant shift when compared to the values of the non-coordinated diphosphinoamine ligands. The concentration of the palladium complex sample solutions proved to be too low due to the low solubility of the compounds, even in dichloroethane, and the $J_{Pd\text{-}P}$ could therefore not be determined.

^{31}P NMR data for these types of compounds provided a quick and easy method to determined if a free PNP-ligand is present or whether a metal-PNP complex was formed.

The single crystal X-ray crystallographic studies of the crystals obtained from the procedures mentioned above are discussed in detail in the following Chapters 4, 5 and 6.

4 Single crystal X-ray crystallographic study of non-coordinated bis(diphenylphosphino)amines

In this chapter...

A series of crystal structures of bis(diphenylphosphino)amine non-coordinated ligands (PNP-ligands) are presented. The different conformations adopted by each ligand are discussed and the various structural parameters are examined and compared to relevant compounds.

4.1 Introduction

The bis(diphenylphosphino)amine ligand systems (PNP-ligands) form an integral part in the ethylene tetramerisation catalytic systems, together with Cr(III) as metal centre. A large number of PNP-ligands with various substituents on both the N and P atoms were evaluated,[1,2,3,4,5] and it was found that the predominant factor in the ethylene tetramerisation catalysis selectivity (in particular the α-selectivity) is the steric bulk on the central nitrogen atom compared to the basicity of the phosphine.

Based on this information, additional PNP ligands have been synthesised and single crystal studies initiated to further evaluate any correlations. A comparison of the crystallographic data of a variety of non-coordinated PNP-ligands with varying activity and selectivity (when complexed with chromium(III)) was made and discussed.

---

[1] Blann, K., Bollmann, A., de Bod, H., Dixon, J.T., Killian, E., Nongodlwana, P., Maumela, M.C., Maumela, H., McConnell, A.E.C., Morgan, D.H., Overett, M.J., Prétorius, M., Kuhlmann, S. and Wasserscheid, P., *J. Catal.*, **2007**, *249*, 244.

[2] Overett, M.J., Blann, K., Bollmann, A., Dixon, J.T., Hess, F.M., Killian, E., Maumela, H., Morgan, D.H., Neveling, A. and Otto, S., *Chem. Commun.*, **2005**, 622.

[3] Blann, K., Bollmann, A., Dixon, J.T., Hess, F.M., Killian, E., Maumela, H., Morgan D.H., Neveling, A., Otto, S. and Overett, M., *Chem. Commun.*, **2005**, 620.

[4] Kuhlmann, S., Blann, K., Bollmann, A., Dixon, J.T., Killian, E., Maumela, M.C., Maumela, H., Morgan, D.H., Prétorius, M., Taccardi, N. and Wasserscheid, P., *J. Catal.*, **2007**, *245*, 277.

[5] Killian, E., Blann, K., Bollmann, A., Dixon, J.T., Kuhlmann, S.E., Maumela, M.C., Maumela, H., Morgan, D.H., Nongodlwana, P., Overett, M.J., Prétorius, M., Höfener, K. and Wasserscheid, P., *J. Mol. Catal. Chem.* **2007**, *270*, 214.

Illustrated in **Figure 4.1** are the PNP-ligands that are evaluated in this crystallographic study.

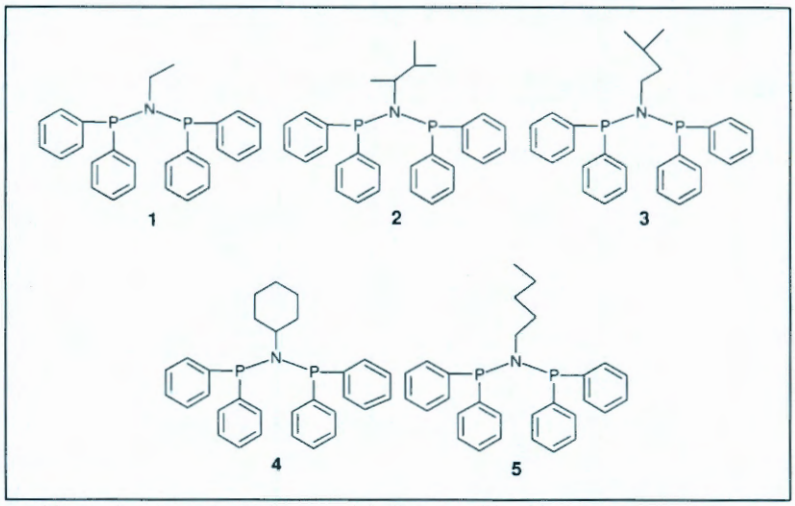

Figure 4.1: The diphosphinoamine ligands (PNP-ligands) discussed in this single crystal X-ray crystallographic study. (1) Bis(diphenylphosphino)ethylamine (PNP-Ethyl); (2) Bis(diphenylphosphino)1,2-dimethylpropylamine (PNP-Dimprop); (3) Bis(diphenylphosphino)isopentylamine (PNP-*i*-Pent); (4) Bis(diphenylphosphino)-cyclohexylamine (PNP-Cychex); (5) Bis(diphenylphosphino)-*n*-pentylamine (PNP-*n*-Pent).

An interesting aspect of the non-coordinated disphosphinoamine ligands is the different possible conformations it can adopt in the solid state (**Figure 4.2**).[6] It is generally thought that conformations of the type $C_{2V'}$ would suffer severe steric interactions and is not expected to be a significant part of the conformation equilibrium. Conformations C_{2v} and C_S (and slight deviations thereof) is therefore expected for these type of compounds. It has been postulated that as the steric bulk of the R group increases, it is more likely that the diphosphinoamine will have conformation C_S in order to relieve major steric interactions.[6] The ideal geometries of the conformers of the diphosphinoamine ligands were theoretically calculated, see **Table 4.1** for the ideal torsion angles of these conformers.

The conformation adopted by of each of the free PNP-ligands in solid state will be further discussed in following paragraphs.

[6] Keat, R., Manojlovic-Muir, L., Muir, K.W. and Rycroft, D.S., *J. Chem. Soc. Dalton Trans.*,**1981**, 2192.

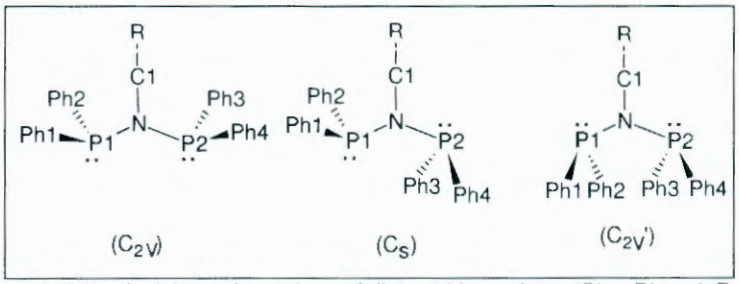

Figure 4.2: The possible principle conformations of diphosphineamines. (Ph = Phenyl, R = alkyl group).

Table 4.1: The torsion angles (°) of the ideal principle conformations of diphosphinoamines (theoretically calculated)[a].

Torsion components	C_{2V}	C_S	$C_{2V'}$
C1 – N – P1 – C11[(b)]	-45	-50	-136
C1 – N – P1 – C21[(b)]	55	50	120
C1 – N – P2 – C31[(b)]	-55	-130	-151
C1 – N – P2 – C41[(b)]	45	130	106

a) Calculations were performed using the using the Gaussian 03 software suite[7] and the B3LYP/LANL2DZ basis set.
b) C11, C21, C31 and C41 are the phosphorous-coordinated carbon atoms of the phenyl groups: Ph1, Ph2, Ph3 and Ph4 (see **Figure 4.2**) respectively.

4.2 Crystallographic data

The compounds prepared as described in §3.2.1-5 were investigated by single crystal X-ray crystallography and are summarized in **Table 4.2**. Molecular diagrams (using DIAMOND 3.0[8]) of the compounds are presented. Graphical representations of overlays of selected complexes are also presented (using Hyperchem 7.52[9]). Selected bond lengths, angles and torsion angles tabulated with a discussion highlighting some of the important aspects of each particular structure thereafter. Additional correlations with other relevant structures are done in §4.3

[7] Gaussian 03, Revision C.01, Frisch, M. J., Trucks, G. W., Schlegel, H. B., Scuseria, G. E., Robb, M. A., Cheeseman, J. R., Montgomery, Jr., J. A., Vreven, T., Kudin, K. N., Burant, J. C., Millam, J. M., Iyengar, S. S., Tomasi, J., Barone, V., Mennucci, B., Cossi, M., Scalmani, G., Rega, N., Petersson, G. A., Nakatsuji, H., Hada, M., Ehara, M., Toyota, K., Fukuda, R., Hasegawa, J., Ishida, M., Nakajima, T., Honda, Y., Kitao, O., Nakai, H., Klene, M., Li, X., Knox, J. E., Hratchian, H. P., Cross, J. B., Adamo, C., Jaramillo, J., Gomperts, R., Stratmann, R. E., Yazyev, O., Austin, A. J., Cammi, R., Pomelli, C., Ochterski, J. W., Ayala, P. Y., Morokuma, K., Voth, G. A., Salvador, P., Dannenberg, J. J., Zakrzewski, V. G., Dapprich, S., Daniels, A. D., Strain, M. C., Farkas, O., Malick, D. K., Rabuck, A. D., Raghavachari, K., Foresman, J. B., Ortiz, J. V., Cui, Q., Baboul, A. G., Clifford, S., Cioslowski, J., Stefanov, B. B., Liu, G., Liashenko, A., Piskorz, P., Komaromi, I., Martin, R. L., Fox, D. J., Keith, T., Al-Laham, M. A., Peng, C. Y., Nanayakkara, N., Challacombe, M., Gill, P. M. W., Johnson, B., Chen, W., Wong, M. W., Gonzalez, C., & Pople, J. A., Gaussian, Inc.,Pittsburgh PA, **2003**.

[8] Brandenburg, K. and Putz, H., **2005**, DIAMOND. Release 3.0c. Crystal Impact GbR, Bonn, Germany.

[9] Hyperchem ™ Release 7.52, Windows Molecular Modeling System, Hypercube, Inc., **2002**.

Table 4.2: General crystal data for the following compounds, PNP-Ethyl (1), PNP-Dimprop (2), PNP-*i*-Pent (3), PNP-*n*-Pent (4) and PNP-Cychex (5).

Identification code	**PNP-Ethyl (1)**	**PNP-Dimprop (2)**	**PNP-*i*-Pent (3)**	**PNP-*n*-Pent (4)**	**PNP-Cychex (5)**
Empirical formula	$C_{26}H_{25}P_2N$	$C_{29}H_{31}P_2N$	$C_{29}H_{31}P_2N$	$C_{29}H_{31}P_2N$	$C_{30}H_{31}P_2N$
Formula weight	413.43	455.51	455.51	455.51	467.50
Crystal system, space group	Monoclinic, $P2_1/n$	Triclinic, $P\bar{1}$	Orthorombic, $P2_12_12_1$	Triclinic, $P\bar{1}$	Monoclinic, $P2_1/n$
Unit cell dimensions:					
a(Å)	9.570(5)	9.242(5)	9.0563(3)	13.0867(5)	15.8170(17)
b(Å)	13.441(5)	10.454(5)	10.0353(3)	13.5688(5)	10.3420(12
c(Å)	16.907(5)	12.899(5)	27.5493(8)	15.0806(6)	15.8170(17)
α (°)	90.000	91.031(5)	90.000	75.836(2)	90.000
β (°)	91.647(5)	98.188(5)	90.000	75.371(2)	107.33(2)
γ (°)	90.000	102.775(5)	90.000	80.012(2)	90.000
Volume ($Å^3$)	2173.9(15)	1201.4(10)	2503.75(13)	2494.44(17)	2469.8(5)
Z	4	2	4	4	4
Calculated density (Mg/m^3)	1.373	1.259	1.208	1.213	1.257
Absorption coefficient (mm^{-1})	0.219	0.199	0.191	0.191	0.195
F(000)	944	484	968	968	992
Crystal size (mm)	0.39 x 0.13 x 0.11	0.47 x 0.29 x 0.14	0.39 x 0.41 x 0.57	0.45x 0.33x0.32	0.14 x 0.13 x 0.13
θ range / completeness of collection (°)	1.94-28.3 / 99.9	1.60-28.27 / 99.7	1.48-28.26 / 99.9	1.6-28.4 / 99.2	1.60-28.34 / 80.5
	-12<=h<=12	-12<=h<=12	-11<=h<=12	-17<=h<=17	-20<=h<=21
Limiting indices	-17<=k<=17	-13<=k<=13	-13<=k<=13	-18<=k<=18	-12<=k<=13
	-22<=l<=22	-17<=l<=17	-36<=l<=36	-20<=l<=20	-21<=l<=15
Reflections collected / unique / observed (I>2σ(I))	25117 / 5401	24124 / 5947	19224 / 6180	123188 / 12382	14416 / 4964
	R(int) = 0.0460	R(int) = 0.0313	R(int) = 0.0339	R(int) = 0.0372	R(int) = 0.0828
Max. and min. transmission	0.9715 and 0.9690	0.9727 and 0.9125	0.9793 and 0.9294	0.9413 and 0.9189	0.9745 and 0.9723
Data / restraints / parameters	5401 / 0 / 262	5947 / 4 / 298	6180 / 0 / 309	12382 / 0 / 577	4964 / 0 / 298
Goodness of fit on F^2	1.055	1.089	1.066	1.038	1.636
Final R indices (I>2σ(I))	R1 = 0.0379	R1 = 0.0425	R1 = 0.0356	R1 = 0.0321	R1 = 0.0855
	wR2 = 0.0862	wR2 = 0.1102	wR2 = 0.0918	wR2 = 0.0809	wR2 = 0.1670
R indices(all data)	R1 = 0.0522	R1 = 0.0482	R1 = 0.0390	R1 = 0.0384	R1 = 0.1380
	wR2 = 0.0938	wR2 = 0.1141	wR2 = 0.0978	wR2 = 0.0854	wR2 = 0.2266
$\Delta\rho_{min}$, $\Delta\rho_{max}$ ($e.Å^{-3}$)	0.431 and -0.260	0.557 and -0.514	0.535 and -0.218	0.380 and -0.291	0.927 and -0.741

4.2.1 Bis(diphenylphosphino)ethylamine (1)

The compound bis(diphenylphosphino)-ethylamine ligand (PNP-Ethyl) (1) (see **Figure 4.2**) crystallizes in a monoclinic crystal system and in the $P2_1/n$ space group. The number of formula units per unit cell $Z = 4$.

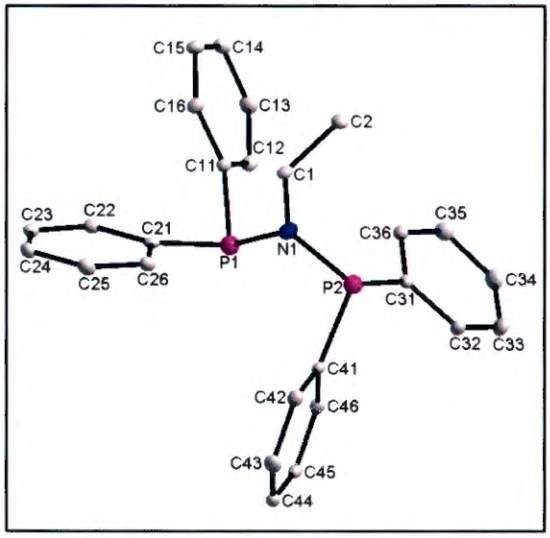

Figure 4.3: Graphical representation of PNP-Ethyl (1) at 50% probability. (H-atoms were omitted for clarity.)

Table 4.3: Selected torsion angles (°) for the compound PNP-Ethyl (1).

Atoms	Torsion angle (°)
C1 – N1 – P1 – C11	50.9(1)
C1 – N1 – P1 – C21	-53.5(1)
C1 – N1 – P2 – C31	-116.4(1)
C1 – N1 – P2 – C41	137.4(1)

The diphenylphosphine groups for PNP-Ethyl are staggered relative to the PNP backbone, as further illustrated by the torsion angles (see **Table 4.3**). This geometry indicates the preferred conformation for this compound in the solid state to be the approximate conformation C_S (see **Figure 4.2** and **Table 4.1**). This is unexpected as this conformation is usually adopted for diphosphinoamines with relatively bulky

nitrogen-bonded alkyl groups and in this case the alkyl is considered a relatively small ethyl substituent.

Table 4.4: Selected geometric parameters (Å, °) for the compound PNP-Ethyl (1).

Atoms	Bond length (Å)	Atoms	Bond angle (°)
P1 – N	1.712(1)	P1 – N1 – P2	123.7(1)
P2 – N	1.713(1)	C1 – N1 – P1	122.3(1)
N1 – C1	1.485(2)	C1 – N1 – P2	114.0(1)
P1 – C11	1.847(2)	C11 – P1 – C21	100.4(1)
P1 – C21	1.836(2)	N1 – P1 – C11	104.8(1)
P2 – C32	1.825(2)	N1 – P1 – C21	102.6(1)
P2 – C41	1.833(2)	C31 – P2 – C41	100.8(1)
		N1 – P2 – C31	105.6(1)
		N1 – P2 – C41	105.5(1)

All bond distances and angles are considered to be normal and fall within the range reported for similar complexes. [6,10,11] The geometry around the phosphorous ligands is distorted from tetrahedral geometry with C-P-C angles being the most distorted (varying from 100.4(1)° to 100.8(1) °). This is as expected due to the extra space needed by the lone electron pair on the two phosphorous atoms, forcing the three substituents coordinated to each phosphorous atom to move closer to each other and therefore deviating from the ideal tetrahedral bond angle of 109.5 °.

The distance of N1 from the P1-P2-C1 plane was calculated as 0.023(1) Å. This indicates that the nitrogen atom had to adapt an almost planar geometry with the two P atoms and the C atom attached to it. A distorted tetrahedral geometry was consequently adopted (with angles at the nitrogen varying between 114.0(1) and 123.7(1) °) in order to accommodate the steric bulk of the phenyl groups and the alkyl group.

[10] Cotton, F.A., Kuhn, F.E. and Yokochi, A., *Inorg. Chim. Acta*, **1996**, *252*, 251.

[11] Fei, Z., Scopeleti and R. Dyson, P.J., *J. Chem. Soc. Dalton Trans.*, **2003**, 2772.

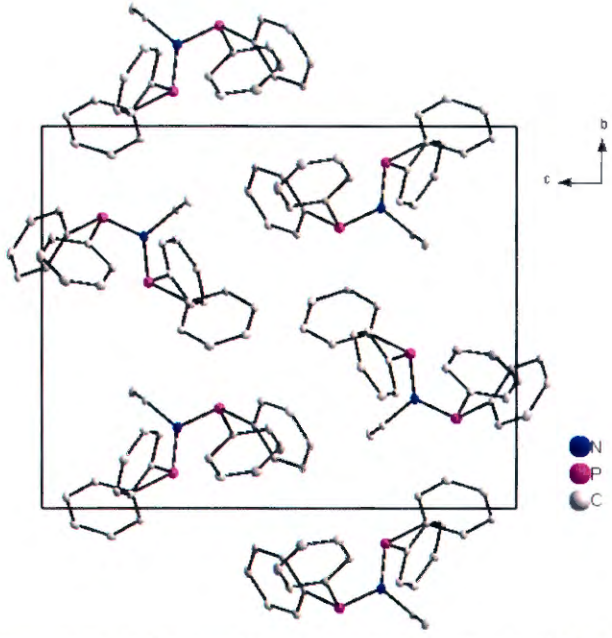

Figure 4.4: Graphical representation of the perspective view of the unit cell of PNP-Ethyl (1) along the a-axis. (H-atoms were omitted for clarity.)

There are no classical intermolecular hydrogen interactions present for this compound. The PNP-Ethyl molecules are packed in vertical layers across the bc plane in a head to tail manner (see **Figure 4.4**).

Correlations of the title compound with other relevant compounds are done in §4.3. Complete supplementary data of the title compound is given in Appendix A, Table A1-5.

4.2.2 Bis(diphenylphosphino)-1,2-dimethylpropylamine (2)[12]

The free bis(diphenylphosphino)-1,2-dimethylpropylamine ligand (PNP-Dimprop) (2) crystallizes in a triclinic crystal system and in the $P\bar{1}$ space grouap. The number of formula units per unit cell Z = 2. Three of the five carbon atoms in the nitrogen-coordinated 1,2-dimethylpropyl moiety are disordered over two positions in a 9:1 ratio.

[12] Cloete, N., Visser, H.G., Roodt, A., Dixon, J.T. and Blann, K., *Acta Cryst.*, **2008**, *E64*, o480.

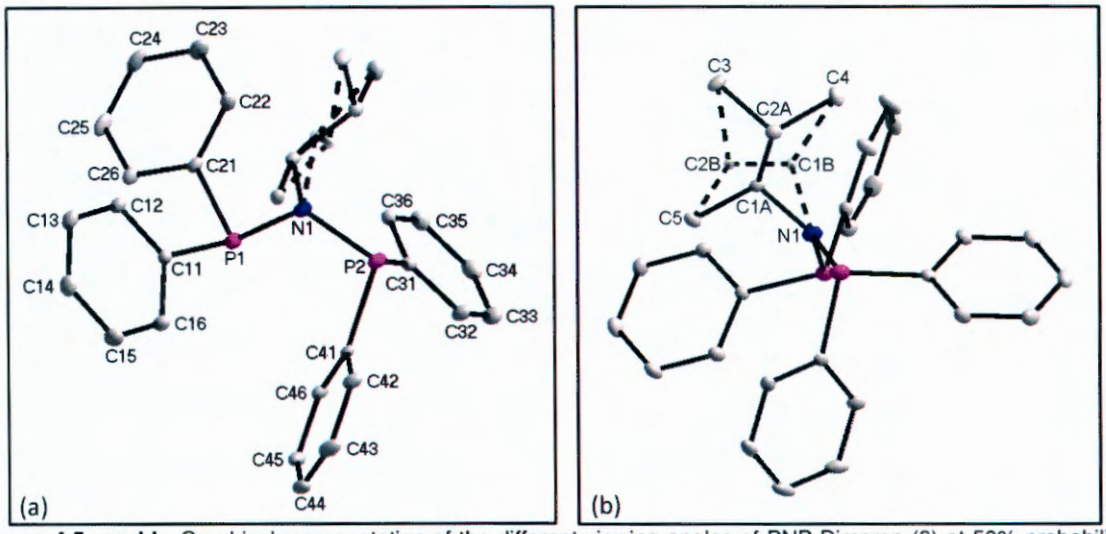

Figure 4.5a and b: Graphical representation of the different viewing angles of PNP-Dimprop (2) at 50% probability. A/B indicates the disordered carbon atoms in the 1,2-dimethylpropyl alkyl group. Disordered parts belonging together are numbered A and B respectively. (H-atoms were omitted for clarity).

Table 4.5: Selected torsion angles (°) for the compound PNP-Dimprop (2).

Atoms	Torsion angle (°)	Atoms	Torsion angle (°)
C1A – N1 – P1 – C11	-39.6(1)	C1B – N1 – P1 – C11	-77.9(5)
C1A – N1 – P1 – C21	65.4(1)	C1B – N1 – P1 – C21	27.1(5)
C1A – N1 – P2 – C31	114.8(1)	C1B – N1 – P2 – C31	121.6(5)
C1A – N1 – P2 – C41	-140.1(1)	C1B – N1 – P2 – C41	-105.5(5)

The distorted 1,2-dimethylpropyl group requires a relatively large space above the nitrogen atom, making it necessary for the compound to adopt conformation C_S (see **Figure 4.2** and **Table 4.1**) with the phenyl groups staggered with regard to the PNP-backbone. In spite of this, there are some degrees of freedom present which is manifested in the fact that the alkyl substituent crystallizes in a disordered position. The orientation of the phenyl groups relative to the N1-C1A/B bond is further demonstrated by the torsion angles in **Table 4.5**.

Table 4.6: Selected geometric parameters (Å, °) for the compound PNP-Dimprop (2).

Atoms	Bond length (Å)	Atoms	Bond angle (°)
P1 – N	1.721(2)	P1 – N1 – P2	117.9(1)
P2 – N	1.727(2)	C1A – N1 – P1	121.6(1)
N1 – C1A	1.515(2)	C1B – N1 – P1	130.1(4)
N1 – C1B	1.520(2)	C1A – N1 – P2	115.5(1)
P1 – C11	1.831(2)	C1B – N1 – P2	111.2(4)
P1 – C21	1.839(2)	C11 – P1 – C21	99.6(1)
P2 – C32	1.826(2)	N1 – P1 – C11	104.9(1)
P2 – C41	1.836(2)	N1 – P1 – C21	106.6(1)
		C31 – P2 – C41	99.7(1)
		N1 – P2 – C31	110.4(1)
		N1 – P2 – C41	105.0(1)

All bond distances and angles are considered to be normal and fall within the range reported for similar complexes.[6,10,11] The distortion of the phosphorous geometry is evident from the C-P-C angles that range between 99.6(1) and 99.7(1) °. The distances of N1 from the P1-P2-C1A and P1-P2-C1B planes were calculated as 0.216(1) and 0.090(1) Å respectively. This indicates the distortion of the tetrahedral geometry of the nitrogen atom in order to accommodate the steric bulk of the substituents coordinated to this atom (angles ranging between 111.2(4) and 130.1(4) °).

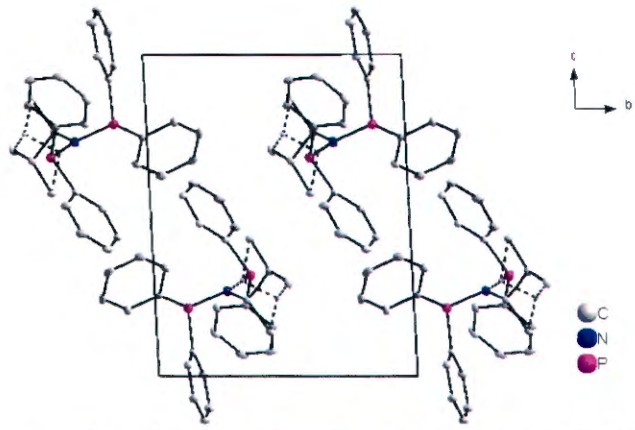

Figure 4.6: Graphical representation of a perspective view of the unit cell of PNP-Dimprop along the a-axis. (H-atoms were omitted for clarity.)

There are no classical intermolecular hydrogen interactions observed for the PNP-Dimprop compound. The molecules are packed in diagonal layers across the bc plane in a head-to-tail fashion (see **Figure 4.6)**.

Correlations of the title compound with other relevant compounds are done in §4.3. Complete supplementary data of the title compound is given in Appendix A, Table A6-10.

4.2.3 Bis(diphenylphosphino)-isopentylamine (3)

The bis(Diphenylphosphino)-isopentylamine non-coordinated ligand (PNP-*i*-Pent) (3) crystallizes in an orthorhombic crystal system and in a $P2_12_12_1$ space group. The number of formula units per unit cell $Z = 4$.

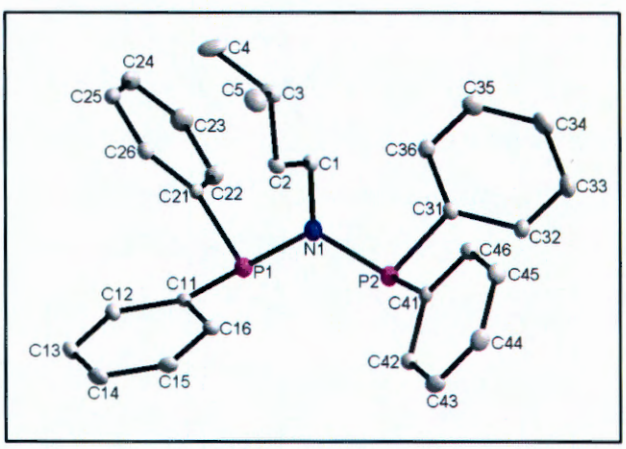

Figure 4.7: Graphical representation of PNP-i-Pent (3) at 50% probability. (H-atoms were omitted for clarity.)

Table 4.7: Selected torsion angles (°) for the compound PNP-*i*-Pent (3).

Atoms	Torsion angle (°)
C1 – N1 – P1 – C11	-72.2(2)
C1 – N1 – P1 – C21	37.0(2)
C1 – N1 – P2 – C31	-50.3(2)
C1 – N1 – P2 – C41	58.2(2)

The non-coordinated PNP-*i*-Pent ligand adopted the approximate conformation C_{2v} (see **Figure 4.2** and **Table 4.1**), see **Table 4.7** for torsion angles which further describes the orientation of the phenyl rings. This indicates that enough space is available in the solid state for both sets of phosphorous-bonded phenyl rings to be turned upwards towards the nitrogen-bonded alkyl group.

Table 4.8: Selected geometric parameters (Å, °) for the compound PNP-*i*-Pent (3).

Atoms	Bond length (Å)	Atoms	Bond angle (°)
P1 – N	1.712(2)	P1 – N1 – P2	111.0(1)
P2 – N	1.703(2)	C1 – N1 – P1	125.0(1)
N1 – C1	1.483(2)	C1 – N1 – P2	123.7(1)
P1 – C11	1.830(2)	C11 – P1 – C21	104.0(1)
P1 – C21	1.830(2)	N1 – P1 – C11	105.7(1)
P2 – C32	1.832(2)	N1 – P1 – C21	103.9(1)
P2 – C41	1.829(2)	C31 – P2 – C41	103.2(1)
		N1 – P2 – C31	104.9(1)
		N1 – P2 – C41	105.3(1)

All bond distances and angles are considered to be normal and fall within the range reported for similar complexes.[6,10,11] The geometry of the phosphorous atoms is distorted from the ideal tetrahedral arrangement, with C-P-C angles ranging from 103.2(1) to 104.0(1) °. The distance of N1 from the P1-P2-C1 plane was calculated as 0.055(2) Å. The angles at N1 which range between 111.0(1) and 125.0(1) ° indicate a distortion from the ideal tetrahedral geometry.

There is a weak hydrogen interaction present between C35-H35···P2 (distance between H35 and P2 is 2.946(2) Å) (see **Figure 4.8**).

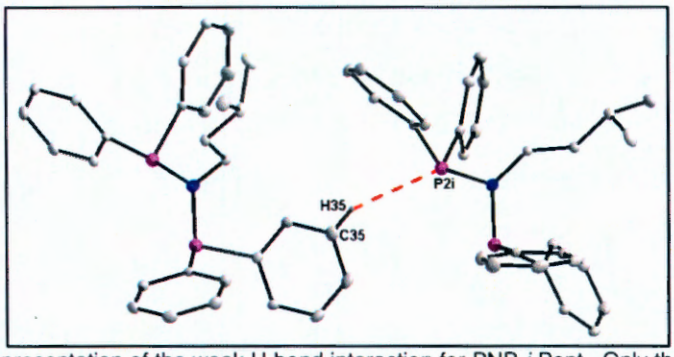

Figure 4.8: Graphical representation of the weak H-bond interaction for PNP-*i*-Pent. Only the applicable H atom with relevance to the H-bond interaction is indicated. The red fragmented line indicates the weak intermolecular hydrogen interaction between the PNP-*i*-Pent molecules ((i) = 0.5-x, -y, 0,5+z).

The PNP-*i*-Pent molecules are packed in vertical lines across the ac plane in a head-to-tail fashion (see **Figure 4.8**).

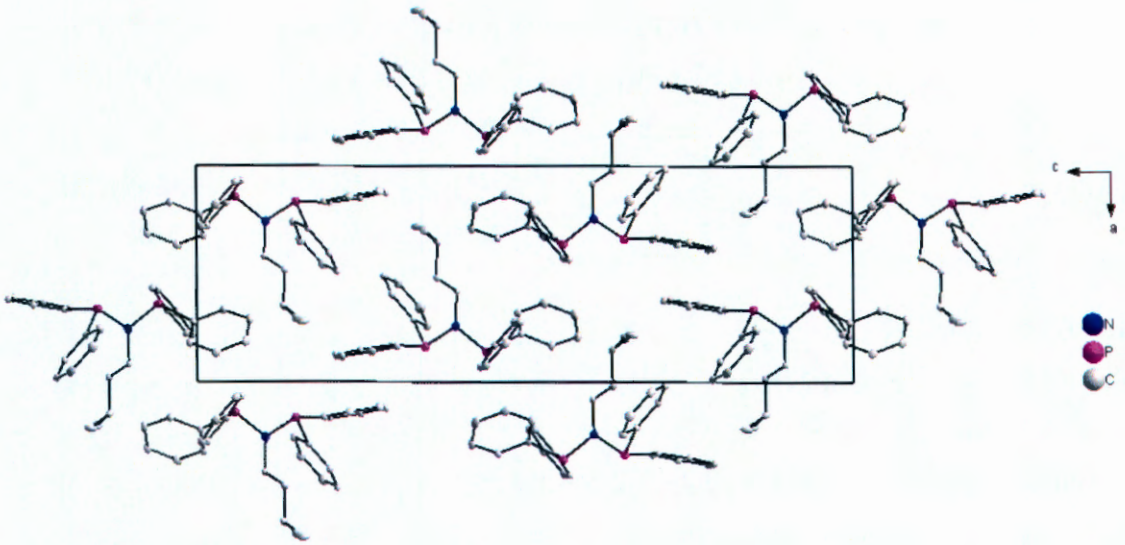

Figure 4.8: Graphical representation of a perspective view of the unit cell of PNP-*i*-Pent along the b-axis. (H-atoms were omitted for clarity.)

Correlations of the title compound with other relevant compounds are done in §4.3. Complete supplementary data of the title compound is given in Appendix A, Table A10-15.

4.2.4 Bis(diphenylphosphino)-cyclohexylamine (PNP-Cychex) (4)

The bis(diphenylphosphino)cyclohexylamine (PNP-Cychex) (4) complex crystallizes in the monoclinic crystal system in the $P2_1/n$ space group. The number of formula units per unit cell $Z = 4$.

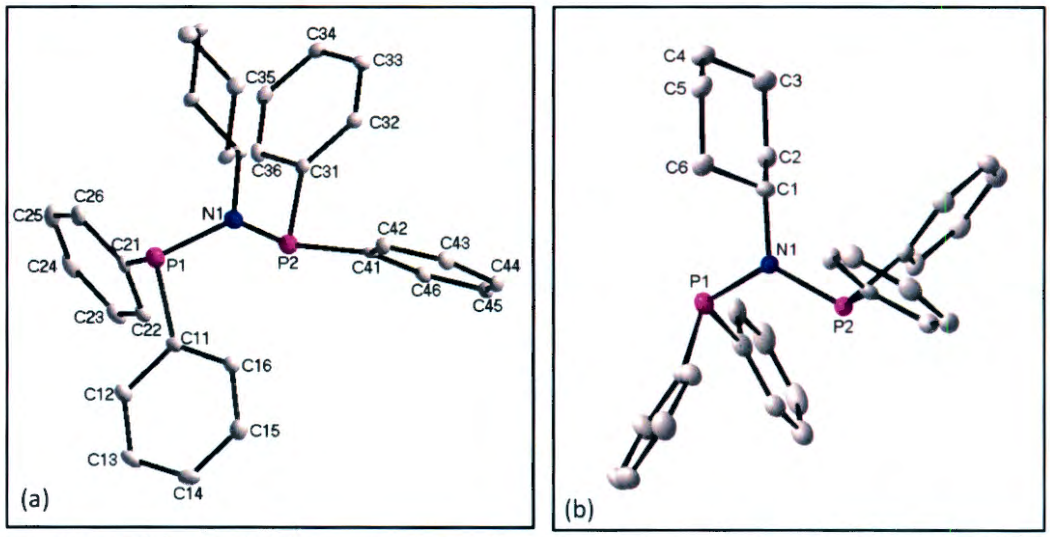

Figure 4.9a and b: Graphical representation of the different viewing angles of PNP-Cychex (4) at 50% probability. (H-atoms were omitted for clarity).

Table 4.9: Selected torsion angles (°) for the compound PNP-Cychex (4).

Atoms	Torsion angle (°)
C1 – N1 – P1 – C11	-135.6(1)
C1 – N1 – P1 – C21	117.2(1)
C1 – N1 – P2 – C31	-38.8(1)
C1 – N1 – P2 – C41	66.2(1)

The PNP-Cychex compound adopted the approximate conformation C_S (see **Figure 4.2** and **Table 4.1**) in the solid state, which is as expected for a diphosphinoamine with a sterically bulky substituent such as the cyclohexyl group. The orientation of the phenyl rings are further illustrated by the torsion angles in **Table 4.9**.

Table 4.10: Selected geometric parameters (Å, °) for the compound PNP-Cychex (4).

Atoms	Bond length (Å)	Atoms	Bond angle (°)
P1 – N	1.758(4)	P1 – N1 – P2	119.0(2)
P2 – N	1.686(5)	C1 – N1 – P1	115.1(1)
N1 – C1	1.502(6)	C1 – N1 – P2	122.0(2)
P1 – C11	1.819(5)	C11 – P1 – C21	102.6(2)
P1 – C21	1.836(6)	N1 – P1 – C11	104.1(1)
P2 – C31	1.850(5)	N1 – P1 – C21	105.5(1)
P2 – C41	1.848(5)	C31 – P2 – C41	99.0(2)
		N1 – P2 – C31	103.9(1)
		N1 – P2 – C41	105.9(1)

All bond distances and angles are considered to be normal and fall within the range reported for similar complexes.[6,10,11] The distortion of the phosphorous atom is apparent from the C-P-C angles which deviate from the ideal 109.5 ° with values that range from 99.0(2) to 102.6(2) °. The distance of N1 from the P1-P2-C1 plane was calculated as 0.173(1) Å and angles of N1 vary between 115.1(1) and 122.0(2) °. There are no classical intermolecular interactions.

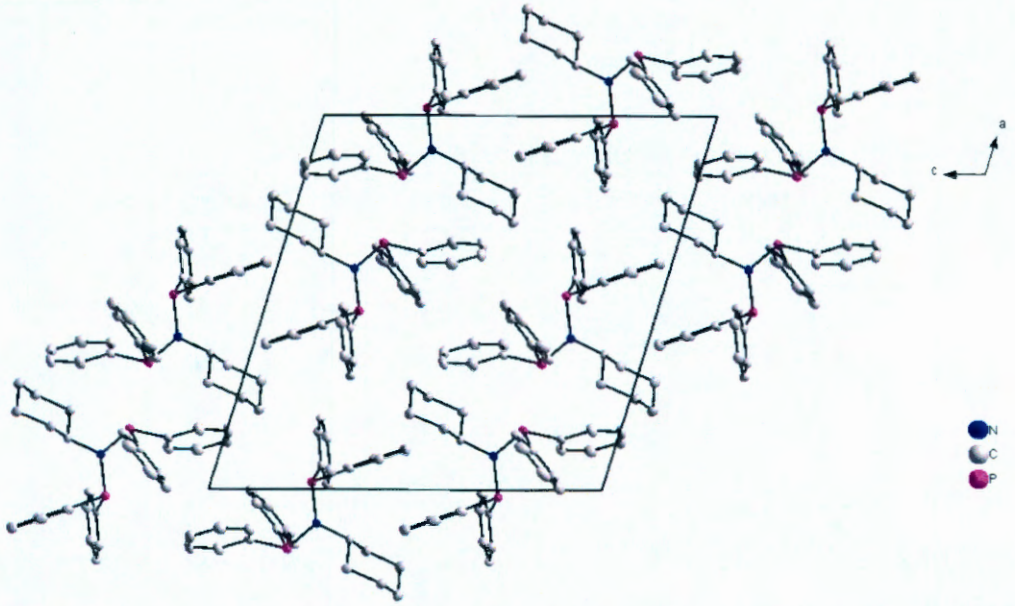

Figure 4.10: Graphical representation of a perspective view of the unit cell of PNP-Cychex (4) along the b-axis. (H-atoms were omitted for clarity.)

The packing pattern of PNP-Cychex reveals that the molecules are packed in diagonal layers across the ac-plane with the molecules alternating the direction in which the cyclohexyl moieties are pointing (see **Figure 4.10**).

Correlations of the title compound with other relevant compounds are done in §4.3. Complete supplementary data of the title compound is given in Appendix A, Table A16-20.

4.2.5 Bis(diphenylphosphino)-*n*-pentylamine (5)

The bis(diphenylphosphino)-pentylamine (PNP-*n*-Pent) (6) compound crystallizes with two crystallographically independent molecules in the asymmetric unit, in the triclinic crystal system and in the $P\bar{1}$ space group. The number of formula units per unit cell is Z = 4. The two molecules are described in the following paragraphs as PNP-*n*-Pent I (5I) (molecule containing N1, see **Figure 4.11**) and PNP-*n*-Pent I (5II) (molecule containing N2, see **Figure 4.11**).

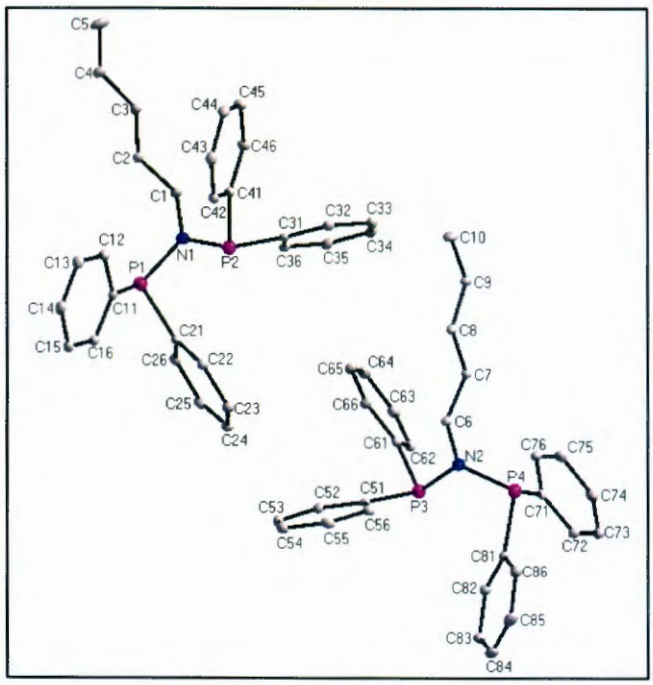

Figure 4.11: Graphical representation of PNP-*n*-Pent I (5I) and PNP-*n*-Pent II (5II) at 50% probability. (H-atoms were omitted for clarity.)

Table 4.11: Selected torsion angles (°) for the compound PNP-*n*-Pent I (5I) and PNP-n-Pent II (5II).

Atoms	Torsion angle (°)	Atoms	Torsion angle (°)
C1 – N1 – P1 – C11	-121.8(1)	C6 – N1 – P4 – C71	-127.7(1)
C1 – N1 – P1 – C21	131.7(1)	C6 – N1 – P4 – C81	126.7(1)
C1 – N1 – P2 – C31	-56.1(1)	C6 – N1 – P3 – C51	-54.0(1)
C1 – N1 – P2 – C41	49.4(1)	C6 – N1 – P3 – C61	51.4(1)

Both PNP-*n*-Pent molecules in the asymmetric unit adopted the approximate conformation C_S (see **Figure 4.2** and **Table 4.1**), with only small differences in lengths and angles between the two molecules. The torsion angles of the two independent molecules (see **Table 4.11**) show that the orientation of the corresponding phenyl rings are very similar with only small differences between the respective torsion angles. These structural similarities indicate that these two crystallographic independent molecules in the asymmetric unit are almost mirror images of each other. An overlay of the two molecules illustrating the similarities is presented in **Figure 4.12** (with P1, N1 and P2 overlayed on P4, N2 and P3 respectively).

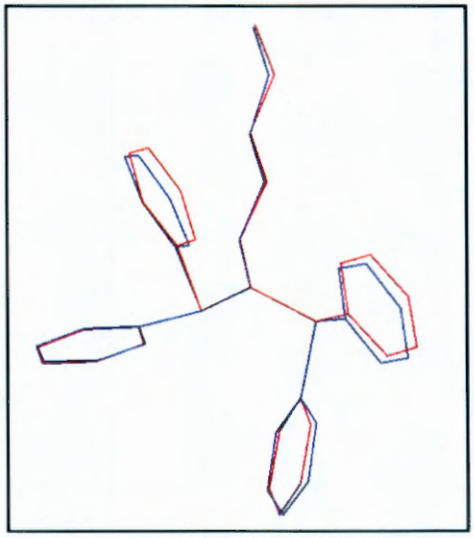

Figure 4.12: Graphical representation of an overlay of the PNP-*n*-Pent I (5I) (blue) and PNP-*n*-Pent II (5II) (red) using Hyperchem 7.52[9]

Table 4.12: Selected geometric parameters (Å, °) for the compound PNP-*n*-Pent I (5I).

Atoms	Bond length (Å)	Atoms	Bond angle (°)
P1 – N1	1.713(1)	P1 – N1 – P2	123.4(1)
P2 – N1	1.712(1)	C1 – N1 – P1	116.0(1)
N1 – C1	1.482(1)	C1 – N1 – P2	123.4(1)
P1 – C11	1.828(1)	C11 – P1 – C21	101.5(1)
P1 – C21	1.830(1)	N1 – P1 – C11	104.1(1)
P2 – C31	1.834(1)	N1 – P1 – C21	105.7(1)
P2 – C41	1.836(1)	C31 – P2 – C41	101.1(1)
		N1 – P2 – C31	102.9(1)
		N1 – P2 – C41	105.2(1)

Table 4.13: Selected geometric parameters (Å, °) for the compound PNP-*n*-Pent II (5II).

Atoms	Bond length (Å)	Atoms	Bond angle (°)
P3 – N2	1.708(1)	P3 – N2 – P4	120.5(1)
P4 – N2	1.718(1)	C6 – N2 – P3	123.8(1)
N2 – C6	1.483(1)	C6 – N2 – P4	115.7(1)
P3 – C51	1.834(1)	C51 – P3 – C61	100.7(1)
P3 – C61	1.840(1)	N1 – P3 – C51	102.2(1)
P4 – C71	1.825(1)	N1 – P3 – C61	107.2(1)
P4 – C81	1.838(1)	C71 – P4 – C81	100.7(1)
		N1 – P4 – C71	103.4(1)
		N1 – P4 – C81	106.1(1)

All bond distances and angles are considered to be normal and fall within the range reported for similar complexes.[6,10,11] Both PNP-*n*-Pent molecules exhibit distortion of the geometry at the phosphorous atoms, with C-P-C angles that range between 100.7(1) and 101.5(1) ° for both molecules. The distance of N1 from the P1-P2-C1 plane was calculated as 0.010(1) Å and the distance calculated of N2 from the P3-P4-C6 plane

was 0.025(1) Å. The distortion of the geometry at the nitrogen atoms are further illustrated by the angles that vary between 115.7(1) and 123.8(1) °.

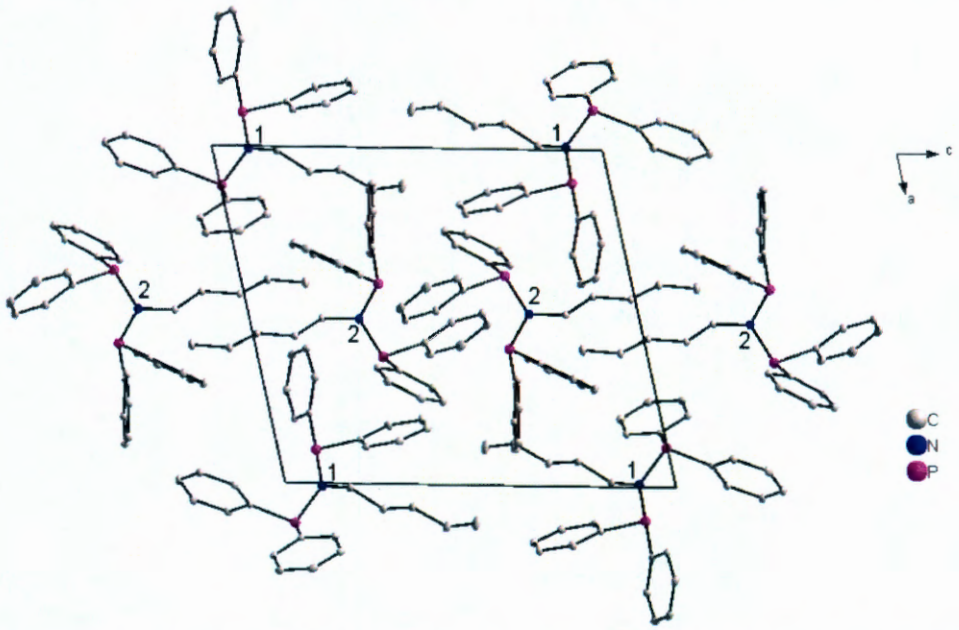

Figure 4.13: Graphical representation of a perspective view of the unit cell of PNP-*n*-Pent along the b-axis. The molecules containing N1 is labeled as '1' and the second PNP-*n*-Pent molecule in the asymmetric unit containing N2 is labeled as '2'. (H-atoms were omitted for clarity.)

There are no classical intermolecular interactions present for the PNP-*n*-Pent compound. The molecules are packed in horizontal layers across the ac-plane. The molecules containing N1 is labeled as 1 in the **Figure 4.13** and the second molecule in the asymmetric unit containing N2 is labeled 2. It is clear from **Figure 4.13** that the horizontal layers alternate between a row of molecules 1 and molecules 2 of the PNP-*n*-Pent compound.

Correlations of the title compound with other relevant compounds are done in §4.3. Complete supplementary data of the title compound is given in Appendix A, Table A20-25.

4.3 Discussion

All five free ligands reported in this study are similar except for the substituent on the nitrogen atom. The largest and most profound effect of changing the substituents from one ligand to another was the change in the P-N-P angle. This observation is further illustrated when compared to two other diphenylphosphinoamine ligands from literature, bis(diphenylphosphino)-isopropylamine[6] (PNP-*i*-Prop) (see **Figure 4.14**) and bis(diphenylphosphino)phenylamine[11] (PNP-Phen) (see **Figure 4.15**) in **Table 4.14**.

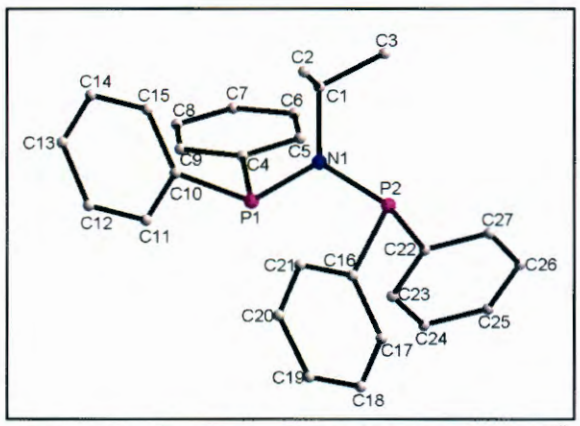

Figure 4.14: Graphical representation of (PNP-*i*-Prop)[6] at 50% probability. (H-atoms were omitted for clarity.)

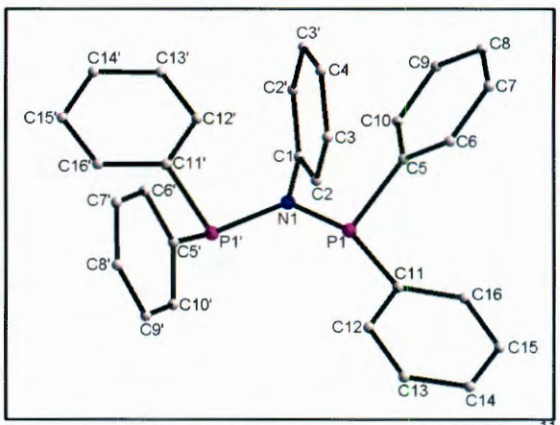

Figure 4.15: Graphical representation of (PNP-Phen)[11] at 50% probability. (H-atoms were omitted for clarity.)

Table 4.14: The P-N-P angle (°) and conformation adopted for various free bis(diphenylphosphino)amine ligands.

Compound	Bond angle (°) P – N – P	Conformation (See Figure 4.2)
PNP-Ethyl	123.7(1)	C_S
PNP-*n*-Pent	123.4(1) and 120.5(1)	C_S
PNP-*i*-Prop[6]	122.8(3)	C_S
PNP-Cychex	119.0(1)	C_S
PNP-Dimprop[12]	117.9(1)	C_S
PNP-Phen[11]	113.2(2)	C_{2V}
PNP-*i*-Pent	111.0(1)	C_{2V}

It appears that the bulkiness of the nitrogen-coordinated substituent affects the P-N-P bond angle of the compound. There seems to be a tendency for the P–N–P bond angles (PNP-Phen = 113.2(2)°, PNP-Dimprop = 117,9(1) °, PNP-*i*-Prop = 122.8(3) °, PNP-Ethyl = 123.7(1) °) to increase as the substituent on the N atom becomes smaller (PNP-Phen > PNP-Dimprop > PNP-*i*-Prop > PNP-Ethyl) in the non-coordinated ligand. This indicates that the P-N-P bond angle is forced to close somewhat in order to accommodate the larger nitrogen-bound substituent.

The P-N-P bond angles for PNP-Ethyl (123.7(1)°) and PNP-*n*-Pent (123.4(1) and 120.5(1) °) are very similar, which is as expected, since these two compounds both have linear unbranched alkyl groups as nitrogen-substituents and adopted a similar conformation.

The PNP-*i*-Pent has a substantially smaller P-N-P bond angle (111.0(1) °) even though the compounds contain a relatively bulky substituent coordinated to the nitrogen atom. The compound adopts conformation C_{2V} in the solid state, which could explain the large difference in the P-N-P angles in comparison with the five other PNP ligands with C_S conformations (PNP-Ethyl, PNP-*n*-Pent, PNP-*i*-Prop, PNP-Dimprop and PNP-Cychex).

Table 4.15: Selected bond lengths for various free bis(diphenylphosphino)amine ligands.

Compound	C1-N1 (Å)	P1-N1 (Å)	P2-N1 (Å)
PNP-Ethyl	1.485(2)	1.712(1)	1.713(1)
PNP-*n*-Pent I	1.482(1)	1.713(1)	1.712(1)
PNP-*i*-Pent	1.483(2)	1.712(2)	1.703(2)
PNP-Cychex	1.502(6)	1.758(4)	1.686(5)
PNP-Dimprop[12]	1.515(2)	1.721(2)	1.727(2)

Selected bond lengths of the various non-coordinated PNP ligands (see **Table 4.15**) indicate also that the P-N bond lengths increase as the steric bulk of the alkyl moieties increase. This is evident when the P1-N1 and P2-N1 bonds lengths for PNP-Dimprop (1.712(1) and 1.713(1) °) and PNP-Ethyl (1.721(2) and 1.727(2) °) are compared. The same trend is observed for the C-N bonds of the various free PNP ligands (see **Table 4.14**). The bond lengths are clearly longer in order to accommodate the larger alkyl groups and to prevent substantial steric crowding.

It has been shown by this crystallographic study of the free bis(diphenylphosphino)amine ligands, that it is not merely the steric bulkiness of the nitrogen-coordinated substituent atom that affects the conformation of the PNP compounds in solid state. The P-N-P angle and selected bond lengths were shown to be affected by the steric bulk of such a substituent.

Possible isomers of the non-coordinated PNP-ligands were identified through the use of theoretical calculations. The optimized isomers with the lowest relative energy was then compared to the crystal structure of the corresponding PNP ligand. This study is presented and discussed in Chapter 7.

5 Single crystal X-ray crystallographic study of Pt(II)-PNP and Pd(II)-PNP complexes

In this chapter...

The crystallographic data of a series of [$PtCl_2$(PNP-alkyl)] and [$PdCl_2$(PNP-alkyl)] complexes were collected and are discussed in detail. The phenyl rings of the PNP ligands arrange itself in one of two modes, namely basket- and fan-like orientations.

5.1 Introduction

An important part of this investigation is concerned with the synthesis and evaluation of the solid state characteristics of the PNP ligands used with Cr(III) as pre-catalyst systems for ethylene tetramerisation. Ideally a whole range of Cr(III)-PNP compounds has to be synthesized and crystallized so that X-ray crystallographic data could be obtained. This could then be used to evaluate the structural factors that govern the selectivity of the catalyst systems. Unfortunately the synthesis of the PNP complexes with chromium(III) (Cr(III)) is very complicated, necessitating stringent anaerobic conditions. To date only one Cr(III)-PNP complex has been reported in literature.[1]

In order to negate the complications experienced with Cr(III), it was decided to extend the knowledge of the PNP ligands in general and to investigate the coordination chemistry of these ligands at other, more stable metal centres. A number of square planar complexes of Pt(II) and Pd(II) coordinated with various diphosphinoamine ligands have been reported in literature.[2, 3, 4, 5, 6, 7] Similar metal complexes were therefore

[1] Bollmann, A., Blann, K., Dixon, J.T., Hess, F. M., Killian, E., Maumela, H., McGuinness, D. S., Morgan, D. H., Neveling, A., Otto, S., Overett, M.J., Slawin, A.M.Z., Wasserscheid, P. and Kuhlmann, S., *J. Am. Chem. Soc.*, **2004**, *126*, 14712.
[2] Browning, C.S., Farrar, D.H. and Frankel, D.C., *Acta Cryst.*, **1992**, *C48*, 806.
[3] Calabrò, G., Drommi, D., Graiff, C., Faraone, F. and Tiripicchio, A., *Eur. J. Inorg., Chem.*, **2004**, 1447.

synthesized to act as model complexes for chromium(III) and to investigate the steric and electronic properties and the effects induced by the PNP-ligands, systematically. The complexes proved to be fairly easy to synthesize and were not air or moisture sensitive like the Cr(III)-PNP counterparts.

5.2 Crystallographic data

Single crystals suitable for study by single crystal X-ray crystallography were obtained as described in §3.2.1-10. **Scheme 5.1** and **5.2** provides a summary of the complexes that form part of this study, while the general crystal data is summarised **in Table 5.1** and **Table 5.27**. A molecular diagram showing the numbering scheme (using DIAMOND 3.0[8]) of each compound is presented, also with selected bond lengths, angles and torsion angles. Graphical representations of overlays of selected complexes are also presented (using Hyperchem7.52[9]). A discussion highlighting some of the important aspects of each particular structure is presented thereafter.

Please note: additional correlations with other relevant structures are however done in §5.3.1-5.3.2. For the sake of brevity and to prevent tedium, the general features are summarised in §5.3.3, while differences like hydrogen bonding, packing and disorders in the structures are discussed in detail for each separate structure.

[4] Tooke, D.M., Zijp, E.J., van der Vlugt, J.I., Vogt, D. and Spek, A., *Acta. Cryst.*, **2007**, *E63*, m86.
[5] Durap, F., Biricik, N., Gümgüm, B., Özkar, S., Ang, W.H., Fei, Z. and Scopelliti, R., *Polyhedron*, **2008**, *27*, 196.
[6] Babu, R.P.K., Krishnamurthy, S.S. and Nethaji, M., *Tetrahedron*, **1995**, *6*, 427.
[7] Fei, Z., Han Ang, W., Zhao, D., Scopelliti, R. and Dyson, P.J., *Inorg. Chim. Acta*,, **2006**, *359*, 2635.
[8] Brandenburg, K. and Putz, H., **2005**, DIAMOND. Release 3.0c. Crystal Impact GbR, Bonn, Germany.
[9] Hyperchem ™ Release 7.52, Windows Molecular Modeling System, Hypercube, Inc., **2002**.

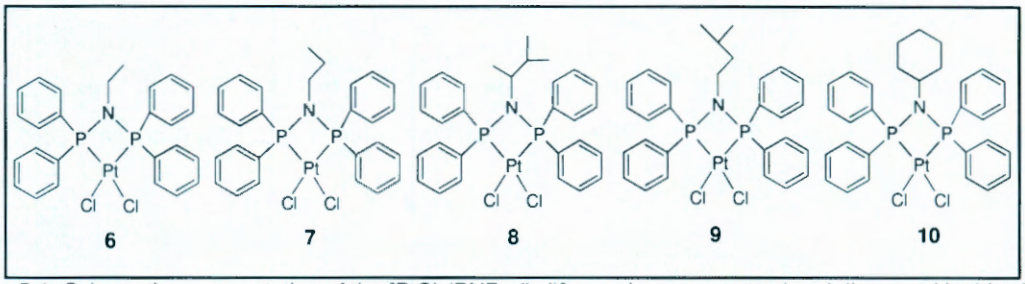

Scheme 5.1: Schematic representation of the [$PtCl_2$(PNP-alkyl)] complexes presented and discussed in this chapter:
6: Dichlorido-bis(diphenylphosphino)-ethylamine-platinum(II) ([$PtCl_2$(PNP-Ethyl)]),
7: Dichlorido-bis(diphenylphosphino)-*n*-propylamine-platinum(II) ([$PtCl_2$(PNP-*n*-Prop)]),
8: Dichlorido-bis(diphenylphosphino)-1,2-dimethylpropylamine-platinum(II) ([$PtCl_2$(PNP-Dimprop)]),
9: Dichlorido-bis(diphenylphosphino)-isopentylamine-platinum(II) ([$PtCl_2$(PNP-*i*-Pent)]),
10: Dichlorido-bis(diphenylphosphino)-cyclohexylamine-platinum(II) ([$PtCl_2$(PNP-Cychex)]).

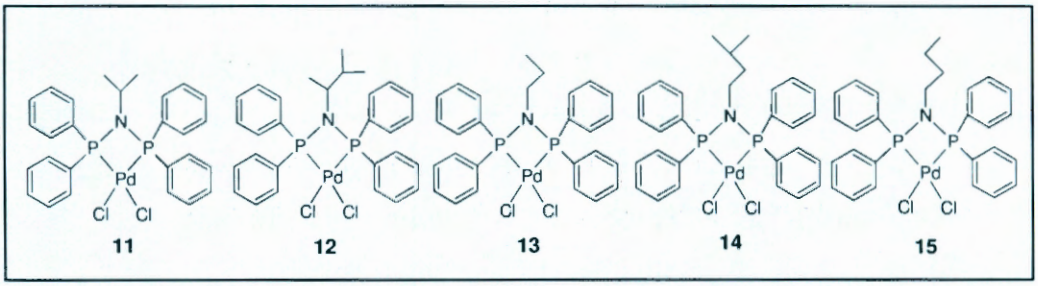

Scheme 5.2: Schematic representation of the [$PdCl_2$(PNP-alkyl)] complexes presented and discussed in this chapter:
11: Dichlorido-bis(diphenylphosphino)-isopropylamine-palladium(II) ([$PdCl_2$(PNP-*i*-Prop)]),
12: Dichlorido-bis(diphenylphosphino)-1,2-dimethylpropylamine-palladium(II) ([$PdCl_2$(PNP-Dimprop)]),
13: Dichlorido-bis(diphenylphosphino)-*n*-propylamine-palladium(II) ([$PdCl_2$(PNP-*n*-Prop)]),
14: Dichlorido-bis(diphenylphosphino)-isopentyl-palladium(II) ([$PdCl_2$(PNP-*i*-Pent)]),
15: Dichlorido-bis(diphenylphosphino)-*n*-butylamine-palladium(II) ([$PdCl_2$(PNP-*n*-Butyl)]).

Table 5.1: General crystal data for the following compounds , [$PtCl_2$(PNP-Ethyl)] (6), [$PtCl_2$(PNP-Dimprop)] (7), [$PtCl_2$(PNP-*i*-Pent)] (8), [$PtCl_2$(PNP-*n*-Prop)] (9) and [$PtCl_2$(PNP-Cychex)] (10).

Identification code	[$PtCl_2$(PNP-Ethyl)] (6)	[$PtCl_2$(PNP-*n*-Prop)] (7)	[$PtCl_2$(PNP-Dimprop)] (8)	[$PtCl_2$(PNP-*i*-Pent)] (9)	[$PtCl_2$(PNP-Cychex] (10)
Empirical formula	$PtNP_2Cl_2C_{26}H_{25}$	$PtNP_2Cl_2C_{27}H_{27}$	$PtNP_2Cl_2C_{29}H_{31}$	$PtNP_2Cl_2C_{29}H_{31}$	$PtNP_2Cl_2C_{30}H_{30}$
Formula weight	679.40	693.43	721.51	721.51	732.48
Crystal system, space group	Orthorhombic, $P2_1/c$	Monoclinic, $P2_1/n$	Monoclinic, $P2_1/n$	Orthorhombic, *Pnma*	Monoclinic, $P2_1/n$
Unit cell dimensions:					
a(Å)	9.362(1)	10.6301(4)	10.0154(9)	20.6687(12)	11.0839(9)
b(Å)	9.774(1)	18.812(1)	14.838(1)	17.3609(11)	17.238(2)
c(Å)	27.858(3)	12.765(1)	18.000(2)	8.3412(4)	14.842(1)
α (°)	90.000	90.000	90.000	90.000	90.000
β (°)	90.000	97.326(1)	94.892(3)	90.000	100.329(2)
γ (°)	90.000	90.000	90.000	90.000	90.000
Volume ($Å^3$)	2549.2(4)	2531.8(2)	2665.2(4)	2993.0(3)	2789.8(4)
Z	4	4	4	4	4
Calculated density (Mg/m^3)	1.770	1.819	1.833	1.601	1.744
Absorption coefficient (mm^{-1})	5.854	5.897	5.608	4.991	5.357
F(000)	1320	1352	1444	1416	1436
Crystal size (mm)	0.20 x 0.19 x 0.08	0.38 x 0.10 x 0.02	0.22 x 0.07 x 0.05	0.05 x 0.15 x 0.38	0.48 x 0.23 x 0.18
Θ range / completeness of collection (°)	1.46-28.63/ 66.3	2.17-28.32/ 99.6	1.78-26.00/ 99.5	2.29-28.29/ 99.9	2.12-28.30/ 99.7
	-12<=h<=12	-14<=h<=14	-11<=h<=12	-27<=h<=27	-14<=h<=14
Limiting indices	-13<=k<=13	-25<=k<=25	-17<=k<=18	-23<=k<=23	-22<=k<=22
	-37<=l<=37	-17<=l<=17	-22<=l<=22	-10<=l<=11	-19<=l<=19
Reflections collected / unique / observed (I>2σ(I))	29858 / 4341	50743 / 6276	21499 / 5216	54400 / 3837	43257 / 6929
	R(int) = 0.0427	R(int) = 0.0522	R(int) = 0.0432	[R(int) = 0.0483]	R(int) = 0.0584
Data / restraints / parameters	4341 / 0 / 289	6276 / 0 / 299	5216 / 0 / 319	3837 / 0 / 173	6929 / 0 / 325
Goodness of fit on F^2	1.093	1.042	1.066	1.107	1.033
Final R indices (I>2σ(I))	R1 = 0.0230	R1 = 0.0219	R1 = 0.0525	R1 = 0.0235	R1 = 0.0260
	wR2 = 0.0497	wR2 = 0.0492	wR2 = 0.1380	wR2 = 0.0570	wR2 = 0.0526
R indices(all data)	R1 = 0.0303	R1 = 0.0303	R1 = 0.0615	R1 = 0.0287	R1 = 0.0333
	wR2 = 0.0585	wR2 = 0.0528	wR2 = 0.1491	wR2 = 0.0596	wR2 = 0.0549
$\Delta\rho_{min}$, $\Delta\rho_{max}$ ($e.Å^{-3}$)	1.000 and -0.643	1.554 and -0.633	8.974 and -4.437	2.300 and -0.730	1.997 and -1.094

5.2.1 Dichlorido-bis(diphenylphosphino)-ethylamine-platinum(II) (6)

The title complex, [$PtCl_2$(PNP-Ethyl)], (see **Figure 5.1**) crystallizes in an orthorhombic crystal system in the $P2_1/c$ space group with 4 molecules per unit cell.

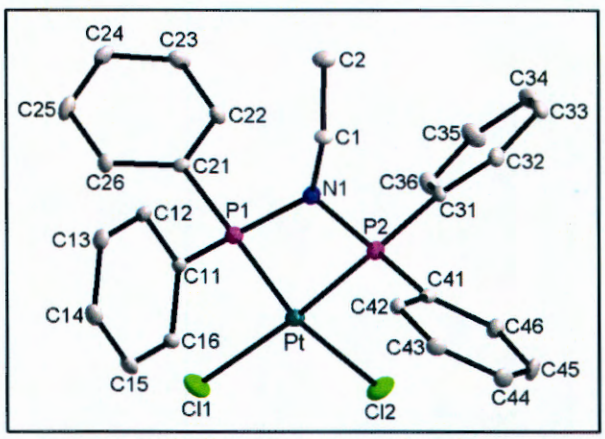

Figure 5.1: Graphical representation of [$PtCl_2$(PNP-Ethyl)] (6) at 50% probability. (H-atoms were omitted for clarity).

Table 5.2: Selected geometric parameters (Å, °) for [$PtCl_2$(PNP-Ethyl)] (6).

Atoms	Bond length (Å)	Atoms	Bond angle (°)
Pt – P1	2.210(1)	P1 – Pt – P2	72.1(1)
Pt – P2	2.186(1)	Cl1 – Pt – Cl2	91.7(1)
Pt – Cl1	2.333(1)	P1 – N1 – P2	100.0(2)
Pt – Cl2	2.343(1)	C1 – N1 – P1	131.7(3)
N1 – C1	1.475(5)	C1 – N1 – P2	127.7(3)
N1 – P1	1.692(4)	N1 – P1 – C11	109.2(2)
N1 – P2	1.686(3)	N1 – P1 – C21	108.4(2)
P1 – C11	1.791(4)	N1 – P2 – C31	108.9(2)
P1 – C21	1.807(4)	N1 – P2 – C41	108.7(2)
P2 – C31	1.793(5)	C11 – P1 – C21	107.0(2)
P2 – C41	1.809(5)	C31 – P2 – C41	106.5(2)

The P1-Pt-P2, P1-N1-P2 and Cl1-Pt-Cl2 angles are 72.1(2), 100.1(2) and 91.7(1) ° respectively for complex 1. The Pt-Cl bonds are of the expected lengths in these type of complexes.[3, 4, 5, 6, 7]

Table 5.3: Selected torsion angles (°) for [$PtCl_2$(PNP-Ethyl)] (6).

Atoms	Torsion angle (°)
Pt – P1 – C11 – C12	175.2(3)
Pt – P1 – C21 – C22	-63.6(4)
Pt – P2 – C31 – C32	-172.8(3)
Pt – P2 – C41 – C42	-80.8(4)

The phenyl rings are arranged in a 'fan-like' fashion which could be due to the fact that the ethyl substituent does not take significant amount of space (see **Figure 5.1**). This orientation is further illustrated by the torsion angles, Pt-P1-C11-C12 (175.2(3) °) and Pt-P1-C31-C32 (-172.8(3) °) (see **Table 5.3**) and will be discussed in detail in §5.3.3. The space which is occupied by the ethyl moiety is illustrated by **Figure 5.2** in which the alkyl group is displayed using space-filling atoms (the hydrogen and carbon atoms of the alkyl moiety is displayed as light and dark blue spheres respectively) and the remaining atoms of [$PtCl_2$(PNP-Ethyl)] is displayed in stick-wire formation.

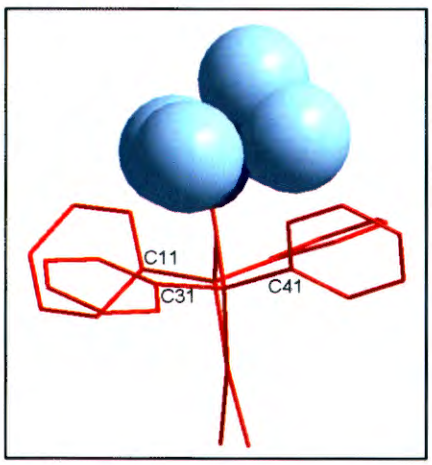

Figure 5.2: Graphical representation of [$PtCl_2$(PNP-Ethyl)] (6) using space-filling and stick-wire representation of the atoms (light blue = hydrogen atoms, dark blue = carbon atoms).

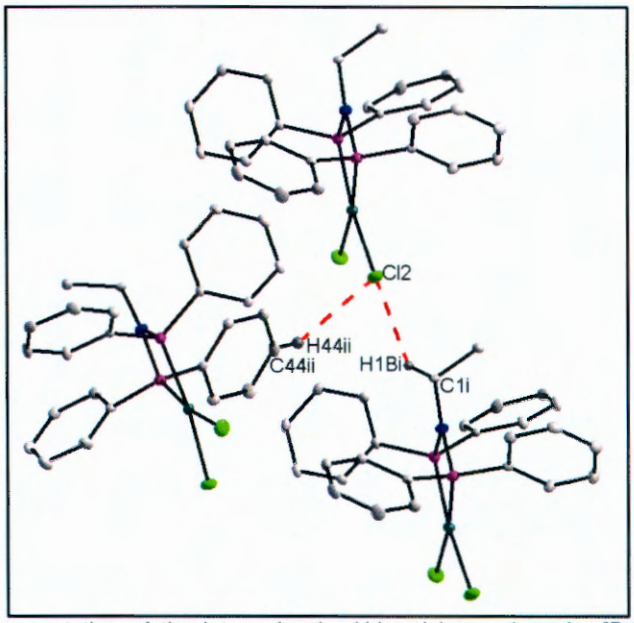

Figure 5.3: Graphical representation of the intermolecular H-bond interactions for [$PtCl_2$(PNP-Ethyl)] (6). Only applicable H atoms with relevance to the H-bond interactions are indicated. The red fragmented lines indicate the intermolecular hydrogen bonding between the [$PtCl_2$(PNP-Ethyl)] molecules. ((i) (-1+x, y, z) and (ii) (-1/2+x, 1-y, 1/2-z))

Table 5.4 : Hydrogen bonds for [$PtCl_2$(PNP-Ethyl)] (6) (Å and °).

D-H...A	d(D-H)	d(H...A)	D(D...A)	<(DHA)
C1-H1B...Cl2(i)	0.99	2.66	3.383(4)	130.4
C33-H33...Cl2(ii)	0.95	2.72	3.594(6)	152.9

Symmetry transformations used to generate equivalent atoms:
(i) (-1+x, y, z), (ii) (-1/2+x, 1-y, 1/2-z)

Intermolecular C-H···Cl hydrogen interactions exists between the [$PtCl_2$(PNP-Ethyl)] complexes, (see **Figure 5.3**) and these hydrogen bonds and angles are given in **Table 5.4**. The H-bond intermolecular interactions appear to be the dominant factor in the packing pattern of the [$PtCl_2$(PNP-Ethyl)] complex as seen in **Figure 5.4**. The molecules are packed in a head-to-tail fashion in vertical layers across the ac plane, with each layer pointing in the opposite direction relative to one another.

Complete supplementary data of the title compound is given in Appendix B, Table B1-5.

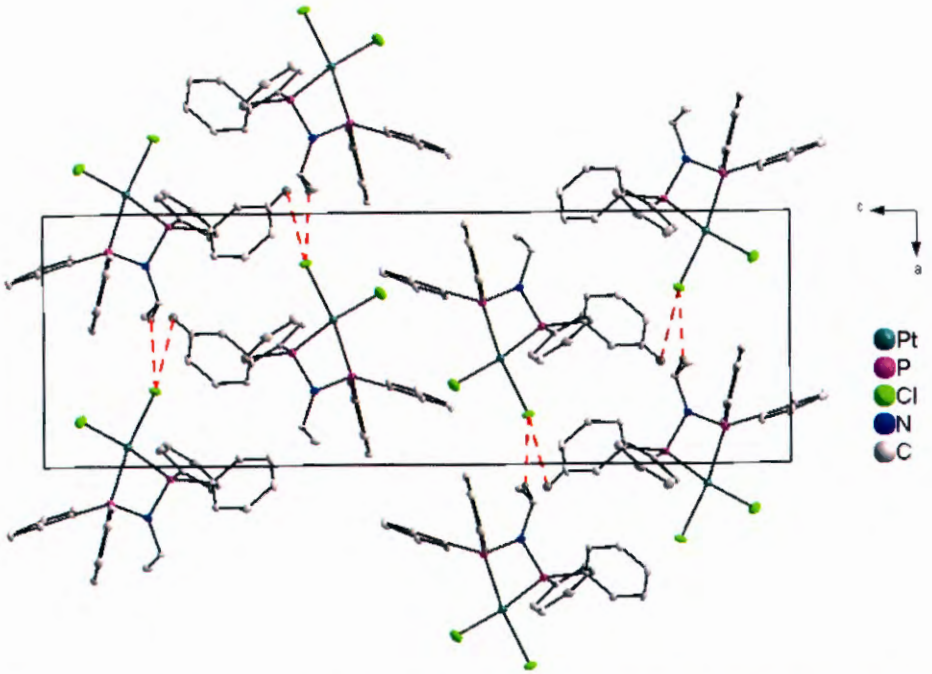

Figure 5.4: Perspective view of the unit cell of [$PtCl_2$(PNP-Ethyl)] (6) along the b-axis. H-atoms were omitted for clarity. Only applicable H atoms with relevance to the H-bond interactions are indicated. The red fragmented lines indicate the intermolecular hydrogen interactions between the [$PtCl_2$(PNP-Ethyl)] molecules.

5.2.2 Dichlorido-bis(diphenylphosphino)-*n*-propylamine-platinum(II) (7)

The title compound, [$PtCl_2$(PNP-*n*-Prop)] (7), (see **Figure 5.5**) crystallizes in a monoclinic crystal system in the $P2_1/n$ space group with 4 molecules per unit cell.

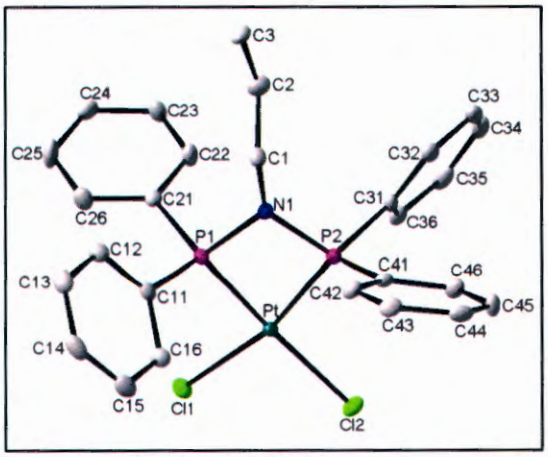

Figure 5.5: Graphical representation of [$PtCl_2$(PNP-*n*-Prop)] (7) at 50% probability. (H-atoms were omitted for clarity).

Table 5.5: Selected geometric parameters (Å, °) for [$PtCl_2$(PNP-*n*-Prop)] (7).

Atoms	Bond length (Å)	Atoms	Bond angle (°)
Pt – P1	2.193(1)	P1 – Pt – P2	72.4(1)
Pt – P2	2.602(1)	Cl1 – Pt – Cl2	92.7(1)
Pt – Cl1	2.346(1)	P1 – N1 – P2	100.1(1)
Pt – Cl2	2.353(1)	C1 – N1 – P1	126.4(2)
N1 – C1	1.484(3)	C1 – N1 – P2	132.5(2)
N1 – P1	1.699(2)	N1 – P1 – C11	108.5(1)
N1 – P2	1.695(2)	N1 – P1 – C21	110.3(1)
P1 – C11	1.804(3)	N1 – P2 – C31	112.0(1)
P1 – C21	1.804(3)	N1 – P2 – C41	107.4(1)
P2 – C31	1.810(3)	C11 – P1 – C21	110.3(1)
P2 – C41	1.804(3)	C31 – P2 – C41	103.5(1)

The bond angles P1-Pt-P2, P1-N1-P2 and Cl1-Pt-Cl2 for [$PtCl_2$(PNP-*n*-Prop)] are 72.4(2), 100.1(1) and 92.7(2) ° respectively. The Pt-Cl bonds are of the expected lengths in these type of complexes.[3, 4, 5, 6, 7]

Table 5.6: Selected torsion angles (°) for [$PtCl_2$(PNP-*n*-Prop)] (7).

Atoms	Torsion angle (°)
Pt – P1 – C11 – C12	-178.1(2)
Pt – P1 – C21 – C22	-60.1(2)
Pt – P2 – C31 – C32	176.6(2)
Pt – P2 – C41 – C42	-76.7(2)

The phenyl rings are orientated in a "fan-like" manner as illustrated by the torsion angles Pt-PP1-C11-C12 (-178.1(2) °) and Pt-P2-C31-C32 (176.6(2) °) (see **Table 5.6**) and as seen in **Figure 5.5**. A relatively small space is occupied by the propyl moiety, creating enough space for the phenyl rings to arrange in this manner. The space which is occupied by the propyl substituent and the orientation of the phenyl rings are illustrated

in **Figure 5.6**. The orientation of the phenyl rings for this complex will be discussed in §5.3.3.

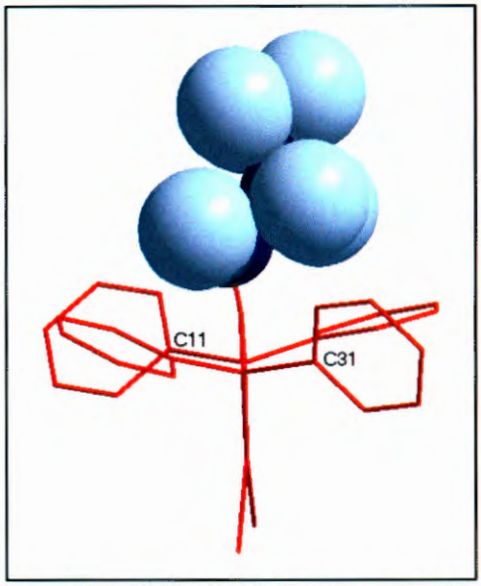

Figure 5.6: Graphical representation of [$PtCl_2$(PNP-*n*-Prop)] (7) using space-filling and stick-wire representation of the atoms (light blue spheres = hydogen atoms, dark blue spheres = carbon atoms).

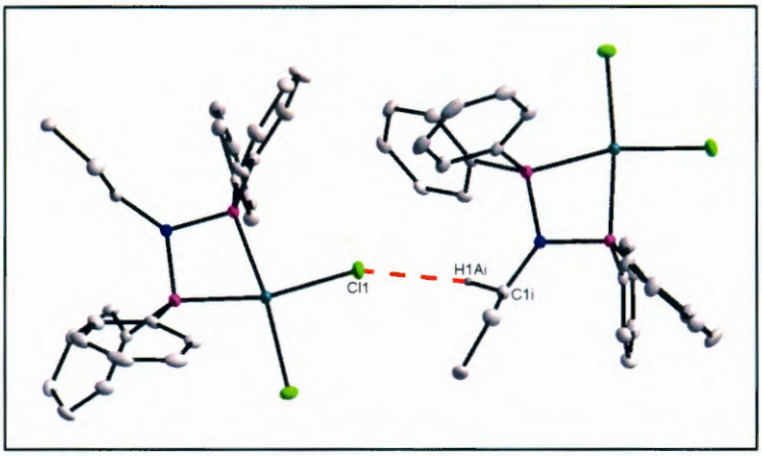

Figure 5.7: Graphical representation of the intermolecular H-bond interactions for [$PtCl_2$(PNP-*n*-Prop)] (7). Only applicable H atoms with relevance to the H-bond interactions are indicated. The red fragmented lines indicate the intermolecular hydrogen bonding between the [$PtCl_2$(PNP-*n*-Prop)] molecules. ((i) (1/2+x, 1/2-y, -1/2+z))

Table 5.7: Hydrogen interaction for [$PtCl_2$(PNP-*n*-Prop)] (Å and °).

D-H...A	d(D-H)	d(H...A)	D(D...A)	<(DHA)
C1-H1A...Cl1(i)	0.99	2.64	3.512(3)	147.1

Symmetry transformations used to generate equivalent atoms:

(i) (1/2+x, 1/2-y, -1/2+z)

Intermolecular C-H···Cl hydrogen interactions exists in the solid state of the [$PtCl_2$(PNP-*n*-Prop)] complex (see **Figure 5.7**). The hydrogen bonding interactions is given in **Table 5.7**. The molecules are packed in horizontal layers across the ac plane in a staggered head-to-tail fashion (see **Figure 5.8**). The packing pattern appears to be significantly influenced by the H-bond interactions.

Complete supplementary data of the title compound is given in Appendix B, Table B6-10.

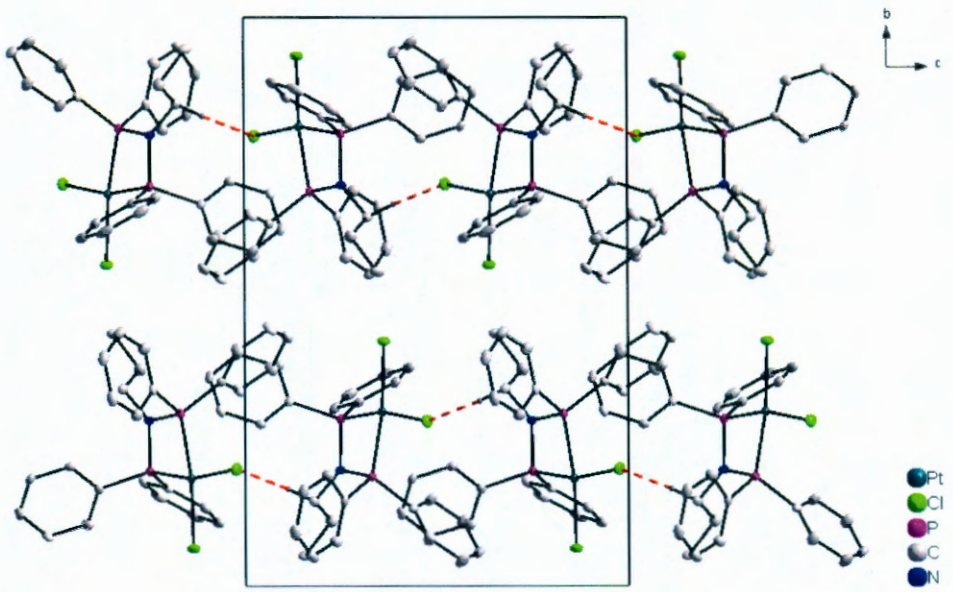

Figure 5.8: Perspective view of the unit cell of [$PtCl_2$(PNP-*n*-Prop)] (7) along the a-axis. H-atoms were omitted for clarity. Only applicable H atoms with relevance to the H-bond interactions are indicated. The red fragmented lines indicate the intermolecular hydrogen bonding between the [$PtCl_2$(PNP-*n*-Prop)] molecules.

5.2.3 Dichlorido-bis(diphenylphosphino)-1,2-dimethylpropylamine-platinum(II) (8)

The title compound, [$PtCl_2$(PNP-Dimprop)] (8), (see **Figure 5.9a** and **b**) crystallizes in a monoclinic crystal system in the $P2_1/n$ space group. The crystal structure has a 90% occupancy disorder for the alkyl group coordinated to the nitrogen atom with 4 molecules per unit cell.

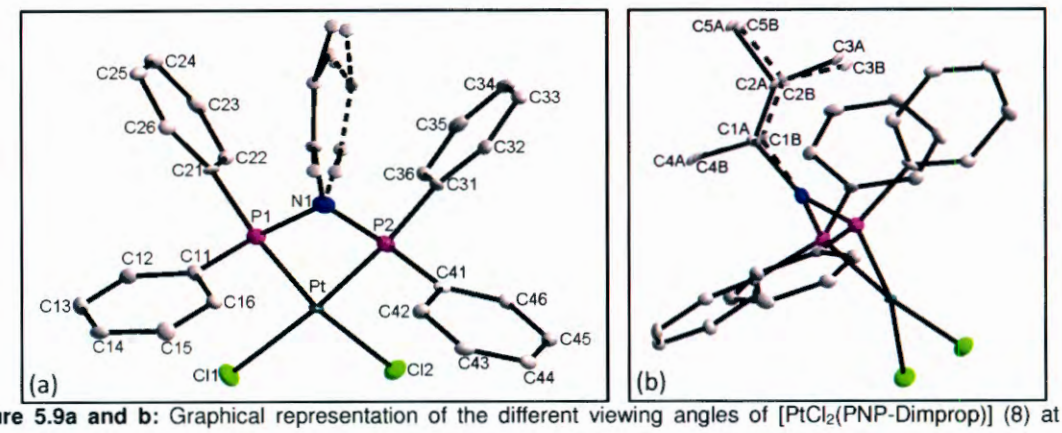

Figure 5.9a and b: Graphical representation of the different viewing angles of [$PtCl_2$(PNP-Dimprop)] (8) at 50% probability. A/B indicates the disordered carbon atoms in the 1,2-dimethylpropyl alkyl group. Disordered parts belonging together are numbered A and B respectively. (H-atoms were omitted for clarity).

Table 5.8: Selected geometric parameters (Å, °) for [$PtCl_2$(PNP-Dimprop)] (8).

Atoms	Bond length (Å)	Atoms	Bond angle (°)
Pt – P1	2.205(2)	P1 – Pt – P2	72.3(1)
Pt – P2	2.211(2)	Cl1 – Pt – Cl2	90.8(1)
Pt – Cl1	2.347(2)	P1 – N1 – P2	98.6(4)
Pt – Cl2	2.362(2)	C1A – N1 – P1	120.0(9)
N1 – C1A	1.55(2)	C1B – N1 – P1	140.7(9)
N1 – C1B	1.52(2)	C1A – N1 – P2	140.4(9)
N1 – P1	1.716(7)	C1B – N1 – P2	119.7(9)
N1 – P2	1.720(7)	N1 – P1 – C11	111.9(4)
P1 – C11	1.819(8)	N1 – P1 – C21	109.7(4)
P1 – C21	1.800(8)	N1 – P2 – C31	111.5(4)
P2 – C31	1.801(8)	N1 – P2 – C41	111.0(4)
P2 – C41	1.820(8)	C11 – P1 – C21	104.6(4)
		C31 – P2 – C41	105.1(4)

The P1-Pt-P2, P1-N1-P2 and Cl1-Pt-Cl2 angles for [$PtCl_2$(PNP-Dimprop)] (8) is 72.3(1), 98.6(4) 90.8(1) ° respectively. The Pt-Cl bonds, which range between 2.347(2) and 2.362(2) °, are of the expected lengths in these type of complexes.[3, 4, 5, 6, 7]

Table 5.9: Selected torsion angles (°) for [$PtCl_2$(PNP-Dimprop)] (8).

Atoms	Torsion angle (°)
Pt – P1 – C11 – C12	-98.4(2)
Pt – P1 – C21 – C22	-11.8(3)
Pt – P2 – C31 – C32	-174.4(2)
Pt – P2 – C41 – C42	-78.2(2)

The phenyl rings are arranged in such a manner that space is created for the 1,2-dimethylpropyl group to have degrees of freedom and consequently has a 50% occupancy disorder (see **Figure 5.9**). The phenyl rings atoms are twisted away from one another in such a manner that ring 2 (ring containing atom C21) and ring 3 (ring containing atom C31) is creating a space, almost 'basket-like' or similar to two 'hands', to accommodate the alkyl group bonded to the nitrogen atom. This orientation is further described by the torsion angles Pt-P1-C21-C22 (-11.8(3) °) and Pt-P2-C31-C32 (-174.4(2) °, see **Table 5.9**. The relatively large space occupied by the alkyl group is illustrated in **Figure 5.10** in which the alkyl group is displayed using space-filling atoms and the remaining atoms of [$PtCl_2$(PNP-Dimprop)] is displayed in stick-wire formation. The orientation of the phenyl rings is further discussed in §5.3.3.

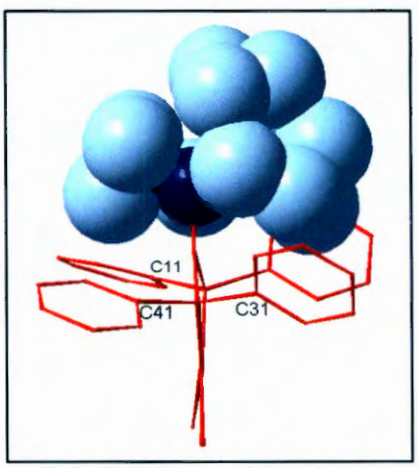

Figure 5.10: Graphical representation of [$PtCl_2$(PNP-Dimprop)] (8) using space-filling and stick-wire representation of the atoms (light blue spheres = hydrogen atoms, dark blue spheres = carbon atoms).

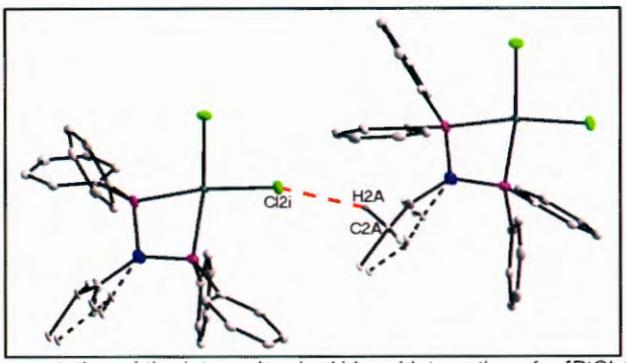

Figure 5.11: Graphical representation of the intermolecular H-bond interactions for [$PtCl_2$(PNP-Dimprop)] (8) at 50% probability. The black fragmented lines represent the 50% occupancy disorder in the 1,2-dimethylpropyl group. Only applicable H atoms with relevance to the H-bond interactions are indicated. The red fragmented lines indicate the intermolecular hydrogen bonding between the [$PtCl_2$(PNP-Dimprop)] molecules.((i) (1/2+x, 1/2-y, 1/2+z))

Table 5.10 : Hydrogen bond for [$PtCl_2$(PNP-Dimprop)] (8) (Å and °).

D-H...A	d(D-H)	d(H...A)	d(D...A)	<(DHA)
C2A-H2A...Cl2(i)	0.98	2.8	3.65(2)	145.6

Symmetry transformations used to generate equivalent atoms:
(i) (1/2+x, 1/2-y, 1/2+z)

Intermolecular C-H···Cl hydrogen inteactions exist between the molecules of the [$PtCl_2$(PNP-Dimprop)] complex (see **Figure 5.11**). The bond distances and angles for the hydrogen bonding are presented in **Table 5.10**. The molecules are packed in horizontal layers across the ab-plane in a head-to-tail fashion (see **Figure 5.12**).

Complete supplementary data of the title compound is given in Appendix B, Table B11-15.

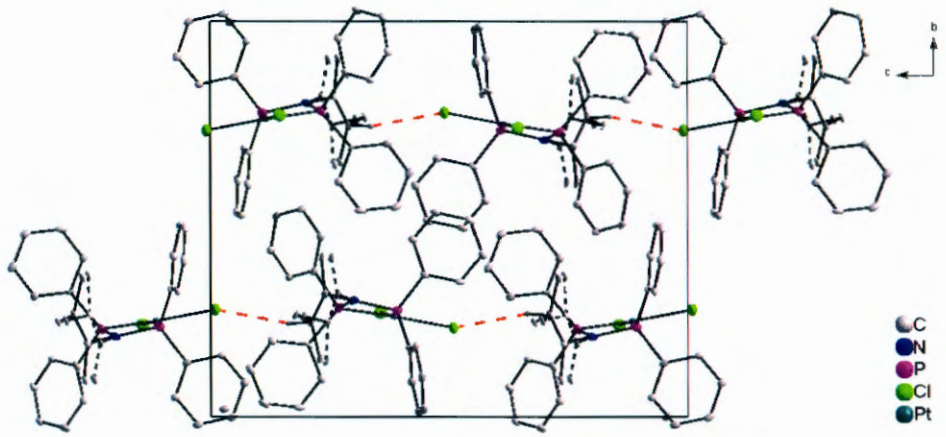

Figure 5.12: Perspective view of the unit cell of [$PtCl_2$(PNP-Dimprop)] (8) along the a-axis. H-atoms were omitted for clarity. Only applicable H atoms with relevance to the H-bond interactions are indicated. The red fragmented lines indicate the intermolecular hydrogen bonding between the [$PtCl_2$(PNP-Dimprop)] molecules. The black fragmented lines represent the 50% occupancy disorder in the 1,2-dimethylpropyl group.

5.2.4 Dichlorido-bis(diphenylphosphino)-isopentylamine-platinum(II) (9)

The title compound, [$PtCl_2$(PNP-*i*-Pent)] (9) (see **Figure 5.13**) crystallizes in an orthorhombic crystal system in the *Pnma* space group. The nitrogen bonded isopentyl moiety is 50% disordered with 4 molecules per unit cell.

It is evident from **Figure 5.13** that there is a mirror plane running through the centre of the Pt, N1, C1 and C3 atoms. The C2 atom is disordered (50% occupancy) around this mirror plane (can be split into C2A and C2B). The methyl groups on the periphery of the isopentyl moiety, C4 and C5, are also disordered as can be seen from **Figure 5.13**. C4 was split into C4A and C4B' across the mirror plane (50% occupancy), C5 was split in the same manner into C5A and C5B' (50% occupancy). The first part of the disorder of the alkyl group consists of C1, C2A, C3, C4A, C5A' and the second part of C1, C2B', C3, C4B', C5B.

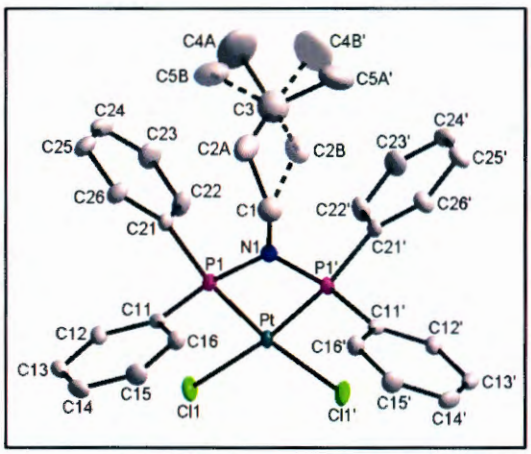

Figure 5.13: Graphical representation of[$PtCl_2$(PNP-*i*-Pent)] (9) at 50% probability. A/B indicates the disordered carbon atoms in the isopentyl alkyl group. Disordered parts belonging together are numbered A and B respectively. (H-atoms were omitted for clarity).

Table 5.11: Selected geometric parameters (Å, °) for [$PtCl_2$PNP-*i*-Pent] (9).

	Bond length (Å)		**Bond angle (°)**
Pt – P1	2.201(1)	P1 – Pt – P1'	72.2(1)
Pt – P1'	2.201(1)	Cl1 – Pt – Cl1'	91.3(1)
Pt – Cl1	2.351(1)	P1 – N1 – P1'	99.5(2)
Pt – Cl1'	2.351(1)	C1 – N1 – P1	130.2(1)
N1 – C1	1.488(7)	C1 – N1 – P1'	130.2(1)
N1 – P1	1.699(3)	N1 – P1 – C11	110.1(2)
N1 – P1'	1.699(3)	N1 – P1 – C21	111.0(2)
P1 – C11	1.800(3)	N1 – P1' – C11'	110.1(2)
P1 – C21	1.804(3)	N1 – P1' – C21'	111.0(2)
P2 – C11'	1.800(3)	C11 – P1 – C21	105.6(2)
P2 – C21'	1.804(3)	C11' – P1' – C21'	105.6(2)

The bond angles, P1-Pt-P1', P1-N1-P1' and Cl1-Pt-Cl1', are 72.2(1), 99.5(2) and 91.3(1) ° respectively for the complex. The Pt-Cl bonds are comparable to other similar complexes.[3, 4, 5, 6, 7]

Table 5.12: Selected torsion angles (°) for [$PtCl_2$(PNP-*i*-Pent)] (9).

Atoms	Torsion angle (°)
Pt– P1 – C11 – C12	-88.3(1)
Pt– P1 – C21 – C22	-15.8(2)
Pt – P1' – C11' – C12'	88.3(1)
Pt – P1'– C21' – C22'	15.8(2)

The phenyl rings 2 (ring containing C21) and ring 3 (ring containing C21') bonded to the phosphorous atoms are therefore twisted away from one another in a 'basket-like' manner to accommodate the disordered alkyl moiety (see **Figure 5.13**). The space required by the alkyl moiety is further illustrated by the space-filling and stick representation of the complex, see **Figure 5.14**. The orientations of the phenyl rings are further illustrated by the torsion angles Pt-P1-C21-C22 (-15.8(2) °) and Pt-P1'-C21'-C22' (15.8(2) °), see **Table 5.12**. The orientation of the phenyl rings are discussed in more detail in §5.3.3.

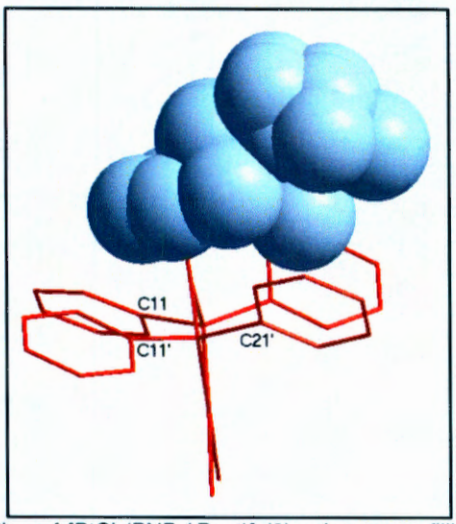

Figure 5.14: Graphical representation of [$PtCl_2$(PNP-*i*-Pent)] (9) using space-filling and stick-wire representation of the atoms (light blue spheres = hydrogen atoms, dark blue = carbon atoms.

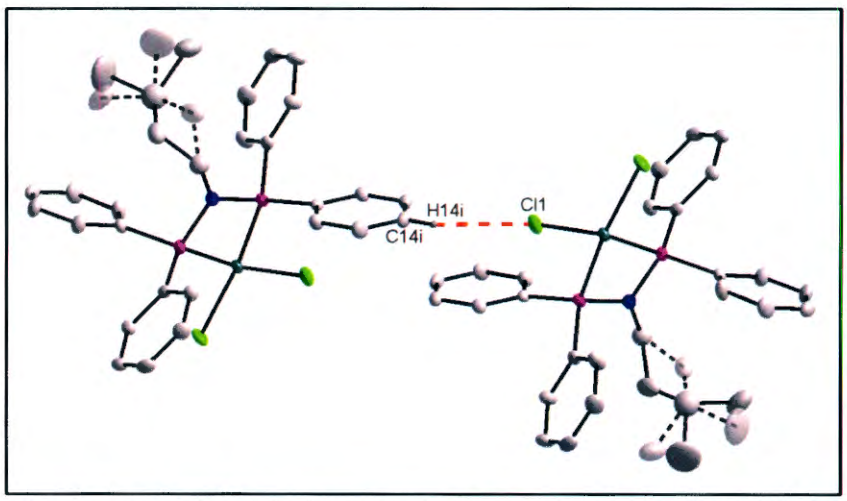

Figure 5.15: Graphical representation of the intermolecular H-bond interactions for [$PtCl_2$(PNP-*i*-Pent)] (9) at 50% probability. Only applicable H atoms with relevance to the H-bond interactions are indicated. The black fragmented lines represent the 50% occupancy disorder in the isopentyl group. The red fragmented lines indicate the intermolecular hydrogen bonding between the [$PtCl_2$(PNP-*i*-Pent)] molecules. ((i) (1-x, -y, 1-z))

Table 5.13 : Hydrogen bond for [$PtCl_2$PNP-*i*-Pent] (9) (Å and °).

D-H...A	d(D-H)	d(H...A)	D(D...A)	<(DHA)
C14-H14...Cl1(i)	0.93	2.77	3.612(4)	151.0

Symmetry transformations used to generate equivalent atoms:
(i) (1-x, -y, 1-z)

There are C-H···Cl intermolecular hydrogen interactions present for $PtCl_2$(PNP-*i*-Pent)] (see **Figure 5.15**). A list of H-bond interactions is given in **Table 5.13**. The molecules are packed in horizontal layers across the ab plane in a head-to-tail fashion (see **Figure 5.16**). The packing is clearly influenced by the hydrogen bonding interactions.

Complete supplementary data of the title compound is given in Appendix B, Table B16-20.

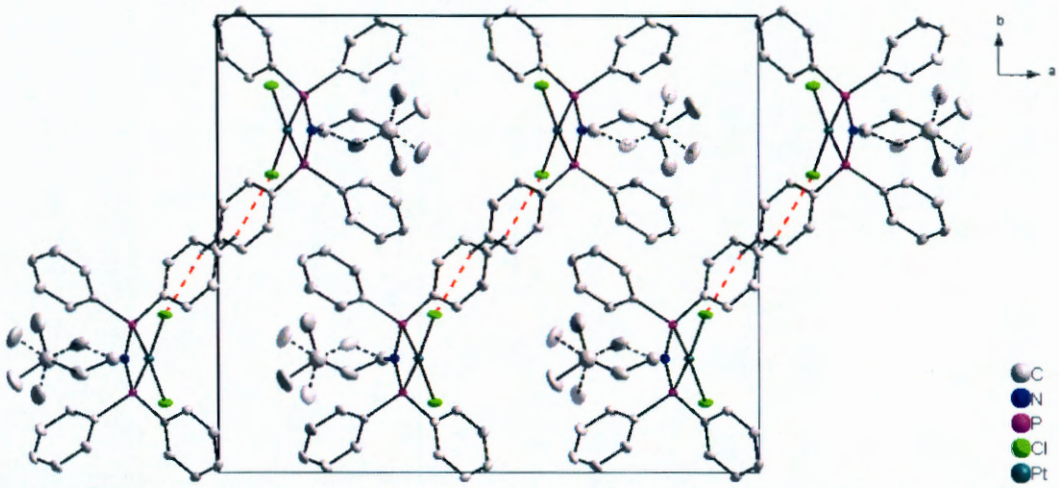

Figure 5.16: Perspective view of the unit cell of [$PtCl_2$(PNP-*i*-Pent)] (9) along the c axis. H-atoms were omitted for clarity. Only applicable H atoms with relevance to the H-bond interactions are indicated. The black fragmented lines represent the 50% occupancy disorder. The red fragmented lines indicate the intermolecular hydrogen bonding between the [$PtCl_2$(PNP-*i*-Pent)] molecules. The black fragmented lines represent the 50% occupancy disorder in the isopentyl group.

5.2.5 Dichlorido-bis(diphenylphosphino)-cyclohexylamine-platinum(II) (10)

The title compound, [$PtCl_2$(PNP-Cychex)] (10), (see **Figure 5.17**) crystallizes in a monoclinic crystal system in the $P2_1/n$ space group with 4 molecules per unit cell.

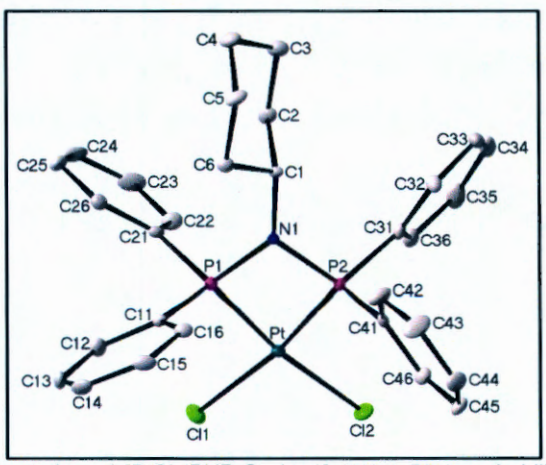

Figure 5.17: Graphical representation of [$PtCl_2$(PNP-Cychex)] (10)at 50% probability. (H-atoms were omitted for clarity).

Table 5.14: Selected geometric parameters (Å, °) for [$PtCl_2$PNP-Cychex] (10).

Atoms	Bond length (Å)	Atoms	Bond angle (°)
Pt – P1	2.214(1)	P1 – Pt – P2	71.9(1)
Pt – P2	2.200(1)	Cl1 – Pt – Cl2	91.8(1)
Pt – Cl1	2.357(7)	P1 – N1 – P2	99.3(1)
Pt – Cl2	2.361(1)	C1 – N1 – P1	132.5(2)
N1 – C1	1.489(4)	C1 – N1 – P2	127.0(2)
N1 – P1	1.697(3)	N1 – P1 – C11	110.9(1)
N1 – P2	1.704(3)	N1 – P1 – C21	111.5(1)
P1 – C11	1.801(3)	N1 – P2 – C31	110.5(1)
P1 – C21	1.799(3)	N1 – P2 – C41	109.3(1)
P2 – C31	1.800(3)	C11 – P1 – C21	106.2(1)
P2 – C41	1.808(3)	C31 – P2 – C41	105.4(1)

The P1-Pt-P2, P1-N1-P2 and Cl1-Pt-Cl2 angles of the [$PtCl_2$PNP-Cychex] is 71.9(1), 99.3(1) and 91.8(1) ° respectively (see **Table 5.14**). The Pt-Cl bonds are of the expected lengths in these type of complexes.[3, 4, 5, 6, 7]

Table 5.15: Selected torsion angles (°) for [$PtCl_2$PNP-Cychex] (10).

Atoms	Torsion angle (°)
Pt – P1 – C11 – C12	-87.6(3)
Pt – P1 – C21 – C22	-19.7(3)
Pt – P2 – C31 – C32	173.5(2)
Pt – P2 – C41 – C42	-128.0(3)

It is shown by the torsion angles, Pt-P1-C21-C22 (-19.7(3) °) and Pt-P2-C31-C32 (173.5(2) °) (see **Table 5.15**) that the phenyl rings are orientated in a 'basket-like' fashion, with ring 2 (phenyl ring containing C21) and ring 3 (phenyl ring containing C31) twisted toward each other to accommodate the sterically bulky cyclohexyl group, this is further illustrated by the space-filling and stick-wire representation of the complex (see

Figure 5.18). The torsion angles and the orientation of the phenyl rings are further discussed in §5.3.3.

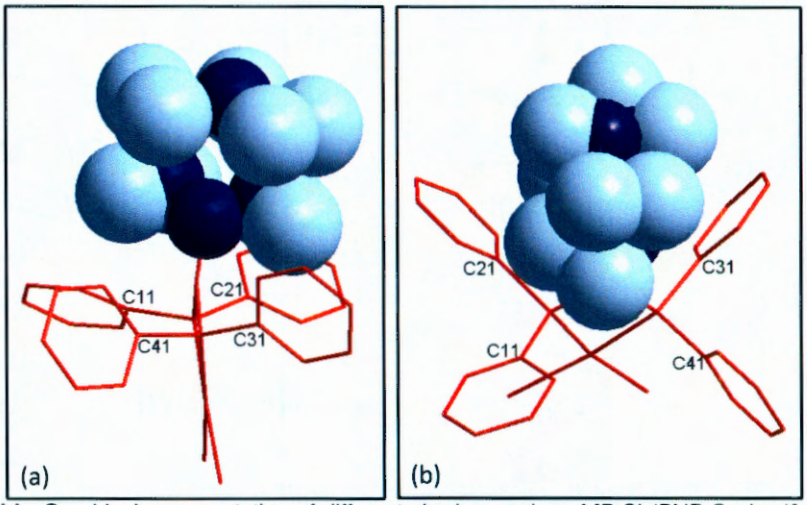

Figure 5.18a and b: Graphical representation of different viewing angles of [$PtCl_2$(PNP-Cychex)] (10) using space-filling and stick-wire representation of the atoms (light blue spheres = hydrogen atoms, dark blue spheres = carbon atoms).

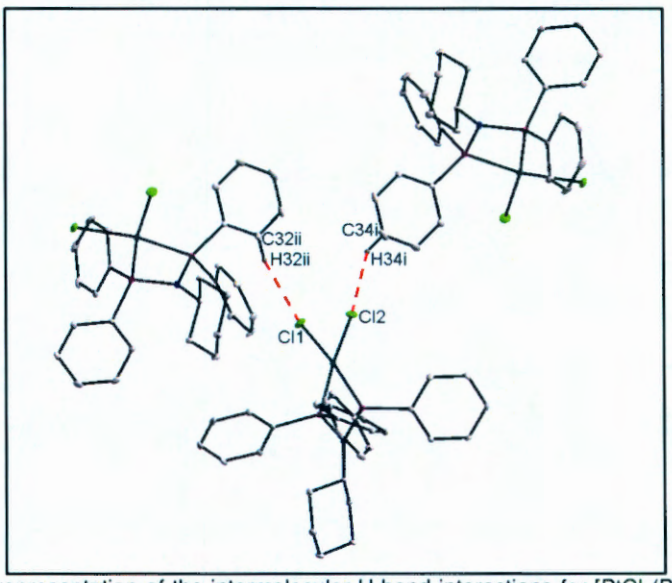

Figure 5.19: Graphical representation of the intermolecular H-bond interactions for [$PtCl_2$(PNP-Cychex)] (10). Only applicable H atoms with relevance to the H-bond interactions are indicated. The red fragmented lines indicate the intermolecular hydrogen bonding between the [$PtCl_2$(PNP- Cychex)] molecules. ((i) (-1/2+x, 1/2-y, -1/2+z) and (ii) (1/2-x, -1/2+y, 3/2-z))

Table 5.16 : Hydrogen bonds for [$PtCl_2$PNP-Cychex] (10) (Å and °).

D-H...A	d(D-H)	d(H...A)	D(D...A)	<(DHA)
C32-H32...Cl1(i)	0.95	2.73	3.619(3)	156.0
C34-H34...Cl2(ii)	0.95	2.75	3.663(3)	152.1

Symmetry transformations used to generate equivalent atoms:

(i) (-1/2+x, 1/2-y, -1/2+z), (ii) (1/2-x, -1/2+y, 3/2-z)

Intermolecular C-H···Cl hydrogen interactions are present in the [$PtCl_2$PNP-Cychex] complex (see **Figure 5.19**). The bond distances and angles for the hydrogen bonding are presented in **Table 5.16**. The molecules are packed in vertical layers across the bc plane in a staggered head-to-tail fashion (see **Figure 5.20**). Once again the packing pattern appears to be determined by the H-bond interactions.

Complete supplementary data of the title compound is given in Appendix B, Table B21-25.

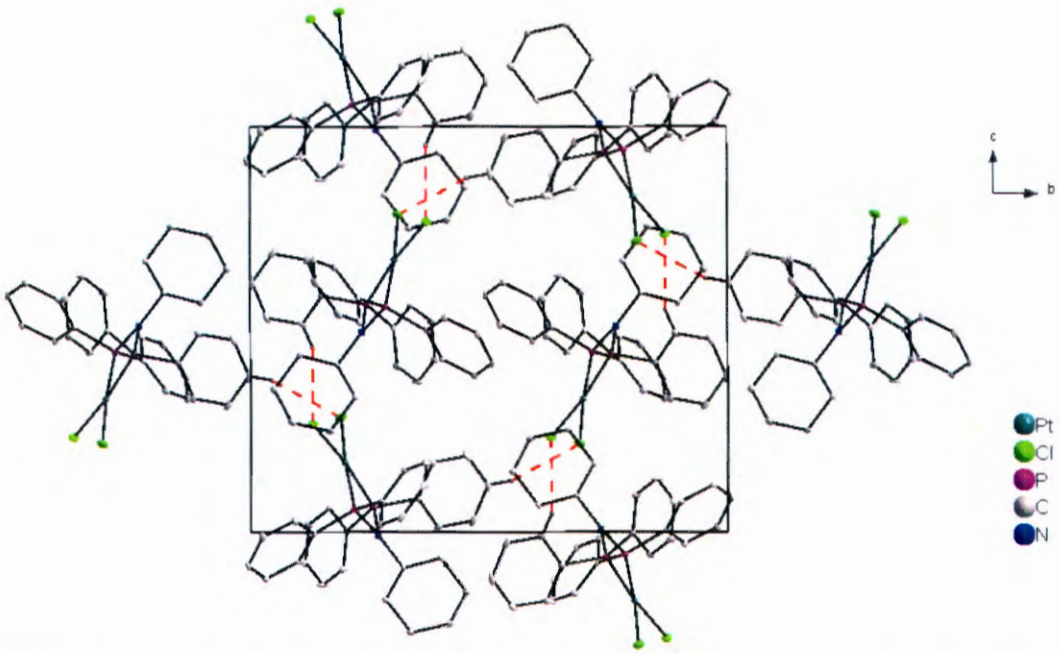

Figure 5.20: Perspective view of the unit cell of [$PtCl_2$(PNP-Cychex)] (10) along the a axis. H-atoms were omitted for clarity. Only applicable H atoms with relevance to the H-bond interactions are indicated. The red fragmented lines indicate the intermolecular hydrogen bonding between the [$PtCl_2$(PNP-Cychex)] molecules.

Table 5.17: General crystal data for the following compounds, $[PdCl_2(PNP\text{-}i\text{-}Prop)]$ (11), $[PdCl_2(PNP\text{-}Dimprop)]$ (12), $[PdCl_2(PNP\text{-}n\text{-}Prop)]$ (13), $[PdCl_2(PNP\text{-}i\text{-}Pent)]$ (14), $[PdCl_2(PNP\text{-}n\text{-}Butyl)]$ (15).

Identification code	$[PdCl_2(PNP\text{-}i\text{-}Prop)]$ (11)	$[PdCl_2(PNP\text{-}Dimprop)]$ (12)	$[PdCl_2(PNP\text{-}n\text{-}Prop)]$ (13)	$[PdCl_2(PNP\text{-}i\text{-}Pent)$ (14)	$[PdCl_2(PNP\text{-}n\text{-}Butyl)]$ (15)
Empirical formula	$PdNP_2Cl_2C_{27}H_{27}$	$PdNP_2Cl_2C_{29}H_{31}$	$PdNP_2Cl_2C_{27}H_{27}$	$PdNP_2Cl_2C_{29}H_{31}$	$PdNP_2Cl_2C_{28}H_{29}$
Formula weight	604.74	632.79	604.74	632.79	618.76
Crystal system, space group	Orthorhombic, *Pbca*	Monoclinic, *P121/n*	Monoclinic, *C12/c*	Orthorhombic, *Pnma*	Triclinic, $P\bar{1}$
Unit cell dimensions:					
a(Å)	16.631(5)	10.062(5)	10.797(5)	20.654(5)	11.290(5)
b(Å)	14.856(5)	14.922(5)	16.583(5)	17.441(5)	13.851(6)
c(Å)	20.258(5)	18.126(5)	14.888(5)	8.264(5)	17.633(8)
α (°)	90.000(5)	90.000(5)	90.000(5)	90.000(5)	81.93(2)
β (°)	90.000(5)	94.877(5)	95.093(5)	90.000(5)	84.77(2)
γ (°)	90.000(5)	90.000(5)	90.000(5)	90.000(5)	78.61(2)
Volume ($Å^3$)	5005(3)	2712(2)	2655(2)	2977(2)	2671(2)
Z	8	4	4	8	4
Calculated density (Mg/m^3)	1.605	1.550	1.513	1.412	1.539
Absorption coefficient (mm^{-1})	1.100	1.019	1.037	0.928	1.033
F(000)	2448	1288	1224	1288	1256
Crystal size (mm)	0.04 x 0.18 x 0.30	0.05 x 0.12 x 0.22	0.02 x 0.11 x 0.38	0.07 x 0.15 x 0.19	0.08 x 0.20 x 0.26
Θ range / completeness of collection (°)	2.01 to 28.30/99.9	2.26 to 33.2/91.3	2.26 to 33.11/92.0	1.97 to 28.27/99.7	1.17 to 28.61/94.9
	-22<=h<=22	-14<=h<=15	-16<=h<=16	-27<=h<=27	-14<=h<=15
Limiting indices	-19<=k<=18	-14<=k<=22	-25<=k<=25	-22<=k<=23	-18<=k<=14
	27<=l<=27	-26<=l<=27	-22<=l<=9	-9<=l<=10	23<=l<=23
Reflections collected / unique / observed (I>2σ(I))	66201/6212	27460 / 9491	13541 / 4647	23800 / 3790	36127 / 12996
	[R(int) = 0.0503]	[R(int) = 0.0835]	[R(int) = 0.0727]	[R(int) = 0.0499]	[R(int) = 0.2201]
Data / restraints / parameters	6212 / 0 / 298	9491 / 0 / 303	4647 / 0 / 152	3790 / 0 / 160	12996 / 0 / 338
Goodness of fit on F^2	1.057	0.953	0.836	1.103	1.027
Final R indices (I>2σ(I))	R1 = 0.0238	R1 = 0.1020	R1 = 0.0647	R1 = 0.0588	R1 = 0.1263
	wR2 = 0.0543	wR2 = 0.2544	wR2 = 0.1513	wR2 = 0.1748	wR2 = 0.2935
R indices(all data)	R1 = 0.0324,	R1 = 0.1885	R1 = 0.1580	R1 = 0.0724	R1 = 0.2896
	wR2 = 0.0591	wR2 = 0.3008	wR2 = 0.1831	wR2 = 0.1912	wR2 = 0.3711
$\Delta\rho_{min}$, $\Delta\rho_{max}$ ($e.Å^{-3}$)	0.501 and -0.437	6.053 and -1.096	2.577 and -1.578	4.373 and -2.136	2.185 and -1.604

5.2.6 Dichlorido-bis(diphenylphosphino)-isopropylamine-palladium(II) (11)

The title compound, [$PdCl_2$(PNP-i-Prop)] (11) (see **Figure 5.21**) crystallizes in an orthorombic crystal system in the *Pbca* space group with 8 molecules per unit cell.

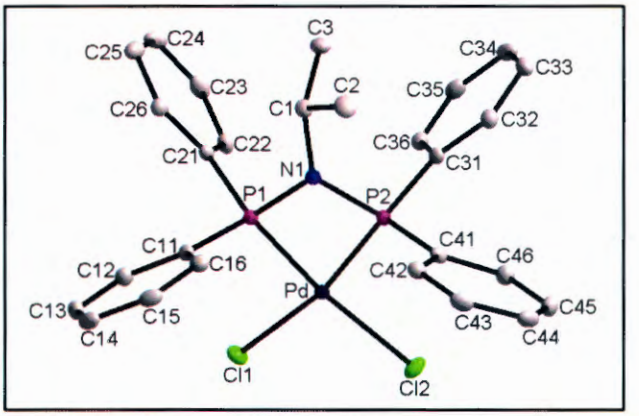

Figure 5.21: Graphical representation of [$PdCl_2$(PNP-*i*-Prop)] (11) at 50% probability. (H-atoms were omitted for clarity).

Table 5.18: Selected geometric parameters (Å, °) for [$PdCl_2$PNP-*i*-Prop] (11).

Atoms	Bond length (Å)	Atoms	Bond angle (°)
Pd – P1	2.207(1)	P1 – Pd – P2	71.3(1)
Pd – P2	2.219(1)	Cl1 – Pd – Cl2	95.6(1)
Pd – Cl1	2.358(1)	P1 – N1 – P2	98.6(1)
Pd – Cl2	2.371(1)	C1 – N1 – P1	124.5(1)
N1 – C1	1.504(2)	C1 – N1 – P2	132.7(1)
N1 – P1	1.800(2)	N1 – P1 – C11	109.3(1)
N1 – P2	1.704(2)	N1 – P1 – C21	108.6(1)
P1 – C11	1.793(2)	N1 – P2 – C31	112.9(1)
P1 – C21	1.799(2)	N1 – P2 – C41	110.1(1)
P2 – C31	1.801(2)	C11 – P1 – C21	106.1(1)
P2 – C41	1.795(2)	C31 – P2 – C41	105.7(1)

The [$PdCl_2$PNP-*i*-Prop] complex has P1-Pt-P2, P1-N1-P2 and Cl1-Pt-Cl2 angles of 71.3(1), 95.6(1) and 100.1(1) ° respectively. The Pd-Cl bonds, which range between 2.358(1) and 2.371(1) ° are of the expected lengths in these type of complexes.[2, 5, 6, 7]

Table 5.19: Selected torsion angles (°) for [$PdCl_2$PNP-*i*-Prop] (11).

Atoms	Torsion angle (°)
Pd– P1 – C11 – C12	-85.2(1)
Pd– P1 – C21 – C22	-9.6(1)
Pd – P2 – C31 – C32	-163.6(1)
Pd – P2 – C41 – C42	-87.3

The phenyl rings bonded to the phosphorous atoms are twisted away from one another in such a manner that ring 2 (ring containing atom C21) and ring 3 (ring containing atom C31) is creating a space, almost 'basket-like', to accommodate the alkyl group bonded to the nitrogen atom (see **Figure 5.21**). The space utilised by the isopropyl moiety is illustrated by the space-filling and stick-wire representation of [$PdCl_2$(PNP-*i*-Prop)], see **Figure 5.22**. The orientations of the phenyl rings is further demonstrated by the torsion angles Pd-P1-C21-C22 (-9.6(1) °) and Pd-P2-C31-C31 (-163.6(1) °) (see **Table 5.19**). The rings 1 and 4 are twisted towards each other to create space for the alkyl group.

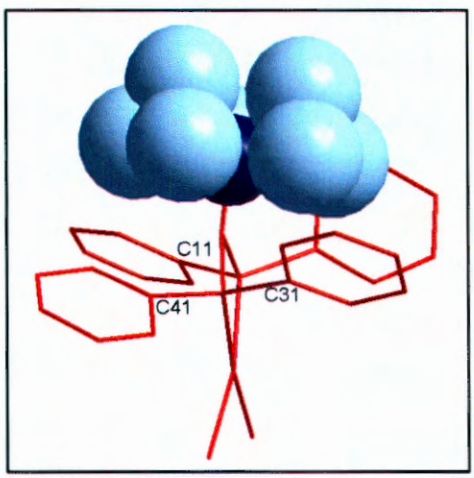

Figure 5.22: Graphical representation of [$PdCl_2$(PNP-*i*-Prop)] (11) using space-filling and stick-wire representation of the atoms (light blue spheres = hydrogen atoms, dark blue spheres = carbon atoms).

The [$PdCl_2$PNP-*i*-Prop] molecules pack in horizontal layers across the ac plane (see **Figure 5.23**). There are no classical intermolecular hydrogen bonding interactions for this complex.

Complete supplementary data of the title compound is given in Appendix B, Table B26-30.

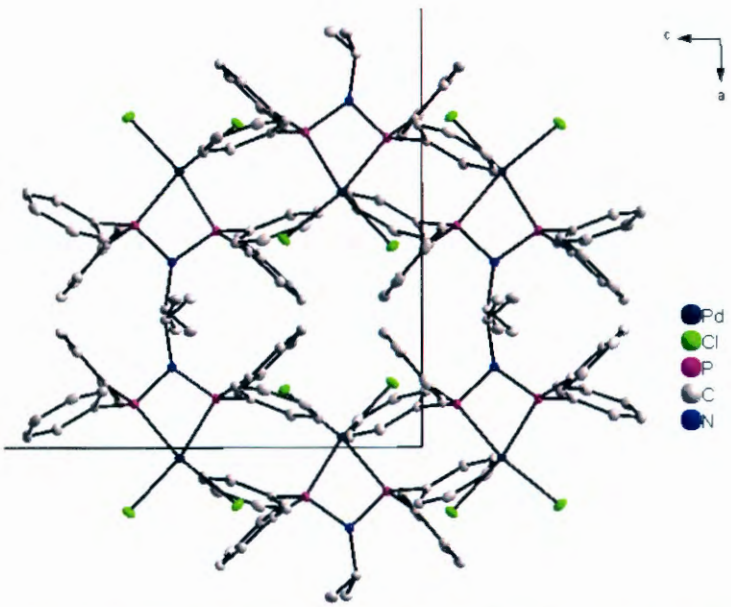

Figure 5.23: Perspective view of a fraction of the unit cell of [$PdCl_2$(PNP-*i*-Prop)] (11) along the b axis. H-atoms were omitted for clarity. Only applicable H atoms with relevance to the H-bond interactions are indicated. The red fragmented lines indicate the intermolecular hydrogen interaction between the [$PdCl_2$(PNP-*i*-Prop)] molecules.

5.2.7 Dichlorido-bis(diphenylphosphino)-1,2-dimethylpropylamine-palladium(II) (12)

The title complex, [$PdCl_2$(PNP-Dimprop)] (12), (see **Figure 5.24a** and **b**), crystallizes in a monoclinic crystal system in the $P2_1/n$ space group with 4 molecules per unit cell.

A 50% disorder on the N-substituent is present in the structure and the second carbon atom of the alkyl moiety (bonded to C1 and C3) occupies two positions, C2A and C2B (50% occupancy each).

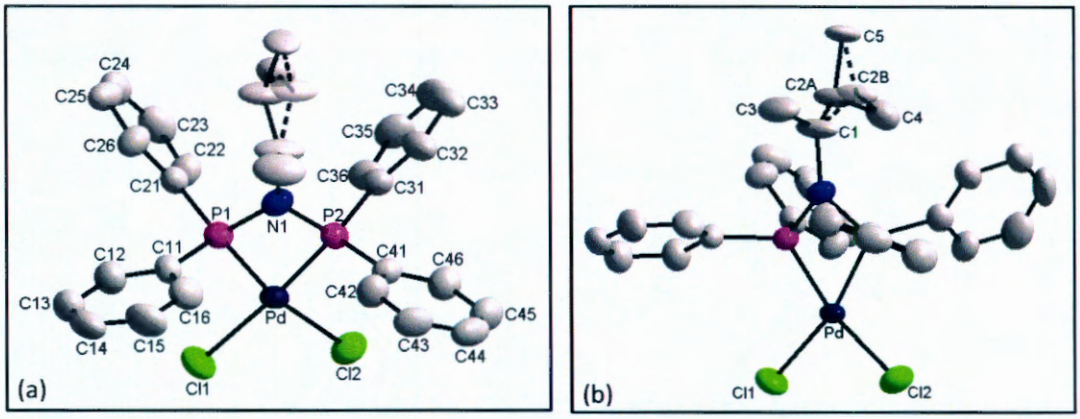

Figure 5.24a and b: Graphical representation of the different viewing angles of [$PdCl_2$(PNP-Dimprop)] (12) at 50% probability. A/B indicates the disordered carbon atoms in the 1,2-dimethylpropyl alkyl group. Disordered parts belonging together are numbered A and B respectively. (H-atoms were omitted for clarity).

Table 5.20: Selected geometric parameters (Å, °) for [$PdCl_2$PNP-Dimprop] (12).

Atoms	Bond length (Å)	Atoms	Bond angle (°)
Pd – P1	2.216(2)	P1 – Pd – P2	71.6(1)
Pd – P2	2.221(2)	Cl1 – Pd – Cl2	94.0(1)
Pd – Cl1	2.338(2)	P1 – N1 – P2	99.7(3)
Pd – Cl2	2.357(2)	C1 – N1 – P1	130.1(6)
N1 – C1	1.530(9)	C1 – N1 – P2	129.4(6)
N1 – P1	1.691(6)	N1 – P1 – C11	111.8(3)
N1 – P2	1.706(6)	N1 – P1 – C21	111.2(3)
P1 – C11	1.805(7)	N1 – P2 – C31	112.0(3)
P1 – C21	1.813(8)	N1 – P2 – C41	110.8(3)
P2 – C31	1.790(8)	C11 – P1 – C21	105.3(4)
P2 – C41	1.803(7)	C31 – P2 – C41	105.0(4)

The P1-Pt-P2, P1-N1-P2 and Cl1-Pt-Cl2 angles of the complex is 71.6(1), 99.7(3) and 94.0(1) ° respectively. The Pd-Cl bonds, which range from 2.338(2) to 2.357(2) °, are of the expected lengths in these type of complexes.[2, 5, 6, 7]

Table 5.21: Selected torsion angles (°) for [$PdCl_2$PNP-Dimprop] (12).

Atoms	Torsion angle (°)
Pd– P1 – C11 – C12	-95.7(6)
Pd– P1 – C21 – C22	-13.5(7)
Pd – P2 – C31 – C32	-174.6(6)
Pd – P2 – C41 – C42	-79.6(7)

The phenyl rings 2 (ring containing C21) and 3 (ring containing C31) is twisted in such a manner that the basket-like arrangement is adopted to accommodate the 50% disordered alkyl moiety. **Figure 5.25** illustrates the space required by the alkyl group in the space-filling and stick-wire representation of [$PdCl_2$(PNP-Dimprop). This arrangement is similar to that of [$PdCl_2$(PNP-Dimprop)] (see §5.2.2). The torsion angles Pd-P1-C21-C22 (-13.5(7) °) and Pd-P2-C31-C32 (-174.6(6) °) further describes the orientation of the phenyl rings (see **Table 5.21**). The orientations of the phenyl rings are further described and discussed in §5.3.3.

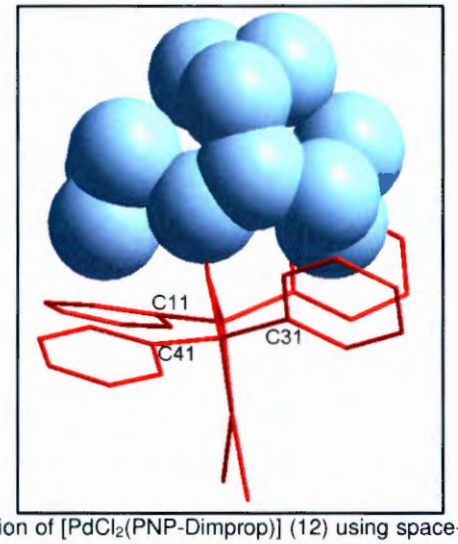

Figure 5.25: Graphical representation of [$PdCl_2$(PNP-Dimprop)] (12) using space-filling and stick-wire representation of the atoms (light and dark blue sphere = hydrogen and carbon atoms respectively).

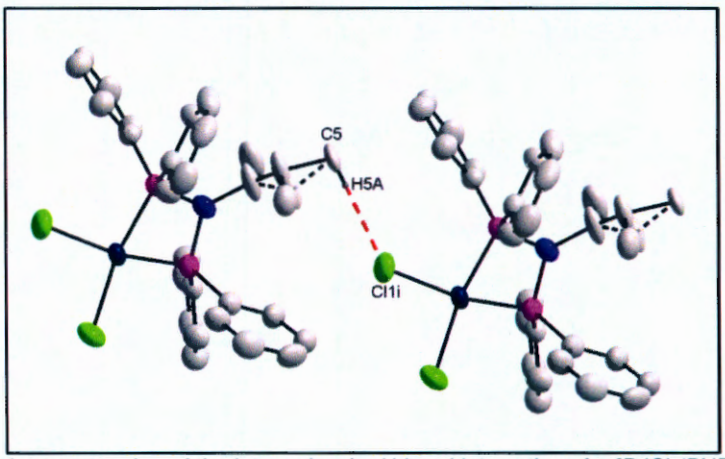

Figure 5.26: Graphical representation of the intermolecular H-bond interactions for [$PdCl_2$(PNP-Dimprop)] (12). The black fragmented lines indicate the 50% occupancy disorder in the 1,2-dimethylpropyl group. The red fragmented lines indicate the intermolecular hydrogen bonding. Only applicable H atoms with relevance to the H-bond interactions are indicated. ((i) (1+x, y, z))

Table 5.22: Hydrogen bond for [$PdCl_2$PNP-Dimprop] (12) (Å and °).

D-H...A	d(D-H)	d(H...A)	D(D...A)	<(DHA)
C5-H5B...Cl1(i)	0.96	2.76	3.715(9)	172.0

Symmetry transformations used to generate equivalent atoms:
(i) (1+x, y, z)

Intermolecular C-H···Cl hydrogen bonding interactions is present between (see **Figure 5.26**). The hydrogen bond distances and angles are given in **Table 5.22**. The molecules are packed in vertical layers across the ab-plane with hydrogen bonding linking the vertical layers (see **Figure 5.27**).

Complete supplementary data of the title compound is given in Appendix B, Table B31-35.

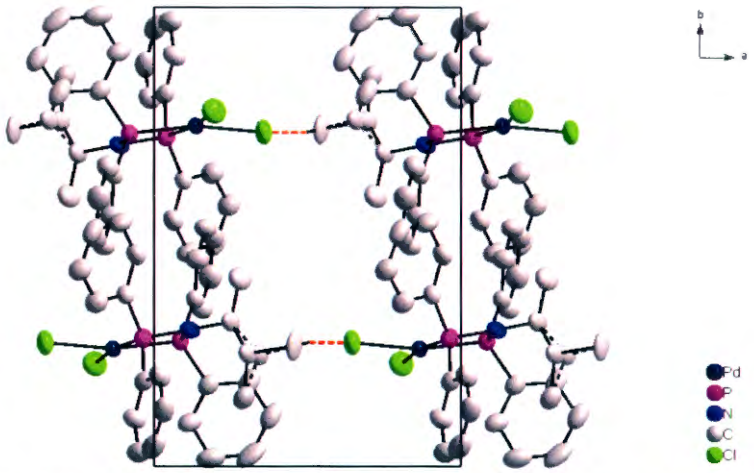

Figure 5.27: Perspective view of the unit cell of [$PdCl_2$(PNP-Dimprop)] (12) along the c axis. H-atoms were omitted for clarity. Only applicable H atoms with relevance to the H-bond interactions are indicated. The red fragmented lines indicate the intermolecular hydrogen interactions between the [$PdCl_2$(PNP-Dimprop)] molecules. The black fragmented lines indicate the 50% occupancy disorder in the 1,2-dimethylpropyl group.

5.2.8 Dichlorido-bis(diphenylphosphino)-*n*-propylamine-palladium(II) (13)

The title the complex, [$PdCl_2$(PNP-*n*-Prop)] (13), crystallizes in a monoclinic crystal system in a *P2/c* space group with 4 molecules per unit cell.

The complex lies on a two-fold rotation axis as can be seen in **Figure 5.28a** and **b**. The nitrogen coordinated carbon atom is disordered and was split into C1A, C1B, C1A', C1B' each with 25% occupancy. The carbon atom bonded to C1 is disordered (50% occupancy) around this two fold axis (occupies two positions, C2A and C2B'). The C3 atom lies on the two-fold axis and was therefore split into C3A, C3B and C3A'. The C3B atom has a 50% occupancy and C3A and C3A' each has a 25% occupancy. The propyl moiety is consequently disordered four-fold (part 1: C1A, C2A, C3A; part 2: C1B, C2, C3B; part 3: C1A',C2B', C3A'; part 4: C1B', C2B', C3B). No hydrogen atoms were placed on the disordererd alkyl moiety, due to the uncertainty of the hydrogen atom positions.

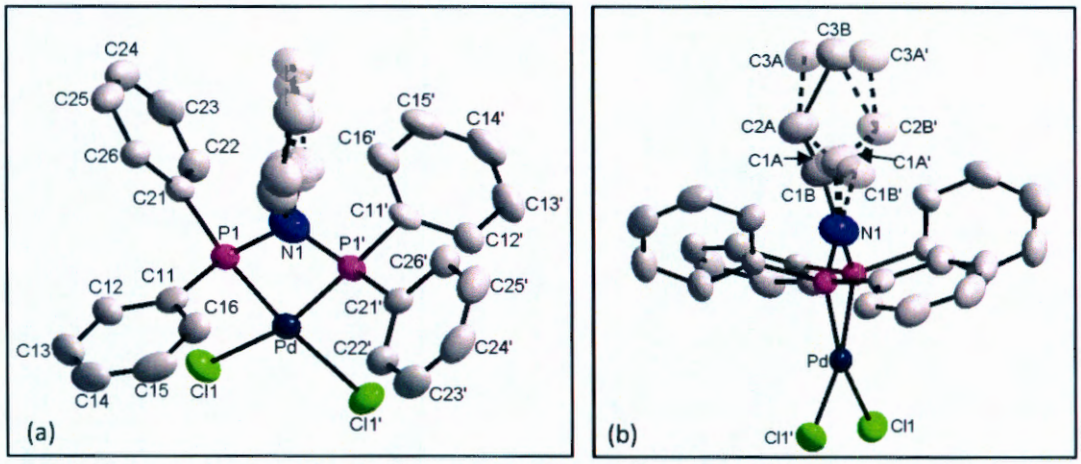

Figure 5.28a and b: Graphical representation of the different viewing angles of [Bis(diphenylphosphino)-*n*-propylamine]dichloridopalladium(II) [$PdCl_2$(PNP-*n*-Prop)] (12). A/B indicates the disordered carbon atoms in the propyl moiety. Disordered parts belonging together are numbered A and B respectively. The atoms generated by the 2-fold axis symmetry operation is labeled with an accent. (H-atoms were omitted for clarity).

Table 5.23: Selected geometric parameters (Å, °) for [$PdCl_2$PNP-*n*-Prop] (13).

Atoms	Bond length (Å)	Atoms	Bond angle (°)
Pd – P1	2.223(2)	P1 – Pd – P1'	71.5(1)
Pd – P1'	2.223(2)	Cl1 – Pd – Cl1'	94.9(1)
Pd – Cl1	2.347(2)	P1 – N1 – P1'	100.8(5)
Pd – Cl1'	2.347(2)	N1 – P1 – C11	111.4(2)
N1 – C1A	1.40(3)	N1 – P1 – C11'	111.4(2)
N1 – C1A'	1.40(3)	N1 – P1' – C21	106.6(2)
N1 – C1B	1.47(3)	N1 – P1' – C21'	106.6(2)
N1 – C1B'	1.47(3)	C11 – P1 – C21	107.5(2)
N1 – P1	1.686(6)	C11' – P1' – C21'	107.5(2)
N1 – P1'	1.686(6)		
P1 – C11	1.797(5)		
P1 – C11'	1.797(5)		
P2 – C21	1.792(5)		
P2 – C21'	1.792(5)		

The bond angles, P1-Pd-P1', P1-N1-P1' and Cl1-Pd-Cl1', is 71.7(2), 100.8(5) and 94.9(1) ° respectively. The Pd-Cl bonds are of the expected lengths in these type of complexes.[2, 5, 6, 7]

Table 5.24: Selected torsion angles (°) for [$PdCl_2$PNP-*n*-Prop] (13).

Atoms	Torsion angle (°)
Pd– P1 – C11 – C12	-97.0(4)
Pd– P1 – C21 – C22	-17.4(5)
Pd – P1' – C11' – C12'	-97.0(4)
Pd – P1' – C21' – C22'	-17.4(5)

The phosphorous-bonded phenyl rings are arranged in a 'fan-like' manner, but with the rings orientated more horizontally relative to the disordered propyl moiety (see **Figure 5.28**), which creates enough space for the propyl substituent to be able to have enough degrees of freedom and consequently be disordered. The torsion angles Pd-P1-C11-C12 (-97.0(4) °) and Pd-P1'-C11'-C12' (97.0(4) °) (see **Table 5.24**) further illustrate the orientation of the phenyl rings.

The [$PdCl_2$(PNP-*n*-Prop)] molecules are packed in horizontal layers across the bc plane in a head-to-tail fashion (see **Figure 5.29**). No intermolecular hydrogen interactions were observed for this complex.

Complete supplementary data of the title compound is given in Appendix B, Table B35-40.

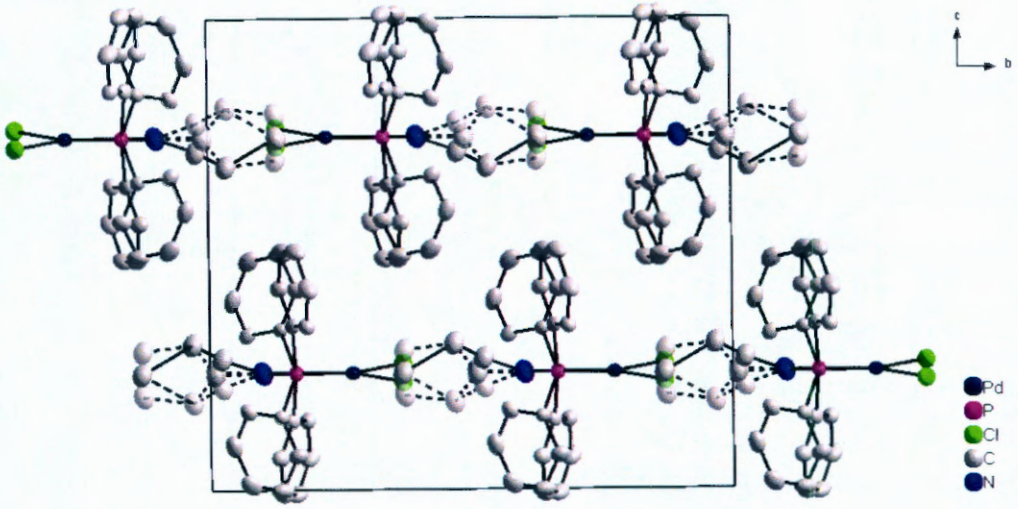

Figure 5.29: Perspective view of the unit cell of [$PdCl_2$(PNP-*n*-Prop)] (13) along the a axis. H-atoms were omitted for clarity. Only applicable H atoms with relevance to the H-bond interactions are indicated. The red fragmented lines indicate the intermolecular hydrogen bonding between the [$PdCl_2$(PNP-*n*-Prop)] molecules. The black fragmented lines indicate the 50% occupancy disorder in the propyl group.

5.2.9 Dichlorido-bis(diphenylphosphino)-isopentylamine-palladium(II) (14)

The title compound, [$PdCl_2$(PNP-*i*-Pent)] (14), crystallizes in an orthorhombic crystal system in the *Pnma* space group with 8 molecules per unit cell.

A mirror plane is present and runs through the centre of the Pd, N1, C1 and C3 atoms (see **Figure 5.30a** and **b**). The C2 atom is disordered (50% occupancy) across the mirror plane (can be split into C2A and C2B). The methyl groups, C4 and C5, are also disordered, C4 was split into C4A and C4B' across the mirror plane (50% occupancy) and C5 was split in the same manner into C5A and C5B' (50% occupancy). The first part of the disorder of the alkyl group consists of C1, C2A, C3, C4A, C5A' and the second part of C1, C2B', C3, C4B', C5B.

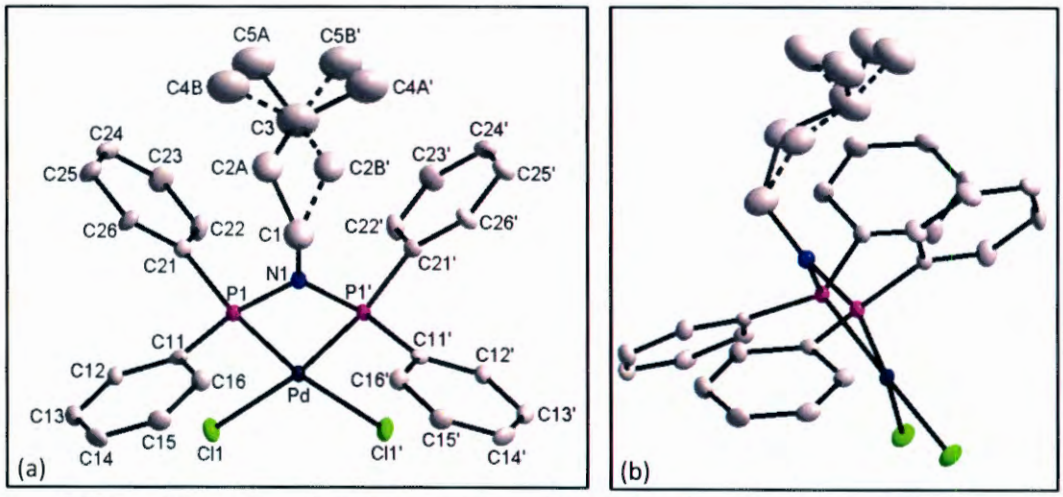

Figure 5.30a and b: Graphical representation of the different viewing angles of [Bis(diphenylphosphino)isopentylamine]dichloridopalladium(II) [$PdCl_2$(PNP-*i*-Pent)] (14). A/B indicates the disordered carbon atoms in the isopentyl moiety. Disordered parts belonging together are numbered A and B respectively. (H-atoms were omitted for clarity).

Table 5.25: Selected geometric parameters (Å, °) for [$PdCl_2$PNP-*i*-Pent] (14).

Atoms	Bond length (Å)	Atoms	Bond angle (°)
Pd – P1	2.211(1)	P1 – Pd – P1'	71.7(1)
Pd – P1'	2.211(1)	Cl1 – Pd – Cl1'	95.0(1)
Pd – Cl1	2.353(1)	P1 – N1 – P1'	99.5(3)
Pd – Cl1'	2.353(1)	C1 – N1 – P1	130.3(2)
N1 – C1	1.488(1)	C1 – N1 – P1'	130.3(2)
N1 – P1	1.696(4)	N1 – P1 – C11	110.4(2)
N1 – P1'	1.696(4)	N1 – P1 – C11'	110.4(2)
P1 – C11	1.797(5)	N1 – P1' – C21	111.7(2)
P1 – C11'	1.797(5)	N1 – P1' – C21'	111.7(2)
P2 – C21	1.806(5)	C11 – P1 – C21	106.2(2)
P2 – C21'	1.806(5)	C11' – P1' – C21'	106.2(2)

The P1-Pd-P1', P1-N1-P1' and Cl1-Pd-Cl1' angles of [$PdCl_2$(PNP-*i*-Pent)] is 71.7(1), 99.5(3) and 95.0(1) ° respectively (see **Table 5.25**). The Pd-Cl bonds are comparable to similar complexes.[2, 5, 6, 7]

Table 5.26: Selected torsion angles (°) for [$PdCl_2$PNP-*i*-Pent] (14).

Atoms	Torsion angle (°)
Pd– P1 – C11 – C12	-88.0(4)
Pd– P1 – C21 – C22	-17.2(5)
Pd – P1' – C11' – C12'	88.0(4)
Pd – P1' – C21' – C22'	17.2(5)

The phenyl rings bonded to the phosphorous atoms are twisted away from one another in such a manner that ring 2 (ring containing atom C21) and ring 3 (ring containing atom C31) is creating a space, almost 'basket-like', to accommodate the large alkyl group bonded to the nitrogen atom (see **Figure 5.30a** and **b**). The rings 1 and 4 are twisted towards each other in order to create space for the alkyl group. This can also be illustrated by the torsion angles Pd-Pd-P1-C11-C12 (-88.0(4) °) and Pd-P1'-C11'-C12' (88.0(4) °), see **Table 5.26**. The space utilised by the alkyl moiety is illustrated by **Figure 5.31**.

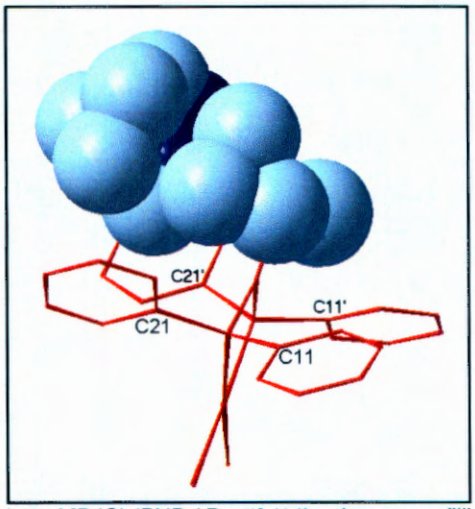

Figure 5.31: Graphical representation of [$PdCl_2$(PNP-*i*-Pent)] (14) using space-filling and stick-wire representation of the atoms (light blue spheres = hydrogen atoms, dark blue spheres = carbon atoms).

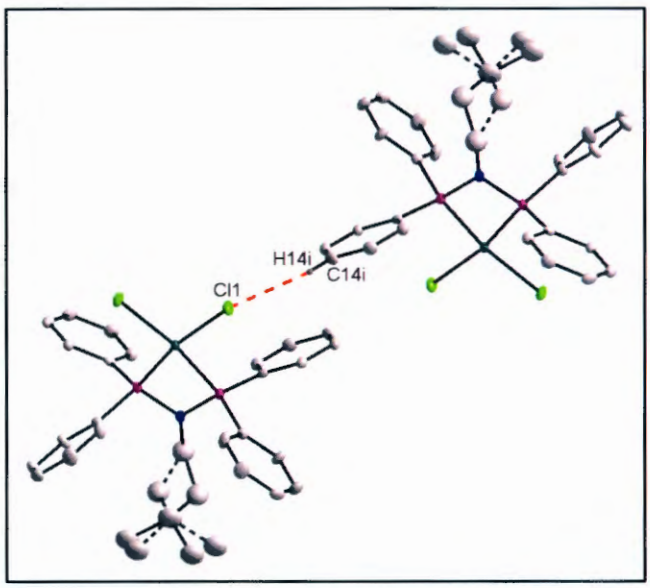

Figure 5.32: Graphical representation of the intermolecular H-bond interactions for [$PdCl_2$(PNP-*i*-Pent)] (14). Only applicable H atoms with relevance to the H-bond interactions are indicated. The red fragmented lines indicate the intermolecular hydrogen interactions between the [$PdCl_2$(PNP-*i*-Pent)] molecules. The black fragmented lines indicate the 50% occupancy disorder in the isopentyl group. ((i) (1-x,- y,1- z))

Table 5.27 : Hydrogen bond for [$PdCl_2$PNP-*i*-Pent] (14) (Å and °).

D-H...A	d(D-H)	d(H...A)	D(D...A)	<(DHA)
C14-H14...Cl1(i)	0.93	2.75	3.592(5)	150

Symmetry transformations used to generate equivalent atoms:
(i) (1-x,- y,1- z)

Intermolecular C-H···Cl hydrogen bonding is present between H14 and Cl1 and consequently also H14' and Cl1' (due to the mirror-plane present) for [$PdCl_2$(PNP-*i*-Pent)] (see **Figure 5.32**). The hydrogen bond distances and angle are presented in **Table 5.27**. The molecules are packed in horizontal layers across the ab plane in a head-to-tail manner with hydrogen bonding linking the horizontal layers (see **Figure 5.33**).

Complete supplementary data of the title compound is given in Appendix B, Table B41-45.

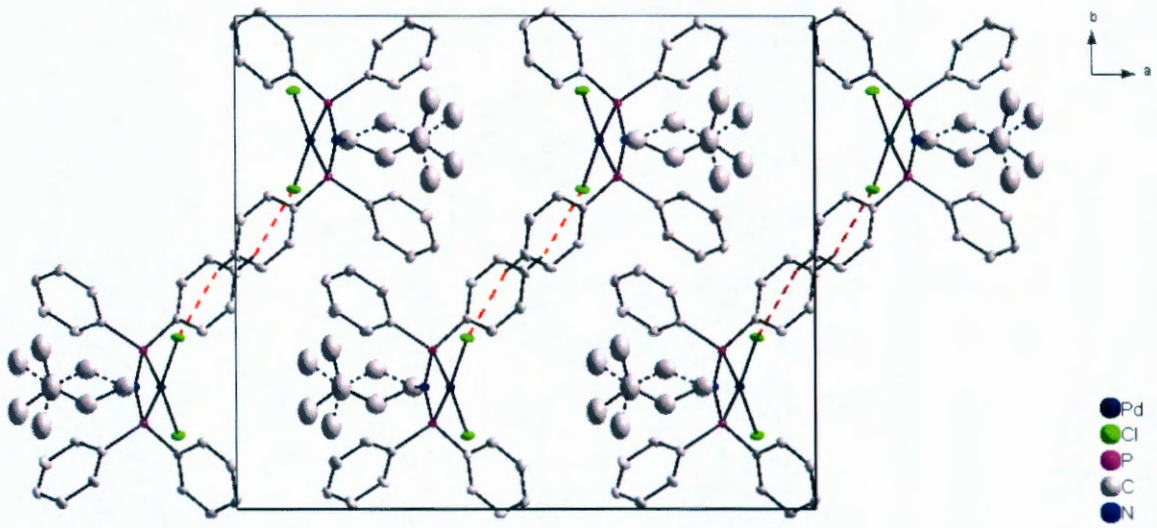

Figure 5.25 : Perspective view of the unit cell of [$PdCl_2$(PNP-*i*-Pent)] (14) along the c axis. H-atoms were omitted for clarity. Only applicable H atoms with relevance to the H-bond interactions are indicated. The red fragmented lines indicate the intermolecular hydrogen bonding between the [$PdCl_2$(PNP-*i*-Pent)] molecules. The black fragmented lines indicate the 50% occupancy disorder in the isopentyl group.

5.2.10 Dichlorido-bis(diphenylphosphino)-*n*-butylamine-palladium(II) (15)

The title complex, [$PdCl_2$(PNP-*n*-Butyl)] (15), crystallizes with two crystallographically independent molecules in the asymmetric unit and is referred to as [$PdCl_2$(PNP-*n*-Butyl)] (I) (15I) for the molecule containing Pd1 (see **Figure 5.34a**) and [$PdCl_2$(PNP-*n*-Butyl)] (II) (15II) for the molecule containing Pd2 (see **Figure 5.34b**).

The ([$PdCl_2$(PNP-*n*-Butyl)]) compound crystallizes in a triclinic crystal system in the $P\bar{1}$ space group with 4 molecules per unit cell.

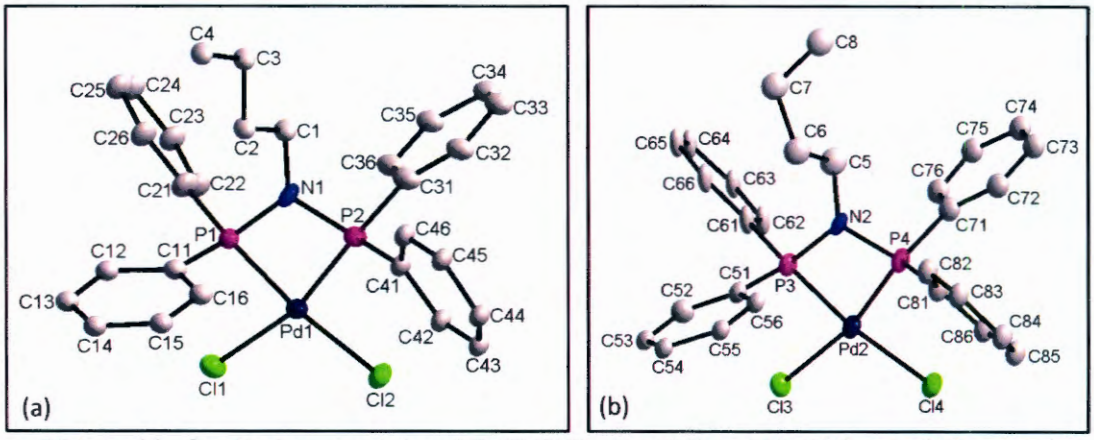

Figure 5.34a and b: Graphical representation of [$PdCl_2$(PNP-*n*-Butyl)] (I) and (II) (15(I) and 15(II)) respectively at 50% probability. (H-atoms were omitted for clarity).

The two [$PdCl_2$(PNP-*n*-Butyl)] molecules in the asymmetric unit have insignificant differences in bond lengths and angles (see **Table 5.28** and **5.29**).

Table 5.28: Selected geometric parameters (Å, °) for the compound [$PdCl_2$(PNP-*n*-Butyl)] (I) (15I).

Atoms	Bond length (Å)	Atoms	Bond angle (°)
Pd1– P1	2.205(4)	P1 – Pd1 – P2	71.3(2)
Pd1 – P2	2.227(4)	Cl1 – Pd1 – Cl2	93.8(2)
Pd1 – Cl1	2.345(4)	P1 – N1 – P2	99.6(6)
Pd1 – Cl2	2.346(4)	C1 – N1 – P1	129.2(7)
P1 – N1	1.69(1)	C1 – N1 – P2	129.0(6)
P2 – N1	1.69(1)	N1 – P1 – C11	107.3(7)
N1 – C1	1.46(2)	N1 – P1 – C21	108.8(7)
P1 – C11	1.79(2)	N1 – P2 – C31	108.6(7)
P1 – C21	1.76(2)	N1 – P2 – C41	109.3(7)
P2 – C31	1.83(2)	C11 – P1 – C21	109.0(8)
P2 – C41	1.75(2)	C31 – P2 – C41	107.2(8)

Table 5.29: Selected geometric parameters (Å, °) for the compound [$PdCl_2$(PNP-*n*-Butyl) (II) (15II).

Atoms	Bond length (Å)	Atoms	Bond angle (°)
Pd2– P3	2.201(4)	P3 – Pd2 – P4	71.5(2)
Pd2 – P4	2.223(4)	Cl3 – Pd2 – Cl4	94.6(2)
Pd2 – Cl3	2.364(4)	P3 – N2 – P4	101.3(7)
Pd2 – Cl4	2.360(4)	C5 – N2 – P3	127.0(6)
P3 – N2	1.67(2)	C5 – N2 – P4	127.5(6)
P4 – N2	1.67(1)	N1 – P3 – C51	108.4(7)
N2 – C5	1.48(2)	N1 – P3 – C61	108.3(7)
P3 – C51	1.80(2)	N1 – P4 – C71	108.9(7)
P3 – C61	1.80(2)	N1 – P4 – C81	111.0(7)
P4 – C71	1.80(2)	C51 – P3 – C61	108.3(7)
P4 – C81	1.81(2)	C71 – P4 – C81	107.0(7)

The P-Pd-P, P-N-P, Cl-Pd-Cl angles for [$PdCl_2$(PNP-*n*-Butyl)] (I) are 71.3(2), 99.6(6) and 93.8(2) ° respectively (see **Table 5.28**). The corresponding angles for [$PdCl_2$(PNP-*n*-Butyl)] (II) are 71.5(2), 101.3(7) and 94.6(2) ° respectively (see **Table 5.29**). The Pd-Cl bonds for both molecules in the asymmetric unit are of the expected lengths in these type of complexes.[2, 5, 6, 7]

Table 5.30: Selected torsion angles (°) for the compound [$PdCl_2$(PNP-*n*-Butyl)] (I) (15I) and (II) (15II) .

Atoms	Torsion angle (°)	Atoms	Torsion angle (°)
Pd1– P1 – C11 – C12	-113.2(5)	Pd2– P3 – C51 – C52	-94.5(5)
Pd1– P1 – C21 – C22	-4.8(5)	Pd2– P3 – C61 – C62	-8.9(5)
Pd1 – P2 – C31 – C32	-157.3(4)	Pd2 – P4 – C71 – C72	-151.4(4)
Pd1 – P2 – C41 – C42	49.1(5)	Pd2 – P4 – C81 – C82	-119.9(5)

The torsion angles of ring 4 (phenyl ring containing C41) of molecule 1 (49.1(5) °) and ring 8 (phenyl ring containing C81) of molecule 2 (-119.9(5) °) are significantly different. The orientations of the other three sets of phenyl rings of the corresponding phenyl rings of the two [$PdCl_2$(PNP-*n*-Butyl)] molecules are comparable as can be seen from the torsion angles (see **Table 5.30**). Both [$PdCl_2$(PNP-*n*-Butyl)] molecules adopted

variations of the 'basket-like' orientation for the phenyl groups. This is further illustrated by the torsion angles Pd1-P1-C21-C22 (-4.8(5) °) and Pd1-P2-C41-C42 (49.1(5) °) for molecule 1 and Pd2-P3-C61-C62 (-8.9(5) °) and Pd2-P4-C81-C82 (-119.9(5) °) for molecule 2. An overlay of the two independent molecules illustrating the differences is presented in **Figure 5.35** (with P1, N1 and P2 overlayed on P3, N2 and P4 respectively). The space consumed by the butyl moieties for the two molecules are illustrated by the space-filling and stick-wire representation of the two molecules in **Figure 5.36 a** and **b**.

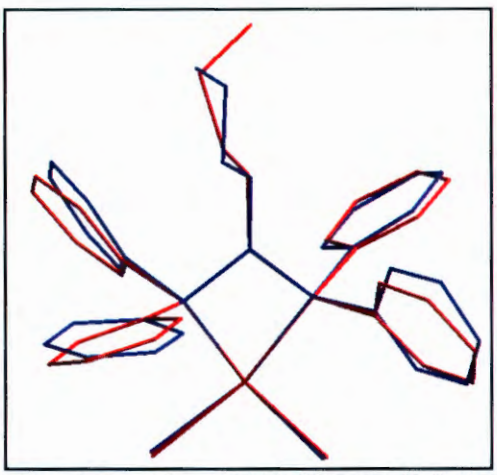

Figure 5.35: Graphical representation of an overlay of [$PdCl_2$(PNP-Butyl)] (i) (15I) (blue) and (ii) (15II) (red) using Hyperchem 7.52.[9]

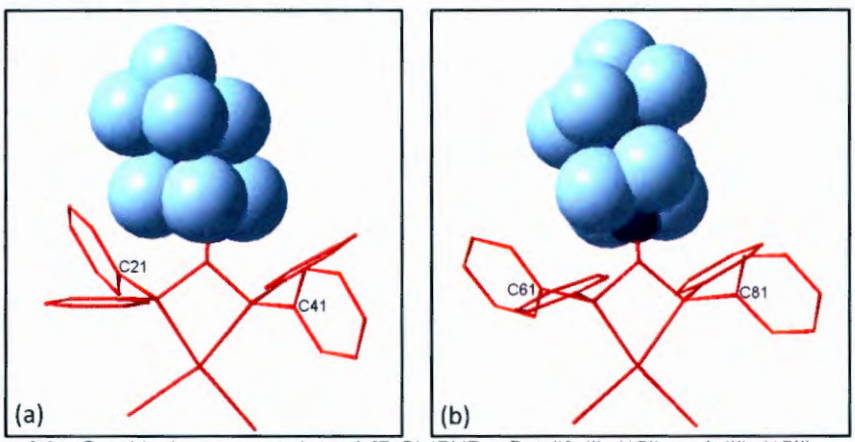

Figure 5.36a and b: Graphical representation of [$PtCl_2$(PNP-*n*-Butyl)] (I) (15I) and (II) (15II) respectively using space-filling and stick-wire representation of the atoms (light blue spheres = hydrogen atoms, dark blue spheres = carbon atoms).

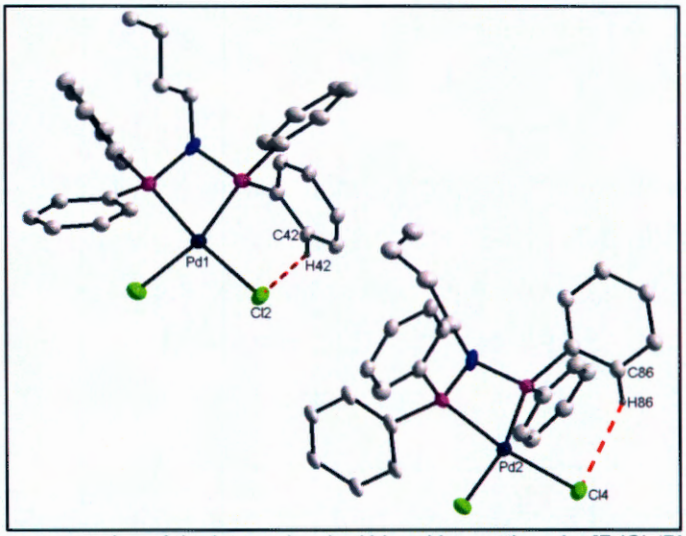

Figure 5.37: Graphical representation of the intramolecular H-bond interactions for [$PdCl_2$(PNP-*n*-Butyl)] (I) (15I) and (I) (15II). Only applicable H atoms with relevance to the H-bond interactions are indicated. The red fragmented lines indicate the intermolecular hydrogen interactions between the [$PdCl_2$(PNP-*n*-Butyl)] molecules.

Table 5.32 : Hydrogen bond for [$PdCl_2$PNP-*n*-Butyl] (I) (15I) and (II) (15II) (Å and °).

D-H...A	d(D-H)	d(H...A)	D(D...A)	<(DHA)
C42-C42...Cl2(i)	0.93	2.76	3.607(2)	151.1
C86-H86...Cl4(i)	0.93	2.80	3.541(2)	137.3
C35-H35...Cl1(ii)	0.93	2.78	3.697(2)	169.9
C65-H65...Cl2(i)	0.93	2.82	3.547(2)	135.5

Symmetry transformations used to generate equivalent atoms:
(i) (x, y, z), (ii) (1-x, -y, 2-z)

Intramolecular CH···Cl hydrogen bonding is present for both independent molecules (see **Figure 5.37**). The hydrogen bonding distances and angle is presented in **Table 5.32**.

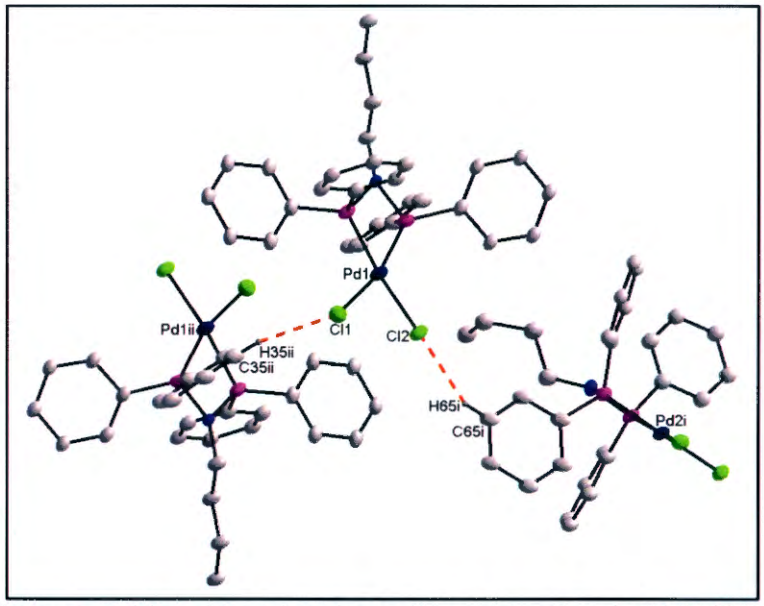

Figure 5.38: Graphical representation of the Intermolecular H-bond interactions for [$PdCl_2$(PNP-Butyl)] (I) (15I) and (II) (15II). Only applicable H atoms with relevance to the H-bond interactions are indicated. The red fragmented lines indicate the intermolecular hydrogen interactions between the [$PdCl_2$(PNP-*n*-Butyl)] molecules. ((ii) (1-x, -y, 2-z))

Intermolecular C-H···Cl hydrogen bonding is also present between the molecules of [$PdCl_2$(PNP-*n*-Butyl)] (see **Figure 5.38**). A list of H-bond interactions is given in **Table 5.32**.

The molecules are packed in vertical layers across the bc plane in a slightly staggered head-to-tail fashion with hydrogen bonding stabilizing the crystal packing (see **Figure 5.39**).

Complete supplementary data of the title compound is given in Appendix B, Table B46-50.

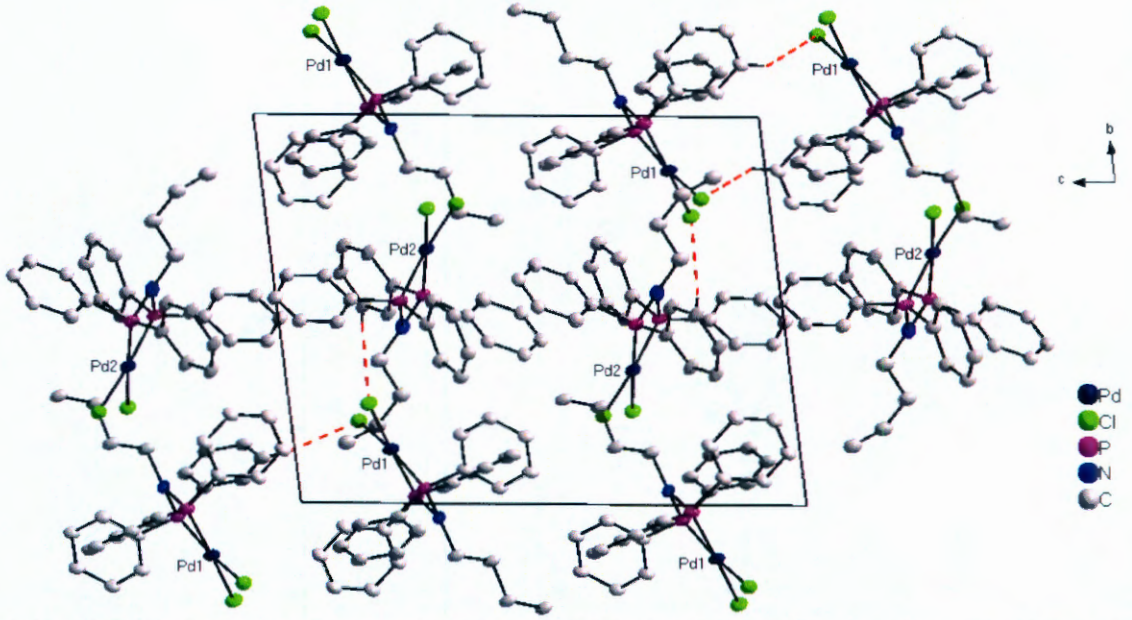

Figure 5.39: Perspective view of the unit cell of [$PdCl_2$(PNP-*n*-Butyl)] (I) and (II) along the a axis. H-atoms were omitted for clarity. Only applicable H atoms with relevance to the H-bond interactions are indicated. The red fragmented lines indicate the intermolecular hydrogen bonding between the [$PdCl_2$(PNP-*n*-Butyl)] molecules.

5.3 Discussion

5.3.1 [$PtCl_2$(PNP-alkyl)] complexes

Five [$PtCl_2$(PNP-alkyl)] complexes, [$PtCl_2$(PNP-Ethyl)] (6), [$PtCl_2$(PNP-*n*-Prop)] (7), [$PtCl_2$(PNP-Dimprop)] (8), [$PtCl_2$(PNP-*i*-Pent)] (9), and [$PtCl_2$(PNP-Cychex)] (10) have been synthesized and single crystal X-ray crystallographic data have been collected. The only difference between the complexes are the different alkyl moieties bonded to the nitrogen atom of the diphosphinoamine ligand which is coordinated to the platinum(II) centre.

The crystal structure specific geometric parameters of the various [$PtCl_2$(PNP-alkyl)] complexes were briefly discussed in §5.2.1-5.2.5. It was noted that stable chelate complexes were formed despite the strain caused by the formation of the four-membered Pt-P-N-P ring. The strain is evident from the bond angles around the

platinum metal centre; the ideal square planar geometry of all these complexes are distorted with P-Pt-P bond angles that range from 71.9(1) ° to 72.4(1) ° (see **Table 5.33**) and Cl-Pt-Cl angles that range between 90.8(1) ° and 92.7(1) °. The corresponding geometric parameters are comparable to other structurally characterised platinum(II) diphosphinoamine complexes. [3, 4, 5, 6, 7]

The P1-Pt-P2 bond angles of the various [$PtCl_2$(PNP-alkyl)] complexes reported are similar within experimental error (see **Table 5. 33**), which illustrates the rigidity of the P-N-P frame upon coordination. Similarly, the P-N-P angles decreased upon coordination, from the much larger P-N-P angle observed for the non-coordinated P-N-P ligands, in order to accommodate coordination to the platinum centre. There is a tendency of the P-N-P angle to slightly decrease as the steric bulk of the nitrogen-coordinated alkyl moiety increases. The P-N-P angle of the complexes with relatively bulky nitrogen-coordinated alkyl groups, [$PtCl_2$(PNP-Cychex)] (99.3(1) °) and [$PtCl_2$(PNP-Dimprop)] (98.6(4) °) are smaller than the complexes which have less bulky alkyl groups, [$PtCl_2$(PNP-Ethyl)] (100.0(2) °) and [$PtCl_2$(PNP-*n*-Prop)] (100.1(1) °). This is further illustrated when comparing these values to that of the similar complex, [($PtCl_2$((PPh_2)$_2$NMethyl)] which has a methyl group coordinated to the nitrogen atom and has a P-N-P angle of 102.4(3).[2] This trend is as expected, as a bulkier alkyl substituent on the nitrogen atom forces the P-N-P angle to become smaller in order to accommodate the larger moiety.

The most significant differences that are observed between the various [$PtCl_2$(PNP-alkyl)] complexes are the changes in the P-N-P angles and the values of the torsion angles for the platinum complexes. This indicates that the orientations of the phenyl rings are influenced by the changes in steric bulk of the various nitrogen-bonded alkyl substituents. This is further discussed in δ5.3.3.

Table 5.33: Selected geometric parameters (bond angles (°)) for [$PtCl_2$(PNP-alkyl)].

	P1 – Pt – P2 (°)	P1 –N1–P2 (°)	Cl1–Pt–Cl2 (°)
[$PtCl_2$(PNP-Ethyl)]	72.1(1)	100.0(2)	91.7(1)
[$PtCl_2$(PNP-*n*-Prop]	72.4(1)	100.1(1)	92.7(1)
[$PtCl_2$(PNP-*i*-Pent]	72.2(1)	99.5(2)	91.3(1)
[$PtCl_2$(PNP-Cychex)]	71.9(1)	99.3(1)	91.8(1)
[$PtCl_2$(PNP-Dimprop)]	72.3(1)	98.6(4)	90.8(1)

5.3.2 [$PdCl_2$(PNP-alkyl)] complexes

Five [$PdCl_2$(PNP-alkyl)] complexes, [$PdCl_2$(PNP-*i*-Prop)] (11), [$PdCl_2$(PNP-Dimprop)] (12), [$PdCl_2$(PNP-*n*-Prop)] (13), [$PdCl_2$(PNP-*i*-Pent)] (14), and [$PdCl_2$(PNP-*n*-Butyl)] (15) have been synthesized and crystallographic data collected. The only difference between the complexes are the different alkyl moieties coordinated to the nitrogen atom of the diphosphinoamine ligand.

The crystal structure specific geometric parameters of the five [$PdCl_2$(PNP-alkyl)] complexes were briefly discussed in §5.3.1-5.3.5 and clearly indicate distorted square planar geometries for all five reported Pd(II)-PNP complexes, with P-Pd-P bite angles ranging between 71.3(1) ° and 71.7(1) ° (see **Table 5.34**). The Cl-Pd-Cl angles for the complexes also deviate from the ideal angle of 90° with values between 93.8(2) ° and 95.6(1) °. These distortions from the ideal geometry of the palladium(II) centre originate from the formation of the four-membered chelate ring, P-N-P-Pd. The geometric parameters of the palladium complexes reported correspond well with other similar palladium(II) diphosphinoamine complexes.[2, 5, 6, 7]

The bond lengths of the palladium(II)-PNP complexes reported are comparable within experimental error. The P-N-P angles for the five Pd(II)-PNP complexes are also similar within experimental error, even though the steric bulk of the nitrogen-bonded alkyl groups vary substantially from one complex to another.

Table 5.34: Selected geometric parameters (bond angles (°)) for [$PdCl_2$(PNP-alkyl)].

	P1 – Pd – P2	P1 –N1–P2	Cl1–Pd–Cl2
[$PdCl_2$(PNP-*i*-Prop)]	71.3(1)	98.6(1)	95.6(1)
[$PdCl_2$(PNP-*n*-Prop)]	71.5(1)	100.8(5)	94.9(1)
[$PdCl_2$(PNP-Dimprop]	71.6(1)	99.7(3)	94.0(1)
[$PdCl_2$(PNP-*i*-Pent)]	71.7(1)	99.5(3)	95.0(1)
[$PdCl_2$(PNP-*n*-Butyl] (I)	71.3(2)	99.6(6)	93.8(2)
[$PdCl_2$(PNP-*n*-Butyl] (II)	71.5(2)	101.3(7)	94.6(2)

The torsion angles and the arrangement of the phenyl rings for the various [$PdCl_2$(PNP-alkyl)] complexes are further discussed in δ5.3.3.

5.3.3 Comparison of solid state parameters of [$PtCl_2$(PNP-alkyl)] and [$PdCl_2$(PNP-alkyl) complexes

Both platinum(II) and palladium(II) are d-block metal cations, which typically form four coordinated square-planar complexes. The [($PtCl_2$(PNP-alkyl)] and [($PdCl_2$(PNP-alkyl)] series of complexes both produced distorted square-planar geometry upon the formation of the four-membered chelate ring, causing strain within structures of the metal compounds. The slightly larger P-Pt-P bite-angles (ranging between 71.9(1) ° and 72.4(1) °) than the corresponding angles of the Pd(II)-PNP complexes which range from 71.3(1) ° to 71.7(1) ° originate from the greater size of the platinum centre when compared to palladium. The phosphorous-bonded phenyl rings are consequently spread out more widely for the platinum complexes, resulting in greater steric interactions with the chloride ligands. This results in smaller Cl-Pt-Cl angles (90.8(1) ° to 92.7(1) °) in comparison to the corresponding angles of the palladium complexes which range between 93.8(2) ° and 95.6(1) °.

There are three sets Pt(II) and Pd(II) compounds which share the same PNP-ligand ([$PtCl_2$(PNP-Dimprop)] and [$PdCl_2$(PNP-Dimprop)], [$PtCl_2$(PNP-*i*-Pent)] and [$PdCl_2$(PNP-*i*-Pent)], [$PtCl_2$(PNP-*n*-Prop)] and [$PdCl_2$(PNP-*n*-Prop)]. The [$PtCl_2$(PNP-Dimprop)] and [$PdCl_2$(PNP-Dimprop)] complexes are isomorphous in solid state with virtually identical phenyl ring orientations. This is also observed for the [$PtCl_2$(PNP-*i*-Pent)] and [$PdCl_2$(PNP-*i*-Pent)] complexes. [$PtCl_2$(PNP-*n*-Prop)] and [$PdCl_2$(PNP-*n*-Prop)] have slight differences with regards to the orientation of the respective phenyl ring and it is important to note that the propyl substituent for the palladium complex is highly disordered. The substituent will as a result occupy a larger space and create a significant steric interference with the phenyl groups which will influence the orientation of the rings. This is in contrast to the propyl group of the platinum complex which is not disordered and necessitates a smaller space.

General summary of geometric parameters for the [$PtCl_2$(PNP-alkyl)] and [$PdCl_2$(PNP-alkyl)] complexes

It is clear that there are some similarities for all the structures presented in this chapter. Firstly, all the complexes presented in this chapter contain a metal centre (platinum(II)/palladium(III)) which is coordinated by two phosphorous atoms from the diphosphinoamine ligand (PNP-ligand) and two chlorido ligands that complete the coordination sphere (see **Scheme 5.1** and **5.2** for a summary of the complexes presented in this chapter). The square-planar geometry at the metal centre (platinum(II)/palladium(II)) is severely distorted as illustrated by the P-M-P (M = Pt(II)/Pd(II)) bite angles which vary from 71.3(1) to 72.4(1) °. This distortion influences the geometry at the phosphorous atoms and the P-N-P angles as well as the C-P-C angles, which vary between 103.5(1) and 110.3(1) ° as opposed to the expected value of 109.5 °. The P-N-P angles of the coordinated bidentate ligands vary between 98.6(1) and 101.3(7) ° compared to the free ligands which vary between 111.0(1) and 123.4(1) ° (see Chapter 4). These P-N-P angles indicate a severe distortion from the ideal trigonal-planar angle expected at the sp^2-hybridized nitrogen. The bond lengths and angles for all these complexes correspond well to other similar complexes.[2, 3, 4, 5, 6, 7]

Another interesting aspect to consider when investigating the series of [$PtCl_2$(PNP-alkyl)]] and [$PdCl_2$(PNP-alkyl)] complexes are the orientation of the phenyl rings. It is noticeable that there are two prominent conformations ('basket'- and 'fan-like') with regards to the orientations of the phenyl rings for these square-planar complexes. The first is the 'basket-like' conformation (see **Figure 5.40a** and **b**) in which rings 2 (phenyl rings containing C21) and ring 3 (ring containing C31) have torsion angles (Pt/Pd-P1-C21-C22 and Pt/Pd-P2-C31-C32 respectively) that are approximately -10° and ±180 ° respectively (see **Table 5.35**). This type of conformation in which the phenyl rings 2 and 3 are twisted towards each other, encompasses (in a 'basket-like' manner) the sterically bulky alkyl moiety. The complexes that have the 'basket-like' conformation and slight variations thereof are: [$PtCl_2$(PNP-Dimprop)], [$PdCl_2$(PNP-*i*-Prop)], [$PdCl_2$(PNP-Dimprop)], [$PtCl_2$(PNP-*i*-Pent)], [$PdCl_2$(PNP-*i*-Pent)] and [$PtCl_2$(PNP-Cychex)] (see entries 1-6, **Tables 5.35**). [$PdCl_2$(PNP-*n*-Butyl)] (I) (see entry 7, **Table 5.35**) adopted as a variation of the basket conformation, with values of -4.8(5) and 157.3(4) ° for Pt-P1-C31-C32 and Pt-P2-C31-C32 respectively.

Table 5.35: Selected torsion angles (°) for [$PtCl_2$(PNP-Cychex)], [$PtCl_2$(PNP-Dimprop)], [$PtCl_2$(PNP-Cychex)], and [$PdCl_2$(PNP-Dimprop)].

Entries	Compounds	M-P1-C11-C12 (°)	M-P1-C21-C22 (°)	M-P2-C31-C32 (°)	M-P1-C41-C42 (°)
1	[$PtCl_2$(PNP-Dimprop)]	-98.4(2)	-11.8(3)	-174.4(2)	-78.2(2)
2	[$PdCl_2$(PNP-*i*-Prop)]	-85.2(1)	-9.6(1)	163.6(1)	-87.3(1)
3	[$PdCl_2$(PNP-Dimprop)]	-95.7(6)	-13.5(7)	-174.6(6)	-79.6(7)
4	[$PtCl_2$(PNP-*i*-Pent)]*	-88.3(1)	-15.8(2)	-164.4(2)	-86.1(3)
5	[$PdCl_2$(PNP-*i*-Pent)]*	-88.0(4)	-17.2(5)	-162.9(4)	-85.6(4)
6	[$PtCl_2$(PNP-Cychex)]	-87.6(3)	-19.7(3)	173.5(2)	-128.0(3)
7	[$PdCl_2$(PNP-*n*-Butyl)] (I)	-113.2(5)	-4.8(5)	-157.3(4)	49.1(5)
8	[$PdCl_2$(PNP-*n*-Prop)]#	-97.0(4)	17.4(5)	-97.0(4)	17.4(5)
9	[$PtCl_2$(PNP-Ethyl)]	175.2(3)	-63.6(4)	-172.8(3)	-80.8(4)
10	[$PtCl_2$(PNP-*n*-Prop)]	-178.1(2)	-60.1(2)	176.6(2)	-76.7(2)

M = Pt(II) or Pd(II)

* The torsion components for both [$PtCl_2$(PNP-*i*-Pent)] and [$PdCl_2$(PNP-*i*-Pent)] are as follows: M-P1'-C21'-C26' and M-P1'-C11'-C16' instead of M-P2-C31-C32 and M-P2-C41-C42 respectively.

The torsion components for [$PdCl_2$(PNP-*n*-Prop)] is as follows: M-P1'-C11'-C12' and M-P1'-C21'-C22' instead of M-P2-C31-C32 and M-P2-C41-C42 respectively.

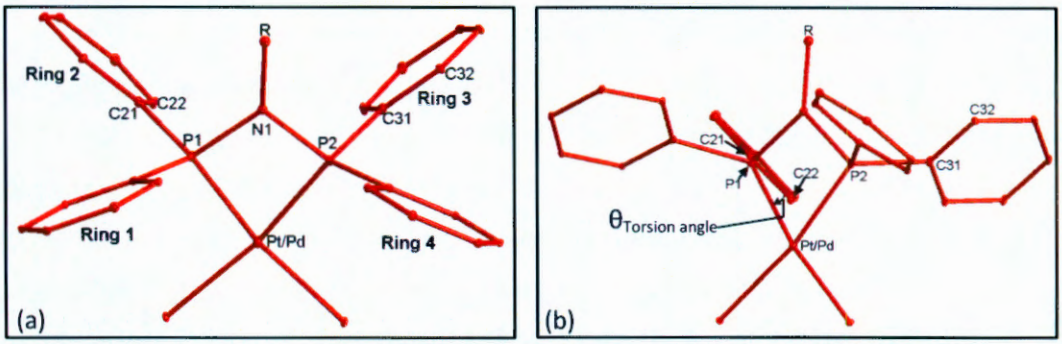

Figure 5.40a and b: Graphical representation of different viewing angles of the 'basket-like' conformation as adopted by selected platinum(II) and palladium(II) PNP-ligand coordinated complexes. The Pt/Pd-P1-C21-C22 torsion angle is illustrated by viewing along the P1-C21 bond in (b). (R = alkyl moiety.)

The phenyl rings of $[PtCl_2(PNP\text{-}alkyl)]$ and $[PdCl_2(PNP\text{-}alkyl)]$ complexes with alkyl moieties that are less sterically bulky have more degrees of freedom. The 'fan-like' orientation of the phenyl groups (see **Figure 5.41**) is consequently adopted. This type of conformation typically has Pt/Pd-P1-C21-C22 and Pt/Pd-P1-C41-C42 torsion angles of approximately ±60.0° for both rings. The Pt/Pd-P2-C11-C12 and Pt/Pd-P2-C31-C32 torsion angles are approximately ±180.0 ° (see **Table 5.44**). Complexes that adopts this arrangement for the phenyl rings are: $[PtCl_2(PNP\text{-}Ethyl)]$ and $[PtCl_2(PNP\text{-}n\text{-}Prop)]$ (see entries 9 and 10, **Table 5.44**).

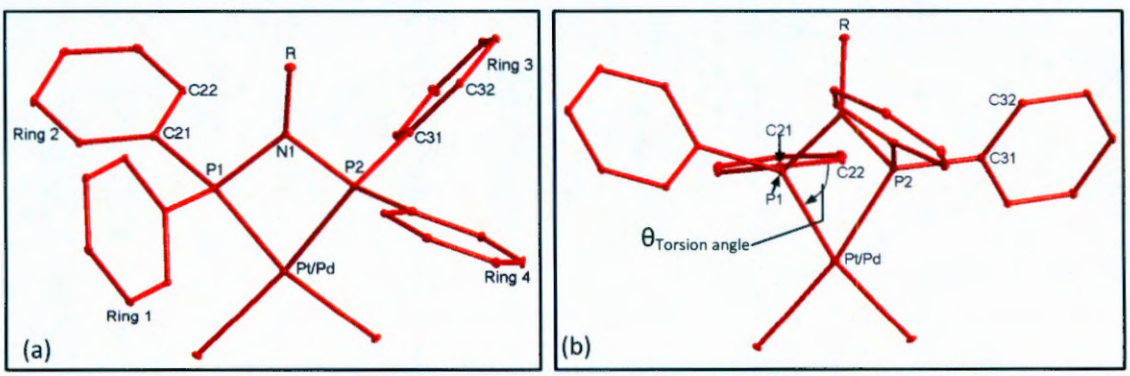

Figure 5.41a and b: Graphical representation of dfferent viewing angles of the 'fan-like' conformation of adopted by selected platinum(II) and palladium(II) PNP-ligand coordinated complexes. The Pt/Pd-P1-C21-C22 torsion angle is illustrated by viewing along the P1-C21 bond in (b). (R = alkyl moiety.)

It is evident that the steric bulkiness of the alkyl group plays a significant role in the orientation of the phenyl rings of the [$PtCl_2$(PNP-alkyl)] and [$PdCl_2$(PNP-alkyl)] complexes in solid state.

Theoretical calculations were performed on all the [$PtCl_2$(PNP-alkyl)] and [$PdCl_2$(PNP-alkyl)] discussed above. These optimised structures are presented, discussed and compared to the crystal structures of the corresponding complexes in Chapter 8.

6 Single crystal X-ray Crystallographic study of Cr(III)-PNP complexes

In this chapter...

The X-ray crystallographic data of three Cr(III)-PNP complexes were collected and are discussed in detail. Several geometric parameters are examined and evaluated. Comparisons with similar complexes from the literature are made.

6.1 Introduction

The selective tetramerisation of ethylene was first reported in 2004[1] by Sasol Technology as mentioned in Chapter 2. The catalytic runs associated therewith were typically performed *in situ*, but it was also possible to achieve good yield results with preformed Cr(III)-PNP complexes. One such complex was synthesised and crystallographically studied. The crystal structure revealed a chloride-bridged dimer, $[CrCl_2(\mu\text{-}Cl)(PNP\text{-}Ph)]_2$ (PNP-Ph = bis(diphenylphosphino)phenylamine, see **Figure 6.1**).

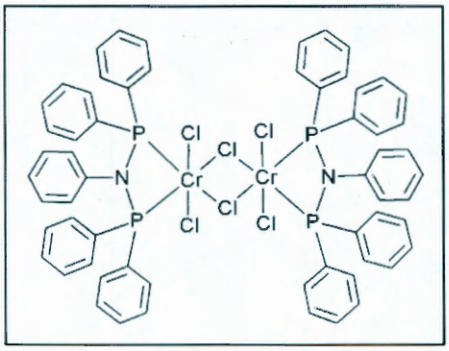

Figure 6.1: Schematic representation of $[CrCl_2(\mu\text{-}Cl)(PNP\text{-}Ph)]_2$.[1]

[1] Bollmann, A., Blann, K., Dixon, J.T., Hess, F. M., Killian, E., Maumela, H.; McGuinness, D. S.; Morgan, D. H.; Neveling, A.; Otto, S.; Overett, M.J.; Slawin, A.M.Z.; Wasserscheid, P. and Kuhlmann, S. *J. Am. Chem. Soc.* **2004**, *126*, 14712.

In an attempt to understand the catalytic process better it is necessary to investigate how the PNP-ligands interact with Cr(III) and what effects are induced. Thus, a range of possible Cr(III)-PNP complexes were therefore synthesized and crystallographically studied. These structures of the Cr(III)-PNP complexes are then compared to determine the changes that occur within the structure when the nitrogen-coordinated alkyl moiety is changed from one PNP-ligand to another.

6.2 Crystallographic data

Single crystals, suitable for X-ray crystallography, were obtained as described in §3.2.5.1-3. A summary of the general crystal data is reported **in Table 6.1**. A schematic view of the asymmetric unit of each complex and molecular diagrams (using DIAMOND 3.0[2]) of the compounds are presented, while graphical representations of overlays of selected complexes are also presented (using Hyperchem7.52[3]). Selected geometric parameters are reported and discussed, any additional correlations with other relevant structures are done in §6.3.

The following complexes are reported and discussed in this chapter:

16) (*n*-Pentylammonium)(tetrachlorido-bis(diphenylphosphino)-*n*-pentylamine-chromate(III))-ditoluene solvate ([*n*-Pent-NH_3][$CrCl_4$(PNP-*n*-Pent)]·$2C_7H_8$)
17) (Isopentylammonium)(tetrachlorido-bis(diphenylphosphino)-isopentylamine-chromate(III))ditoluene solvate ([*i*-Pent-NH_3][$CrCl_4$(PNP-*i*-Pent)]·$2C_7H_8$)
18) (*n*-Butyl-ammonium)(tetrachlorido-bis(diphenylphosphino)-*n*-butylamine-chromate(III))-ditoluene solvate ([*n*-Butyl-NH_3][$CrCl_4$(PNP-*n*-Butyl)]·$2C_7H_8$)

[2] Brandenburg, K. and Putz, H., **2005**, DIAMOND. Release 3.0c. Crystal Impact GbR, Bonn, Germany.
[3] Hyperchem ™ Release 7.52, Windows Molecular Modeling System, Hypercube, Inc., **2002**.

Table 6.1: General crystal data for the following compounds, [*n*-Pent-NH_3]$_2$[$CrCl_4$(PNP-Pent)]$_2$·4C_7H_8 **(16)**, ([*i*-Pent-NH_3]$_2$[$CrCl_4$(PNP-*i*-Pent)]$_2$·4C_7H_8) **(17)** and [*n*-Butyl-NH_3]$_4$[$CrCl_4$(PNP-*n*-Butyl)]$_4$·8C_7H_8 **(18)**.

Identification code	(16)	(17)	(18)
Empirical formula	$Cr_2P_4N_4Cl_8C_{96}H_{116}$	$Cr_2P_4N_4Cl_8C_{103}H_{124}$	$Cr_4P_8N_8Cl_{16}C_{184}H_{216}$
Formula weight	1837.4	1929.5	3562.6
Crystal system, space group	Triclinic, $P\bar{1}$	Triclinic, $P\bar{1}$	Triclinic, $P\bar{1}$
Unit cell dimensions:			
a(Å)	14, 992(5)	14.369(5)	17.7196(5)
b(Å)	18.605(5)	15.025(5)	17.7751(5)
c(Å)	18.855(5)	25.696(5)	31.2552(5)
α (°)	93.861(5)	80.096(5)	88.432(2)
β (°)	110.769(5)	85.170(5)	81.404(2)
γ (°)	103.578(5)	68.900(5)	71.938(2)
Volume (Å^3)	4714(2)	5097(3)	9252.2(4)
Z	2	2	8
Calculated density (Mg/m^3)	1.294	1.258	5.112
Absorption coefficient (mm^{-1})	0.286	0.265	0.290
F(000)	964	984	1864
Crystal size (mm)	0.24 x 0.26 x 0.45	0.10 x 0.13 x 0.15	0.15 x 0.16 x 0.20
θ range / completeness of collection (°)	1.14-28.45/ 98.9	1.47-28.41/ 98.7	1.21-28.40/ 99.2
	-20<=h<=20	-18<=h<=19	-23<=h<=23
Limiting indices	-24<=k<=24	-18<=k<=20	-22<=k<=23
	-25<=l<=25	-34<=l<=34	-41<=l<=41
Reflections collected / unique / observed (I>2σ(I))	76455/ 23517	63799 / 25306	130946 / 46075
	R(int) = 0.0698	R(int) = 0.0869	R(int) = 0.0556
Data / restraints / parameters	23517/0/1021	25306/238/1098	46075/0/1733
Goodness of fit on F^2	0.961	1.009	0.969
Final R indices (I>2σ(I))	R1 = 0.0531	R1 = 0.0682	R1 = 0.0751
	wR2 = 0.1349	wR2 = 0.1546	wR2 = 0.1716
R indices(all data)	R1 = 0.1512	R1 = 0.1662	R1 = 0.1297
	wR2 = 0.1839	wR2 = 0.2059	wR2 = 0.2097
$\Delta\rho_{min}$, $\Delta\rho_{max}$ (e.Å^{-3})	0.566 and -0.566	1.387 and -0.645	3.392 and -4.860

6.2.1 [*n*-Pent-NH_3][$CrCl_4$(PNP-*n*-Pent)]·2C_7H_8 (16)

The title compound crystallizes in a triclinic crystal system in the $P\bar{1}$ spacegroup. The asymmetric unit consists of two mono-anionic chromium(III) complexes, two non-coordinated *n*-pentylammonium cations and four non-coordinated toluene solvate molecules. The complexity of the crystal structure is shown in a schematic view of the

asymmetric unit [*n*-Pent-NH_3][$CrCl_4$(PNP-*n*-Pent)]·2C_7H_8 in **Scheme 6.1** A molecular diagram of the complex is presented in **Figure 6.2.**

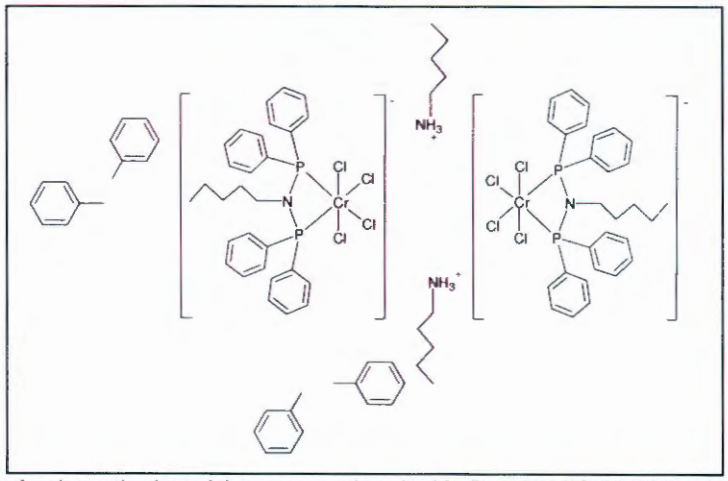

Scheme 6.1: A schematic view of the asymmetric unit of [*n*-Pent-NH_3][$CrCl_4$(PNP-*n*-Pent)]·2C_7H_8.

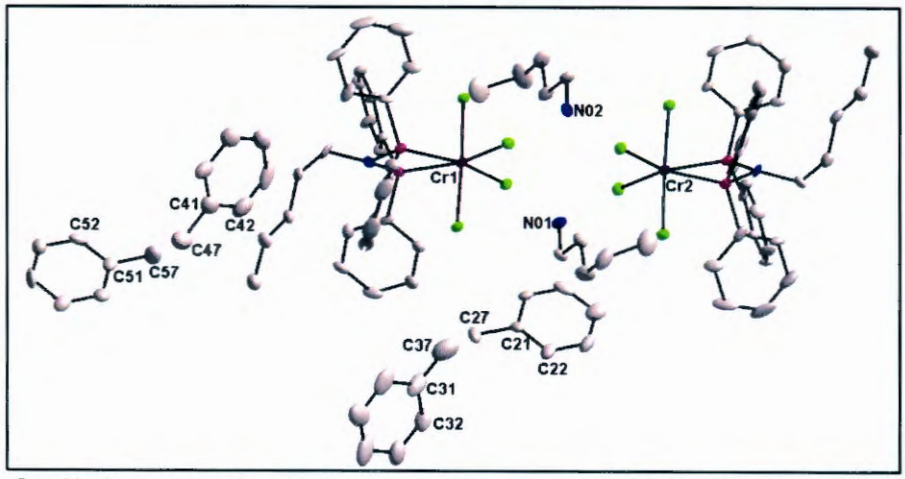

Figure 6.2: Graphical representation of the asymmetric unit [n-Pent-NH_3][$CrCl_4$(PNP-*n*-Pent)]·2C_7H_8 at 50% probability. (H-atoms were omitted for clarity.)

Figure 6.3 illustrates the numbering for the toluene solvate molecules and the non-coordinated pentylammonium molecules in the asymmetric unit.

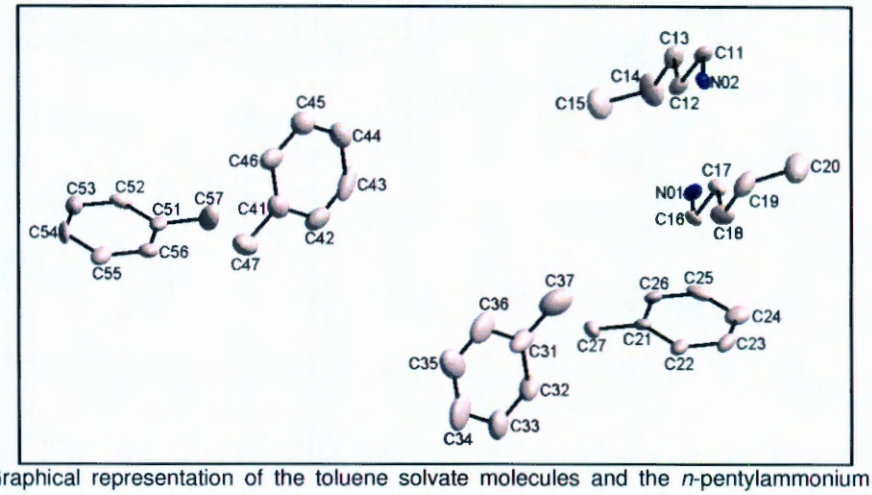

Figure 6.3: Graphical representation of the toluene solvate molecules and the *n*-pentylammonium [*n*-Pent-NH_3]$^+$ molecules in the asymmetric unit of the complex, [n-Pent-NH_3][CrCl4(PNP-*n*-Pent)]·2C_7H_8 at 50% probability. (H-atoms were omitted for clarity.)

The two independent chromium(III) complexes will be referred to as [$CrCl_4$(PNP-*n*-Pent)]$^-$ (16I) (molecule containing Cr1) (see **Figure 6.4a** and **b**) and [$CrCl_4$(PNP-*n*-Pent)]$^-$ (16II) (molecule containing Cr2), see **Figure 6.5a** and **b**.

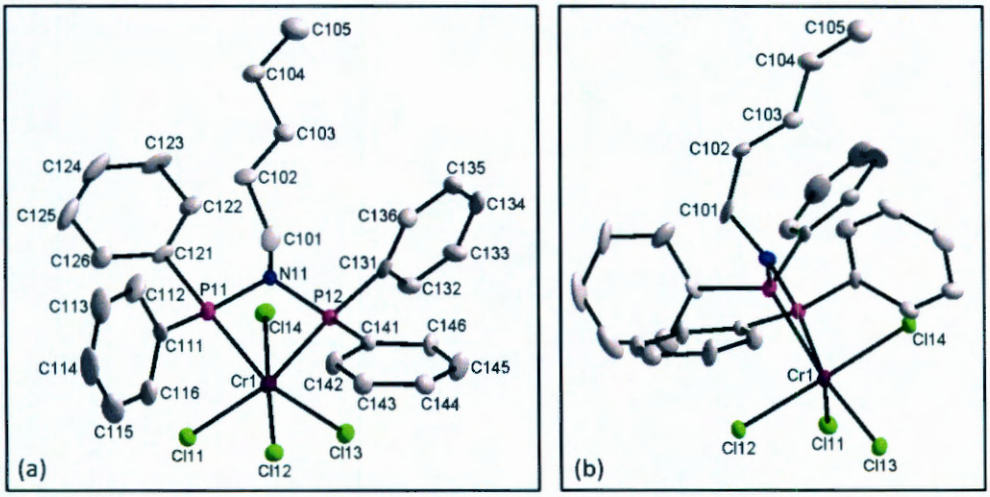

Figure 6.4 a and b: Graphical representation of different viewing angles of [$CrCl_4$(PNP-*n*-Pent)]$^-$ (I) (16I) at 50% probability. (H-atoms were omitted for clarity.)

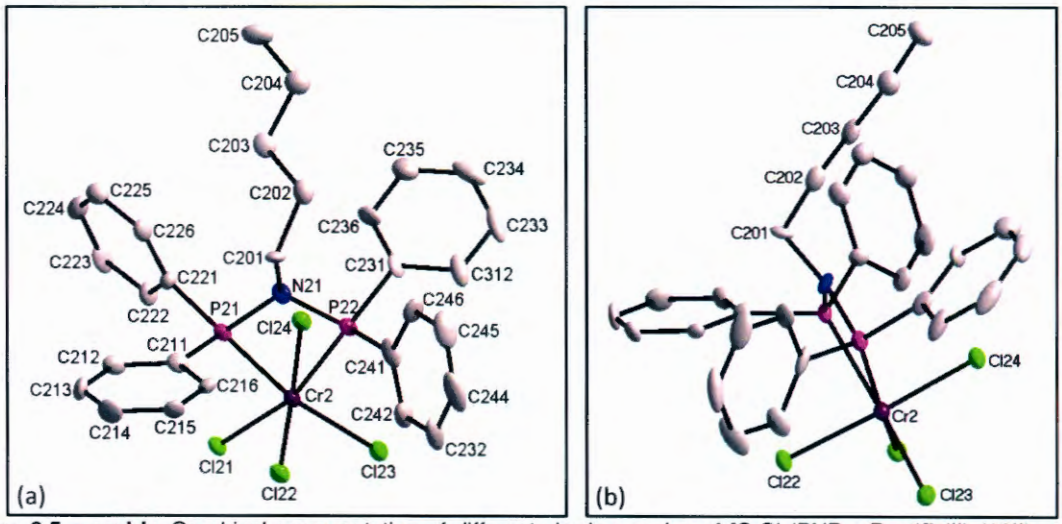

Figure 6.5 a and b: Graphical representation of different viewing angles of $[CrCl_4(PNP\text{-}n\text{-}Pent)]^-$ (II) (16II) at 50% probability. (H-atoms were omitted for clarity.)

Table 6.2: Selected bond angles (°) for $[CrCl_4(PNP\text{-}n\text{-}Pent)]^-$ (I) (16I) and (II) (16(II).

Atoms	Bond angle (°)	Atoms	Bond angle (°)
P11 – Cr1 – P12	66.7(1)	P21 – Cr2 – P22	66.9(1)
Cl11 – Cr1– Cl12	90.2(1)	Cl21 – Cr2– Cl22	90.2(1)
Cl13 – Cr1 – Cl14	89.9(1)	Cl23 – Cr2 – Cl24	89.9(1)
Cl12 – Cr1 – Cl14	177.3(1)	Cl22 – Cr1 – Cl24	177.3(1)
Cl13 – Cr1 – P11	163.8(1)	Cl23 – Cr2 – P21	163.1(1)
Cl11 – Cr1 – P12	163.0(1)	Cl21 – Cr2 – P22	163.9(1)
P11 – N11 – P12	106.0(3)	P21 – N21 – P22	106.6(4)
C101 – N11 – P11	125.2(6)	C201 – N21 – P21	124.1(5)
C101 – N11 – P12	125.2(5)	C201 – N21 – P22	124.7(6)
N11 – P11 – C111	107.5(3)	N21 – P21 – C211	104.6(4)
N11 – P11 – C121	107.8(4)	N21 – P21 – C221	112.1(4)
N11 – P12 – C131	110.9(3)	N21 – P22 – C231	107.1(3)
N11 – P12 – C141	104.594)	N21 – P22 – C241	107.8(3)
C111 – P11 – C121	101.5(4)	C211 – P21 – C221	102.8(4)
C131 – P12 – C141	101.7(4)	C231 – P22 – C241	102.0(4)

The $[CrCl_4(PNP\text{-}n\text{-}Pent)]^-$ (I) (16I) and (II) (16II) have distorted octahedral geometries at the chromium(III) centres with P-Cr-P angles 66.7(1) and 66.9(1) ° respectively (see **Table 6.2**). The small P-Cr-P bite angles of the coordinated ligands compress the P-N-P angles to 106.0(3) ° and 106.6(4) ° (for $[CrCl_4(PNP\text{-}n\text{-}Butyl)]^-$ (I) and (I) respectively). This illustrates the severe distortion at the nitrogen atoms from the ideal trigonal-planar angle expected at the sp^2-hybridized nitrogen atoms. The phosphorous atoms are also distorted from the ideal tetrahedral geometry with C-P-C angles varying from 101.5(4) to 102.8(4) ° for the two mono-anionic complexes.

Table 6.3: Selected bond lengths (Å) for $[CrCl_4(PNP\text{-}n\text{-}Pent)]^-$ (I) (16I) and (II) (16II).

Atoms	Bond length (Å)	Atoms	Bond length (Å)
Cr1 – P11	2.496(3)	Cr2 – P22	2.493(3)
Cr1 – P12	2.466(2)	Cr2 – P21	2.474(2)
Cr1 – Cl11	2.342(2)	Cr2 – Cl21	2.329(3)
Cr1 – Cl12	2.316(2)	Cr2 – Cl22	2.318(2)
Cr1 – Cl13	2.329(3)	Cr2 – Cl23	2.310(2)
Cr1 – Cl14	2.313(2)	Cr2 – Cl24	2.341(2)
N11 – C101	1.482(9)	N21 – C201	1.496(9)
N11 – P11	1.712(6)	N21 – P21	1.712(6)
N11 – P12	1.706(7)	N21 – P22	1.701(7)
P11 – C111	1.834(8)	P21 – C211	1.811(8)
P11 – C121	1.808(8)	P21 – C221	1.820(8)
P12 – C131	1.813(8)	P22 – C231	1.823(8)
P12 – C141	1.823(8)	P22 – C241	1.823(9)

The bond lengths are similar for $[CrCl_4(PNP\text{-}n\text{-}Pent)]^-$ (I) and (II) (see **Table 6.3**) within experimental error.

Table 6.4: Selected torsion angles (°) for $[CrCl_4(PNP\text{-}n\text{-}Pent)]^-$ (I) (16I) and (II) (16II).

Atoms	Torsion angle (°)	Atoms	Torsion angle (°)
Cr1 – P11 – C111 – C112	170.0(3)	Cr2 – P22 – C241 – C242	11.7(4)
Cr1– P11 – C121 – C122	-70.6(4)	Cr2 – P21 – C211 – C212	-114.1(3)
Cr1 – P12 – C131 – C132	-26.2(4)	Cr2 – P21 – C221 – C222	24.7(4)
Cr1 – P12 – C141 – C142	-64.1(4)	Cr2 – P22 – C231 – C232	-106.0(3)

The orientations of the phosphorous coordinated phenyl groups for the anionic complexes are described by the torsion angles in **Table 6.4**. It is clear from comparing the corresponding torsion angles that the phenyl rings are arranged differently for the two complexes, see **Figure 6.6** for a graphical representation of an overlay of $[CrCl_4(PNP\text{-}n\text{-}Pent)]^-$ (I) and (II) (with P11-Cr1-P12 placed on P21-Cr2-P22). Even though the orientations differ significantly for the two complexes, it still appears that both complexes adopted a variation of the 'fan-like' arrangement for the phenyl rings as described in Chapter 5.

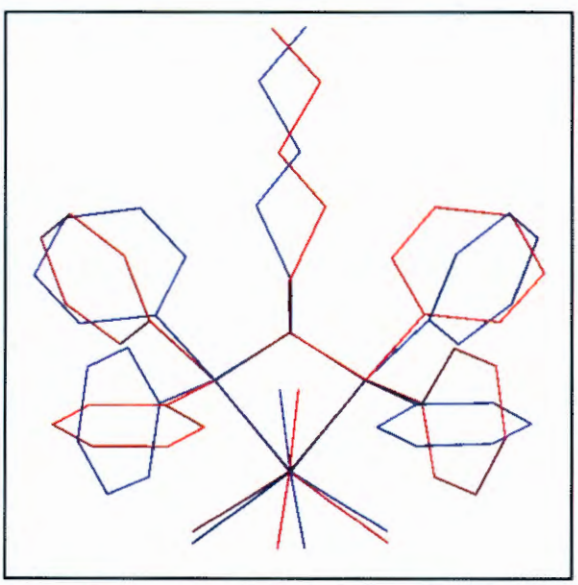

Figure 6.6: Graphical representation of an overlay of $[CrCl_4(PNP\text{-}n\text{-}Pent)]^-$ (I) (16I) (blue) and (II) (16II) (red).

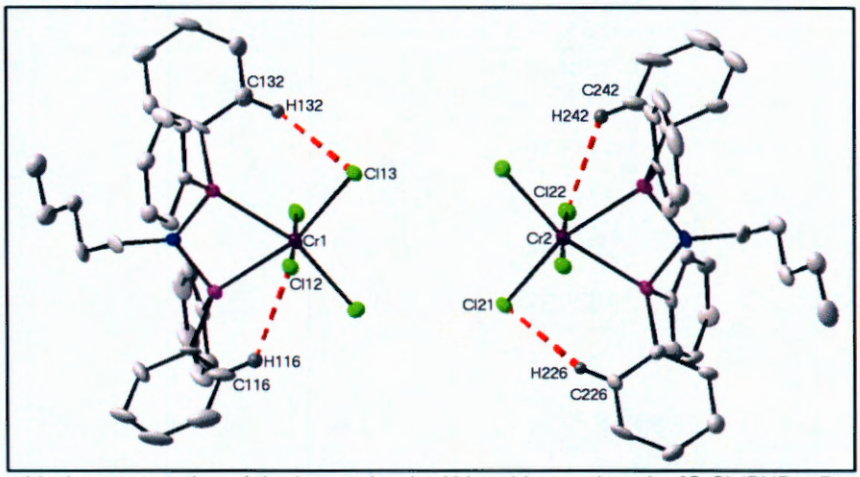

Figure 6.7: Graphical representation of the intramolecular H-bond interactions for $[CrCl_4(PNP\text{-}n\text{-}Pent)]^-$ (I) (16I) and (II) (16II) molecules at 50% probability. Only applicable H- atoms with relevance to the H-bond interactions are indicated. The red fragmented lines indicate the intramolecular hydrogen bonding interactions.

Intramolecular C-H···Cl hydrogen bonding interactions exist within both the $[CrCl_4(PNP\text{-}n\text{-}Pent)]^-$ complexes (see **Figure 6.7**). The relevant bond data is presented in **Table 6.5**.

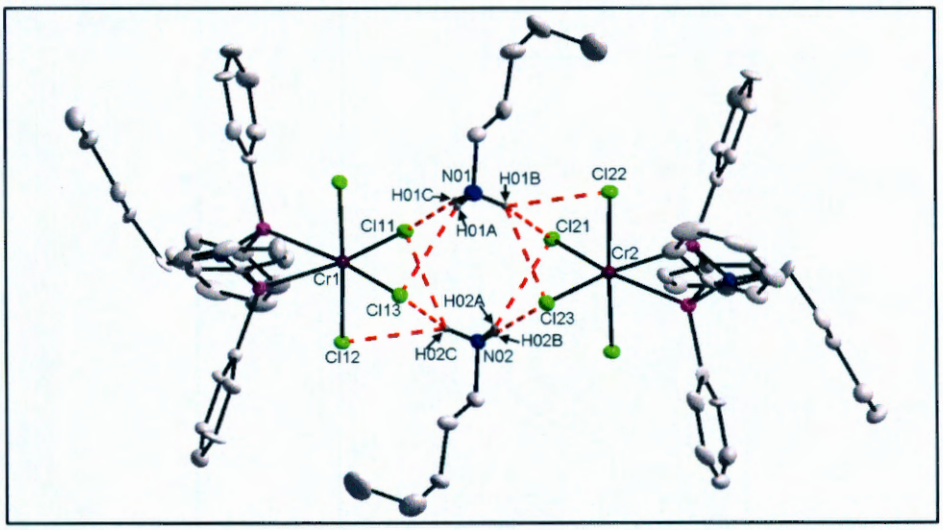

Figure 6.8: Graphical representation of the intermolecular H-bond interactions between two $[CrCl_4(PNP\text{-}n\text{-}Pent)]^-$ (I) (16II) and (II) (16II) within the asymmetric unit at 50% probability. Only applicable H atoms with relevance to the H-bond interactions are indicated. The red fragmented lines indicate the intermolecular hydrogen interactions.

There are multiple N-H···Cl hydrogen bonding interactions present between $[CrCl_4(PNP\text{-}n\text{-}Pent)]^-$ (I) and (II) and the two *n*-pentylammonium cations of the asymmetric unit (see **Figure 6.8**).

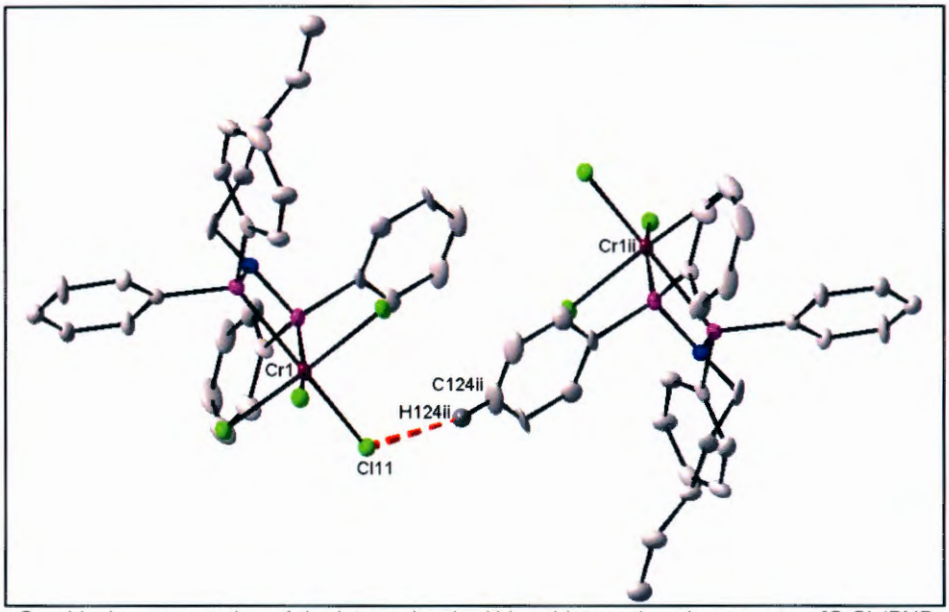

Figure 6.9: Graphical representation of the intermolecular H-bond interactions between two $[CrCl_4(PNP\text{-}n\text{-}Pent)]^-$ (I) (16l) complexes at 50% probability. Only applicable H atoms with relevance to the H-bond interactions are indicated. The red fragmented lines indicate the intermolecular hydrogen bonding interactions. ((ii) 1-x, 1-y, 1-z)

There is also a C-H···Cl intermolecular hydrogen bonding interaction observed between $[CrCl_4(PNP\text{-}n\text{-}Pent)]^-$ (I) complexes (see **Figure 6.9**).

The relevant bond data, including the interaction bond distances and angles, is presented in **Table 6.5**.

Table 6.5: Hydrogen bonds for $[CrCl_4(PNP\text{-}n\text{-}Pent)]^-$ (I) (16I) and (II) (16II) (Å and °).

D-H...A	d(D-H)	d(H...A)	D(D...A)	<(DHA)
N01-H01A...Cl13(i)	0.89	2.70	3.267	122
N01-H01B...Cl21(i)	0.89	2.69	3.292	126
N01-H01B...Cl22(i)	0.89	2.71	3.489	146
N01-H01B...Cl23(i)	0.89	2.80	3.456	131
N01-H01C...Cl11(i)	0.89	2.37	3.254	173
N02-H02A...Cl21(i)	0.89	2.71	3.287	123
N02-H02B...Cl23(i)	0.89	2.38	3.261	172
N02-H02C...Cl11(i)	0.89	2.82	3.465	131
N02-H02C...Cl12(i)	0.89	2.68	3.477	149
N02-H02C...Cl13(i)	0.89	2.71	3.288	123
C116-H116...Cl12(i)	0.93	2.63	3.36(1)	135
C124-H124...Cl11(ii)	0.93	2.75	3.64(1)	162
C132-H132...Cl13(i)	0.93	2.78	3.640(9)	154
C226-H226...Cl21(i)	0.93	2.81	3.66(9)	151
C242-H242...Cl22(i)	0.93	2.68	3.36(1)	131

Symmetry transformations used to generate equivalent atoms:
(i) (x, y, z), (ii) (1-x, 1-y, 1-z)

It appears that the packing of the $[NH_3\text{-Pentyl}][CrCl_4(PNP\text{-}n\text{-}Pent)]\cdot 2C_7H_8$ compounds to be largely influenced by the various intermolecular hydrogen bonding interactions between the cations, anionic complexes (see **Figure 6.10**). There appears to be no intermolecular hydrogen interactions between the toluene solvate molecules with one another or any of the cations or anionic complexes.

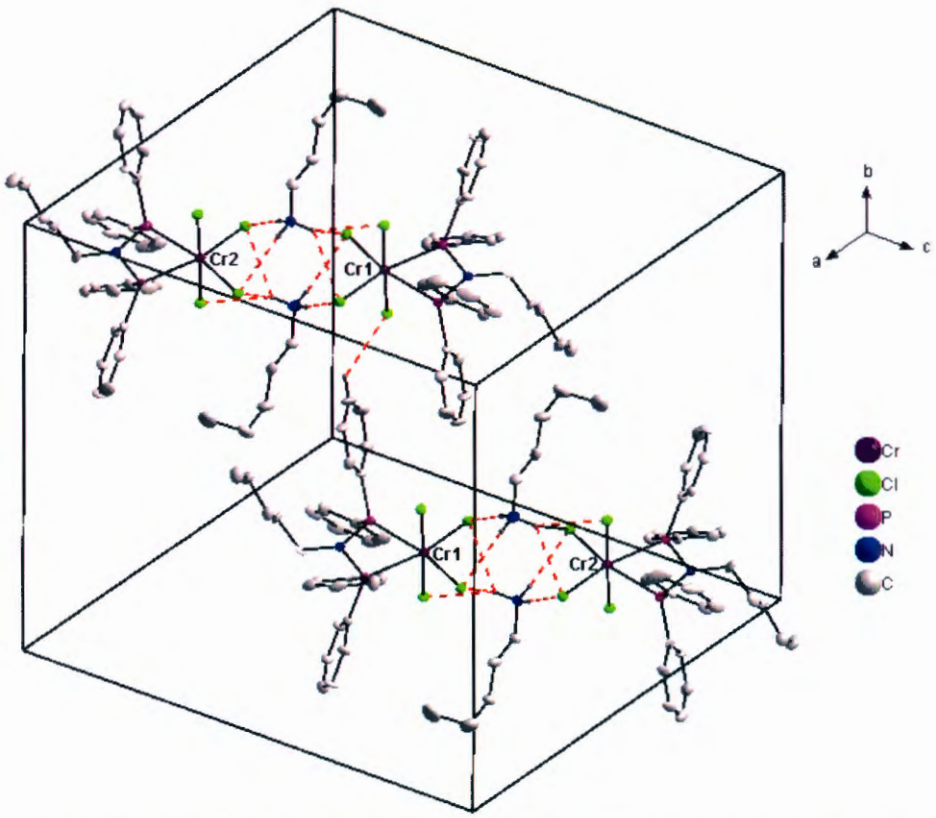

Figure 6.10: Perspective view of the unit cell of [*n*-Pent-NH_3][$CrCl_4$(PNP-*n*-Pent)]·2C_7H_8. H-atoms were omitted for clarity. Only applicable H atoms with relevance to the H-bond interactions are indicated. The solvate toluene molecules were omitted for clarity. The red fragmented lines indicate the intermolecular hydrogen bonding interactions.

6.2.2 [*i*-Pent-NH_3][$CrCl_4$(PNP-*i*-Pent)]·2C_7H_8

The title compound crystallizes in a triclinic crystal system in the $P\bar{1}$ spacegroup. The asymmetric unit of the crystal structure for [*i*-Pent-NH_3][$CrCl_4$(PNP-*i*-Pent)]·2C_7H_8 contains two mono-anionic chromium(III)-complexes, two non-coordinated isopentylammonium cations and four toluene solvate molecules. One of the isopentylammonium cations and a toluene molecule are disordered (50% occupancy for both disorders).

The asymmetric unit is presented in **Scheme 6.2** as a two-dimensional presentation for clarity. The molecular diagram is presented in **Figure 6.10**.

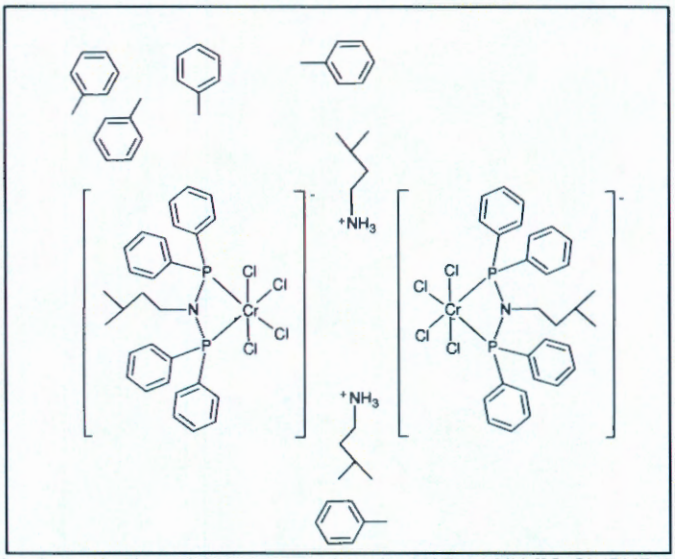

Scheme 6.2: A schematic view of the asymmetric unit of [*i*-Pent-NH_3][$CrCl_4$(PNP-*i*-Pent)]$2C_7H_8$.

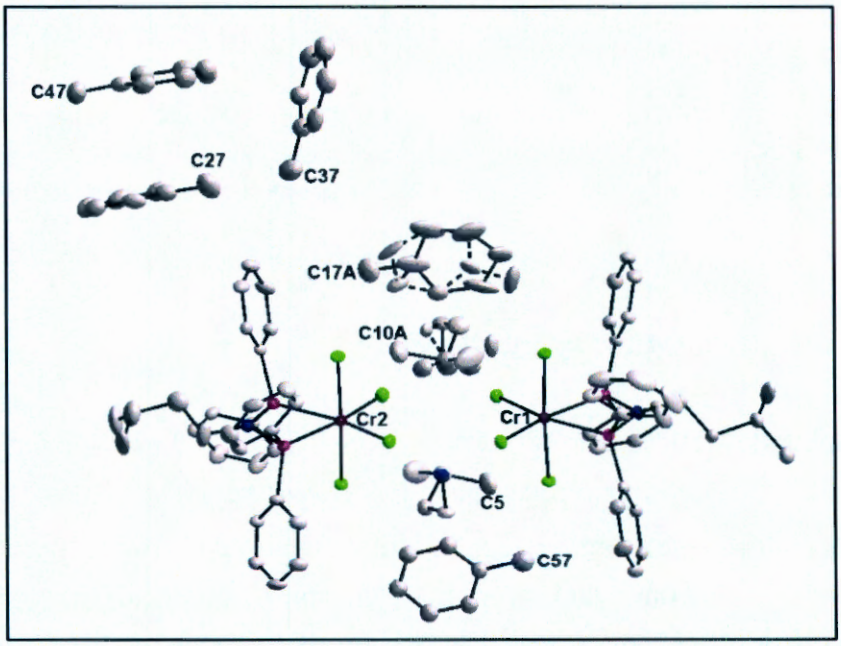

Figure 6.11: Graphical representation of [*i*-Pent-NH_3][$CrCl_4$(PNP-*i*-Pent)]$2C_7H_8$ at 50% probability. (H-atoms were omitted for clarity).

The 50% occupancy disorder of the isopentylammonium cation (containing N02) is illustrated in **Figure 6.12**.

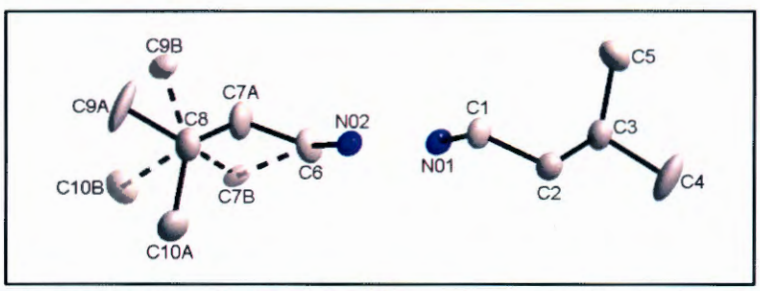

Figure 6.12: Graphical representation of the isopentylammonium molecules in the asymmetric unit of [*i*-Pent-NH_3][$CrCl_4$(PNP-*i*-Pent)]·2C_7H_8 at 50% probability. A/B indicates the disordered carbon atoms in the isopentyl alkyl group. Disordered parts belonging together are numbered A and B respectively. (H-atoms were omitted for clarity.)

The 50% occupancy disorder of one of the toluene molecules (molecule containing C17A and B) is presented in **Figure 6.13**. The numbering schemes of the other toluene solvate molecules are also illustrated in **Figure 6.13**.

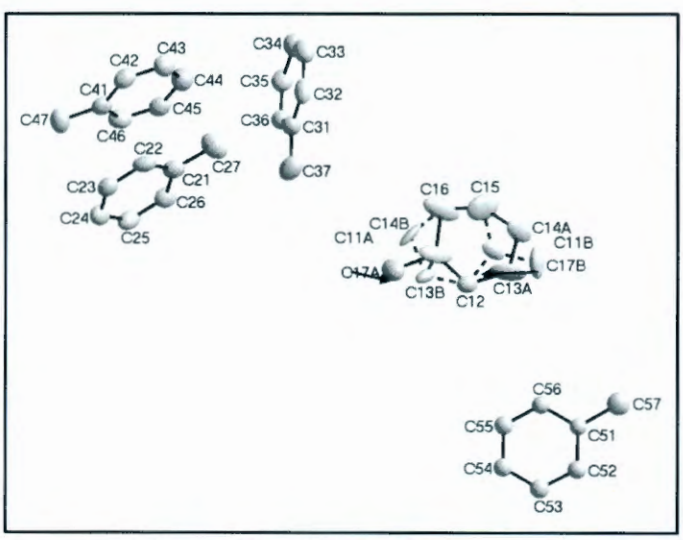

Figure 6.13: Graphical representation of the toluene solvato molecules in the asymmetric unit of [*i*-Pent-NH_3][$CrCl_4$(PNP-*i*-Pent)]·2C_7H_8 at 50% probability. A/B indicates the disordered carbon atoms in the. Disordered parts belonging together are numbered A and B respectively. (H-atoms were omitted for clarity.)

The two $[CrCl_4(PNP\text{-}i\text{-}Pent)]^-$ complexes in the asymmetric unit are referred to as $[CrCl_4(PNP\text{-}i\text{-}Pent)]^-$ (I) (17I) (molecule containing Cr1, see **Figure 6.14a** and **b**) and $[CrCl_4(PNP\text{-}i\text{-}Pent)]^-$ (II) (17II) (molecule containing Cr2, see **Figure 6.15a** and **b**).

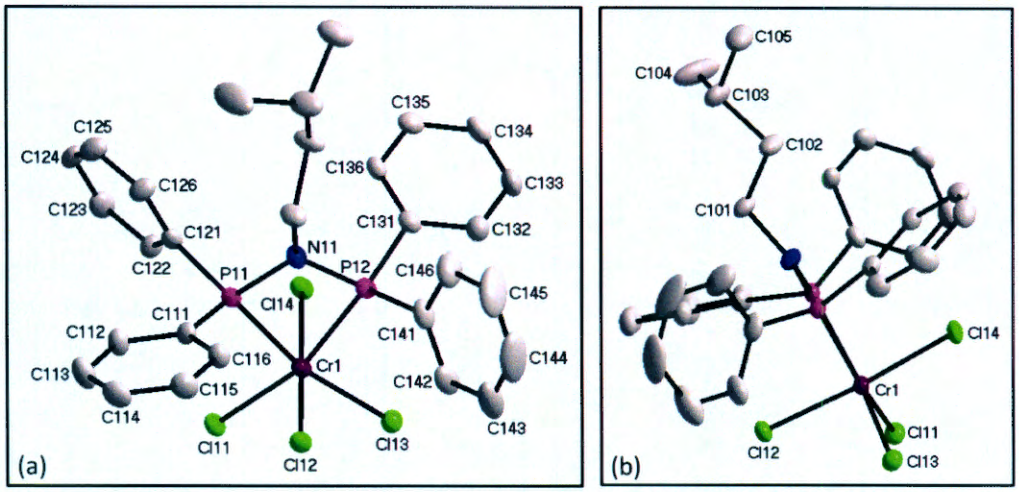

Figure 6.14 a and b: Graphical representation of different viewing angles of $[CrCl_4(PNP\text{-}i\text{-}Pent)]^-$ (I) (17I) at 50% probability. (H-atoms were omitted for clarity.)

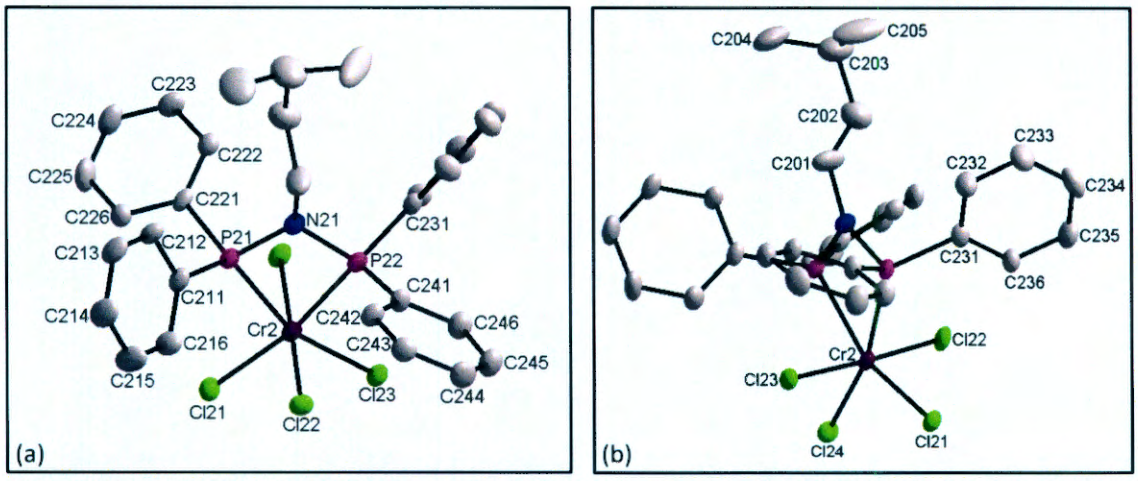

Figure 6.15 a and b: Graphical representation of different viewing angles of $[CrCl_4(PNP\text{-}i\text{-}Pent)]^-$ (II) (17II) at 50% probability. (H-atoms were omitted for clarity.)

Table 6.6: Selected bond angles (°) for $[CrCl_4(PNP\text{-}i\text{-}Pent)]^-$ (I) (17I) and (II) (17II).

Atoms	Bond angle (°)	Atoms	Bond angle (°)
P11 – Cr1 – P12	67.1(1)	P21 – Cr2 – P22	66.8(1)
Cl11 – Cr1– Cl12	90.6(1)	Cl21 – Cr2– Cl22	90.5(1)
Cl13 – Cr1 – Cl14	91.5(1)	Cl23 – Cr2 – Cl24	91.2(1)
Cl12 – Cr1 – Cl14	175.9(1)	Cl22 – Cr1 – Cl24	177.6(1)
Cl13 – Cr1 – P11	163.1(1)	Cl23 – Cr2 – P21	159.8(1)
Cl11 – Cr1 – P12	163.1(1)	Cl21 – Cr2 – P22	165.3(1)
P11 – N11 – P12	106.5(2)	P21 – N21 – P22	105.9(2)
C101 – N11 – P11	124.7(3)	C201 – N21 – P22	124.5(3)
C101 – N11 – P12	127.2(3)	C201 – N21 – P21	128.2(4)
N1 – P11 – C111	106.6(2)	N21 – P21 – C211	107.1(2)
N1 – P11 – C121	109.9(2)	N21 – P21 – C221	109.1(2)
N1 – P12 – C131	109.5(2)	N21 – P22 – C231	108.4(2)
N1 – P12 – C141	109.0(2)	N21 – P22 – C241	107.5(2)
C111 – P11 – C121	102.3(2)	C211 – P21 – C221	102.4(2)
C131 – P12 – C141	102.3(2)	C231 – P22 – C241	103.5(2)

The bond angles of $[CrCl_4(PNP\text{-}i\text{-}Pent)]^-$ (I) and (II) are similar within experimental error (see **Table 6.6**).

The P-Cr-P bite angles of $[CrCl_4(PNP\text{-}i\text{-}Pent)]^-$ (I) and (II) (66.8(1) and 67.1(1) ° respectively) are significantly smaller than 90 ° of an ideal octahedral geometry at the chromium(III) centre. The strain experienced in the complexes is further illustrated by the distorted geometries at the nitrogen atoms with angles that range between 105.9(2) (P21-N21-P22) and 128.2(4) ° (C201-N21-P21) for both chromium(III) complexes. The C-P-C angles range between 102.3(2) and 103.5(2) ° for the two anionic complexes.

Table 6.7: Selected bond lengths (Å) for $[CrCl_4(PNP\text{-}i\text{-}Pent)]^-$ (I) (17I) and (II) (17II).

Atoms	Bond length (Å)	Atoms	Bond length (Å)
Cr1 – P11	2.462(2)	Cr2 – P22	2.458(2)
Cr1 – P12	2.470(1)	Cr2 – P21	2.480(1)
Cr1 – Cl11	2.335(1)	Cr2 – Cl21	2.328(2)
Cr1 – Cl12	2.316(2)	Cr2 – Cl22	2.317(2)
Cr1 – Cl13	2.326(2)	Cr2 – Cl23	2.324(1)
Cr1 – Cl14	2.298(1)	Cr2 – Cl24	2.298(1)
N11 – C101	1.478(5)	N21 – C201	1.475(6)
N11 – P11	1.701(4)	N21 – P21	1.697(4)
N11 – P12	1.702(4)	N21 – P22	1.709(4)
P11 – C111	1.808(5)	P21 – C211	1.816(5)
P11 – C121	1.806(5)	P21 – C221	1.809(5)
P12 – C131	1.816(5)	P22 – C231	1.813(5)
P12 – C141	1.811(5)	P22 – C241	1.810(5)

The corresponding angles for $[CrCl_4(PNP\text{-}i\text{-}Pent)]^-$ (I) and (II) are similar within experimental error (see **Table 6.7**).

Table 6.8: Selected torsion angles (°) for $[CrCl_4(PNP\text{-}i\text{-}Pent)]^-$ (I) (17I) and (II) (17II).

Atoms	Torsion angle (°)	Components	Torsion angle (°)
Cr1 – P11 – C111 – C112	-106.4(4)	Cr2 – P21 – C221 – C222	-78.4(4)
Cr1– P11 – C121 – C122	19.3(5)	Cr2 – P21 – C211 – C212	174.0(3)
Cr1 – P12 – C131 – C132	-101.4(4)	Cr2 – P22 – C241 – C242	-82.0(4)
Cr1 – P12 – C141 – C142	16.6(5)	Cr2 – P22 – C231 – C232	-179.1(3)

It is evident from the corresponding torsion angles in **Table 6.8** that the arrangements of the phenyl rings for the two anionic complexes are significantly different. Different variations of the 'fan-like' arrangement of the rings are however adopted for both complexes. **Figure 6.16** displays an overlay of $[CrCl_4(PNP\text{-}i\text{-}Pent)]^-$ (I) and (II), (with

P11-Cr1-P12 placed on P21-Cr2-P22) illustrating the differences between the anionic complexes .

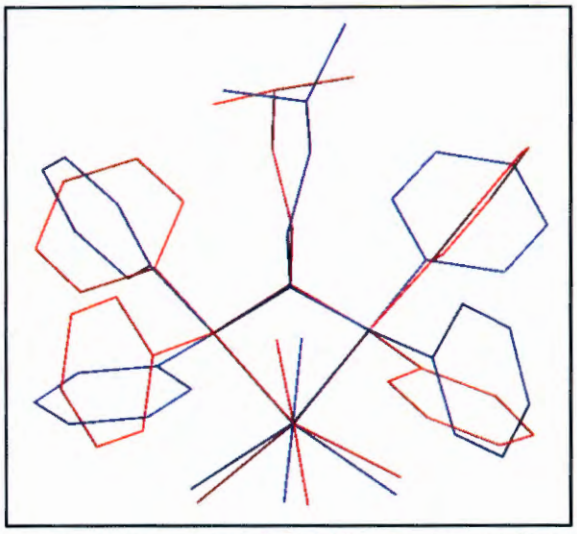

Figure 6.16: Graphical representation of an overlay of $[CrCl_4(PNP\text{-}n\text{-}Pent)]^-$ (I) (17II) (blue) and (II) (17II) (red).

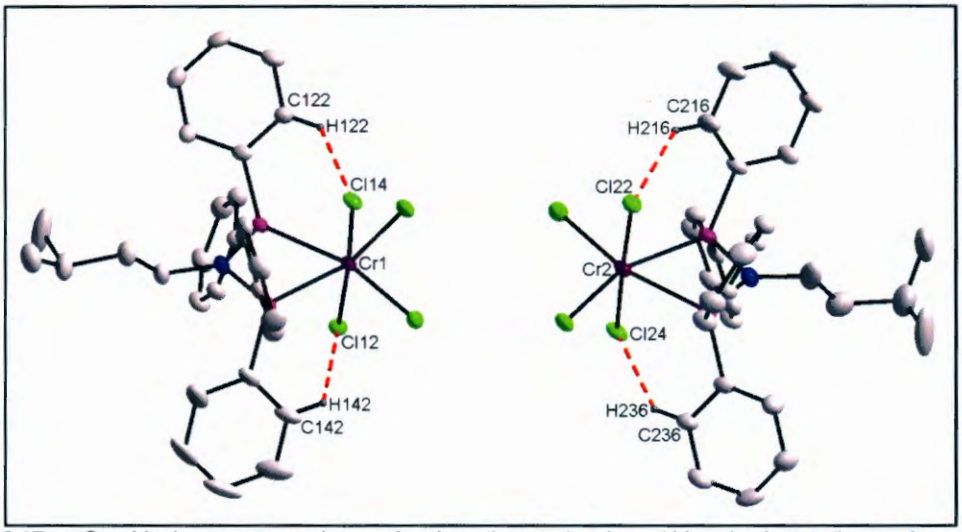

Figure 6.17: Graphical representation of the intramolecular H-bond interactions for the two $[CrCl_4(PNP\text{-}i\text{-}Pent)]^-$ molecules at 50% probability. Only applicable H atoms with relevance to the H-bond interactions are indicated. The red fragmented lines indicate the intramolecular hydrogen interactions.

Intramolecular C-H···Cl hydrogen bonding interactions exist within both the $[CrCl_4(PNP\text{-}i\text{-}Pent)]^-$ complexes (see **Figure 6.17**). The bond distances and angles for the hydrogen bonding interactions are presented in **Table 6.9**.

Table 6.9: Hydrogen bonds for $[CrCl_4(PNP\text{-}i\text{-}Pent)]^-$ (I) (17I) and (II) (17II) (Å and °).

D-H...A	d(D-H)	d(H...A)	D(D...A)	<(DHA)
C112-H112...Cl14(i)	0.93	2.73	3.346(5)	125
C142-H142...Cl12(i)	0.93	2.75	3.335(6)	122
C216-H216...Cl22(i)	0.93	2.67	3.414(6)	138
C236-H236...Cl24(i)	0.93	2.65	3.405(6)	139

Symmetry transformations used to generate equivalent atoms:

(i) (x, y, z)

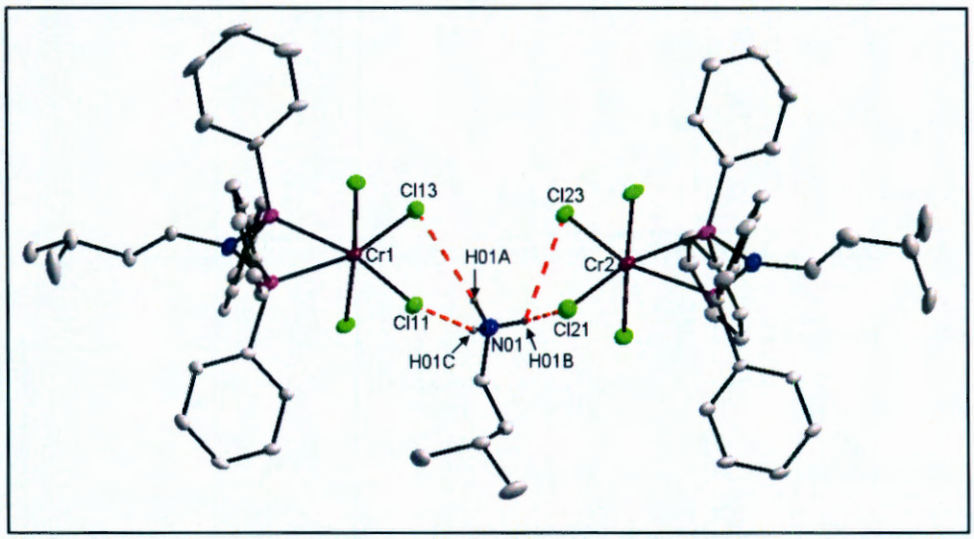

Figure 6.18: Graphical representation of the intermolecular H-bond interactions between an isopentylammonium and $[CrCl_4(PNP\text{-}i\text{-}Pent)]^-$ (I) (17I) and (II) (17II) (50% probability for all atoms). Only applicable H atoms with relevance to the H-bond interactions are indicated. The red fragmented lines indicate the intermolecular hydrogen interactions.

The N-H···Cl intermolecular hydrogen bonding interactions between the complexes $[CrCl_4(PNP\text{-i-Pent})]^-$ (I), (II) and one of the isopentylammonium cation (cation containing N01) is illustrated in **Figure 6.18**, the hydrogen bond distances and angles are presented in **Table 6.10**.

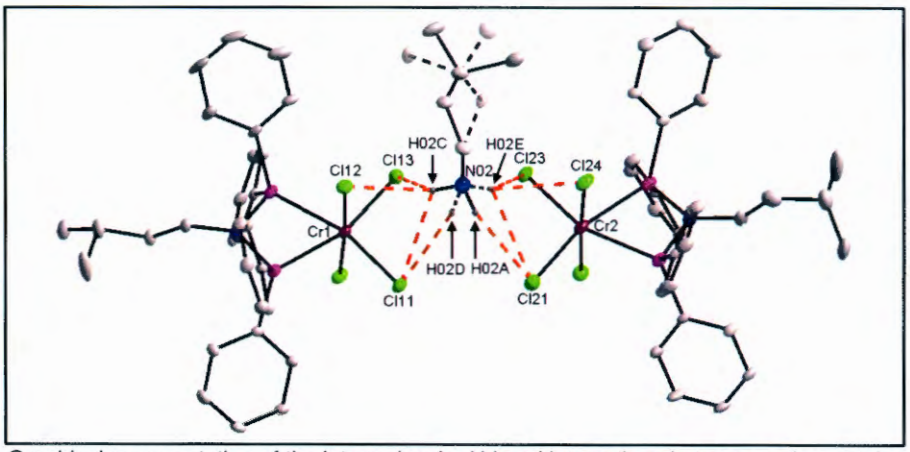

Figure 6.19: Graphical representation of the intermolecular H-bond interactions between an isopentylammonium and $[CrCl_4(PNP\text{-}i\text{-}Pent)]^-$ molecule (I) (17I) and (II) (17II) (50% probability) for all atoms. Only applicable H atoms with relevance to the H-bond interactions are indicated. The red fragmented lines indicate the intermolecular hydrogen interactions.

Additonal N-H···Cl hydrogen interactions exist between the two isopentylammonium cations and the $[CrCl_4(PNP\text{-}i\text{-}Pent)]^-$ (I) and (II) molecules in the asymmetric unit (see **Figure 6.19**). A list of H-bond interactions is given in **Table 6.10**.

Table 6.10: Hydrogen bond for $[i\text{-}Pent\text{-}NH_3][CrCl_4(PNP\text{-}i\text{-}Pent)]\cdot 2C_7H_8$ (Å and °).

D-H...A	d(D-H)	d(H...A)	D(D...A)	<(DHA)
N02A-H02A...Cl21(i)	0.89	2.74	3.428	135
N02A-H02B...Cl23(i)	0.89	2.41	3.265	161
N02A-H02C...Cl12(i)	0.89	2.53	3.334	150
N02A-H02C...Cl13(i)	0.89	2.72	3.322	126
N02A-H02D...Cl11(i)	0.89	2.73	3.394	132
N02A-H02E...Cl23(i)	0.89	2.63	3.265	130
N02A-H02E...Cl24(i)	0.89	2.67	3.453	148
N02A-H02F...Cl13(i)	0.89	2.47	3.322	160
N01-H01A...Cl13(i)	0.89	2.64	3.381	141
N01-H01A...Cl21(i)	0.89	2.78	3.316	120
N01-H01A...Cl22(i)	0.89	2.48	3.312	156
N01-H01A...Cl23(i)	0.89	2.80	3.343	120
N01-H01A...Cl11(i)	0.89	2.40	3.239	158

Symmetry transformations used to generate equivalent atoms

(i) (x, y, z)

It appears that the intermolecular hydrogen bonding interactions between the $[CrCl_4(PNP\text{-}i\text{-}Pent)]^-$ molecules and the cationic isopentylammonium molecules have a significant effect on the packing of $[i\text{-}Pent\text{-}NH_3][CrCl_4(PNP\text{-}i\text{-}Pent)]\cdot 2C_7H_8$ in solid state (see **Figure 6.20**). The chromium(III) complexes and the isopentylammonium molecules are packed in diagonal layers across the ac plane. The toluene solvato molecules fill the spaces in between the layers.

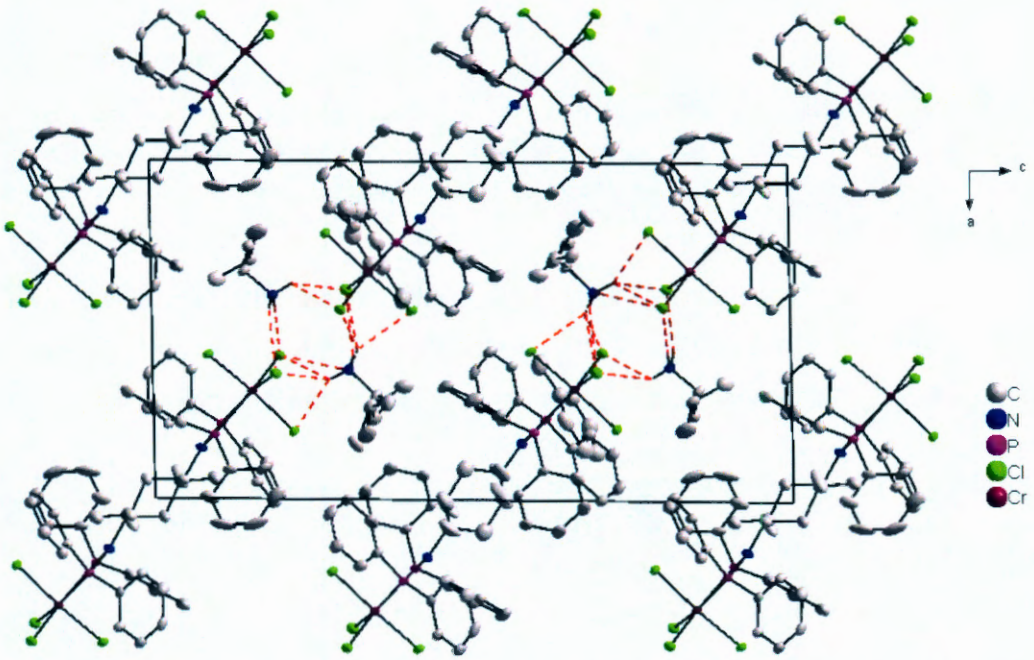

Figure 6.20: Perspective view of the unit cell of $[i\text{-}Pent\text{-}NH_3][CrCl_4(PNP\text{-}i\text{-}Pent)]\cdot 2C_7H_8$ along the b axis at 50% probability. H-atoms were omitted for clarity. Only applicable H atoms with relevance to the H-bond interactions are indicated. The solvate toluene molecules were omitted for clarity. The red fragmented lines indicate the intermolecular hydrogen bonding interactions.

6.2.3 $[n\text{-Butyl-}NH_3][CrCl_4(PNP\text{-}n\text{-Butyl})]\cdot 2C_7H_8$

The title compound crystallizes in a triclinic crystal system in the $P\bar{1}$ spacegroup. The asymmetric unit of the crystal structure for the title compound contains four independent mono-anionic chromium(III)-complexes, four *n*-butylammonium cations and eight

toluene solvate molecules. The asymmetric unit of is presented in **Scheme 6.3** as a two-dimensional scheme for clarity, while a molecular diagram is presented in **Figure 6.21**.

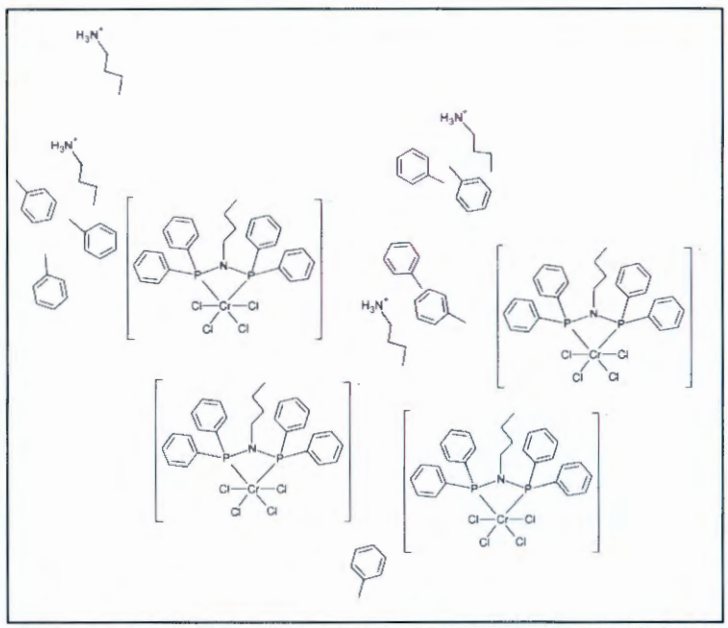

Scheme 6.3: Two dimensional representation of the asymmetric of [*n*-Butyl-NH_3][$CrCl_4$(PNP-*n*-Butyl)]·2C_7H_8.

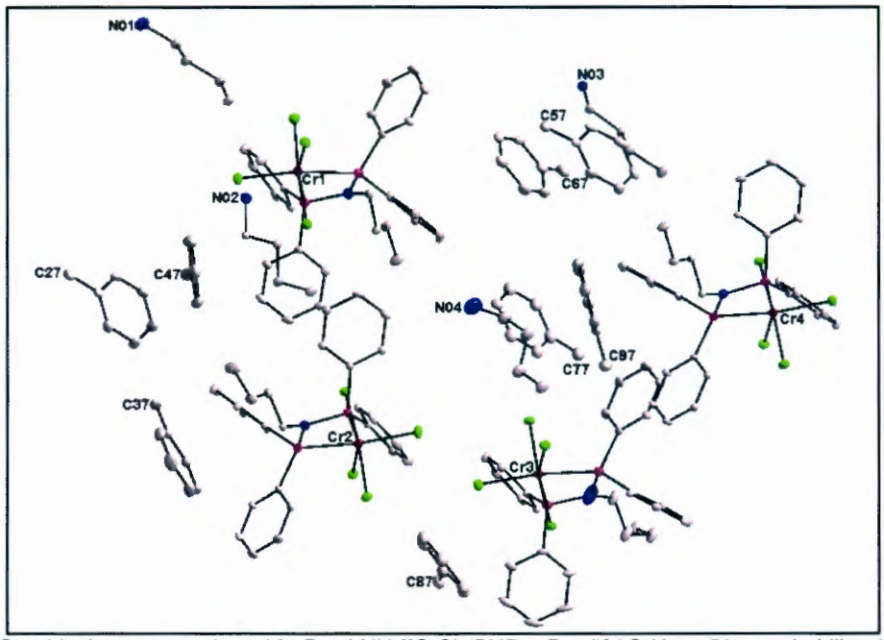

Figure 6.21: Graphical representation of [*n*-Butyl-NH_3][$CrCl_4$(PNP-*n*-Butyl)]·2C_7H_8 at 50% probability. (H-atoms were omitted for clarity).

The numbering of the non-coordinated butylammonium cations and the toluene solvato molecules are illustrated in **Figure 6.22**.

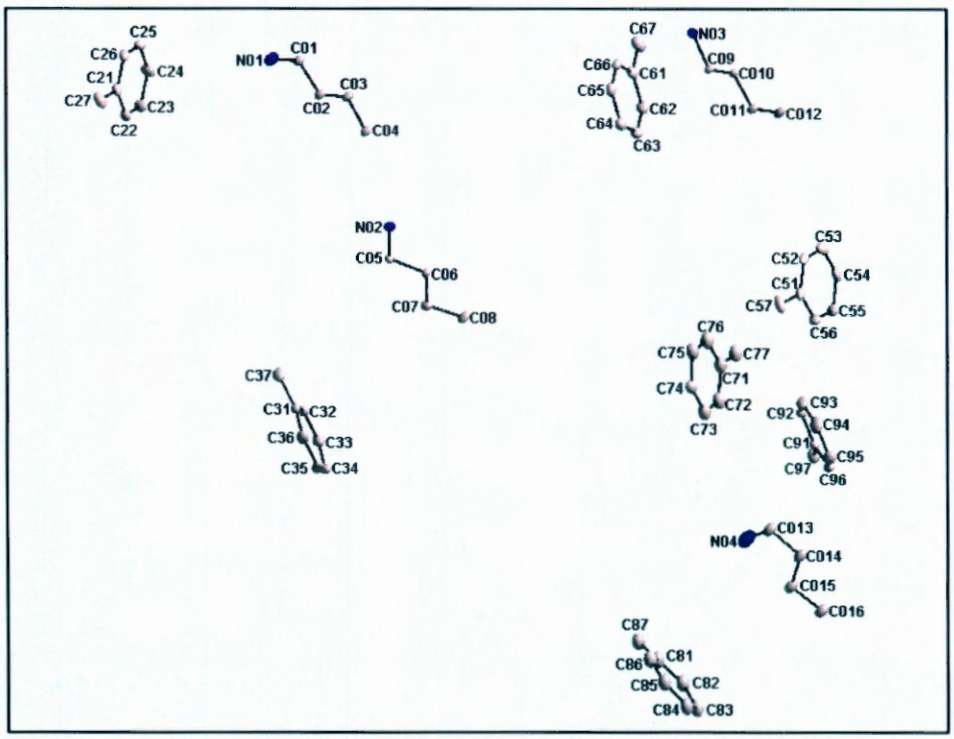

Figure 6.22: Graphical representation of the toluene solvato molecules and the *n*-butylammonium molecules in the asymmetric unit of [*n*-Butyl-NH_3][$CrCl_4$(PNP-*n*-Butyl)]·2C_7H_8 at 50% probability. (H-atoms were omitted for clarity.)

The four independent chromium(III) anionic complexes in the asymmetric unit will be referred to as [$CrCl_4$(PNP-*n*-Butyl)]$^-$ (I) (18I) (see **Figure 6.23)**, (II) (18II), (III) (18II) and (IV) (18IV) (molecules containing atoms Cr1, Cr2, Cr3 and Cr4 respectively).

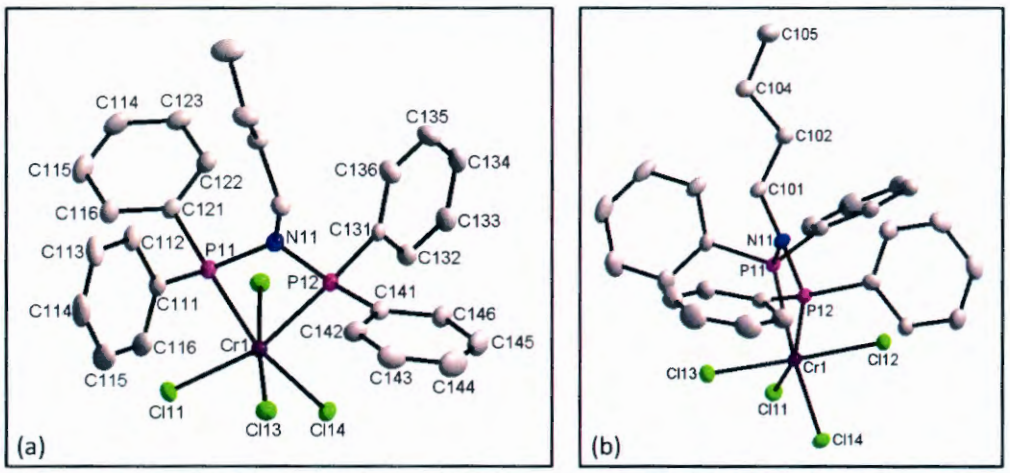

Figure 6.23a and b: Graphical representation of different viewing angles of $[CrCl_4(PNP\text{-}n\text{-}Butyl)]^-$ (I) (18I) at 50% probability. (H-atoms were omitted for clarity.)

Table 6.11: Selected bond angles (°) for $[CrCl_4(PNP\text{-}n\text{-}Butyl)]^-$ (I) (18I), $[CrCl_4(PNP\text{-}n\text{-}Butyl)]^-$ (II) (18II), $[CrCl_4(PNP\text{-}n\text{-}Butyl)]^-$ (III) (18III) and $[CrCl_4(PNP\text{-}n\text{-}Butyl)]^-$ (IV) (18IV).

Atoms	18I (°)	18II (°)	18III (°)	18IV (°)
Pn1 – Crn – Pn2	66.9(1)	66.9(1)	67.2(1)	67.1(1)
Cln1 – Crn– Cln2	92.2(1)	92.5(1)	90.5(1)	91.8(1)
Cln3 – Crn – Cln4	90.2(1)	89.5(1)	92.8(1)	90.2(1)
Pn1 – Nn1 – Pn2	105.3(2)	105.2(2)	106.1(2)	105.4(2)
Cn01 – Nn1 – Pn1	125.2(3)	125.7(3)	127.1(4)	125.7(3)
Cn01 – Nn1 – Pn2	127.0(3)	126.0(3)	125.3(4)	127.2(3)
Nn1 – Pn1 – Cn11	108.2(2)	106.6(2)	108.3(2)	106.4(2)
Nn1 – Pn1 – Cn21	107.9(2)	109.8(2)	108.6(3)	110.0(2)
Nn1 – Pn2 – Cn31	109.8(2)	108.3(2)	110.3(2)	108.1(2)
Nn1 – Pn2 – Cn41	106.5(2)	107.8(2)	105.6(2)	108.9(2)
Cn11 – Pn1 – Cn21	104.0(2)	104.8(2)	103.6(2)	102.8(2)
Cn31 – Pn2 – Cn41	103.7(2)	103.0(2)	103.6(2)	104.4(2)

n = 1/ 2/ 3/ 4 for $[CrCl_4(PNP\text{-}n\text{-}Butyl)]^-$ (I), (II), (III) and (IV) respectively.

The four mono anionic chromium complexes ($[CrCl_4(PNP\text{-}n\text{-}Butyl)]^-$ (I), (II), (III) and (IV)) in the asymmetric unit have similar bond angles and distances (see **Table 6.11** and

6.12). All four chromium(III) complexes display distorted octahedral geometries at the respective chromium(III) centres, this is evident from the small bite angles P-Cr-P (66.9(1), 66.9(1), 67.2(1) and 67.1(1) ° for $[CrCl_4(PNP\text{-}Butyl)]^-$ (I), (II), (III) and (IV) respectively). The coordination of the diphosphinoamine ligands for the respective complexes forces the P-N-P angles which range between 105.2(2) and 106.1(2) ° for the four monomeric complexes to close and the geometry at the nitrogen atom is consequently distorted from its ideal geometry. The strain experienced by the anionic complex is further illustrated by the distortion of the tetrahedral geometry at the phosphorous atoms with C-P-C angles that range from 102.8(2) to 104.8(2) ° for the four anionic complexes.

Table 6.12: Selected bond lengths (Å) for $[CrCl_4(PNP\text{-}n\text{-}Butyl)]^-$ (I) (18I), $[CrCl_4(PNP\text{-}n\text{-}Butyl)]^-$ (II) (18II), $[CrCl_4(PNP\text{-}n\text{-}Butyl)]^-$ (III) (18III) and $[CrCl_4(PNP\text{-}n\text{-}Butyl)]^-$ (IV) (18IV).

Atoms	(18I) (Å)	(18II) (Å)	(18III) (Å)	(18IV) (Å)
Crn – Pn1	2.458(1)	2.457(1)	2.453(1)	2.457(1)
Crn – Pn2	2.461(1)	2.461(1)	2.461(2)	2.461(1)
Crn– Cln1	2.313(1)	2.297(1)	2.316(1)	2.312(1)
Crn – Cln2	2.304(1)	2.317(1)	2.344(1)	2.324(1)
Crn – Cln3	2.307(1)	2.351(1)	2.317(12)	2.324(1)
Crn – Cln4	2.335(1)	2.301(1)	2.302(1)	2.327(1)
Nn1 – Cn01	1.474(6)	1.482(6)	1.482(7)	1.475(6)
Nn1 – Pn1	1.712(4)	1.697(4)	1.702(5)	1.701(4)
Nn1 – Pn2	1.699(4)	1.714(4)	1.700(5)	1.705(4)
Pn1 – Cn11	1.817(4)	1.810(5)	1.812(4)	1.811(5)
Pn1 – Cn21	1.813(5)	1.814(5)	1.810(5)	1.813(5)
Pn2 – Cn31	1.813(5)	1.807(5)	1.818(5)	1.804(5)
Pn2 – Cn41	1.808(5)	1.808(4)	1.807(5)	1.811(4)

n = 1/ 2/ 3/ 4 for $[CrCl_4(PNP\text{-}n\text{-}Butyl)]^-$ (I), (II), (III) and (IV) respectively.

The corresponding bond lengths for the four chromium(III) complexes are similar within experimental error, see **Table 6.12**.

Table 6.13: Selected torsion angles (°) for $[CrCl_4(PNP\text{-}n\text{-}Butyl)]^-$ (I) (18I), $[CrCl_4(PNP\text{-}n\text{-}Butyl)]^-$ (II) (18II), $[CrCl_4(PNP\text{-}n\text{-}Butyl)]^-$ (III) (18III) and $[CrCl_4(PNP\text{-}n\text{-}Butyl)]^-$ (IV) (18IV).

Atoms	(18I) (°)	(18II) (°)	(18III) (°)	(18IV) (°)
Crn-Pn1-Cn11-Cn12	176.9(1)	-110.1(1)	172.8(1)	-110.7(1)
Crn-Pn1-Cn21-Cn22	-75.1(1)	-135.8(1)	-78.3(1)	-144.5(1)
Crn-Pn2-Cn31-Cn32	-43.8(1)	-91.5(1)	-34.0(1)	-93.3(1)
Crn-Pn2-Cn41-Cn42	-65.8(1)	4.5(1)	-62.3(1)	17.1(1)

n = 1/ 2/ 3/ 4 for $[CrCl_4(PNP\text{-}n\text{-}Butyl)]^-$ (I), (II), (III) and (IV) respectively.

The torsion angles for the four independent $[CrCl_4(PNP\text{-}n\text{-}Butyl]^-$ molecules in the asymmetric unit (see **Table 6.13**) indicate that $[CrCl_4(PNP\text{-}n\text{-}Butyl]^-$ (I) and (III) have similar orientations for the respective phenyl rings. An overlay of $[CrCl_4(PNP\text{-}n\text{-}Butyl]^-$ (I) and (III) (with P11-Cr1-P12 placed on P31-Cr3-P32) is presented in **Figure 6.25**. The ring orientations for $[CrCl_4(PNP\text{-}n\text{-}Butyl]^-$ (II) and (IV) are also similar with similar torsion angles for the corresponding rings, this similarity is further illustrated by the overlay of the two molecules (with P21-Cr2-P22 placed on P41-Cr4-P42) in **Figure 6.26**. The orientations of the phenyl rings of all four molecules are slight variations of the 'fan-like' arrangements as described before.

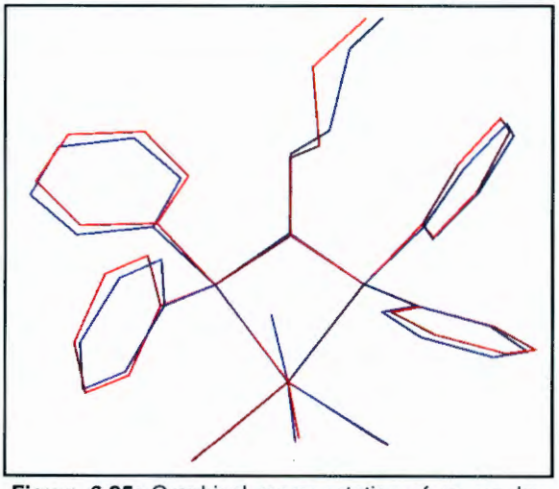

Figure 6.25: Graphical representation of an overlay of $[CrCl_4(PNP\text{-}n\text{-}Butyl)]^-$ (I) (18I) (blue) and (III) (18III) (red).

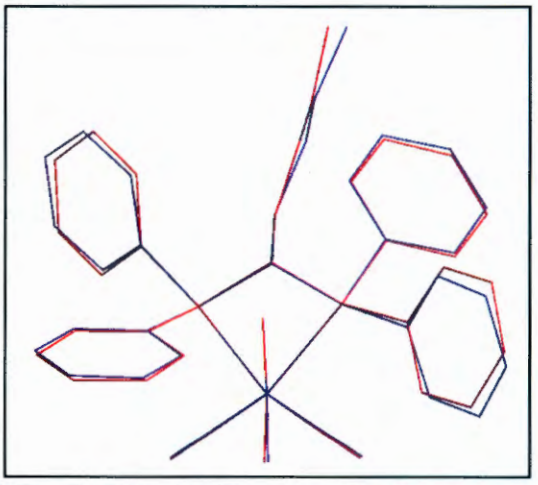

Figure 6.26: Graphical representation of an overlay of $[CrCl_4(PNP\text{-}n\text{-}Butyl)]^-$ (II) (18II) (blue) and (IV) (18IV) (red).

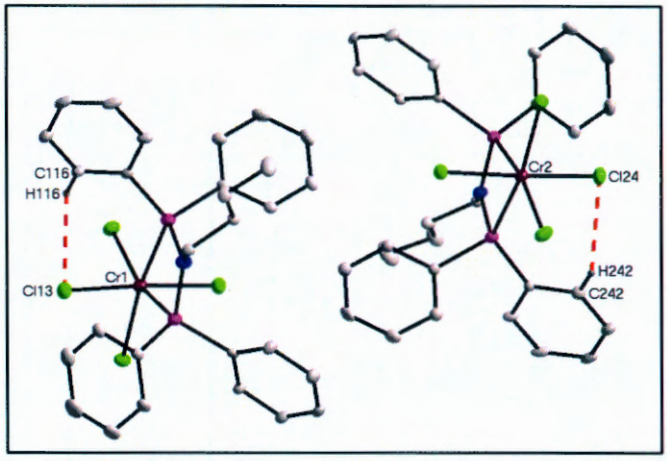

Figure 6.27: Graphical representation of the intramolecular H-bond interactions for $[CrCl_4(PNP\text{-}n\text{-}Butyl)]^-$ (I) (18I) and (II) (18II) at 50% probability. Only applicable H atoms with relevance to the H-bond interactions are indicated. The red fragmented lines indicate the intramolecular hydrogen bonding interactions.

Intramolecular C-H···Cl hydrogen bonding interactions are present for $[CrCl_4(PNP\text{-}n\text{-}Butyl]^-$ (I) and (II) as illustrated in **Figure 6.27**. The hydrogen bonding distances and angles for the two complexes are presented in **Table 6.14**.

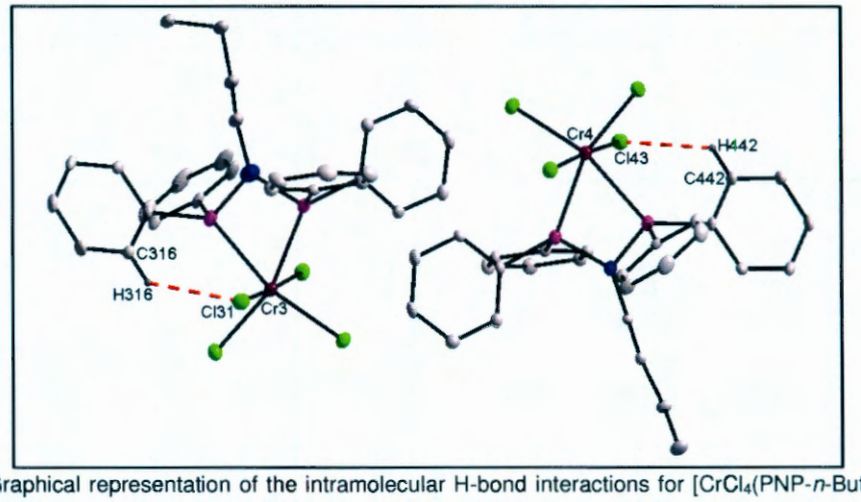

Figure 6.28: Graphical representation of the intramolecular H-bond interactions for $[CrCl_4(PNP\text{-}n\text{-}Butyl)]^-$ (III) (18III) and (IV) (18IV) at 50% probability. Only applicable H atoms with relevance to the H-bond interactions are indicated. The red fragmented lines indicate the intramolecular hydrogen interactions.

$[CrCl_4(PNP\text{-}n\text{-}Butyl)]^-$ (III) and (IV) also have intramolecular C-H···Cl hydrogen bonding interactions stabilizing the complexes in solid state (see **Figure 6.28**). The complete list of intramolecular hydrogen interactions are presented in **Table 6.14**.

Table 6.14: Intramolecular hydrogen bonding interactions for $[NH_3\text{-}i\text{-Pent}][CrCl_4(PNP\text{-}i\text{-Pent})]\cdot 2C_7H_8$. (Å and °).

D-H...A	d(D-H)	d(H...A)	D(D...A)	<(DHA)
C116-H116...Cl13(i)	0.93	2.60	3.315(5)	134
C242-H242...Cl24(i)	0.93	2.64	3.349(5)	134
C316-H316...Cl31(i)	0.93	2.63	3.347(5)	134
C442-H442...Cl43(i)	0.93	2.75	3.314(5)	120

Symmetry transformations used to generate equivalent atoms:

(i) (x, y, z)

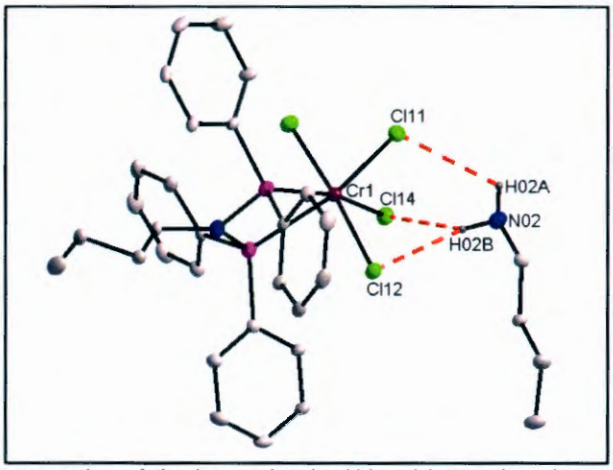

Figure 6.29: Graphical representation of the intermolecular H-bond interactions between $[CrCl_4(PNP\text{-}n\text{-Butyl})]^-$ (I) (18I) and an isopentylammonium cation at 50% probability. Only applicable H atoms with relevance to the H-bond interactions are indicated. The red fragmented lines indicate the intramolecular hydrogen interactions.

Intermolecular N-H···Cl hydrogen bonding interactions that are present between a isopentylammonium cation (molecule containing N02) and $[CrCl_4(PNP\text{-}n\text{-Butyl})]^-$ (I) are illustrated in **Figure 6.29**. The hydrogen bonding distances and angles are presented in **Table 6.15**.

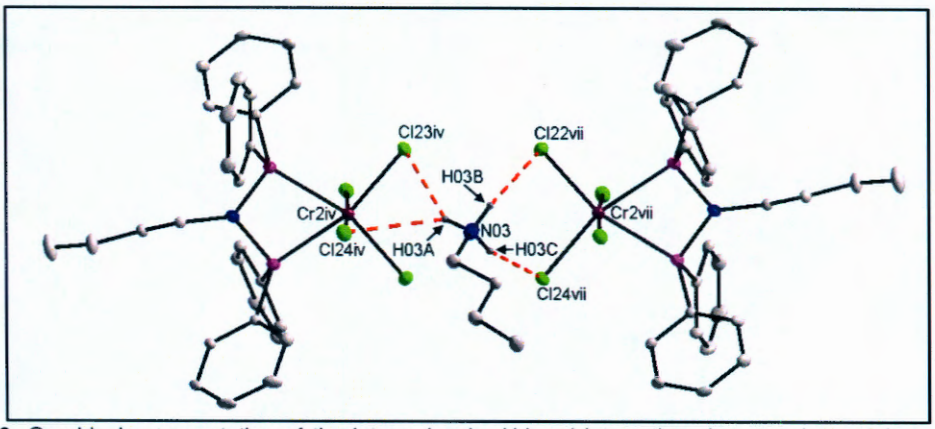

Figure 6.30: Graphical representation of the intermolecular H-bond interactions between isopentylammonium and two $[CrCl_4(PNP\text{-}n\text{-}Butyl)]^-$ (II) (18II) molecules at 50% probability. Only applicable H atoms with relevance to the H-bond interactions are indicated. The red fragmented lines indicate the intramolecular hydrogen interactions. ((iv) (-1+x, y , z) and (vii) (1-x, -y , 1-z))

Additional N-H···Cl hydrogen bonding interactions are present between a isopentylammonium cation and two $[CrCl_4(PNP\text{-}n\text{-}Butyl)]^-$ (I) molecules (see **Figure 6.30**). The hydrogen bonding distances and angles are presented in **Table 6.15**.

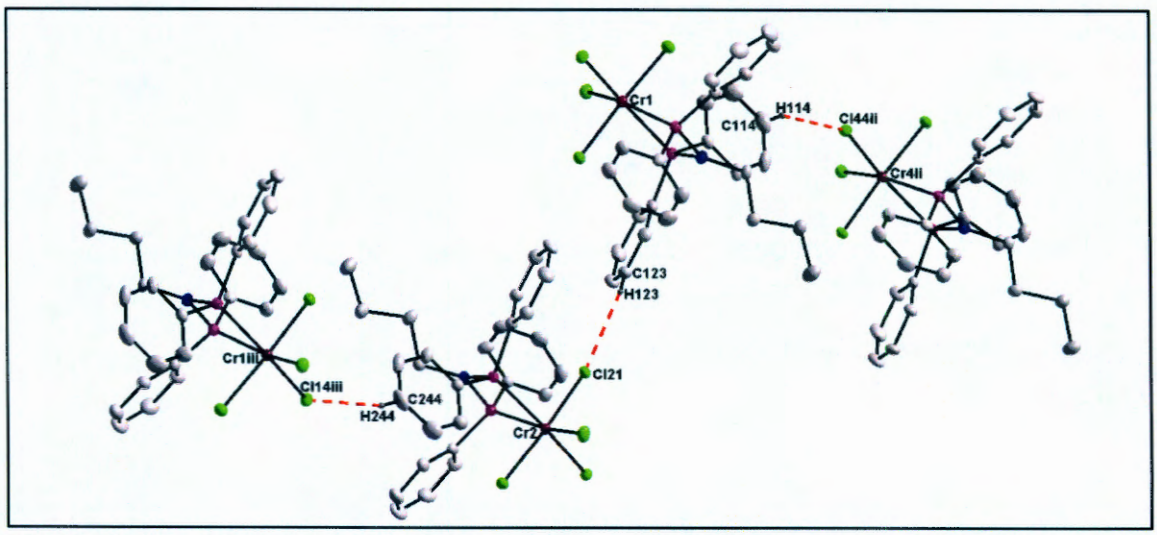

Figure 6.31: Graphical representation of the intermolecular H-bond interactions between $[CrCl_4(PNP\text{-}n\text{-}Butyl)]^-$ (I) (18I), (I) (18II) and (IV) (18IV) molecules at 50% probability. Only applicable H atoms with relevance to the H-bond interactions are indicated. The red fragmented lines indicate the intramolecular hydrogen bonding interactions. ((ii) (1-x, -y, 1-z) and ((iii) (1-x, 1-y, 1-z))

The intermolecular hydrogen bonding interactions (C-H···Cl) between $[CrCl_4(PNP\text{-}n\text{-}Butyl)]^-$ (I) and (II) is illustrated in **Figure 6.31**. The hydrogen bonding interaction distances and angles are presented in **Table 6.15**.

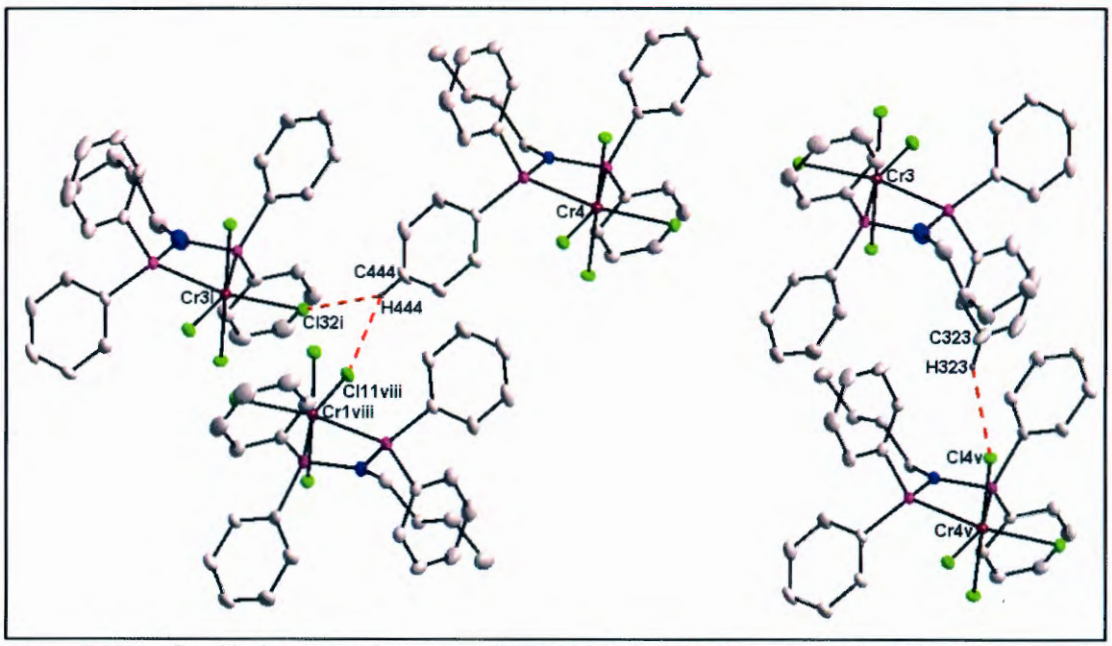

Figure 6.32: Graphical representation of the intermolecular H-bond interactions between $[CrCl_4(PNP\text{-}n\text{-}Butyl)]^-$ (I) (18I), (III) (18III) and (IV) (18IV) at 50% probability. Only applicable H atoms with relevance to the H-bond interactions are indicated. The red fragmented lines indicate the intramolecular hydrogen interactions. ((v) (1+x, y , z) and (viii) (x, y, -1+z))

Additional C-H···Cl intermolecular hydrogen bonding interactions between $[CrCl_4(PNP\text{-}n\text{-}Butyl)]^-$ (III) and (IV) molecules are presented in **Figure 6.32**. A complete list of hydrogen bonding interactions is given in **Table 6.15**.

Table 6.15: Hydrogen bonds for [*n*-Butyl-NH_3][$CrCl_4$(PNP-*n*-Butyl)]·$2C_7H_8$. (Å and °).

D-H...A	d(D-H)	d(H...A)	D(D...A)	<(DHA)
N02-H02A...Cl11(ix)	0.89	2.80	3.310(4)	118
N02-H02B...Cl12(ix)	0.89	2.60	3.335(4)	141
N02-H02B...Cl14(ix)	0.89	2.62	3.359(4)	141
N03-H03A...Cl23(iv)	0.89	2.60	3.396(5)	150
N03-H03A...Cl24(iv)	0.89	2.74	3.398(5)	132
N03-H03A...Cl22(vii)	0.89	2.70	3.247(5)	121
N03-H03A...Cl23(vii)	0.89	2.43	3.284(6)	160
C114-H114...Cl44(ii)	0.93	2.76	3.629(5)	156
C244-H224...Cl14(iii)	0.93	2.76	3.637(5)	158
C314-H314...Cl23(vi)	0.93	2.79	3.643(5)	153
C323-H323...Cl41(v)	0.93	2.83	3.618(7)	143
C444-H444...Cl11(viii)	0.93	2.79	3.465(5)	130
C444-H444...Cl32(i)	0.93	2.78	3.591(5)	146

Symmetry transformations used to generate equivalent atoms:
(i) (1-x,1- y, -z), (ii) (1-x, -y, 1-z), (iii) (1-x, 1-y , 1-z), (iv) (-1+x, y , z), (v) (1+x, y , z), (vi) (2-x, -y , 1-z), (vii) (1-x, -y , 1-z), (viii) (x, y, -1+z) and (ix) (x, y, z)

The packing pattern of [*n*-Butyl-NH_3][$CrCl_4$(PNP-*n*-Butyl)]·$2C_7H_8$ in solid state is significantly influenced by hydrogen bonding interactions. The [$CrCl_4$(PNP-*n*-Butyl)]$^-$ complexes are packed in diagonal layers across the ac plane (see **Figure 6.33**) with intermolecular hydrogen bonding interactions dominating the arrangement of the mono-anionic complexes within the unit cell.

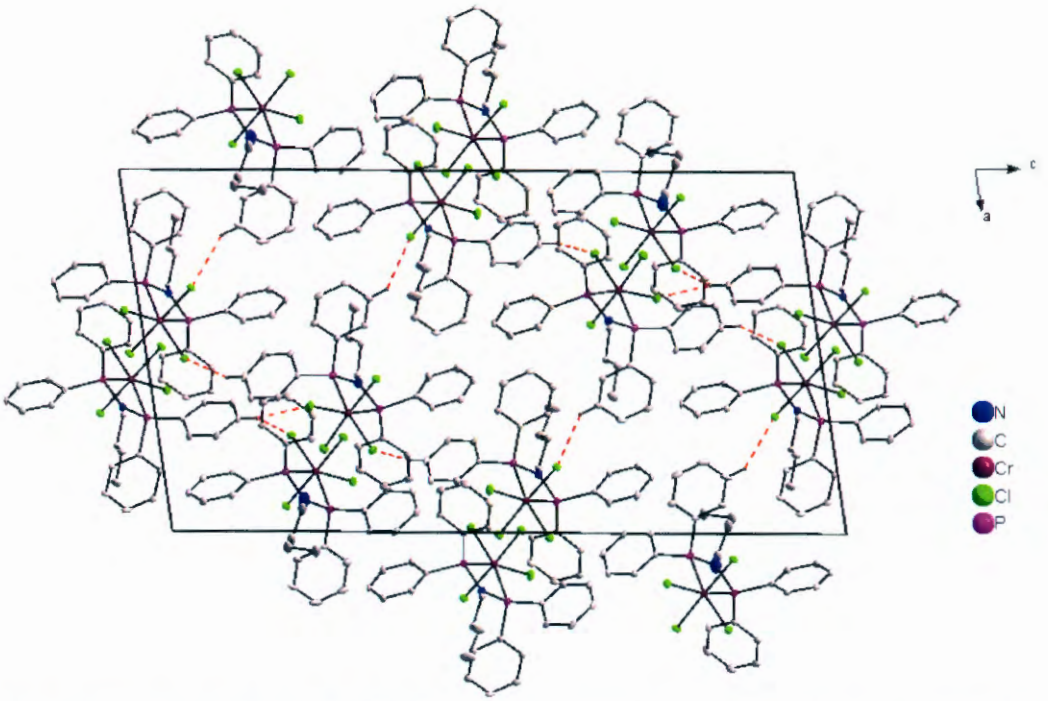

Figure 6.33: Perspective view of the unit cell of $[CrCl_4(PNP\text{-}n\text{-}Pent)]^-$ anions along the b axis at 50% probability. H-atoms were omitted for clarity. Only applicable H atoms with relevance to the H-bond interactions are indicated. The red fragmented lines indicate the intramolecular hydrogen bonding interactions.

6.3 Discussion

The asymmetric units of the crystal structures for the three chromium(III)-PNP complexes reveal monomeric Cr(III)-PNP complexes with non-coordinated alkylammonium cations as well as non-coordinated toluene molecules, this is in contrast with the dimeric species $[CrCl_2(\mu\text{-}Cl)(P_2NC_{30}H_{25})]_2$[1] (see **Figure 6.34**). Each respective Cr(III)-complex has a PNP-ligand and four chloride atoms bonded to the central Cr(III) atom. During the synthesis of these complexes no additional alkyl-ammonium chloride was added. It is possible that during the synthesis of the PNP-ligand systems the alkyl-ammonium chloride was retained as an impurity even after consecutive purification steps

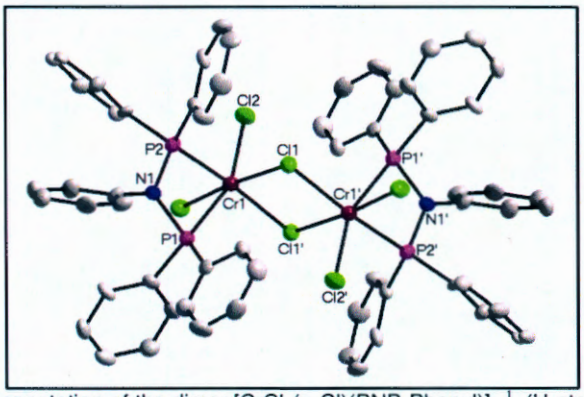

Figure 6.34: Graphical representation of the dimer $[CrCl_2(\mu\text{-}Cl)(PNP\text{-}Phenyl)]_2$.[1] (H-atoms were omitted for clarity.)

The geometric parameters for the various chromium(III) complexes investigated reveal that the bond angles are similar within experimental error (see **Table 6.16**). The monomeric anionic complexes display distorted octahedral geometries at the metal centre with P-Cr-P angles that range from 66.7(1) to 67.2(1) °. These small bite angles are attributed to the formation of the four-membered ring (Cr-P-N-P) upon coordination of the diphosphinoamine ligand for each respective chromium-PNP complex. The P-N-P angles which range between 105.9(2) and 106.6(4) ° for $[CrCl_4(PNP\text{-}n\text{-}Pent)]^-$ (I) (16I), (II) (16II), $[CrCl_4(PNP\text{-}i\text{-}Pent)]^-$ (I) (17I) and (II) (17II) (see **Table 6.16**) are significantly smaller than the corresponding angles of the PNP-*n*-Pent and PNP-*i*-Pent ligands, when not coordinated, which range from 111.0(1) to 123.4(1) ° (see Chapter 4). The strain experienced by the complexes is further illustrated by the distortion of the ideal tetrahedral geometries at the phosphorous atoms with C-P-C angles that range between 101.5(4) and 104.8(2) °.

The geometric parameters for the various chromium(III) complexes investigated reveal that the bond angles are similar within experimental error (see **Table 6.16**). It appears that the different PNP-ligands for the respective monomeric chromium complexes do not have a significant influence on the bond angles or lengths of the complexes.

Table 6.16: Selected bond angles (°) for the complexes, $[CrCl_4(PNP\text{-}n\text{-}Pent)]^-$ (I) (16I), (II) (16II), $[CrCl_4(PNP\text{-}i\text{-}Pent)]^-$ (I) (17I), (II) (17II), $[CrCl_4(PNP\text{-}n\text{-}Butyl)]^-$ (I) (18I), (II) (18II), (III) (18III), (IV) (18IV) and $[CrCl_2(\mu\text{-}Cl)(PNP\text{-}Phenyl)]_2$.[1]

Complex	P-Cr-P (°)	P-N-P (°)
$[CrCl_4(PNP\text{-}n\text{-}Pent)]^-$ (I) (16I)	66.7(1)	106.0(3)
$[CrCl_4(PNP\text{-}n\text{-}Pent)]^-$ (II) (16II)	66.7(1)	106.6(4)
$[CrCl_4(PNP\text{-}i\text{-}Pent)]^-$ (I) (17I)	67.1(1)	106.5(2)
$[CrCl_4(PNP\text{-}i\text{-}Pent)]^-$ (II) (17II)	66.8(1)	105.9(2)
$[CrCl_4(PNP\text{-}n\text{-}Butyl)]^-$ (I) (18I)	66.9(1)	105.3(2)
$[CrCl_4(PNP\text{-}n\text{-}Butyl)]^-$ (II) (18II)	66.9(1)	105.2(2)
$[CrCl_4(PNP\text{-}n\text{-}Butyl)]^-$ (III) (18III)	67.2(1)	106.1(2)
$[CrCl_4(PNP\text{-}n\text{-}Butyl)]^-$ (IV) (18IV)	67.1(1)	105.4(2)
$[CrCl_2(\mu\text{-}Cl)(PNP\text{-}Phen]_2$[1]	66.6(7)	106.5(3)

The most noteworthy changes observed between the complexes were the torsion angles, defining the relative orientation of the phenyl rings at the P-atoms. These torsion angles for each respective $[CrCl_4(PNP\text{-}alkyl)]^-$ complex reveal that each complex had different variations of the 'fan-like' arrangement of the phenyl rings.

It is evident from this chapter and chapters 4 and 5 that the steric bulk of the nitrogen-coordinated alkyl moiety has a significant influence on the structure of the compounds in the solid state. To date, the size of the alkyl moiety has been estimated. A steric parameter was therefore introduced in which the steric bulk of the nitrogen-coordinated alkyl moiety is determined and further quantified. This parameter is presented and discussed in Chapter 10.

Theoretical calculations were performed on the $[CrCl_4(PNP\text{-}alkyl)]^-$ complexes and are presented, discussed and compared with the crystallographic data of the corresponding complexes in Chapter 9.

7 Theoretical study of non-coordinated bis(diphenylphosphino)amine ligands

In this chapter...

Possible isomers of selected non-coordinated PNP-ligands were identified using theoretical caculations. The isomer(s) with the lowest relative energy were re-optimized at a higher level of theory and compared with the crystallographic data of the corresponding ligands.

7.1 Introduction

Computational chemistry can be described as using a set of techniques for the investigation of chemical problems on a computer, for example the determination of molecular geometry, energies of molecules, transition states and chemical reactivity. Various methods exist for solving these problems and these can be classified into five broad classes.[1]

1. Molecular mechanics (MM)
2. Ab initio calculations
3. Semiempirical (SE) calculations
4. Density functional calculations (DFT)
5. Molecular dynamics

The study is based on DFT calculations and therefore the focus will be on this specific model of computational chemistry.

DFT calculations are not based on the wavefunction, but rather on the electron density function and this originated with a theorem by Hoenburg and Kohn.[2] In this formulation

[1] Lewars, E., **2004**, *Computational Chemistry, Introduction to the theory and Application of molecular and quantum mechanics.* Kluwer academic publishers New York, Boston, Dordrecht, London, Moscow.
[2] Hohenberg, P. and Kohn, W., *Phys Rev.*, **1964**, *136*, B864.

the electron density is expressed as a linear combination of basis functions similar in mathematical form to HF (Hartree-Fock) orbitals. A determinant is formed from these functions called Kohn-Sham orbitals and the electron density of these orbitals is used to compute the energy.[3] Although these orbitals describe electron behaviour they are not mathematically equivalent to either HF or natural orbitals. Subsequently a density functional is used to obtain the energy for the electron density noting that a functional is a function of a function. Density functionals can be broken down into several classes, with the simplest called the Xα method, introduced by J. C. Slater in an attempt to make an approximation to Hartree-Fock. Some of the more widely used functionals are listed in **Table 7.1**[4,5,6,7].

Table 7.1: Selected functionals used in computational chemistry.

Acronyms	Name	Type
Xα	X alpha	Exchange only
HFS	Hartree-Fock Slater	HF with LDA exchange
VWN	Vosko, Wilks and Nusair	LDA
BLYP	Becke correlation functional with Lee, Yang and Parr exchange	Gradient corrected
B3LYP	Becke 3 term with Lee, Yang and Parr exchange	Hybrid

DFT calculations must use a basis set and each unique pairing of a method with a basis set represents a different approximation to the Schrödinger equation. A basis set is a mathematical representation of the molecular orbital within an orbital. The basis set can be interpreted as restricting each electron to a particular region of space. Larger basis sets impose fewer constraints on electrons and more accurately approximate exact molecular obitals, but they require correspondingly more computational resources.

Minimal basis sets contain the minimum number of basis functions needed for each atom for example, carbon: 1s, 2s, $2p_x$, $2p_y$, $2p_z$. Minimal basis sets use fixed-sized

[3] Kohn, W. and Sham, J. L., *Phys. Rev.*, **1965**, *140*, A1133.
[4] Young, D. C., **2001**, *Computational Chemistry: A Practical Guide for Applying Techniques to Real-World Problems, John Wiley & Sons, Inc.*
[5] Jensen, F., **1999**. *Introduction to Computational Chemistry*, John Wiley & Sons, New York.
[6] Koch, W, and Holthausen, M. C., **2000**, *A Chemist's Guide to Density Functional Theory*, Wiley-VCH, Weinheim.
[7] Dobson, J. F., Vignale, G. and Das, M. P., **1998**, *Electronic Density Functional Theory Recent Progress and New Directions*. Plenum, New York.

atomic-type orbitals. An example of a minimal basis set is STO-3G ('Slater Type Orbitals' using three Gaussian primitives per basis function).

The first way to make a basis set larger is to increase the number of basis functions per atom. Split valence sets, such as 3-21G and 6-31G have two or more sizes of basis functions for each valence orbital. The example of the carbon is represented as 1s, 2s, 2s', $2p_x$, $2p_y$, $2p_z$, $2p_x$', $2p_y$', $2p_z$' where the primed and unprimed orbitals differ in size. Basis sets like 6-311G use three sizes of contracted functions for each orbital.

Split valence basis sets allow orbitals to change size, but not shape. Polarized basis sets remove this limitation by adding orbitals with angular momentum beyond what is required for the ground state to the description of each atom, for example polarized basis sets add d-functions to carbon, f-functions to transition metals and can also add p-functions to hydrogen atoms. The basis set 6-31G(d,p), also known as 6-31G**, adds p-functions to hydrogens and d functions to main group atoms.

Basis sets can also have diffuse functions which are large sized versions of s- and p-type functions. They allow orbitals to occupy a larger region of space. Basis sets with diffuse functions are important for systems where electrons are relatively far from the nucleus, molecules with lone pairs, anions and other systems with significant negative charges.

Basis sets for atoms beyond the third row of the periodic table are handled somewhat differently. Electrons near the nucleus are treated in an approximate way, *via* ECP's, which include some relativistic effects. The LANL2DZ basis set is the best known of these.

7.2 Experimental

Possible isomers of selected non-coordinated PNP-ligands were identified through molecular dynamics calculations and calculated at the B3LYP/LANL2DZ level to

determine if the conformers are global minima. The isomer with the lowest energy as calculated with LANL2DZ was then further optimised at a B3LYP/6-,31+G(d,p) level of theory with more calculated degrees of freedom and is therefore a more accurate representation of the specific isomer. All calculations were carried out using the Gaussian 03 software suite[8]. The re-optimized structures were then compared to the crystallographic data of the particular non-coordinated PNP-ligand. Molecular diagrams (using DIAMOND 3.0[9]) of the structures are presented. Graphical representations of overlays of selected complexes are also presented (using Hyperchem7.52[10])

Theoretical calculations were performed on the following non-coordinated bis(diphenylphosphino)amine ligands (PNP-ligands):

1) Bis(diphenylphosphino)-ethylamine (PNP-Ethyl)
2) Bis(diphenylphosphino)-1,2-dimethylpropylamine (PNP-Dimprop)
3) Bis(diphenylphosphino)-isopentylamine (PNP-*i*-Pent)
4) Bis(diphenylphosphino)-cyclohexylamine (PNP-Cychex)
5) Bis(diphenylphosphino)-*n*-pentylamine (PNP-*n*-Pent)

The crystal structures are denoted with numerical values, for example PNP-Ethyl, PNP-Dimprop and PNP-i-Pent are indicated as 1, 2 and 3 respectively. The corresponding calculated structures (the isomer with the lowest normalized ΔEnergy which was re-optimized at a B3LYP/6-,31+G(d,p) level) are indicated for example as 1^*, 2^* and 3^* and so forth.

[8] Gaussian 03, Revision C.01, Frisch, M. J., Trucks, G. W., Schlegel, H. B., Scuseria, G. E., Robb, M. A., Cheeseman, J. R., Montgomery, Jr., J. A., Vreven, T., Kudin, K. N., Burant, J. C., Millam, J. M., Iyengar, S. S., Tomasi, J., Barone, V., Mennucci, B., Cossi, M., Scalmani, G., Rega, N., Petersson, G. A., Nakatsuji, H., Hada, M., Ehara, M., Toyota, K., Fukuda, R., Hasegawa, J., Ishida, M., Nakajima, T., Honda, Y., Kitao, O., Nakai, H., Klene, M., Li, X., Knox, J. E., Hratchian, H. P., Cross, J. B., Adamo, C., Jaramillo, J., Gomperts, R., Stratmann, R. E., Yazyev, O., Austin, A. J., Cammi, R., Pomelli, C., Ochterski, J. W., Ayala, P. Y., Morokuma, K., Voth, G. A., Salvador, P., Dannenberg, J. J., Zakrzewski, V. G., Dapprich, S., Daniels, A. D., Strain, M. C., Farkas, O., Malick, D. K., Rabuck, A. D., Raghavachari, K., Foresman, J. B., Ortiz, J. V., Cui, Q., Baboul, A. G., Clifford, S., Cioslowski, J., Stefanov, B. B., Liu, G., Liashenko, A., Piskorz, P., Komaromi, I., Martin, R. L., Fox, D. J., Keith, T., Al-Laham, M. A., Peng, C. Y., Nanayakkara, N., Challacombe, M., Gill, P. M. W., Johnson, B., Chen, W., Wong, M. W., Gonzalez, C., & Pople, J. A., Gaussian, Inc.,Pittsburgh PA, **2003**.

[9] Brandenburg, K. and Putz, H., **2005**, DIAMOND. Release 3.0c. Crystal Impact GbR, Bonn, Germany.

[10] Hyperchem ™ Release 7.52, Windows Molecular Modeling System, Hypercube, Inc., **2002**.

7.3 Theoretical calculations on non-coordinated PNP-ligands

7.3.1 PNP-Ethyl (1 *vs.* 1*)

Nine possible isomers of the PNP-Ethyl non-coordinated ligand were identified and optimized at the B3LYP/LANL2DZ level. The varying ΔEnergy values of each of the isomers are illustrated in **Figure 7.1**.

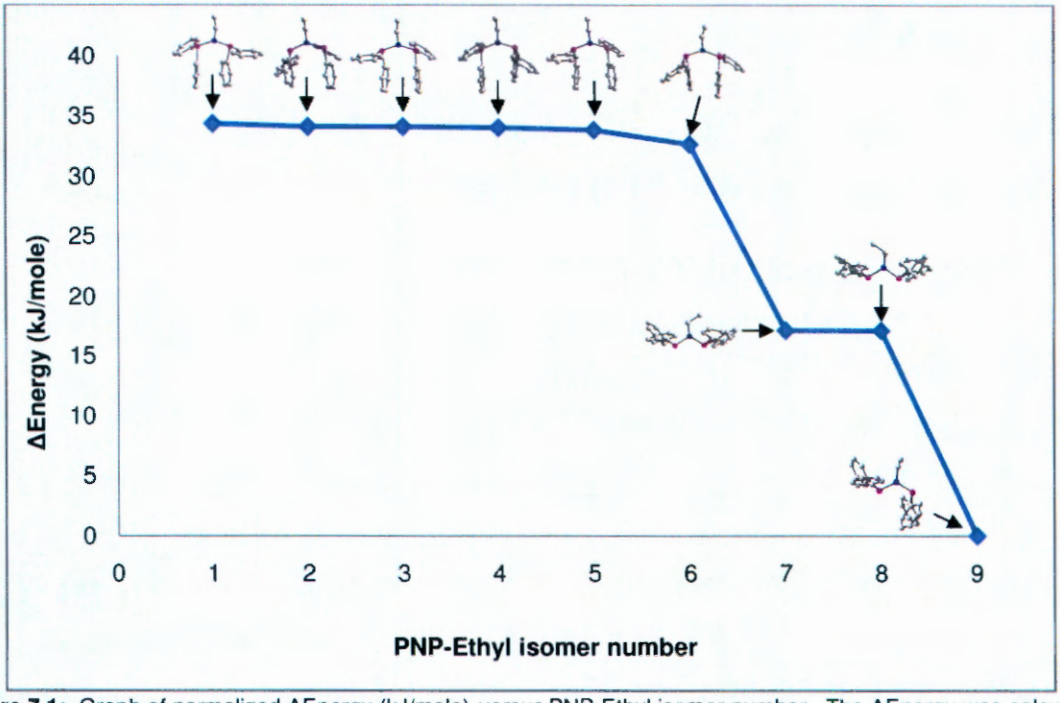

Figure 7.1: Graph of normalized ΔEnergy (kJ/mole) *versus* PNP-Ethyl isomer number. The ΔEnergy was calculated using the B3LYP/LANL2DZ basis set.

The structure of the PNP-Ethyl isomer 9, which has the lowest ΔEnergy value (normalized to 0 kJ/mole) was re-optimized at a higher level of theory (B3LYP/6-,31+G(d,p) level). An overlay of the structure calculated using the lower basis set, B3LYP/LAN2DZ, and the re-optimized structure using the B3LYP/6-,31+G(d,p) basis set is presented in **Figure 7.2**.

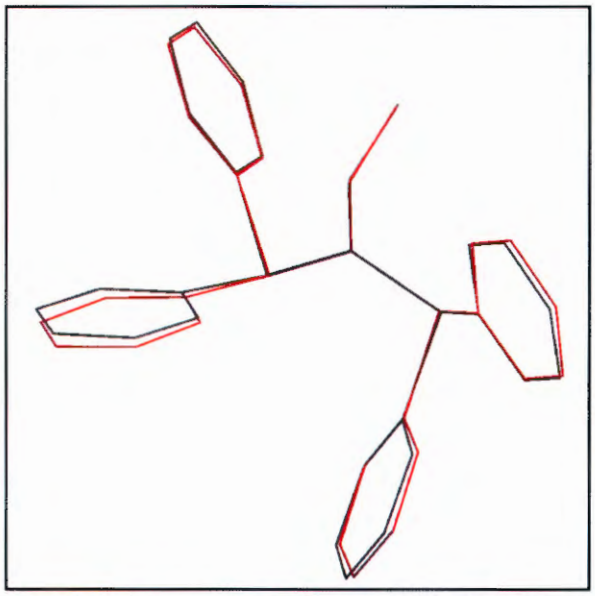

Figure 7.2: Graphical representation of an overlay of the calculated structures of PNP-Ethyl isomer 9 using the B3LYP/LANL2DZ basis set (black) and the B3LYP/6-31+G(d,p) basis set (red).

The re-optimized structure of PNP-Ethyl isomer 9 (will be referred to as 1*) was then compared to the crystallographic data of PNP-Ethyl (1) (see §4.2.1) and **Figure 7.3** illustrates an overlay of the two structures.

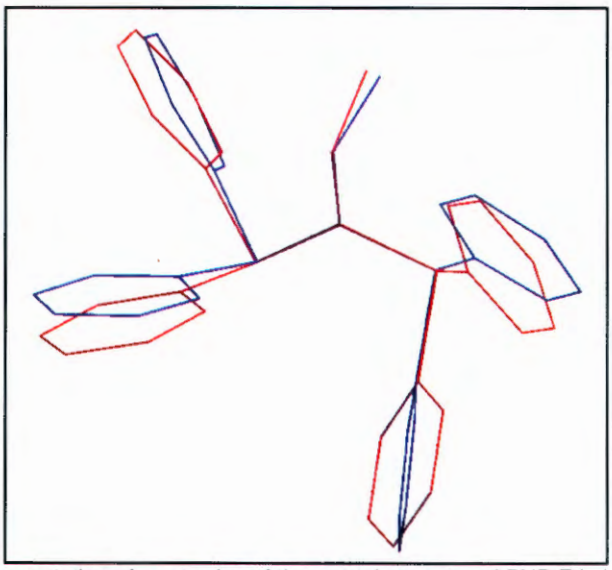

Figure 7.3: Graphical representation of an overlay of the crystal strucutre of PNP-Ethyl (1) (blue) and the calculated structure of PNP-Ethyl isomer 9 using the B3LYP/6-31+G(d,p) basis set (1*) (red).

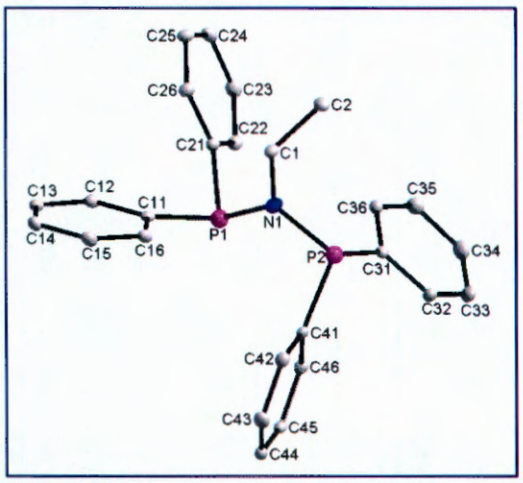

Figure 7.4: Graphical representation of the crystal structure of PNP-Ethyl (1) at 50% probability. (H-atoms were omitted for clarity).

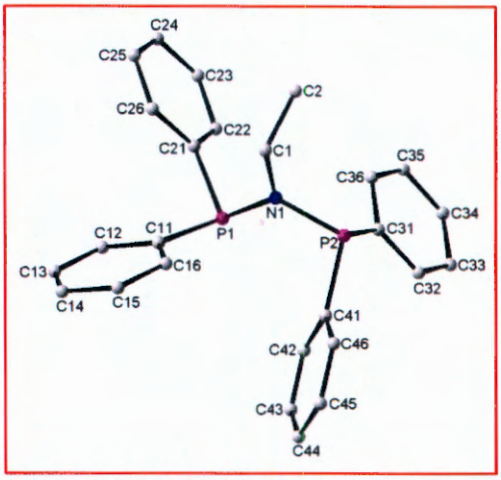

Figure 7.5: Graphical representation of the re-optimized structure of PNP-Ethyl isomer 9, using the B3LYP/6-,31+G(d,p) basis set (1*). (H-atoms were omitted for clarity).

It can be seen from **Figures 7.4** and **7.5** that the crystal structure has virtually the same conformation as the calculated PNP-Ethyl isomer (approximate conformation C_S, see **Figure 4.2** in Chapter 4). It is surprising that both these structures indicate this geometry to be adopted as the ethyl moiety is seen as a relatively small alkyl group since it would be expected that this compound could adopt the C_{2V} conformation. Interestingly the second lowest isomer of the calculated PNP-Ethyl isomers indicates C_{2V} conformation with a difference of 15 kJ/mole difference between these two isomers, 8 and 9.

Table 7.1: Selected bond angles (°) for the crystal structure of PNP-Ethyl (1) and the calculated PNP-Ethyl isomer 9 (1*).

Bond angles (°)	1	1*
P1-N1-P2	123.7(1)	122.8
C11-P1-C21	100.4(1)	101.2
C31-P2-C41	100.8(1)	102.2
C1-N1-P1	122.3(1)	122.5
C1-N1-P2	114.0(1)	114.6

The P-N-P bond angle for the calculated structure (122.8°) is only 1.1 ° larger than that of the solid state crystal structure (123.7(1) °). The rest of the bond angles as reported in **Table 7.1** are similar within experimental error, with the largest difference being 2.4 ° (C31-P2-C41).

Table 7.2: Selected bond lengths (Å) for the crystal structure of PNP-Ethyl (1) and the calculated PNP-Ethyl isomer 9 (1*).

Bond Length (Å)	1	1*
P1-N1	1.713(2)	1.744
P2-N1	1.713(2)	1.749
N1-C1	1.486(2)	1.487
P1-C11	1.837(1)	1.856
P1-C21	1.848(2)	1.864
P2-C31	1.826(2)	1.850
P2-C41	1.833(2)	1.857

The P-N bond lengths of the crystal structure is slightly shorter (1.713(1) **Å**) than that of the calculated structure (1.744 Å and 1.749 Å for bond lengths, P1-N1 and P2-N1 respectively). This is the same case for the C-P bonds that are shorter for the crystal structure (1.826(2) – 1.848(2) (Å)) than the calculated structure (1. 850 - 1.864 Å).

Table 7.3: Selected torsion angles (°) for the crystal structure of PNP-Ethyl (1) and the calculated PNP-Ethyl isomer 9 (1*).

Torsion angles (°)	1	1*
N1-P1-C11-C12	155.2(1)	163.6
N1-P1-C21-C22	109.4(1)	101.6
N1-P2-C31-C32	-170.3(1)	-152.6
N1-P2-C41-C42	90.9(1)	70.8

The corresponding torsion angles of the two structures are in the same order, indicating that the orientation of the phenyl rings are similar with slight variations observed (see **Table 7.3** and **Figure 7.3**). These comparable torsion angles are as expected, because the two structures adopted the same conformation.

7.3.2 PNP-Dimprop (2 *vs.* 2*)

Eleven possible isomers of the PNP-Dimprop non-coordinated ligand were identified and optimized at a B3LYP/LANL2DZ level. The varying ΔEnergy values of each of the isomers are illustrated in **Figure 7.6**.

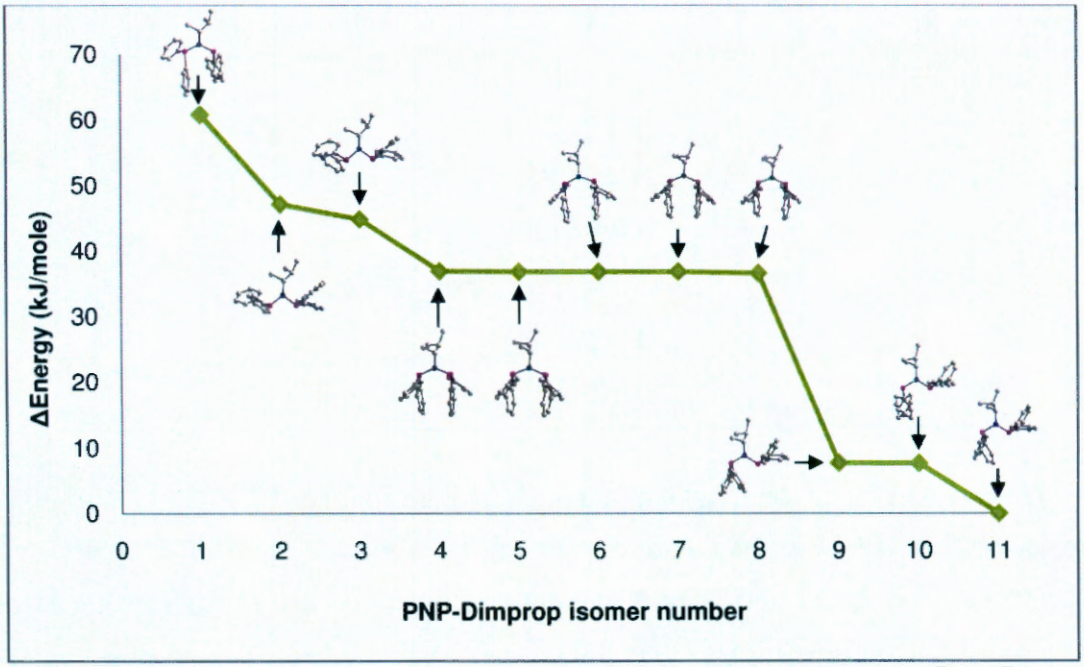

Figure 7.6: Graph of normalized ΔEnergy (kJ/mole) *versus* PNP-Dimprop isomer number. The ΔEnergy was calculated using the B3LYP/LANL2DZ basis set.

The structure of PNP-Dimprop isomer 11 (normalized to 0 kJ/mol) was re-optimized at a B3LYP/6-,31+G(d,p) level. An overlay of the two structures calculated by using the B3LYP/LAN2DZ and B3LYP/6-,31+G(d,p) basis sets is presented in **Figure 7.7**.

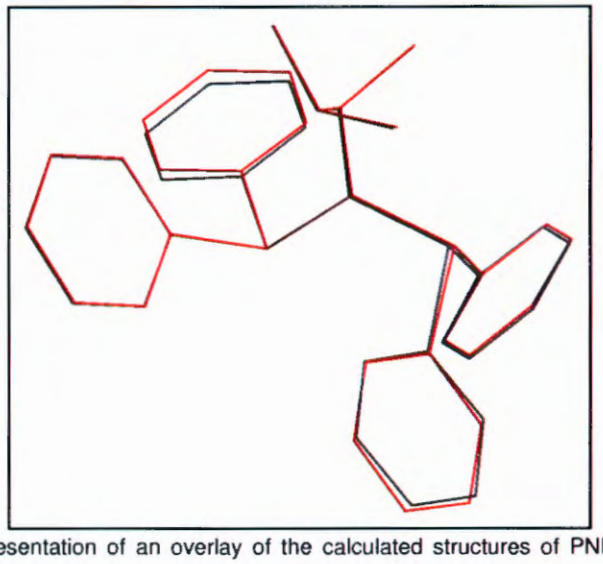

Figure 7.7: Graphical representation of an overlay of the calculated structures of PNP-Dimprop isomer 11 using the B3LYP/LANL2DZ basis set (black) and the B3LYP/6-31+G(d,p) basis set (red).

The crystal structure of PNP-Dimprop (2) (see §4.2.2) was compared with the re-optimized structure (will be reffered to as 2*) and an overlay of the calculated and re-optimized structures illustrate the differences between the structures (see **Figures 7.8**).

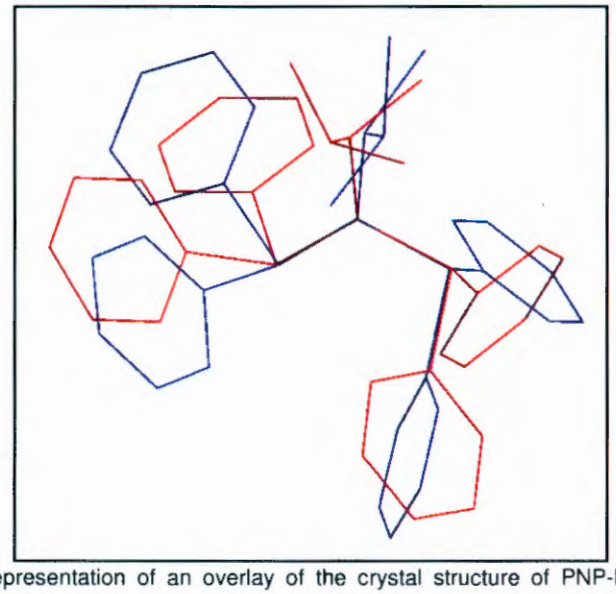

Figure 7.8: Graphical representation of an overlay of the crystal structure of PNP-Dimprop (2) (blue) and the calculated structure of PNP-Dimprop isomer 11 using the B3LYP/6-31+G(d,p) basis set (2*) (red).

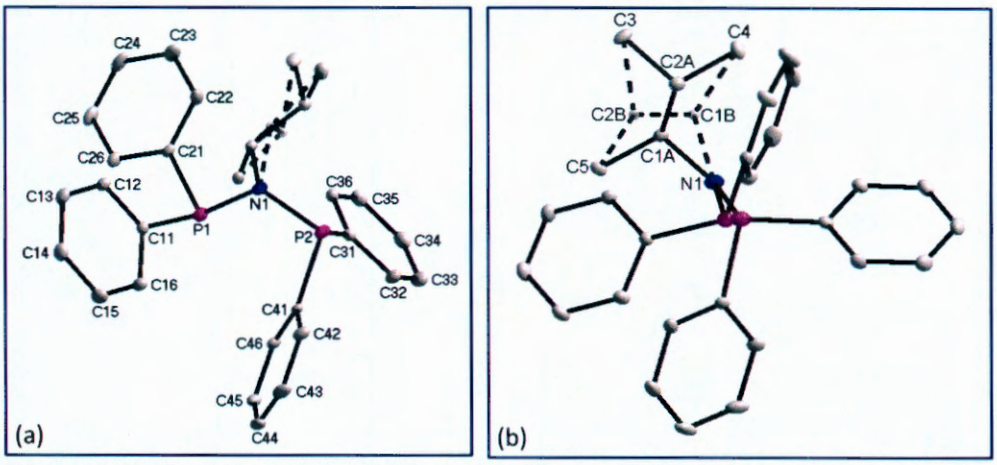

Figure 7.9a and b: Graphical representation of the different viewing angles of the crystal structure of PNP-Dimprop (2) at 50% probability. A/B indicates the disordered carbon atoms in the 1,2-dimethylpropyl alkyl group. Disordered parts belonging together are numbered A and B respectively. (H-atoms were omitted for clarity).

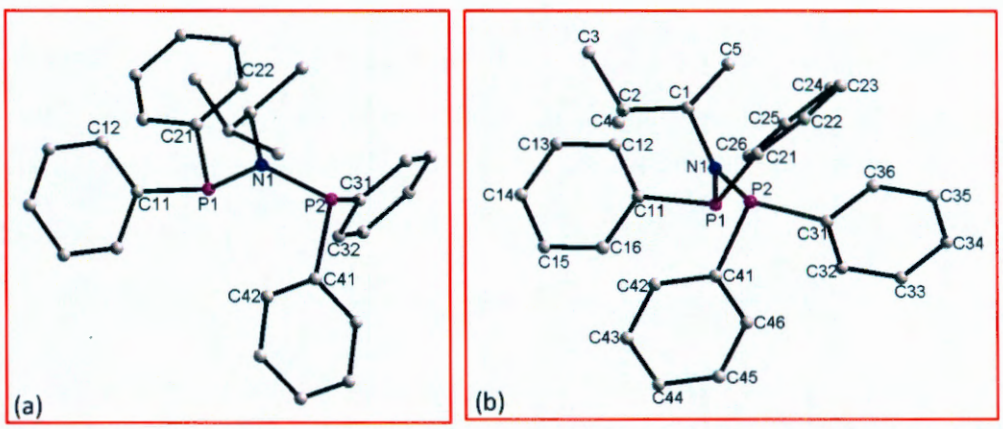

Figure 7.10a and b: Graphical representation of the different viewing angels of the re-optimized structure of PNP-Dimprop isomer 11 (2˙), using the B3LYP/6-,31+G(d,p) basis set. (H-atoms were omitted for clarity).

Both the crystal structure and the calculated structure display conformation (C_S), see **Figures 7.9** and **7.10**. This is expected as the alkyl substituent on the nitrogen atom is quite bulky and by adopting this conformation the steric hindrance is somewhat relieved. It is interesting to note that PNP-Dimprop isomer 2 and 3 (see **Figure 7.6**) display conformations (C_{2V}) and these have a much higher energy than that of isomer 11.

Table 7.4: Selected bond angles (°) for the crystal structure of PNP-Dimprop (2) and the calculated PNP-Dimprop isomer 11 (2*).

Bond angle (°)	2	2*
P1 – N1 – P2	117.9(1)	120.0
C1A – N1 – P1	121.6(1)	121.6
C1B – N1 – P1	130.1(4)	-
C1A – N1 – P2	115.5(1)	118.4
C1B – N1 – P2	111.2(4)	-
C11 – P1 – C21	99.6(1)	101.2
N1 – P1 – C11	104.9(1)	106.0
N1 – P1 – C21	106.6(1)	104.5
C31 – P2 – C41	99.7(1)	102.1
N1 – P2 – C31	110.4(1)	105.8
N1 – P2 – C41	105.0(1)	105.1

The P-N-P bond angle for the calculated structure (120.0°) is slightly larger than that in the crystal structure (117.9(1) °). The smaller C1A-N1-P2 and C1B-N1-P2 angles in the crystal structure (115.5(1)° and 111.2(1)°) indicate that the alkyl group is more tilted towards P2 than the alkyl group of the calculated structure (118.4°). The rest of the bond angles as reported in **Table 7.4** are similar within experimental error.

Table 7.5: Selected bond angles (°) for the crystal structure of PNP-Dimprop (2) and the calculated PNP-Dimprop isomer 11 (2*).

Bond length (Å)	2	2*
P1 – N	1.721(2)	1.752
P2 – N	1.727(2)	1.753
N1 – C1A	1.515(2)	1.505
N1 – C1B	1.520(2)	-
P1 – C11	1.831(2)	1.865
P1 – C21	1.839(2)	1.857
P2 – C32	1.826(2)	1.860
P2 – C41	1.836(2)	1.850

The P-N bond lengths in the crystal structure is slightly shorter (1.721(2) - 1.727(2) (Å)) than that of the calculated structure (1.752 - 1.753 (Å)). This is the same case for the C-P bonds which are shorter in the crystal structure (1.826(2) – 1.839(2) (Å)) than the calculated structure (1.850 – 1.865 (Å)).

Table 7.6: Selected torsion angles (°) for the crystal structure of PNP-Dimprop (2) and the calculated PNP-Dimprop isomer 11 (2*).

Torsion angles (°)	2	2*
N1-P1-C11-C12	86.2(1)	77.3
N1-P1-C21-C22	17.4(1)	32.7
N1-P2-C31-C32	-168.2(1)	-72.8
N1-P2-C41-C42	-103.4(1)	-35.4

Phenyl rings 1 (ring containing C11) for the two structures are orientated similarly for both the crystal structure and the calculated structure of PNP-Dimprop as can be seen from the torsion angle N1-P1-C11-C12 (86.2(1) and 77.3 ° respectively) (see **Table 7.6** and **Figure 7.8**). Similar orientations of ring 2 (ring containing C21) for both structures are observed, with N1-P1-C21-C22 angles of 17.4(1) and 32.7 in the crystal and calculated structure respectively. The other two phenyl rings have different orientations when comparing the two structures as is apparent from the torsion angles listed in **Table 7.6**.

7.3.3 PNP-*i*-Pent (3 *vs.* 3*)

Eleven possible isomers of the PNP-*i*-Pent non-coordinated ligand were identified and optimized at the B3LYP/LANL2DZ level. The varying ΔEnergy values of each of the isomers are illustrated in **Figure 7.11**.

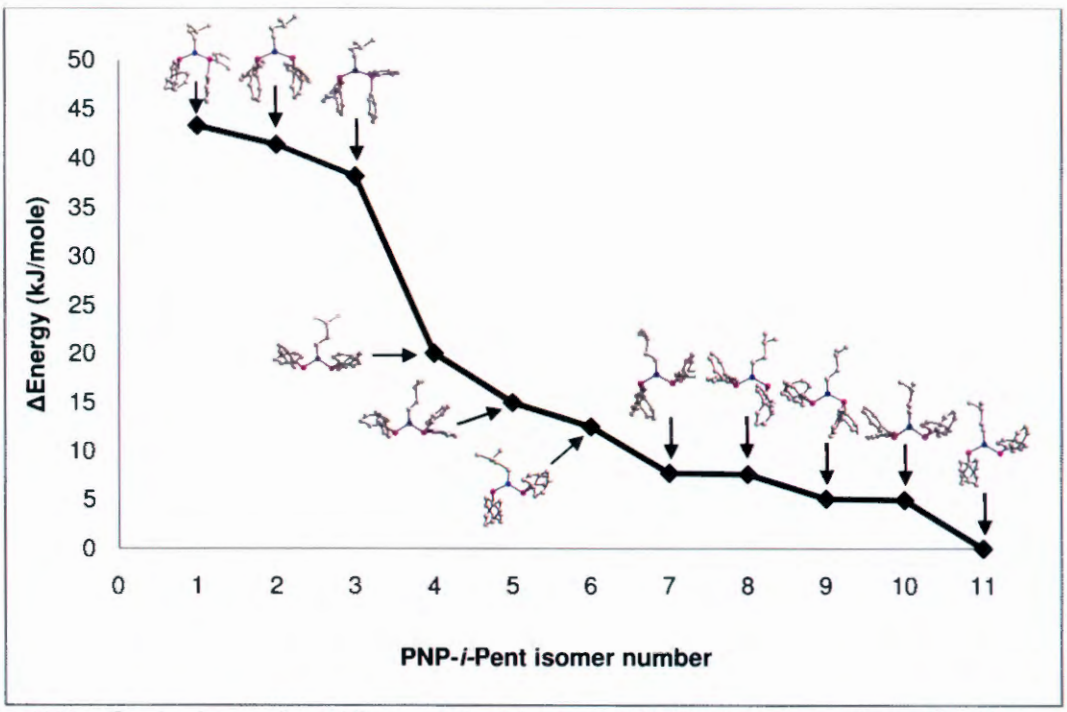

Figure 7.11: Graph of normalized ΔEnergy (kJ/mole) *versus* PNP-*i*-Pent isomer number. The ΔEnergy was calculated using the B3LYP/LANL2DZ basis set.

The overlay of the two structures (isomer 11, which was normalised to 0 kJ/mole) calculated using B3LYP/LAN2DZ and B3LYP/6-,31+G(d,p) is presented in **Figure 7.12**.

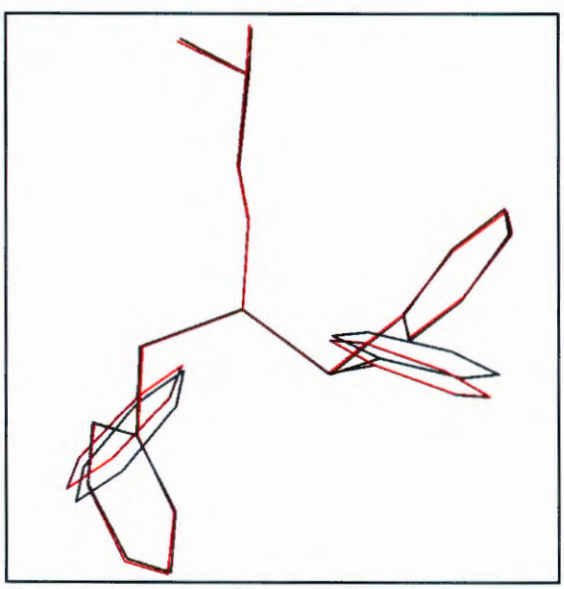

Figure 7.12: Graphical representation of an overlay of the calculated structures of PNP-*i*-Pent isomer 11 using the B3LYP/LANL2DZ basis set (black) and the B3LYP/6-31+G(d,p) basis set (red).

The re-optimized structure (at B3LYP/6-,31+G(d,p) level) of the PNP-*i*-Pent isomer with the lowest ΔEnergy (PNP-*i*-Pent isomer 11) (will be referred to as 3*) was compared to the crystallographic structure of PNP-*i*-Pent (3) (see §4.2.3) ,see **Figure 7.13** for an overlay of the two structures.

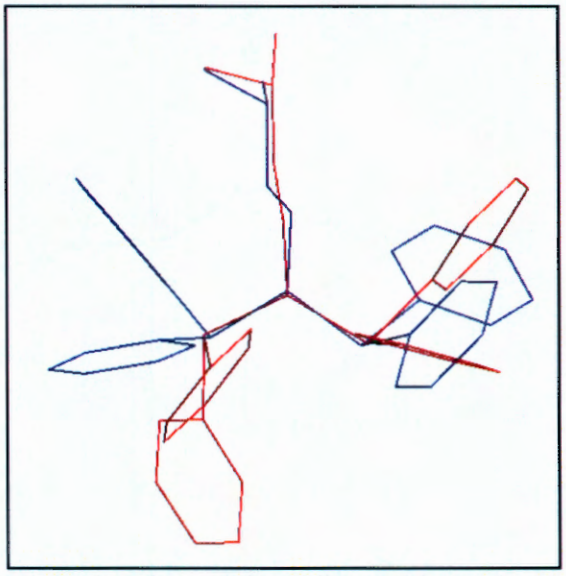

Figure 7.13: Graphical representation of an overlay of the crystal strucutre of PNP-*i*-Pent (3) (blue) and the calculated structure of PNP-*i*-Pent isomer 11 using the B3LYP/6-31+G(d,p) basis set (3*) (red).

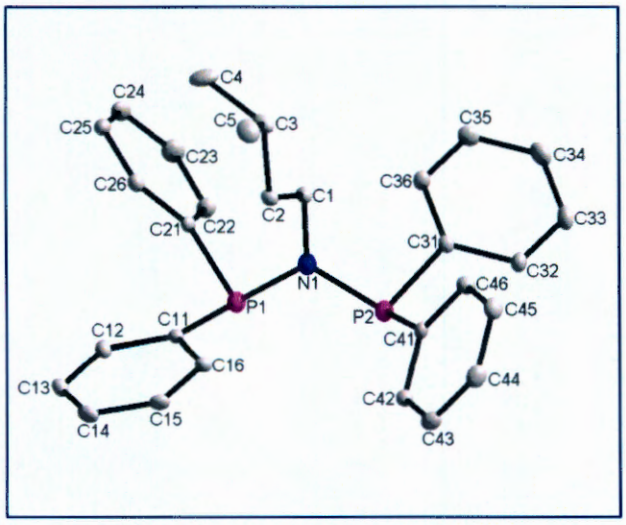

Figure 7.14: Graphical representation of the crystal structure of PNP-*i*-Pent (3) at 50% probabilty. (H-atoms were omitted for clarity).

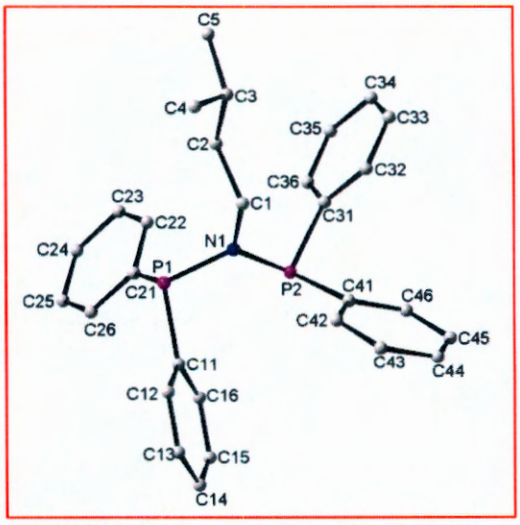

Figure 7.15: Graphical representation of the re-optimized structure of PNP-*i*-Pent isomer 11, using the B3LYP/6-,31+G(d,p) basis set (3*). (H-atoms were omitted for clarity).

The crystal structure of PNP-*i*-Pent adopted approximate C_{2V} conformation (see **Figure 7.14**), while the optimized calculated structure adopted an approximate conformation C_S (see **Figure 7.15**). Interestingly, isomer 10 displays the same conformation as the crystal structure, but the energy of this isomer is not the lowest of the 11 isomers calculated (see **Figure 7.11**).

Table 7.7: Selected bond angles (°) for the crystal structure of PNP-*i*-Pent (3) and the calculated PNP-*i*-Pent isomer 11 (3*).

Bond angles (°)	3	3*
P1-N1-P2	111.0(1)	122.6
C11-P1-C21	104.0(1)	102.2
C31-P2-C41	103.2(1)	101.1
C1-N1-P1	125.0(1)	114.4
C1-N1-P2	123.7(1)	122.8

The P-N-P angle for the calculated structure is substantially larger (122.6 °) than that in the crystal structure (111.0(1) °) (see **Table 7.7**). This is due to the different conformations adopted by the two structures. The crystal structure requires space for the sterically bulky phenyl rings in the approximate C_{2V} conformation by forcing the P-N-P angle to a smaller value. The calculated structure requires steric hindrance due to its approximate C_S conformation and a larger P-N-P angle is observed.

Table 7.8: Selected bond lengths (Å) for the crystal structure of PNP-*i*-Pent (3) and the calculated PNP-*i*-Pent isomer 11 (3*).

Bond Length (Å)	3	3*
P1-N1	1.712(2)	1.749
P2-N1	1.703(2)	1.744
N1-C1	1.483(2)	1.488
P1-C11	1.830(2)	1.857
P1-C21	1.830(2)	1.850
P2-C31	1.832(2)	1.863
P2-C41	1.829(2)	1.856

The bond lengths in the crystal structure are overall shorter than the bond lengths for the predicted structure of the calculated PNP-*i*-Pent isomer 11 structure (see **Table 7.8**).

Table 7.9: Selected torsion angles (°) for the crystal structure of PNP-*i*-Pent (3) and the calculated PNP-*i*-Pent isomer 11 (3*).

Torsion angles (°)	3	3*
N1-P1-C11-C12	159.2(1)	106.4
N1-P1-C21-C22	95.5(1)	-33.8
N1-P2-C31-C32	169.2(1)	80.4
N1-P2-C41-C42	96.1(1)	22.2

The phenyl rings of the two structures have noticeably different orientations due to the different conformations that were adopted (see **Figure 7.13**). This is further illustrated by the large differences in the torsion angles of the respective structures (see **Table 7.9**).

7.3.4 PNP-Cychex (4 *vs.* 4*)

Seven possible isomers of the PNP-Cychex non-coordinated ligand were identified and optimized at a B3LYP/LANL2DZ level. The varying ΔEnergy values of each of the isomers are illustrated in **Figure 7.16.**

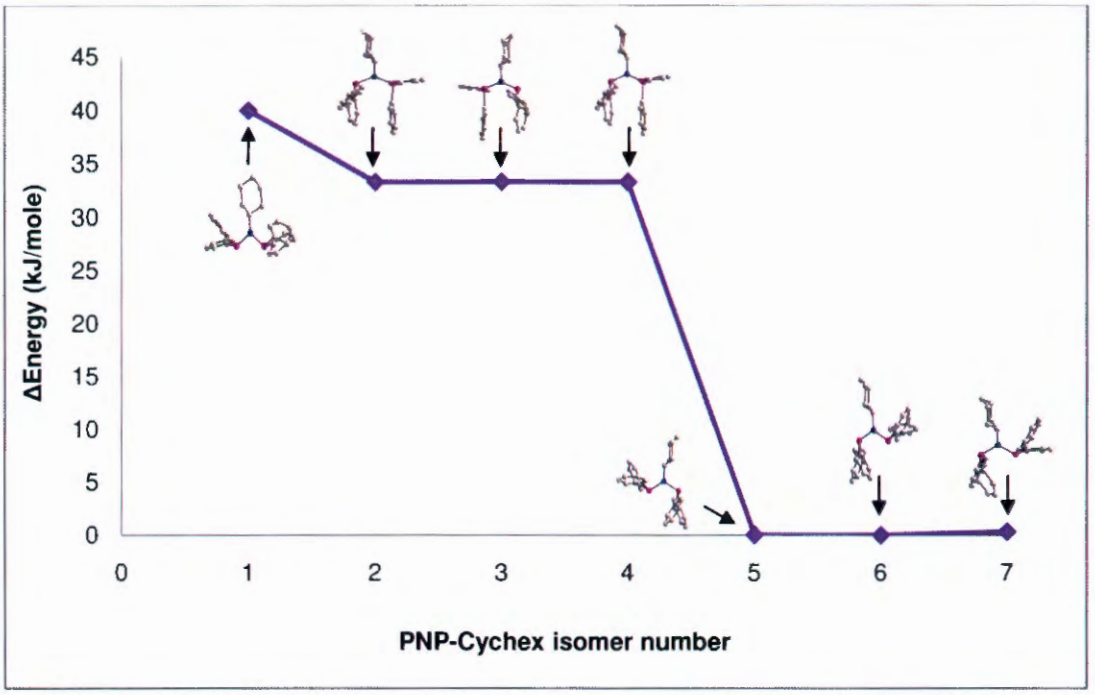

Figure 7.16: Graph of normalized ΔEnergy (kJ/mole) *versus* PNP-Cychex isomer number. The ΔEnergy was calculated using the B3LYP/LANL2DZ basis set.

The PNP-Cychex isomer 7, which has the lowest ΔEnergy (normalized to 0 kJ/mole) was re-optimized at a higher level of theory using the B3LYP/6-,31+G(d,p) basis set. An overlay of the two structures calculated using the B3LYP/LAN2DZ and B3LYP/6-,31+G(d,p) basis sets is presented in **Figure 7.17**.

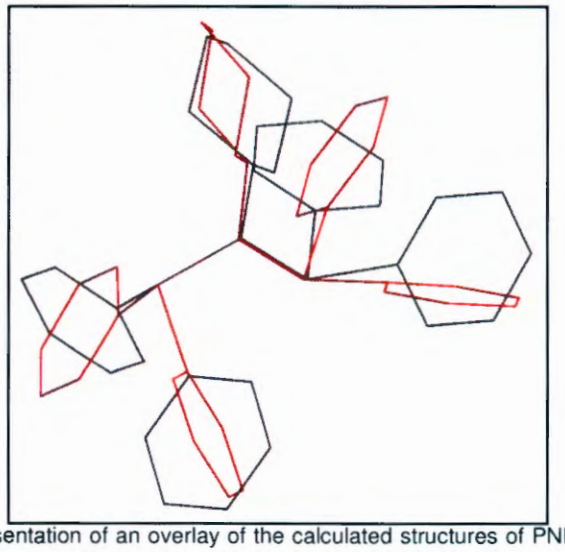

Figure 7.17: Graphical representation of an overlay of the calculated structures of PNP-Cychex isomer 7 using the B3LYP/LANL2DZ basis set (black) and the B3LYP/6-31+G(d,p) basis set (red).

A comparison is made between the crystal structure of PNP-Cychex (4) (see §4.2.4) and the re-optimized structure (will be referred to as 4*) of the corresponding compound, an overlay of these structures illustrates the differences observed in **Figure 7.18**.

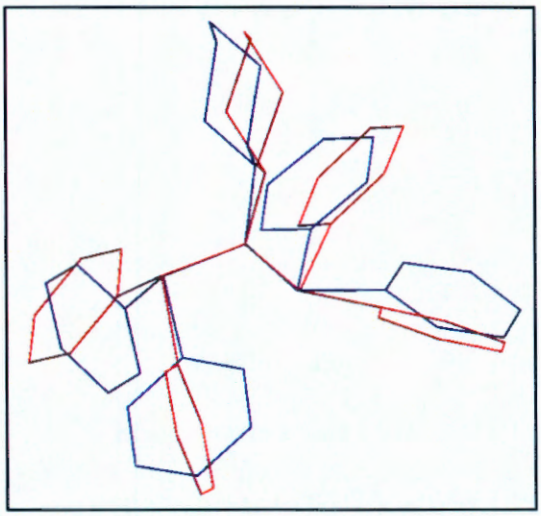

Figure 7.18: Graphical representation of an overlay of the crystal strucutre of PNP-Cychex (4) (blue) and the calculated structure of PNP-Cychex isomer 7 using the B3LYP/6-31+G(d,p) basis set (4*) (red).

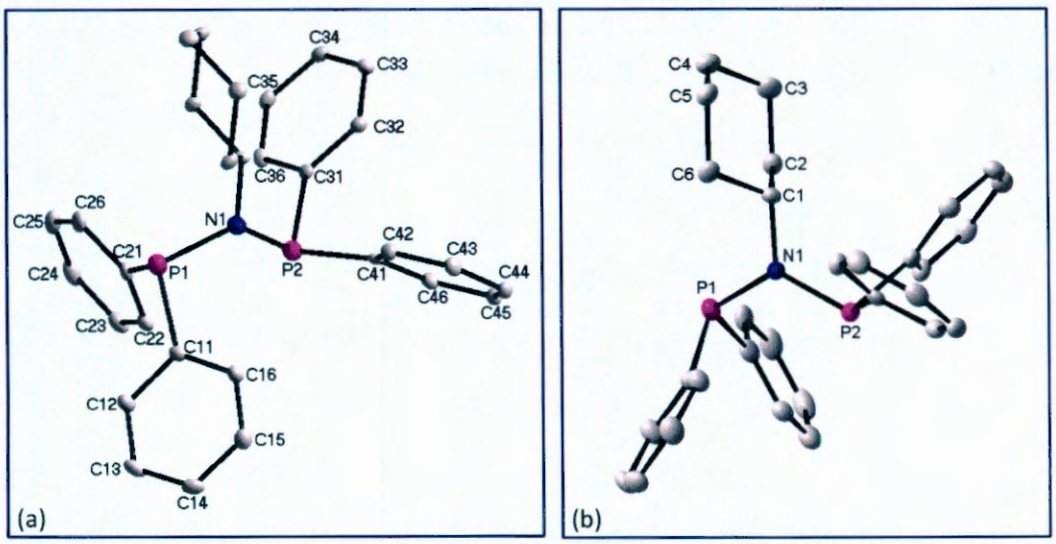

Figure 7.19a and b: Graphical representation of the different viewing angles of the crystal structure of PNP-Cychex (4) at 50% probability. (H-atoms were omitted for clarity).

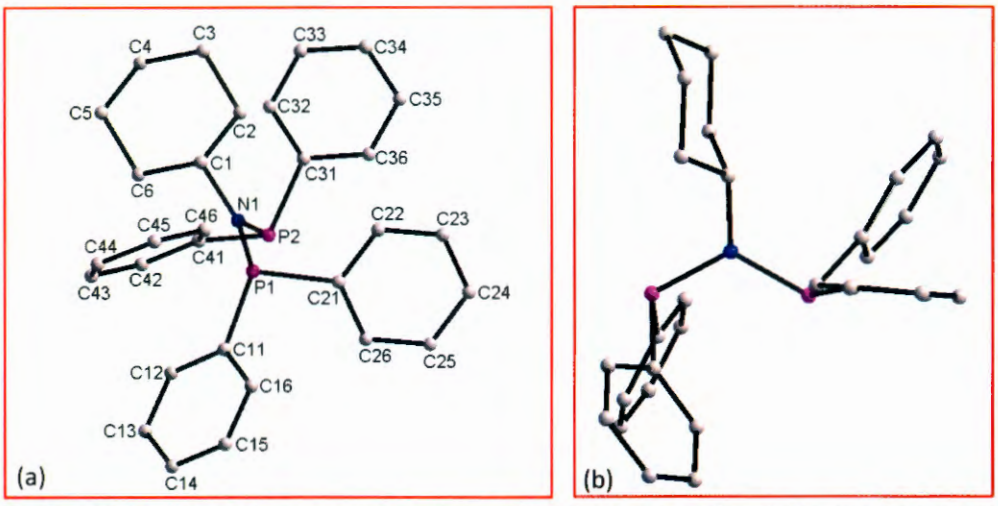

Figure 7.20a and b: Graphical representation of the different viewing angles of the re-optimized structure of PNP-Cychex isomer 7, using the B3LYP/6-,31+G(d,p) basis set (4*). (H-atoms were omitted for clarity).

It is clear from **Figures 7.19** and **7.20** that the crystal structure has the same conformation as the calculated isomer 7 (approximate conformation C_S). This is as expected since the alkyl substituent bonded to the nitrogen is sterically bulky and this conformation has to be adopted to create space for this. This is further illustrated by the fact that calculated isomer 1 (see **Figure 7.16**) has the highest relative energy, this conformation creates the least space for a nitrogen bonded alkyl group.

Table 7.10: Selected bond angles (°) for the crystal structure of PNP-Cychex (4) and the calculated PNP-Cychex isomer 7 (4*).

Bond angles (°)	4	4*
P1-N1-P2	119.5(2)	121.3
C11-P1-C21	102.2(2)	102.6
C31-P2-C41	100.0(2)	101.4
C1-N1-P1	115.1(2)	116.7
C1-N1-P2	122.1(2)	121.9

The P-N-P bond angle for the calculated structure (121.3 °) is slightly larger than that of the crystal structure (119.5 °). The smaller C1-N1-P1 angle for the crystal structure (115.1(1)°) indicate that the alkyl group is more tilted towards P1 than the alkyl group of the calculated structure (116.7°). The rest of the bond angles as reported in **Table 7.10** are relatively similar.

Table 7.11: Selected bond lengths (Å) for the crystal structure of PNP-Cychex (4) and the calculated PNP-Cychex isomer 7 (4').

Bond Length (Å)	4	4'
P1-N1	1.731(2)	1.752
P2-N1	1.703(3)	1.749
N1-C1	1.502(3)	1.499
P1-C11	1.834(3)	1.858
P1-C21	1.836(3)	1.850
P2-C31	1.851(3)	1.865
P2-C41	1.836(3)	1.856

The P-N bond lengths of the crystal structure is slightly shorter (1.703(3) -1.731(2) (Å)) than that of the calculated structure (1.749 – 1.752 (Å)). This is the also the case for the C-P bonds that are shorter for the crystal structure (1.834(3) – 1.851(3) (Å)) than the calculated structure (1.850 – 1.865 (Å)).

Table 7.12: Selected torsion angles (°) for the crystal structure of PNP-Cychex (4) and the calculated PNP-Cychex isomer 7 (4').

Torsion angles (°)	4	4'
N1-P1-C11-C12	-161.8(1)	111.6
N1-P1-C21-C22	80.6(1)	-44.1
N1-P2-C31-C32	91.9(1)	32.5
N1-P2-C41-C42	5.1(1)	77.6

Even though the crystal structure and the calculated structure display similar conformations it can be seen from **Table 7.12** that there are large differences in torsion angles, which indicates that the orientation of the phenyl rings are different. Slight differences in the orientation of the phenyl rings is possibly due to packing effects in the crystal structure, whereas the optimised structure is calculated in gaseous form.

7.3.5 PNP-*n*-Pent (5 *vs.* 5*)

Ten possible isomers of the PNP-*n*-Pent non-coordinated ligand were identified and optimized at a B3LYP/LANL2DZ level. The varying ΔEnergy values of each of the isomers are illustrated in **Figure 7.21**.

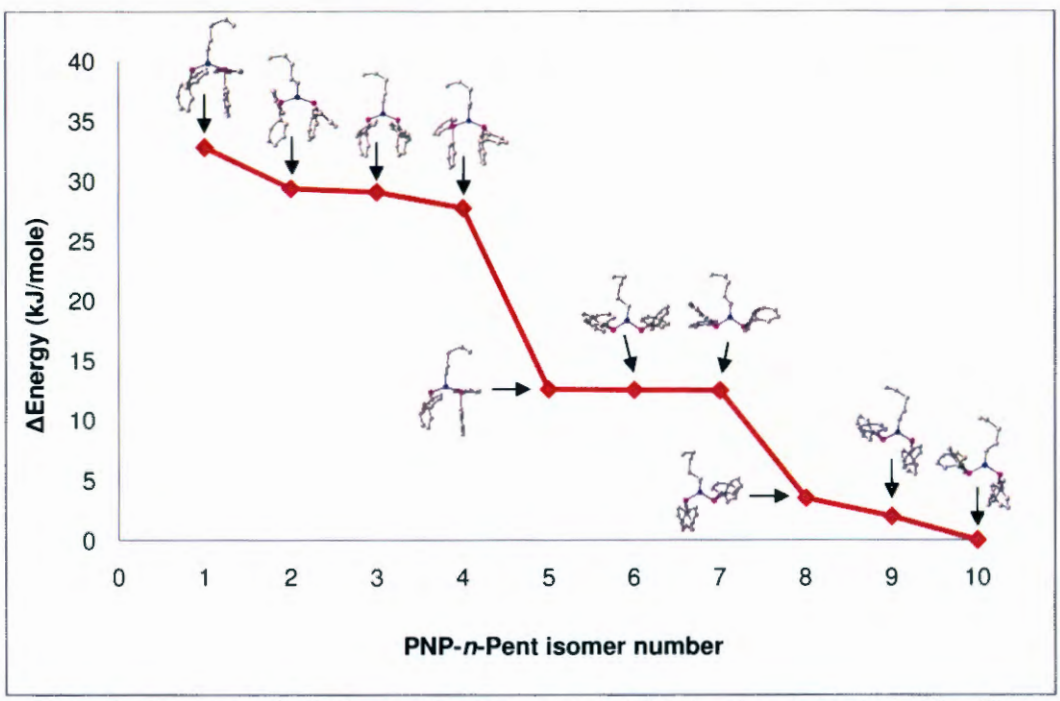

Figure 7.21: Graph of normalised ΔEnergy (kJ/mole) *versus* PNP-*n*-Pent isomer number. The ΔEnergy was calculated using the B3LYP/LANL2DZ basis set.

The PNP-*n*-Pent isomer 10 (normalized to 0 kJ/mole) was re-optimized using the B3LYP/6-,31+G(d,p) basis set. An overlay of the PNP-*n*-Pent structures calculated using the basis sets, B3LYP/LAN2DZ and B3LYP/6-,31+G(d,p) respectively can be seen in **Figure 7.22**.

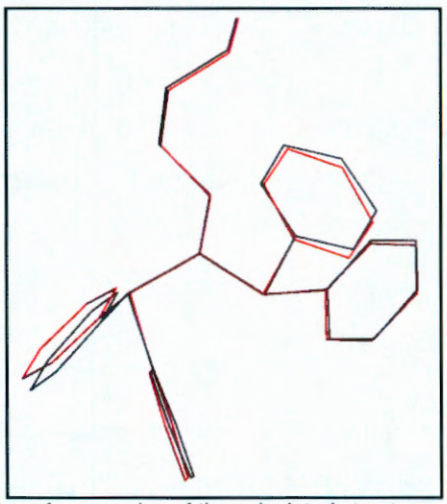

Figure 7.22: Graphical representation of an overlay of the calculated structures of PNP-*n*-Pent isomer 10 using the B3LYP/LANL2DZ basis set (black) and the B3LYP/6-31+G(d,p) basis set (red).

There are two crystallographically independent molecules in the asymmetric unit of the PNP-*n*-Pent crystal structure (5I and 5II) (see §4.2.5). These two molecules are both compared with the re-optimized structure of PNP-*n*-Pent isomer 10 (will be referred to as 5*). The differences between the re-optimized structure and the crystal structure are further illustrated by the overlay of the calculated structure with each of the two independent molecules of the crystal structure (see **Figures 7.23** and **7.24**).

Figure 7.23: Graphical representation of an overlay of the crystal strucutre of PNP-*n*-Pent (I) (5I) (blue) and the calculated structure of PNP-*n*-Pent isomer 10 using the B3LYP/6-31+G(d,p) basis set (5*) (red).

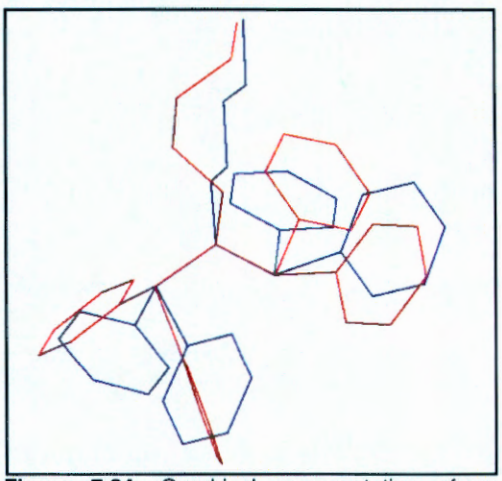

Figure 7.24: Graphical representation of an overlay of the crystal strucutre of PNP-*n*-Pent (II) (5II) (blue) and the calculated structure of PNP-*n*-Pent isomer 10 using the B3LYP/6-31+G(d,p) basis set (5*) (red).

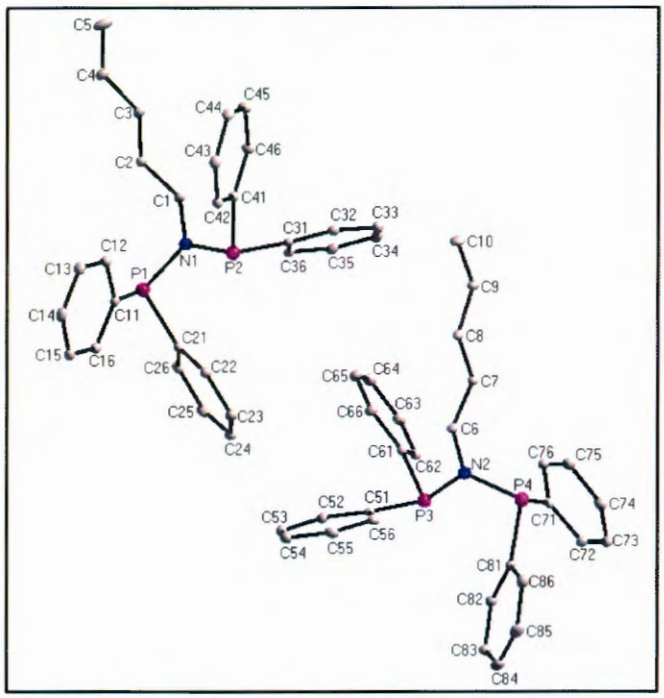

Figure 7.25: Graphical representation of the crystal structure of PNP-*n*-Pent (I and II) at 50% probability. (H-atoms were omitted for clarity).

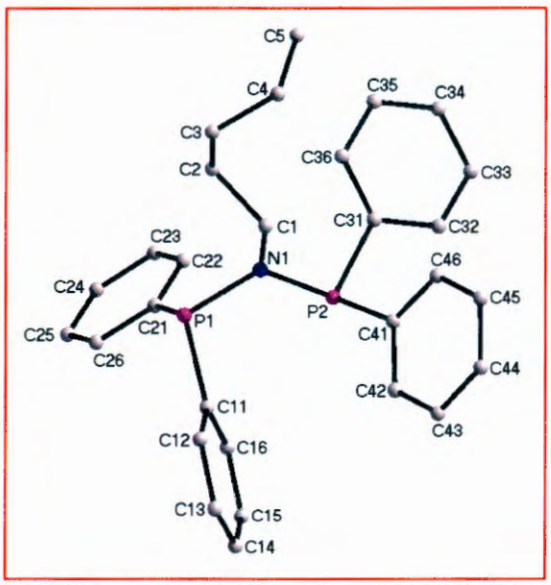

Figure 7.26: Graphical representation of the re-optimized structure of PNP-*n*-Pent isomer 10, using the B3LYP/6-,31+G(d,p) basis set (5*). (H-atoms were omitted for clarity).

The two molecules of the crystal structure and the calculated structure (see **Figures 7.25** and **7.26**) adopted an approximate conformation C_S (see **Figure 4.2** in §4.1 and).

Table 7.13: Selected bond angles (°) for the crystal structure of PNP-*n*-Pent I and II (5I and 5II) and the calculated PNP-*n*-Pent isomer 10 (5*).

Bond angles (°)	5I and 5II	5*
P1 – N1 – P2	123.4(1)	121.1
P3 – N2 – P4	120.5(1)	-
C1 – N1 – P1	116.0(1)	113.5
C6 – N2 – P3	123.8(1)	-
C1 – N1 – P2	123.4(1)	120.7
C6 – N2 – P4	115.7(1)	-
C11 – P1 – C21	101.5(1)	102.1
C51 – P3 – C61	100.7(1)	-
C31 – P2 – C41	101.1(1)	101.5
C71 – P4 – C81	100.7(1)	-

The bond angles of the calculated structure are closer to the corresponding angles of the first molecule (the PNP-*n*-Pent molecule containing N1, see **Figure 7.25**) (see **Table 7.13**). The C1-N1-P1 angle of the crystal structure (molecule 1) and the calculated structure (116.0(1) and 113.5 ° respectively) indicate that the pentyl group is tilted towards P1 for both these structures. The distortion at the phosphorous atoms are also predicted for the calculated PNP-*n*-Pent isomer 10 as is illustrated by the C-P-C angles that range between 101.5 and 102.1 ° which is significantly smaller than the ideal 109.5 ° of a tetrahedral geometry.

Table 7.14: Selected bond lengths (Å) for the crystal structure of PNP-*n*-Pent I and II (5I and 5II) and the calculated PNP-*n*-Pent isomer 10 (5˙).

Bond length (Å)	5I and 5II	5˙
P1 – N1	1.713(1)	1.736
P3 – N2	1.708(1)	-
P2 – N1	1.712(1)	1.728
P4 – N2	1.718(1)	-
N1 – C1	1.482(1)	1.483
N2 – C6	1.483(1)	-
P1 – C11	1.828(1)	1.849
P3 – C51	1.834(1)	-
P1 – C21	1.830(1)	1.843
P3 – C61	1.840(1)	-
P2 – C31	1.834(1)	1.848
P4 – C71	1.825(1)	-
P2 – C41	1.836(1)	1.855
P4 – C81	1.838(1)	-

The P-C bonds range between 1.825(1) and 1.840(1) Å in the crystal structure which is shorter than the corresponding angles of the calculated structure that range between 1.843 and 1.855 Å for the calculated structure. A similar trend is observed for the P-N bond lengths, with longer bond lengths for the crystal structure (1.708 and 1.713 Å) in comparison to the calculated structure (1.728 – 1.736 Å).

Table 7.15: Selected torsion angles (°) for the crystal structure of PNP-*n*-Pent I and II (5I and 5II) and the calculated PNP-*n*-Pent isomer 10 (5*).

Torsion angles (°)	5I and 5II	5*
N1 – P1 – C11 – C12	37.9(1)	-10.3
N1 – P3 – C51 – C52	-158.5(1)	-
N1 – P1 – C21 – C22	69.3(1)	98.7
N1 – P3 – C61 – C62	-114.6(1)	-
N1 – P2 – C31 – C32	108.9(1)	172.7
N1 – P4 – C71 – C72	147.9(1)	-
N1 – P2 – C41 – C42	159.5(1)	96.1
N1 – P4 – C81 – C82	-65.6(1)	-

The torsion angles listed in **Table 7.15** indicate that all three structures (two molecules of the crystal structure and the calculated structure) have very different orientations for all the corresponding phenyl rings. It appears that even though all three structures (two crystallographic structures and the re-optimized PNP-n-Pent isomer 10) adopted approximate C_S conformations, the phenyl rings have degrees of freedom to arrange differently for the three structures.

7.4 Discussion

The theoretical structures for the various compounds (PNP-Ethyl, PNP-Dimprop, PNP-*i*-Pent, PNP-*n*-Pent and PNP-Cychex) were successfully calculated and optimised. The conformations of the compounds were correctly predicted by theory for four of the five compounds (see **Table 7.16**) with PNP-*i*-Pent being the only compound to adopt an approximate C_{2v} conformation in contrast to the predicted C_S conformation.

Table 7.16: Conformations (see **Figure 4.2** in §4.1) for the crystal structures and the calculated structures of PNP-Ethyl, PNP-Dimprop, PNP-*i*-Pent, PNP-*n*-Pent and PNP-Cychex.

		Conformation
Crystal structure:	PNP-Ethyl (1)	C_S
Calculated structure:	PNP-Ethyl isomer 9 (1*) [a]	C_S
Crystal structure:	PNP-Dimprop (2)	C_S
Calculated structure:	PNP-Dimprop isomer 11 (2*)[b]	C_S
Crystal structure:	PNP-*i*-Pent (3)	C_S
Calculated structure:	PNP-*i*-Pent isomer 11 (3*)[c]	C_{2v}
Crystal structure:	PNP-Cychex (4)	C_S
Calculated structure:	PNP-Cychex isomer 7 (4*)[d]	C_S
Crystal structure:	PNP-*n*-Pent (5)	C_S
Calculated structure:	PNP-*n*-Pent isomer 10 (5*)[e]	C_S

(a) See Figure 7.5; (b) See Figure 7.10; (c) See Figure 7.15; (d) See Figure 7.20; (e) See Figure 7.26

The conformation of the crystal structure of PNP-i-Pent (approximate C_{2v}) is possibly influenced by the (C35-H35···P2) weak intermolecular hydrogen interaction described in §4.2.3 (see Chapter 4). The structure of the calculated PNP-*i*-Pent isomer 11 does however not take intermolecular interactions into account, since the calculations are performed as if the compound is in ideal gaseous state. This could explain why the optimized structure adopted the approximate conformation C_{2v}. The bond and torsion angles are consequently significantly different due to the difference in adopted conformations for the two structures.

It was shown that even though the conformations were similar for the crystal and calculated structures, deviations between the corresponding structures were present. These deviations are clearly illustrated by the torsion angles for the different structures that indicated different orientations of the phenyl rings of the corresponding structures. The differences between the crystallographic data and the corresponding calculated structure are possibly due to packing effects within a crystal structure where intermolecular interactions could significantly influence the structure of the compound.

In contrast the calculated structures are optimized as if in the gaseous form with no intermolecular interactions present.

The isomers of PNP-Ethyl, PNP-Dimprop, PNP-*i*-Pent and PNP-*n*-Pent that were re-optimized using the higher level of theory, corresponded very well to the relevant crystal structures with regards to bond angles. A trend was observed for the series of free PNP-alkyl ligand crystals (as discussed in Chapter 4) in which the P-N-P angle became smaller as the steric bulk of the alkyl moiety increased. A similar trend is observed for the calculated PNP-alkyl structures, with the P-N-P angle of PNP-Ethyl (122.8 °) that is larger than the corresponding angles of PNP-Cychex (121.3 °) and PNP-Dimprop (120.0 °) which have more sterically bulky alkyl substituents.

The bond lengths for all the isomers of the lowest ΔEnergy which were re-optimized, were longer than the corresponding bond lengths of the related crystal structures. It is inherent of the technique, when performing theoretical calculations, to over-estimate the bond lengths for the structures calculated. This overestimation is however only approximately 1% when comparing the bond lengths of the calculated structures to the related crystal structures.

Table 7.17: Selected bond lengths (Å) for the calculated (isomer with lowest energy which was re-optimized at B3LYP/6-,31+G(d,p) level) and crystal structures of PNP-Ethyl, PNP-Dimprop, PNP-*i*-Pent, PNP-*n*-Pent and PNP-Cychex.

Bond lengths (Å)	P1-N1 (Calc)	P1-N1 (XRD)	P2-N1 (Calc)	P2-N1 (XRD)	N1-C1 (Calc)	N1-C1 (XRD)
PNP-*n*-Pent	1.736	1.713(1)	1.728	1.712(1)	1.488	1.482(1)
PNP-Ethyl	1.744	1.712(1)	1.749	1.713(1)	1.487	1.485(2)
PNP-*i*-Pent	1.749	1.712(2)	1.744	1.703(2)	1.488	1.483(2)
PNP-Cychex	1.752	1.758(4)	1.749	1.686(5)	1.499	1.502(6)
PNP-Dimprop	1.752	1.721(2)	1.753	1.727(2)	1.505	1.515(2)

Calc = calculated structure , XRD = crystal structure

It appears that selected bond lengths (P1-N1, P2-N1 and N1-C1) for the calculated and re-optimized free PNP-ligands increase in length as the alkyl moiety of the PNP-ligands

become more sterically bulky (see **Table 7.17**). The above-mentioned bond lengths are for example slightly longer for PNP-Dimprop in comparison to the corresponding bond lengths of PNP-Ethyl. It is possible that the bonds are calculated to be longer in order to provide space for the sterically bulky alkyl groups. It is of interest to note that a similar trend with regards to the bond lengths was observed and discussed in the crystallographic study of the non-coordinated PNP-ligands (see Chapter 4).

This chapter described the theoretical study on the free ligands The theoretical study on the various platinum(II)- and palladium(II) coordinated bis(diphenylphosphino)amine complexes are presented, described and compared to the corresponding crystal structures in Chapter 8.

8 Theoretical study of Pt-PNP and Pd-PNP complexes

In this chapter...

The theoretical calculations of the crystal structures of the [$PtCl_2$(PNP-alkyl)] and the [$PdCl_2$(PNP-alkyl)] complexes are presented. The calculated structures are compared with the crystallographic data of the corresponding complexes.

8.1 Introduction

Theoretical calculations are increasingly being used to gather information involving metal ions in coordination and organometallic chemistry.[1,2,3] Various platinum(II) and palladium(II) complexes have been optimized using density functional theory (DFT) calculations and compared to the corresponding single crystal X-ray crystallographic data, in order to better understand the factors which determine the adopted structure in solid state.[4,5,6]

The DFT optimized geometric structures for the [$PtCl_2$(PNP-alkyl)] and [$PdCl_2$(PNP-alkyl)] complexes in this PhD study are compared with the X-ray crystallographic data in conjunction with the free ligands (Chapter 7). This study was undertaken to determine from the differences and similarities what influences the geometry of the square planar complexes as the alkyl substituents of the coordinated diphosphinoamine ligands change from one complex to another.

8.2 Experimental

The structures of the [$PtCl_2$(PNP-alkyl)] and [$PdCl_2$(PNP-alkyl)] complexes were fully optimized with the density functional theory (DFT) using the Becke3-Lee-Yang-Parr

---

[1] Woo, T., Folga, E. and Ziegler, T., *Organometallics*, **1993**, *12*, 1289.
[2] Branchadell, V., Moreno-Manas, M., Pajuelo, F. and Pleixtas, R., *Organometallics*, **1999**, *18*, 4934.
[3] Burckhardt, U., Casty, G.L., Tilley, T.D., Woo, T. and Rothlisberger, U., *Organometallics*, **2000**, *19*, 3830.
[4] Magistrato, A., Merlin, M., Pregosin, P.S. and Rothlisberger, U., *Organometallics*, **2000**, 19, 3591.
[5] Atesin, T.A., Oster, S.S., Skugrud, K. and Jones, W.D., *Inorg. Chim. Acta*, **2006**, *359*, 2798.
[6] Zhao, X., Pan, Q., Li, M., Xia, B. and Zhang, H., *J. Mol. Struc.*, **2007**, *822*, 65.

(B3LYP)[7] functionals supplemented with the standard 6-31G(d,p) and LANL2DZ basis sets. All calculations were carried out using the Gaussian 03 software suite[8].

These optimized structures were then compared to the crystallographic data of the corresponding complexes. Molecular diagrams of the structures (using DIAMOND 3.0[9]) are presented and overlays of the calculated structures with the corresponding crystal structures (using Hyperchem 7.52[10]). Selected geometric parameters of the calculated structures and corresponding crystal structures are presented and discussed. Theoretical calculations were performed on the following complexes (see Chapter 5 for the abbreviations):

6) [$PtCl_2$(PNP-Ethyl)]
7) [$PtCl_2$(PNP-*n*-Propyl)]
8) [$PtCl_2$(PNP-Dimprop)]
9) [$PtCl_2$(PNP-*i*-Pent)]
10) [$PtCl_2$(PNP-Cychex)]
11) [$PdCl_2$(PNP-*i*-Prop)])
12) [$PdCl_2$(PNP-Dimprop)]
13) [$PdCl_2$(PNP-*n*-Prop)
14) [$PdCl_2$(PNP-*i*-Pent)]
15) [$PdCl_2$(PNP-*n*-Butyl)]

Each of the crystal structures are denoted with numerical values for example 6, 7 and 8, while the corresponding calculated structures at B3LYP/6-,31+G(d,p) are indicated as 6^*, 7^*, 8^* and so forth.

[7] Lee, C., Yang, W. and Parr, R. G., *Phys. Rev.* B, **1988**, *37*, 785.
[8] Gaussian 03, Revision C.01, Frisch, M. J., Trucks, G. W., Schlegel, H. B., Scuseria, G. E., Robb, M. A., Cheeseman, J. R., Montgomery, Jr., J. A., Vreven, T., Kudin, K. N., Burant, J. C., Millam, J. M., Iyengar, S. S., Tomasi, J., Barone, V., Mennucci, B., Cossi, M., Scalmani, G., Rega, N., Petersson, G. A., Nakatsuji, H., Hada, M., Ehara, M., Toyota, K., Fukuda, R., Hasegawa, J., Ishida, M., Nakajima, T., Honda, Y., Kitao, O., Nakai, H., Klene, M., Li, X., Knox, J. E., Hratchian, H. P., Cross, J. B., Adamo, C., Jaramillo, J., Gomperts, R., Stratmann, R. E., Yazyev, O., Austin, A. J., Cammi, R., Pomelli, C., Ochterski, J. W., Ayala, P. Y., Morokuma, K., Voth, G. A., Salvador, P., Dannenberg, J. J., Zakrzewski, V. G., Dapprich, S., Daniels, A. D., Strain, M. C., Farkas, O., Malick, D. K., Rabuck, A. D., Raghavachari, K., Foresman, J. B., Ortiz, J. V., Cui, Q., Baboul, A. G., Clifford, S., Cioslowski, J., Stefanov, B. B., Liu, G., Liashenko, A., Piskorz, P., Komaromi, I., Martin, R. L., Fox, D. J., Keith, T., Al-Laham, M. A., Peng, C. Y., Nanayakkara, N., Challacombe, M., Gill, P. M. W., Johnson, B., Chen, W., Wong, M. W., Gonzalez, C., & Pople, J. A., Gaussian, Inc,Pittsburgh PA, **2003**.
[9] Brandenburg, K. and Putz, H., **2005**, DIAMOND. Release 3.0c. Crystal Impact GbR, Bonn, Germany.
[10] Hyperchem ™ Release 7.52, Windows Molecular Modeling System, Hypercube, Inc., **2002**.

8.3 Theoretical calculations on [$PtCl_2$(PNP-alkyl)] complexes.

8.3.1 [$PtCl_2$(PNP-Ethyl)] (6 *vs.* 6*)

The [$PtCl_2$(PNP-Ethyl)] (6) crystal structure, see §5.2.1 (see **Figure 8.1**) is compared to the corresponding calculated structure (6*) (see **Figure 8.2**).

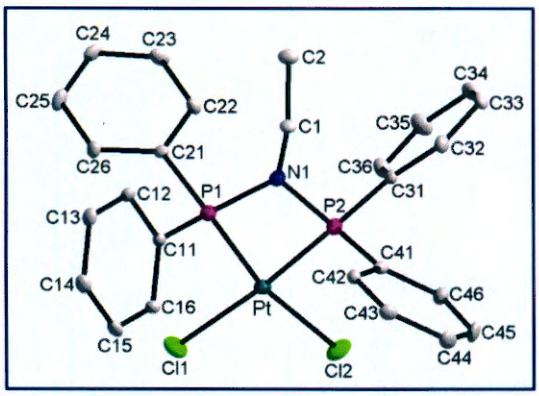

Figure 8.1: Graphical representation of the crystal structure of [$PtCl_2$PNP-Ethyl] (6) at 50% probability. (H-atoms were omitted for clarity.)

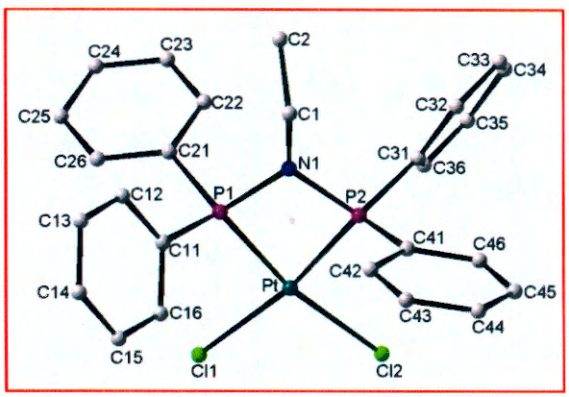

Figure 8.2: Graphical representation of the calculated structure of [$PtCl_2$PNP-Ethyl] (6*). (H-atoms were omitted for clarity.)

Table 8.1: Selected bond angles(°) for the crystal structure of [$PtCl_2$PNP-Ethyl] (6) and the calculated [$PtCl_2$PNP-Ethyl] structure (6*).

Bond angles (°)	6	6*
P1 – Pt - P2	72.1(1)	72.8
Cl1 – Pt - Cl2	91.7(1)	94.7
P1 - N1 - P2	100.0(2)	101.4
C11 - P1 - C21	107.0(2)	106.8
C31 - P2 - C41	106.5(2)	106.4

Both crystallographic and calculated structures indicate a distorted square-planar geometry for the platinum complex, with P-Pt-P and Cl-Pt-Cl angles all deviating from the ideal 90 °. The P-Pt-P angle for the calculated [$PtCl_2$(PNP-Ethyl)] complex is only slightly larger (0.7 ° difference) than the corresponding angle of the crystal structure (see **Table 8.1**). The angles of the two structures are comparable within experimental error.

Table 8.2: Selected torsion angles(°) for the crystal structure of [$PtCl_2$PNP-Ethyl] (6) and the calculated [$PtCl_2$PNP-Ethyl] structure (6*).

Torsion angles (°)	6	6*
Pt – P1 – C11 – C12	175.2(3)	174.5
Pt – P1 – C21 – C22	-63.6(4)	-63.9
Pt – P2 – C31 – C32	-172.8(3)	173.1
Pt – P2 – C41 – C42	-80.8(4)	-67.5

The orientation of ring 4 (phenyl ring containing C41) displays the most significant difference for the two structures, with the torsion angles, Pt-P1-C31-C32, for the crystal structure (-80.8(4) °) and the calculated structure (-67.5 °). The other three rings have very similar torsion angles (see **Table 8.2**), indicating similar phenyl ring orientations of corresponding rings. The torsion angles also indicate a 'fan-like' arrangement (see Chapter 5 for defintion) of the phenyl rings for the crystal and the calculated structure. An overlay of the two structures is presented in **Figure 8.3**.

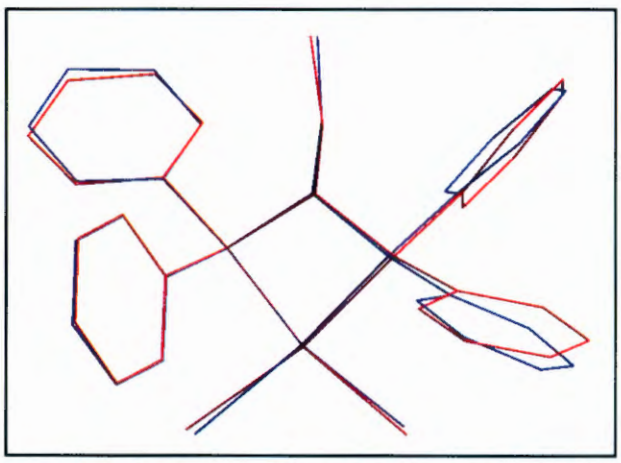

Figure 8.3: Graphical representation of an overlay of the crystal structure of [$PtCl_2$(PNP-Ethyl)] (6) (blue) and the calculated structure of [$PtCl_2$(PNP-Ethyl)] (6*) using the B3LYP/6-31+G(d,p) basis set (red).

Table 8.3: Selected bond lengths (Å) for the crystal structure of [$PtCl_2$PNP-Ethyl] (6) and the calculated [$PtCl_2$PNP-Ethyl] structure (6*).

Bond Length (Å)	6	6*
Pt-P1	2.210(1)	2.256
Pt-P2	2.186(1)	2.255
Pt-Cl1	2.333(1)	2.403
Pt-Cl2	2.343(1)	2.404
P1-N1	1.692(4)	1.732
P2-N1	1.686(3)	1.730
N1-C1	1.475(5)	1.472
P1-C11	1.791(4)	1.823
P1-C21	1.807(4)	1.823
P2-C31	1.793(5)	1.824
P2-C41	1.809(5)	1.824

The bond lengths for the calculated [$PtCl_2$(PNP-Ethyl)] structure are in general slightly longer for the optimised structure when comparing it to the crystal structure (see **Table 8.3**). The N1-C1 bond is however slightly longer for the crystal structure (1.475(5) Å) than the calculated structure (1.472 Å).

8.3.2 [$PtCl_2$(PNP-*n*-Prop)] (7 *vs.* 7*)

The predicted structure for [$PtCl_2$(PNP-*n*-Prop)] (7*) is illustrated in **Figure 8.5** and the crystal structure (7) (see §5.2.2) to which it is compared is shown in **Figure 8.4**.

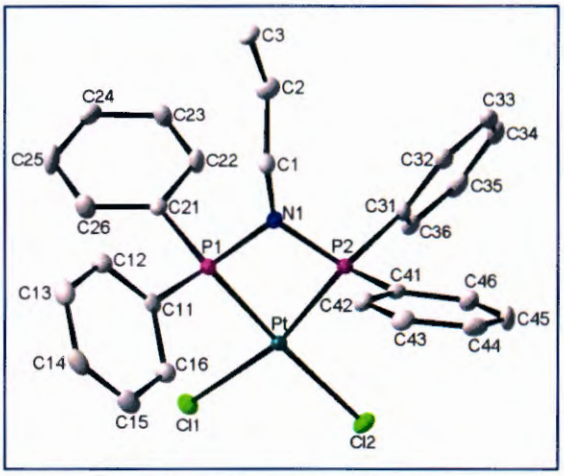

Figure 8.4: Graphical representation of the crystal structure of [$PtCl_2$(PNP-*n*-Prop)] (7) at 50% probability. (H-atoms were omitted for clarity.)

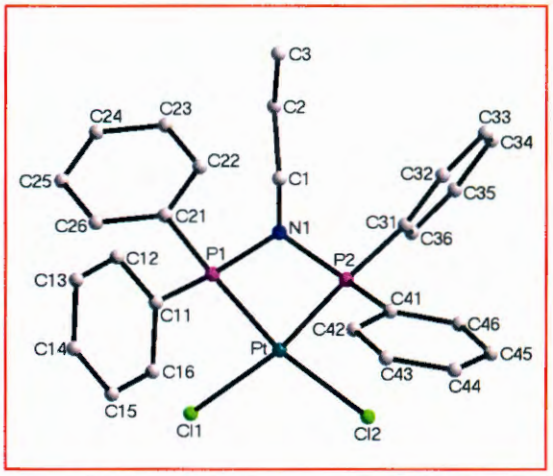

Figure 8.5: Graphical representation of the calculated structure of [$PtCl_2$(PNP-*n*-Prop)] (7*). (H-atoms were omitted for clarity.)

Table 8.4: Selected bond angles(°) for the crystal structure of [$PtCl_2$PNP-*n*-Prop] (7) and the calculated [$PtCl_2$PNP-*n*-Prop] structure (7*) .

Bond angles (°)	7	7*
P1 – Pt - P2	72.4(1)	72.8
Cl1 – Pt - Cl2	92.7(1)	94.8
P1 - N1 - P2	100.1(1)	101.3
C11 - P1 - C21	110.3(1)	106.7
C31 - P2 - C41	103.5(1)	106.3

The P1-Pt-P2 bite angle for the calculated structure (72.8°) is slightly larger than the corresponding angles of crystal structure (72.4(1) °) (see **Table 8.4**). The Cl1-Pt-Cl2 angle in the crystal structure and the calculated structure has a difference of only 2.1 °. The distortion of the square planar geometry of the Pt-PNP complex is evident from the above-mentioned angles which all deviate from the ideal geometry. The C-P-C bond angles of the calculated structure are very similar (106.7 ° and 106.3 ° respectively) whereas the C-P-C angles for the crystal structure differ substantially (110.3(1) ° and 103.5(1) °).

Table 8.5: Selected torsion angles(°) for the crystal structure of [$PtCl_2$(PNP-*n*-Prop)] (7) and the calculated [$PtCl_2$(PNP-*n*-Prop)] structure (7*).

Torsion angles (°)	7	7*
Pt – P1 – C11 – C12	-178.1(2)	-174.7
Pt – P1 – C21 – C22	-60.1(2)	-65.1
Pt – P2 – C31 – C32	176.6(2)	173.6
Pt – P2 – C41 – C42	-76.7(2)	-68.1

The orientation of the phenyl rings for the calculated and crystal structure are very similar as can be seen in **Figure 8.6** in which the overlay of the two structures is illustrated. The torsion angles (**Table 8.5**) also further illustrate the similarity of the phenyl ring orientations, with the difference in angles ranging from 3.0 ° to 8.6 °. The torsion angles also indicate that the phenyl rings are arranged in the 'fan-like' fashion for both structures.

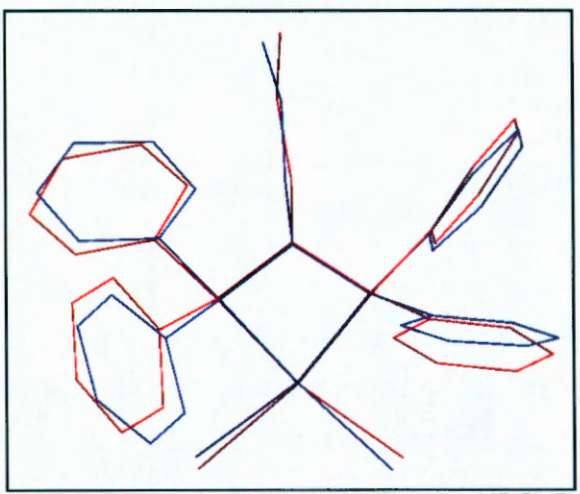

Figure 8.6: Graphical representation of an overlay of the crystal structure of [$PtCl_2$(PNP-*n*-Prop)] (7) (blue) and the calculated structure of [$PtCl_2$(PNP-*n*-Prop)] (7*) using the B3LYP/6-31+G(d,p) basis set (red). RMS= 3.620 x 10^{-2} Å.

Table 8.6: Selected bond lengths (Å) for the crystal structure of [$PtCl_2$(PNP-*n*-Prop)] (7) and the calculated [$PtCl_2$(PNP-*n*-Prop)] structure (7*).

Bond Length (Å)	7	7*
Pt-P1	2.193(1)	2.256
Pt-P2	2.602(1)	2.255
Pt-Cl1	2.346(1)	2.403
Pt-Cl2	2.353(1)	2.404
P1-N1	1.699(2)	1.733
P2-N1	1.695(2)	1.730
N1-C1	1.484(3)	1.471
P1-C11	1.804(3)	1.823
P1-C21	1.804(3)	1.823
P2-C31	1.810(3)	1.824
P2-C41	1.804(3)	1.823

The bond lengths are larger for all the angles of the calculated structure in comparison to the corresponding bond lengths of the crystal structure, except for N1-C1 in the calculated structure which is slightly smaller (1.471 °) than the N1-C1 bond in the crystal structure (1.484(3) °) (see **Table 8.6**).

8.3.3 [$PtCl_2$(PNP-Dimprop)] (8 *vs.* 8*)

The crystal structure of [$PtCl_2$PNP(Dimprop)] (8) (see §5.2.3) contains a 90% occupancy disorder of the alkyl moiety (see **Figure 8.7**), this structure is compared to the calculated structure (8*) (see **Figure 8.8**).

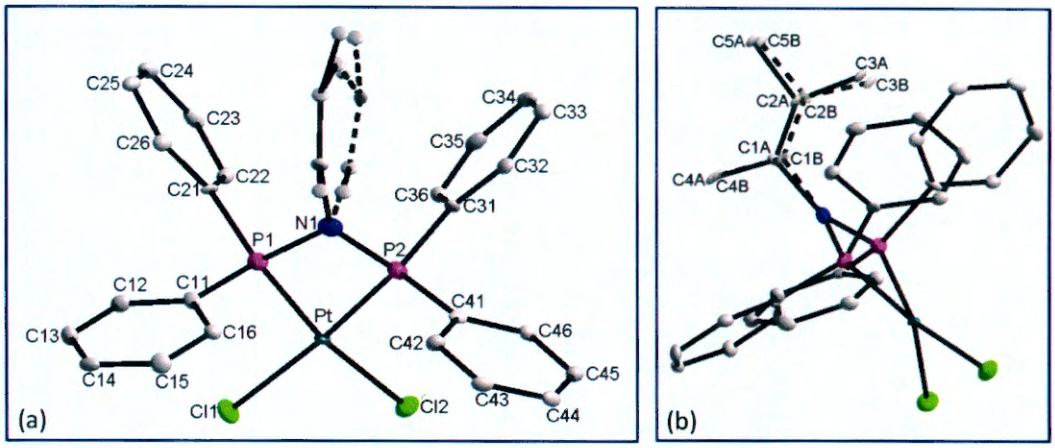

Figure 8.7a and b: Graphical representation of the different viewing angles of the crystal structure of [$PtCl_2$(PNP-Dimprop)] (8) at 50% probability. A/B indicates the disordered carbon atoms in the 1,2-dimethylpropyl alkyl group. Disordered parts belonging together are numbered A and B respectively. (H-atoms were omitted for clarity).

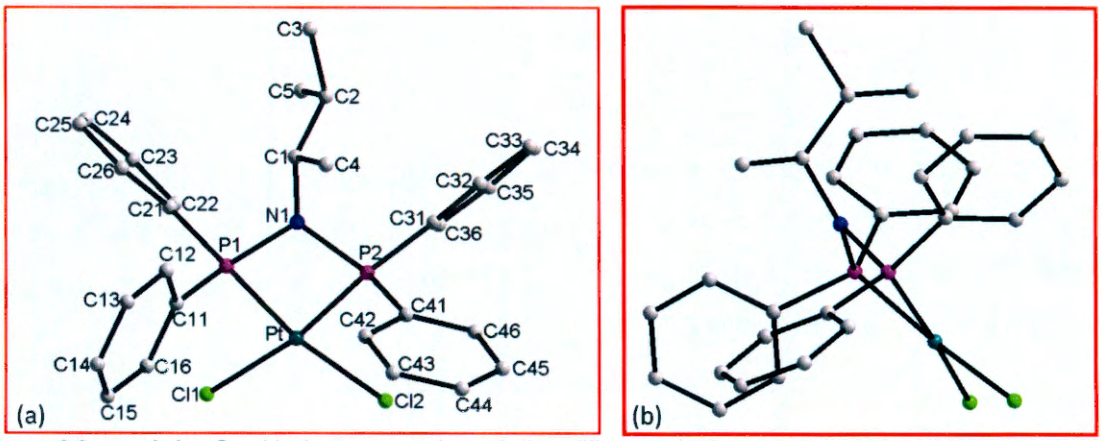

Figure 8.8a and b: Graphical representation of the different viewing angles of the calculated structure of [$PtCl_2$(PNP-Dimprop)] (8*). (H-atoms were omitted for clarity.)

Table 8.7: Selected bond angles(°) for the crystal structure of [$PtCl_2$(PNP-Dimprop)] (8) and the calculated [$PtCl_2$(PNP-Dimprop)] structure (8*).

Bond angles (°)	8	8*
P1-Pt-P2	71.6(1)	74.0
Cl1-Pt-Cl2	91.5(1)	94.5
P1-N1-P2	98.8(1)	102.5
C11-P1-C21	104.8(1)	106.3
C31-P2-C41	105.1(1)	106.8

The P1-Pt-P2 bite angle for the calculated structure (74.0°) is larger than that of the crystal structure (71.6°), but both indicate a significant deviation from the 90° angle expected for a square planar complex. The rest of the bond angles as reported in **Table 8.7** show to be slightly larger for the calculated structure in comparison to the angles of the crystal structure, with the largest difference being 3.7 ° (P1-N1-P2).

Table 8.8: Selected torsion angles(°) for the crystal structure of [$PtCl_2$(PNP-Dimprop)] (8) and the calculated [$PtCl_2$(PNP-Dimprop)] (8*) structure.

Torsion angles (°)	8	8*
Pt-P1-C11-C12	-98.4	139.4
Pt-P1-C21-C22	-11.8	-5.5
Pt-P2-C31-C32	-174.3	-177.6
Pt-P2-C41-C42	-78.2	-66.0

The torsion angles in ring 1, Pt-P1-C11-C12 for the crystal structure and the calculated structure are substantially different, -98.4 and 139.4° respectively. There are only small differences between the other torsion angles in **Table 8.8**, when comparing the crystal and calculated structures. This indicates that the orientations of three of the four phenyl rings are similar and both structures adopted a 'basket-like' orientation (see Chapter 5 for definition) for the phenyl rings. An overlay of the crystal structure (with only the A part of the 90% occupancy disorder illustrated) and the optimized structure further illustrates the phenyl ring arrangements for the two structures (see **Figure 8.9**).

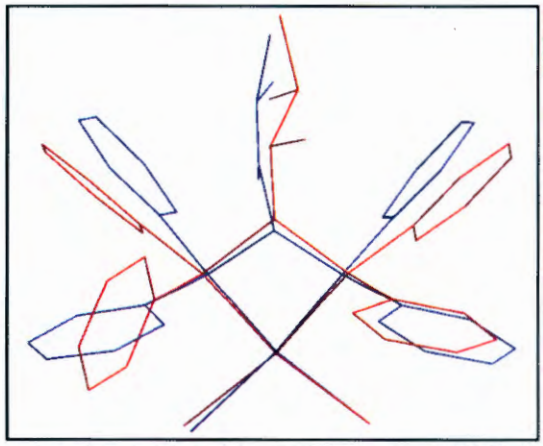

Figure 8.9: Graphical representation of an overlay of the crystal structure of [$PtCl_2$(PNP-Dimprop)] (8) (blue) and the calculated structure of [$PtCl_2$(PNP-Dimprop)] (8*) using the B3LYP/6-31+G(d,p) basis set (red).

Table 8.9: Selected bond lengths (Å) for the crystal structure [$PtCl_2$(PNP-Dimprop)] (8) and the calculated [$PtCl_2$(PNP-Dimprop)] structure (8*).

Bond Length (Å)	8	8*
Pt-P1	2.232(2)	2.339
Pt-P2	2.217(1)	2.350
Pt-Cl1	2.344(1)	2.437
Pt-Cl2	2.337(2)	2.428
P1-N1	1.713(1)	1.806
P2-N1	1.717(1)	1.810
N1-C1A	1.553(2)	1.498
N1-C1B	1.524(2)	-
P1-C11	1.813(1)	1.870
P1-C21	1.802(1)	1.860
P2-C31	1.802(1)	1.862
P2-C41	1.817(1)	1.867

The bond lengths are in general slightly longer for the calculated structure when comparing it to the crystal structure (see **Table 8.9**). The only exception to be observed is the N1-C1 bond which is slightly longer for the crystal structure (range between 1.524(2) and 1.553(2) Å) and the calculated structure (1.498 Å).

8.3.4 [$PtCl_2$(PNP-*i*-Pent)] (9 *vs.* 9*)

The [$PtCl_2$(PNP-*i*-Pent)] (9) crystal structure displays a 50% occupancy disorder of the isopentyl substituent, see §5.2.4 (see **Figure 8.10**). The calculated structure (9*) of the title compound is numbered in a similar fashion for simplicity (see **Figure 8.11**).

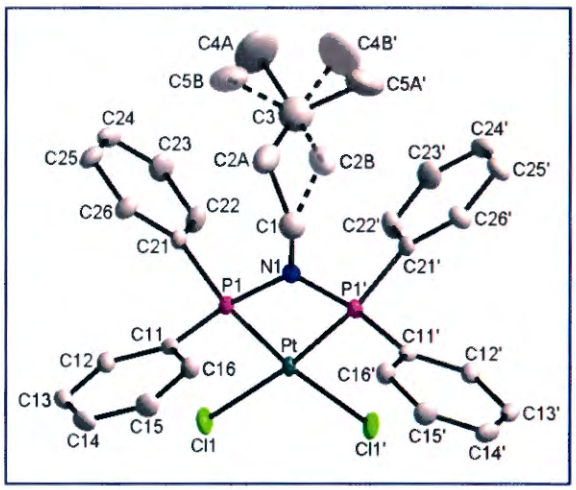

Figure 8.10: Graphical representation of the crystal structure of [$PtCl_2$(PNP-*i*-Pent)] (9) at 50% probability. A/B indicates the disordered carbon atoms in the isopentyl alkyl group. Disordered parts belonging together are numbered A and B respectively. (H-atoms were omitted for clarity).

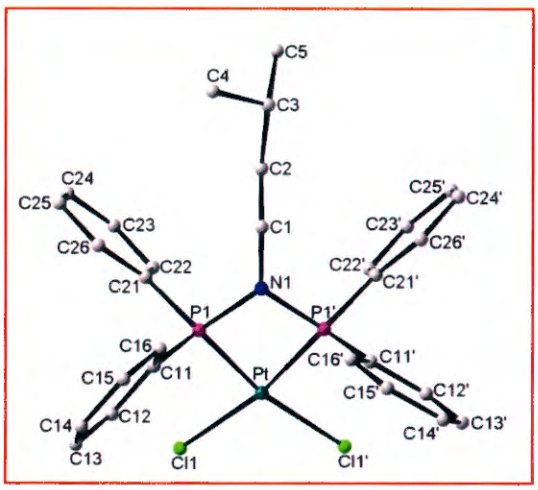

Figure 8.11: Graphical representation of the calculated structure of [$PtCl_2$(PNP-*i*-Pent)] (9*). (H-atoms were omitted for clarity.)

Table 8.10: Selected bond angles(°) for the crystal structure of [$PtCl_2$PNP-*i*-Pent] (9) and the calculated [$PtCl_2$PNP-*i*-Pent] structure (9*).

Bond angles (°)	9	9*
P1 – Pt – P1'	72.2(1)	72.6
Cl1 – Pt – Cl1'	91.3(1)	94.7
P1 - N1 – P1'	99.5(2)	100.7
C11 - P1 - C21	105.6(2)	105.5
C11' – P1' – C21'	105.6(2)	105.3

The bite angle, P1-Pt-P2, of the calculated structure (72.6 °) is only slightly larger than the corresponding angle in the calculated structure (72.2(1) °). The Cl-Pt-Cl angles for the two structures do differ, with the calculated structure being larger (94.7 °) than the corresponding angle of the crystal structure (91.3(1) °). The rest of the angles as reported in **Table 8.10** correspond well for the two structures.

Table 8.11: Selected torsion angles(°) for the crystal structure of [$PtCl_2$PNP-*i*-Pent] (9) and the calculated [$PtCl_2$PNP-*i*-Pent] structure (9*).

Torsion angles (°)	9	9*
Pt – P1 – C11 – C12	-88.3(1)	-59.5
Pt – P1 – C21 – C22	-15.8(2)	-11.7
Pt – P1' – C21' – C22'	88.3(1)	8.5
Pt – P1' – C11' – C12'	15.8(2)	78.5

The torsion angles (see **Table 8.11**) of rings 2 (ring containing C21) and 3 (ring containing C21') of the calculated and crystal structures, indicate that the orientations for these rings are similar. Ring 2 and 3 for the two structures both display the 'basket-like' orientation with the phenyl rings pointing towards each other to accommodate the isopentyl moieties of the respective structures. **Figure 8.12** illustrates the overlay of the two structures (part A of the 50% occupancy disorder is presented).

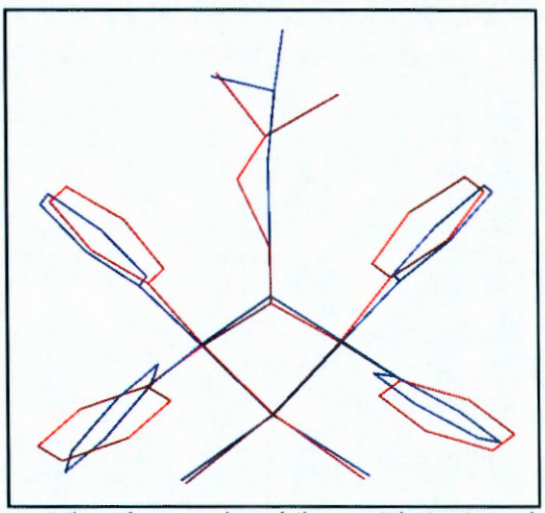

Figure 8.12: Graphical representation of an overlay of the crystal structure of [$PtCl_2$(PNP-*i*-Pent)] (blue) and the calculated structure of [$PtCl_2$(PNP-*i*-Pent)] using the B3LYP/6-31+G(d,p) basis set (red).

Table 8.12: Selected bond lengths (Å) for the crystal structure of [$PtCl_2$PNP-*i*-Pent] (9) and the calculated [$PtCl_2$PNP-*i*-Pent] structure (9*).

Bond Length (Å)	9	9*
Pt-P1	2.201(1)	2.254
Pt-P1'	2.201(1)	2.253
Pt-Cl1	2.351(1)	2.409
Pt-Cl1'	2.351(1)	2.405
P1-N1	1.699(3)	1.733
P1'-N1	1.699(3)	1.732
N1-C1	1.488(7)	1.476
P1-C11	1.800(3)	1.825
P1-C21	1.804(3)	1.822
P1'-C21'	1.800(3)	1.823
P1'-C11'	1.804(3)	1.822

The bond length N1-C1 for the calculated structure (1.476 °) is similar within experimental error to the corresponding bond length of the crystal structure (1.488(7) °) than N1-C1 bond for the crystal structure. The rest of the bond lengths (see **Table 8.12**) for the calculated structure of [$PtCl_2$PNP-*i*-Pent] is longer than the corresponding angles of the crystal structures.

8.3.5 [$PtCl_2$(PNP-Cychex)] (10 *vs.* 10*)

The similarity between the calculated (10*) and crystal structure of [$PtCl_2$(PNP-Cychex)] (10) (see §5.2.5) can be observed in **Figure 8.14** and **8.13** respectively.

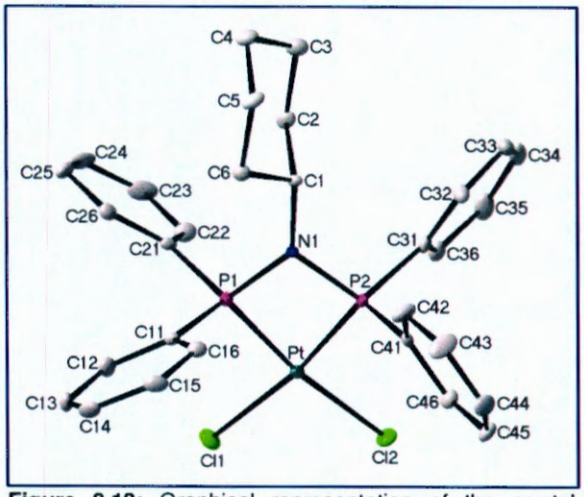

Figure 8.13: Graphical representation of the crystal structure of [$PtCl_2$(PNP-Cychex)] (10) at 50% probability. (H-atoms were omitted for clarity.)

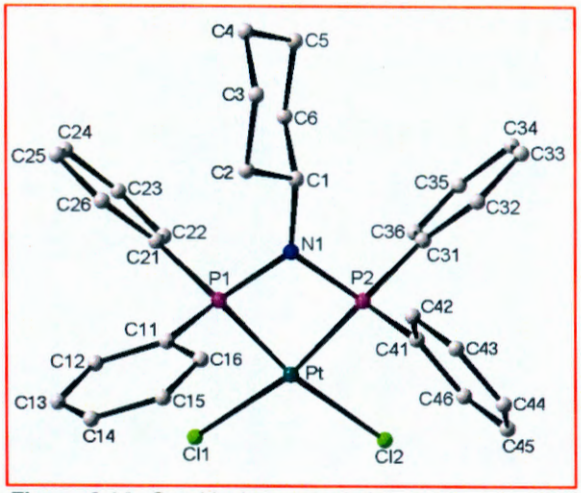

Figure 8.14: Graphical representation of the calculated structure of [$PtCl_2$(PNP-Cychex)] (10*). (H-atoms were omitted for clarity.)

Table 8.13: Selected bond angles(°) for the crystal structure of [$PtCl_2$(PNP-Cychex)] (10) and the calculated [$PtCl_2$(PNP-Cychex)] structure (10*).

Bond angles (°)	10	10*
P1-Pt-P2	71.9(1)	72.6
Cl1-Pt-Cl2	99.3(1)	94.4
P1-N1-P2	99.3(2)	100.3
C11-P1-C21	106.2(2)	106.6
C31-P2-C41	105.4(1)	105.4

The P1-Pt-P2 bite angle for the calculated structure (72.6°) is only 0.7° larger than that of the crystal structure (71.9°), both angles indicating a distortion of the square planar complex, due to the constraints placed on the complex by the coordination of the bidentate PNP ligand. The Cl1-Pt-Cl2 angle for the crystal structure (99.3(2) °) is substantially larger than the respective angle for the calculated structure (94.4°), both showing distortion from the expected angle 90 °. This indicates that enough space is created around the platinum metal centre by the orientation of the phenyl rings for the two platinum-coordinated chloride atoms to be placed further apart, enabling a larger bond angle. The rest of the bond angles as reported in **Table 8.13** show slightly larger

bond angles for the calculated structure in comparison to the angles of the crystal structure, with the largest difference being 1.1 ° (Cl1-Pt-Cl2).

Table 8.14: Selected torsion angles(°) for the crystal structure of [$PtCl_2$(PNP-Cychex)] (10) and the calculated [$PtCl_2$(PNP-Cychex)] structure (10*).

Torsion angles (°)	10	10*
Pt-P1-C11-C12	-87.6(1)	-94.9
Pt-P1-C21-C22	-19.8(1)	-9.6
Pt-P2-C31-C32	173.6(2)	-169.9
Pt-P2-C41-C42	-127.9(2)	-121.7

The torsion angles of the optimized structure indicate the 'basket-like' arrangement of the phenyl rings, which is similar to that found in the crystal structure. There are fairly small differences between the other torsion angles in **Table 8.14**, when comparing the crystal and calculated structures, with the largest difference of 10.2° (Pt-P1-C21-C22). **Figure 8.15** illustrates the overlay of the two structures.

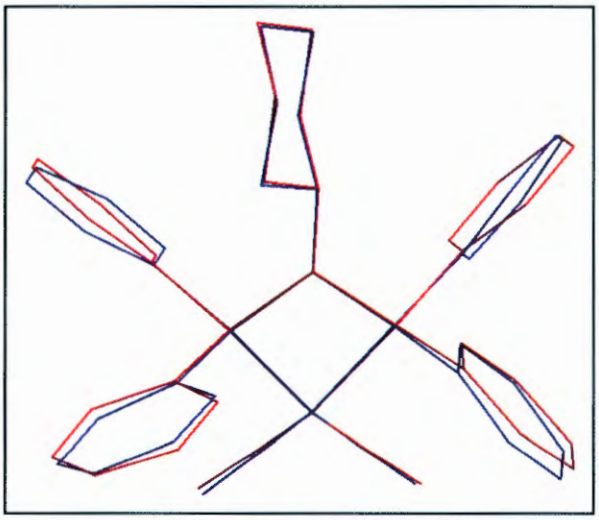

Figure 8.15: Graphical representation if an overlay of the crystal structure of [$PtCl_2$(PNP-Cychex)] (10) (blue) and the calculated structure of [$PtCl_2$(PNP-Cychex)] (10*) using the B3LYP/6-31+G(d,p) basis set (red).

Table 8.15: Selected bond lengths (Å) for the crystal structure of [$PtCl_2$(PNP-Cychex)] (10) and the calculated [$PtCl_2$(PNP-Cychex)] structure (10*).

Bond Length (Å)	10	10*
Pt-P1	2.214(2)	2.258
Pt-P2	2.200(2)	2.247
Pt-Cl1	2.357(2)	2.402
Pt-Cl2	2.361(2)	2.411
P1-N1	1.697(3)	1.740
P2-N1	1.704(3)	1.736
N1-C51	1.489(4)	1.487
P1-C11	1.801(2)	1.824
P1-C21	1.799(2)	1.825
P2-C31	1.808(3)	1.823
P2-C41	1.799(2)	1.826

The bond lengths are in general slightly longer for the calculated structure when comparing it to the crystal structure (see **Table 8.15**).

8.4 Theoretical calculations on [$PdCl_2$(PNP-alkyl)] complexes.

8.4.1 [$PdCl_2$(PNP-*i*-Prop)] (11 *vs.* 11*)

The optimized [$PdCl_2$(PNP-*i*-Prop)] (11*) structure is compared to the (see **Figure 8.17**) the corresponding crystal structure (11), see §5.2.6 (see **Figure 8.16**).

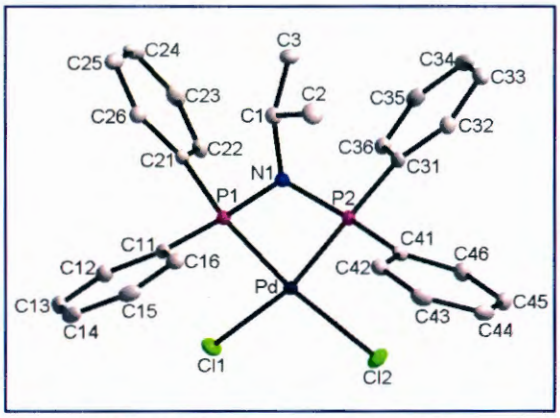

Figure 8.16: Graphical representation of the crystal structure of [$PdCl_2$(PNP-*i*-Prop)] (11) at 50% probability. (H-atoms were omitted for clarity.)

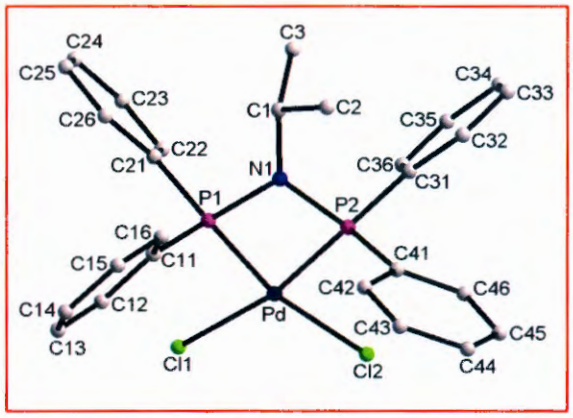

Figure 8.17: Graphical representation of the calculated structure of [$PdCl_2$(PNP-*i*-Prop)] (11*). (H-atoms were omitted for clarity.)

Table 8.16: Selected bond angles (°) for the crystal structure of [$PdCl_2$(PNP-*i*-Prop)] (11) and the calculated [$PdCl_2$(PNP-*i*-Prop)] structure (11*).

Bond angles (°)	11	11*
P1-Pd-P2	71.3(1)	72.2
Cl1-Pd-Cl2	95.6(1)	98.2
P1-N1-P2	98.6(1)	100.8
C11-P1-C21	106.1(1)	105.2
C31-P2-C41	105.7(1)	106.6

The Cl1-Pt-Cl2 angles for the calculated and crystal structure of [$PtCl_2$PNP-*i*-Prop] (98.2 and 95.6 ° respectively, see **Table 8.16**) both deviate significantly from the ideal 90 ° of a square-planar geometry. A similar deviation from the ideal geometry is observed for the P1-Pd-P2 angles of the crystal structure (71.3(1) °) and the calculated structure (72.2 °). The P-N-P angles of the two complexes (crystal structure: 98.6(1) ° and calculated structure: 100.8 °) differ with only 2.2 ° and both are considerably smaller than the corresponding angle of the crystal structure's non-coordinated PNP-*i*-Prop (122.8(3) °, see Chapter 4). The rest of the angles only have small differences.

Table 8.17: Selected torsion angles(°) for the crystal structure of [$PdCl_2$(PNP-*i*-Prop)] (11) and the calculated [$PtCl_2$(PNP-*i*-Prop)] structure (11*).

Torsion angles (°)	11	11*
Pd-P1-C11-C12	-85.2(1)	-60.7
Pd-P1-C21-C22	-9.6(1)	-8.2
Pd-P2-C31-C32	-163.6(1)	-170.3
Pd-P2-C41-C42	-87.3	-76.5

The similarity of the torsion angles when comparing the calculated and crystal structure (see **Table 8.17**) indicates that the orientation of the phenyl rings are comparable (see **Figures 8.18**) and both structures adopted a 'basket-like' arrangement of the phenyl rings. The largest difference in torsion angles is the Pd-P1-C11-C12 angle with a difference of 24.5 ° between the two structures.

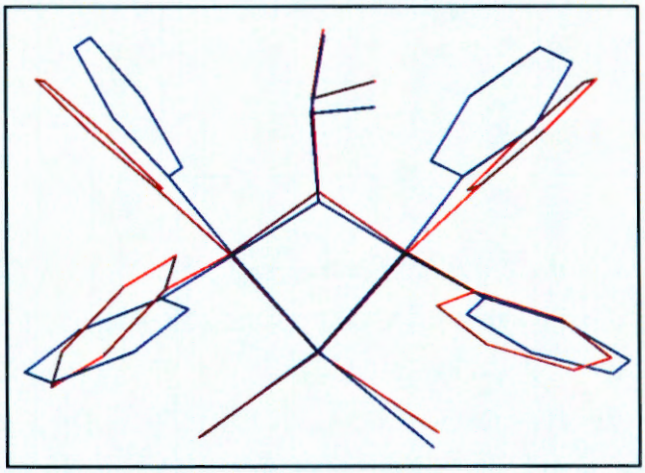

Figure 8.18: Graphical representation of an overlay of the crystal structure of [$PdCl_2$(PNP-*i*-Prop)] (blue) and the calculated structure of [$PdCl_2$(PNP-*i*-Prop)] using the B3LYP/6-31+G(d,p) basis set (red).

Table 8.18: Selected bond lengths (Å) for the crystal structure of [$PtCl_2$(PNP-*i*-Prop)] (11) and the calculated [$PtCl_2$(PNP-*i*-Prop)] structure (11*).

Bond Length (Å)	11	11*
Pd-P1	2.207(1)	2.271
Pd-P2	2.219(1)	2.278
Pd-Cl1	2.358(1)	2.394
Pd-Cl2	2.371(1)	2.387
P1-N1	1.800(2)	1.736
P2-N1	1.704(2)	1.741
N1-C1	1.504(2)	1.492
P1-C11	1.793(2)	1.826
P1-C21	1.799(2)	1.827
P2-C31	1.801(2)	1.827
P2-C41	1.795(2)	1.824

The N1-C1 bond length for the crystal structure of [$PtCl_2$PNP-*i*-Prop] (1.504(2) °) is slightly shorter than that of the calculated structure (1.492 °) (see **Table 8.18**). The rest of the bond lengths of the calculated structure are all longer than the corresponding bond lengths of the crystal structure.

8.4.2 [$PdCl_2$(PNP-Dimprop)] (12 vs. 12*)

The 50% occupancy disorder of the alkyl moiety of the [$PdCl_2$(PNP-Dimprop)] (12) (see §5.2.7) is illustrated in **Figure 5.19a** and **b**. This structure is compared to the corresponding calculated structure (12*) (see **Figure 5.20**).

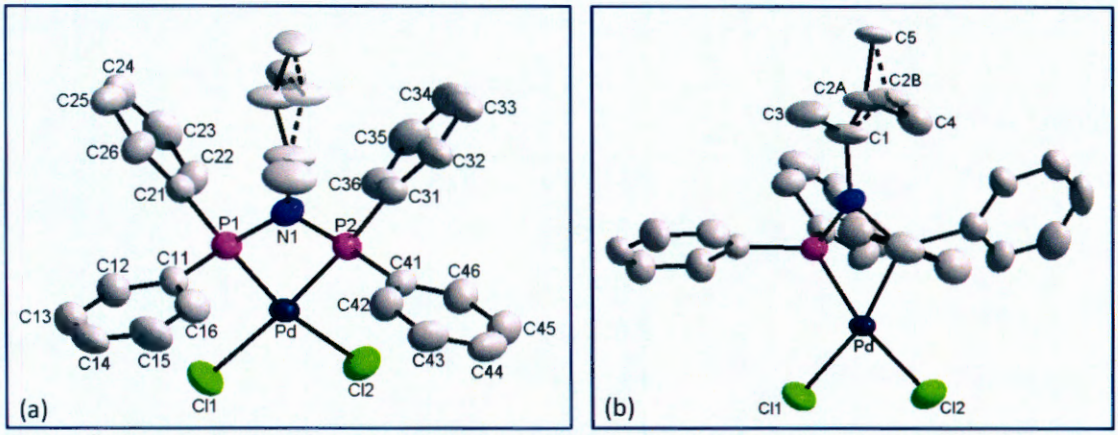

Figure 5.19a and b: Graphical representation of the different viewing angles of the crystal structure of [$PdCl_2$(PNP-Dimprop)] (12) at 50% probability. A/B indicates the disordered carbon atoms in the 1,2-dimethylpropyl alkyl group. Disordered parts belonging together are numbered A and B respectively. (H-atoms were omitted for clarity).

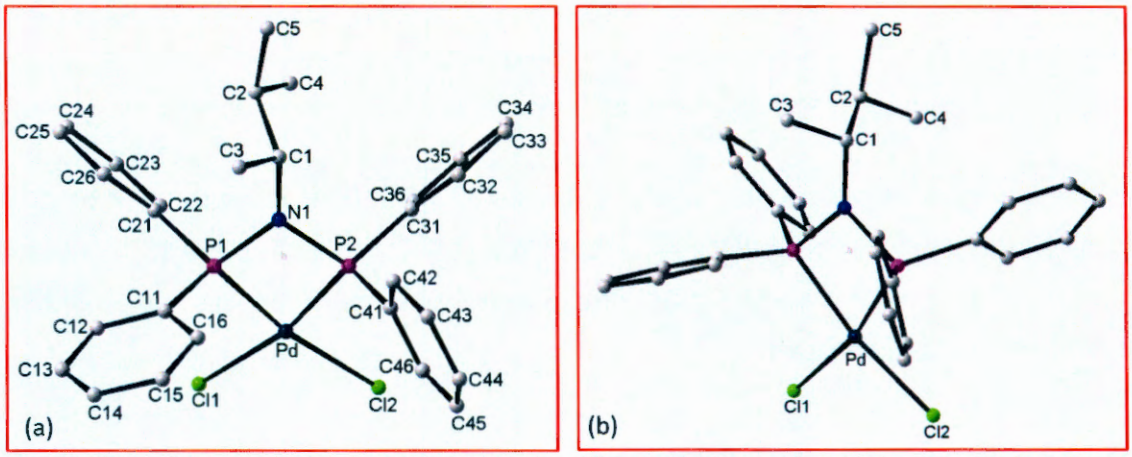

Figure 8.20a and b: Graphical representation of the different viewing angles of the calculated structure of [$PdCl_2$(PNP-Dimprop)] (12*). (H-atoms were omitted for clarity.)

Table 8.19: Selected bond angles (°) for the crystal structure of [$PdCl_2$(PNP-Dimprop)] (12) and the calculated [$PdCl_2$(PNP-Dimprop)] structure (12*).

Bond angles (°)	12	12*
P1-Pd-P2	71.6(1)	72.1
Cl1-Pd-Cl2	94.0(1)	97.4
P1-N1-P2	99.7(3)	100.6
C11-P1-C21	105.3(4)	106.5
C31-P2-C41	105.0(4)	105.1

The distorted square planar geometry of the calculated structure of [$PdCl_2$(PNP-Dimprop)] is evident from the P1-Pd-P2 angle (72.1 °) and the Cl1-Pd-Cl2 angle (97.4 °) (see **Table 8.19**). These values compare well with the corresponding values of the crystal structure, 71.6(1) ° and 97.4 ° respectively. The P1-N1-P2 angle for the two structures only differ by 0.9 °, with the angle being larger for the calculated structure.

Table 8.20: Selected torsion angles(°) for the crystal structure of [$PdCl_2$(PNP-Dimprop)] (12) and the calculated [$PdCl_2$(PNP-Dimprop)] structure (12*).

Torsion angles (°)	12	12*
Pd-P1-C11-C12	-95.7(6)	-101.3
Pd-P1-C21-C22	-13.5(7)	-5.7
Pd-P2-C31-C32	-174.6(6)	-170.7
Pd-P2-C41-C42	-79.6(7)	-137.2

The torsion angles shown in **Table 8.20** indicate that ring 4 (phenyl rings containing C41) is the only ring with a significant difference in orientation (Pd-P2-C41-C42 for the calculated structure is -137.2 ° and -79.6(7) °) for the corresponding angle of the crystal structure. The other phenyl rings of the calculated and crystal structure are similar, with the largest difference of only 7.8 °. A similar "basket-like" orientation for rings 2 and 3 (rings containing C21 and C31 respectively) are observed for both structures (see **Figures 8.17** and **8.18**) to accommodate the sterically bulky alkyl moiety. The overlay of the two structures further illustrates the similarity of the orientation of some of the phenyl rings (see **Figure 8.21**) (only part A of the 50% occupancy disorder of the crystal structure is presented).

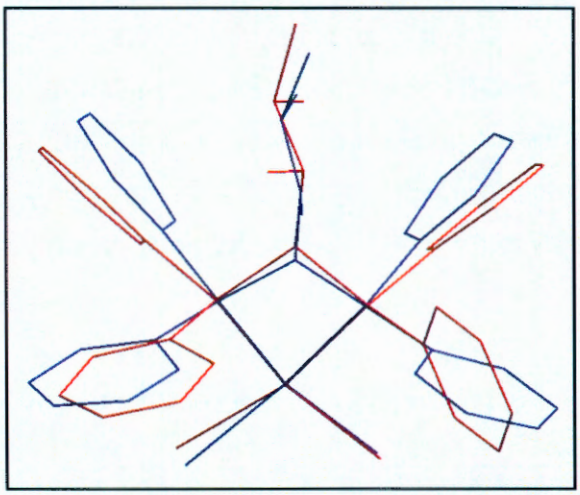

Figure 8.21: Graphical representation of an overlay of the crystal structure of [$PdCl_2$(PNP-Dimprop)] (12) (blue) and the calculated structure of [$PdCl_2$(PNP-Dimprop)] (12*) using the B3LYP/6-31+G(d,p) basis set (red).

Table 8.21: Selected bond lengths (Å) for the crystal structure of [$PdCl_2$(PNP-Dimprop)] (12) and the calculated [$PdCl_2$(PNP-Dimprop)] structure (12*).

Bond Length (Å)	12	12*
Pd-P1	2.216(2)	2.277
Pd-P2	2.221(2)	2.277
Pd-Cl1	2.338(2)	2.387
Pd-Cl2	2.357(2)	2.394
P1-N1	1.691(6)	1.742
P2-N1	1.706(6)	1.742
N1-C1	1.530(9)	1.495
P1-C11	1.805(7)	1.828
P1-C21	1.813(8)	1.826
P2-C31	1.790(8)	1.825
P2-C41	1.803(7)	1.833

The N1-C1 bond length in the crystal structure of [$PdCl_2$PNP-Dimprop] (1.530(9) °) is slightly longer than that of the calculated structure (1.495 °). The rest of the bond lengths of the calculated structure are all longer than the corresponding bond lengths of the crystal structure (see **Table 8.21**).

8.4.3 [$PdCl_2$(PNP-*n*-Prop)] (13 vs. 13*)

The crystal structure complex (13) lies on a two-fold rotation axis as can be seen in **Figure 8.22a** and **b,** see §5.2.8. The structure also has a four-fold disorder present for the alkyl moiety. The predicted structure (13*) of the corresponding complex is illustrated in **Figure 8.23** (the structure is numbered in a similar fashion than the crystal structure in order to simplify the comparison).

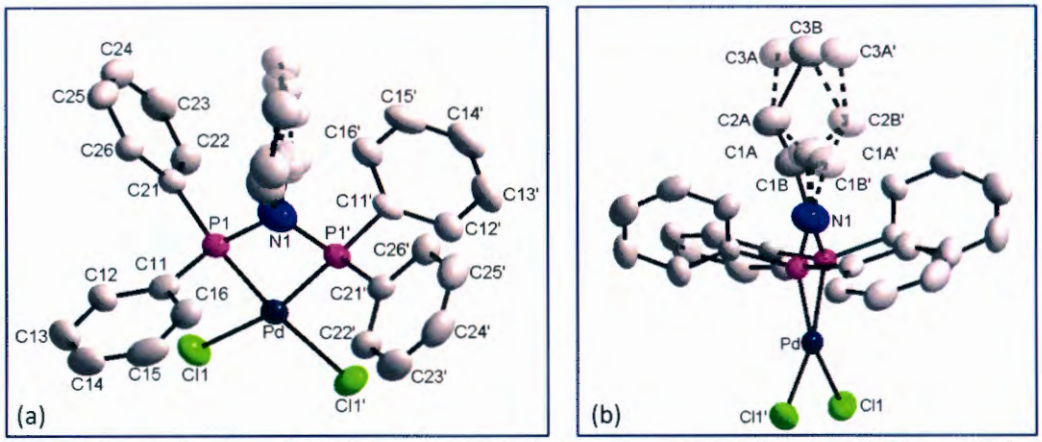

Figure 8.22a and b: Graphical representation of the different viewing angles of the crystal structure of [$PdCl_2$(PNP-*n*-Prop)] (13). A/B indicates the disordered carbon atoms in the propyl moiety. Disordered parts belonging together are numbered A and B respectively. The atoms generated by the 2-fold axis symmetry operation is labeled with an accent. (H-atoms were omitted for clarity).

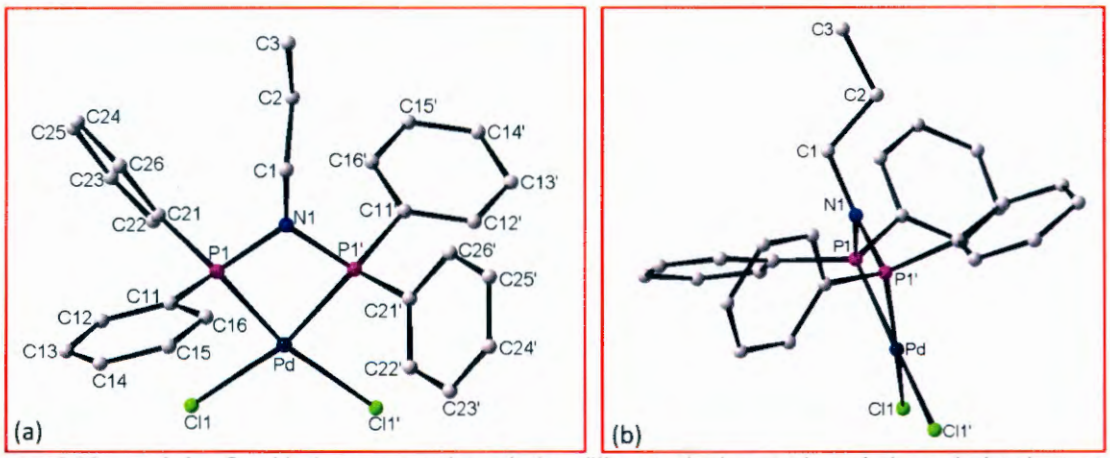

Figure 8.23a and b: Graphical representation of the different viewing angles of the calculated structure of [$PdCl_2$(PNP-*n*-Prop)] (13*) (H-atoms were omitted for clarity.)

Table 8.22: Selected bond angles (°) for the crystal structure of [$PdCl_2$(PNP-*n*-Prop)] (13) and the calculated [$PdCl_2$(PNP-*n*-Prop)] structure (13*).

Bond angles (°)	13	13*
P1-Pd-P1'	71.5(1)	72.4
Cl1-Pd-Cl1'	94.9(1)	98.7
P1-N1-P1'	100.8(5)	101.9
C11-P1-C21	107.5(2)	106.1
C11'-P1'-C21'	107.5(2)	106.8

The calculated [$PdCl_2$(PNP-*n*-Prop)] complex adopted a distorted square planar geometry, similar to that of the crystal structure. This is illustrated by the very similar P-Pd-P angle of the calculated structure (72.4 °) and the crystal structure (71.5(1) °) (see **Table 8.22**). The Cl-Pd-Cl angle for the calculated structure (98.7 °) is larger than the corresponding angle of the crystal structure (94.9(1) °).

Table 8.23: Selected torsion angles (°) for the crystal structure of [$PdCl_2$(PNP-*n*-Prop)] (13) and the calculated [$PdCl_2$(PNP-*n*-Prop)] structure (13*).

Torsion angles (°)	13	13*
Pd-P1-C11-C12	-97.0(4)	-99.2
Pd-P1-C21-C22	-17.4(5)	3.4
Pd-P1'-C11'-C12'	-97.0(4)	-105.4
Pd-P1'-C21'-C22'	-17.4(5)	3.3

The torsion angles of the two structures indicate similar orientations for phenyl rings 1 (rings containing C11) and 3 (ring containing C11') (see **Table 8.23**). The largest difference in torsion angles is observed for the Pd-P1-C21-C22 torsion angle (3.4 °) and the corresponding torsion angle Pd-P1'-C11'-C12' (-17.4(5) °). The overlay of the two structures is presented in **Figure 8.24** (only part A of the disorder for the crystal structure is illustrated). The 'fan-like' orientation of phenyl rings was adopted for both structures.

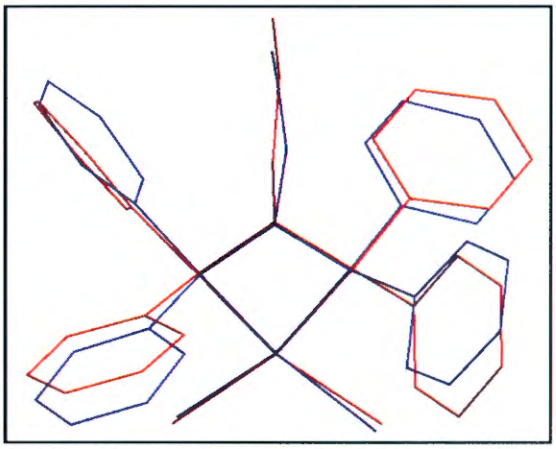

Figure 8.24: Graphical representation of an overlay of the crystal structure of [$PdCl_2$(PNP-*n*-Prop)] (13) (blue) and the calculated structure of [$PdCl_2$(PNP-*n*-Prop)] (13*) using the B3LYP/6-31+G(d,p) basis set (red).

Table 8.24: Selected bond lengths (Å) for the crystal structure of [$PdCl_2$(PNP-*n*-Prop)] (13) and the calculated [$PdCl_2$(PNP-*n*-Prop)] structure (13*).

Bond Length (Å)	13	13*
Pd-P1	2.223(2)	2.276
Pd-P1'	2.223(2)	2.279
Pd-Cl1	2.347(2)	2.388
Pd-Cl1'	2.347(2)	2.385
P1-N1	1.686(6)	1.728
P1'-N1	1.686(6)	1.734
N1-C1A	1.40(3)	1.474
N1-C1A'	1.40(3)	-
N1-C1B	1.47(3)	-
N1-C1B'	1.47(3)	-
P1-C11	1.797(5)	1.827
P1-C21	1.797(5)	1.825
P1'-C11'	1.792(5)	1.823
P1'-C21'	1.792(5)	1.824

The bond lengths of the crystal structure is slightly shorter overall than the corresponding bond lengths of the calculated [$PdCl_2$(PNP-*n*-Prop)], see **Table 8.24**.

8.4.4 [$PdCl_2$(PNP-*i*-Pent)] (14 *vs.* 14*)

The calculated [$PdCl_2$(PNP-*i*-Pent)] (14*) structure, (see **Figure 8.26**) is compared to the crystal structure (14), see §5.2.9, which contains a 50% occupancy disorder of the alkyl substituent (see **Figure 8.25a** and **b**)

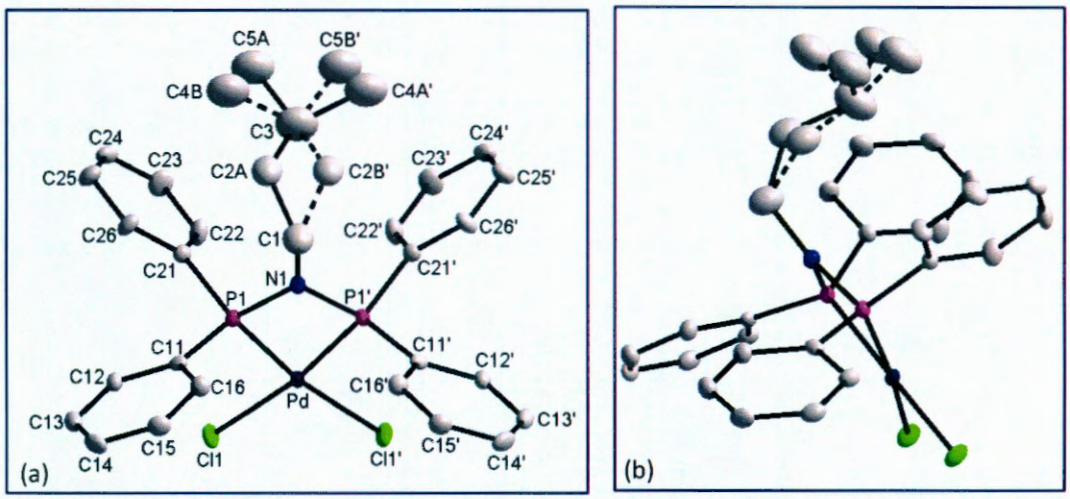

Figure 8.25a and b: Graphical representation of the different viewing angles of the crystal structure of [$PdCl_2$(PNP-*i*-Pent)] (14) at 50 % probability. A/B indicates the disordered carbon atoms in the isopentyl moiety. Disordered parts belonging together are numbered A and B respectively. (H-atoms were omitted for clarity).

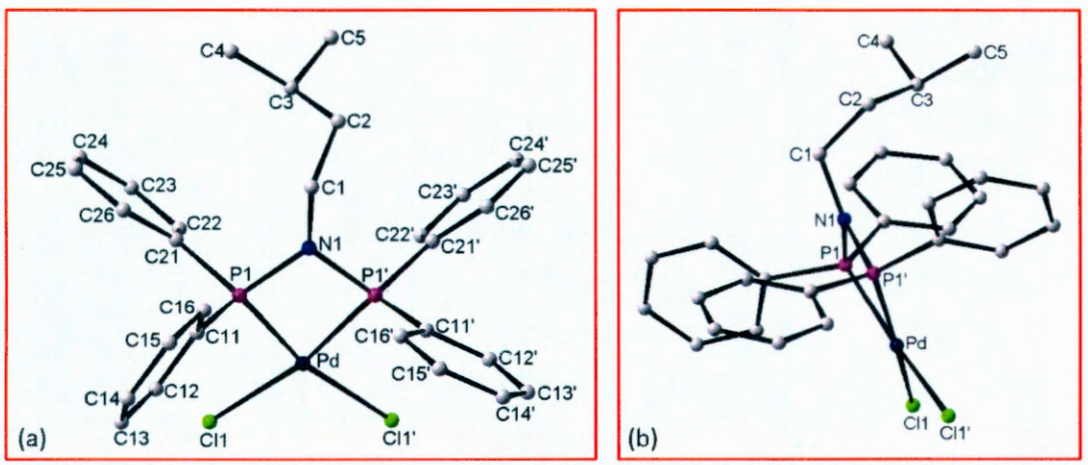

Figure 8.26a and b: Graphical representation of the different viewing angles of the calculated structure of [$PdCl_2$(PNP-*i*-Pent)] (14*). (H-atoms were omitted for clarity.)

Table 8.25: Selected bond angles(°) for the crystal structure of [$PdCl_2$(PNP-*i*-Pent)] (14) and the calculated [$PdCl_2$(PNP-*i*-Pent)] structure (14*).

Bond angles (°)	14	14*
P1-Pd-P1'	71.7(1)	72.1
Cl1-Pd-Cl1'	95.0(1)	98.0
P1-N1-P1'	99.5(3)	101.0
C11-P1-C21	106.2(2)	105.3
C21'-P1'-C11'	106.2(2)	105.9

The calculated structure for [$PdCl_2$(PNP-*i*-Pent)] adopted a distorted square planar geometry with a P-Pd-P angle of 72.1 °, which is similar to the corresponding crystal structure (71.7(1) °) (see **Table 8.25**). The P-N-P angle for the calculated structure (101.0 °) is slightly larger than the equivalent angle of the crystal structure (99.5(3) °). The rest of the angles reported in **Table 8.25** for the two complexes compare well.

Table 8.26: Selected torsion angles(°) for the crystal structure of [$PdCl_2$(PNP-*i*-Pent)] (14) and the calculated [$PdCl_2$(PNP-*i*-Pent)] structure (14*).

Torsion angles (°)	14	14*
Pd-P1-C11-C12	-88.0(4)	-53.9
Pd-P1-C21-C22	-17.2(5)	-15.4
Pd-P1'-C21'-C22'	17.2(5)	11.7
Pd-P1'-C11'-C12'	88.0(4)	87.2

The orientation of the phenyl rings of the two structures are very similar (see **Table 8.26**). It is only ring 1 (rings containing C11) that differ slightly with regards to their orientations, with ring 1 of the calculated structure that has a Pd-P1-C11-C12 torsion angle of -53.9 ° in comparison to the corresponding angle of the crystal structure (-88.0(4) °). **Figure 8.31** illustrates the overlay of the two structures (only part A of the 50% occupancy disorder is shown).

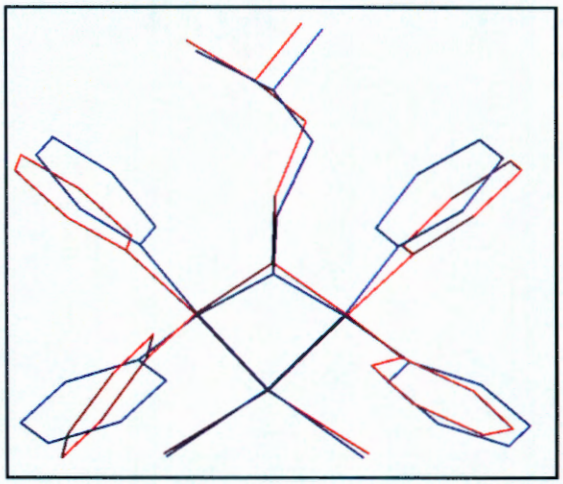

Figure 8.27: Graphical representation of an overlay of the crystal structure of [$PdCl_2$(PNP-*i*-Pent)] (14) (blue) and the calculated structure of [$PdCl_2$(PNP-*i*-Pent)] (14˙) using the B3LYP/6-31+G(d,p) basis set (red).

Table 8.27: Selected bond lengths (Å) for the crystal structure of [$PdCl_2$(PNP-*i*-Pent)] (14) and the calculated [$PdCl_2$(PNP-*i*-Pent)] structure (14˙).

Bond Length (Å)	14	14˙
Pd-P1	2.211(1)	2.277
Pd-P1'	2.211(1)	2.274
Pd-Cl1	2.353(1)	2.393
Pd-Cl1'	2.353(1)	2.388
P1-N1	1.488(1)	1.482
P1'-N1	1.696(4)	1.735
N1-C1	1.696(4)	1.738
P1-C11	1.797(5)	1.830
P1-C21	1.797(5)	1.823
P1'-C21'	1.806(5)	1.827
P1'-C11'	1.806(5)	1.823

Slightly longer bond lengths are predicted for the [$PdCl_2$(PNP-*i*-Pent)] calculated structure in comparison to the corresponding bond lengths of the crystal structure, see **Table 8.27**.

8.4.5 [$PdCl_2$(PNP-*n*-Butyl)] (15 *vs.* 15*)

The asymmetric unit of the title compound contains two crystallographically independent molecules and are refered to as [$PdCl_2$(PNP-*n*-Butyl)] (I) (15I) and (II) (15II), see §5.2.10 (see **Figure 8.28a** and **b**). These two structures are compared to the calculated [$PdCl_2$(PNP-*n*-Butyl)] structure (15*) (see **Figure 8.29**).

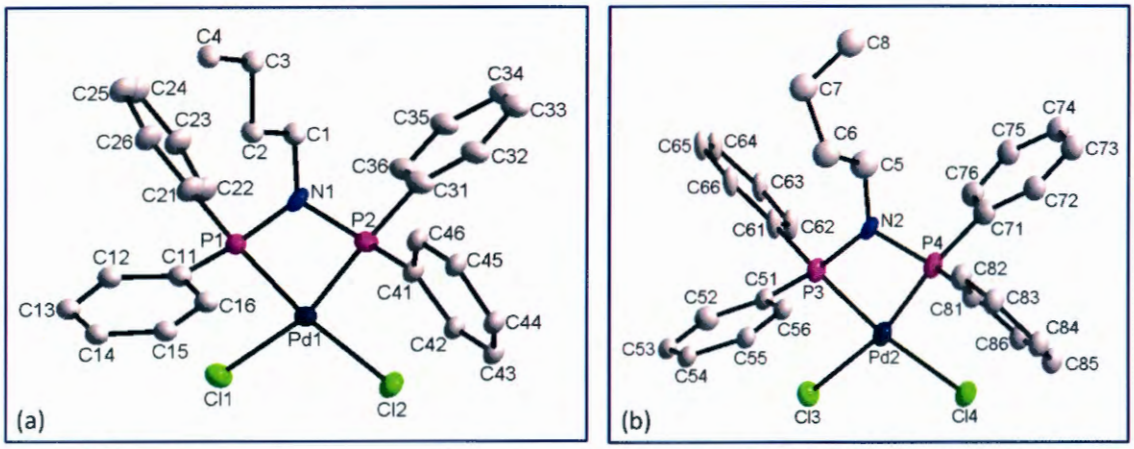

Figure 8.28a and b: Graphical representation of the crystal structure of [$PdCl_2$(PNP-*n*-Butyl)] (I) (15I) and (II) (15II) respectively at 50% probability. (H-atoms were omitted for clarity).

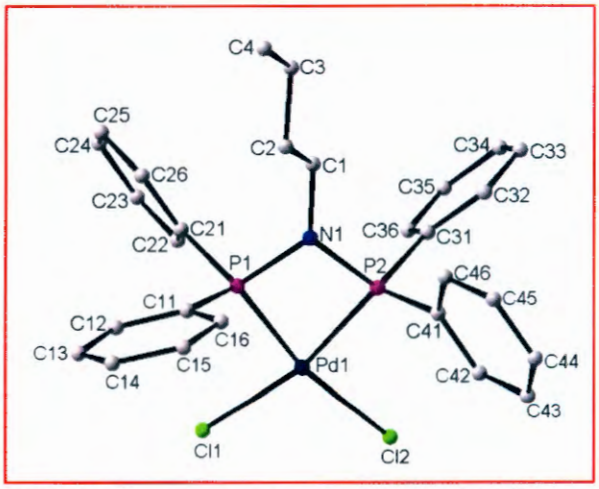

Figure 8.29: Graphical representation of the calculated structure of [$PdCl_2$(PNP-*n*-Butyl)] (15*). (H-atoms were omitted for clarity.)

Table 8.28: Selected bond angles (°) for the crystal structure of [$PdCl_2$(PNP-*n*-Butyl)] (I) (15I) and (II) (15II) and the calculated [$PdCl_2$(PNP-*n*-Butyl)] structure (15*).

Bond angles (°)	15I and 15II	15*
P1-Pd1-P2	71.3(2)	72.2
P3-Pd2-P4	71.5(2)	-
Cl1-Pd1-Cl2	93.8(2)	97.8
Cl3-Pd2-Cl4	94.6(2)	-
P1-N1-P2	99.6(6)	101.2
P3-N2-P4	101.3(7)	-
C11-P1-C21	109.0(8)	106.6
C51-P3-C61	108.3(7)	-
C31-P2-C41	107.2(8)	105.8
C71-P4-C81	107.0(7)	-

A distorted square-planar geometry at the palladium(II) centre is predicted for the calculated [$PdCl_2$(PNP-*n*-Butyl)] complex which is evident from the P-Pd-P angle of 72.2 ° (see **Table 8.28**). The rest of the bond angles compare well with the corresponding angles of the [$PdCl_2$(PNP-*n*-Butyl) (I) and (II).

Table 8.29: Selected torsion angles(°) for the crystal structure of [$PdCl_2$(PNP-*n*-Butyl)] (I) (15I) and (II) (15II) and the calculated [$PdCl_2$(PNP-*n*-Butyl)] structure (15*).

Torsion angles (°)	15I and 15II	15*
Pd1-P1-C11-C12	-113.2(5)	-96.6
Pd2-P3-C51-C52	-94.5(5)	-
Pd1-P1-C21-C22	-4.8(5)	2.12
Pd2-P3-C61-C62	-8.9(5)	-
Pd1-P2-C31-C32	-157.3(4)	-166.9
Pd2-P4-C71-C72	-151.4(4)	-
Pd1-P2-C41-C42	49.1(5)	51.1
Pd2-P4-C81-C82	-119.9(5)	-

The torsion angles of the calculated structure indicates that the orientations of the phenyl rings are the most similar to that of [$PdCl_2$(PNP-n-Butyl)] (I) (see **Table 8.29**). Both these structures adopted the 'fan-like' arrangement for the phenyl rings. An overlay of the calculated structure with each of the crystal structure molecules are presented in **Figure 8.30** and **8.31** respectively.

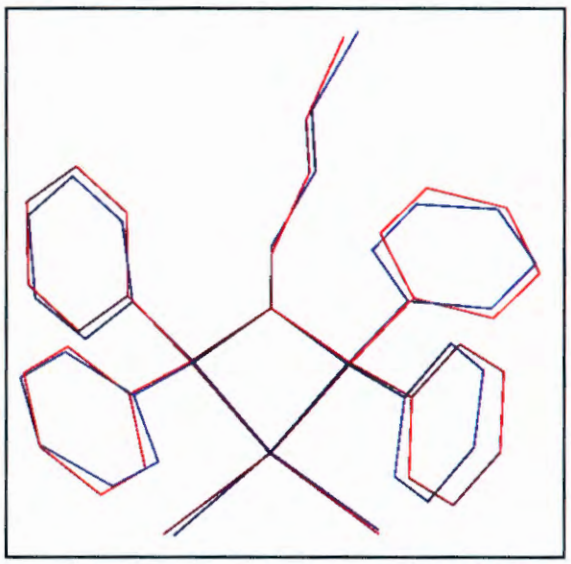

Figure 8.30: Graphical representation of an overlay of the crystal structure of [$PdCl_2$(PNP-*n*-Butyl)] (I) (15I) (blue) and the calculated structure of [$PdCl_2$(PNP-*n*-Butyl)] (15*) using the B3LYP/6-31+G(d,p) basis set (red).

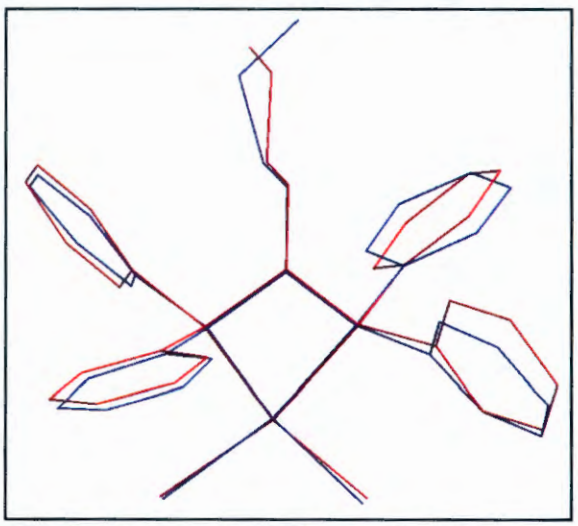

Figure 8.31: Graphical representation of an overlay of the crystal strucutre of [$PdCl_2$(PNP-*n*-Butyl)] (II) (15II) (blue) and the calculated structure of [$PdCl_2$(PNP-*n*-Butyl)] (15*) using the B3LYP/6-31+G(d,p) basis set (red).

Table 8.30: Selected bond lengths (Å) for the crystal structure of [$PdCl_2$(PNP-*n*-Butyl)] (I) (15I) and (II) (15II) and the calculated [$PdCl_2$(PNP-*n*-Butyl)] (15*) structure.

Bond Length (Å)	15I and 15II	15*
Pd1-P1	2.205(4)	2.275
Pd2-P3	2.201(4)	-
Pd1-P2	2.227(4)	2.280
Pd2-P4	2.223(4)	-
Pd1-Cl1	2.345(4)	2.387
Pd2-Cl3	2.364(4)	-
Pd1-Cl2	2.346(4)	2.392
Pd2-Cl4	2.360(4)	-
P1-N1	1.69(1)	1.736
P3-N2	1.67(2)	-
P2-N1	1.69(1)	1.737
P4-N2	1.67(2)	-
N1-C1	1.46(2)	1.476
N2-C6	1.48(2)	-
P1-C11	1.79(2)	1.822
P3-C51	1.80(2)	-
P1-C21	1.76(2)	1.825
P3-C61	1.80(2)	-
P2-C31	1.83(2)	1.827
P4-C71	1.80(2)	-
P2-C41	1.75(2)	1.825
P4-C81	1.81(2)	-

The bond lengths (see **Table 8.30**) reveal slightly longer bond lengths for the calculated [$PdCl_2$(PNP-*n*-Butyl)] complex in comparison with the corresponding bond lengths of the molecules of the crystal structure.

8.5 Discussion

The structures of the various [$PtCl_2$(PNP-alkyl)] and [$PdCl_2$(PNP-alkyl)] compounds were successfully calculated and optimized.

The bond angles for the various [$PtCl_2$(PNP-alkyl)] calculated complexes compare well to the corresponding crystal structures. The P-Pt-P bite angles for the optimized complexes range between 72.6 and 74.0 ° (see **Table 8.31**). The small bite angles of the optimized structures indicate a significantly distorted square planar geometry at the platinum(II) centre, which is due to the formation of the four-membered ring (Pt-P-N-P). The strain within the calculated complexes are further illustrated by the P-N-P angles that range from 100.3 to 102.5 °, these values are significantly smaller than the corresponding angles of the free PNP-alkyl ligand structures (isomers with the lowest ΔEnergy) which were calculated optimized to be between 121.1 and 122.8 ° (see Chapter 7). The distortion of the tetrahedral geometry at the phosphorous atoms is evident from the C-P-C angles of the calculated structures which range from 105.3 to 106.8 °. The distortions predicted for the calculated [$PtCl_2$(PNP-alkyl)] complexes are similar to that of the corresponding crystal complexes as discussed in Chapter 5.

Table 8.31: Selected bond angles (°) for the calculated and crystal [$PtCl_2$(PNP-alkyl)] complexes.

Bond angles (°)	P–Pt–P (Calc)	P–Pt–P (XRD)	P–N–P (Calc)	P–N–P (XRD)	Cl–Pt–Cl (Calc)	Cl–Pt–Cl (XRD)
[$PtCl_2$(PNP-Ethyl)]	72.8	72.1(1)	101.4	100.0(2)	94.7	91.7(1)
[$PtCl_2$(PNP-*n*-Prop]	72.8	72.4(1)	101.3	100.1(1)	94.8	92.7(1)
[$PtCl_2$(PNP-*i*-Pent]	72.6	72.2(1)	100.7	99.5(2)	94.7	91.3(1)
[$PtCl_2$(PNP-Cychex)]	72.6	71.9(1)	101.3	99.3(1)	94.4	91.8(1)
[$PtCl_2$(PNP-Dimprop)]	74.0	72.3(1)	102.5	98.6(4)	94.5	90.8(1)

Calc = calculated structure, XRD = crystal structure

The bond angles for the predicted structures of the [$PdCl_2$(PNP-alkyl)] complexes are comparable to the bond angles of the respective compounds in solid state. The distortion of the square planar complexes are predicted to be similar to that of the

crystal structures. This is illustrated by the P-Pd-P angles which range between 72.1 and 72.4 and the Cl-Pd-Cl angles that range from 97.4 to 98.7 ° (see **Table 8.32**).

Table 8.32: Selected bond angles (°) for calculated and crystal [$PdCl_2$(PNP-alkyl)] complexes.

Bond angles (°)	P–Pd–P (Calc)	P–Pd–P (XRD)	P–N–P (Calc)	P–N–P (XRD)	Cl–Pd–Cl (Calc)	Cl–Pd–Cl (XRD)
[$PdCl_2$(PNP-*i*-Prop)]	72.2	71.3(1)	100.8	98.6(1)	98.2	95.6(1)
[$PdCl_2$(PNP-*n*-Prop)]	72.4	71.5(1)	101.9	100.8(5)	98.7	94.9(1)
[$PdCl_2$(PNP-*n*-Butyl]	72.2	71.3(2)	101.2	99.6(6)	97.8	93.8(2)
[$PdCl_2$(PNP-Dimprop]	72.1	71.6(1)	100.6	99.7(3)	97.4	94.0(1)
[$PdCl_2$(PNP-*i*-Pent)]	72.1	71.7(1)	101.0	99.5(3)	98.0	95.0(1)

Calc = calculated structure, XRD = crystal structure

The bond lengths for all the optimized structures are slightly longer than the corresponding bond lengths of the related crystal structures. It is inherent of the technique, when performing theoretical calculations, to over-estimate the bond lengths for the structures calculated.

It is important to note that the arrangement of the phenyl rings (with regards to the 'fan'- and 'basket-like' orientations) were in essence correctly predicted for each of the ten calculated complexes discussed in this chapter. The optimizations for the various complexes do however not take intra- and intermolecular interactions into account when calculating the complexes. It is clear that in spite of this, the agreement is remarkable. The only difference when comparing the calculated [$PtCl_2$(PNP-alkyl)] complexes are the alkyl moieties that are modified from one complex to another. It is the same with regards to the various optimized [$PdCl_2$(PNP-alkyl)] complexes. This clearly indicates that it is the various alkyl moieties and subsequent change in steric bulk, that influence the arrangement of the phenyl rings of the square-planar complexes and that the packing had little or no effect and that the solid state behaviour in the systems could be well predicted by theoretical calculations.

An additional theoretical study of Cr(III)-PNP complexes is presented and discussed in the next chapter.

9 Theoretical study of Cr(III)-PNP complexes

In this chapter...

The optimized geometric structures of the [$CrCl_4$(PNP-alkyl)] complexes are presented. A comparison of the calculated structure and the crystallographic data of the corresponding complexes are made and the similarities and differences are discussed in detail.

9.1 Introduction

Theoretical calculations on various organometallic compounds have been performed recently [1,2,3,4,5,6], including chromium(III) complexes.[7,8] This novel technique provides additional insight into the basic chemistry associated with metal coordinated complexes, especially when compared to the solid state data of the compounds. It was therefore decided to investigate the structures of the chromium(III)-PNP complexes in conjunction with the free ligands (Chapter 7) and the Pt(II)/Pd(II) complexes (Chapter 8), to acquire more knowledge on the structures of these anionic complexes.

The optimized geometries of the [$CrCl_4$(PNP-alkyl)]$^-$ complexes were calculated using density functional theory methods (DFT). The geometric parameters of the various calculated structures are compared to the solid state crystal structure counterparts to determine from the differences and similarities what influences the geometry of the [$CrCl_4$(PNP-alkyl)]$^-$ complexes as the alkyl substituents change from one complex to another.

---

[1] Woo, T., Folga, E. and Ziegler, T., *Organometallics*, **1993**, *12*, 1289.
[2] Branchadell, V., Moreno-Manas, M., Pajuelo, F. and Pleixtas, R., *Organometallics*, **1999**, *18*, 4934.
[3] Burckhardt, U., Casty, G.L., Tilley, T.D., Woo, T. and Rothlisberger, U., *Organometallics*, **2000**, *19*, 3830.
[4] Magistrato, A., Merlin, M., Pregosin, P.S. and Rothlisberger, U., Organometallics, **2000**, 19, 3591.
[5] Atesin, T.A., Oster, S.S., Skugrud, K. and Jones, W.D., *Inorg. Chim. Acta*, **2006**, *359*, 2798.
[6] Zhao, X., Pan, Q., Li, M., Xia, B. and Zhang, H., *J. Mol. Struc.*, **2007**, *822*, 65
[7] Kar, T., Liao, M., Biswas, S., Sarkar, S., Dey, K., Yap, G.P.A. and Kreisel, K., *Spectrochimica Acta*, **2006**, *A65*, 882.
[8] Gonzalez-Baro, A.C., Pis-Diez, R., Piro, O.E. and Parajon-Costa, B.S., *Polyhedron*, **2008**, *27*, 502.

9.2 Experimental

The structures of the $[CrCl_4(PNP\text{-}alkyl)]^-$ complexes were optimized with the density functional theory (DFT) using the Becke3-Lee-Yang-Parr (B3LYP)[9] functionals supplemented with the LANL2DZ basis set. Due to limited computational power the Cr(III) complexes were only optimised using the LANL2DZ basis set. The optimised structures obtained with the use of the LANL2DZ basis set is therefore compared to the crystallographic data of the corresponding complexes. All calculations were carried out using the Gaussian 03 software suite[10]. No countercations were taken into account in the calculations of the complexes.

Molecular diagrams of the structures (using DIAMOND 3.0[11]) are presented as well as overlays of the calculated structures with the corresponding crystal structures (using Hyperchem 7.52[12]). Selected geometric parameters of the calculated structures and corresponding crystal structures are presented and discussed. Each of the crystal structures is denoted with numerical values for example 16, 17 and 18, while the corresponding calculated structures at B3LYP/LANL2DZ level are indicated as 16*, 17* and 18* (see §9.3.1 to §9.3.3 for numbering structures). Theoretical calculations were performed on the following complexes (see Chapter 6 for the abbreviations of the chromium(III)-PNP complexes):

16) $[CrCl_4(PNP\text{-}n\text{-}Pent)]^-$

17) $[CrCl_4(PNP\text{-}i\text{-}Pent)]^-$

18) $[CrCl_4(PNP\text{-}n\text{-}Butyl)]^-$

---

[9] Lee, C., Yang, W. and Parr, R. G.,*Phys. Rev.* B, **1988**, *37*, 785.

[10] Gaussian 03, Revision C.01, Frisch, M. J., Trucks, G. W., Schlegel, H. B., Scuseria, G. E., Robb, M. A., Cheeseman, J. R., Montgomery, Jr., J. A., Vreven, T., Kudin, K. N., Burant, J. C., Millam, J. M., Iyengar, S. S., Tomasi, J., Barone, V., Mennucci, B., Cossi, M., Scalmani, G., Rega, N., Petersson, G. A., Nakatsuji, H., Hada, M., Ehara, M., Toyota, K., Fukuda, R., Hasegawa, J., Ishida, M., Nakajima, T., Honda, Y., Kitao, O., Nakai, H., Klene, M., Li, X., Knox, J. E., Hratchian, H. P., Cross, J. B., Adamo, C., Jaramillo, J., Gomperts, R., Stratmann, R. E., Yazyev, O., Austin, A. J., Cammi, R., Pomelli, C., Ochterski, J. W., Ayala, P. Y., Morokuma, K., Voth, G. A., Salvador, P., Dannenberg, J. J., Zakrzewski, V. G., Dapprich, S., Daniels, A. D., Strain, M. C., Farkas, O., Malick, D. K., Rabuck, A. D., Raghavachari, K., Foresman, J. B., Ortiz, J. V., Cui, Q., Baboul, A. G., Clifford, S., Cioslowski, J., Stefanov, B. B., Liu, G., Liashenko, A., Piskorz, P., Komaromi, I., Martin, R. L., Fox, D. J., Keith, T., Al-Laham, M. A., Peng, C. Y., Nanayakkara, N., Challacombe, M., Gill, P. M. W., Johnson, B., Chen, W., Wong, M. W., Gonzalez, C., & Pople, J. A., Gaussian, Inc, Pittsburgh PA, **2003**.

[11] Brandenburg, K. and Putz, H., **2005**, DIAMOND. Release 3.0c. Crystal Impact GbR, Bonn, Germany.

[12] Hyperchem ™ Release 7.52, Windows Molecular Modeling System, Hypercube, Inc., **2002**.

9.3 Theoretical calculations on $[CrCl_4(PNP\text{-}alkyl)]^-$ complexes.

9.3.1 $[CrCl_4(PNP\text{-}n\text{-}Pent)]^-$ (16 *vs.* 16*)

Two independent monomeric $[CrCl_4(PNP\text{-}n\text{-}Pent)]^-$ complexes are present in the asymmetric unit of the crystal structure of $[n\text{-}Pent\text{-}NH_3][CrCl_4(PNP\text{-}n\text{-}Pent)]\cdot 2C_7H_8$ (see §6.2.1), and are referred to as $[CrCl_4(PNP\text{-}n\text{-}Pent)]^-$ (I) (16I) (see **Figure 9.1a** and **b**) and $[CrCl_4(PNP\text{-}n\text{-}Pent)]^-$ (II) (16II). Both anionic complexes are compared to the optimised structure of $[CrCl_4(PNP\text{-}n\text{-}Pent)]^-$ (16*)(see **Figure 9.2**).

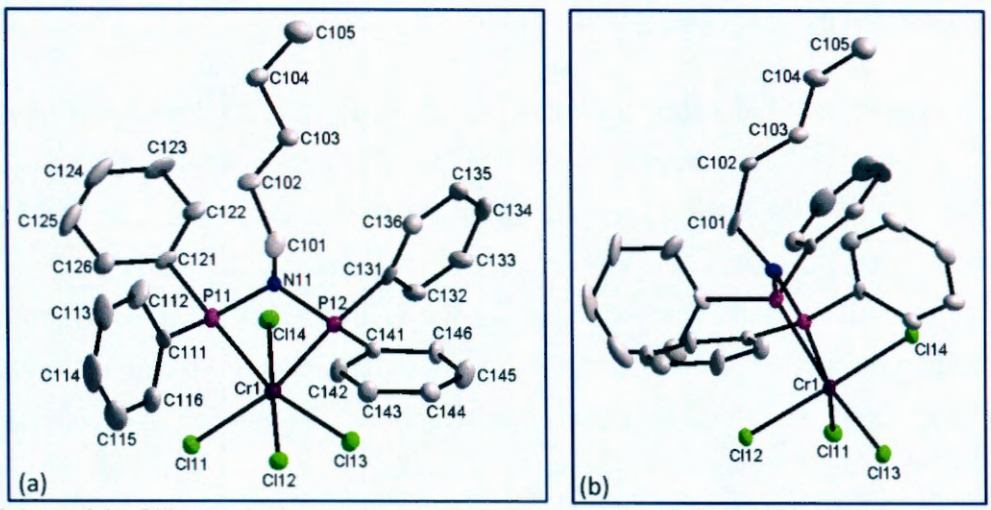

Figure 9.1a and b: Different viewing angles of the crystal structure of $[CrCl_4(PNP\text{-}n\text{-}Pent)]^-$ (I) (16I) at 50% probability. (H-atoms were omitted for clarity.)

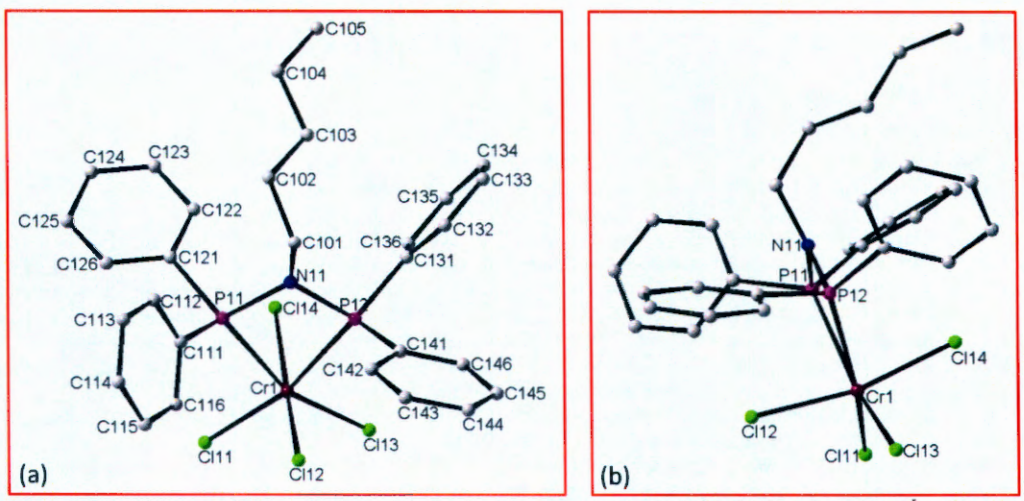

Figure 9.2a and b: Different viewing angles of the calculated structure of $[CrCl_4(PNP\text{-}n\text{-}Pent)]^-$ (16*). (H-atoms were omitted for clarity.)

Table 9.1: Selected bond angles (°) for crystal structures, $[CrCl_4(PNP\text{-}n\text{-}Pent)]^-$ (I) **(16I)**, $[CrCl_4(PNP\text{-}n\text{-}Pent)]^-$ (II) **(16II)** and the calculated structure of $[CrCl_4(PNP\text{-}n\text{-}Pent)]^-$ (16*)

Bond angles (°)	16I	16II	16*
Pn1-Crn-Pn2	66.7(1)	66.9(1)	64.9
Cln1-Crn-Cln2	90.2(1)	90.2(1)	93.3
Cln3-Crn-Cln4	89.9(1)	89.9(1)	93.4
Pn1-Nn1-Pn2	106.0(3)	106.6(4)	108.7
Cn11-Pn1-Cn21	101.5(4)	102.8(4)	101.1
Cn31-Pn2-Cn41	101.7(4)	102.0(4)	101.0

n = 1/ 2 for (16I) and (16II) respectively and n = 1 for calculated structure of $[CrCl_4(PNP\text{-}n\text{-}Pent)]^-$.

The bite angle, P-Cr-P of the optimized structure (64.9 °) illustrates a distorted octahedral geometry at chromium(III) of the calculated structure and is slightly smaller than the corresponding angles of $[CrCl_4(PNP\text{-}n\text{-}Pent)]^-$ (I) and (II) (66.7(1) and 66.9(1) ° respectively) (see **Table 9.1**). The P-N-P angle for the calculated structure (108.7 °) is significantly smaller than the corresponding angle for the optimised structure of the free PNP-*n*-Pent isomer 10 (121.1 °, see Chapter 7). This trend for the P-N-P angle to close significantly upon coordination of the PNP-ligand is similar to that observed for the crystal structures of $[CrCl_4(PNP\text{-}n\text{-}Pent)]^-$ (I) and (II) (106.0(3) and 106.6(4) ° respectively) and PNP-*n*-Pent (123.4(1) and 120.5(1) ° for the two crystallographic independent molecules).

Table 9.2: Selected torsion angles (°) for crystal structures, $[CrCl_4(PNP\text{-}n\text{-}Pent)]^-$ (I) **(16I)**, $[CrCl_4(PNP\text{-}n\text{-}Pent)]^-$ (II) **(16II)** and the calculated structure of $[CrCl_4(PNP\text{-}n\text{-}Pent)]^-$(16*).

Torsion angles (°)	16I	16II	16*
Crn-Pn1-Cn11-Cn12	170.0(3)	-114.1(3)	172.9
Crn -Pn1-Cn21-Cn22	-70.6(4)	24.7(4)	-62.6
Crn -Pn2-Cn31-Cn32	-26.2(4)	-106.0(3)	-174.6
Crn -Pn2-Cn41-Cn42	-64.1(4)	11.7(4)	-75.4

n = 1/ 2 for 16I and 16II respectively and n = 1 for calculated structure of $[CrCl_4(PNP\text{-}n\text{-}Pent)]^-$.

It is evident from the torsion angles in **Table 9.2** that the calculated $[CrCl_4(PNP\text{-}n\text{-}Pent)]^-$ structure has a similar arrangement of the phenyl rings than the crystal structure $[CrCl_4(PNP\text{-}n\text{-}Pent)]^-$ (I). Phenyl rings 3 (molecule containing C131 for both the calculated and the crystal structure) show the most significant difference with torsion angles of -174.6 and -26.2(4) ° respectively). The torsion angles of the calculated structure also indicate a 'fan-like' arrangement of the rings.

An overlay of the calculated structure and the crystal structure $[CrCl_4(PNP\text{-}n\text{-}Pent)]^-$ (I) and (II) is displayed in **Figures 9.3** and **9.4** respectively and illustrates the similarity between the calculated structure and $[CrCl_4(PNP\text{-}n\text{-}Pent)]^-$ (I).

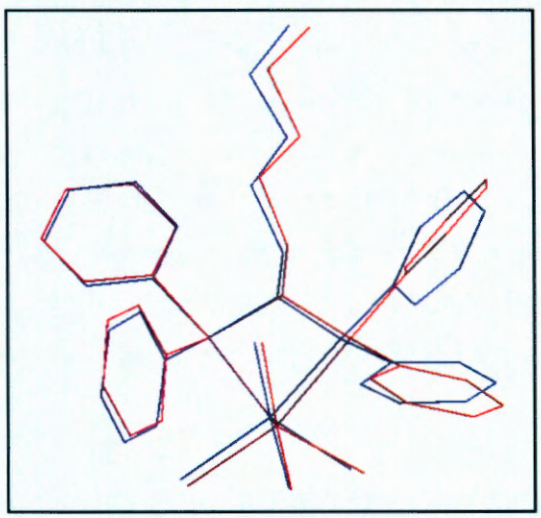

Figure 9.3: Graphical representation of an overlay of the $[CrCl_4(PNP\text{-}n\text{-}Pent)]^-$ (I) crystal structure (16I) (blue) and the calculated structure of $[CrCl_4(PNP\text{-}n\text{-}Pent)]^-$ (16*) (red).

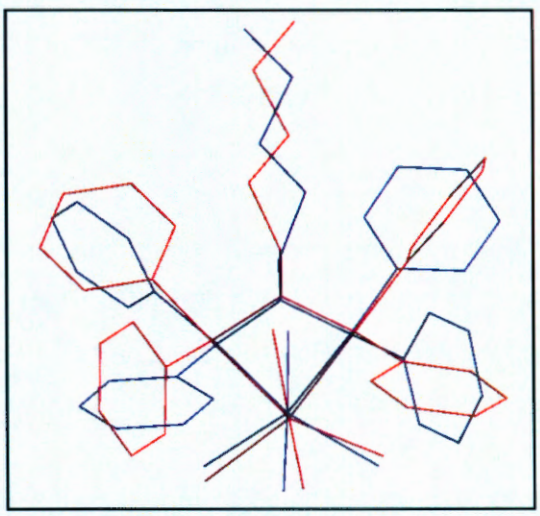

Figure 9.4: Graphical representation of an overlay of the $[CrCl_4(PNP\text{-}n\text{-}Pent)]^-$ (II) crystal structure (16II) (blue) and the calculated structure of $[CrCl_4(PNP\text{-}n\text{-}Pent)]^-$ (16*) (red).

Table 9.3: Selected bond lengths (Å) for crystal structures, $[CrCl_4(PNP\text{-}n\text{-}Pent)]^-$ (I) **(16I)**, $[CrCl_4(PNP\text{-}n\text{-}Pent)]^-$ (II) **(16II)** and the calculated structure of $[CrCl_4(PNP\text{-}n\text{-}Pent)]^-$ **(16*)**.

Bond Length (Å)	16I	16II	16*
Crn-Pn1	2.496(3)	2.474(2)	2.764
Crn -Pn2	2.466(2)	2.493(3)	2.698
Crn -Cln1	2.342(2)	2.329(3)	2.319
Crn -Cln2	2.316(2)	2.318(2)	2.391
Crn -Cln3	2.329(3)	2.310(2)	2.324
Crn –Cln4	2.313(2)	2.341(2)	2.398
Pn1-Nn1	1.712(6)	1.712(6)	1.806
Pn2-Nn1	1.706(7)	1.701(7)	1.801
Nn1-Cn01	1.482(9)	1.496(9)	1.486
Pn1-Cn11	1.834(8)	1.811(8)	1.895
Pn1-Cn21	1.808(8)	1.820(8)	1.887
Pn2-Cn31	1.813(8)	1.823(8)	1.893
Pn2-Cn41	1.823(8)	1.823(9)	1.884

n = 1/ 2 for (16I), (16II) respectively and n = 1 for calculated structure of $[CrCl_4(PNP\text{-}n\text{-}Pent)]^-$.

The bond lengths for the calculated structure are overall slightly longer than the corresponding bond lengths of the $[CrCl_4(PNP\text{-}n\text{-}Pent)]^-$ (I) and (II) (see **Table 9.3**).

9.3.2 $[CrCl_4(PNP\text{-}i\text{-}Pent)]^-$ (17 vs. 17*)

The two crystallographic independent anionic complexes $[CrCl_4(PNP\text{-}i\text{-}Pent)]^-$ (I) (17I) (see **Figure 9.5a** and **b**) and $[CrCl_4(PNP\text{-}i\text{-}Pent)]^-$ (II) (17II) (see §6.2.2) are compared to the calculated $[CrCl_4(PNP\text{-}i\text{-}Pent)]^-$ structure (17*) (see **Figure 9.6a** and **b**).

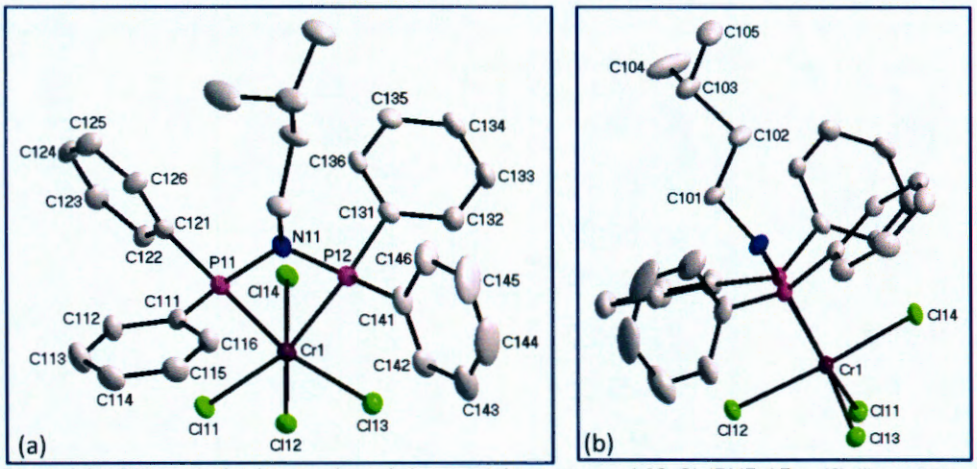

Figure 9.5a and b: Different viewing angles of the crystal structure of $[CrCl_4(PNP\text{-}i\text{-}Pent)]^-$ (I) at 50% probability. (H-atoms were omitted for clarity.)

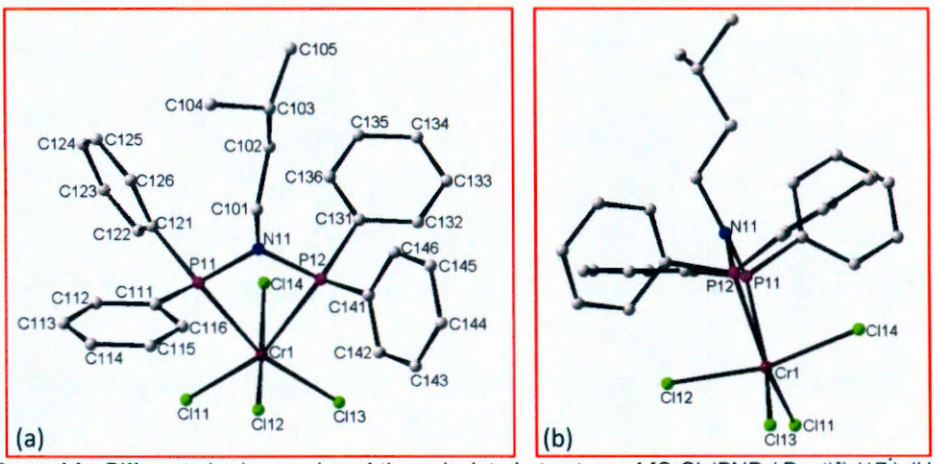

Figure 9.6a and b: Different viewing angles of the calculated structure of $[CrCl_4(PNP\text{-}i\text{-}Pent)]^-$ (17^*) (H-atoms were omitted for clarity.)

Table 9.4: Selected bond angles (°) for crystal structures, $[CrCl_4(PNP\text{-}i\text{-}Pent)]^-$ (I) **(17I)**, $[CrCl_4(PNP\text{-}i\text{-}Pent)]^-$ (II) **(17II)** and the calculated structure of $[CrCl_4(PNP\text{-}i\text{-}Pent)]^-$ (17^*).

Bond angles (°)	17I	17II	17^*
Pn1-Crn-Pn2	67.1(1)	66.8(1)	65.4
Cln1-Crn-Cln2	90.6(1)	90.5(1)	94.5
Cln3-Crn-Cln4	91.5(1)	91.2(1)	94.7
Pn1-Nn1-Pn2	106.5(2)	105.9(2)	109.1
Cn11-Pn1-Cn21	102.3(2)	102.4(2)	101.0
Cn31-Pn2-Cn41	102.3(2)	103.5(2)	101.2

n = 1/ 2 for (17I), (17II) respectively and n = 1 for calculated structure of $[CrCl_4(PNP\text{-}i\text{-}Pent)]^-$.

A similar distortion of the octahedral geometry at the chromium(III) centre is observed for the molecules of the crystal structure and the calculated structure with P-Cr-P angles of 67.1(1), 66.8(1) and 65.4 ° respectively (see **Table 9.4**) which all deviate significantly from the ideal 90 °. The P-N-P angle for the optimized structure (109.1 °) is larger than the corresponding angles of the crystal structure which range between 105.9(2) and 106.5(2) °, all these angles indicate a significant distortion at the nitrogen atoms.

Table 9.5: Selected torsion angles (°) for crystal structures, $[CrCl_4(PNP\text{-}i\text{-}Pent)]^-$ (I) (17I), $[CrCl_4(PNP\text{-}i\text{-}Pent)]^-$ (II) **(17II)** and the calculated structure of $[CrCl_4(PNP\text{-}i\text{-}Pent)]^-$ (17*).

Torsion angles (°)	17I	17II	17*
Crn-Pn1-Cn11-Cn12	-106.4(4)	174.0(3)	-112.0
Crn -Pn1-Cn21-Cn22	19.3(5)	-78.4(4)	17.3
Crn -Pn2-Cn31-Cn32	-101.4(4)	-179.1(3)	-105.6
Crn -Pn2-Cn41-Cn42	16.6(5)	-82.0(4)	6.0

n = 1/ 2 for 17I and 17II respectively and n = 1 for calculated structure of $[CrCl_4(PNP\text{-}i\text{-}Pent)]^-$.

The calculated structure of $[CrCl_4(PNP\text{-}i\text{-}Pent)]^-$ adopted a variation of the 'fan-like' arrangement of the phenyl rings as is demonstrated by the torsion angles in **Table 9.5** These torsion angles are also similar to the corresponding angles of $[CrCl_4(PNP\text{-}i\text{-}Pent)]^-$ (I) with the largest difference observed for ring 4 (ring containing C141 for both structures). The overlays of the calculated structure with each of the molecules are illustrated in **Figures 9.7** and **9.8** respectively.

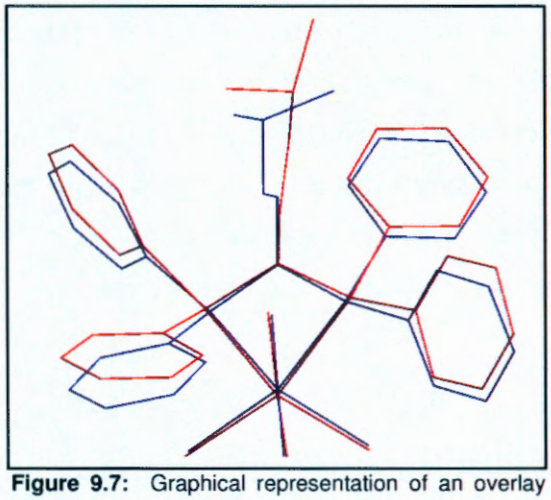

Figure 9.7: Graphical representation of an overlay of the $[CrCl_4(PNP\text{-}i\text{-}Pent)]^-$ (I) crystal structure (17I) (blue) and the calculated structure of $[CrCl_4(PNP\text{-}i\text{-}Pent)]^-$ (17^*) (red).

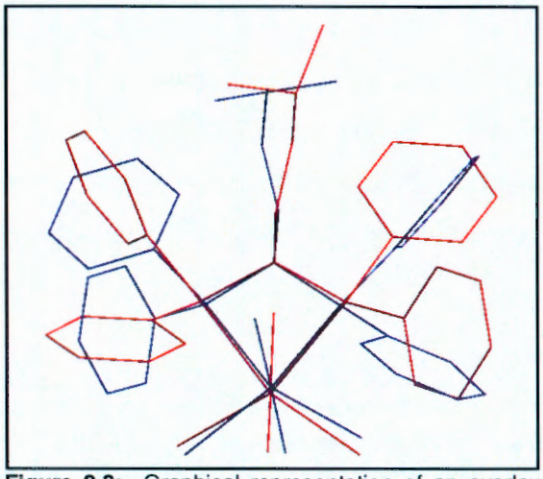

Figure 9.8: Graphical representation of an overlay of the $[CrCl_4(PNP\text{-}i\text{-}Pent)]^-$ (II) crystal structure (17II) (blue) and the calculated structure of $[CrCl_4(PNP\text{-}i\text{-}Pent)]^-$ (17^*) (red).

Table 9.6: Selected bond lengths (Å) for crystal structures, $[CrCl_4(PNP\text{-}i\text{-}Pent)]^-$ (I) (17I), $[CrCl_4(PNP\text{-}i\text{-}Pent)]^-$ (II) **(17II)** and the calculated structure of $[CrCl_4(PNP\text{-}i\text{-}Pent)]^-$ (17^*).

Bond Length (Å)	17I	17II	17^*
Crn-Pn1	2.462(2)	2.480(1)	2.707
Crn -Pn2	2.470(1)	2.458(2)	2.715
Crn -Cln1	2.335(1)	2.328(2)	2.327
Crn -Cln2	2.316(2)	2.317(2)	2.400
Crn -Cln3	2.326(2)	2.324(1)	2.323
Crn –Cln4	2.298(1)	2.298(1)	2.390
Pn1-Nn1	1.701(4)	1.697(4)	1.797
Pn2-Nn1	1.702(4)	1.709(4)	1.798
Nn1-Cn01	1.478(5)	1.475(6)	1.483
Pn1-Cn11	1.808(5)	1.816(5)	1.885
Pn1-Cn21	1.806(5)	1.809(5)	1.892
Pn2-Cn31	1.816(5)	1.813(5)	1.886
Pn2-Cn41	1.811(5)	1.810(5)	1.890

n = 1/ 2 for (17I) and (17II) respectively and n = 1 for calculated structure of $[CrCl_4(PNP\text{-}i\text{-}Pent)]^-$

It is evident from **Table 9.6** that the bond lengths for $[CrCl_4(PNP\text{-}i\text{-}Pent)]^-$ (I) and (II) are overall shorter than the bond lengths of the corresponding calculated structure.

9.3.3 $[CrCl_4(PNP\text{-}n\text{-}Butyl)]^-$ (18 *vs.* 18*)

The crystal structure of $[n\text{-}Butyl\text{-}NH_3][CrCl_4(PNP\text{-}n\text{-}Butyl)]\cdot 2C_7H_8$ revealed four crystallographic independent monomeric chromium(III) complexes (see §6.2.3). These complexes $[CrCl_4(PNP\text{-}n\text{-}Butyl)]^-$ (1) (18I), see §6.2.3 (see **Figure 9.9a** and **b**), (II) (18II), (III) (18III) and (IV) (18IV) are all compared to the calculated $[CrCl_4(PNP\text{-}n\text{-}Butyl)]^-$ structure (see **Figure 9.10a** and **b**).

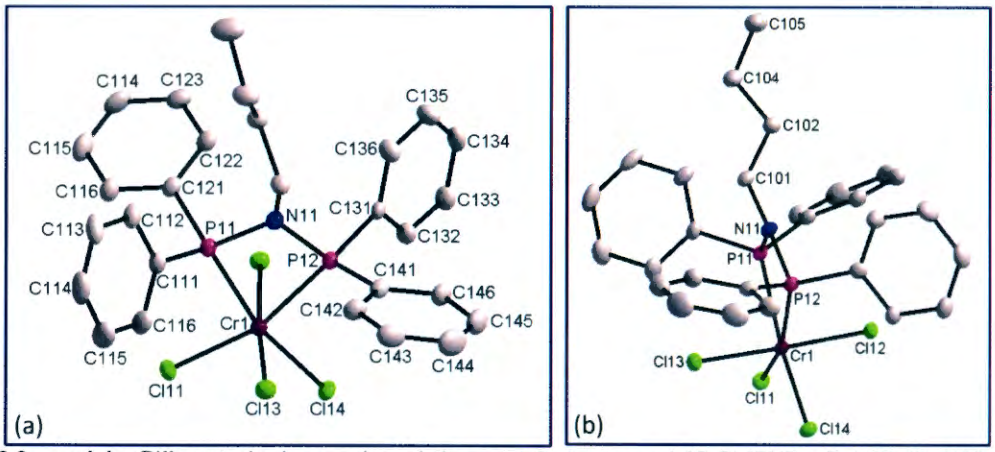

Figure 9.9a and b: Different viewing angles of the crystal structure of $[CrCl_4(PNP\text{-}n\text{-}Butyl)]^-$ (I) (18I) at 50% probability. (H-atoms were omitted for clarity.)

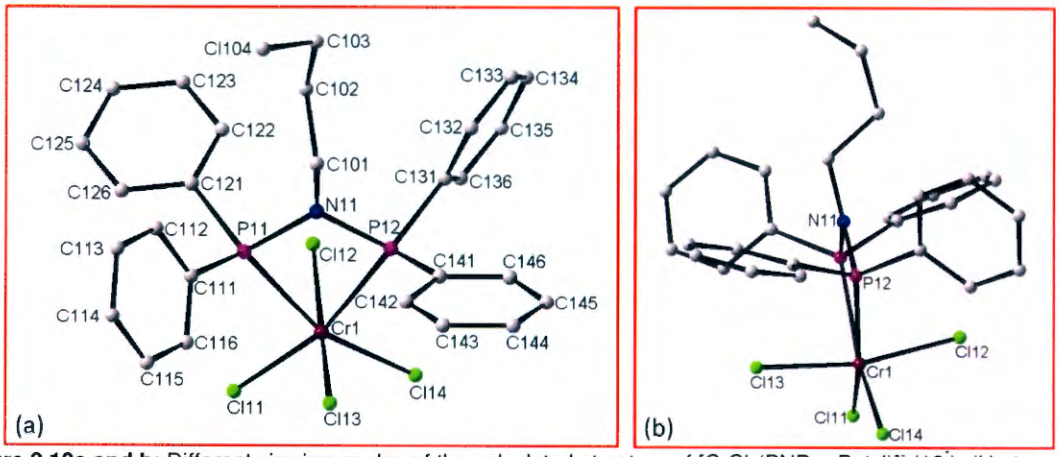

Figure 9.10a and b: Different viewing angles of the calculated structure of $[CrCl_4(PNP\text{-}n\text{-}Butyl)]^-$ (18*). (H-atoms were omitted for clarity.)

Table 9.7: Selected bond angles (°) for crystal structures, $[CrCl_4(PNP\text{-}n\text{-}Butyl)]^-$ (I) (18I), $[CrCl_4(PNP\text{-}n\text{-}Butyl)]^-$ (II) (18II), $[CrCl_4(PNP\text{-}n\text{-}Butyl)]^-$ (III) (18III) and $[CrCl_4(PNP\text{-}n\text{-}Butyl)]^-$ (IV) (18IV) and the calculated structure of $[CrCl_4(PNP\text{-}n\text{-}Butyl)]^-$ (18*).

Bond angles (°)	18I	18II	18III	18IV	18*
Pn1 – Crn – Pn2	66.9(1)	66.9(1)	67.2(1)	67.1(1)	65.2
Cln1 – Crn– Cln2	92.2(1)	92.5(1)	90.5(1)	91.8(1)	94.4
Cln3 – Crn – Cln4	90.2(1)	89.5(1)	92.8(1)	90.2(1)	94.6
Pn1 – Nn1 – Pn2	105.3(2)	105.2(2)	106.1(2)	105.4(2)	109.4
Cn11 – Pn1 – Cn21	104.0(2)	104.8(2)	103.6(2)	102.8(2)	101.1
Cn31 – Pn2 – Cn41	103.7(2)	103.0(2)	103.6(2)	104.4(2)	101.0

n=1/ 2/ 3/ 4 for 18I, 18II, 18III, and 18IV respectively and n=1 for calculated structure of $[CrCl_4(PNP\text{-}n\text{-}Butyl)]^-$.

The P-Cr-P angle for the calculated $[CrCl_4(PNP\text{-}n\text{-}Butyl)]^-$ structure is slightly smaller than the corresponding angles of the four monomeric chromium(III) complexes of $([n\text{-}Butyl\text{-}NH_3]_4[CrCl_4(PNP\text{-}n\text{-}Butyl)]_4 \cdot 8C_7H_8$ which range between 66.9(1) and 67.2(1) ° (see **Table 9.7**). The small bite angles for all the structures show distortion of the octahedral geometry at the chromium(III) centres. The P-N-P angle of the calculated structure (109.4 °) is closer to ideal tetrahedral geometry at the nitrogen atom in comparison to the smaller corresponding angles of the complexes of the crystal structure which range from 105.2(2) to 106.1(2) °. The C-P-C angles of the calculated structure (101.0 °) illustrate the strain experienced in the structure.

Table 9.8: Selected torsion angles (°) for crystal structures, $CrCl_4(PNP\text{-}n\text{-}Butyl)]^-$ (I) (18I), $[CrCl_4(PNP\text{-}n\text{-}Butyl)]^-$ (I) (18II), $[CrCl_4(PNP\text{-}n\text{-}Butyl)]^-$ (III) (18III) and $[CrCl_4(PNP\text{-}n\text{-}Butyl)]^-$ (IV) (18IV) and the calculated structure of $[CrCl_4(PNP\text{-}n\text{-}Butyl)]^-$ (18*).

Torsion angles (°)	18I	18II	18III	18IV	18*
Crn-Pn1-Cn11-Cn12	176.9(1)	-110.1(1)	172.8(1)	-110.7(1)	175.9
Crn-Pn1-Cn21-Cn22	-75.1(1)	-135.8(1)	-78.3(1)	-144.5(1)	-65.1
Crn-Pn2-Cn31-Cn32	-43.8(1)	-91.5(1)	-34.0(1)	-93.3(1)	169.0
Crn-Pn2-Cn41-Cn42	-65.8(1)	4.5(1)	-62.3(1)	17.1(1)	-66.7

n=1/ 2/ 3/ 4 for 18I, 18II, 18III and 18IV respectively and n=1 for calculated structure of $[CrCl_4(PNP\text{-}n\text{-}Butyl)]^-$.

It is evident from the torsion angles of the calculated structure (see **Table 9.8**) that a 'fan-like' arrangement of the phenyl rings is adopted. The ring orientations of the calculated structure is similar to $[CrCl_4(PNP\text{-}n\text{-}Butyl)]^-$ (I) and (III) as is illustrated by the similar corresponding torsion angles. Ring 3 of calculated structure (ring containing C131) is the only ring to show a significantly different orientation with a torsion angle of 169.0 ° in comparison to Cr1-P12-C131-C132 (-43.8(1) °) and Cr3-P32-C331-C332 (-34.0(1) °). An overlay of the calculated structure with each of the four complexes of the crystal structure is illustrated in **Figures 9.11**, **9.12**, **9.13** and **9.14** respectively.

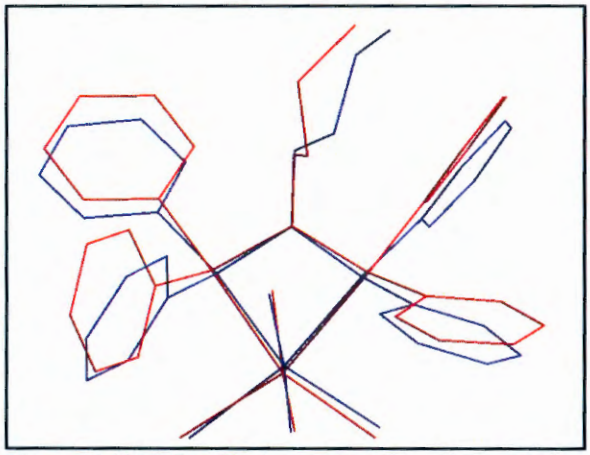

Figure 9.11: Graphical representation of an overlay of the $[CrCl_4(PNP\text{-}n\text{-}Butyl)]^-$ (I) crystal structure (blue) (18I) and the calculated structure of $[CrCl_4(PNP\text{-}i\text{-}Pent)]^-$ (18*) (red).

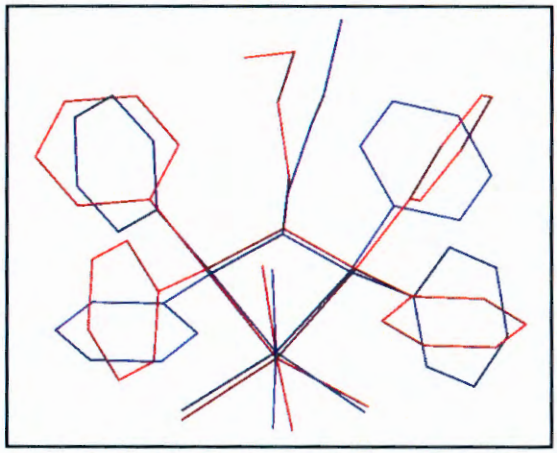

Figure 9.12: Graphical representation of an overlay of the $[CrCl_4(PNP\text{-}n\text{-}Butyl)]^-$ (II) crystal structure (18II) (blue) and the calculated structure of $[CrCl_4(PNP\text{-}i\text{-}Pent)]^-$ (18*) (red).

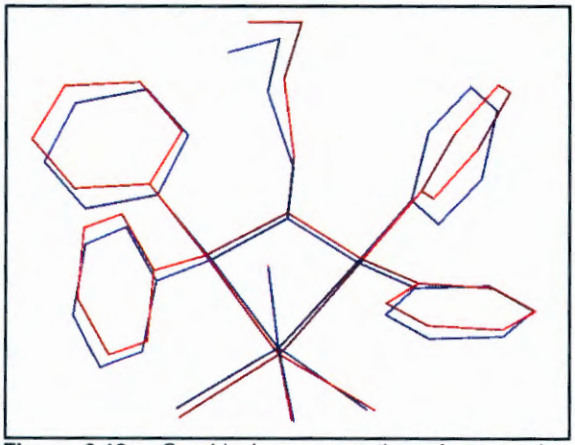

Figure 9.13: Graphical representation of an overlay of the $[CrCl_4(PNP\text{-}n\text{-}Butyl)]^-$ (III) crystal structure (18III) (blue) and the calculated structure of $[CrCl_4(PNP\text{-}i\text{-}Pent)]^-$ (18*) (red).

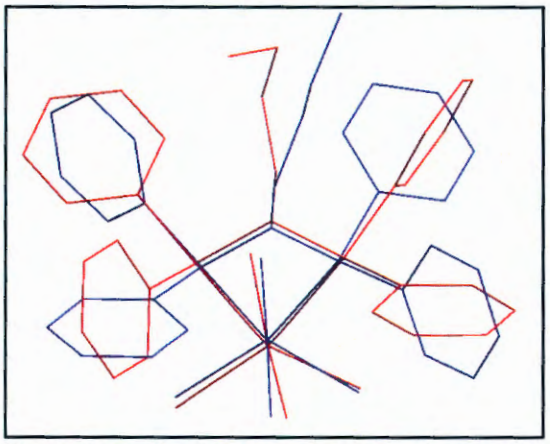

Figure 9.14: Graphical representation of an overlay of the $[CrCl_4(PNP\text{-}n\text{-}Butyl)]^-$ (IV) crystal structure (18IV) (blue) and the calculated structure of $[CrCl_4(PNP\text{-}i\text{-}Pent)]^-$ (18*) (red).

Table 9.9: Selected bond lengths (Å) for crystal structures, $CrCl_4$(PNP-*n*-Butyl)]$^-$ (I) (18I), [$CrCl_4$(PNP-*n*-Butyl)]$^-$ (II) (18II), [$CrCl_4$(PNP-*n*-Butyl)]$^-$ (III) (18III) and [$CrCl_4$(PNP-*n*-Butyl)]$^-$ (IV) (18IV) and the calculated structure of [$CrCl_4$(PNP-*n*-Butyl)]$^-$ (18*).

Bond Length (Å)	18I	18II	18III	18IV	18*
Crn – Pn1	2.458(1)	2.457(1)	2.453(1)	2.457(1)	2.745
Crn – Pn2	2.461(1)	2.461(1)	2.461(2)	2.461(1)	2.697
Crn– Cln1	2.313(1)	2.297(1)	2.316(1)	2.312(1)	2.320
Crn – Cln2	2.304(1)	2.317(1)	2.344(1)	2.324(1)	2.394
Crn – Cln3	2.307(1)	2.351(1)	2.317(12)	2.324(1)	2.396
Crn – Cln4	2.335(1)	2.301(1)	2.302(1)	2.327(1)	2.327
Nn1 – Pn1	1.712(4)	1.697(4)	1.702(5)	1.701(4)	1.799
Nn1 – Pn2	1.699(4)	1.714(4)	1.700(5)	1.705(4)	1.795
Nn1 – Cn01	1.474(6)	1.482(6)	1.482(7)	1.475(6)	1.482
Pn1 – Cn11	1.817(4)	1.810(5)	1.812(4)	1.811(5)	1.893
Pn1 – Cn21	1.813(5)	1.814(5)	1.810(5)	1.813(5)	1.887
Pn2 – Cn31	1.813(5)	1.807(5)	1.818(5)	1.804(5)	1.892
Pn2 – Cn41	1.808(5)	1.808(4)	1.807(5)	1.811(4)	1.885

n=1/ 2/ 3/ 4 for 18I 18II, 18III and 18IV respectively and n=1 for calculated structure of [$CrCl_4$(PNP-*n*-Butyl)]$^-$.

The bond lengths, as seen in **Table 9.9**, of the calculated [$CrCl_4$(PNP-*n*-Butyl)]$^-$ are longer than the corresponding bond lengths of the four anionic complexes

9.4 Discussion

The structures of [$CrCl_4$(PNP-*n*-Pent)]$^-$, [$CrCl_4$(PNP-*i*-Pent)]$^-$ and [$CrCl_4$(PNP-*n*-Butyl)]$^-$ were successfully optimized by theoretical calculations

The bond angles overall compared well to the corresponding bond angles of the complexes of the crystal structures. The P-Cr-P bite angles of the three calculated structures range between 64.9 and 65.4 ° whereas the angles for the complexes of the

crystal structures range from 66.7(1) and 67.1(1) °. Even though the bite angles of the calculated structures are slightly smaller than the corresponding angles of the crystal structures, the bond angles still indicate a distorted octahedral geometry at the chromium(III) centre. The P-N-P angles for the calculated structures range between 108.7 and 109.4 ° and the C-P-C angels range from 101.0 to 101.2 °. These angles, which all deviate from the ideal tetrahedral geometry, indicate the distortion at the nitrogen and phosphorous atoms respectively. The strain experienced within the complexes of the $[CrCl_4(PNP\text{-}alkyl)]^-$ crystal structures as described in Chapter 6 is clearly emulated in the corresponding calculated structures.

The bond lengths for the optimized structures are in some cases longer than the corresponding bond lengths of the related crystal structures, in fact the Cr-P distances are overestimated by approximately 10%. This is inherent of the technique, when performing theoretical calculations, to over-estimate the bond lengths for the structures calculated.

The torsion angles of the calculated Cr(III) structures all revealed variations of the 'fan-like' orientation of the phenyl rings which is the same type of arrangement that was adopted by the crystal structures. Interestingly, the monomeric $[CrCl_4(PNP\text{-}alkyl)]^-$ complexes of the crystal structures have various intramolecular C-H···Cl hydrogen bonding interactions between the hydrogen atoms of the phenyl rings and the chloride atoms (see Chapter 6) which could have an influence on the arrangement of the phenyl rings. Despite the absence of any hydrogen bonding interactions for the calculated structures, the optimized structures had a very similar arrangement for the phenyl rings for at least one of the complexes in the asymmetric unit of the respective crystal structures. It therefore appears that the arrangements of the phenyl rings for these complexes are not determined by the intra- or intermolecular interactions.

Factors which possibly affect the arrangement of the phenyl rings are presented in Chapter 10 in which a steric parameter measuring the steric bulk of the alkyl moieties of the various diphoshinoamine ligands is described.

In spite of the differences observed between the solid state structures and the theoretically calculated ones, the fair to good agreement between these two techniques were highlighted by the results presented in this chapter.

10 Effective Tolman based study on the steric effect of the N-substituent in the PNP-ligands

In this chapter...

A steric parameter is defined to measure the steric bulk of the alkyl group bonded to the nitrogen atom of the bis(diphenylphosphino)alkylamine ligands. Correlations between this measured steric parameter of the various PNP ligands and the ethylene oligomerisation catalytic selectivity of the ligand system, when combined with $[CrCl_3(THF)_3]$ or $[Cr(acac)_3]$ and MMAO as catalyst system, are presented and discussed.

10.1 Introduction

The Tolman cone angle[1] is a measure of the steric demand induced by a ligand. Tertiary phosphines are commonly classified using this parameter, but the method can be applied to any ligand. Tolman proposed to measure the steric bulk of a phosphine ligand from CPK models in the following way: from the metal centre, located at a distance of 2.28 Å from the phosphorous atom in the appropriate direction, a cone is constructed with the sides' tangent to the van der Waals radii of the outermost atoms on the substituents on the phosphorous atom (see **Figure 10.1**).

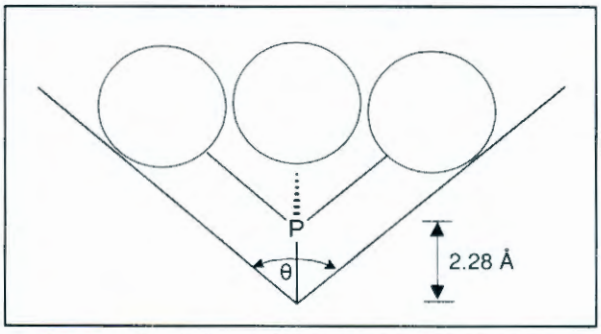

Figure 10.1: Representation for the calculation of the Tolman cone angles in symmetrical phosphines.

[1] C.A. Tolman, *Chem. Rev.*, 1977, **77**, *313*,

In the case of non-symmetrical $PX_1X_2X_3$ ligands (X_1 – X_3 different alkyl, aryl *etc.* substituents) it is assumed that $\theta_i/2$ would be the same as $P(X_i)_3$ (see **Figure 10.2**).

With use of the equation:

$$\theta = \left(\frac{2}{3}\right)\sum_{i=1}^{3}\frac{\theta i}{2} \qquad (10.1)$$

the steric parameter of a non-symmetrical phosphine can be estimated.

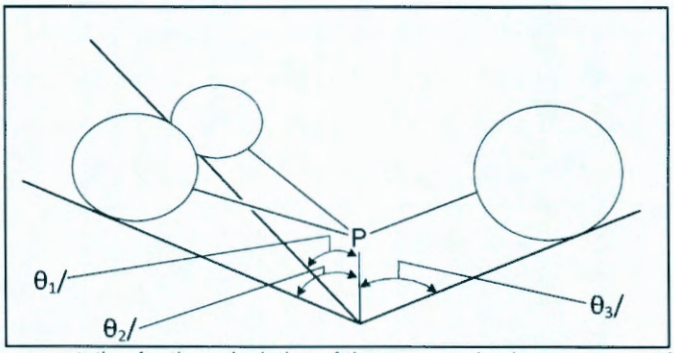

Figure 10.2: Representation for the calculation of the cone angles in non-symmetrical phosphines.

It was mentioned in Chapter 2 that the selective tetramerisation of ethylene to 1-octene was first reported in 2004.[2] The evaluation of the catalytic behaviour of a large number of diphosphinoamine (PNP) ligands with various substituents on both the N and P atoms followed this discovery.[3,4,5,6,7] It was found that a predominant factor in the catalysis selectivity (in particular the 1-olefin) is the steric bulk on the central nitrogen atom compared to the basicity of the phosphine. Based on this information, additional

[2] Bollmann, A., Blann, K., Dixon, J.T., Hess, F. M., Killian, E.; Maumela, H., McGuinness, D. S., Morgan, D. H., Neveling, A., Otto, S., Overett, M.J., Slawin, A.M.Z., Wasserscheid, P. and Kuhlmann, S., *J. Am. Chem. Soc.*, **2004**, *126*, 14712.

[3] Blann, K., Bollmann, A., de Bod, H., Dixon, J.T., Killian, E., Nongodlwana, P., Maumela, M.C., Maumela, H., McConnell, A.E., Morgan, D.H., Overett, M.J., Prétorius, M., Kuhlmann, S. and Wasserscheid, P., *J. Catal.*, **2007**, *249*, 244.

[4] Overett, M.J., Blann, K., Bollmann, A., Dixon, J.T., Hess, F.M., Killian, E., Maumela, H., Morgan, D.H., Neveling, A. and Otto, S., *Chem. Commun.*, **2005**, 622.

[5] Blann, K., Bollmann, A., Dixon, J.T., Hess, F.M., Killian, E., Maumela, H., Morgan D.H., Neveling, A., Otto, S. and Overett, M., *Chem. Commun.*, **2005**, 620.

[6] Kuhlmann, S., Blann, K., Bollmann, A., Dixon, J.T., Killian, E., Maumela, M.C., Maumela, H., Morgan, D.H., Prétorius, M., Taccardi, N. and Wasserscheid, P., *J. Catal.*, **2007**, *245*, 277.

[7] Killian, E., Blann, K., Bollmann, A., Dixon, J.T., Kuhlmann, S.E., Maumela, M.C., Maumela, H., Morgan, D.H., Nongodlwana, P., Overett, M.J., Prétorius, M., Höfener, K. and Wasserscheid, P., *J. Mol. Catal. Chem.*, **2007**, *270*, 214.

EFFECTIVE TOLMAN-BASED-N-SUB STERIC EFFECT OF PNP-LIGANDS

PNP ligands have been synthesised in which the alkyl group bonded to the nitrogen atom was varied in a systematic way to evaluate the stereo-electronic properties thus induced.

In order to define a steric parameter for the alkyl group, a modification of the Tolman cone angle is used, the Effective Tolman-based N-substituent steric effect ($\theta_{N\text{-}sub}$) is used in this crystallographic study of the diphosphinoamine (PNP) ligand systems. This parameter is constructed from the nitrogen atom with the sides' tangent to the Van der Waals radii of the outermost atoms on the substituents on the nitrogen-bonded carbon atom (C_1) (see **Figure 10.3**). The calculations of $\theta_{N\text{-}sub}$ were performed using **Equation 10.1**. These calculated $\theta_{N\text{-}sub}$ values for the various PNP ligands investigated in this study is then compared with the catalytic data of the corresponding Cr(III)-PNP catalyst systems.

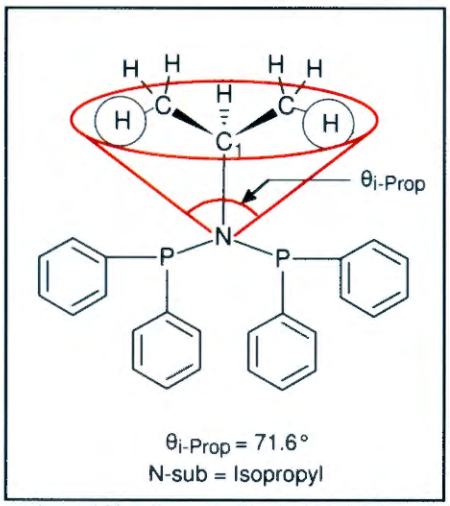

Figure10.3: Effective Tolman-based N-sub steric effect of bis(diphenylphosphino)-isopropylamine.

10.2 Experimental

As noted above, the $\theta_{N\text{-}Sub}$ parameter was calculated for the non-coordinated PNP ligands, $[PtCl_2(PNP\text{-}alkyl)]$ complexes, $[PdCl_2PNP\text{-}alkyl)]$ complexes and the $[CrCl_4(PNP\text{-}alkyl)]^-$ anionic compounds using the corresponding crystallographic data. A comparison of the $\theta_{N\text{-}Sub}$ values and the 1-hexene (1-C6) and 1-octene (1-C8) selectivity for the various PNP ligands was made (see **Table 10.1**). The Effective Tolman based study on the steric effect of the N-substituent was also calculated from the theoretically optimised structures ($\theta_{N\text{-}Sub}^*$) and is also included in **Table 10.1**.

All catalytic reations were conducted in a 300 ml Parr reactor (see **Table 10.1** for data).

The catalytic procedure associated with the ligands for entry numbers 6, 7, 11, 14 and 15 (see **Table 10.1**) is as follows:[2] 0.033 mmol $CrCl_3(THF)_3$ (THF = tetrahydrofuran), 0.10 mmol PNP-ligand, and 300 equivalents MMAO-3A (modified methylaluminoxane) with 100 ml toluene as solvent. The reaction was started by pressurisation with ethylene to the desired pressure (30 bar) with a reaction temperature of 65 °C. After the specified reaction time (30 minutes) the reaction was terminated by shutting off the ethylene feed, after which the autoclave was cooled rapidly to 0 °C.

The catalytic procedure associated with the ligands of entry numbers 1, 2, 3, 4, 5, 8, 9, 10, 12 and 13 (see **Table 10.1**) is as follows: 0.025 mmol $(Cr(acac)_3$ (acac = acetyl-acetonato) 0.030 mmol PNP-ligand, and 300 equivalents MMAO-3A (modified methylaluminoxane) with 100 ml methylcyclohexane as solvent.[3,8] The reaction was started by pressurisation with ethylene to the desired pressure (45 bar) with a reaction temperature of 60 °C. After the specified reaction time (30 minutes)

[8] Unpublished. Catalysis performed by Dr. W Gabrielli and N. Cloete on 08-08-2007

the reaction was terminated by shutting off the ethylene feed, after which the autoclave was cooled rapidly to 0 °C.

Comparative studies using different Cr precursors have shown that the nature of the Cr precursor employed does not have a significant influence on the catalytic behavior.[3]

Solvents were purchased from Aldrich and percolated through neutral alumina. $[Cr(acac)_3]$ (97 % purity) and $[CrCl_3(THF)_3]$ (99 %) were obtained from Sigma-Aldrich and used without further purification. See Chapter 3 for the synthesis and characterization of the PNP ligands. MMAO-3A was obtained from Akzo-Nobel.

The ethylene oligomerisation products were analysed by GC-MS and GC-FID (% reported in **Table 10.1** = weight %). The GC-MS spectra were recorded on a Varian Saturn 2100T. GC/FID analyses were carried out on a Hewlett-Packard 5890 chromatograph using a J&W Scientific 50 m x 0.2 mm x PONA column.[2,3]

10.3 Results

The correlation between the catalytic data and the $\theta_{N\text{-}sub}$ values are reported in increased values of $\theta_{N\text{-}sub}$ in **Table 10.1**.

It is clear from the data reported in **Table 10.1** that the $\theta_{N\text{-}sub}$ values calculated from the X-ray data of either the free or coordinated ligand, to any of the Pt(II), Pd(II) or Cr(III) complexes, show excellent agreement.

Table 10.1: Calculated $\theta_{N\text{-}sub}$ (°) and selected ethylene oligomerisation catalytic data for various PNP-ligand systems.

Nr.	Crystalline compound[a]	PNP-ligand used in catalysis	N-Sub	$\theta_{N\text{-}Sub}$ (°) (crystal data)[b]	$\theta_{N\text{-}Sub}$ (°)* (optmised structures)[c]	Phenyl ring orient.[d]	% C_6	% 1-C_6	% C_8	% 1-C_8
1	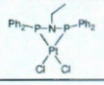	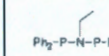	Pt-Ethyl	62.8	61.8	Fan	17.5[(3)]	40.7[(3)]	63.0[(3)]	97.3[(3)]
2			Ethyl	62.9	63.8	Fan	17.5[(3)]	40.7[(3)]	63.0[(3)]	97.3[(3)]
3			Cr-*n*-Butyl	63.0	64.7	Fan	18.5[(8)]	41.2[(8)]	61.1[(8)]	96.3[(8)]
4	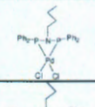	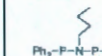	Pd-*n*-Butyl	63.2	64.4	Fan	18.5[(8)]	41.2[(8)]	61.1[(8)]	96.3[(8)]
5	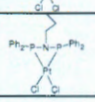	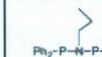	Pt-*n*-Prop	63.2	64.6	Fan	18.5[(8)]	41.2[(8)]	61.3[(8)]	96.3[(8)]
6	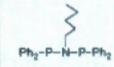		*n*-Pent	63.2	64.6	-	24.9[(3)]	54.7[(3)]	58.1[(3)]	96.8[3)]
7		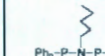	Cr-*n*-Pent	63.5	64.2	Fan	24.9[(3)]	54.7[(3)]	58.1[(3)]	96.8[(3)]
8		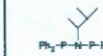	Pt-Dimprop	67.6	69.4	Basket	24.3[(3)]	85.1[(3)]	65.7[(3)]	99.5[(3)]
9	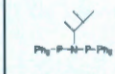	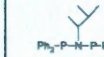	Dimprop	67.8	71.7	-	24.3[(3)]	85.1[(3)]	65.7[(3)]	99.5[(3)]
10		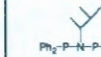	Pd-Dimprop	68.8	69.6	Basket	24.3[(3)]	85.1[(3)]	65.7[(3)]	99.5[(3)]
11		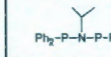	Pd-*i*-Prop	69.1	70.9	Basket	32.7[(3)]	86.5[(3)]	60.6[(3)]	99.2[(3)]
12			Pt-Cychex	69.4	71.0	Basket	19.4[(3)]	75.0[(3)]	68.3[(3)]	99.0[(3)]
13	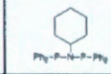		Cychex	69.5	70.5	-	19.4[(3)]	75.0[(3)]	68.3[(3)]	99.0[(3)]
14	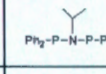	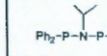	*i*-Prop	71.6	70.3	-	32.7[(3)]	86.5[(3)]	60.6[(3)]	99.2[(3)]
15	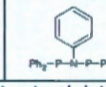		Phenyl	49.8	51.3	-	27.3[(2)]	67.8[(2)]	61.6[(2)]	97.8[(2)]

(a) Structural data used to calculate $\theta_{N\text{-}sub}$.

(b) $\theta_{N\text{-}Sub}$ determined from the crystallographic data, see Chapters 4, 5 and 6.

(c) $\theta_{N\text{-}Sub}$* determined from the optimized structures, see Chapters 7, 8 and 9.

(d) Phenyl ring orientation (phosphorous-coordinated) when PNP-ligands are coordinated to a metal centre (Pt(II)/ Pd(II)/ Cr(III).

(Ph = Phenyl substituent, orient. = orientation)

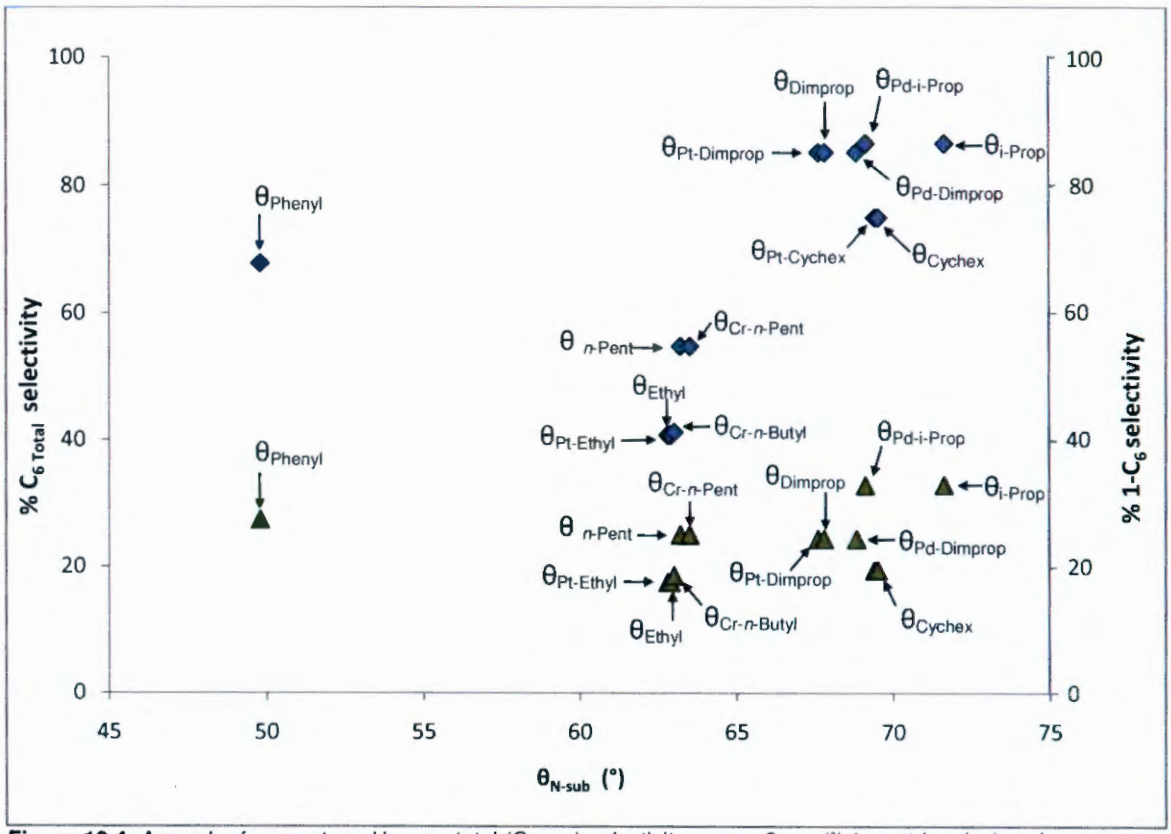

Figure 10.4: A graph of percentage Hexene total ($C_{6\ Total}$) selectivity *versus* $\theta_{N\text{-}sub}$ (°) (grey triangles) and percentage 1-Hexene (1-C_6) selectivity *versus* $\theta_{N\text{-}sub}$ (°) (blue diamonds).

It is clear from **Table 10.1** that the 1-C_6 selectivity of the PNP-ligand system (when coordinated with Cr(III)) increases as the $\theta_{N\text{-}sub}$ becomes larger (see **Figure 10.4**). It is interesting to note that with an increase of only 8.8°, from $\theta_{Pt\text{-}Ethyl}$ (62.8 °) to $\theta_{i\text{-}Prop}$ (71.6 °), the 1-C_6 selectivity increases dramatically from 40.7 % to 86.6 %, i.e. it more than doubled. This confirms and quantifies to some extent the $\theta_{N\text{-}sub}$ parameter for use in this reaction, that the steric bulkiness ($\theta_{N\text{-}sub}$) has a significant effect on the 1-hexene selectivity. The total C_6 selectivity also increases from around 17 % to 24 % with this 8.8 ° increase in the $\theta_{N\text{-}sub}$.

It is of interest to note that the $\theta_{N\text{-}sub}$* for the various theoretically optimized structures are similar to the corresponding $\theta_{N\text{-}sub}$ values for the crystallographic data (see

Table 10.1). The largest difference is observed for the PNP-Dimprop ligand with values of 67.8 and 71.7 ° for $\theta_{Dimprop}$ and $\theta_{NDimprop}$* respectively. A trend of an increase for the total C_6 and the 1-C_6 selectivity as the $\theta_{N\text{-}sub}$* becomes larger is observed, which is similar to that of the crystallographically determined steric parameters ($\theta_{N\text{-}sub}$).

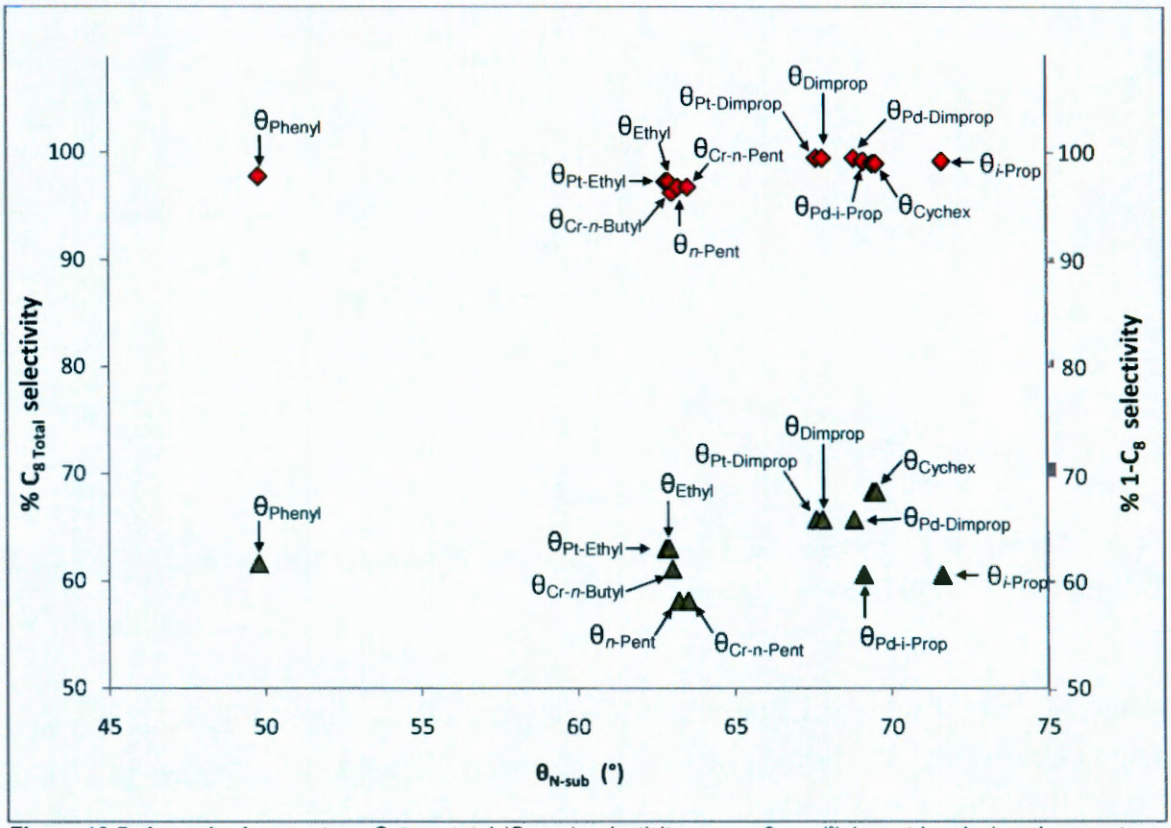

Figure 10.5: A graph of percentage Octene total ($C_{8\ Total}$) selectivity *versus* $\theta_{N\text{-}sub}$ (°) (grey triangles) and percentage 1-Octene (1-C_8) selectivity *versus* $\theta_{N\text{-}sub}$ (°) (red diamonds).

The 1-octene (1-C_8) selectivity also appears to increase as the $\theta_{N\text{-}sub}$ becomes larger (see **Table 10.1** and **Figure 10.5**). The effect is however less dramatic with the selectivity only increasing from 97.3 % to 99.2 % for $\theta_{Pt\text{-}Ethyl}$ (62.8 °) and $\theta_{i\text{-}Prop}$ (71.6 °) respectively. The total C_8 selectivity varies in a fluctuating way by only 8 % with a systematic increase in $\theta_{N\text{-}sub}$.

Similar tendencies for $\theta_{N\text{-}Sub}^*$ is observed with an increase of the total C_8 and 1-C_8 selectivities as the $\theta_{N\text{-}Sub}^*$ increases (see **Table 10.1**).

The θ_{Phenyl} (49.8 °) for the free PNP-Phenyl is distinctly smaller than the rest of the $\theta_{N\text{-}sub}$ values reported (see **Figure 10.4** and **Figure 10.5**), the θ_{Phenyl}^* (51.3 °) is also significantly smaller than the other $\theta_{N\text{-}Sub}^*$ reported. Both cases are attributed to the fact that the nitrogen-coordinated carbon of the phenyl moiety on the PNP-Phenyl compound only contains two substituents and consequently does not strictly adhere to the Tolman cone angle hypothesis in which three substituents must be present.

10.4 Discussion

The Effective Tolman-based steric effect ($\theta_{N\text{-}sub}$) (determined from the crystallographic data) of the alkyl substituent on the nitrogen atom varies considerably for the various compounds of the different PNP-ligand systems. This change is significant when branching is present at the nitrogen coordinated C1 atom, as apparent from θ_{Ethyl} (62.9 °) for the PNP-Ethyl that is dramatically smaller than $\theta_{i\text{-}Prop}$ (71.6 °). It is again noted that $\theta_{N\text{-}sub}$ is accurately determined from structural data of either the coordinated or free ligand. It is again underlined by the different value pairs in **Table 10.1** for example small differences in $\theta_{N\text{-}sub}$ were observed between the coordinated and the non-coordinated PNP-ligands for example $\theta_{Pt\text{-}Ethyl}$ (62.8 °) and θ_{Ethyl} (62.9 °). Relatively small differences between the corresponding $\theta_{N\text{-}Sub}$ and $\theta_{N\text{-}Sub}^*$ values were also observed.

The crystal structures of the various compounds in **Table 10.1** show only small changes in bond angles and bond lengths within each of the various PNP-compounds as discussed previously in Chapters 4, 5 and 6. The most significant differences between the crystal structures of the metal-coordinated PNP-compounds, were the orientation of

the phenyl rings as the substituents on the nitrogen atom changed from one compound to the other.

The data obtained from the Pt(II)- and Pd(II)-PNP complexes (see Chapter 5) illustrate how the orientation of the phenyl rings are affected by the steric bulkiness of the nitrogen-coordinated alkyl group. The following complexes, $[PtCl_2(PNP\text{-}Dimprop)]$, $[PdCl_2(PNP\text{-}i\text{-}Prop,)]$, $[PdCl_2(PNP\text{-}Dimprop)]$ and $[PtCl_2(PNP\text{-}Cychex)]$ have $\theta_{N\text{-}Sub}$ values that range between 67.6 and 69.4 °. All these complexes have the 'basket-like' orientation (see **Figure 10.6**) of the phenyl rings in the solid state (as discussed in Chapter 5), which create space for the alkyl groups of the respective complexes. A significant difference in the orientations of the respective phenyl rings is however observed for $[PtCl_2(PNP\text{-}n\text{-}Prop)]$, $[PtCl_2(PNP\text{-}Ethyl)]$ and $[PdCl_2(PNP\text{-}n\text{-}Butyl)]$ in solid state, these complexes have $\theta_{N\text{-}Sub}$ that vary between 62.8 and 63.2 °. These complexes adopted the 'fan-like' orientation for the phenyl rings of the respective complexes as defined in Chapter 5.

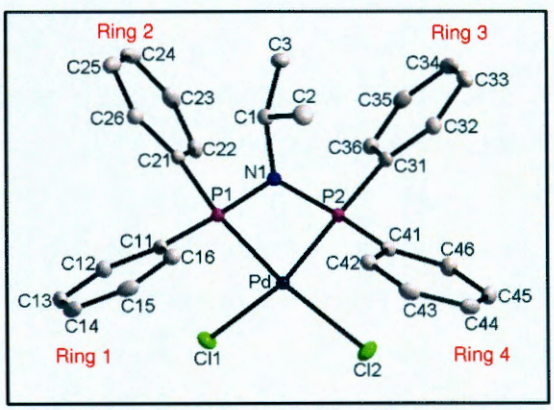

Figure 10.6: Graphical representation of the crystal structure of $[PdCl_2(PNP\text{-}i\text{-}Prop)]$ at 50 % probability. (H-atoms were omitted for clarity).

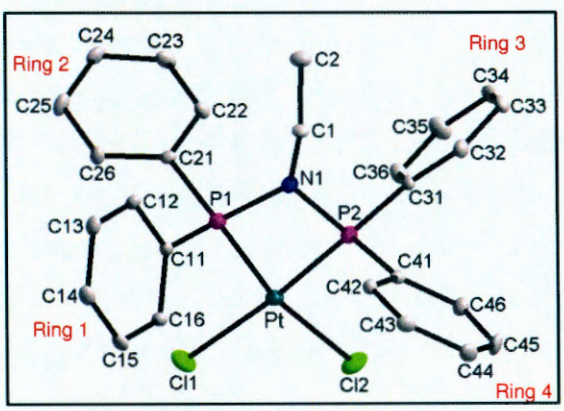

Figure 10.7: Graphical representation of the crystal structure of $[PtCl_2(PNP\text{-}Ethyl)]$ at 50 % probability. (H-atoms were omitted for clarity).

It appears that the steric bulk of the nitrogen-bonded alkyl group is not substantially affecting the bond angles, but it is influencing the orientation of the phenyl rings of the PNP-ligands when bonded to a metal centre. This could then ultimately influence the

metallocycle formation and therefore the selectivity after which reductive elimination liberates 1-hexene and 1-octene.

In an effort to assess the space occupied by the phosphorous coordinated phenyl rings in the crystal structures of the metal-PNP compounds, it was decided to measure the angle created by the outermost hydrogen atom of phenyl ring 1 (ring containing C11), the metal centre and the outermost hydrogen atom of phenyl ring 4 (ring containing C41) (σ_{14}, see **Figure 10.8**). The second angle (σ_{23}) consists of the outermost hydrogen atom of phenyl ring 2, the metal centre and the outermost hydrogen atom of phenyl ring 3, see **Figure 10.8**. The σ_{14} and σ_{23} angles for selected metal-PNP compounds are presented in **Table 10.2**.

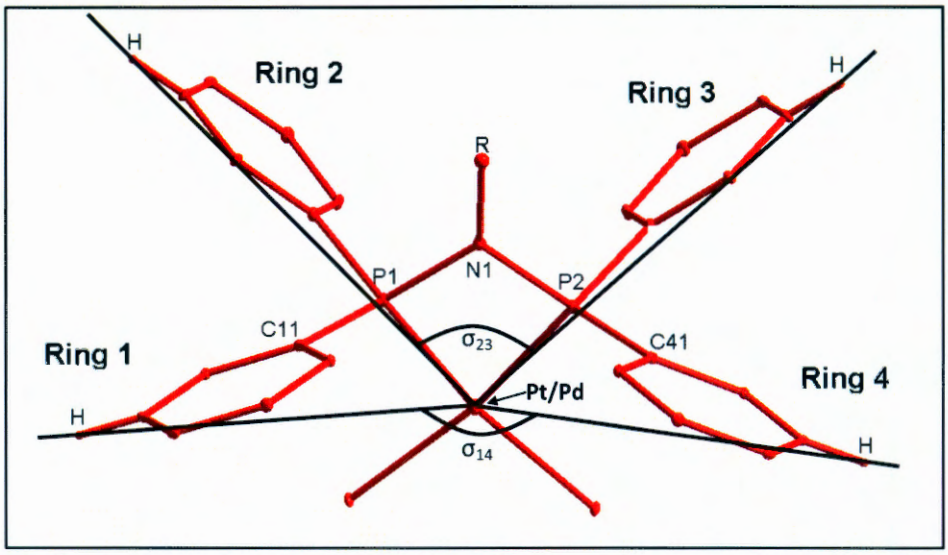

Figure 10.8: Graphical representation of the measured σ_{14} and σ_{23} angles for [$PtCl_2$(PNP-alkyl)] and [$PdCl_2$(PNP-alkyl)] complexes. (metal = Pt(II)/ Pd(II), R = alkyl group.)

Table 10.2: The $\theta_{N\text{-}Sub}$, σ_{14} and σ_{23} angles (°) for selected [$PtCl_2$(PNP-alkyl)] and [$PdCl_2$(PNP-alkyl)] complexes obtained from crystallographic data.

Complex	Phenyl ring orientation	$\theta_{N\text{-}Sub}$ (°) (crystal data)	σ_{14} (°)	σ_{23} (°)
[$PtCl_2$(PNP-Ethyl)]	Fan	62.8	111.1(2)	110.0(2)
[$PtCl_2$(PNP-*n*-Prop)]	Fan	63.2	101.9(2)	99.8(2)
[$PtCl_2$(PNP-Dimprop)]	Basket	67.6	132.2(3)	82.3(3)
[$PdCl_2$(PNP-Dimprop)]	Basket	68.8	132.4(3)	83.3(3)
[$PdCl_2$(PNP-*i*-Prop)]	Basket	69.1	132.0(2)	84.2(2)
[$PtCl_2$(PNP-Cychex)]	Basket	69.4	121.2(2)	101.1(2)

It can be seen in **Table 10.2** that the σ_{23} angles for the complexes with the basket-like orientation are significantly smaller (range from 82.3(3) to 101.1(2) °) than σ_{14} of the same complexes. The σ_{14} and σ_{23} for the complexes with the fan-like phenyl ring arrangement are however very similar. The σ_{14} angles for the complexes with the basket-like phenyl ring arrangement is significantly larger (range between 121.2(2) and 132.0(2) °) than the corresponding angles for the complexes which adopted a fan-like orientation, which range from 101.9(2) to 111.1(2) °. When taking into consideration that the steric bulk of the nitrogen-coordinated alkyl moieties point towards phenyl rings 2 and 3 and away from rings 1 and 4, it is clear that the complexes with large $\theta_{N\text{-}Sub}$ (i.e. sterically bulky alkyl moieties), which adopted the basket-like arrangement, have phenyl rings 1 and 4 placed further apart with a large σ_{14} angle. In contrast, σ_{23} is significantly smaller for these complexes as the sterically bulky alkyl group compels rings 2 and 3 to envelope the alkyl substituent, which creates more rigidity in the arrangement of these phenyl rings. In the case of the complexes which adopted the fan-like orientations for the phenyl rings, the rings have more degrees of freedom as the alkyl moieties are smaller (with smaller $\theta_{N\text{-}Sub}$ values) and the phenyl rings are spread in a similar manner with comparable σ_{14} and σ_{23} values. The 1-hexene and 1-octene selectivity clearly increased for the PNP ligands with the larger $\theta_{N\text{-}Sub}$ values (see **Table 10.1**) and these ligands which proved to be the most selective (PNP-i-Prop, PNP-Cychex, PNP-Dimprop) formed metal-PNP complexes which adopted basket-like arrangement for the phosphorous coordinated phenyl rings. It is therefore possible to

consider that the phenyl ring arrangement, which is noticeably affected by the steric bulk of the nitrogen-coordinated alkyl group of the PNP ligands, is playing a role in the selectivity of the catalytic process when these ligands are used as part of the catalyst system (together with Cr(III) and an aluminoxane activator).

Finally, it is concluded that, as illustrated above, the introduction of the $\theta_{N\text{-}sub}$ steric parameter calculated for the different catalytic systems concerned, that quite a good correlation was found. This should be extended in future, also utilizing computational techniques, specifically molecular mechanics for prediction of activities in these ligand/ catalyst systems.

11 Substitution kinetic study of the [PtCl$_2$(PNP-*i*-Pent)] complex

In this chapter...

The reactions of [PtCl$_2$(PNP-i-Pent)] with Br$^-$ and the resulting substitution of the two chlorido ligands in two consecutive steps, was investigated. The activation parameters for the substitution reactions were determined by a temperature study of the reactions.

11.1 Introduction

The preceding chapters discussed different structural properties as obtained from solid state and theoretical studies. This chapter looks at a preliminary study of the reactivity induced by the PNP-ligands *via* classic kinetics.

Investigations of the substitution reactions at square planar platinum(II) centres have contributed considerably to the understanding of reaction mechanisms and ligand effects.[1,2,3] It has been shown that these type of complexes typically involve a reversible substitution with an observable solvent pathway[4] (see **Scheme 11.1**). The rate of substitution depends on many factors such as the nature of the metal, the ligand coordinated *trans* to the substituted ligand and the incoming nucleophile.[5,6]

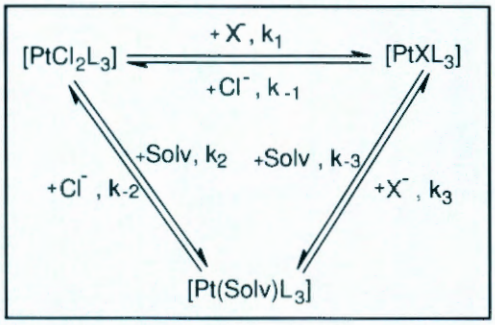

Scheme 11.1: Schematic representation of an example for the mechanism for square planar substitution showing both the direct pathway (k_2) and the parallel solvent assisted pathway (k_1)[1] (L =monodentate ligand, Solv = solvent species).

[1] Otto, S. and Roodt, A., *J. Organomet. Chem.*, **2006**, *691*, 4626.
[2] Romeo, R., Grassi, A. and Monsù Scolaro, L., *Inorg. Chem.*, **1992**, *31*, 4383.
[3] Basolo, F., Chatt, J., Gray, H.B., Pearson, R.G. and Shaw, B.L., *J. Chem. Soc.*, **1961**, 2207.
[4] Wendt, O.F. and Elding, L.I., *Inorg. Chem.*, **1997**, *36*, 6028.
[5] Vranckx, J. and Vanquickenborne, L.G., *Inorg. Chim. Acta*, **1974**, *11*, 159.
[6] Burdett, J., *Inorg. Chem.*, **1977**, *16*, 3031.

The substitution reactions of [$PtCl_2$(PNP-*i*-Pent)] with mono-anionic bromide (Br^-) was therefore studied to investigate the solution and kinetic behaviour of the complex.

11.2 Experimental

All kinetic experiments were carried out in air and all solvents were pre-dried over aluminiumoxide and distilled. The [$PtCl_2$(PNP-*i*-Pent)] metal complex was synthesized, characterized as described in Chapter 3.

^{31}P NMR spectra were recorded on a 600 MHz Bruker spectrometer ^{31}P chemical shifts are reported relative to 85 % H_3PO_4 (0 ppm). UV/Vis absorbance spectra were collected on a Varian Cary 50 Conc spectrophotometer in a 1.000 ± 0.001 cm quartz cuvette, which was equipped with a temperature cell regulator accurate within 0.1 °C.

The [Br^-] solutions (added as PPh_4Br) were ten to eighty fold in excess compared to the platinum(II) complex, ensuring *pseudo* first-order conditions. A constant amount of [Cl^-] (ten-fold excess, added as PPh_4Cl, compared to the platinum(II) complex) was also added to each of the [PPh_4Br] solutions to ensure that a constant [Cl^-] is maintained during the reaction.

The reactions were first monitored over a UV/Vis wavelength region to determine a suitable point at which to conduct the substitution. Once a wavelength is selected, an absorbance *vs.* time graph can be constructed and used to determine the observed rate constant for a specific temperature and [PPh_4Br] concentration. Kinetic data was analyzed with the Scientist[7] software package using a first-order rate equation as defined below (**Equation 11.1**). Rate laws and kinetic activation parameters are given in Appendix D.

$$A_{obs} = A_f - (A_f - A_i)e^{-(kobs)t} \qquad (11.1)$$

A_{obs} = observed absorbance, A_f = final absorbancem A_i, = initial absorbance, k_{obs} = pseudo first-order rate constant and t = time.

[7] Scientist for Windows (32), Micromath Inc., Version 2.01, **1986-1995**.

11.3 Reaction mechanism

Two consecutive reactions were observed when the reaction between [$PtCl_2$(PNP-*i*-Pent)] and [PPh_4Br] was monitored over a wavelength region 280 to 380 nm (see **Figures 11.1** and **11.2**).

The initial reaction shows an increase in absorbance (see **Figure 11.1**) at around 10 minutes with a subsequent decrease in absorbance for the second reaction (see **Figure 11.2**). These two reactions have significantly different reaction rates differing by approximately an order of magnitude, with the first reaction that is significantly faster than the second. The difference in rates makes it possible to accurately analyse each reaction separately.

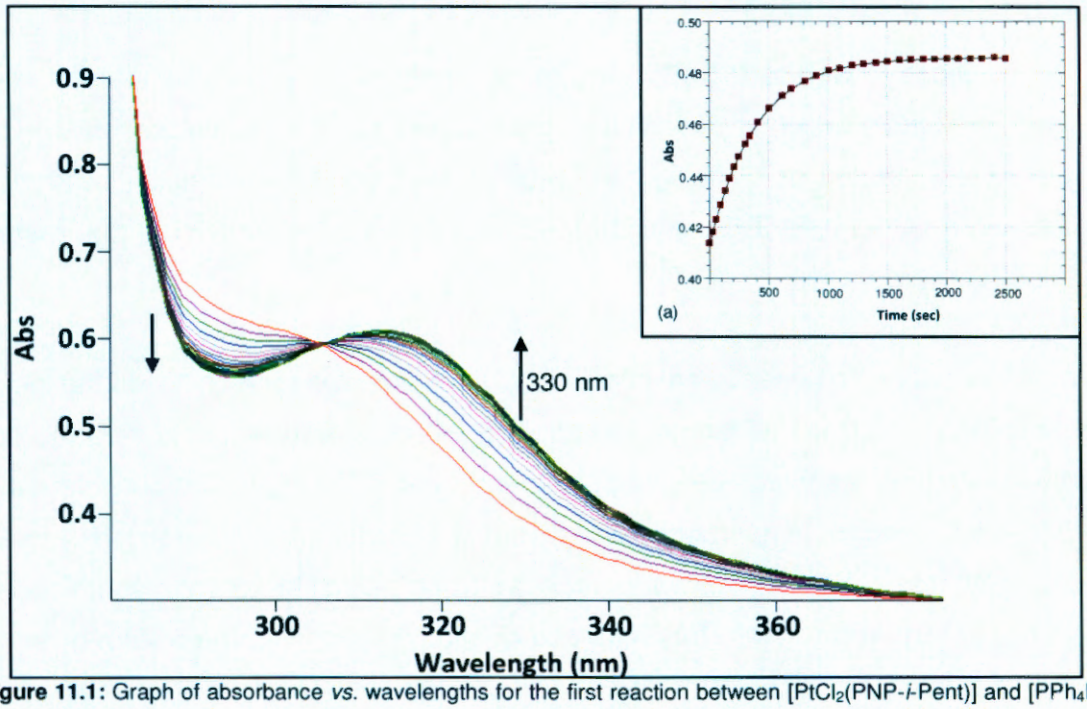

Figure 11.1: Graph of absorbance *vs.* wavelengths for the first reaction between [$PtCl_2$(PNP-*i*-Pent)] and [PPh_4Br] in 1,2-dichloroethane, at 15 °C. [$PtCl_2$(PNP-i-Pent)] = 2.5 x 10^{-4} M and [PPh_4Br] = 2.5 x 10^{-3} M. Insert (a) is a graph of absorbance vs. time (seconds) of the first-order fit reaction between [$PtCl_2$(PNP-*i*-Pent)] and [PPh_4Br] at 330 nm, experimental points observed , as well as the fitted line is shown.

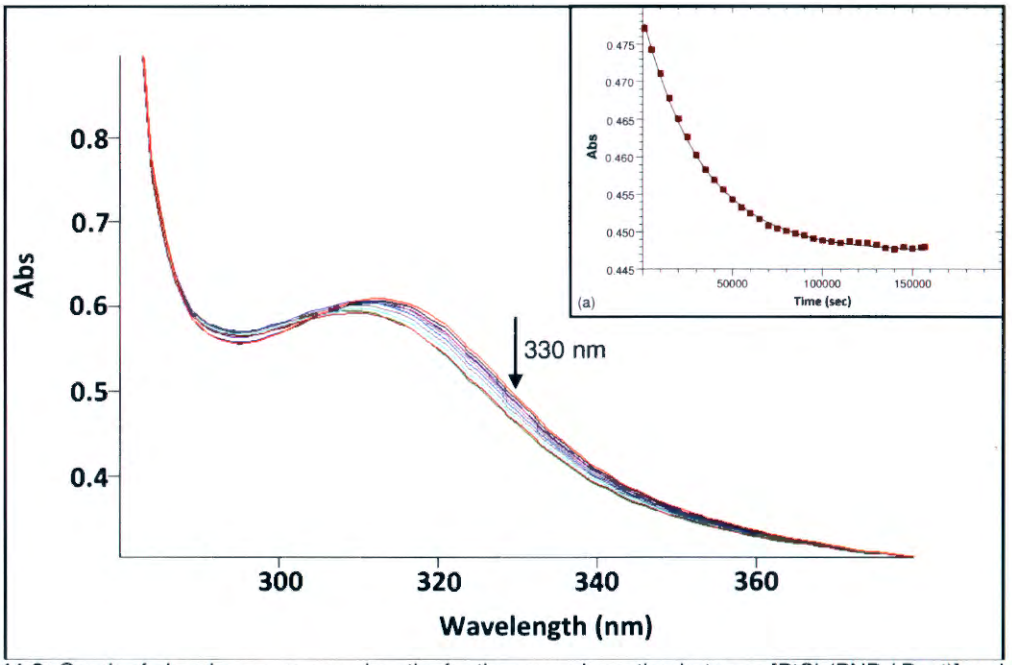

Figure 11.2: Graph of absorbance *vs.* wavelengths for the second reaction between [$PtCl_2$(PNP-*i*-Pent)] and PPh_4Br in 1,2-dichloroethane, at 30 °C. [$PtCl_2$(PNP-i-Pent)] = 2.5 x 10^{-4} M and [PPh_4Br] = 2.5 x 10^{-3} M. Insert (a) is a graph of absorbance vs. time (seconds) of the second reaction between [$PtCl_2$(PNP-*i*-Pent)] and [PPh_4Br] at 330 nm, experimental points observed, as well as the fitted line is shown.

The final products of the consecutive reactions were analysed by ^{31}P NMR. The ^{31}P NMR data of the reaction mixture after the completion of the reactions between [$PtCl_2$(PNP-*i*-pent)] (0.04 M) and [PPh_4Br] (0.178 M) (see **Figures 11.3** and **11.4**) revealed the presence of three distinctive platinum(II) species in solution. The chemical shift of the starting complex [$PtCl_2$(PNP-*i*-Pent)] is 15.8 ppm (see §3.2.4.3) as observed in the absence of added [Br^-], which correlates well with the strong singlet observed at 15.8 ppm (see **Figure 11.4**). The four peaks at 14.9, 15.1, 15.9 and 16.1 ppm represents a doublet of doublets and are attributed to the [PtClBr(PNP-*i*-Pent)] intermediate, with the P-P coupling clearly observed as a result of the non-symmetrical nature of the complex ($J_{P\text{-}P}$ = 39.1 Hz). The [$PtBr_2$(PNP-*i*-Pent)] product is also observed at 15.2 ppm.

The presence of the final product, [$PtBr_2$(PNP-*i*-Pent)], is further established by the presence of the two peaks (doublet) at 8.5 and 21.7 ppm (see **Figure 11.3**) induced by the Pt-P coupling (J_{Pt-P} = 3194 Hz). The slightly larger peak at 9.1 ppm is one of the peaks of the doublet for the [$PtCl_2$(PNP-*i*-Pent)] starting complex, with the second peak possibly being obscured by the peaks of the [PPh_4Br] (δ 22.7 ppm). The Pt-P coupling constant can however be determined as J_{Pt-P} = 3243 Hz, which correlates well to the corresponding value of [$PtCl_2$(PNP-i-Pent)] as reported in Chapter 3 (J_{Pt-P} =3240.0 Hz).

The existence of these complexes in solution long after the second rection is complete (time for second reaction is approximately 2 days , spectrum was collected after 7 days) clearly indicates the presence of an equilibrium of [$PtCl_2$(PNP-*i*-Pent)], [PtClBr(PNP-*i*-Pent)] and [$PtBr_2$(PNP-*i*-Pent)] in solution.

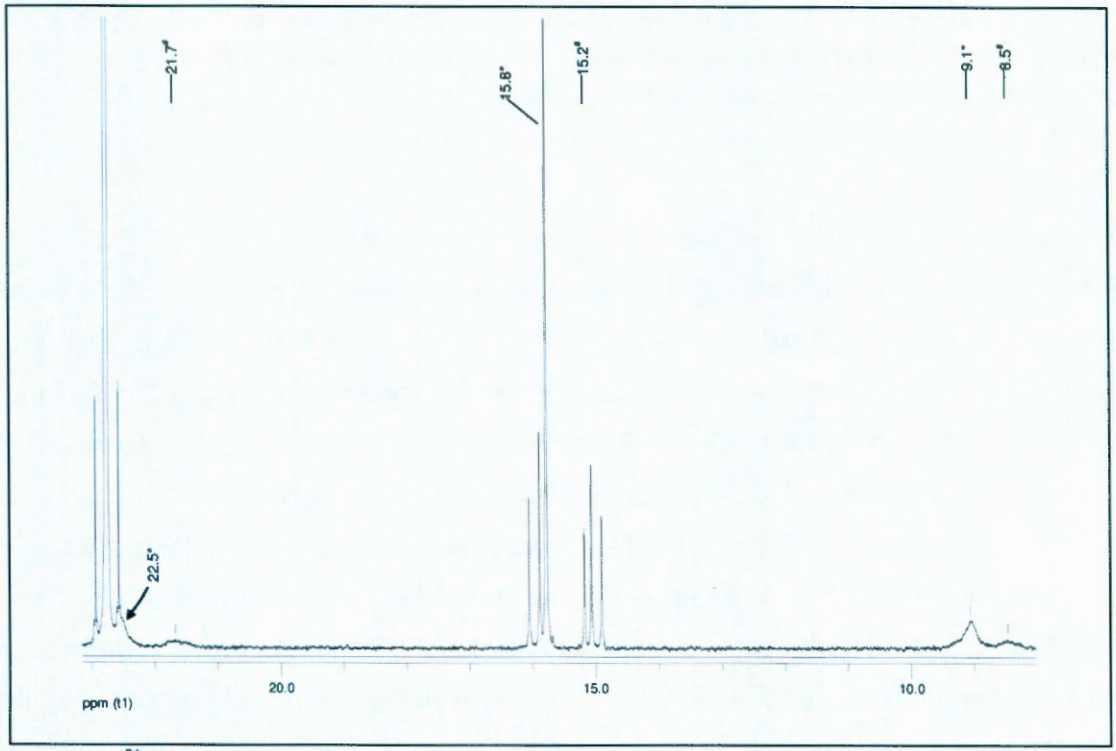

Figure 11.3: ^{31}P NMR of the reaction mixture after the completion of both substitution reactions between [$PtCl_2$(PNP-*i*-pent)] and PPh_4Br in 1,2-dichloroethane and $CDCl_3$. [$PtCl_2$(PNP-*i*-Pent)] = 4.0 x 10^{-2} M, [PPh_4Br] = 0.178 M at 25 °C (* denotes the peaks for [$PtCl_2$(PNP-*i*-Pent)], # denotes the peaks for [PtBr(PNP-*i*-Pent)]).

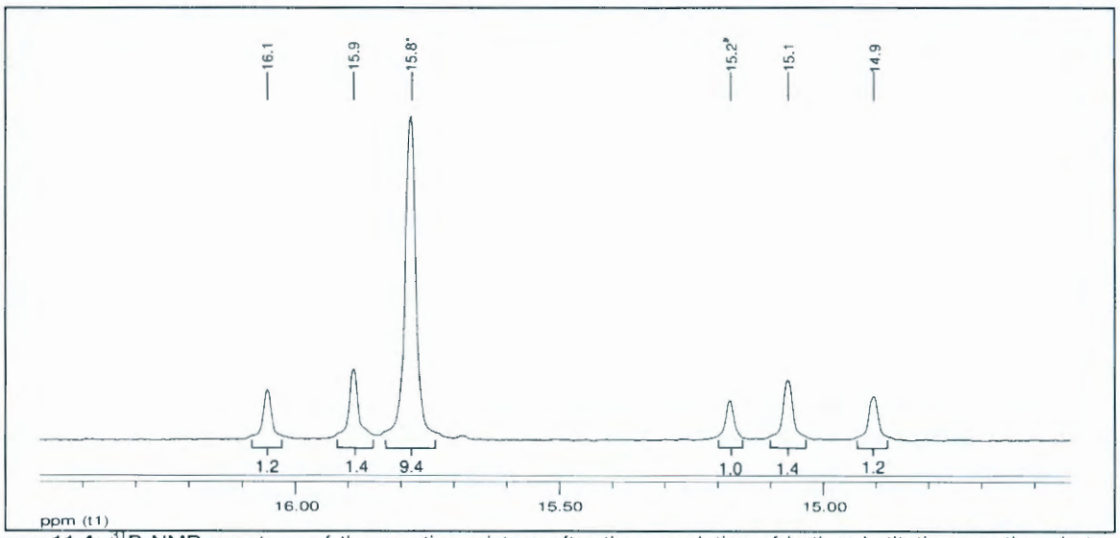

Figure 11.4: ^{31}P NMR spectrum of the reaction mixture after the completion of both substitution reactions between $[PtCl_2(PNP\text{-}i\text{-}pent)]$ and PPh_4Br in dichloroethane and $CDCl_3$. $[PtCl_2(PNP\text{-}i\text{-}Pent)] = 4.0 \times 10^{-2}$ M, $[PPh_4Br] = 0.178$ M at 25 °C (* denotes the peak for $[PtCl_2(PNP\text{-}i\text{-}Pent)]$, # denotes the peak for $[PtBr(PNP\text{-}i\text{-}Pent)]$).

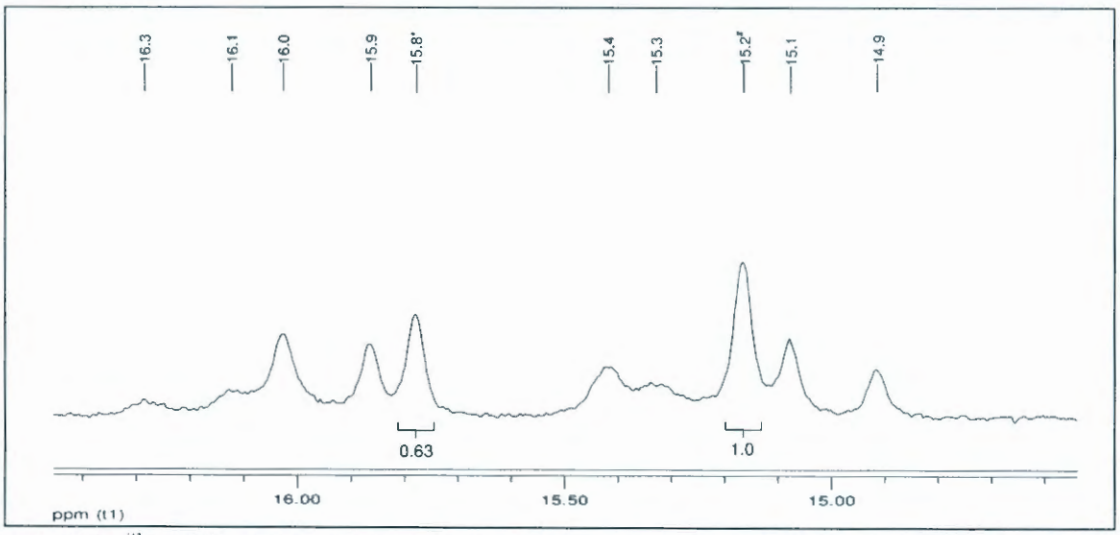

Figure 11.5: ^{31}P NMR of the reaction mixture after the completion of both substitution reactions between $[PtCl_2(PNP\text{-}i\text{-}pent)]$ and PPh_4Br in dichloroethane and $CDCl_3$. $[PtCl_2(PNP\text{-}i\text{-}Pent)] = 4.0 \times 10^{-2}$ M, $[PPh_4Br] = 0.40$ M at 25 °C (* denotes the peak for $[PtCl_2(PNP\text{-}i\text{-}Pent)]$, # denotes the peak for $[PtBr(PNP\text{-}i\text{-}Pent)]$).

$[Br^-]$ (as PPh_4Br] of a higher concentration was added to react with $[PtCl_2(PNP\text{-}i\text{-}Pent)]$ in order to further establish the presence of an equilibrium reaction species. The ^{31}P

NMR data of the reaction mixture after the completion of the reactions between [$PtCl_2$(PNP-*i*-pent)] (0.04 M) and [PPh_4Br] (0.40 M) (i.e. much higher [Br^-] however showed the presence of additional phosphorous-containing species (see **Figure 11.5,** peaks at 16.3, 16.1, 15.4 and 15.3 ppm), which could not be identified. It was consequently decided to only follow reactions up to 0.02 M of [PPh_4Br] with 2.5 x 10^{-4} M [$PtCl_2$(PNP-*i*-Pent)] for the kinetic study where there were clearly only the intermediate ([PtClBr(PNP-*i*-Pent)]) and final product ([$PtBr_2$(PNP-*i*-Pent)]) formed (see §11.4). Despite the presence of the additional species the extra [PPhBr] added to the reaction mixture did provide further evidence that equilibra are present, with an increase of the [$PtBr_2$(PNP-*i*-Pent)]: [$PtCl_2$(PNP-*i*-Pent)] ratio of 1.0:0.63 (from integration values for the different species, see **Figure 11.5**) in comparison to the corresponding ratio obtained from the spectrum in **Figure 11.4** which is 1:9.4.

The equilibrium constants for the two consecutive equilibria was calculated for the reactions between 0.178 M of [PPh_4Br] with 0.04 M [$PtCl_2$(PNP-*i*-Pent)] from the ^{31}P NMR data (see **Figure 11.4**). The concentrations for the different species in solution was calculated using the relative integrals of the compounds and the known concentration of [$PtCl_2$(PNP-*i*-Pent)] (0.04 M) which was added. The equilibrium constants were calculated for the first and second reaction (second **Scheme 11.2**) using **Equations 11.2** and **11.3** respectively.

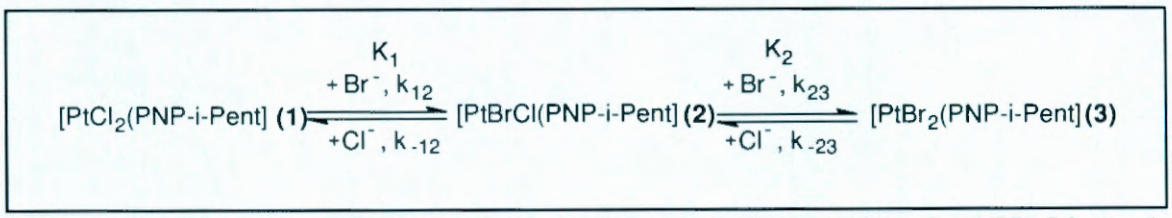

Scheme 11.2: Schematic view of the two consecutive reactions between [$PtCl_2$(PNP-i-Pent)] and [PPh_4Br] according to the ^{31}P NMR data.

$$K_1 = \frac{[2][Cl]}{[1][Br]} \qquad (11.2)$$

and

$$K_2 = \frac{[3][Cl]}{[2][Br]} \qquad (11.3)$$

In Equation 11.1 and 11.2 [Cl^-] and [Br^-] represent the equilibrium concentration of the halide species, with [1], [2] and [3] the equilibrium concentration of the [$PtCl_2$(PNP-*i*-Pent)], [PtBrCl(PNP-*i*-Pent)] and [$PtBr_2$(PNP-*i*-Pent)] complexes respectively.

$K_{1(NMR)}$ was calculated as 0.06, $K_{2(NMR)}$ as 0.02 and the overall equilibrium constant ($K_{(NMR)Total}$) was calculated as 0.001.

The equilibrium constants for the reactions between [$PtCl_2$(PNP-*i*-Pent)] and Br^- ions were also determined spectrophotometrically at 15, 25, 30 and 40 °C (see §11.4 for the data used) using **Equation 11.4** (see Appendix D).

$$\Delta A = \frac{A_0 + A_f[Br^-]K}{[Cl^-] + K[Br^-]} \qquad (11.4)$$

ΔA is the absorbance difference ($|A_f - A_0|$) at a given [Br^-], K is the equilibrium constant, A_0 and A_f are the absorbance of [$PtCl_2$(PNP-*i*-Pent)] and [PtClBr(PNP-*i*-Pent)] respectively. The absorbance *versus* [Br^-] data were fitted to **Equation 11.1** using a least-squares program (Scientist®) to determine equilibrium constants for the two consecutive reactions, see **Figures 11.6** and **11.7** for an example fit for the first and second reaction respectively. See **Table 11.1** for the equilibrium constant values calculated for the two reactions at different temperatures.

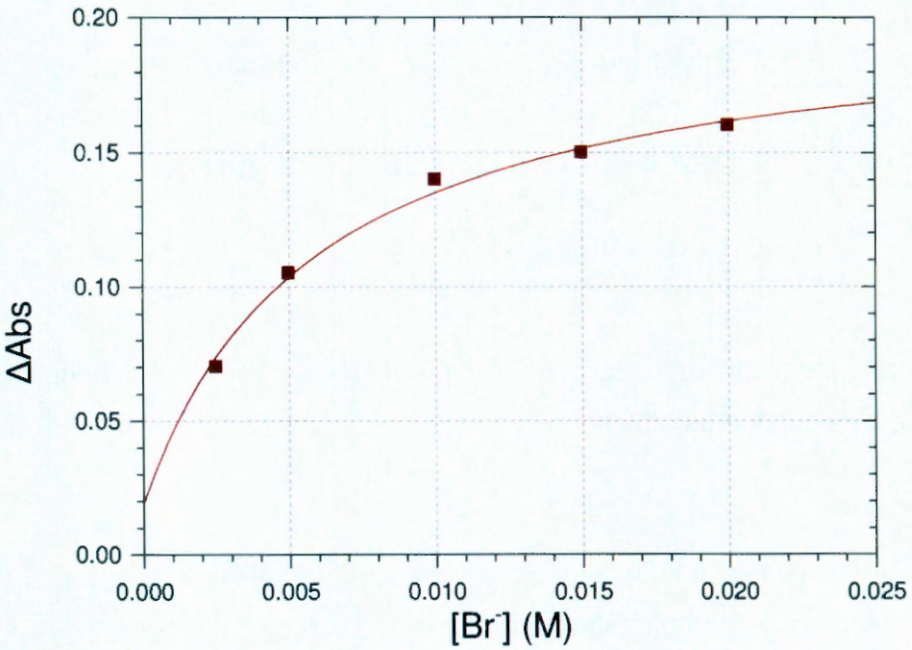

Figure 11.6: Graph of the Scientist fit of [Br^-] vs. ΔAbs (change in absorbance) for the first reaction between [$PtCl_2$(PNP-i-Pent)] and PPh_4Br in 1,2-dichloroethane, i.e. the formation of the [PtBrCl(PNP-*i*-Pent)] complex. λ = 330 nm, 15 °C, [$PtCl_2$(PNP-i-Pent)] = 2.5 x 10^{-4} M.

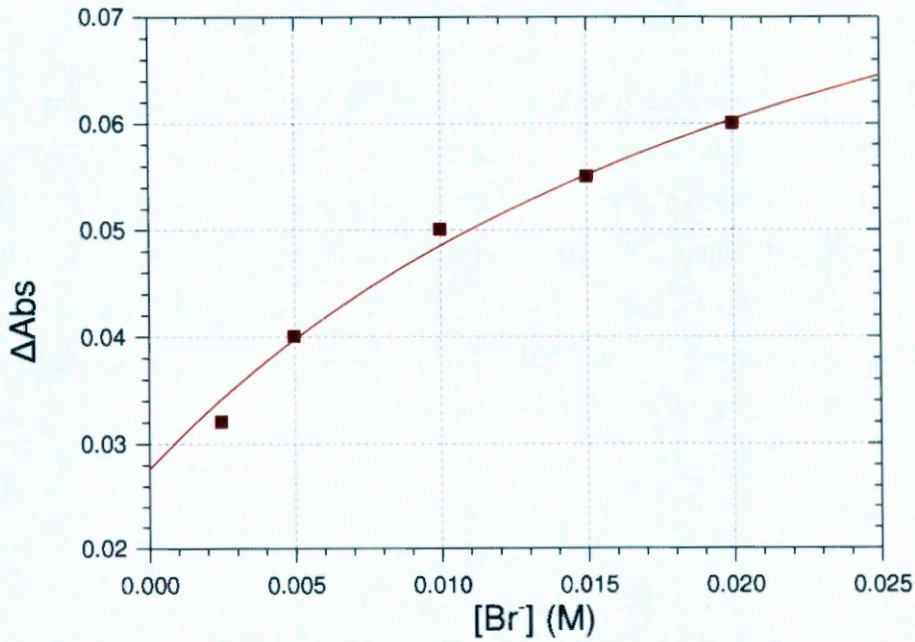

Figure 11.7: Graph of the Scientist fit of [Br^-] vs. ΔAbs (change in absorbance) for the second reaction between [$PtCl_2$(PNP-i-Pent)] and PPh_4Br in 1,2-dichloroethane, i.e. formation of the final product, [$PtBr_2$(PNP-*i*-Pent)]. λ = 330 nm, 30 °C, [$PtCl_2$(PNP-i-Pent)] = 2.5 x 10^{-4} M.

Table 11.1: The equilibrium constants determined spectrophotometrically and calculated for the first and second reaction between $[PtCl_2(PNP\text{-}i\text{-}Pent)]$ and PPh_4Br at various temperatures.

Temperature (°C)	$K_1^{\#}$	$K_2^{\#}$
15.0	0.42(5)	0.10(4)
25.0	0.37(5)	0.1(1)
30.0	0.37(5)	0.09(4)
40.0	0.42(8)	0.10(4)

$^{\#}$Spetophotometrically determined

The average $K_1^{\#}$ ($K_1^{\#}{}_{average}$) value was calculated as 0.4(1) M^{-1} and the average $K_2^{\#}$ ($K_2^{\#}{}_{average}$) was calculated as 0.1(1) M^{-1}. The total equilibrium constant for both reactions ($K_{12}^{\#}$) as 0.04(4) M^{-1} (calculated from the $K_1^{\#}{}_{average}$ and $K_2^{\#}{}_{average}$ values).

Table 11.2: Summary of the equilibrium constants obtained through the use of ^{31}P NMR and spectophotometrically.

	$K_{first\ reaction}$	$K_{second\ reaction}$	K_{Total}
^{31}P NMR	0.04	0.03	0.001
Spectophotometrically[a]	0.39(5)	0.1(1)	0.04(4)

a) The average equilibrium constant values are reported.

Reaction rate law for the first reaction, i.e. the formation of the [PtBrCl(PNP-i-Pent)] complex.

As stated previously in §11.1 these type of complexes typically include a solvent assisted pathway (k_{14}) (see **Scheme 11.3**).

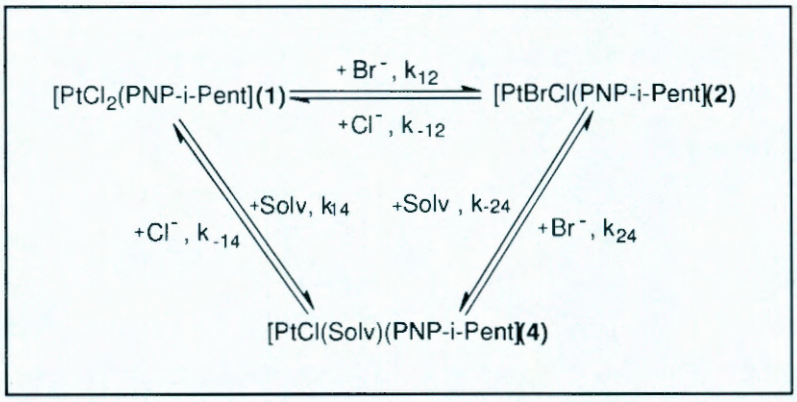

Scheme 11.3: Schematic view of the reaction mechanism for the first reaction between [$PtCl_2$(PNP-*i*-Pent)] and [PPh_4Br] with the solvent assisted pathway included.

By incorporating the reversibility in the equilibria, the expression for the *pseudo* first-order rate constant for the first reaction can therefore be deduced as give in **Equation 11.5** (see Appendix D for complete derivation):

$$k_{obs} = k_{12}[Br^-] + k_{-12}[Cl^-] + \frac{k_{-24}k_{-14}[Cl^-]+k_{24}k_{14}[Br^-]}{k_{-24}[Cl^-]+k_{-14}[Br^-]} \qquad (11.5)$$

The reactions were performed under *pseudo* first-order conditions and the [Cl^-] was kept constant.

The graph of k_{obs} *vs.* [Br^-] (see §11.4) at various temperatures yielded straight lines with non-zero intercepts. The non-zero intercept can be attributed to a combination of the contribution by the solvent assisted path-way (see **Scheme 11.3**) and the equilibrium (it has already been established that an equilibrium is present, see above) or there is no solvent assisted pathway and the intercept only represents the equilibrium contribution.

The equilibrium constants determined from the ^{31}P NMR data ($K_{1(NMR)}$) and spectrophotometrically ($K_1^{\#}{}_{average}$) for the first substitution reaction were determined and correlated fairly well. If a solvent assisted pathway was present it would be expected that the intercept values of the graphs of k_{obs} *vs.* [Br^-] would be much larger than seen in §11.4, **Figure 11.8**. The solvent which was used, 1,2-dichloroethane was also chosen

for this study as it is a non-coordinative solvent.[8] Due to all this evidence it is concluded that a solvent assisted pathway is negligible for the reaction and **Equation11.5** can be simplified to **Equation 11.6**.

$$k_{obs} = k_{12}[Br^-] + k_{-12}[Cl^-] \quad (11.6)$$

Reaction rate law for the second reaction, i.e. formation of the [$PtBr_2$(PNP-i-Pent)] complex

The reaction mechanism, including the solvent assisted pathway (k_{25}), for the second reaction observed between [$PtCl_2$(PNP-*i*-Pent)] and [PPh_4Br] is presented in (see **Scheme 11.4**)

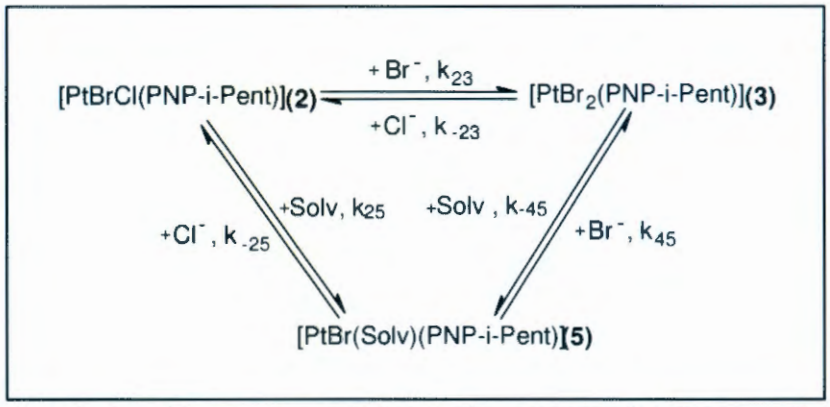

Scheme 11.4: Schematic view of the reaction mechanism for the second reaction between [$PtCl_2$(PNP-i-Pent)] and [PPh_4Br] with the solvent assisted pathway included.

By incorporating the reversibility and the equilibria, the expression for the *pseudo* first-order rate constant for the second reaction can therefore be deduced as give in **Equation 11.7** (see Appendix D for complete derivation):

$$k_{obs2} = k_{24}[Br^-] + k_{-24}[Cl^-] + \frac{k_{-25}k_{-45}[Cl^-]+k_{25}k_{45}[Br^-]}{k_{-25}[Cl^-]+k_{-45}[Br^-]} \quad (11.7)$$

[8] Weiner, H. and Finke, R.G., *J. Am. Chem. Soc.*, **1999**, *121*, 9831.

Equation 11.7 can be simplified to **Equation 11.8** for the same reasons as stated for the first reaction, with $K_2^{\#}{}_{average}$ value that compares fairly well with $K_{2(NMR)}$ (from ^{31}P NMR data) and the non-zero intercepts of the graphs of k_{obs} *vs.* [Br^-] for the second reaction (see §11.4, **Figure 11.9**) which are not large enough to incorporate a solvent assisted pathway and only represents the equilibrium contribution.

$$k_{obs} = k_{23}[Br^-] + k_{-23}[Cl^-] \qquad (11.8)$$

11.4 Results and discussion

Formation of the [PtBrCl(PNP-i-Pent)] complex

A graph of k_{obs} vs. [Br^-] (as defined by the rate expession in **Equation 11.5**) at various temperatures is presented in **Figure 11.8**. The k_{12} and k_{-12} values are reported in **Table 11.3**.

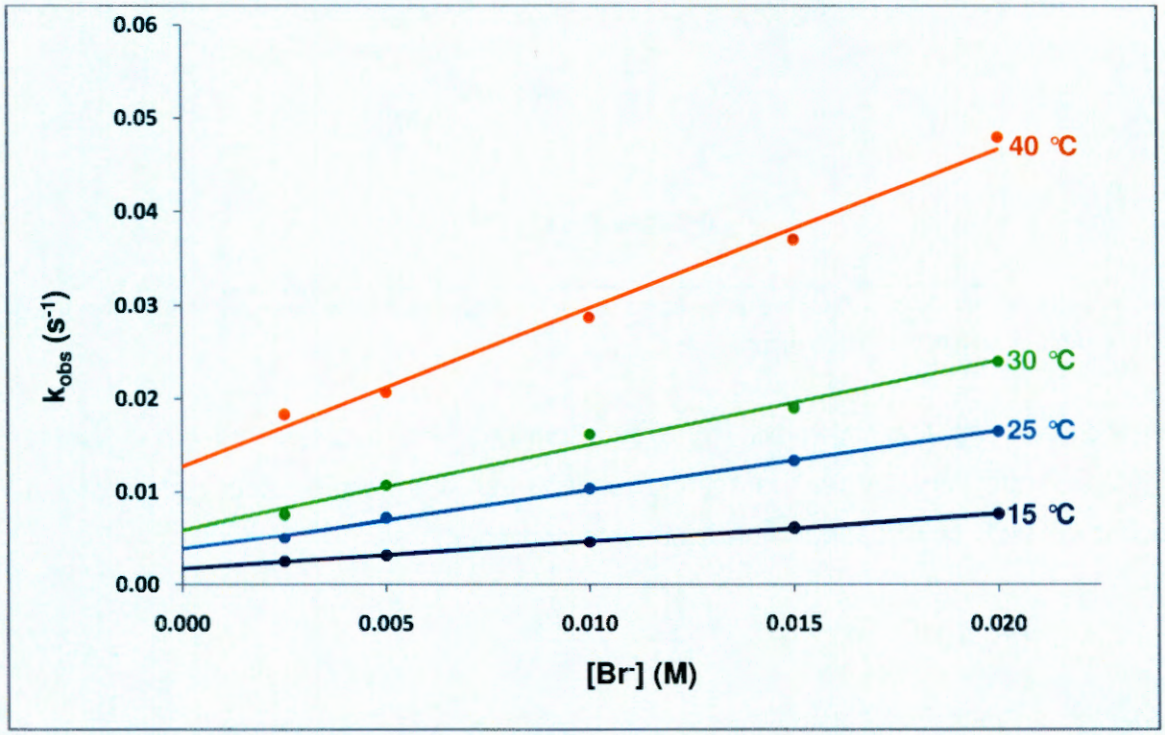

Figure 11.8: Temperature and [PPh_4Br] dependence of the pseudo first order rate constant for the first reaction between [$PtCl_4$(PNP-i-Pent)] and PPh_4Br in 1,2-dichloroethane (λ = 330 nm) [$PtCl_2$(PNP-*i*-Pent)] = 2.5 x 10^{-4} M and [PPh_4Cl] = 2.5 x 10^{-3} M. (Appendix D, Table D1)

Table 11.3: UV/Vis kinetic data obtained from **Figure 11.8** for the first substitution reaction of [$PtCl_2$(PNP-*i*-Pent)] with PPh_4Br at different temperatures in 1,2-dichloroethane.

Temperature (°C)	k_{12} (M^1s^{-1})	Intercept ($k_{-12}[Cl^-]$)	k_{-12} ($M^{-1}s^{-1}$)	K_1[a]
15.0	0.300(5)	0.0017(2)	0.68(5)	0.44(3)
25.0	0.64(2)	0.004(2)	1.6(8)	0.4(2)
30.0	0.90(6)	0.0060(7)	2.4(3)	0.38(4)
40.0	1.7(1)	0.013(1)	5.2(5)	0.3(3)

a) Kinetically determined $K_1 = k_{12}/k_{-12}$.

The average equilibrium constant ($K_{1average}$) was calculated as 0.4(2).

The second substitution reaction, i.e. formation of [$PtBr_2$(PNP-i-Pent)]

A graph of k_{obs} vs. [Br^-] (according to the rate law in **Equation 11.7**) at various temperatures is presented in **Figure 11.9**. The k_{23} and k_{-23} values are reported in **Table 11.4**.

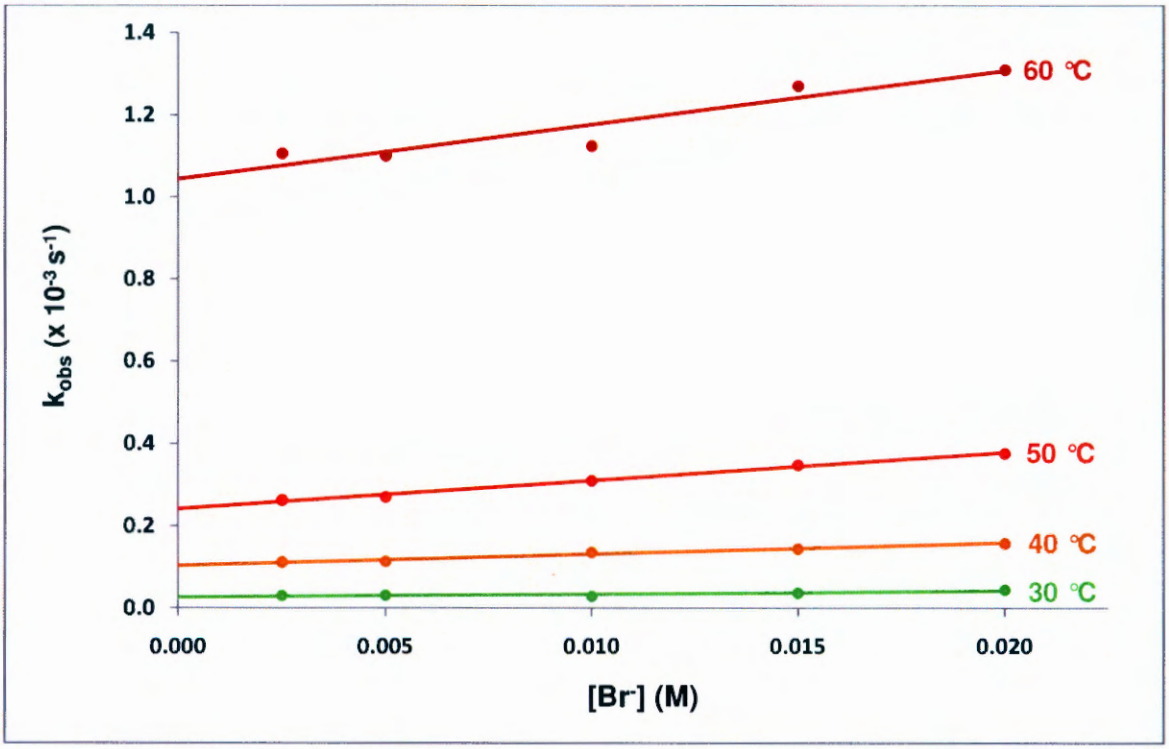

Figure 11.9: Temperature and [PPh_4Br] dependence of the pseudo first order rate constant for the second reaction between [$PtCl_4$(PNP-i-Pent)] and PPh_4Br in 1,2-dichloroethane (λ = 330 nm) [$PtCl_2$(PNP-*i*-Pent)] = 2.5 x 10^{-4} M and [PPh_4Cl] = 2.5 x 10^{-3} M. (Appendix D, Table D2)

Table 11.4: UV/Vis kinetic data obtained from **Figure 11.9** for the second substitution reaction of [$PtCl_2$(PNP-*i*-Pent)] with PPh_4Br at different temperatures in 1,2-dichloroethane.

Temperature (°C)	k_{23} (x 10^{-3} M^1s^{-1})	Intercept (x 10^{-3}) ($k_{-23}[Cl^-]$)	k_{-23} ($M^{-1}s^{-1}$)	K_2[a]
30.0	0.8(3)	0.025(3)	0.010(1)	0.07(3)
40.0	2.8(3)	0.10(3)	0.04(1)	0.07(2)
50.0	0.68(3)	0.241(4)	0.096(2)	0.071(3)
60.0	1.3(3)	1.10(5)	0.42(2)	0.031(7)

a) Kinetically determined $K_1 = k_{23}/k_{-23}$.

The average equilibrium constant (K_2) was calculated as 006(1).

The total equilibrium constant for both substitution reactions (K_{Total}) was calculated as 0.02(1) (from K_1 and K_2).

Table 11.5: Summary of the equilibrium constants obtained through the use of various methods (^{31}P NMR, spectrophotometrically and kinetically).

	^{31}P NMR[a]	Spectophotometrically[b]	Kinetically[c]
K_1	0.040	0.39(5)	0.4(2)
K_2	0.030	0.1(1)	0.06(1)
K_{Total}	0.001	0.04(4)	0.02(1)

a) See Table 11.2
b) See Table 11.2
c) See Tables 11.3 and 11.4
K_1 = equilibrium constant for the first reaction, i.e. formation of [PtBrCl(PNP-*i*-Pent)].
K_2 = equilibrium constant for the second reaction, i.e. formation of [$PtBr_2$(PNP-*i*-Pent)].
$K_{Total} = K_1 \times K_2$

The correlation of the equilibrium constants obtained through the use of different methods compare fairly well within experimental error. This is further evidence that a solvent assisted pathway is not present during these consecutive reactions.

Activation parameters

The activation entropy ($\Delta S^{\neq}$) and the activation enthalpy ($\Delta H^{\neq}$) were determined for both reactions from the temperature study by using the Eyring equation (**Equation 11.9**).

$$ln\frac{k_1}{T} = \ln\frac{k_B}{h} + \frac{\Delta S}{R} - \frac{\Delta H}{RT} \qquad (11.9)$$

Where T = temperature (K), R = 8,314 $J.mol^{-1}.K^{-1}$ (gas constant), k_B = 1.38 x 10^{-23} $J.K^{-1}$ (Boltzmann's constant), h = 6.63 x 10^{-34} J.s (Plank's constant) and $k_1 = k_{12}$ for the first substitution reaction and $k_1 = k_{23}$ for the second substitution reaction.

The Gibbs free energy of activation ($\Delta G^{\neq}$) for the reaction was calculated by using **Equation 11.10**:

$$\Delta G^{\neq} = \Delta H^{\neq} - T\Delta S^{\neq} \qquad (11.10)$$

The obtained and fitted results for both substitution reactions are illustrated in **Figure 11.10** and **11.11** and summarized in **Table 11.5**.

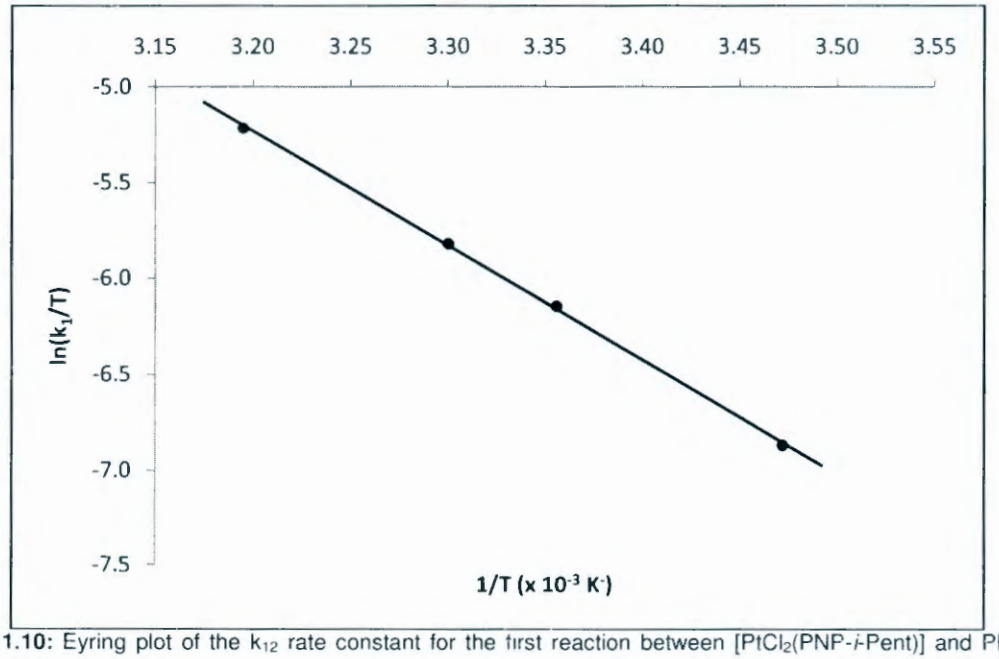

Figure 11.10: Eyring plot of the k_{12} rate constant for the first reaction between [$PtCl_2$(PNP-*i*-Pent)] and PPh_4Br in 1,2-dichloroethane. (Appendix D, Table D3)

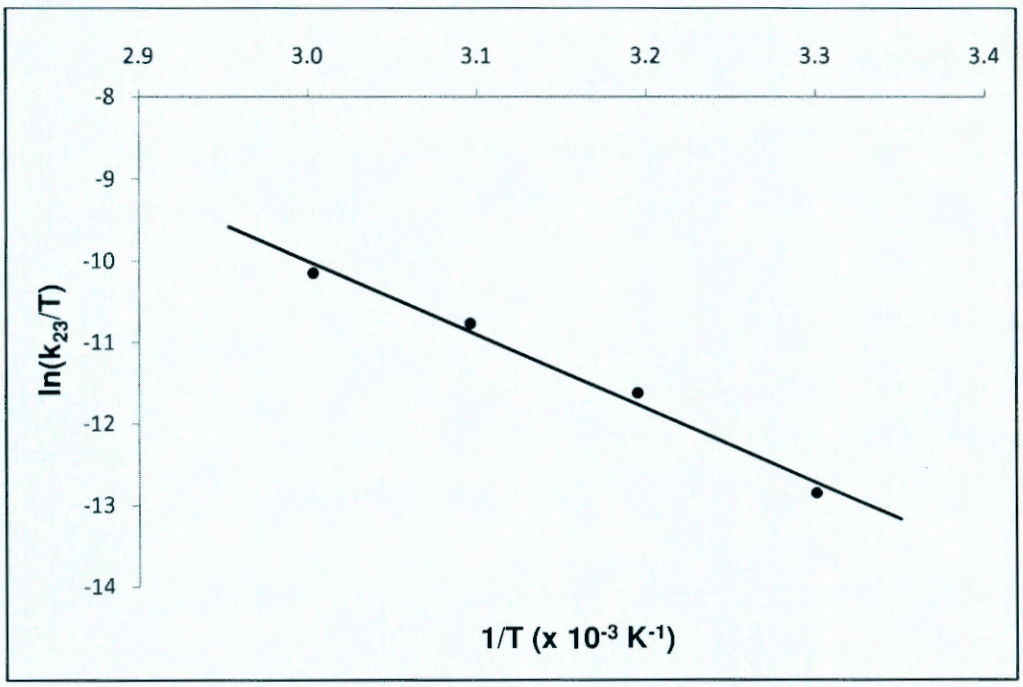

Figure 11.11: Eyring plot of the k_{23} rate constant for the second reaction between [$PtCl_2$(PNP-*i*-Pent)] and PPh_4Br in 1,2-dichloroethane. (Appendix D, Table D4)

Table 11.5: Kinetic data obtained from the Eyring equation (see **Equation 11.9**, **Figures 11.5** and **11.6**).

Reaction	$\Delta H^{\neq}$ (kJ.mol^{-1})	$\Delta S^{\neq}$ (J.K^{-1}.mol^{-1})	$\Delta G^{\neq}$ (30 °C) (kJ.mol^{-1})
First reaction	49.5(8)	-82(3)	74.4
Second reaction	75(6)	-54(20)	91.4

The activation parameters for the first reaction between [$PtCl_2$(PNP-*i*-Pent)] with Br^- is typical of an associatively activated process, which is characterised by a low enthalpy and large negative entropy (see **Table 11.3**). The activation parameters indicate that very little bond breaking has occurred in the transition state.

The kinetic measurements of the second substitution reaction also indicate the expected associative mode of activation as supported by a large negative entropy of activation and a low enthalpy (see **Table 11.3**).

11.4 Conclusion

The kinetics of the two consecutive reactions between [$PtCl_2$(PNP-*i*-Pent)] and Br^- were successfully investigated. Two consecutive reactions were observed and analysed separately, in which the two chlorido ligands of the staring platinum(II) complex is substituted with two Br^-, forming [PtBrCl(PNP-*i*-Pent)] and [$PtBr_2$(PNP-*i*-Pent)] for the first and second reaction respectively. Both these reactions proved to be reversible through the use of ^{31}P NMR. Three Pt(II) species in solution were identified after the completion of the two reactions, namely [($PtCl_2$(PNP-*i*-Pent)], [(PtBrCl(PNP-*i*-Pent)] and [($PtBr_2$(PNP-*i*-Pent)]. The presence of the equilibria were further established by spectrophotometric and kinetic methods. No solvent pathway was observed for either of these reactions. An associative mechanism was identified for both reactions which indicate the formation of a 5-coordinate intermediate species.

It is interesting to note that these equilibria were identified for these relatively simple substitution processes, of which the steric bulk of the PNP-ligands (obviously not the only contributing factor) is a prime contributor. This emphasizes the fact that subtle changes in steric demand of the PNP ligand should have significant influence on the coordination and subsequent insertion process as operative in the selective oligomerisation reactions.

12 Evaluation of study

In this chapter...

A summary of the success, results obtained and scientific importance of this study as well as a discussion of some future possibilities are discussed.

1.1 Introduction

One of the original motivations for this study was to gain further insight into the chemistry and properties of the PNP ligands used as part of the catalyst system in homogeneous catalysis and evaluate any correlations between the solid state structural parameters and the ethylene oligomerisation selectivity of these ligands (when complexed to Cr(III)). The findings of this investigation are discussed below.

1.2 Evaluation

Single crystal X-ray crystallographic study

It was stated in literature that the steric bulk of the nitrogen-bonded alkyl group of the PNP ligands has a significant effect on the catalytic selectivity, especially towards the formation of 1-C_6 and 1-C_8. The focus of this study was therefore to investigate the structural effects when the nitrogen-coordinated alkyl substituents are systematically varied for a range of diphosphinoamine ligands, which have varying catalytic activity and selectivity (when complexed to chromium(III). This lead to a successful synthesis and characterization of a range of PNP ligands which have varying nitrogen-coordinated moieties. The solid state study of selected free ligands revealed that there is a correlation between the steric bulk and the P-N-P angle, with a decrease of the angle as the steric bulk increases.

The coordination mode of these ligands were also investigated and a range of metal-PNP complexes (metal = Pt(II), Pd(II) and Cr(III)) was consequently synthesized and characterized. The single crystal X-ray crystallographic studies on these complexes revealed that the bond angles and bond lengths of the coordination polyhedron are not significantly affected by the different nitrogen-coordinated alkyl moieties. The most noticeable differences for the various compounds were however that the orientations of the phenyl rings were affected when the steric bulk of the alkyl group is increased. It appears that a "basket-like" arrangement (as defined in Chapter 5) is adopted for ligands with a relatively sterically bulky nitrogen alkyl substituent and a "fan-like" arrangement for the less bulky moieties.

Computational chemistry

A number of possible isomers were identified for each of the free PNP ligands (of which crystal structures were also obtained) by theoretical calculations (DFT calculations). The isomer with the lowest relative energy was identified (and re-optimised at a higher level of theory) for each ligand and was compared with the crystallographic data of the corresponding compound. A good correlation was observed between the conformations adopted in solid state and the predicted conformations, with comparable bond lengths and angles. Slight variations in the orientation of the phenyl rings were however observed between the optimized lowest energy isomer and the crystal structure due to relatively large degrees of freedom of the phenyl rings these free ligands.

The results from the theoretical study (DFT calculations) of the metal-coordinated PNP compounds (metal = Pt(II), Pd(II) and Cr(III)) were successfully compared with the crystallographic data of the corresponding compounds. The optimized structures revealed that the theoretically calculated structures had similar phenyl ring arrangements ("basket" or "fan-like" as defined in Chapter 5) than the corresponding compounds, even though no intermolecular interactions were considered in the

theoretical calculations. It was consequently concluded that the arrangement of the phenyl rings, is largely influenced by the steric bulk of the alkyl substituents and thus of the overall steric bulk, introducing a knock-on effect in the ligands.

Catalytic selectivity vs. crystallographic data

A steric parameter was defined (Effective Tolman-based N-substituent steric effect ($\theta_{N\text{-}sub}$)) in which the steric bulk of the nitrogen-coordinated alkyl substituent is quantified. A comparison between $\theta_{N\text{-}sub}$ for various diphosphinoamine ligands (free and metal-coordinated) and the catalytic selectivity (for 1-C_6 and 1-C_8) revealed a relatively good correlation with the catalytic selectivity increasing (1-hexene and 1-octene) as $\theta_{N\text{-}sub}$ for the varying ligands increased. It was also possible to compare the $\theta_{N\text{-}sub}^*$ (from theoretically calculated structures) with the catalytic selectivity and a similar trend was observed for the optimized structures than the solid state structures ($\theta_{N\text{-}sub}$).

Substitution kinetics

The kinetics of the substitution of two chlorido ligands from the [$PtCl_2$(PNP-*i*-Pent)] complex with Br^- was successfully investigated. Two consecutive reversible reactions were observed and analysed separately. Three platinum(II) species [($PtCl_2$(PNP-*i*-Pent)], [(PtBrCl(PNP-*i*-Pent)] and [($PtBr_2$(PNP-*i*-Pent)], are present in equilibrium after the completion of the two reactions and was characterized with ^{31}P NMR. The fact that these equilibria were identified for even these simple substitution processes, of which the steric bulk of the PNP-ligands (obviously not the only contributing factor) is a prime contributor, underlines the fact that subtle changes in steric demand of the PNP ligand should have significant influence on coordination and the subsequent insertion process as operative in the oligomerisation reations. An

associative mechanism was also identified for both reactions, indicating the formation of 5-coordinate intermediate species.

1.3 Future work

Perform even more detailed theoretical calculations for other variations of PNP-ligands, determine the $\theta_{N\text{-}sub}$* and then synthesize the corresponding ligands. Ethylene oligomerisation catalysis, using these novel ligands (together with Cr(III)), should be executed to determine to what extent the catalytic behavior can be predicted.

Define a steric parameter which will accurately determine the space occupied by the phosphorous coordinated phenyl rings of the PNP ligands (when metal coordinated) and investigate any further correlations between the catalytic selectivity (when complexed with Cr(III)) and this newly defined parameter.

The substitution kinetic study should be expanded by investigating additional crystallographically characterized [$PtCl_2$(PNP-alkyl)] complexes. It could present the opportunity to investigate the effect of the different PNP ligands on the solution and kinetic behaviour of these ligands when coordinated and perhaps gain insight into the catalytic behaviour of these PNP ligands (when complexed with Cr(III)).

Isolation of intermediates in the catalytic cycle, e.g. metallocycles, and study the solution properties.

Appendix A

Table A1: Atomic coordinates (x 10^4) and equivalent isotropic displacement parameters ($Å^2$ x 10^3) for PNP-Ethyl U(eq) is defined as one third of the trace of the orthogonalize Uij tensor.

	x	y	z	U(eq)
N(1)	3510(1)	2123(1)	7148(1)	16(1)
P(1)	4131(1)	933(1)	7242(1)	16(1)
P(2)	2941(1)	2632(1)	6267(1)	15(1)
C(1)	3484(2)	2824(1)	7827(1)	18(1)
C(2)	2014(2)	3060(1)	8084(1)	25(1)
C(11)	3209(2)	409(1)	8092(1)	17(1)
C(12)	2204(2)	-319(1)	7933(1)	20(1)
C(13)	1434(2)	-742(1)	8534(1)	23(1)
C(14)	1660(2)	-433(1)	9309(1)	23(1)
C(15)	2670(2)	280(1)	9482(1)	23(1)
C(16)	3449(2)	696(1)	8883(1)	21(1)
C(21)	5879(2)	1123(1)	7692(1)	17(1)
C(22)	6509(2)	357(1)	8139(1)	19(1)
C(23)	7876(2)	430(1)	8419(1)	20(1)
C(24)	8647(2)	1279(1)	8274(1)	22(1)
C(25)	8044(2)	2046(1)	7832(1)	22(1)
C(26)	6682(2)	1965(1)	7536(1)	20(1)
C(31)	1370(2)	1937(1)	5976(1)	17(1)
C(32)	795(2)	2090(1)	5214(1)	22(1)
C(33)	-414(2)	1606(1)	4969(1)	28(1)
C(34)	1098(2)	977(1)	5480(1)	28(1)
C(35)	-562(2)	840(1)	6240(1)	25(1)
C(36)	659(2)	1317(1)	6487(1)	20(1)
C(41)	4163(2)	2188(1)	5530(1)	16(1)
C(42)	5294(2)	2801(1)	5371(1)	21(1)
C(43)	6214(2)	2552(1)	4780(1)	25(1)
C(44)	6006(2)	1691(1)	4345(1)	23(1)
C(45)	4893(2)	1070(1)	4498(1)	20(1)
C(46)	3976(2)	1318(1)	5090(1)	18(1)

Table A2. Bond lengths [Å] and angles [°] for PNP-Ethyl.

Atoms	Bond length (Å)	Atoms	Bond angle (°)
N(1)-C(1)	1.4856(18)	C(1)-N(1)-P(1)	122.29(10)
N(1)-P(1)	1.7127(14)	C(1)-N(1)-P(2)	114.00(10)
N(1)-P(2)	1.7130(13)	P(1)-N(1)-P(2)	123.65(7)
P(1)-C(21)	1.8369(18)	N(1)-P(1)-C(21)	102.58(7)
P(1)-C(11)	1.8478(15)	N(1)-P(1)-C(11)	104.81(7)
P(2)-C(31)	1.8255(17)	C(21)-P(1)-C(11)	100.36(7)

P(2)-C(41)	1.8331(16)	N(1)-P(2)-C(31)	105.59(7)
C(1)-C(2)	1.518(2)	N(1)-P(2)-C(41)	105.52(7)
C(1)-H(1A)	0.99	C(31)-P(2)-C(41)	100.78(7)
C(1)-H(1B)	0.99	N(1)-C(1)-C(2)	112.95(13)
C(2)-H(2A)	0.98	N(1)-C(1)-H(1A)	109
C(2)-H(2B)	0.98	C(2)-C(1)-H(1A)	109
C(2)-H(2C)	0.98	N(1)-C(1)-H(1B)	109
C(11)-C(12)	1.393(2)	C(2)-C(1)-H(1B)	109
C(11)-C(16)	1.403(2)	H(1A)-C(1)-H(1B)	107.8
C(12)-C(13)	1.394(2)	C(1)-C(2)-H(2A)	109.5
C(12)-H(12)	0.95	C(1)-C(2)-H(2B)	109.5
C(13)-C(14)	1.385(2)	H(2A)-C(2)-H(2B)	109.5
C(13)-H(13A)	0.95	C(1)-C(2)-H(2C)	109.5
C(14)-C(15)	1.386(2)	H(2A)-C(2)-H(2C)	109.5
C(14)-H(14)	0.95	H(2B)-C(2)-H(2C)	109.5
C(15)-C(16)	1.392(2)	C(12)-C(11)-C(16)	118.04(14)
C(15)-H(15)	0.95	C(12)-C(11)-P(1)	117.34(11)
C(16)-H(16)	0.95	C(16)-C(11)-P(1)	124.63(12)
C(21)-C(26)	1.397(2)	C(11)-C(12)-C(13)	121.46(14)
C(21)-C(22)	1.403(2)	C(11)-C(12)-H(12)	119.3
C(22)-C(23)	1.382(2)	C(13)-C(12)-H(12)	119.3
C(22)-H(22)	0.95	C(14)-C(13)-C(12)	119.74(15)
C(23)-C(24)	1.385(2)	C(14)-C(13)-H(13A)	120.1
C(23)-H(23)	0.95	C(12)-C(13)-H(13A)	120.1
C(24)-C(25)	1.388(2)	C(13)-C(14)-C(15)	119.70(14)
C(24)-H(24)	0.95	C(13)-C(14)-H(14)	120.2
C(25)-C(26)	1.387(2)	C(15)-C(14)-H(14)	120.2
C(25)-H(25)	0.95	C(14)-C(15)-C(16)	120.56(15)
C(26)-H(26)	0.95	C(14)-C(15)-H(15)	119.7
C(31)-C(36)	1.391(2)	C(16)-C(15)-H(15)	119.7
C(31)-C(32)	1.402(2)	C(15)-C(16)-C(11)	120.48(15)
C(32)-C(33)	1.380(2)	C(15)-C(16)-H(16)	119.8
C(32)-H(32)	0.95	C(11)-C(16)-H(16)	119.8
C(33)-C(34)	1.386(2)	C(26)-C(21)-C(22)	117.87(15)
C(33)-H(33)	0.95	C(26)-C(21)-P(1)	122.22(12)
C(34)-C(35)	1.382(2)	C(22)-C(21)-P(1)	119.53(12)
C(34)-H(34)	0.95	C(23)-C(22)-C(21)	121.29(15)
C(35)-C(36)	1.387(2)	C(23)-C(22)-H(22)	119.4
C(35)-H(35)	0.95	C(21)-C(22)-H(22)	119.4
C(36)-H(36)	0.95	C(22)-C(23)-C(24)	120.15(15)
C(41)-C(42)	1.393(2)	C(22)-C(23)-H(23)	119.9
C(41)-C(46)	1.394(2)	C(24)-C(23)-H(23)	119.9
C(42)-C(43)	1.391(2)	C(23)-C(24)-C(25)	119.44(16)

C(42)-H(42)	0.95	C(23)-C(24)-H(24)	120.3
C(43)-C(44)	1.384(2)	C(25)-C(24)-H(24)	120.3
C(43)-H(43)	0.95	C(26)-C(25)-C(24)	120.55(15)
C(44)-C(45)	1.383(2)	C(26)-C(25)-H(25)	119.7
C(44)-H(44)	0.95	C(24)-C(25)-H(25)	119.7
C(45)-C(46)	1.391(2)	C(25)-C(26)-C(21)	120.67(15)
C(45)-H(45)	0.95	C(25)-C(26)-H(26)	119.7
C(46)-H(46)	0.95	C(21)-C(26)-H(26)	119.7
		C(36)-C(31)-C(32)	118.21(15)
		C(36)-C(31)-P(2)	123.55(12)
		C(32)-C(31)-P(2)	118.08(12)
		C(33)-C(32)-C(31)	120.61(15)
		C(33)-C(32)-H(32)	119.7
		C(31)-C(32)-H(32)	119.7
		C(32)-C(33)-C(34)	120.51(16)
		C(32)-C(33)-H(33)	119.7
		C(34)-C(33)-H(33)	119.7
		C(35)-C(34)-C(33)	119.42(16)
		C(35)-C(34)-H(34)	120.3
		C(33)-C(34)-H(34)	120.3
		C(34)-C(35)-C(36)	120.32(15)
		C(34)-C(35)-H(35)	119.8
		C(36)-C(35)-H(35)	119.8
		C(35)-C(36)-C(31)	120.88(15)
		C(35)-C(36)-H(36)	119.6
		C(31)-C(36)-H(36)	119.6
		C(42)-C(41)-C(46)	118.76(14)
		C(42)-C(41)-P(2)	116.96(12)
		C(46)-C(41)-P(2)	124.14(12)
		C(43)-C(42)-C(41)	120.57(15)
		C(43)-C(42)-H(42)	119.7
		C(41)-C(42)-H(42)	119.7
		C(44)-C(43)-C(42)	119.90(15)
		C(44)-C(43)-H(43)	120.1
		C(42)-C(43)-H(43)	120.1
		C(45)-C(44)-C(43)	120.33(14)
		C(45)-C(44)-H(44)	119.8
		C(43)-C(44)-H(44)	119.8
		C(44)-C(45)-C(46)	119.69(15)
		C(44)-C(45)-H(45)	120.2
		C(46)-C(45)-H(45)	120.2
		C(45)-C(46)-C(41)	120.75(14)
		C(45)-C(46)-H(46)	119.6

C(41)-C(46)-H(46)	119.6

Table A3. Anisotropic displacement parameters ($A^2 \times 10^3$) for PNP-Ethyl. The anisotropic displacement factor exponent takes the form: -2 pi [$h^2 a^{*2} U11 + ... + 2 h k a^* b^* U12$]

	U11	U22	U33	U23	U13	U12
N(1)	19(1)	16(1)	11(1)	-2(1)	-1(1)	1(1)
P(1)	21(1)	15(1)	12(1)	0(1)	1(1)	0(1)
P(2)	18(1)	16(1)	12(1)	0(1)	1(1)	0(1)
C(1)	22(1)	18(1)	13(1)	-3(1)	-1(1)	0(1)
C(2)	25(1)	32(1)	19(1)	-6(1)	1(1)	5(1)
C(11)	20(1)	17(1)	15(1)	1(1)	1(1)	2(1)
C(12)	24(1)	18(1)	19(1)	-1(1)	0(1)	0(1)
C(13)	21(1)	20(1)	28(1)	1(1)	2(1)	-3(1)
C(14)	23(1)	24(1)	24(1)	5(1)	8(1)	4(1)
C(15)	29(1)	25(1)	16(1)	1(1)	5(1)	2(1)
C(16)	24(1)	21(1)	16(1)	0(1)	0(1)	-2(1)
C(21)	20(1)	19(1)	12(1)	-1(1)	4(1)	2(1)
C(22)	24(1)	17(1)	18(1)	0(1)	5(1)	1(1)
C(23)	23(1)	22(1)	16(1)	3(1)	5(1)	6(1)
C(24)	17(1)	26(1)	22(1)	0(1)	3(1)	3(1)
C(25)	20(1)	21(1)	25(1)	3(1)	7(1)	0(1)
C(26)	21(1)	20(1)	18(1)	4(1)	5(1)	4(1)
C(31)	16(1)	19(1)	15(1)	-2(1)	0(1)	3(1)
C(32)	20(1)	31(1)	16(1)	3(1)	1(1)	2(1)
C(33)	22(1)	42(1)	20(1)	-2(1)	-6(1)	2(1)
C(34)	20(1)	31(1)	32(1)	-4(1)	-4(1)	-4(1)
C(35)	22(1)	25(1)	27(1)	1(1)	2(1)	-3(1)
C(36)	18(1)	24(1)	17(1)	0(1)	-1(1)	2(1)
C(41)	17(1)	20(1)	11(1)	2(1)	-1(1)	2(1)
C(42)	19(1)	23(1)	19(1)	1(1)	-1(1)	-2(1)
C(43)	18(1)	30(1)	26(1)	5(1)	5(1)	-1(1)
C(44)	20(1)	34(1)	16(1)	6(1)	3(1)	9(1)
C(45)	24(1)	24(1)	13(1)	-1(1)	-1(1)	7(1)
C(46)	19(1)	20(1)	16(1)	2(1)	1(1)	0(1)

Table A4: Atomic coordinates ($\times 10^4$) and equivalent isotropic displacement parameters ($A^2 \times 10^3$) for PNP-Dimprop. U(eq) is defined as one third of the trace of the orthogonalized Uij tensor.

	X	Y	z	U(eq)
N(1)	7880(1)	2798(1)	2706(1)	14(1)
P(1)	7006(1)	1261(1)	2151(1)	13(1)
P(2)	6779(1)	3741(1)	3183(1)	15(1)
C(1)	9338(1)	3556(1)	2396(1)	17(1)

C(2)	10316(1)	4479(1)	3300(1)	19(1)
C(1A)	9539(13)	3412(10)	3029(9)	0(2)
C(2A)	9969(11)	4724(10)	2470(9)	0(2)
C(3)	11800(1)	5188(1)	2963(1)	24(1)
C(4)	10609(2)	3781(1)	4300(1)	24(1)
C(5)	9075(1)	4360(1)	1405(1)	19(1)
C(11)	7231(1)	1355(1)	758(1)	16(1)
C(12)	8484(1)	1131(1)	360(1)	19(1)
C(13)	8621(1)	1286(1)	-692(1)	23(1)
C(14)	7502(2)	1671(1)	1363(1)	26(1)
C(15)	6245(2)	1889(1)	-980(1)	27(1)
C(16)	6097(1)	1723(1)	69(1)	22(1)
C(21)	8260(1)	172(1)	2565(1)	16(1)
C(22)	7890(1)	-1091(1)	2085(1)	22(1)
C(23)	8651(2)	-2040(1)	2445(1)	28(1)
C(24)	9823(2)	-1738(1)	3273(1)	30(1)
C(25)	10208(2)	-491(2)	3741(1)	34(1)
C(26)	9421(1)	452(1)	3396(1)	25(1)
C(31)	5053(1)	3490(1)	2229(1)	16(1)
C(32)	4916(1)	4497(1)	1552(1)	22(1)
C(33)	3657(1)	4372(2)	788(1)	30(1)
C(34)	2534(1)	3248(2)	696(1)	31(1)
C(35)	2640(1)	2249(1)	1372(1)	28(1)
C(36)	3885(1)	2370(1)	2141(1)	21(1)
C(41)	6038(1)	2843(1)	4266(1)	17(1)
C(42)	4879(1)	3258(1)	4670(1)	25(1)
C(43)	4322(1)	2697(2)	5541(1)	29(1)
C(44)	4920(2)	1718(1)	6027(1)	27(1)
C(45)	6069(2)	1307(1)	5641(1)	24(1)
C(46)	6632(1)	1862(1)	4769(1)	20(1)

Table A5. Bond lengths [Å] and angles [°] for PNP-Dimprop.

Atoms	Bond length (Å)	Atoms	Bond angle (°)
N(1)-C(1)	1.5148(16)	C(1)-N(1)-C(1A)	32.0(4)
N(1)-C(1A)	1.520(11)	C(1)-N(1)-P(1)	121.56(8)
N(1)-P(1)	1.7220(11)	C(1A)-N(1)-P(1)	130.1(4)
N(1)-P(2)	1.7278(11)	C(1)-N(1)-P(2)	115.53(8)
P(1)-C(21)	1.8317(13)	C(1A)-N(1)-P(2)	111.2(5)
P(1)-C(11)	1.8404(14)	P(1)-N(1)-P(2)	117.82(6)
P(2)-C(41)	1.8267(13)	N(1)-P(1)-C(21)	106.56(6)
P(2)-C(31)	1.8367(13)	N(1)-P(1)-C(11)	104.93(5)
C(1)-C(2)	1.5432(17)	C(21)-P(1)-C(11)	99.56(5)

C(1)-C(5)	1.5629(18)	N(1)-P(2)-C(41)	104.99(6)
C(1)-H(1)	1	N(1)-P(2)-C(31)	106.17(6)
C(2)-C(4)	1.5137(19)	C(41)-P(2)-C(31)	99.75(6)
C(2)-C(3)	1.5335(18)	N(1)-C(1)-C(2)	112.35(10)
C(2)-H(2)	1	N(1)-C(1)-C(5)	112.30(9)
C(1A)-C(2A)	1.561(13)	C(2)-C(1)-C(5)	109.53(10)
C(1A)-C(4)	1.778(12)	N(1)-C(1)-H(1)	107.5
C(2A)-C(5)	1.495(10)	C(2)-C(1)-H(1)	107.5
C(2A)-C(3)	1.680(9)	C(5)-C(1)-H(1)	107.5
C(3)-H(3A)	0.98	C(4)-C(2)-C(3)	110.46(11)
C(3)-H(3B)	0.98	C(4)-C(2)-C(1)	113.05(11)
C(3)-H(3C)	0.98	C(3)-C(2)-C(1)	110.49(11)
C(4)-H(4A)	0.98	C(4)-C(2)-H(2)	107.5
C(4)-H(4B)	0.98	C(3)-C(2)-H(2)	107.5
C(4)-H(4C)	0.98	C(1)-C(2)-H(2)	107.5
C(5)-H(5A)	0.98	N(1)-C(1A)-C(2A)	109.7(8)
C(5)-H(5B)	0.98	N(1)-C(1A)-C(4)	130.0(8)
C(5)-H(5C)	0.98	C(2A)-C(1A)-C(4)	102.9(7)
C(11)-C(12)	1.3946(17)	C(5)-C(2A)-C(1A)	101.1(7)
C(11)-C(16)	1.4005(17)	C(5)-C(2A)-C(3)	135.9(8)
C(12)-C(13)	1.3890(18)	C(1A)-C(2A)-C(3)	99.9(7)
C(12)-H(12A)	0.95	C(2)-C(3)-C(2A)	40.6(4)
C(13)-C(14)	1.3865(19)	C(2)-C(3)-H(3A)	109.5
C(13)-H(13)	0.95	C(2A)-C(3)-H(3A)	70
C(14)-C(15)	1.387(2)	C(2)-C(3)-H(3B)	109.5
C(14)-H(14)	0.95	C(2A)-C(3)-H(3B)	114.7
C(15)-C(16)	1.3892(19)	H(3A)-C(3)-H(3B)	109.5
C(15)-H(15A)	0.95	C(2)-C(3)-H(3C)	109.5
C(16)-H(16)	0.95	C(2A)-C(3)-H(3C)	133.1
C(21)-C(26)	1.3817(16)	H(3A)-C(3)-H(3C)	109.5
C(21)-C(22)	1.3977(17)	H(3B)-C(3)-H(3C)	109.5
C(22)-C(23)	1.3879(19)	C(2)-C(4)-C(1A)	41.8(3)
C(22)-H(22)	0.95	C(2)-C(4)-H(4A)	109.5
C(23)-C(24)	1.386(2)	C(1A)-C(4)-H(4A)	81.2
C(23)-H(23A)	0.95	C(2)-C(4)-H(4B)	109.5
C(24)-C(25)	1.377(2)	C(1A)-C(4)-H(4B)	150.3
C(24)-H(24A)	0.95	H(4A)-C(4)-H(4B)	109.5
C(25)-C(26)	1.392(2)	C(2)-C(4)-H(4C)	109.5
C(25)-H(25A)	0.95	C(1A)-C(4)-H(4C)	91.7
C(26)-H(26)	0.95	H(4A)-C(4)-H(4C)	109.5
C(31)-C(32)	1.3949(17)	H(4B)-C(4)-H(4C)	109.5
C(31)-C(36)	1.3967(16)	C(2A)-C(5)-C(1)	47.3(4)
C(32)-C(33)	1.3939(17)	C(2A)-C(5)-H(5A)	156.6

C(32)-H(32)	0.95	C(1)-C(5)-H(5A)	109.5
C(33)-C(34)	1.376(2)	C(2A)-C(5)-H(5B)	81.3
C(33)-H(33)	0.95	C(1)-C(5)-H(5B)	109.5
C(34)-C(35)	1.384(2)	H(5A)-C(5)-H(5B)	109.5
C(34)-H(34)	0.95	C(2A)-C(5)-H(5C)	85
C(35)-C(36)	1.3887(17)	C(1)-C(5)-H(5C)	109.5
C(35)-H(35)	0.95	H(5A)-C(5)-H(5C)	109.5
C(36)-H(36)	0.95	H(5B)-C(5)-H(5C)	109.5
C(41)-C(46)	1.3943(17)	C(12)-C(11)-C(16)	118.45(11)
C(41)-C(42)	1.4020(18)	C(12)-C(11)-P(1)	123.89(9)
C(42)-C(43)	1.3866(19)	C(16)-C(11)-P(1)	117.61(9)
C(42)-H(42)	0.95	C(13)-C(12)-C(11)	121.03(11)
C(43)-C(44)	1.387(2)	C(13)-C(12)-H(12A)	119.5
C(43)-H(43)	0.95	C(11)-C(12)-H(12A)	119.5
C(44)-C(45)	1.380(2)	C(14)-C(13)-C(12)	119.98(12)
C(44)-H(44)	0.95	C(14)-C(13)-H(13)	120
C(45)-C(46)	1.3893(18)	C(12)-C(13)-H(13)	120
C(45)-H(45)	0.95	C(13)-C(14)-C(15)	119.66(12)
C(46)-H(46)	0.95	C(13)-C(14)-H(14)	120.2
		C(15)-C(14)-H(14)	120.2
		C(14)-C(15)-C(16)	120.53(12)
		C(14)-C(15)-H(15A)	119.7
		C(16)-C(15)-H(15A)	119.7
		C(15)-C(16)-C(11)	120.33(12)
		C(15)-C(16)-H(16)	119.8
		C(11)-C(16)-H(16)	119.8
		C(26)-C(21)-C(22)	117.98(11)
		C(26)-C(21)-P(1)	124.65(9)
		C(22)-C(21)-P(1)	116.87(9)
		C(23)-C(22)-C(21)	120.90(12)
		C(23)-C(22)-H(22)	119.6
		C(21)-C(22)-H(22)	119.6
		C(24)-C(23)-C(22)	120.33(12)
		C(24)-C(23)-H(23A)	119.8
		C(22)-C(23)-H(23A)	119.8
		C(25)-C(24)-C(23)	119.10(12)
		C(25)-C(24)-H(24A)	120.5
		C(23)-C(24)-H(24A)	120.5
		C(24)-C(25)-C(26)	120.59(12)
		C(24)-C(25)-H(25A)	119.7
		C(26)-C(25)-H(25A)	119.7
		C(21)-C(26)-C(25)	121.07(12)
		C(21)-C(26)-H(26)	119.5

C(25)-C(26)-H(26)	119.5
C(32)-C(31)-C(36)	118.55(10)
C(32)-C(31)-P(2)	117.02(8)
C(36)-C(31)-P(2)	124.43(9)
C(33)-C(32)-C(31)	120.69(11)
C(33)-C(32)-H(32)	119.7
C(31)-C(32)-H(32)	119.7
C(34)-C(33)-C(32)	119.98(13)
C(34)-C(33)-H(33)	120
C(32)-C(33)-H(33)	120
C(33)-C(34)-C(35)	120.07(12)
C(33)-C(34)-H(34)	120
C(35)-C(34)-H(34)	120
C(34)-C(35)-C(36)	120.28(12)
C(34)-C(35)-H(35)	119.9
C(36)-C(35)-H(35)	119.9
C(35)-C(36)-C(31)	120.41(12)
C(35)-C(36)-H(36)	119.8
C(31)-C(36)-H(36)	119.8
C(46)-C(41)-C(42)	118.27(11)
C(46)-C(41)-P(2)	124.52(9)
C(42)-C(41)-P(2)	116.96(9)
C(43)-C(42)-C(41)	120.97(13)
C(43)-C(42)-H(42)	119.5
C(41)-C(42)-H(42)	119.5
C(42)-C(43)-C(44)	119.95(13)
C(42)-C(43)-H(43)	120
C(44)-C(43)-H(43)	120
C(45)-C(44)-C(43)	119.65(12)
C(45)-C(44)-H(44)	120.2
C(43)-C(44)-H(44)	120.2
C(44)-C(45)-C(46)	120.77(13)
C(44)-C(45)-H(45)	119.6
C(46)-C(45)-H(45)	119.6
C(45)-C(46)-C(41)	120.39(12)
C(45)-C(46)-H(46)	119.8
C(41)-C(46)-H(46)	119.8

Table A6. Anisotropic displacement parameters ($A^2 \times 10^3$) for PNP-Dimprop. The anisotropic displacement factor exponent takes the form: -2 pi [h^2 a*^2 U11 + ... + 2 h k a* b* U12]

	U11	U22	U33	U23	U13	U12
N(1)	11(1)	13(1)	19(1)	-1(1)	1(1)	6(1)
P(1)	12(1)	13(1)	15(1)	0(1)	2(1)	5(1)
P(2)	12(1)	15(1)	18(1)	0(1)	1(1)	7(1)
C(1)	13(1)	18(1)	20(1)	-1(1)	3(1)	5(1)
C(2)	17(1)	22(1)	21(1)	-2(1)	2(1)	6(1)
C(3)	15(1)	23(1)	33(1)	-5(1)	7(1)	-1(1)
C(4)	32(1)	26(1)	15(1)	2(1)	4(1)	10(1)
C(5)	21(1)	21(1)	16(1)	-1(1)	-1(1)	12(1)
C(11)	16(1)	16(1)	16(1)	0(1)	1(1)	6(1)
C(12)	19(1)	21(1)	21(1)	2(1)	4(1)	9(1)
C(13)	26(1)	24(1)	23(1)	2(1)	10(1)	10(1)
C(14)	33(1)	30(1)	17(1)	1(1)	6(1)	10(1)
C(15)	27(1)	38(1)	19(1)	3(1)	-1(1)	15(1)
C(16)	19(1)	30(1)	19(1)	1(1)	2(1)	12(1)
C(21)	17(1)	16(1)	17(1)	3(1)	5(1)	8(1)
C(22)	21(1)	17(1)	29(1)	1(1)	6(1)	7(1)
C(23)	35(1)	16(1)	39(1)	3(1)	15(1)	12(1)
C(24)	44(1)	32(1)	26(1)	13(1)	14(1)	29(1)
C(25)	42(1)	43(1)	22(1)	1(1)	-3(1)	31(1)
C(26)	32(1)	26(1)	20(1)	-3(1)	-4(1)	18(1)
C(31)	14(1)	22(1)	16(1)	0(1)	3(1)	10(1)
C(32)	20(1)	30(1)	22(1)	8(1)	6(1)	13(1)
C(33)	28(1)	49(1)	19(1)	10(1)	4(1)	23(1)
C(34)	24(1)	52(1)	22(1)	-8(1)	-6(1)	23(1)
C(35)	16(1)	31(1)	37(1)	-12(1)	-4(1)	10(1)
C(36)	17(1)	21(1)	27(1)	-1(1)	2(1)	10(1)
C(41)	16(1)	21(1)	15(1)	-1(1)	0(1)	6(1)
C(42)	22(1)	35(1)	21(1)	2(1)	3(1)	15(1)
C(43)	23(1)	46(1)	22(1)	0(1)	6(1)	12(1)
C(44)	27(1)	35(1)	16(1)	1(1)	4(1)	1(1)
C(45)	30(1)	24(1)	18(1)	2(1)	-1(1)	6(1)
C(46)	21(1)	21(1)	17(1)	-1(1)	0(1)	8(1)

Table A7: Atomic coordinates (x 10^4) and equivalent isotropic displacement parameters ($Å^2 \times 10^3$) for PNP-i-Pent U(eq) is defined as one third of the trace of the orthogonalize Uij tensor.

	X	Y	z	U(eq)
N(1)	7568(2)	155(2)	1051(1)	16(1)
P(1)	6642(1)	929(1)	1514(1)	15(1)
P(2)	6408(1)	-205(1)	583(1)	15(1)
C(1)	9191(2)	-43(2)	1031(1)	17(1)

C(2)	9811(2)	1169(2)	1341(1)	19(1)
C(3)	11500(2)	1223(2)	1329(1)	24(1)
C(4)	12193(2)	-101(2)	1628(1)	36(1)
C(5)	12042(2)	2564(2)	1523(1)	30(1)
C(11)	6702(2)	-230(2)	2026(1)	17(1)
C(12)	6485(2)	240(2)	2499(1)	20(1)
C(13)	6221(2)	-636(2)	2878(1)	25(1)
C(14)	6180(2)	1995(2)	2795(1)	26(1)
C(15)	6397(2)	-2482(2)	2330(1)	23(1)
C(16)	6637(2)	-1609(2)	1948(1)	20(1)
C(21)	7880(2)	2282(2)	1696(1)	17(1)
C(22)	7578(2)	3512(2)	1483(1)	25(1)
C(23)	8425(3)	4625(2)	1593(1)	32(1)
C(24)	9558(2)	4523(2)	1924(1)	30(1)
C(25)	9871(2)	3310(2)	2140(1)	27(1)
C(26)	9043(2)	2193(2)	2026(1)	22(1)
C(31)	7231(2)	616(2)	54(1)	17(1)
C(32)	6681(2)	329(2)	-410(1)	23(1)
C(33)	7109(2)	1078(2)	-809(1)	28(1)
C(34)	8106(2)	2119(2)	-755(1)	29(1)
C(35)	8647(2)	2421(2)	-297(1)	25(1)
C(36)	8203(2)	1687(2)	105(1)	20(1)
C(41)	6695(2)	-1975(2)	456(1)	16(1)
C(42)	5683(2)	-2833(2)	678(1)	20(1)
C(43)	5731(2)	-4204(2)	600(1)	24(1)
C(44)	6790(2)	-4722(2)	289(1)	25(1)
C(45)	7808(2)	-3882(2)	70(1)	24(1)
C(46)	7766(2)	-2522(2)	152(1)	22(1)

Table A8. Bond lengths [Å] and angles [°] for PNP-i-Pent.

Atoms	Bond length (Å)	Atoms	Bond angle (°)
N(1)-C(1)	1.484(2)	C(1)-N(1)-P(2)	123.65(11)
N(1)-P(2)	1.7036(15)	C(1)-N(1)-P(1)	125.02(11)
N(1)-P(1)	1.7124(15)	P(2)-N(1)-P(1)	110.99(8)
P(1)-C(11)	1.8296(17)	N(1)-P(1)-C(11)	105.73(8)
P(1)-C(21)	1.8309(18)	N(1)-P(1)-C(21)	103.87(8)
P(2)-C(41)	1.8288(17)	C(11)-P(1)-C(21)	103.98(8)
P(2)-C(31)	1.8321(18)	N(1)-P(2)-C(41)	105.26(8)
C(1)-C(2)	1.523(2)	N(1)-P(2)-C(31)	104.85(8)
C(1)-H(1A)	0.99	C(41)-P(2)-C(31)	103.16(8)
C(1)-H(1B)	0.99	N(1)-C(1)-C(2)	116.32(15)
C(2)-C(3)	1.531(3)	N(1)-C(1)-H(1A)	108.2

C(2)-H(2A)	1.04(2)	C(2)-C(1)-H(1A)	108.2
C(2)-H(2B)	1.02(3)	N(1)-C(1)-H(1B)	108.2
C(3)-C(5)	1.530(3)	C(2)-C(1)-H(1B)	108.2
C(3)-C(4)	1.530(3)	H(1A)-C(1)-H(1B)	107.4
C(3)-H(3A)	0.91(2)	C(1)-C(2)-C(3)	112.50(15)
C(4)-H(4A)	0.98	C(1)-C(2)-H(2A)	108.4(14)
C(4)-H(4B)	0.98	C(3)-C(2)-H(2A)	108.1(13)
C(4)-H(4C)	0.98	C(1)-C(2)-H(2B)	107.4(14)
C(5)-H(5A)	0.98	C(3)-C(2)-H(2B)	111.3(14)
C(5)-H(5B)	0.98	H(2A)-C(2)-H(2B)	109(2)
C(5)-H(5C)	0.98	C(5)-C(3)-C(4)	109.13(17)
C(11)-C(12)	1.399(2)	C(5)-C(3)-C(2)	110.14(16)
C(11)-C(16)	1.402(2)	C(4)-C(3)-C(2)	111.88(16)
C(12)-C(13)	1.386(2)	C(5)-C(3)-H(3A)	110.6(15)
C(12)-H(12)	0.95	C(4)-C(3)-H(3A)	107.8(15)
C(13)-C(14)	1.383(3)	C(2)-C(3)-H(3A)	107.3(16)
C(13)-H(13)	0.95	C(3)-C(4)-H(4A)	109.5
C(14)-C(15)	1.385(3)	C(3)-C(4)-H(4B)	109.5
C(14)-H(14)	0.95	H(4A)-C(4)-H(4B)	109.5
C(15)-C(16)	1.388(2)	C(3)-C(4)-H(4C)	109.5
C(15)-H(15)	0.95	H(4A)-C(4)-H(4C)	109.5
C(16)-H(16)	0.95	H(4B)-C(4)-H(4C)	109.5
C(21)-C(26)	1.394(3)	C(3)-C(5)-H(5A)	109.5
C(21)-C(22)	1.394(3)	C(3)-C(5)-H(5B)	109.5
C(22)-C(23)	1.388(3)	H(5A)-C(5)-H(5B)	109.5
C(22)-H(22)	0.95	C(3)-C(5)-H(5C)	109.5
C(23)-C(24)	1.377(3)	H(5A)-C(5)-H(5C)	109.5
C(23)-H(23)	0.95	H(5B)-C(5)-H(5C)	109.5
C(24)-C(25)	1.385(3)	C(12)-C(11)-C(16)	118.00(16)
C(24)-H(24)	0.95	C(12)-C(11)-P(1)	120.02(14)
C(25)-C(26)	1.385(3)	C(16)-C(11)-P(1)	120.50(13)
C(25)-H(25)	0.95	C(13)-C(12)-C(11)	120.83(17)
C(26)-H(26)	0.95	C(13)-C(12)-H(12)	119.6
C(31)-C(36)	1.396(2)	C(11)-C(12)-H(12)	119.6
C(31)-C(32)	1.402(2)	C(14)-C(13)-C(12)	120.34(18)
C(32)-C(33)	1.387(3)	C(14)-C(13)-H(13)	119.8
C(32)-H(32)	0.95	C(12)-C(13)-H(13)	119.8
C(33)-C(34)	1.389(3)	C(13)-C(14)-C(15)	119.82(18)
C(33)-H(33)	0.95	C(13)-C(14)-H(14)	120.1
C(34)-C(35)	1.386(3)	C(15)-C(14)-H(14)	120.1
C(34)-H(34)	0.95	C(14)-C(15)-C(16)	120.08(17)
C(35)-C(36)	1.390(2)	C(14)-C(15)-H(15)	120
C(35)-H(35)	0.95	C(16)-C(15)-H(15)	120

C(36)-H(36)	0.95	C(15)-C(16)-C(11)	120.90(17)
C(41)-C(46)	1.395(3)	C(15)-C(16)-H(16)	119.5
C(41)-C(42)	1.398(2)	C(11)-C(16)-H(16)	119.5
C(42)-C(43)	1.393(3)	C(26)-C(21)-C(22)	118.66(17)
C(42)-H(42)	0.95	C(26)-C(21)-P(1)	126.43(14)
C(43)-C(44)	1.386(3)	C(22)-C(21)-P(1)	114.90(13)
C(43)-H(43)	0.95	C(23)-C(22)-C(21)	120.81(18)
C(44)-C(45)	1.389(3)	C(23)-C(22)-H(22)	119.6
C(44)-H(44)	0.95	C(21)-C(22)-H(22)	119.6
C(45)-C(46)	1.384(3)	C(24)-C(23)-C(22)	119.77(19)
C(45)-H(45)	0.95	C(24)-C(23)-H(23)	120.1
C(46)-H(46)	0.95	C(22)-C(23)-H(23)	120.1
		C(23)-C(24)-C(25)	120.16(19)
		C(23)-C(24)-H(24)	119.9
		C(25)-C(24)-H(24)	119.9
		C(24)-C(25)-C(26)	120.21(18)
		C(24)-C(25)-H(25)	119.9
		C(26)-C(25)-H(25)	119.9
		C(25)-C(26)-C(21)	120.37(18)
		C(25)-C(26)-H(26)	119.8
		C(21)-C(26)-H(26)	119.8
		C(36)-C(31)-C(32)	118.30(16)
		C(36)-C(31)-P(2)	121.52(13)
		C(32)-C(31)-P(2)	119.20(14)
		C(33)-C(32)-C(31)	120.78(18)
		C(33)-C(32)-H(32)	119.6
		C(31)-C(32)-H(32)	119.6
		C(32)-C(33)-C(34)	120.31(18)
		C(32)-C(33)-H(33)	119.8
		C(34)-C(33)-H(33)	119.8
		C(35)-C(34)-C(33)	119.43(17)
		C(35)-C(34)-H(34)	120.3
		C(33)-C(34)-H(34)	120.3
		C(34)-C(35)-C(36)	120.49(18)
		C(34)-C(35)-H(35)	119.8
		C(36)-C(35)-H(35)	119.8
		C(35)-C(36)-C(31)	120.66(17)
		C(35)-C(36)-H(36)	119.7
		C(31)-C(36)-H(36)	119.7
		C(46)-C(41)-C(42)	118.48(16)
		C(46)-C(41)-P(2)	126.54(14)
		C(42)-C(41)-P(2)	114.93(13)
		C(43)-C(42)-C(41)	121.29(17)

C(43)-C(42)-H(42)	119.4
C(41)-C(42)-H(42)	119.4
C(44)-C(43)-C(42)	119.24(17)
C(44)-C(43)-H(43)	120.4
C(42)-C(43)-H(43)	120.4
C(43)-C(44)-C(45)	120.01(17)
C(43)-C(44)-H(44)	120
C(45)-C(44)-H(44)	120
C(46)-C(45)-C(44)	120.63(18)
C(46)-C(45)-H(45)	119.7
C(44)-C(45)-H(45)	119.7
C(45)-C(46)-C(41)	120.34(17)
C(45)-C(46)-H(46)	119.8
C(41)-C(46)-H(46)	119.8

Table A9. Anisotropic displacement parameters ($A^2 \times 10^3$) for PNP-i-Pent. The anisotropic displacement factor exponent takes the form: -2 pi [h^2 a*^2 U11 + ... + 2 h k a* b* U12]

	U11	U22	U33	U23	U13	U12
N(1)	17(1)	19(1)	13(1)	-1(1)	-1(1)	1(1)
P(1)	17(1)	16(1)	13(1)	-1(1)	0(1)	0(1)
P(2)	17(1)	16(1)	13(1)	0(1)	-1(1)	0(1)
C(1)	17(1)	19(1)	15(1)	1(1)	1(1)	2(1)
C(2)	18(1)	19(1)	19(1)	3(1)	1(1)	1(1)
C(3)	21(1)	29(1)	22(1)	8(1)	5(1)	6(1)
C(4)	19(1)	34(1)	54(1)	9(1)	-6(1)	-4(1)
C(5)	30(1)	29(1)	32(1)	5(1)	1(1)	11(1)
C(11)	13(1)	22(1)	15(1)	1(1)	0(1)	-3(1)
C(12)	19(1)	24(1)	17(1)	-1(1)	1(1)	1(1)
C(13)	22(1)	35(1)	17(1)	2(1)	4(1)	-1(1)
C(14)	24(1)	32(1)	24(1)	10(1)	2(1)	-5(1)
C(15)	21(1)	21(1)	26(1)	4(1)	1(1)	-7(1)
C(16)	19(1)	24(1)	19(1)	0(1)	2(1)	-3(1)
C(21)	20(1)	18(1)	15(1)	-4(1)	2(1)	-4(1)
C(22)	28(1)	22(1)	24(1)	2(1)	-3(1)	-2(1)
C(23)	42(1)	19(1)	35(1)	2(1)	1(1)	-4(1)
C(24)	37(1)	26(1)	28(1)	-9(1)	6(1)	-14(1)
C(25)	22(1)	39(1)	20(1)	-6(1)	1(1)	-10(1)
C(26)	22(1)	25(1)	17(1)	1(1)	2(1)	-1(1)
C(31)	20(1)	16(1)	16(1)	1(1)	0(1)	3(1)
C(32)	25(1)	25(1)	18(1)	-2(1)	-2(1)	-2(1)
C(33)	36(1)	30(1)	17(1)	1(1)	-2(1)	5(1)
C(34)	37(1)	26(1)	22(1)	10(1)	5(1)	6(1)
C(35)	30(1)	14(1)	30(1)	4(1)	3(1)	0(1)

C(36)	26(1)	16(1)	19(1)	1(1)	-1(1)	-1(1)
C(41)	20(1)	16(1)	14(1)	-2(1)	-2(1)	-2(1)
C(42)	19(1)	23(1)	19(1)	0(1)	0(1)	0(1)
C(43)	24(1)	21(1)	26(1)	6(1)	-4(1)	-4(1)
C(44)	31(1)	15(1)	29(1)	-1(1)	-5(1)	4(1)
C(45)	27(1)	22(1)	24(1)	-3(1)	2(1)	5(1)
C(46)	22(1)	21(1)	23(1)	1(1)	2(1)	0(1)

Table A10: Atomic coordinates (x 10^4) and equivalent isotropic displacement parameters ($Å^2$ x 10^3) for PNP-Cychex U(eq) is defined as one third of the trace of the orthogonalize Uij tensor.

	X	Y	z	U(eq)
N(1)	4085(2)	8406(2)	1983(2)	17(1)
P(1)	3406(1)	7708(1)	2535(1)	18(1)
P(2)	5204(1)	8307(1)	2427(1)	16(1)
C(1)	3654(2)	8652(3)	1014(2)	17(1)
C(2)	3346(2)	7399(3)	500(2)	20(1)
C(3)	2933(2)	7661(3)	-485(2)	24(1)
C(4)	2168(2)	8608(3)	-655(2)	27(1)
C(5)	2479(2)	9853(3)	-147(2)	23(1)
C(6)	2881(2)	9596(3)	854(2)	21(1)
C(11)	3635(2)	8617(3)	3564(2)	19(1)
C(12)	3390(2)	8066(3)	4276(2)	26(1)
C(13)	3429(2)	8781(3)	5034(2)	29(1)
C(14)	3708(2)	10049(3)	5097(2)	27(1)
C(15)	3940(2)	10609(3)	4404(2)	28(1)
C(16)	3908(2)	9903(3)	3644(2)	23(1)
C(21)	3907(2)	6133(3)	2920(2)	22(1)
C(22)	4624(2)	5934(3)	3671(2)	24(1)
C(23)	4950(2)	4696(3)	3899(2)	29(1)
C(24)	4574(3)	3653(3)	3386(3)	32(1)
C(25)	3863(2)	3836(3)	2639(2)	30(1)
C(26)	3529(2)	5060(3)	2413(2)	26(1)
C(31)	5566(2)	7435(3)	1573(2)	17(1)
C(32)	5821(2)	8031(3)	895(2)	20(1)
C(33)	6078(2)	7312(3)	284(2)	22(1)
C(34)	6090(2)	5977(3)	333(2)	22(1)
C(35)	5839(2)	5367(3)	994(2)	21(1)
C(36)	5587(2)	6085(3)	1614(2)	20(1)
C(41)	5632(2)	9927(3)	2317(2)	17(1)
C(42)	5123(2)	11013(3)	2004(2)	21(1)
C(43)	5512(2)	12230(3)	2043(2)	22(1)
C(44)	6410(2)	12377(3)	2405(2)	21(1)

C(45)	6929(2)	11302(3)	2709(2)	21(1)
C(46)	6547(2)	10094(3)	2661(2)	20(1)

Table A11. Bond lengths [Å] and angles [°] for PNP-Cychex.

Atoms	Bond length (Å)	Atoms	Bond angle (°)
N(1)-C(1)	1.502(4)	C(1)-N(1)-P(2)	122.09(19)
N(1)-P(2)	1.703(3)	C(1)-N(1)-P(1)	115.11(19)
N(1)-P(1)	1.731(2)	P(2)-N(1)-P(1)	119.46(14)
P(1)-C(11)	1.820(3)	N(1)-P(1)-C(11)	104.29(13)
P(1)-C(21)	1.834(3)	N(1)-P(1)-C(21)	105.45(13)
P(2)-C(41)	1.836(3)	C(11)-P(1)-C(21)	102.15(14)
P(2)-C(31)	1.851(3)	N(1)-P(2)-C(41)	105.86(13)
C(1)-C(6)	1.526(4)	N(1)-P(2)-C(31)	103.77(13)
C(1)-C(2)	1.530(4)	C(41)-P(2)-C(31)	99.91(13)
C(2)-C(3)	1.523(4)	N(1)-C(1)-C(6)	112.0(2)
C(3)-C(4)	1.517(5)	N(1)-C(1)-C(2)	112.0(2)
C(4)-C(5)	1.521(4)	C(6)-C(1)-C(2)	110.0(3)
C(5)-C(6)	1.544(4)	C(3)-C(2)-C(1)	111.4(3)
C(11)-C(16)	1.392(4)	C(4)-C(3)-C(2)	111.9(3)
C(11)-C(12)	1.415(4)	C(3)-C(4)-C(5)	109.7(3)
C(12)-C(13)	1.394(4)	C(4)-C(5)-C(6)	111.4(3)
C(13)-C(14)	1.378(5)	C(1)-C(6)-C(5)	110.1(2)
C(14)-C(15)	1.382(5)	C(16)-C(11)-C(12)	117.5(3)
C(15)-C(16)	1.393(4)	C(16)-C(11)-P(1)	123.3(2)
C(21)-C(22)	1.391(5)	C(12)-C(11)-P(1)	118.3(2)
C(21)-C(26)	1.396(4)	C(13)-C(12)-C(11)	121.2(3)
C(22)-C(23)	1.387(4)	C(14)-C(13)-C(12)	119.9(3)
C(23)-C(24)	1.373(5)	C(13)-C(14)-C(15)	119.7(3)
C(24)-C(25)	1.380(5)	C(14)-C(15)-C(16)	120.9(3)
C(25)-C(26)	1.377(5)	C(11)-C(16)-C(15)	120.7(3)
C(31)-C(32)	1.396(4)	C(22)-C(21)-C(26)	118.3(3)
C(31)-C(36)	1.398(4)	C(22)-C(21)-P(1)	125.3(3)
C(32)-C(33)	1.373(4)	C(26)-C(21)-P(1)	116.5(3)
C(33)-C(34)	1.382(4)	C(23)-C(22)-C(21)	120.3(3)
C(34)-C(35)	1.378(4)	C(24)-C(23)-C(22)	120.6(3)
C(35)-C(36)	1.380(4)	C(23)-C(24)-C(25)	119.8(3)
C(41)-C(42)	1.385(4)	C(26)-C(25)-C(24)	120.0(3)
C(41)-C(46)	1.396(4)	C(25)-C(26)-C(21)	121.1(3)
C(42)-C(43)	1.393(4)	C(32)-C(31)-C(36)	117.9(3)
C(43)-C(44)	1.372(4)	C(32)-C(31)-P(2)	124.6(2)
C(44)-C(45)	1.381(4)	C(36)-C(31)-P(2)	117.4(2)
C(45)-C(46)	1.380(4)	C(33)-C(32)-C(31)	121.0(3)

C(32)-C(33)-C(34)	120.3(3)
C(35)-C(34)-C(33)	119.9(3)
C(34)-C(35)-C(36)	120.1(3)
C(35)-C(36)-C(31)	120.8(3)
C(42)-C(41)-C(46)	117.6(3)
C(42)-C(41)-P(2)	125.7(2)
C(46)-C(41)-P(2)	116.4(2)
C(41)-C(42)-C(43)	121.0(3)
C(44)-C(43)-C(42)	120.4(3)
C(43)-C(44)-C(45)	119.4(3)
C(46)-C(45)-C(44)	120.3(3)
C(45)-C(46)-C(41)	121.3(3)

Table A12. Anisotropic displacement parameters ($A^2 \times 10^3$) for PNP-Cychex. The anisotropic displacement factor exponent takes the form: -2 pi [h^2 a*^2 U11 + ... + 2 h k a* b* U12]

	U11	U22	U33	U23	U13	U12
N(1)	14(1)	22(1)	14(1)	0(1)	5(1)	0(1)
P(1)	18(1)	19(1)	20(1)	-2(1)	9(1)	-2(1)
P(2)	15(1)	18(1)	16(1)	1(1)	5(1)	0(1)
C(1)	17(2)	21(2)	13(2)	0(1)	4(1)	1(1)
C(2)	20(2)	21(2)	19(2)	-6(1)	5(1)	-1(1)
C(3)	26(2)	26(2)	20(2)	-7(1)	5(1)	-2(1)
C(4)	24(2)	34(2)	21(2)	0(2)	2(1)	-1(1)
C(5)	19(2)	28(2)	21(2)	0(1)	4(1)	1(1)
C(6)	19(2)	20(2)	22(2)	-5(1)	4(1)	-2(1)
C(11)	16(2)	25(2)	19(2)	1(1)	7(1)	2(1)
C(12)	32(2)	24(2)	27(2)	-1(2)	16(2)	-3(2)
C(13)	35(2)	34(2)	22(2)	3(2)	16(2)	5(2)
C(14)	30(2)	32(2)	20(2)	-4(1)	9(2)	4(2)
C(15)	29(2)	25(2)	31(2)	-4(2)	12(2)	-4(2)
C(16)	25(2)	22(2)	23(2)	0(1)	11(1)	-1(1)
C(21)	22(2)	23(2)	24(2)	1(1)	12(1)	-4(1)
C(22)	25(2)	26(2)	23(2)	0(1)	10(1)	-2(1)
C(23)	30(2)	32(2)	28(2)	8(2)	14(2)	6(2)
C(24)	38(2)	22(2)	48(2)	8(2)	29(2)	6(2)
C(25)	30(2)	21(2)	46(2)	-6(2)	19(2)	-5(2)
C(26)	20(2)	29(2)	33(2)	-1(2)	13(2)	-2(1)
C(31)	13(2)	20(2)	18(2)	0(1)	4(1)	1(1)
C(32)	22(2)	18(2)	20(2)	-2(1)	6(1)	-1(1)
C(33)	25(2)	26(2)	16(2)	-1(1)	8(1)	-1(1)
C(34)	22(2)	25(2)	20(2)	-7(1)	6(1)	-3(1)
C(35)	20(2)	13(2)	30(2)	-1(1)	5(1)	1(1)

C(36)	17(2)	20(2)	23(2)	4(1)	7(1)	1(1)
C(41)	21(2)	20(2)	12(1)	-2(1)	8(1)	0(1)
C(42)	18(2)	23(2)	24(2)	1(1)	9(1)	1(1)
C(43)	28(2)	16(2)	25(2)	1(1)	12(1)	0(1)
C(44)	25(2)	20(2)	21(2)	-5(1)	10(1)	-5(1)
C(45)	17(2)	30(2)	18(2)	1(1)	5(1)	-5(1)
C(46)	20(2)	24(2)	18(2)	2(1)	6(1)	2(1)

Table A13: Atomic coordinates (x 10^4) and equivalent isotropic displacement parameters ($Å^2$ x 10^3) for PNP-n-Pent U(eq) is defined as one third of the trace of the orthogonalize Uij tensor.

	X	Y	z	U(eq)
N(1)	9915(1)	2385(1)	9070(1)	15(1)
N(2)	15106(1)	2552(1)	12810(1)	15(1)
P(1)	8818(1)	2416(1)	9972(1)	14(1)
P(2)	10989(1)	2973(1)	9025(1)	14(1)
P(3)	14053(1)	1944(1)	13504(1)	14(1)
P(4)	16236(1)	2489(1)	13214(1)	15(1)
C(1)	9874(1)	1810(1)	8364(1)	17(1)
C(2)	9256(1)	2422(1)	7630(1)	18(1)
C(3)	9320(1)	1841(1)	6866(1)	19(1)
C(4)	8752(1)	2439(1)	6098(1)	24(1)
C(5)	8869(1)	1850(1)	5330(1)	34(1)
C(6)	15101(1)	3198(1)	11863(1)	16(1)
C(7)	15651(1)	2646(1)	11073(1)	18(1)
C(8)	15588(1)	3325(1)	10115(1)	20(1)
C(9)	16027(1)	2758(1)	9317(1)	24(1)
C(10)	15947(1)	3436(1)	8366(1)	35(1)
C(11)	8366(1)	3780(1)	9899(1)	15(1)
C(12)	8418(1)	4453(1)	9027(1)	18(1)
C(13)	7968(1)	5466(1)	8960(1)	21(1)
C(14)	7455(1)	5826(1)	9766(1)	21(1)
C(15)	7381(1)	5160(1)	10636(1)	20(1)
C(16)	7828(1)	4148(1)	10705(1)	17(1)
C(21)	9328(1)	2080(1)	11044(1)	15(1)
C(22)	9900(1)	2694(1)	11319(1)	17(1)
C(23)	10255(1)	2354(1)	12148(1)	21(1)
C(24)	10033(1)	1409(1)	12719(1)	25(1)
C(25)	9455(1)	805(1)	12464(1)	24(1)
C(26)	9107(1)	1136(1)	11629(1)	19(1)
C(31)	12081(1)	1924(1)	8992(1)	15(1)
C(32)	13134(1)	2150(1)	8653(1)	18(1)
C(33)	13982(1)	1384(1)	8711(1)	21(1)

C(34)	13800(1)	374(1)	9105(1)	22(1)
C(35)	12762(1)	136(1)	9447(1)	21(1)
C(36)	11910(1)	905(1)	9398(1)	18(1)
C(41)	11315(1)	3726(1)	7822(1)	16(1)
C(42)	11089(1)	4787(1)	7716(1)	17(1)
C(43)	11280(1)	5428(1)	6833(1)	20(1)
C(44)	11681(1)	5013(1)	6043(1)	21(1)
C(45)	11925(1)	3960(1)	6133(1)	22(1)
C(46)	11754(1)	3323(1)	7019(1)	20(1)
C(51)	12968(1)	2999(1)	13547(1)	15(1)
C(52)	11908(1)	2795(1)	13775(1)	18(1)
C(53)	11074(1)	3568(1)	13906(1)	21(1)
C(54)	11277(1)	4566(1)	13800(1)	21(1)
C(55)	12323(1)	4781(1)	13580(1)	21(1)
C(56)	13160(1)	4003(1)	13466(1)	18(1)
C(61)	13648(1)	1220(1)	12792(1)	16(1)
C(62)	13784(1)	157(1)	13085(1)	18(1)
C(63)	13475(1)	-468(1)	12615(1)	22(1)
C(64)	13041(1)	-36(1)	11839(1)	24(1)
C(65)	12905(1)	1021(1)	11534(1)	23(1)
C(66)	13195(1)	1644(1)	12014(1)	20(1)
C(71)	16624(1)	1116(1)	13560(1)	15(1)
C(72)	17130(1)	724(1)	14309(1)	19(1)
C(73)	17529(1)	-302(1)	14507(1)	21(1)
C(74)	17439(1)	-957(1)	13962(1)	22(1)
C(75)	16957(1)	-573(1)	13204(1)	21(1)
C(76)	16553(1)	454(1)	13004(1)	18(1)
C(81)	15789(1)	2837(1)	14367(1)	17(1)
C(82)	15173(1)	2273(1)	15170(1)	21(1)
C(83)	14894(1)	2613(1)	16006(1)	26(1)
C(84)	15236(1)	3507(1)	16059(1)	29(1)
C(85)	15858(1)	4060(1)	15277(1)	28(1)
C(86)	16125(1)	3731(1)	14434(1)	22(1)

Table A14. Bond lengths [Å] and angles [°] for PNP-n-Pent.

Atoms	Bond length (Å)	Atoms	Bond angle (°)
N(1)-C(1)	1.4822(14)	C(1)-N(1)-P(2)	123.40(8)
N(1)-P(2)	1.7115(10)	C(1)-N(1)-P(1)	115.95(7)
N(1)-P(1)	1.7131(10)	P(2)-N(1)-P(1)	120.64(5)
N(2)-C(6)	1.4828(14)	C(6)-N(2)-P(3)	123.77(7)
N(2)-P(3)	1.7075(10)	C(6)-N(2)-P(4)	115.70(7)
N(2)-P(4)	1.7175(10)	P(3)-N(2)-P(4)	120.46(5)

P(1)-C(11)	1.8284(12)	N(1)-P(1)-C(11)	104.12(5)
P(1)-C(21)	1.8304(11)	N(1)-P(1)-C(21)	105.65(5)
P(2)-C(31)	1.8336(12)	C(11)-P(1)-C(21)	101.51(5)
P(2)-C(41)	1.8359(11)	N(1)-P(2)-C(31)	102.85(5)
P(3)-C(51)	1.8340(12)	N(1)-P(2)-C(41)	105.24(5)
P(3)-C(61)	1.8402(11)	C(31)-P(2)-C(41)	101.06(5)
P(4)-C(71)	1.8247(12)	N(2)-P(3)-C(51)	102.20(5)
P(4)-C(81)	1.8378(12)	N(2)-P(3)-C(61)	107.15(5)
C(1)-C(2)	1.5288(16)	C(51)-P(3)-C(61)	100.70(5)
C(1)-H(1A)	0.99	N(2)-P(4)-C(71)	103.41(5)
C(1)-H(1B)	0.99	N(2)-P(4)-C(81)	106.11(5)
C(2)-C(3)	1.5263(16)	C(71)-P(4)-C(81)	100.73(5)
C(2)-H(2A)	0.99	N(1)-C(1)-C(2)	113.49(9)
C(2)-H(2B)	0.99	N(1)-C(1)-H(1A)	108.9
C(3)-C(4)	1.5231(16)	C(2)-C(1)-H(1A)	108.9
C(3)-H(3A)	0.99	N(1)-C(1)-H(1B)	108.9
C(3)-H(3B)	0.99	C(2)-C(1)-H(1B)	108.9
C(4)-C(5)	1.5248(18)	H(1A)-C(1)-H(1B)	107.7
C(4)-H(4A)	0.99	C(3)-C(2)-C(1)	111.75(10)
C(4)-H(4B)	0.99	C(3)-C(2)-H(2A)	109.3
C(5)-H(5A)	0.98	C(1)-C(2)-H(2A)	109.3
C(5)-H(5B)	0.98	C(3)-C(2)-H(2B)	109.3
C(5)-H(5C)	0.98	C(1)-C(2)-H(2B)	109.3
C(6)-C(7)	1.5218(16)	H(2A)-C(2)-H(2B)	107.9
C(6)-H(6A)	0.99	C(4)-C(3)-C(2)	113.63(10)
C(6)-H(6B)	0.99	C(4)-C(3)-H(3A)	108.8
C(7)-C(8)	1.5252(15)	C(2)-C(3)-H(3A)	108.8
C(7)-H(7A)	0.99	C(4)-C(3)-H(3B)	108.8
C(7)-H(7B)	0.99	C(2)-C(3)-H(3B)	108.8
C(8)-C(9)	1.5232(17)	H(3A)-C(3)-H(3B)	107.7
C(8)-H(8A)	0.99	C(3)-C(4)-C(5)	112.05(11)
C(8)-H(8B)	0.99	C(3)-C(4)-H(4A)	109.2
C(9)-C(10)	1.5198(18)	C(5)-C(4)-H(4A)	109.2
C(9)-H(9A)	0.99	C(3)-C(4)-H(4B)	109.2
C(9)-H(9B)	0.99	C(5)-C(4)-H(4B)	109.2
C(10)-H(10A)	0.98	H(4A)-C(4)-H(4B)	107.9
C(10)-H(10B)	0.98	C(4)-C(5)-H(5A)	109.5
C(10)-H(10C)	0.98	C(4)-C(5)-H(5B)	109.5
C(11)-C(12)	1.3994(16)	H(5A)-C(5)-H(5B)	109.5
C(11)-C(16)	1.4015(16)	C(4)-C(5)-H(5C)	109.5
C(12)-C(13)	1.3880(17)	H(5A)-C(5)-H(5C)	109.5
C(12)-H(12)	0.95	H(5B)-C(5)-H(5C)	109.5
C(13)-C(14)	1.3895(18)	N(2)-C(6)-C(7)	113.51(9)

C(13)-H(13)	0.95	N(2)-C(6)-H(6A)	108.9
C(14)-C(15)	1.3897(17)	C(7)-C(6)-H(6A)	108.9
C(14)-H(14)	0.95	N(2)-C(6)-H(6B)	108.9
C(15)-C(16)	1.3867(17)	C(7)-C(6)-H(6B)	108.9
C(15)-H(15)	0.95	H(6A)-C(6)-H(6B)	107.7
C(16)-H(16)	0.95	C(6)-C(7)-C(8)	111.67(10)
C(21)-C(26)	1.3963(16)	C(6)-C(7)-H(7A)	109.3
C(21)-C(22)	1.4023(16)	C(8)-C(7)-H(7A)	109.3
C(22)-C(23)	1.3886(16)	C(6)-C(7)-H(7B)	109.3
C(22)-H(22)	0.95	C(8)-C(7)-H(7B)	109.3
C(23)-C(24)	1.3907(18)	H(7A)-C(7)-H(7B)	107.9
C(23)-H(23)	0.95	C(9)-C(8)-C(7)	112.82(10)
C(24)-C(25)	1.3816(19)	C(9)-C(8)-H(8A)	109
C(24)-H(24)	0.95	C(7)-C(8)-H(8A)	109
C(25)-C(26)	1.3916(17)	C(9)-C(8)-H(8B)	109
C(25)-H(25)	0.95	C(7)-C(8)-H(8B)	109
C(26)-H(26)	0.95	H(8A)-C(8)-H(8B)	107.8
C(31)-C(36)	1.3998(16)	C(10)-C(9)-C(8)	112.52(12)
C(31)-C(32)	1.4029(16)	C(10)-C(9)-H(9A)	109.1
C(32)-C(33)	1.3866(17)	C(8)-C(9)-H(9A)	109.1
C(32)-H(32)	0.95	C(10)-C(9)-H(9B)	109.1
C(33)-C(34)	1.3894(18)	C(8)-C(9)-H(9B)	109.1
C(33)-H(33)	0.95	H(9A)-C(9)-H(9B)	107.8
C(34)-C(35)	1.3902(18)	C(9)-C(10)-H(10A)	109.5
C(34)-H(34)	0.95	C(9)-C(10)-H(10B)	109.5
C(35)-C(36)	1.3926(17)	H(10A)-C(10)-H(10B)	109.5
C(35)-H(35)	0.95	C(9)-C(10)-H(10C)	109.5
C(36)-H(36)	0.95	H(10A)-C(10)-H(10C)	109.5
C(41)-C(42)	1.3951(16)	H(10B)-C(10)-H(10C)	109.5
C(41)-C(46)	1.3996(16)	C(12)-C(11)-C(16)	118.33(11)
C(42)-C(43)	1.3906(16)	C(12)-C(11)-P(1)	120.47(9)
C(42)-H(42)	0.95	C(16)-C(11)-P(1)	120.62(8)
C(43)-C(44)	1.3866(17)	C(13)-C(12)-C(11)	120.95(11)
C(43)-H(43)	0.95	C(13)-C(12)-H(12)	119.5
C(44)-C(45)	1.3889(18)	C(11)-C(12)-H(12)	119.5
C(44)-H(44)	0.95	C(12)-C(13)-C(14)	120.13(11)
C(45)-C(46)	1.3903(16)	C(12)-C(13)-H(13)	119.9
C(45)-H(45)	0.95	C(14)-C(13)-H(13)	119.9
C(46)-H(46)	0.95	C(13)-C(14)-C(15)	119.49(11)
C(51)-C(56)	1.3988(16)	C(13)-C(14)-H(14)	120.3
C(51)-C(52)	1.4019(16)	C(15)-C(14)-H(14)	120.3
C(52)-C(53)	1.3879(17)	C(16)-C(15)-C(14)	120.56(11)
C(52)-H(52)	0.95	C(16)-C(15)-H(15)	119.7

C(53)-C(54)	1.3883(18)	C(14)-C(15)-H(15)	119.7
C(53)-H(53)	0.95	C(15)-C(16)-C(11)	120.53(11)
C(54)-C(55)	1.3901(18)	C(15)-C(16)-H(16)	119.7
C(54)-H(54)	0.95	C(11)-C(16)-H(16)	119.7
C(55)-C(56)	1.3916(17)	C(26)-C(21)-C(22)	118.70(10)
C(55)-H(55)	0.95	C(26)-C(21)-P(1)	115.85(9)
C(56)-H(56)	0.95	C(22)-C(21)-P(1)	125.45(9)
C(61)-C(62)	1.3958(16)	C(23)-C(22)-C(21)	120.29(11)
C(61)-C(66)	1.4000(16)	C(23)-C(22)-H(22)	119.9
C(62)-C(63)	1.3930(17)	C(21)-C(22)-H(22)	119.9
C(62)-H(62)	0.95	C(22)-C(23)-C(24)	120.24(12)
C(63)-C(64)	1.3854(18)	C(22)-C(23)-H(23)	119.9
C(63)-H(63)	0.95	C(24)-C(23)-H(23)	119.9
C(64)-C(65)	1.3886(18)	C(25)-C(24)-C(23)	120.01(11)
C(64)-H(64)	0.95	C(25)-C(24)-H(24)	120
C(65)-C(66)	1.3904(17)	C(23)-C(24)-H(24)	120
C(65)-H(65)	0.95	C(24)-C(25)-C(26)	120.02(11)
C(66)-H(66)	0.95	C(24)-C(25)-H(25)	120
C(71)-C(76)	1.3989(16)	C(26)-C(25)-H(25)	120
C(71)-C(72)	1.3992(16)	C(25)-C(26)-C(21)	120.73(11)
C(72)-C(73)	1.3862(17)	C(25)-C(26)-H(26)	119.6
C(72)-H(72)	0.95	C(21)-C(26)-H(26)	119.6
C(73)-C(74)	1.3862(17)	C(36)-C(31)-C(32)	118.10(11)
C(73)-H(73)	0.95	C(36)-C(31)-P(2)	121.93(9)
C(74)-C(75)	1.3910(17)	C(32)-C(31)-P(2)	119.51(9)
C(74)-H(74)	0.95	C(33)-C(32)-C(31)	120.95(11)
C(75)-C(76)	1.3886(17)	C(33)-C(32)-H(32)	119.5
C(75)-H(75)	0.95	C(31)-C(32)-H(32)	119.5
C(76)-H(76)	0.95	C(32)-C(33)-C(34)	120.32(11)
C(81)-C(86)	1.3946(17)	C(32)-C(33)-H(33)	119.8
C(81)-C(82)	1.4035(16)	C(34)-C(33)-H(33)	119.8
C(82)-C(83)	1.3886(17)	C(33)-C(34)-C(35)	119.57(11)
C(82)-H(82)	0.95	C(33)-C(34)-H(34)	120.2
C(83)-C(84)	1.390(2)	C(35)-C(34)-H(34)	120.2
C(83)-H(83)	0.95	C(34)-C(35)-C(36)	120.18(11)
C(84)-C(85)	1.383(2)	C(34)-C(35)-H(35)	119.9
C(84)-H(84)	0.95	C(36)-C(35)-H(35)	119.9
C(85)-C(86)	1.3912(18)	C(35)-C(36)-C(31)	120.86(11)
C(85)-H(85)	0.95	C(35)-C(36)-H(36)	119.6
C(86)-H(86)	0.95	C(31)-C(36)-H(36)	119.6
		C(42)-C(41)-C(46)	118.42(10)
		C(42)-C(41)-P(2)	116.14(8)
		C(46)-C(41)-P(2)	125.44(9)

C(43)-C(42)-C(41)	120.83(11)
C(43)-C(42)-H(42)	119.6
C(41)-C(42)-H(42)	119.6
C(44)-C(43)-C(42)	119.93(11)
C(44)-C(43)-H(43)	120
C(42)-C(43)-H(43)	120
C(43)-C(44)-C(45)	120.16(11)
C(43)-C(44)-H(44)	119.9
C(45)-C(44)-H(44)	119.9
C(44)-C(45)-C(46)	119.69(11)
C(44)-C(45)-H(45)	120.2
C(46)-C(45)-H(45)	120.2
C(45)-C(46)-C(41)	120.91(11)
C(45)-C(46)-H(46)	119.5
C(41)-C(46)-H(46)	119.5
C(56)-C(51)-C(52)	118.00(11)
C(56)-C(51)-P(3)	121.46(9)
C(52)-C(51)-P(3)	120.12(9)
C(53)-C(52)-C(51)	121.05(11)
C(53)-C(52)-H(52)	119.5
C(51)-C(52)-H(52)	119.5
C(52)-C(53)-C(54)	120.28(11)
C(52)-C(53)-H(53)	119.9
C(54)-C(53)-H(53)	119.9
C(53)-C(54)-C(55)	119.46(11)
C(53)-C(54)-H(54)	120.3
C(55)-C(54)-H(54)	120.3
C(54)-C(55)-C(56)	120.29(11)
C(54)-C(55)-H(55)	119.9
C(56)-C(55)-H(55)	119.9
C(55)-C(56)-C(51)	120.88(11)
C(55)-C(56)-H(56)	119.6
C(51)-C(56)-H(56)	119.6
C(62)-C(61)-C(66)	118.42(11)
C(62)-C(61)-P(3)	115.78(8)
C(66)-C(61)-P(3)	125.77(9)
C(63)-C(62)-C(61)	120.74(11)
C(63)-C(62)-H(62)	119.6
C(61)-C(62)-H(62)	119.6
C(64)-C(63)-C(62)	120.07(12)
C(64)-C(63)-H(63)	120
C(62)-C(63)-H(63)	120
C(63)-C(64)-C(65)	120.00(11)

C(63)-C(64)-H(64)	120
C(65)-C(64)-H(64)	120
C(64)-C(65)-C(66)	119.90(11)
C(64)-C(65)-H(65)	120.1
C(66)-C(65)-H(65)	120.1
C(65)-C(66)-C(61)	120.85(11)
C(65)-C(66)-H(66)	119.6
C(61)-C(66)-H(66)	119.6
C(76)-C(71)-C(72)	118.37(11)
C(76)-C(71)-P(4)	120.30(9)
C(72)-C(71)-P(4)	120.76(9)
C(73)-C(72)-C(71)	120.75(11)
C(73)-C(72)-H(72)	119.6
C(71)-C(72)-H(72)	119.6
C(74)-C(73)-C(72)	120.48(11)
C(74)-C(73)-H(73)	119.8
C(72)-C(73)-H(73)	119.8
C(73)-C(74)-C(75)	119.38(11)
C(73)-C(74)-H(74)	120.3
C(75)-C(74)-H(74)	120.3
C(76)-C(75)-C(74)	120.36(11)
C(76)-C(75)-H(75)	119.8
C(74)-C(75)-H(75)	119.8
C(75)-C(76)-C(71)	120.64(11)
C(75)-C(76)-H(76)	119.7
C(71)-C(76)-H(76)	119.7
C(86)-C(81)-C(82)	118.41(11)
C(86)-C(81)-P(4)	115.72(9)
C(82)-C(81)-P(4)	125.85(9)
C(83)-C(82)-C(81)	120.43(12)
C(83)-C(82)-H(82)	119.8
C(81)-C(82)-H(82)	119.8
C(82)-C(83)-C(84)	120.28(12)
C(82)-C(83)-H(83)	119.9
C(84)-C(83)-H(83)	119.9
C(85)-C(84)-C(83)	119.88(12)
C(85)-C(84)-H(84)	120.1
C(83)-C(84)-H(84)	120.1
C(84)-C(85)-C(86)	119.98(12)
C(84)-C(85)-H(85)	120
C(86)-C(85)-H(85)	120
C(85)-C(86)-C(81)	121.01(12)
C(85)-C(86)-H(86)	119.5

C(81)-C(86)-H(86)	119.5	

Table A15. Anisotropic displacement parameters ($A^2 \times 10^3$) for PNP-n-Pent. The anisotropic displacement factor exponent takes the form: -2 pi [h^2 a*^2 U11 + ... + 2 h k a* b* U12]

	U11	U22	U33	U23	U13	U12
N(1)	15(1)	17(1)	14(1)	-6(1)	-3(1)	-3(1)
N(2)	15(1)	18(1)	12(1)	-1(1)	-3(1)	-3(1)
P(1)	14(1)	14(1)	14(1)	-3(1)	-4(1)	-2(1)
P(2)	15(1)	15(1)	13(1)	-4(1)	-2(1)	-2(1)
P(3)	15(1)	16(1)	12(1)	-2(1)	-4(1)	-2(1)
P(4)	14(1)	16(1)	13(1)	-3(1)	-3(1)	-3(1)
C(1)	20(1)	17(1)	16(1)	-7(1)	-6(1)	-1(1)
C(2)	19(1)	20(1)	17(1)	-6(1)	-7(1)	0(1)
C(3)	21(1)	21(1)	18(1)	-6(1)	-7(1)	-2(1)
C(4)	29(1)	25(1)	21(1)	-5(1)	-12(1)	-3(1)
C(5)	54(1)	34(1)	24(1)	-6(1)	-19(1)	-14(1)
C(6)	18(1)	18(1)	12(1)	0(1)	-4(1)	-2(1)
C(7)	17(1)	21(1)	13(1)	-3(1)	-3(1)	-2(1)
C(8)	17(1)	27(1)	13(1)	-2(1)	-4(1)	-2(1)
C(9)	22(1)	37(1)	15(1)	-6(1)	-5(1)	-5(1)
C(10)	33(1)	56(1)	14(1)	-4(1)	-5(1)	-4(1)
C(11)	13(1)	16(1)	18(1)	-3(1)	-5(1)	-2(1)
C(12)	17(1)	20(1)	17(1)	-4(1)	-4(1)	-1(1)
C(13)	21(1)	18(1)	22(1)	1(1)	-7(1)	-2(1)
C(14)	20(1)	16(1)	30(1)	-6(1)	-10(1)	1(1)
C(15)	17(1)	22(1)	22(1)	-9(1)	-5(1)	0(1)
C(16)	16(1)	19(1)	17(1)	-4(1)	-5(1)	-2(1)
C(21)	14(1)	16(1)	13(1)	-4(1)	-2(1)	0(1)
C(22)	18(1)	18(1)	16(1)	-4(1)	-3(1)	-2(1)
C(23)	20(1)	28(1)	18(1)	-7(1)	-5(1)	-2(1)
C(24)	26(1)	30(1)	15(1)	-2(1)	-7(1)	4(1)
C(25)	28(1)	19(1)	19(1)	2(1)	-3(1)	0(1)
C(26)	20(1)	16(1)	18(1)	-3(1)	-2(1)	-2(1)
C(31)	17(1)	18(1)	12(1)	-5(1)	-5(1)	-1(1)
C(32)	19(1)	19(1)	18(1)	-6(1)	-4(1)	-4(1)
C(33)	16(1)	26(1)	23(1)	-11(1)	-5(1)	-1(1)
C(34)	23(1)	23(1)	24(1)	-10(1)	-11(1)	5(1)
C(35)	27(1)	18(1)	20(1)	-3(1)	-11(1)	-2(1)
C(36)	19(1)	20(1)	15(1)	-4(1)	-6(1)	-3(1)
C(41)	16(1)	17(1)	14(1)	-3(1)	-3(1)	-3(1)
C(42)	15(1)	17(1)	19(1)	-6(1)	-4(1)	-1(1)
C(43)	20(1)	16(1)	24(1)	-2(1)	-7(1)	-2(1)

C(44)	22(1)	23(1)	18(1)	1(1)	-5(1)	-4(1)
C(45)	25(1)	24(1)	15(1)	-5(1)	-2(1)	-2(1)
C(46)	25(1)	17(1)	17(1)	-4(1)	-3(1)	0(1)
C(51)	17(1)	18(1)	11(1)	-3(1)	-4(1)	-1(1)
C(52)	19(1)	18(1)	18(1)	-2(1)	-6(1)	-2(1)
C(53)	16(1)	25(1)	20(1)	-3(1)	-5(1)	-1(1)
C(54)	22(1)	22(1)	18(1)	-6(1)	-4(1)	3(1)
C(55)	27(1)	18(1)	18(1)	-6(1)	-2(1)	-2(1)
C(56)	19(1)	21(1)	16(1)	-5(1)	-1(1)	-4(1)
C(61)	14(1)	18(1)	15(1)	-5(1)	-3(1)	-2(1)
C(62)	18(1)	19(1)	17(1)	-3(1)	-3(1)	-2(1)
C(63)	24(1)	18(1)	24(1)	-6(1)	-1(1)	-4(1)
C(64)	23(1)	26(1)	25(1)	-13(1)	-3(1)	-6(1)
C(65)	24(1)	28(1)	20(1)	-8(1)	-10(1)	-2(1)
C(66)	24(1)	18(1)	19(1)	-4(1)	-8(1)	0(1)
C(71)	13(1)	18(1)	15(1)	-3(1)	-2(1)	-2(1)
C(72)	20(1)	21(1)	17(1)	-6(1)	-5(1)	-2(1)
C(73)	22(1)	23(1)	16(1)	-2(1)	-6(1)	1(1)
C(74)	23(1)	17(1)	22(1)	-3(1)	-3(1)	0(1)
C(75)	22(1)	21(1)	22(1)	-9(1)	-4(1)	-2(1)
C(76)	17(1)	22(1)	17(1)	-6(1)	-4(1)	-2(1)
C(81)	16(1)	19(1)	16(1)	-6(1)	-6(1)	0(1)
C(82)	22(1)	24(1)	17(1)	-5(1)	-6(1)	-3(1)
C(83)	25(1)	36(1)	16(1)	-6(1)	-5(1)	-1(1)
C(84)	31(1)	37(1)	23(1)	-16(1)	-11(1)	5(1)
C(85)	33(1)	28(1)	32(1)	-16(1)	-13(1)	-1(1)
C(86)	23(1)	22(1)	24(1)	-7(1)	-8(1)	-2(1)

Appendix B

Table B1: Atomic coordinates (x 10^4) and equivalent isotropic displacement parameters ($Å^2$ x 10^3) for [$PtCl_2$(PNP-Ethyl)] U(eq) is defined as one third of the trace of the orthogonalize Uij tensor.

	x	y	z	U(eq)
Pt(1)	793(1)	2199(1)	1119(1)	12(1)
Cl(1)	1833(1)	971(1)	492(1)	24(1)
Cl(2)	3016(1)	2541(1)	1486(1)	22(1)
N(1)	-2034(3)	3042(4)	1375(1)	13(1)
P(1)	-1455(1)	2220(1)	877(1)	12(1)
P(2)	-485(1)	3170(1)	1680(1)	12(1)
C(1)	-3483(4)	3383(5)	1545(2)	17(1)
C(2)	-4015(5)	4766(5)	1371(2)	24(1)
C(11)	-2396(4)	634(4)	818(2)	15(1)
C(12)	-3855(5)	602(5)	700(2)	17(1)
C(13)	-4537(5)	-647(5)	650(2)	21(1)
C(14)	-3782(5)	-1848(5)	722(2)	22(1)
C(15)	-2352(5)	-1821(5)	846(2)	21(1)
C(16)	-1660(5)	-589(5)	893(2)	18(1)
C(21)	-1907(4)	3247(4)	359(2)	14(1)
C(22)	-1742(5)	4669(5)	380(2)	20(1)
C(23)	-2092(5)	5496(5)	-10(2)	25(1)
C(24)	-2608(5)	4915(5)	-424(2)	22(1)
C(25)	-2710(5)	3487(5)	-458(2)	25(1)
C(26)	-2341(4)	2665(5)	-70(2)	19(1)
C(31)	-197(4)	4928(5)	1838(2)	15(1)
C(32)	-881(5)	5523(5)	2228(2)	21(1)
C(33)	-724(5)	6911(6)	2311(2)	24(1)
C(34)	126(5)	7709(5)	2015(2)	28(1)
C(35)	821(5)	7132(6)	1631(2)	31(1)
C(36)	669(5)	5734(5)	1545(2)	24(1)
C(41)	-654(4)	2240(5)	2238(2)	16(1)
C(42)	-1651(4)	1163(5)	2286(2)	17(1)
C(43)	-1693(5)	390(5)	2705(2)	21(1)
C(44)	-741(5)	640(5)	3070(2)	26(1)
C(45)	260(5)	1682(6)	3019(2)	28(1)
C(46)	300(5)	2480(5)	2609(2)	23(1)

Table B2. Bond lengths [Å] and angles [°] for [$PtCl_2$(PNP-Ethyl)].

Atoms	Bond length (Å)	Atoms	Bond angle (°)
Pt(1)-P(2)	2.1854(12)	P(2)-Pt(1)-P(1)	72.12(4)
Pt(1)-P(1)	2.2099(11)	P(2)-Pt(1)-Cl(1)	171.02(4)
Pt(1)-Cl(1)	2.3328(12)	P(1)-Pt(1)-Cl(1)	99.99(4)

Pt(1)-Cl(2)	2.3428(10)	P(2)-Pt(1)-Cl(2)	96.43(4)
N(1)-C(1)	1.475(5)	P(1)-Pt(1)-Cl(2)	167.91(4)
N(1)-P(2)	1.686(3)	Cl(1)-Pt(1)-Cl(2)	91.70(4)
N(1)-P(1)	1.692(4)	C(1)-N(1)-P(2)	127.7(3)
P(1)-C(11)	1.791(4)	C(1)-N(1)-P(1)	131.7(3)
P(1)-C(21)	1.807(4)	P(2)-N(1)-P(1)	99.96(18)
P(1)-P(2)	2.5874(16)	N(1)-P(1)-C(11)	109.16(19)
P(2)-C(31)	1.793(5)	N(1)-P(1)-C(21)	108.40(19)
P(2)-C(41)	1.809(5)	C(11)-P(1)-C(21)	107.0(2)
C(1)-C(2)	1.520(6)	N(1)-P(1)-Pt(1)	93.41(12)
C(1)-H(1A)	0.99	C(11)-P(1)-Pt(1)	119.26(14)
C(1)-H(1B)	0.99	C(21)-P(1)-Pt(1)	118.16(13)
C(2)-H(2A)	0.98	N(1)-P(1)-P(2)	39.93(11)
C(2)-H(2B)	0.98	C(11)-P(1)-P(2)	124.27(14)
C(2)-H(2C)	0.98	C(21)-P(1)-P(2)	124.97(16)
C(11)-C(16)	1.396(6)	Pt(1)-P(1)-P(2)	53.50(3)
C(11)-C(12)	1.405(6)	N(1)-P(2)-C(31)	108.95(19)
C(12)-C(13)	1.385(7)	N(1)-P(2)-C(41)	108.72(18)
C(12)-H(12)	0.95	C(31)-P(2)-C(41)	106.5(2)
C(13)-C(14)	1.385(7)	N(1)-P(2)-Pt(1)	94.46(13)
C(13)-H(13)	0.95	C(31)-P(2)-Pt(1)	120.61(15)
C(14)-C(15)	1.382(7)	C(41)-P(2)-Pt(1)	116.41(15)
C(14)-H(14)	0.95	N(1)-P(2)-P(1)	40.10(12)
C(15)-C(16)	1.373(6)	C(31)-P(2)-P(1)	127.50(15)
C(15)-H(15)	0.95	C(41)-P(2)-P(1)	122.19(16)
C(16)-H(16)	0.95	Pt(1)-P(2)-P(1)	54.38(4)
C(21)-C(26)	1.385(6)	N(1)-C(1)-C(2)	113.6(3)
C(21)-C(22)	1.400(6)	N(1)-C(1)-H(1A)	108.9
C(22)-C(23)	1.394(6)	C(2)-C(1)-H(1A)	108.9
C(22)-H(22)	0.95	N(1)-C(1)-H(1B)	108.9
C(23)-C(24)	1.374(7)	C(2)-C(1)-H(1B)	108.9
C(23)-H(23)	0.95	H(1A)-C(1)-H(1B)	107.7
C(24)-C(25)	1.402(7)	C(1)-C(2)-H(2A)	109.5
C(24)-H(24)	0.95	C(1)-C(2)-H(2B)	109.5
C(25)-C(26)	1.390(6)	H(2A)-C(2)-H(2B)	109.5
C(25)-H(25)	0.95	C(1)-C(2)-H(2C)	109.5
C(26)-H(26)	0.95	H(2A)-C(2)-H(2C)	109.5
C(31)-C(32)	1.388(7)	H(2B)-C(2)-H(2C)	109.5
C(31)-C(36)	1.395(6)	C(16)-C(11)-C(12)	119.7(4)
C(32)-C(33)	1.385(8)	C(16)-C(11)-P(1)	119.0(3)
C(32)-H(32)	0.95	C(12)-C(11)-P(1)	121.3(3)
C(33)-C(34)	1.385(7)	C(13)-C(12)-C(11)	119.5(4)
C(33)-H(33)	0.95	C(13)-C(12)-H(12)	120.3

C(34)-C(35)	1.372(8)	C(11)-C(12)-H(12)	120.3
C(34)-H(34)	0.95	C(12)-C(13)-C(14)	119.8(4)
C(35)-C(36)	1.395(8)	C(12)-C(13)-H(13)	120.1
C(35)-H(35)	0.95	C(14)-C(13)-H(13)	120.1
C(36)-H(36)	0.95	C(15)-C(14)-C(13)	121.0(4)
C(41)-C(46)	1.384(6)	C(15)-C(14)-H(14)	119.5
C(41)-C(42)	1.414(6)	C(13)-C(14)-H(14)	119.5
C(42)-C(43)	1.390(6)	C(16)-C(15)-C(14)	119.8(4)
C(42)-H(42)	0.95	C(16)-C(15)-H(15)	120.1
C(43)-C(44)	1.376(7)	C(14)-C(15)-H(15)	120.1
C(43)-H(43)	0.95	C(15)-C(16)-C(11)	120.2(4)
C(44)-C(45)	1.391(7)	C(15)-C(16)-H(16)	119.9
C(44)-H(44)	0.95	C(11)-C(16)-H(16)	119.9
C(45)-C(46)	1.383(6)	C(26)-C(21)-C(22)	118.5(4)
C(45)-H(45)	0.95	C(26)-C(21)-P(1)	122.0(3)
C(46)-H(46)	0.95	C(22)-C(21)-P(1)	119.5(4)
		C(23)-C(22)-C(21)	121.1(5)
		C(23)-C(22)-H(22)	119.4
		C(21)-C(22)-H(22)	119.4
		C(24)-C(23)-C(22)	119.9(4)
		C(24)-C(23)-H(23)	120.1
		C(22)-C(23)-H(23)	120.1
		C(23)-C(24)-C(25)	119.5(4)
		C(23)-C(24)-H(24)	120.3
		C(25)-C(24)-H(24)	120.3
		C(26)-C(25)-C(24)	120.4(5)
		C(26)-C(25)-H(25)	119.8
		C(24)-C(25)-H(25)	119.8
		C(21)-C(26)-C(25)	120.4(4)
		C(21)-C(26)-H(26)	119.8
		C(25)-C(26)-H(26)	119.8
		C(32)-C(31)-C(36)	119.3(4)
		C(32)-C(31)-P(2)	121.6(3)
		C(36)-C(31)-P(2)	119.0(4)
		C(33)-C(32)-C(31)	119.5(4)
		C(33)-C(32)-H(32)	120.3
		C(31)-C(32)-H(32)	120.3
		C(32)-C(33)-C(34)	120.9(5)
		C(32)-C(33)-H(33)	119.6
		C(34)-C(33)-H(33)	119.6
		C(35)-C(34)-C(33)	120.3(5)
		C(35)-C(34)-H(34)	119.9
		C(33)-C(34)-H(34)	119.9

C(34)-C(35)-C(36)	119.2(5)
C(34)-C(35)-H(35)	120.4
C(36)-C(35)-H(35)	120.4
C(31)-C(36)-C(35)	120.8(5)
C(31)-C(36)-H(36)	119.6
C(35)-C(36)-H(36)	119.6
C(46)-C(41)-C(42)	118.9(4)
C(46)-C(41)-P(2)	120.0(3)
C(42)-C(41)-P(2)	120.8(3)
C(43)-C(42)-C(41)	120.1(4)
C(43)-C(42)-H(42)	119.9
C(41)-C(42)-H(42)	119.9
C(44)-C(43)-C(42)	120.4(4)
C(44)-C(43)-H(43)	119.8
C(42)-C(43)-H(43)	119.8
C(43)-C(44)-C(45)	119.3(4)
C(43)-C(44)-H(44)	120.3
C(45)-C(44)-H(44)	120.3
C(46)-C(45)-C(44)	121.1(4)
C(46)-C(45)-H(45)	119.5
C(44)-C(45)-H(45)	119.5
C(45)-C(46)-C(41)	120.1(4)
C(45)-C(46)-H(46)	119.9
C(41)-C(46)-H(46)	119.9

Table B3. Anisotropic displacement parameters ($A^2 \times 10^3$) for [$PtCl_2$(PNP-Ethyl)]. The anisotropic displacement factor exponent takes the form: -2 pi [h^2 a*^2 U11 + ... + 2 h k a* b* U12]

	U11	U22	U33	U23	U13	U12
Pt(1)	11(1)	13(1)	13(1)	1(1)	1(1)	1(1)
Cl(1)	25(1)	22(1)	24(1)	-4(1)	8(1)	5(1)
Cl(2)	12(1)	30(1)	26(1)	7(1)	-5(1)	-2(1)
N(1)	10(2)	15(2)	13(2)	-2(2)	-2(1)	1(1)
P(1)	12(1)	12(1)	13(1)	0(1)	-1(1)	0(1)
P(2)	10(1)	15(1)	12(1)	-1(1)	0(1)	0(1)
C(1)	10(2)	19(2)	20(2)	1(2)	2(2)	2(2)
C(2)	18(2)	21(2)	33(3)	3(2)	2(2)	2(2)
C(11)	18(2)	13(2)	12(2)	1(2)	-1(2)	1(2)
C(12)	17(2)	18(2)	15(2)	3(2)	-2(2)	0(2)
C(13)	20(2)	24(2)	19(2)	-1(2)	-3(2)	-6(2)
C(14)	29(2)	16(2)	20(2)	0(2)	2(2)	-6(2)
C(15)	29(2)	12(2)	20(2)	-1(2)	2(2)	0(2)
C(16)	18(2)	17(2)	18(2)	0(2)	-1(2)	3(2)

C(21)	11(2)	15(2)	17(2)	2(2)	0(2)	0(2)
C(22)	28(2)	16(2)	15(2)	-1(2)	2(2)	2(2)
C(23)	35(3)	17(2)	21(3)	6(2)	9(2)	4(2)
C(24)	20(2)	30(3)	15(2)	10(2)	1(2)	1(2)
C(25)	27(2)	35(3)	14(2)	5(2)	-3(2)	-8(2)
C(26)	21(2)	19(2)	18(2)	-1(2)	-2(2)	-4(2)
C(31)	13(2)	17(2)	16(2)	-3(2)	-2(2)	0(2)
C(32)	21(2)	26(3)	15(2)	-1(2)	1(2)	0(2)
C(33)	24(2)	28(3)	21(3)	-11(2)	-1(2)	6(2)
C(34)	26(2)	18(2)	40(3)	-9(2)	-4(2)	-1(2)
C(35)	33(3)	22(3)	38(3)	-3(2)	11(2)	-7(2)
C(36)	22(2)	25(3)	26(3)	-7(2)	6(2)	-4(2)
C(41)	15(2)	18(2)	15(2)	2(2)	2(2)	4(2)
C(42)	17(2)	18(2)	16(2)	-2(2)	-1(2)	1(2)
C(43)	23(2)	18(2)	22(3)	5(2)	4(2)	1(2)
C(44)	40(3)	22(3)	15(2)	5(2)	0(2)	5(2)
C(45)	37(3)	34(3)	14(2)	0(2)	-11(2)	-1(2)
C(46)	22(2)	26(3)	20(2)	0(2)	-4(2)	-1(2)

Table B4: Atomic coordinates (x 10^4) and equivalent isotropic displacement parameters ($Å^2$ x 10^3) for [$PtCl_2$(PNP-n-Prop)] U(eq) is defined as one third of the trace of the orthogonalize Uij tensor.

	X	Y	z	U(eq)
Pt	2501(1)	3089(1)	3575(1)	10(1)
N(1)	3830(2)	2063(1)	2470(2)	12(1)
P(1)	2719(1)	1947(1)	3301(1)	11(1)
P(2)	3954(1)	2961(1)	2493(1)	11(1)
Cl(1)	1004(1)	2921(1)	4754(1)	18(1)
Cl(2)	2300(1)	4334(1)	3623(1)	19(1)
C(1)	4307(3)	1512(2)	1788(2)	15(1)
C(2)	5540(3)	1170(2)	2238(2)	21(1)
C(3)	5846(3)	545(2)	1546(2)	21(1)
C(11)	1349(3)	1525(2)	2579(2)	13(1)
C(12)	1292(3)	799(2)	2354(2)	18(1)
C(13)	254(3)	522(2)	1714(2)	21(1)
C(14)	-725(3)	960(2)	1286(2)	21(1)
C(15)	-678(3)	1684(2)	1507(2)	20(1)
C(16)	354(3)	1966(2)	2150(2)	17(1)
C(21)	3394(3)	1385(2)	4372(2)	12(1)
C(22)	4622(3)	1542(2)	4831(2)	19(1)
C(23)	5195(3)	1152(2)	5679(2)	19(1)
C(24)	4550(3)	600(2)	6087(2)	19(1)
C(25)	3329(3)	446(2)	5647(3)	26(1)
C(26)	2738(3)	839(2)	4798(2)	21(1)

C(31)	5551(3)	3252(2)	2956(2)	13(1)
C(32)	6533(3)	3154(2)	2338(2)	17(1)
C(33)	7734(3)	3393(2)	2709(3)	23(1)
C(34)	7957(3)	3746(2)	3668(3)	25(1)
C(35)	6988(3)	3859(2)	4269(3)	21(1)
C(36)	5776(3)	3606(2)	3920(2)	16(1)
C(41)	3704(3)	3267(2)	1144(2)	12(1)
C(42)	2932(3)	2874(2)	390(2)	15(1)
C(43)	2749(3)	3095(2)	-655(2)	16(1)
C(44)	3346(3)	3702(2)	-948(2)	17(1)
C(45)	4088(3)	4102(2)	-201(2)	18(1)
C(46)	4272(3)	3889(2)	847(2)	17(1)

Table B5. Bond lengths [Å] and angles [°] for [$PtCl_2$(PNP-n-Prop)].

Atoms	Bond length (Å)	Atoms	Bond angle (°)
Pt-P(1)	2.1932(7)	P(1)-Pt-P(2)	72.40(3)
Pt-P(2)	2.2121(7)	P(1)-Pt-Cl(1)	93.70(3)
Pt-Cl(1)	2.3461(7)	P(2)-Pt-Cl(1)	165.96(3)
Pt-Cl(2)	2.3528(7)	P(1)-Pt-Cl(2)	172.11(3)
N(1)-C(1)	1.484(3)	P(2)-Pt-Cl(2)	101.35(3)
N(1)-P(2)	1.695(2)	Cl(1)-Pt-Cl(2)	92.67(3)
N(1)-P(1)	1.699(2)	C(1)-N(1)-P(2)	132.48(19)
P(1)-C(21)	1.804(3)	C(1)-N(1)-P(1)	126.38(19)
P(1)-C(11)	1.804(3)	P(2)-N(1)-P(1)	100.11(12)
P(1)-P(2)	2.6020(10)	N(1)-P(1)-C(21)	107.92(12)
P(2)-C(41)	1.804(3)	N(1)-P(1)-C(11)	108.52(12)
P(2)-C(31)	1.810(3)	C(21)-P(1)-C(11)	110.26(14)
C(1)-C(2)	1.507(4)	N(1)-P(1)-Pt	94.02(8)
C(1)-H(1A)	0.99	C(21)-P(1)-Pt	119.51(10)
C(1)-H(1B)	0.99	C(11)-P(1)-Pt	114.70(10)
C(2)-C(3)	1.530(4)	N(1)-P(1)-P(2)	39.89(8)
C(2)-H(2A)	0.99	C(21)-P(1)-P(2)	123.93(10)
C(2)-H(2B)	0.99	C(11)-P(1)-P(2)	122.36(10)
C(3)-H(3A)	0.98	Pt-P(1)-P(2)	54.13(2)
C(3)-H(3B)	0.98	N(1)-P(2)-C(41)	107.43(13)
C(3)-H(3C)	0.98	N(1)-P(2)-C(31)	111.98(13)
C(11)-C(12)	1.395(4)	C(41)-P(2)-C(31)	103.49(13)
C(11)-C(16)	1.400(4)	N(1)-P(2)-Pt	93.46(8)
C(12)-C(13)	1.388(4)	C(41)-P(2)-Pt	122.17(9)
C(12)-H(12)	0.95	C(31)-P(2)-Pt	117.65(10)
C(13)-C(14)	1.385(4)	N(1)-P(2)-P(1)	40.00(8)
C(13)-H(13)	0.95	C(41)-P(2)-P(1)	126.30(10)

C(14)-C(15)	1.389(4)	C(31)-P(2)-P(1)	126.28(10)
C(14)-H(14)	0.95	Pt-P(2)-P(1)	53.46(2)
C(15)-C(16)	1.389(4)	N(1)-C(1)-C(2)	114.9(2)
C(15)-H(15)	0.95	N(1)-C(1)-H(1A)	108.6
C(16)-H(16)	0.95	C(2)-C(1)-H(1A)	108.6
C(21)-C(26)	1.390(4)	N(1)-C(1)-H(1B)	108.6
C(21)-C(22)	1.393(4)	C(2)-C(1)-H(1B)	108.6
C(22)-C(23)	1.383(4)	H(1A)-C(1)-H(1B)	107.5
C(22)-H(22)	0.95	C(1)-C(2)-C(3)	110.3(3)
C(23)-C(24)	1.383(4)	C(1)-C(2)-H(2A)	109.6
C(23)-H(23)	0.95	C(3)-C(2)-H(2A)	109.6
C(24)-C(25)	1.378(4)	C(1)-C(2)-H(2B)	109.6
C(24)-H(24)	0.95	C(3)-C(2)-H(2B)	109.6
C(25)-C(26)	1.394(4)	H(2A)-C(2)-H(2B)	108.1
C(25)-H(25)	0.95	C(2)-C(3)-H(3A)	109.5
C(26)-H(26)	0.95	C(2)-C(3)-H(3B)	109.5
C(31)-C(36)	1.394(4)	H(3A)-C(3)-H(3B)	109.5
C(31)-C(32)	1.399(4)	C(2)-C(3)-H(3C)	109.5
C(32)-C(33)	1.379(4)	H(3A)-C(3)-H(3C)	109.5
C(32)-H(32)	0.95	H(3B)-C(3)-H(3C)	109.5
C(33)-C(34)	1.387(5)	C(12)-C(11)-C(16)	119.2(3)
C(33)-H(33)	0.95	C(12)-C(11)-P(1)	123.2(2)
C(34)-C(35)	1.377(5)	C(16)-C(11)-P(1)	117.4(2)
C(34)-H(34)	0.95	C(13)-C(12)-C(11)	120.0(3)
C(35)-C(36)	1.392(4)	C(13)-C(12)-H(12)	120
C(35)-H(35)	0.95	C(11)-C(12)-H(12)	120
C(36)-H(36)	0.95	C(14)-C(13)-C(12)	120.6(3)
C(41)-C(46)	1.391(4)	C(14)-C(13)-H(13)	119.7
C(41)-C(42)	1.394(4)	C(12)-C(13)-H(13)	119.7
C(42)-C(43)	1.388(4)	C(13)-C(14)-C(15)	119.8(3)
C(42)-H(42)	0.95	C(13)-C(14)-H(14)	120.1
C(43)-C(44)	1.381(4)	C(15)-C(14)-H(14)	120.1
C(43)-H(43)	0.95	C(16)-C(15)-C(14)	120.0(3)
C(44)-C(45)	1.380(4)	C(16)-C(15)-H(15)	120
C(44)-H(44)	0.95	C(14)-C(15)-H(15)	120
C(45)-C(46)	1.386(4)	C(15)-C(16)-C(11)	120.4(3)
C(45)-H(45)	0.95	C(15)-C(16)-H(16)	119.8
C(46)-H(46)	0.95	C(11)-C(16)-H(16)	119.8
		C(26)-C(21)-C(22)	118.8(3)
		C(26)-C(21)-P(1)	124.0(2)
		C(22)-C(21)-P(1)	117.1(2)
		C(23)-C(22)-C(21)	120.9(3)
		C(23)-C(22)-H(22)	119.6

C(21)-C(22)-H(22)	119.6
C(22)-C(23)-C(24)	120.2(3)
C(22)-C(23)-H(23)	119.9
C(24)-C(23)-H(23)	119.9
C(25)-C(24)-C(23)	119.4(3)
C(25)-C(24)-H(24)	120.3
C(23)-C(24)-H(24)	120.3
C(24)-C(25)-C(26)	120.9(3)
C(24)-C(25)-H(25)	119.6
C(26)-C(25)-H(25)	119.6
C(21)-C(26)-C(25)	119.8(3)
C(21)-C(26)-H(26)	120.1
C(25)-C(26)-H(26)	120.1
C(36)-C(31)-C(32)	120.3(3)
C(36)-C(31)-P(2)	118.8(2)
C(32)-C(31)-P(2)	120.9(2)
C(33)-C(32)-C(31)	119.2(3)
C(33)-C(32)-H(32)	120.4
C(31)-C(32)-H(32)	120.4
C(32)-C(33)-C(34)	120.4(3)
C(32)-C(33)-H(33)	119.8
C(34)-C(33)-H(33)	119.8
C(35)-C(34)-C(33)	120.7(3)
C(35)-C(34)-H(34)	119.7
C(33)-C(34)-H(34)	119.7
C(34)-C(35)-C(36)	119.8(3)
C(34)-C(35)-H(35)	120.1
C(36)-C(35)-H(35)	120.1
C(35)-C(36)-C(31)	119.6(3)
C(35)-C(36)-H(36)	120.2
C(31)-C(36)-H(36)	120.2
C(46)-C(41)-C(42)	119.8(3)
C(46)-C(41)-P(2)	120.8(2)
C(42)-C(41)-P(2)	119.4(2)
C(43)-C(42)-C(41)	120.1(3)
C(43)-C(42)-H(42)	119.9
C(41)-C(42)-H(42)	119.9
C(44)-C(43)-C(42)	119.7(3)
C(44)-C(43)-H(43)	120.1
C(42)-C(43)-H(43)	120.1
C(45)-C(44)-C(43)	120.3(3)
C(45)-C(44)-H(44)	119.8
C(43)-C(44)-H(44)	119.8

C(44)-C(45)-C(46)	120.5(3)
C(44)-C(45)-H(45)	119.7
C(46)-C(45)-H(45)	119.7
C(45)-C(46)-C(41)	119.5(3)
C(45)-C(46)-H(46)	120.2
C(41)-C(46)-H(46)	120.2

Table B6. Anisotropic displacement parameters ($A^2 \times 10^3$) for [$PtCl_2$(PNP-n-Prop)]. The anisotropic displacement factor exponent takes the form: -2 pi [$h^2 a^{*2} U11 + ... + 2 h k a^* b^* U12$]

	U11	U22	U33	U23	U13	U12
Pt	10(1)	10(1)	10(1)	0(1)	2(1)	1(1)
N(1)	15(1)	10(1)	13(1)	1(1)	6(1)	1(1)
P(1)	11(1)	11(1)	10(1)	0(1)	3(1)	0(1)
P(2)	10(1)	11(1)	10(1)	1(1)	1(1)	1(1)
Cl(1)	18(1)	21(1)	18(1)	-1(1)	9(1)	1(1)
Cl(2)	24(1)	12(1)	23(1)	0(1)	2(1)	2(1)
C(1)	18(2)	14(2)	15(2)	-1(1)	7(1)	-1(1)
C(2)	23(2)	21(2)	18(2)	1(1)	1(1)	3(1)
C(3)	25(2)	12(2)	26(2)	2(1)	10(1)	5(1)
C(11)	13(1)	18(2)	8(1)	0(1)	3(1)	-2(1)
C(12)	17(2)	18(2)	19(2)	-2(1)	4(1)	0(1)
C(13)	23(2)	19(2)	22(2)	-6(1)	6(1)	-6(1)
C(14)	16(2)	33(2)	15(2)	-3(1)	2(1)	-8(1)
C(15)	17(2)	30(2)	14(2)	3(1)	1(1)	-1(1)
C(16)	16(2)	17(2)	19(2)	-1(1)	2(1)	-1(1)
C(21)	15(1)	11(1)	12(1)	0(1)	4(1)	2(1)
C(22)	18(2)	19(2)	19(2)	7(1)	2(1)	-5(1)
C(23)	13(2)	24(2)	20(2)	5(1)	0(1)	-4(1)
C(24)	23(2)	17(2)	17(2)	6(1)	2(1)	4(1)
C(25)	30(2)	22(2)	25(2)	10(1)	2(1)	-10(1)
C(26)	16(2)	25(2)	20(2)	3(1)	0(1)	-4(1)
C(31)	12(1)	13(1)	15(2)	5(1)	1(1)	-2(1)
C(32)	18(2)	17(2)	18(2)	7(1)	3(1)	2(1)
C(33)	15(2)	21(2)	32(2)	13(1)	4(1)	2(1)
C(34)	14(2)	20(2)	38(2)	15(1)	-8(1)	-4(1)
C(35)	25(2)	14(2)	19(2)	4(1)	-10(1)	-2(1)
C(36)	18(2)	14(2)	14(2)	4(1)	-2(1)	0(1)
C(41)	13(1)	13(1)	11(1)	1(1)	2(1)	3(1)
C(42)	18(2)	11(1)	16(2)	0(1)	0(1)	1(1)
C(43)	21(2)	16(2)	11(1)	-4(1)	0(1)	3(1)
C(44)	18(2)	22(2)	10(1)	2(1)	0(1)	8(1)
C(45)	18(2)	18(2)	19(2)	7(1)	2(1)	-5(1)
C(46)	16(2)	15(2)	18(2)	1(1)	-4(1)	-2(1)

Table B7: Atomic coordinates (x 10^4) and equivalent isotropic displacement parameters (A^2 x 10^3) for [$PtCl_2$(PNP-Dimprop)]. U(eq) is defined as one third of the trace of the orthogonalized Uij tensor.

	X	Y	z	U(eq)
Pt(1)	3624(1)	2445(1)	1179(1)	9(1)
N(1)	6146(7)	2040(4)	2021(4)	19(2)
P(1)	4586(2)	2235(2)	2314(1)	16(1)
P(2)	5801(2)	2291(2)	1092(1)	16(1)
Cl(1)	1375(2)	2345(2)	1444(1)	22(1)
Cl(2)	2963(2)	2726(2)	-92(1)	21(1)
C(1A)	7350(20)	1874(13)	2601(12)	21(4)
C(2A)	8050(20)	2587(11)	2899(12)	19(2)
C(3A)	7990(30)	3530(20)	2714(16)	19(2)
C(4A)	7660(20)	932(15)	2675(11)	19(2)
C(5A)	9540(30)	2410(20)	3229(13)	19(2)
C(1B)	7590(20)	1884(16)	2332(12)	19(2)
C(2B)	8404(19)	2590(10)	2545(10)	15(3)
C(3B)	7860(30)	3580(20)	2586(16)	19(2)
C(4B)	7890(20)	948(15)	2475(11)	19(2)
C(5B)	9610(30)	2420(20)	3063(13)	19(2)
C(11)	3996(8)	1287(6)	2837(5)	20(2)
C(12)	3063(9)	1458(6)	3347(5)	22(2)
C(13)	2543(9)	753(6)	3738(5)	24(2)
C(14)	2957(9)	-119(6)	3613(5)	22(2)
C(15)	3846(9)	-292(6)	3082(5)	24(2)
C(16)	4359(9)	411(6)	2688(5)	21(2)
C(21)	4664(8)	3161(5)	2962(5)	16(2)
C(22)	4340(9)	4028(6)	2687(5)	22(2)
C(23)	4470(9)	4760(6)	3149(5)	25(2)
C(24)	4982(9)	4654(6)	3895(5)	27(2)
C(25)	5298(9)	3801(6)	4174(5)	25(2)
C(26)	5150(9)	3058(6)	3712(5)	22(2)
C(31)	6729(8)	3262(5)	826(5)	19(2)
C(32)	8081(9)	3203(6)	704(5)	22(2)
C(33)	8806(9)	3976(6)	571(5)	26(2)
C(34)	8175(10)	4806(6)	549(5)	29(2)
C(35)	6820(11)	4874(6)	647(5)	29(2)
C(36)	6101(9)	4093(6)	786(5)	22(2)
C(41)	6323(8)	1378(5)	506(5)	19(2)
C(42)	6356(9)	493(6)	760(5)	23(2)
C(43)	6659(9)	-199(6)	280(5)	24(2)
C(44)	6916(8)	-7(6)	-444(5)	23(2)
C(45)	6857(9)	876(6)	-705(5)	23(2)
C(46)	6561(8)	1569(5)	-231(5)	21(2)

Table B8. Bond lengths [Å] and angles [°] for [$PtCl_2$(PNP-Dimprop)].

Atoms	Bond length (Å)	Atoms	Bond angle (°)
Pt(1)-P(1)	2.205(2)	P(1)-Pt(1)-P(2)	72.26(8)
Pt(1)-P(2)	2.211(2)	P(1)-Pt(1)-Cl(1)	98.84(8)
Pt(1)-Cl(1)	2.347(2)	P(2)-Pt(1)-Cl(1)	167.75(8)
Pt(1)-Cl(2)	2.362(2)	P(1)-Pt(1)-Cl(2)	170.31(8)
N(1)-C(1B)	1.52(2)	P(2)-Pt(1)-Cl(2)	98.42(8)
N(1)-C(1A)	1.55(2)	Cl(1)-Pt(1)-Cl(2)	90.76(8)
N(1)-P(1)	1.716(7)	C(1B)-N(1)-C(1A)	20.9(8)
N(1)-P(2)	1.720(7)	C(1B)-N(1)-P(1)	140.7(9)
P(1)-C(21)	1.800(8)	C(1A)-N(1)-P(1)	120.0(9)
P(1)-C(11)	1.819(8)	C(1B)-N(1)-P(2)	119.7(9)
P(1)-P(2)	2.604(3)	C(1A)-N(1)-P(2)	140.4(9)
P(2)-C(31)	1.801(8)	P(1)-N(1)-P(2)	98.6(4)
P(2)-C(41)	1.820(8)	N(1)-P(1)-C(21)	109.7(4)
C(1A)-C(2A)	1.35(3)	N(1)-P(1)-C(11)	111.9(4)
C(1A)-C(4A)	1.43(3)	C(21)-P(1)-C(11)	104.6(4)
C(1A)-H(1A)	0.98	N(1)-P(1)-Pt(1)	94.4(2)
C(2A)-C(3A)	1.44(3)	C(21)-P(1)-Pt(1)	118.9(3)
C(2A)-C(5A)	1.58(4)	C(11)-P(1)-Pt(1)	117.0(3)
C(2A)-H(2A)	0.98	N(1)-P(1)-P(2)	40.8(2)
C(3A)-H(3A1)	0.96	C(21)-P(1)-P(2)	121.7(3)
C(3A)-H(3A2)	0.96	C(11)-P(1)-P(2)	131.2(3)
C(3A)-H(3A3)	0.96	Pt(1)-P(1)-P(2)	53.98(7)
C(4A)-H(4A1)	0.96	N(1)-P(2)-C(31)	111.5(4)
C(4A)-H(4A2)	0.96	N(1)-P(2)-C(41)	111.0(4)
C(4A)-H(4A3)	0.96	C(31)-P(2)-C(41)	105.1(4)
C(5A)-H(5A1)	0.96	N(1)-P(2)-Pt(1)	94.1(3)
C(5A)-H(5A2)	0.96	C(31)-P(2)-Pt(1)	118.0(3)
C(5A)-H(5A3)	0.96	C(41)-P(2)-Pt(1)	116.9(3)
C(1B)-C(2B)	1.36(3)	N(1)-P(2)-P(1)	40.6(2)
C(1B)-C(4B)	1.44(3)	C(31)-P(2)-P(1)	122.6(3)
C(1B)-H(1B)	0.98	C(41)-P(2)-P(1)	130.0(3)
C(2B)-C(5B)	1.49(3)	Pt(1)-P(2)-P(1)	53.76(7)
C(2B)-C(3B)	1.57(3)	C(2A)-C(1A)-C(4A)	128.8(19)
C(2B)-H(2B)	0.98	C(2A)-C(1A)-N(1)	119.4(16)
C(3B)-H(3B1)	0.96	C(4A)-C(1A)-N(1)	111.4(14)
C(3B)-H(3B2)	0.96	C(2A)-C(1A)-H(1A)	92.2
C(3B)-H(3B3)	0.96	C(4A)-C(1A)-H(1A)	92.2
C(4B)-H(4B1)	0.96	N(1)-C(1A)-H(1A)	92.2
C(4B)-H(4B2)	0.96	C(1A)-C(2A)-C(3A)	131.0(19)
C(4B)-H(4B3)	0.96	C(1A)-C(2A)-C(5A)	117.6(19)
C(5B)-H(5B1)	0.96	C(3A)-C(2A)-C(5A)	106(2)

C(5B)-H(5B2)	0.96	C(1A)-C(2A)-H(2A)	97.9
C(5B)-H(5B3)	0.96	C(3A)-C(2A)-H(2A)	97.9
C(11)-C(16)	1.383(12)	C(5A)-C(2A)-H(2A)	97.9
C(11)-C(12)	1.388(12)	C(2A)-C(3A)-H(3A1)	109.5
C(12)-C(13)	1.387(11)	C(2A)-C(3A)-H(3A2)	109.5
C(12)-H(12)	0.93	H(3A1)-C(3A)-H(3A2)	109.5
C(13)-C(14)	1.383(12)	C(2A)-C(3A)-H(3A3)	109.5
C(13)-H(13)	0.93	H(3A1)-C(3A)-H(3A3)	109.5
C(14)-C(15)	1.385(12)	H(3A2)-C(3A)-H(3A3)	109.5
C(14)-H(14)	0.93	C(1A)-C(4A)-H(4A1)	109.5
C(15)-C(16)	1.384(12)	C(1A)-C(4A)-H(4A2)	109.5
C(15)-H(15)	0.93	H(4A1)-C(4A)-H(4A2)	109.5
C(16)-H(16)	0.93	C(1A)-C(4A)-H(4A3)	109.5
C(21)-C(26)	1.404(12)	H(4A1)-C(4A)-H(4A3)	109.5
C(21)-C(22)	1.406(11)	H(4A2)-C(4A)-H(4A3)	109.5
C(22)-C(23)	1.368(12)	C(2A)-C(5A)-H(5A1)	109.5
C(22)-H(22)	0.93	C(2A)-C(5A)-H(5A2)	109.5
C(23)-C(24)	1.405(13)	H(5A1)-C(5A)-H(5A2)	109.5
C(23)-H(23)	0.93	C(2A)-C(5A)-H(5A3)	109.5
C(24)-C(25)	1.388(13)	H(5A1)-C(5A)-H(5A3)	109.5
C(24)-H(24)	0.93	H(5A2)-C(5A)-H(5A3)	109.5
C(25)-C(26)	1.381(12)	C(2B)-C(1B)-C(4B)	125.6(19)
C(25)-H(25)	0.93	C(2B)-C(1B)-N(1)	120.9(17)
C(26)-H(26)	0.93	C(4B)-C(1B)-N(1)	112.8(17)
C(31)-C(36)	1.383(12)	C(2B)-C(1B)-H(1B)	92.8
C(31)-C(32)	1.393(12)	C(4B)-C(1B)-H(1B)	92.8
C(32)-C(33)	1.390(12)	N(1)-C(1B)-H(1B)	92.8
C(32)-H(32)	0.93	C(1B)-C(2B)-C(5B)	119.0(18)
C(33)-C(34)	1.383(14)	C(1B)-C(2B)-C(3B)	121.9(19)
C(33)-H(33)	0.93	C(5B)-C(2B)-C(3B)	113.3(19)
C(34)-C(35)	1.388(14)	C(1B)-C(2B)-H(2B)	98
C(34)-H(34)	0.93	C(5B)-C(2B)-H(2B)	98
C(35)-C(36)	1.398(12)	C(3B)-C(2B)-H(2B)	98
C(35)-H(35)	0.93	C(2B)-C(3B)-H(3B1)	109.5
C(36)-H(36)	0.93	C(2B)-C(3B)-H(3B2)	109.5
C(41)-C(42)	1.390(12)	H(3B1)-C(3B)-H(3B2)	109.5
C(41)-C(46)	1.397(12)	C(2B)-C(3B)-H(3B3)	109.5
C(42)-C(43)	1.392(12)	H(3B1)-C(3B)-H(3B3)	109.5
C(42)-H(42)	0.93	H(3B2)-C(3B)-H(3B3)	109.5
C(43)-C(44)	1.380(13)	C(1B)-C(4B)-H(4B1)	109.5
C(43)-H(43)	0.93	C(1B)-C(4B)-H(4B2)	109.5
C(44)-C(45)	1.391(12)	H(4B1)-C(4B)-H(4B2)	109.5
C(44)-H(44)	0.93	C(1B)-C(4B)-H(4B3)	109.5

C(45)-C(46)	1.384(11)	H(4B1)-C(4B)-H(4B3)	109.5
C(45)-H(45)	0.93	H(4B2)-C(4B)-H(4B3)	109.5
C(46)-H(46)	0.93	C(2B)-C(5B)-H(5B1)	109.5
		C(2B)-C(5B)-H(5B2)	109.5
		H(5B1)-C(5B)-H(5B2)	109.5
		C(2B)-C(5B)-H(5B3)	109.5
		H(5B1)-C(5B)-H(5B3)	109.5
		H(5B2)-C(5B)-H(5B3)	109.5
		C(16)-C(11)-C(12)	120.2(8)
		C(16)-C(11)-P(1)	121.6(6)
		C(12)-C(11)-P(1)	117.9(6)
		C(13)-C(12)-C(11)	120.1(8)
		C(13)-C(12)-H(12)	120
		C(11)-C(12)-H(12)	120
		C(14)-C(13)-C(12)	119.5(8)
		C(14)-C(13)-H(13)	120.3
		C(12)-C(13)-H(13)	120.3
		C(13)-C(14)-C(15)	120.4(8)
		C(13)-C(14)-H(14)	119.8
		C(15)-C(14)-H(14)	119.8
		C(16)-C(15)-C(14)	120.1(8)
		C(16)-C(15)-H(15)	119.9
		C(14)-C(15)-H(15)	119.9
		C(11)-C(16)-C(15)	119.6(8)
		C(11)-C(16)-H(16)	120.2
		C(15)-C(16)-H(16)	120.2
		C(26)-C(21)-C(22)	119.3(7)
		C(26)-C(21)-P(1)	122.2(6)
		C(22)-C(21)-P(1)	118.3(6)
		C(23)-C(22)-C(21)	120.4(8)
		C(23)-C(22)-H(22)	119.8
		C(21)-C(22)-H(22)	119.8
		C(22)-C(23)-C(24)	120.0(8)
		C(22)-C(23)-H(23)	120
		C(24)-C(23)-H(23)	120
		C(25)-C(24)-C(23)	120.0(8)
		C(25)-C(24)-H(24)	120
		C(23)-C(24)-H(24)	120
		C(26)-C(25)-C(24)	120.2(9)
		C(26)-C(25)-H(25)	119.9
		C(24)-C(25)-H(25)	119.9
		C(25)-C(26)-C(21)	120.1(8)
		C(25)-C(26)-H(26)	120

C(21)-C(26)-H(26)	120
C(36)-C(31)-C(32)	119.5(8)
C(36)-C(31)-P(2)	118.9(6)
C(32)-C(31)-P(2)	121.4(6)
C(33)-C(32)-C(31)	120.3(8)
C(33)-C(32)-H(32)	119.9
C(31)-C(32)-H(32)	119.9
C(34)-C(33)-C(32)	119.7(9)
C(34)-C(33)-H(33)	120.1
C(32)-C(33)-H(33)	120.1
C(33)-C(34)-C(35)	120.7(8)
C(33)-C(34)-H(34)	119.7
C(35)-C(34)-H(34)	119.7
C(34)-C(35)-C(36)	119.1(9)
C(34)-C(35)-H(35)	120.4
C(36)-C(35)-H(35)	120.4
C(31)-C(36)-C(35)	120.6(9)
C(31)-C(36)-H(36)	119.7
C(35)-C(36)-H(36)	119.7
C(42)-C(41)-C(46)	120.2(8)
C(42)-C(41)-P(2)	120.9(7)
C(46)-C(41)-P(2)	118.6(6)
C(41)-C(42)-C(43)	119.6(8)
C(41)-C(42)-H(42)	120.2
C(43)-C(42)-H(42)	120.2
C(44)-C(43)-C(42)	120.1(8)
C(44)-C(43)-H(43)	119.9
C(42)-C(43)-H(43)	119.9
C(43)-C(44)-C(45)	120.4(8)
C(43)-C(44)-H(44)	119.8
C(45)-C(44)-H(44)	119.8
C(46)-C(45)-C(44)	119.9(8)
C(46)-C(45)-H(45)	120.1
C(44)-C(45)-H(45)	120.1
C(45)-C(46)-C(41)	119.8(8)
C(45)-C(46)-H(46)	120.1
C(41)-C(46)-H(46)	120.1

Table B9. Anisotropic displacement parameters ($A^2 \times 10^3$) for [$PtCl_2$(PNP-Dimprop)]. The anisotropic displacement factor exponent takes the form: -2 pi [h^2 a*^2 U11 + ... + 2 h k a* b* U12]

	U11	U22	U33	U23	U13	U12
Pt(1)	6(1)	7(1)	13(1)	0(1)	-4(1)	0(1)
N(1)	22(4)	14(3)	22(4)	3(3)	-3(3)	-2(3)
P(1)	14(1)	19(1)	13(1)	5(1)	-5(1)	-1(1)
P(2)	14(1)	15(1)	19(1)	0(1)	2(1)	1(1)
Cl(1)	13(1)	26(1)	27(1)	1(1)	5(1)	2(1)
Cl(2)	22(1)	26(1)	15(1)	0(1)	-4(1)	3(1)
C(1A)	23(11)	16(8)	24(12)	-1(8)	1(8)	-7(7)
C(2A)	15(3)	26(3)	15(6)	5(4)	-5(3)	-1(2)
C(3A)	15(3)	26(3)	15(6)	5(4)	-5(3)	-1(2)
C(4A)	15(3)	26(3)	15(6)	5(4)	-5(3)	-1(2)
C(5A)	15(3)	26(3)	15(6)	5(4)	-5(3)	-1(2)
C(1B)	15(3)	26(3)	15(6)	5(4)	-5(3)	-1(2)
C(2B)	19(9)	14(8)	11(8)	5(6)	0(7)	-6(6)
C(3B)	15(3)	26(3)	15(6)	5(4)	-5(3)	-1(2)
C(4B)	15(3)	26(3)	15(6)	5(4)	-5(3)	-1(2)
C(5B)	15(3)	26(3)	15(6)	5(4)	-5(3)	-1(2)
C(11)	16(4)	26(4)	15(4)	6(3)	-3(3)	-1(3)
C(12)	27(5)	16(4)	22(4)	3(3)	-1(4)	-2(3)
C(13)	24(5)	25(4)	22(4)	3(3)	5(4)	-1(4)
C(14)	26(5)	19(4)	20(4)	5(3)	-5(4)	-9(3)
C(15)	25(5)	19(4)	27(5)	6(4)	-1(4)	6(4)
C(16)	18(4)	25(4)	20(4)	1(3)	2(3)	0(3)
C(21)	14(4)	13(4)	22(4)	-9(3)	1(3)	2(3)
C(22)	21(5)	24(4)	19(4)	-3(3)	-2(3)	2(4)
C(23)	22(5)	14(4)	42(6)	1(4)	10(4)	1(3)
C(24)	25(5)	23(4)	33(5)	-10(4)	5(4)	-5(4)
C(25)	17(4)	34(5)	23(5)	-9(4)	-3(3)	-1(4)
C(26)	19(4)	22(4)	25(4)	-4(3)	1(4)	4(3)
C(31)	20(4)	15(4)	22(4)	-4(3)	4(3)	-9(3)
C(32)	26(5)	26(4)	14(4)	3(3)	-1(3)	-4(4)
C(33)	24(5)	38(5)	15(4)	3(4)	-1(3)	-11(4)
C(34)	41(6)	27(5)	19(4)	4(4)	-4(4)	-20(4)
C(35)	48(6)	19(4)	20(5)	-1(4)	0(4)	-5(4)
C(36)	21(5)	26(5)	19(4)	2(3)	0(3)	-4(4)
C(41)	11(4)	18(4)	28(5)	-7(3)	-1(3)	5(3)
C(42)	25(5)	19(4)	23(5)	-1(3)	-1(4)	-2(4)
C(43)	19(4)	18(4)	34(5)	-4(4)	-3(4)	0(3)
C(44)	16(4)	22(4)	32(5)	-8(4)	5(4)	-1(3)
C(45)	21(5)	26(4)	23(4)	-5(3)	2(4)	-1(4)
C(46)	19(4)	16(4)	28(5)	-2(3)	3(4)	-1(3)

APPENDIX B

Table B10: Atomic coordinates (x 10^4) and equivalent isotropic displacement parameters ($Å^2$ x 10^3) for [$PtCl_2$(PNP-i-Pent)]. U(eq) is defined as one third of the trace of the orthogonalize Uij tensor.

	X	Y	z	U(eq)
Pt(1)	3705(1)	2500	6180(1)	13(1)
N(1)	3257(2)	2500	2918(4)	16(1)
P(5)	3403(1)	1753(1)	4185(1)	13(1)
Cl(1)	4004(1)	1532(1)	8006(1)	23(1)
C(1A)	3037(3)	2500	1219(7)	33(1)
C(1B)	3037(3)	2500	1219(7)	33(1)
C(2)	2416(5)	2179(5)	831(13)	51(3)
C(3A)	1832(4)	2500	1479(10)	56(2)
C(3B)	1832(4)	2500	1479(10)	56(2)
C(4)	1219(6)	2017(9)	1320(20)	106(6)
C(5)	1652(5)	1712(7)	458(17)	70(4)
C(11)	3995(1)	1114(2)	3327(4)	15(1)
C(12)	4409(2)	1363(2)	2115(4)	20(1)
C(13)	4901(2)	881(2)	1581(4)	24(1)
C(14)	4978(2)	155(2)	2241(4)	24(1)
C(15)	4564(2)	-97(2)	3431(4)	21(1)
C(16)	4074(2)	381(2)	3989(4)	19(1)
C(21)	2685(2)	1178(2)	4466(4)	17(1)
C(22)	2536(2)	560(2)	3467(4)	23(1)
C(23)	1978(2)	134(2)	3722(5)	28(1)
C(24)	1562(2)	328(2)	4967(5)	26(1)
C(25)	1703(2)	942(2)	5951(5)	30(1)
C(26)	2268(2)	1362(2)	5723(5)	26(1)

Table B11. Bond lengths [Å] and angles [°] for [$PtCl_2$(PNP-i-Pent)].

Atoms	Bond length (Å)	Atoms	Bond angle (°)
Pt(1)-P(5)	2.2007(8)	P(5)-Pt(1)-P(5)#1	72.21(4)
Pt(1)-P(5)#1	2.2007(8)	P(5)-Pt(1)-Cl(1)#1	170.39(3)
Pt(1)-Cl(1)#1	2.3511(8)	P(5)#1-Pt(1)-Cl(1)#1	98.23(3)
Pt(1)-Cl(1)	2.3511(8)	P(5)-Pt(1)-Cl(1)	98.23(3)
N(1)-C(1A)	1.488(7)	P(5)#1-Pt(1)-Cl(1)	170.39(3)
N(1)-P(5)#1	1.699(3)	Cl(1)#1-Pt(1)-Cl(1)	91.30(4)
N(1)-P(5)	1.699(3)	C(1A)-N(1)-P(5)#1	130.24(10)
P(5)-C(11)	1.800(3)	C(1A)-N(1)-P(5)	130.24(10)
P(5)-C(21)	1.804(3)	P(5)#1-N(1)-P(5)	99.5(2)
P(5)-P(5)#1	2.5935(15)	N(1)-P(5)-C(11)	110.10(16)
C(1A)-C(2)	1.437(10)	N(1)-P(5)-C(21)	110.97(16)
C(1A)-H(1A1)	0.97	C(11)-P(5)-C(21)	105.63(14)
C(1A)-H(1A2)	0.97	N(1)-P(5)-Pt(1)	94.06(10)

C(2)-C(3A)	1.435(12)	C(11)-P(5)-Pt(1)	118.09(10)
C(2)-H(2A)	0.97	C(21)-P(5)-Pt(1)	117.47(11)
C(2)-H(2B)	0.97	N(1)-P(5)-P(5)#1	40.27(10)
C(3A)-C(4)	1.524(12)	C(11)-P(5)-P(5)#1	128.04(10)
C(3A)-C(5)#1	1.654(12)	C(21)-P(5)-P(5)#1	123.64(10)
C(3A)-H(3A)	0.98	Pt(1)-P(5)-P(5)#1	53.90(2)
C(4)-H(4A)	0.96	C(2)-C(1A)-N(1)	119.1(6)
C(4)-H(4B)	0.96	C(2)-C(1A)-H(1A1)	107.5
C(4)-H(4C)	0.96	N(1)-C(1A)-H(1A1)	107.5
C(5)-H(5A)	0.96	C(2)-C(1A)-H(1A2)	107.5
C(5)-H(5B)	0.96	N(1)-C(1A)-H(1A2)	107.5
C(5)-H(5C)	0.96	H(1A1)-C(1A)-H(1A2)	107
C(11)-C(12)	1.393(4)	C(3A)-C(2)-C(1A)	121.1(8)
C(11)-C(16)	1.397(4)	C(3A)-C(2)-H(2A)	107.1
C(12)-C(13)	1.390(4)	C(1A)-C(2)-H(2A)	107.1
C(12)-H(12)	0.93	C(3A)-C(2)-H(2B)	107.1
C(13)-C(14)	1.384(5)	C(1A)-C(2)-H(2B)	107.1
C(13)-H(13)	0.93	H(2A)-C(2)-H(2B)	106.8
C(14)-C(15)	1.382(5)	C(2)-C(3A)-C(4)	116.9(7)
C(14)-H(14)	0.93	C(2)-C(3A)-C(5)#1	108.5(8)
C(15)-C(16)	1.388(4)	C(4)-C(3A)-C(5)#1	102.9(8)
C(15)-H(15)	0.93	C(2)-C(3A)-H(3A)	109.4
C(16)-H(16)	0.93	C(4)-C(3A)-H(3A)	109.4
C(21)-C(22)	1.393(4)	C(5)#1-C(3A)-H(3A)	109.4
C(21)-C(26)	1.395(5)	C(3A)-C(4)-H(4A)	109.5
C(22)-C(23)	1.386(5)	C(3A)-C(4)-H(4B)	109.5
C(22)-H(22)	0.93	H(4A)-C(4)-H(4B)	109.5
C(23)-C(24)	1.389(5)	C(3A)-C(4)-H(4C)	109.5
C(23)-H(23)	0.93	H(4A)-C(4)-H(4C)	109.5
C(24)-C(25)	1.376(5)	H(4B)-C(4)-H(4C)	109.5
C(24)-H(24)	0.93	H(5A)-C(5)-H(5B)	109.5
C(25)-C(26)	1.390(5)	H(5A)-C(5)-H(5C)	109.5
C(25)-H(25)	0.93	H(5B)-C(5)-H(5C)	109.5
C(26)-H(26)	0.93	C(12)-C(11)-C(16)	119.8(3)
		C(12)-C(11)-P(5)	121.0(2)
		C(16)-C(11)-P(5)	118.9(2)
		C(13)-C(12)-C(11)	119.7(3)
		C(13)-C(12)-H(12)	120.2
		C(11)-C(12)-H(12)	120.2
		C(14)-C(13)-C(12)	120.3(3)
		C(14)-C(13)-H(13)	119.8
		C(12)-C(13)-H(13)	119.8
		C(15)-C(14)-C(13)	120.2(3)

C(15)-C(14)-H(14)	119.9
C(13)-C(14)-H(14)	119.9
C(14)-C(15)-C(16)	120.2(3)
C(14)-C(15)-H(15)	119.9
C(16)-C(15)-H(15)	119.9
C(15)-C(16)-C(11)	119.8(3)
C(15)-C(16)-H(16)	120.1
C(11)-C(16)-H(16)	120.1
C(22)-C(21)-C(26)	119.3(3)
C(22)-C(21)-P(5)	122.0(2)
C(26)-C(21)-P(5)	118.7(2)
C(23)-C(22)-C(21)	120.2(3)
C(23)-C(22)-H(22)	119.9
C(21)-C(22)-H(22)	119.9
C(22)-C(23)-C(24)	120.0(3)
C(22)-C(23)-H(23)	120
C(24)-C(23)-H(23)	120
C(25)-C(24)-C(23)	120.2(3)
C(25)-C(24)-H(24)	119.9
C(23)-C(24)-H(24)	119.9
C(24)-C(25)-C(26)	120.1(3)
C(24)-C(25)-H(25)	119.9
C(26)-C(25)-H(25)	119.9
C(25)-C(26)-C(21)	120.2(3)
C(25)-C(26)-H(26)	119.9
C(21)-C(26)-H(26)	119.9

Table B12. Anisotropic displacement parameters ($A^2 \times 10^3$) for [$PtCl_2$(PNP-i-Pent)]. The anisotropic displacement factor exponent takes the form: -2 pi [h^2 a*^2 U11 + ... + 2 h k a* b* U12]

	U11	U22	U33	U23	U13	U12
Pt(1)	17(1)	9(1)	12(1)	0	2(1)	0
N(1)	16(2)	15(2)	16(2)	0	1(1)	0
P(5)	14(1)	11(1)	14(1)	-1(1)	3(1)	-1(1)
Cl(1)	39(1)	13(1)	18(1)	3(1)	-3(1)	2(1)
C(2)	56(6)	34(4)	62(6)	12(4)	-25(5)	-12(4)
C(4)	45(7)	82(10)	190(20)	12(11)	26(9)	-30(7)
C(5)	40(6)	68(8)	103(10)	-19(7)	-24(6)	-3(5)
C(11)	14(1)	15(1)	15(1)	-5(1)	-2(1)	1(1)
C(12)	20(2)	17(2)	21(2)	-1(1)	3(1)	1(1)
C(13)	21(2)	26(2)	25(2)	-5(1)	7(1)	3(1)
C(14)	19(2)	25(2)	28(2)	-8(1)	-2(1)	8(1)
C(15)	23(2)	17(2)	24(2)	-3(1)	-8(1)	4(1)
C(16)	23(2)	16(1)	17(2)	-1(1)	-3(1)	0(1)

C(21)	17(1)	13(1)	22(2)	3(1)	1(1)	-2(1)
C(22)	23(2)	24(2)	21(2)	-4(1)	1(1)	-5(1)
C(23)	26(2)	25(2)	34(2)	-2(2)	-6(2)	-10(1)
C(24)	18(2)	26(2)	34(2)	12(2)	-2(1)	-7(1)
C(25)	25(2)	28(2)	37(2)	6(2)	12(2)	-5(1)
C(26)	26(2)	19(2)	31(2)	-3(1)	9(2)	-6(1)

Table B13: Atomic coordinates (x 10^4) and equivalent isotropic displacement parameters ($Å^2$ x 10^3) for [$PtCl_2$(PNP-Cychex)] U(eq) is defined as one third of the trace of the orthogonalize Uij tensor.

	X	Y	z	U(eq)
Pt(1)	-448(1)	1975(1)	1712(1)	7(1)
N(1)	-655(2)	2664(2)	-81(2)	7(1)
P(1)	525(1)	2170(1)	552(1)	7(1)
P(2)	-1713(1)	2568(1)	615(1)	6(1)
Cl(1)	1145(1)	1300(1)	2657(1)	16(1)
Cl(2)	-1720(1)	1895(1)	2825(1)	16(1)
C(11)	881(3)	1312(2)	-43(2)	8(1)
C(12)	1979(3)	921(2)	279(2)	14(1)
C(13)	2241(3)	234(2)	-119(2)	14(1)
C(14)	1422(3)	-73(2)	-847(2)	16(1)
C(15)	305(3)	298(2)	-1152(2)	15(1)
C(16)	32(3)	982(2)	-743(2)	12(1)
C(21)	1905(3)	2742(2)	758(2)	9(1)
C(22)	2100(3)	3231(2)	1520(2)	16(1)
C(23)	3151(3)	3681(2)	1708(2)	21(1)
C(24)	4027(3)	3632(2)	1145(2)	23(1)
C(25)	3830(3)	3164(2)	376(2)	18(1)
C(26)	2775(3)	2716(2)	178(2)	14(1)
C(31)	-2346(3)	3498(2)	826(2)	10(1)
C(32)	-3047(3)	3914(2)	117(2)	14(1)
C(33)	-3455(3)	4651(2)	276(3)	20(1)
C(34)	-3230(3)	4963(2)	1155(3)	22(1)
C(35)	-2588(3)	4534(2)	1866(3)	20(1)
C(36)	-2126(3)	3806(2)	1709(2)	14(1)
C(41)	-2993(3)	2003(2)	32(2)	9(1)
C(42)	-3287(3)	1925(2)	-916(2)	17(1)
C(43)	-4311(3)	1492(2)	-1304(2)	22(1)
C(44)	-5030(3)	1134(2)	-756(2)	16(1)
C(45)	-4734(3)	1206(2)	187(2)	13(1)
C(46)	-3722(3)	1639(2)	578(2)	12(1)
C(51)	-731(3)	3185(2)	-889(2)	7(1)

C(52)	-235(3)	2806(2)	-1681(2)	11(1)
C(53)	-485(3)	3339(2)	-2515(2)	14(1)
C(54)	82(3)	4143(2)	-2303(2)	16(1)
C(55)	-365(3)	4509(2)	-1487(2)	16(1)
C(56)	-125(3)	3974(2)	-648(2)	12(1)

Table B14 . Bond lengths [Å] and angles [°] for [$PtCl_2$(PNP-Cychex)].

Atoms	Bond length (Å)	Atoms	Bond angle (°)
Pt(1)-P(2)	2.2003(8)	P(2)-Pt(1)-P(1)	71.89(3)
Pt(1)-P(1)	2.2144(8)	P(2)-Pt(1)-Cl(1)	168.51(3)
Pt(1)-Cl(1)	2.3566(8)	P(1)-Pt(1)-Cl(1)	96.90(3)
Pt(1)-Cl(2)	2.3609(8)	P(2)-Pt(1)-Cl(2)	99.43(3)
N(1)-C(51)	1.489(4)	P(1)-Pt(1)-Cl(2)	171.16(3)
N(1)-P(1)	1.697(3)	Cl(1)-Pt(1)-Cl(2)	91.84(3)
N(1)-P(2)	1.704(3)	C(51)-N(1)-P(1)	132.5(2)
P(1)-C(21)	1.799(3)	C(51)-N(1)-P(2)	127.0(2)
P(1)-C(11)	1.801(3)	P(1)-N(1)-P(2)	99.31(13)
P(1)-P(2)	2.5916(11)	N(1)-P(1)-C(21)	111.47(14)
P(2)-C(31)	1.800(3)	N(1)-P(1)-C(11)	110.85(14)
P(2)-C(41)	1.808(3)	C(21)-P(1)-C(11)	106.17(15)
C(11)-C(16)	1.393(4)	N(1)-P(1)-Pt(1)	94.11(9)
C(11)-C(12)	1.399(4)	C(21)-P(1)-Pt(1)	117.98(11)
C(12)-C(13)	1.377(5)	C(11)-P(1)-Pt(1)	115.86(10)
C(12)-H(12)	0.95	N(1)-P(1)-P(2)	40.44(9)
C(13)-C(14)	1.385(5)	C(21)-P(1)-P(2)	129.72(11)
C(13)-H(13)	0.95	C(11)-P(1)-P(2)	122.00(10)
C(14)-C(15)	1.394(5)	Pt(1)-P(1)-P(2)	53.80(2)
C(14)-H(14)	0.95	N(1)-P(2)-C(31)	110.50(14)
C(15)-C(16)	1.384(5)	N(1)-P(2)-C(41)	109.26(13)
C(15)-H(15)	0.95	C(31)-P(2)-C(41)	105.42(14)
C(16)-H(16)	0.95	N(1)-P(2)-Pt(1)	94.42(9)
C(21)-C(22)	1.396(5)	C(31)-P(2)-Pt(1)	120.09(10)
C(21)-C(26)	1.403(4)	C(41)-P(2)-Pt(1)	116.42(11)
C(22)-C(23)	1.385(5)	N(1)-P(2)-P(1)	40.25(9)
C(22)-H(22)	0.95	C(31)-P(2)-P(1)	130.34(11)
C(23)-C(24)	1.392(5)	C(41)-P(2)-P(1)	120.98(11)
C(23)-H(23)	0.95	Pt(1)-P(2)-P(1)	54.30(2)
C(24)-C(25)	1.384(5)	C(16)-C(11)-C(12)	119.2(3)
C(24)-H(24)	0.95	C(16)-C(11)-P(1)	121.5(2)
C(25)-C(26)	1.388(5)	C(12)-C(11)-P(1)	118.8(2)
C(25)-H(25)	0.95	C(13)-C(12)-C(11)	120.3(3)
C(26)-H(26)	0.95	C(13)-C(12)-H(12)	119.8

C(31)-C(32)	1.390(4)	C(11)-C(12)-H(12)	119.8
C(31)-C(36)	1.395(4)	C(12)-C(13)-C(14)	120.3(3)
C(32)-C(33)	1.382(5)	C(12)-C(13)-H(13)	119.9
C(32)-H(32)	0.95	C(14)-C(13)-H(13)	119.9
C(33)-C(34)	1.391(5)	C(13)-C(14)-C(15)	119.9(3)
C(33)-H(33)	0.95	C(13)-C(14)-H(14)	120.1
C(34)-C(35)	1.377(5)	C(15)-C(14)-H(14)	120.1
C(34)-H(34)	0.95	C(16)-C(15)-C(14)	119.9(3)
C(35)-C(36)	1.391(5)	C(16)-C(15)-H(15)	120
C(35)-H(35)	0.95	C(14)-C(15)-H(15)	120
C(36)-H(36)	0.95	C(15)-C(16)-C(11)	120.2(3)
C(41)-C(46)	1.392(4)	C(15)-C(16)-H(16)	119.9
C(41)-C(42)	1.394(4)	C(11)-C(16)-H(16)	119.9
C(42)-C(43)	1.394(5)	C(22)-C(21)-C(26)	119.5(3)
C(42)-H(42)	0.95	C(22)-C(21)-P(1)	118.2(2)
C(43)-C(44)	1.381(5)	C(26)-C(21)-P(1)	122.4(2)
C(43)-H(43)	0.95	C(23)-C(22)-C(21)	120.3(3)
C(44)-C(45)	1.385(4)	C(23)-C(22)-H(22)	119.9
C(44)-H(44)	0.95	C(21)-C(22)-H(22)	119.9
C(45)-C(46)	1.385(4)	C(22)-C(23)-C(24)	119.8(3)
C(45)-H(45)	0.95	C(22)-C(23)-H(23)	120.1
C(46)-H(46)	0.95	C(24)-C(23)-H(23)	120.1
C(51)-C(56)	1.530(4)	C(25)-C(24)-C(23)	120.4(3)
C(51)-C(52)	1.531(4)	C(25)-C(24)-H(24)	119.8
C(51)-H(51)	1	C(23)-C(24)-H(24)	119.8
C(52)-C(53)	1.527(4)	C(24)-C(25)-C(26)	120.0(3)
C(52)-H(52A)	0.99	C(24)-C(25)-H(25)	120
C(52)-H(52B)	0.99	C(26)-C(25)-H(25)	120
C(53)-C(54)	1.532(5)	C(25)-C(26)-C(21)	119.9(3)
C(53)-H(53A)	0.99	C(25)-C(26)-H(26)	120
C(53)-H(53B)	0.99	C(21)-C(26)-H(26)	120
C(54)-C(55)	1.524(5)	C(32)-C(31)-C(36)	119.6(3)
C(54)-H(54A)	0.99	C(32)-C(31)-P(2)	120.7(2)
C(54)-H(54B)	0.99	C(36)-C(31)-P(2)	119.7(2)
C(55)-C(56)	1.535(5)	C(33)-C(32)-C(31)	120.1(3)
C(55)-H(55A)	0.99	C(33)-C(32)-H(32)	120
C(55)-H(55B)	0.99	C(31)-C(32)-H(32)	120
C(56)-H(56A)	0.99	C(32)-C(33)-C(34)	120.4(3)
C(56)-H(56B)	0.99	C(32)-C(33)-H(33)	119.8
		C(34)-C(33)-H(33)	119.8
		C(35)-C(34)-C(33)	119.5(3)
		C(35)-C(34)-H(34)	120.3
		C(33)-C(34)-H(34)	120.3

C(34)-C(35)-C(36)	120.7(3)
C(34)-C(35)-H(35)	119.6
C(36)-C(35)-H(35)	119.6
C(35)-C(36)-C(31)	119.6(3)
C(35)-C(36)-H(36)	120.2
C(31)-C(36)-H(36)	120.2
C(46)-C(41)-C(42)	119.4(3)
C(46)-C(41)-P(2)	116.9(2)
C(42)-C(41)-P(2)	123.7(2)
C(43)-C(42)-C(41)	119.6(3)
C(43)-C(42)-H(42)	120.2
C(41)-C(42)-H(42)	120.2
C(44)-C(43)-C(42)	120.7(3)
C(44)-C(43)-H(43)	119.7
C(42)-C(43)-H(43)	119.7
C(43)-C(44)-C(45)	119.9(3)
C(43)-C(44)-H(44)	120.1
C(45)-C(44)-H(44)	120.1
C(46)-C(45)-C(44)	119.9(3)
C(46)-C(45)-H(45)	120.1
C(44)-C(45)-H(45)	120.1
C(45)-C(46)-C(41)	120.7(3)
C(45)-C(46)-H(46)	119.7
C(41)-C(46)-H(46)	119.7
N(1)-C(51)-C(56)	112.8(2)
N(1)-C(51)-C(52)	112.6(3)
C(56)-C(51)-C(52)	110.9(3)
N(1)-C(51)-H(51)	106.7
C(56)-C(51)-H(51)	106.7
C(52)-C(51)-H(51)	106.7
C(53)-C(52)-C(51)	109.1(3)
C(53)-C(52)-H(52A)	109.9
C(51)-C(52)-H(52A)	109.9
C(53)-C(52)-H(52B)	109.9
C(51)-C(52)-H(52B)	109.9
H(52A)-C(52)-H(52B)	108.3
C(52)-C(53)-C(54)	111.7(3)
C(52)-C(53)-H(53A)	109.3
C(54)-C(53)-H(53A)	109.3
C(52)-C(53)-H(53B)	109.3
C(54)-C(53)-H(53B)	109.3
H(53A)-C(53)-H(53B)	107.9
C(55)-C(54)-C(53)	111.0(3)

C(55)-C(54)-H(54A)	109.4
C(53)-C(54)-H(54A)	109.4
C(55)-C(54)-H(54B)	109.4
C(53)-C(54)-H(54B)	109.4
H(54A)-C(54)-H(54B)	108
C(54)-C(55)-C(56)	111.2(3)
C(54)-C(55)-H(55A)	109.4
C(56)-C(55)-H(55A)	109.4
C(54)-C(55)-H(55B)	109.4
C(56)-C(55)-H(55B)	109.4
H(55A)-C(55)-H(55B)	108
C(51)-C(56)-C(55)	109.8(3)
C(51)-C(56)-H(56A)	109.7
C(55)-C(56)-H(56A)	109.7
C(51)-C(56)-H(56B)	109.7
C(55)-C(56)-H(56B)	109.7
H(56A)-C(56)-H(56B)	108.2

Table B15. Anisotropic displacement parameters ($A^2 \times 10^3$) for [$PtCl_2$(PNP-Cychex)]. The anisotropic displacement factor exponent takes the form: -2 pi [h^2 a*^2 U11 + ... + 2 h k a* b* U12]

	U11	U22	U33	U23	U13	U12
Pt(1)	8(1)	8(1)	5(1)	0(1)	0(1)	-1(1)
N(1)	6(1)	7(1)	7(1)	2(1)	1(1)	0(1)
P(1)	7(1)	8(1)	6(1)	-1(1)	0(1)	-1(1)
P(2)	7(1)	8(1)	5(1)	0(1)	1(1)	0(1)
Cl(1)	16(1)	17(1)	11(1)	1(1)	-5(1)	4(1)
Cl(2)	19(1)	20(1)	11(1)	4(1)	7(1)	-1(1)
C(11)	9(1)	8(2)	9(1)	0(1)	3(1)	-2(1)
C(12)	9(2)	14(2)	17(2)	-1(1)	0(1)	-2(1)
C(13)	9(2)	12(2)	23(2)	0(1)	5(1)	1(1)
C(14)	23(2)	7(2)	19(2)	-3(1)	10(1)	-3(1)
C(15)	20(2)	12(2)	11(2)	0(1)	-1(1)	-6(1)
C(16)	14(2)	12(2)	8(1)	1(1)	1(1)	-1(1)
C(21)	10(2)	8(2)	10(1)	2(1)	-1(1)	-1(1)
C(22)	18(2)	17(2)	12(2)	0(1)	0(1)	-3(1)
C(23)	29(2)	16(2)	14(2)	-1(2)	-8(2)	-9(2)
C(24)	17(2)	23(2)	24(2)	12(2)	-7(2)	-13(2)
C(25)	10(2)	19(2)	25(2)	9(2)	4(1)	-3(1)
C(26)	11(2)	13(2)	15(2)	3(1)	0(1)	1(1)
C(31)	7(1)	13(2)	11(2)	-2(1)	3(1)	-1(1)
C(32)	14(2)	19(2)	11(2)	4(1)	5(1)	4(1)
C(33)	14(2)	16(2)	30(2)	11(2)	8(2)	5(1)

C(34)	14(2)	9(2)	45(2)	-5(2)	11(2)	-2(1)
C(35)	14(2)	20(2)	26(2)	-13(2)	3(1)	-5(1)
C(36)	10(2)	15(2)	17(2)	-2(1)	3(1)	-3(1)
C(41)	7(1)	7(2)	12(2)	0(1)	1(1)	2(1)
C(42)	16(2)	22(2)	13(2)	3(2)	2(1)	-8(2)
C(43)	22(2)	37(2)	5(2)	3(2)	-2(1)	-10(2)
C(44)	10(2)	20(2)	16(2)	0(1)	-3(1)	-5(1)
C(45)	11(2)	18(2)	13(2)	0(1)	6(1)	-3(1)
C(46)	13(2)	15(2)	9(2)	-2(1)	4(1)	0(1)
C(51)	9(1)	7(2)	7(1)	1(1)	2(1)	0(1)
C(52)	13(2)	11(2)	9(2)	0(1)	2(1)	0(1)
C(53)	17(2)	17(2)	8(2)	0(1)	5(1)	-6(1)
C(54)	22(2)	16(2)	13(2)	4(1)	7(1)	-2(2)
C(55)	21(2)	13(2)	15(2)	1(1)	4(1)	-1(1)
C(56)	16(2)	10(2)	11(2)	-4(1)	4(1)	-3(1)

Table B7: Atomic coordinates (x 10^4) and equivalent isotropic displacement parameters ($Å^2$ x 10^3) for [$PdCl_2$(PNP-i-Prop)]. U(eq) is defined as one third of the trace of the orthogonalize Uij tensor.

	X	Y	z	U(eq)
Pd	5196(1)	2392(1)	6240(1)	9(1)
N(1)	3490(1)	2023(1)	6123(1)	11(1)
P(1)	4180(1)	2313(1)	5542(1)	10(1)
P(2)	4075(1)	2156(1)	6807(1)	10(1)
Cl(1)	6212(1)	2721(1)	5455(1)	16(1)
Cl(2)	6080(1)	2208(1)	7140(1)	17(1)
C(1)	2595(1)	2035(1)	6018(1)	14(1)
C(2)	2187(1)	1289(1)	6406(1)	20(1)
C(3)	2219(1)	2950(1)	6175(1)	18(1)
C(11)	4233(1)	1445(1)	4928(1)	12(1)
C(12)	4657(1)	1632(1)	4349(1)	16(1)
C(13)	4782(1)	956(2)	3888(1)	19(1)
C(14)	4491(1)	95(1)	4007(1)	19(1)
C(15)	4078(1)	-98(1)	4583(1)	18(1)
C(16)	3945(1)	578(1)	5044(1)	15(1)
C(21)	3832(1)	3307(1)	5121(1)	12(1)
C(22)	4124(1)	4152(1)	5309(1)	15(1)
C(23)	3770(1)	4926(1)	5057(1)	19(1)
C(24)	3129(1)	4857(1)	4624(1)	21(1)
C(25)	2853(1)	4019(1)	4421(1)	20(1)
C(26)	3209(1)	3242(1)	4664(1)	15(1)
C(31)	3694(1)	3063(1)	7306(1)	12(1)
C(32)	3124(1)	2917(1)	7800(1)	15(1)
C(33)	2790(1)	3644(1)	8131(1)	18(1)

C(34)	3033(1)	4514(1)	7974(1)	19(1)
C(35)	3608(1)	4663(1)	7492(1)	17(1)
C(36)	3939(1)	3937(1)	7156(1)	14(1)
C(41)	4076(1)	1182(1)	7331(1)	12(1)
C(42)	3858(1)	328(1)	7114(1)	14(1)
C(43)	3911(1)	-402(1)	7540(1)	18(1)
C(44)	4178(1)	-277(1)	8181(1)	18(1)
C(45)	4427(1)	566(1)	8392(1)	18(1)
C(46)	4383(1)	1295(1)	7970(1)	15(1)

Table B8. Bond lengths [Å] and angles [°] for [$PdCl_2$(PNP-i-Prop)].

Atoms	Bond length (Å)	Atoms	Bond angle (°)
Pd-P(1)	2.2068(7)	P(1)-Pd-P(2)	71.31(3)
Pd-P(2)	2.2185(7)	P(1)-Pd-Cl(2)	165.167(18)
Pd-Cl(2)	2.3579(6)	P(2)-Pd-Cl(2)	96.04(3)
Pd-Cl(1)	2.3705(6)	P(1)-Pd-Cl(1)	97.32(3)
N(1)-C(1)	1.504(2)	P(2)-Pd-Cl(1)	168.264(18)
N(1)-P(1)	1.6994(16)	Cl(2)-Pd-Cl(1)	95.62(3)
N(1)-P(2)	1.7036(16)	C(1)-N(1)-P(1)	124.54(12)
P(1)-C(11)	1.7932(19)	C(1)-N(1)-P(2)	132.69(12)
P(1)-C(21)	1.7993(19)	P(1)-N(1)-P(2)	98.57(8)
P(1)-P(2)	2.5794(9)	N(1)-P(1)-C(11)	109.34(9)
P(2)-C(41)	1.7951(19)	N(1)-P(1)-C(21)	108.64(8)
P(2)-C(31)	1.8009(19)	C(11)-P(1)-C(21)	106.09(9)
C(1)-C(2)	1.518(3)	N(1)-P(1)-Pd	94.95(6)
C(1)-C(3)	1.530(3)	C(11)-P(1)-Pd	116.43(6)
C(11)-C(16)	1.395(3)	C(21)-P(1)-Pd	120.36(7)
C(11)-C(12)	1.397(3)	N(1)-P(1)-P(2)	40.77(5)
C(12)-C(13)	1.387(3)	C(11)-P(1)-P(2)	128.85(7)
C(13)-C(14)	1.389(3)	C(21)-P(1)-P(2)	121.52(6)
C(14)-C(15)	1.384(3)	Pd-P(1)-P(2)	54.56(2)
C(15)-C(16)	1.390(3)	N(1)-P(2)-C(41)	112.87(9)
C(21)-C(26)	1.394(3)	N(1)-P(2)-C(31)	110.06(8)
C(21)-C(22)	1.399(3)	C(41)-P(2)-C(31)	105.73(9)
C(22)-C(23)	1.388(3)	N(1)-P(2)-Pd	94.41(6)
C(23)-C(24)	1.385(3)	C(41)-P(2)-Pd	115.66(6)
C(24)-C(25)	1.389(3)	C(31)-P(2)-Pd	117.92(7)
C(25)-C(26)	1.388(3)	N(1)-P(2)-P(1)	40.65(5)
C(31)-C(36)	1.394(3)	C(41)-P(2)-P(1)	131.38(7)
C(31)-C(32)	1.395(3)	C(31)-P(2)-P(1)	120.95(6)
C(32)-C(33)	1.387(3)	Pd-P(2)-P(1)	54.136(17)
C(33)-C(34)	1.392(3)	N(1)-C(1)-C(2)	111.20(16)
C(34)-C(35)	1.385(3)	N(1)-C(1)-C(3)	112.71(16)

C(35)-C(36)	1.389(3)	C(2)-C(1)-C(3)	110.99(17)
C(41)-C(42)	1.391(3)	C(16)-C(11)-C(12)	119.94(17)
C(41)-C(46)	1.401(3)	C(16)-C(11)-P(1)	121.98(14)
C(42)-C(43)	1.387(3)	C(12)-C(11)-P(1)	117.68(15)
C(43)-C(44)	1.386(3)	C(13)-C(12)-C(11)	119.81(19)
C(44)-C(45)	1.386(3)	C(12)-C(13)-C(14)	119.90(19)
C(45)-C(46)	1.383(3)	C(15)-C(14)-C(13)	120.62(18)
		C(14)-C(15)-C(16)	119.81(19)
		C(15)-C(16)-C(11)	119.91(18)
		C(26)-C(21)-C(22)	120.03(17)
		C(26)-C(21)-P(1)	119.79(14)
		C(22)-C(21)-P(1)	119.77(14)
		C(23)-C(22)-C(21)	119.76(19)
		C(24)-C(23)-C(22)	119.90(19)
		C(23)-C(24)-C(25)	120.56(19)
		C(26)-C(25)-C(24)	119.94(19)
		C(25)-C(26)-C(21)	119.72(19)
		C(36)-C(31)-C(32)	119.97(17)
		C(36)-C(31)-P(2)	118.12(14)
		C(32)-C(31)-P(2)	121.74(15)
		C(33)-C(32)-C(31)	119.90(19)
		C(32)-C(33)-C(34)	119.70(19)
		C(35)-C(34)-C(33)	120.72(18)
		C(34)-C(35)-C(36)	119.63(19)
		C(35)-C(36)-C(31)	120.06(18)
		C(42)-C(41)-C(46)	119.79(17)
		C(42)-C(41)-P(2)	123.22(15)
		C(46)-C(41)-P(2)	116.74(14)
		C(43)-C(42)-C(41)	119.98(18)
		C(44)-C(43)-C(42)	119.91(19)
		C(45)-C(44)-C(43)	120.32(18)
		C(46)-C(45)-C(44)	120.18(19)
		C(45)-C(46)-C(41)	119.70(18)

Table B9. Anisotropic displacement parameters ($A^2 \times 10^3$) for [$PdCl_2$(PNP-i-Prop)]. The anisotropic displacement factor exponent takes the form: -2 pi [$h^2 a^{*2} U11 + ... + 2 h k a^* b^* U12$]

	U11	U22	U33	U23	U13	U12
Pd	9(1)	8(1)	10(1)	0(1)	0(1)	0(1)
N(1)	11(1)	11(1)	10(1)	1(1)	0(1)	0(1)
P(1)	10(1)	9(1)	9(1)	0(1)	0(1)	1(1)
P(2)	11(1)	9(1)	9(1)	0(1)	1(1)	0(1)
Cl(1)	14(1)	16(1)	19(1)	1(1)	6(1)	-1(1)
Cl(2)	17(1)	17(1)	19(1)	3(1)	-8(1)	-2(1)

C(1)	11(1)	19(1)	13(1)	-2(1)	-1(1)	-1(1)
C(2)	14(1)	24(1)	22(1)	1(1)	1(1)	-6(1)
C(3)	13(1)	23(1)	19(1)	-1(1)	-1(1)	5(1)
C(11)	14(1)	13(1)	11(1)	-2(1)	-2(1)	2(1)
C(12)	18(1)	15(1)	14(1)	1(1)	0(1)	2(1)
C(13)	20(1)	26(1)	12(1)	-4(1)	0(1)	6(1)
C(14)	19(1)	21(1)	18(1)	-8(1)	-7(1)	7(1)
C(15)	16(1)	13(1)	24(1)	-4(1)	-7(1)	2(1)
C(16)	13(1)	16(1)	15(1)	-1(1)	-2(1)	1(1)
C(21)	13(1)	12(1)	10(1)	2(1)	2(1)	3(1)
C(22)	19(1)	14(1)	12(1)	0(1)	2(1)	1(1)
C(23)	28(1)	11(1)	18(1)	2(1)	7(1)	3(1)
C(24)	20(1)	19(1)	23(1)	10(1)	8(1)	10(1)
C(25)	16(1)	26(1)	18(1)	7(1)	2(1)	4(1)
C(26)	14(1)	16(1)	14(1)	2(1)	0(1)	0(1)
C(31)	15(1)	12(1)	10(1)	-2(1)	-1(1)	2(1)
C(32)	15(1)	16(1)	14(1)	-1(1)	-1(1)	0(1)
C(33)	14(1)	25(1)	14(1)	-4(1)	0(1)	3(1)
C(34)	19(1)	18(1)	18(1)	-8(1)	-5(1)	7(1)
C(35)	22(1)	11(1)	18(1)	0(1)	-5(1)	2(1)
C(36)	16(1)	14(1)	13(1)	0(1)	-1(1)	1(1)
C(41)	13(1)	11(1)	13(1)	3(1)	4(1)	2(1)
C(42)	14(1)	14(1)	15(1)	0(1)	2(1)	1(1)
C(43)	18(1)	11(1)	24(1)	1(1)	5(1)	1(1)
C(44)	18(1)	16(1)	21(1)	8(1)	5(1)	5(1)
C(45)	20(1)	20(1)	13(1)	3(1)	0(1)	3(1)
C(46)	18(1)	13(1)	14(1)	0(1)	0(1)	-1(1)

Table B10: Atomic coordinates (x 10^4) and equivalent isotropic displacement parameters ($Å^2$ x 10^3) for [$PdCl_2$(PNP-Dimprop)]. U(eq) is defined as one third of the trace of the orthogonalize Uij tensor.

	X	Y	z	U(eq)
Pd	3653(1)	2425(1)	1190(1)	35(1)
P(2)	5829(2)	2262(1)	1107(1)	40(1)
P(1)	4627(2)	2195(1)	2317(1)	43(1)
N(1)	6154(6)	2012(4)	2023(3)	43(1)
C(1A)	7491(8)	1837(5)	2465(6)	70(3)
C(2A)	8060(20)	2528(13)	2896(15)	70(3)
C(3A)	7787(10)	896(6)	2567(7)	87(3)
C(4A)	7924(9)	3494(6)	2678(6)	68(2)
C(5A)	9559(8)	2361(6)	3156(5)	67(3)
C(1B)	7491(8)	1837(5)	2465(6)	70(3)
C(2B)	8430(20)	2558(12)	2609(15)	70(3)
C(3B)	7787(10)	896(6)	2567(7)	87(3)
C(4B)	7924(9)	3494(6)	2678(6)	68(2)

C(5B)	9559(8)	2361(6)	3156(5)	67(3)
C(21)	4655(7)	3127(5)	2960(4)	47(2)
C(41)	6323(7)	1352(5)	536(4)	43(2)
C(11)	4053(7)	1247(5)	2820(4)	42(2)
C(31)	6771(8)	3207(5)	838(4)	52(2)
C(26)	5174(8)	3024(5)	3708(4)	53(2)
C(36)	6159(10)	4035(5)	780(5)	61(2)
C(32)	8092(9)	3151(7)	714(5)	68(2)
C(22)	4349(8)	3953(5)	2699(5)	53(2)
C(42)	6399(9)	472(5)	758(5)	56(2)
C(15)	3893(10)	-323(6)	3062(6)	71(3)
C(13)	2572(9)	700(6)	3692(5)	61(2)
C(33)	8808(9)	3896(6)	565(5)	68(2)
C(45)	6816(9)	857(6)	-693(5)	67(2)
C(12)	3106(9)	1404(6)	3304(5)	61(2)
C(16)	4394(8)	368(5)	2681(5)	58(2)
C(14)	2997(9)	-134(6)	3572(5)	64(2)
C(23)	4489(10)	4696(6)	3150(6)	72(3)
C(44)	6910(8)	-6(6)	-438(5)	62(2)
C(46)	6525(8)	1535(5)	-203(5)	57(2)
C(25)	5306(8)	3755(6)	4163(5)	66(2)
C(34)	8166(12)	4737(7)	526(5)	83(3)
C(43)	6662(9)	-195(5)	276(5)	59(2)
C(24)	4960(10)	4566(7)	3898(6)	72(3)
C(35)	6845(12)	4818(6)	635(6)	74(3)
Cl(2)	3058(3)	2750(2)	-68(1)	64(1)
Cl(1)	1443(2)	2290(2)	1483(2)	63(1)

Table B11. Bond lengths [Å] and angles [°] for [$PdCl_2$(PNP-Dimprop)].

Atoms	Bond length (Å)	Atoms	Bond angle (°)
Pd-P(1)	2.216(2)	P(1)-Pd-P(2)	71.61(8)
Pd-P(2)	2.221(2)	P(1)-Pd-Cl(1)	97.56(9)
Pd-Cl(1)	2.338(2)	P(2)-Pd-Cl(1)	165.45(9)
Pd-Cl(2)	2.357(2)	P(1)-Pd-Cl(2)	168.32(9)
P(2)-N(1)	1.706(6)	P(2)-Pd-Cl(2)	97.33(9)
P(2)-C(31)	1.790(8)	Cl(1)-Pd-Cl(2)	93.97(9)
P(2)-C(41)	1.803(7)	N(1)-P(2)-C(31)	112.0(3)
P(2)-P(1)	2.596(3)	N(1)-P(2)-C(41)	110.8(3)
P(1)-N(1)	1.691(6)	C(31)-P(2)-C(41)	105.0(4)
P(1)-C(11)	1.805(7)	N(1)-P(2)-Pd	93.8(2)
P(1)-C(21)	1.813(8)	C(31)-P(2)-Pd	118.7(3)
N(1)-C(1A)	1.530(9)	C(41)-P(2)-Pd	116.3(2)

C(1A)-C(2A)	1.39(2)	N(1)-P(2)-P(1)	39.9(2)
C(1A)-C(3A)	1.443(11)	C(31)-P(2)-P(1)	123.8(3)
C(1A)-H(1A)	0.98	C(41)-P(2)-P(1)	128.8(3)
C(2A)-C(4A)	1.50(2)	Pd-P(2)-P(1)	54.12(6)
C(2A)-C(5A)	1.57(2)	N(1)-P(1)-C(11)	111.8(3)
C(2A)-H(2A)	0.98	N(1)-P(1)-C(21)	111.2(3)
C(3A)-H(3A1)	0.96	C(11)-P(1)-C(21)	105.3(4)
C(3A)-H(3A2)	0.96	N(1)-P(1)-Pd	94.4(2)
C(3A)-H(3A3)	0.96	C(11)-P(1)-Pd	116.9(3)
C(4A)-H(4A1)	0.96	C(21)-P(1)-Pd	117.1(3)
C(4A)-H(4A2)	0.96	N(1)-P(1)-P(2)	40.4(2)
C(4A)-H(4A3)	0.96	C(11)-P(1)-P(2)	130.5(3)
C(5A)-H(5A1)	0.96	C(21)-P(1)-P(2)	122.1(3)
C(5A)-H(5A2)	0.96	Pd-P(1)-P(2)	54.28(7)
C(5A)-H(5A3)	0.96	C(1A)-N(1)-P(1)	130.1(6)
C(2B)-H(2B)	0.98	C(1A)-N(1)-P(2)	129.4(6)
C(21)-C(22)	1.346(10)	P(1)-N(1)-P(2)	99.7(3)
C(21)-C(26)	1.418(11)	C(2A)-C(1A)-C(3A)	125.6(12)
C(41)-C(42)	1.374(10)	C(2A)-C(1A)-N(1)	117.9(10)
C(41)-C(46)	1.400(11)	C(3A)-C(1A)-N(1)	113.3(7)
C(11)-C(12)	1.369(11)	C(2A)-C(1A)-H(1A)	95.9
C(11)-C(16)	1.385(10)	C(3A)-C(1A)-H(1A)	95.9
C(31)-C(32)	1.369(12)	N(1)-C(1A)-H(1A)	95.9
C(31)-C(36)	1.381(11)	C(1A)-C(2A)-C(4A)	123.0(18)
C(26)-C(25)	1.367(10)	C(1A)-C(2A)-C(5A)	113.0(14)
C(26)-H(26)	0.93	C(4A)-C(2A)-C(5A)	107.0(13)
C(36)-C(35)	1.393(12)	C(1A)-C(2A)-H(2A)	103.9
C(36)-H(36)	0.93	C(4A)-C(2A)-H(2A)	103.9
C(32)-C(33)	1.364(11)	C(5A)-C(2A)-H(2A)	103.9
C(32)-H(32)	0.93	C(1A)-C(3A)-H(3A1)	109.5
C(22)-C(23)	1.377(11)	C(1A)-C(3A)-H(3A2)	109.5
C(22)-H(22)	0.93	H(3A1)-C(3A)-H(3A2)	109.5
C(42)-C(43)	1.364(11)	C(1A)-C(3A)-H(3A3)	109.5
C(42)-H(42)	0.93	H(3A1)-C(3A)-H(3A3)	109.5
C(15)-C(16)	1.361(11)	H(3A2)-C(3A)-H(3A3)	109.5
C(15)-C(14)	1.375(13)	C(2A)-C(4A)-H(4A1)	109.5
C(15)-H(15)	0.93	C(2A)-C(4A)-H(4A2)	109.5
C(13)-C(14)	1.340(11)	H(4A1)-C(4A)-H(4A2)	109.5
C(13)-C(12)	1.397(11)	C(2A)-C(4A)-H(4A3)	109.5
C(13)-H(13)	0.93	H(4A1)-C(4A)-H(4A3)	109.5
C(33)-C(34)	1.411(13)	H(4A2)-C(4A)-H(4A3)	109.5
C(33)-H(33)	0.93	C(2A)-C(5A)-H(5A1)	109.5
C(45)-C(44)	1.369(11)	C(2A)-C(5A)-H(5A2)	109.5

C(45)-C(46)	1.393(11)	H(5A1)-C(5A)-H(5A2)	109.5
C(45)-H(45)	0.93	C(2A)-C(5A)-H(5A3)	109.5
C(12)-H(12)	0.93	H(5A1)-C(5A)-H(5A3)	109.5
C(16)-H(16)	0.93	H(5A2)-C(5A)-H(5A3)	109.5
C(14)-H(14)	0.93	C(22)-C(21)-C(26)	119.3(7)
C(23)-C(24)	1.412(14)	C(22)-C(21)-P(1)	119.1(6)
C(23)-H(23)	0.93	C(26)-C(21)-P(1)	121.1(6)
C(44)-C(43)	1.369(12)	C(42)-C(41)-C(46)	117.3(7)
C(44)-H(44)	0.93	C(42)-C(41)-P(2)	124.3(6)
C(46)-H(46)	0.93	C(46)-C(41)-P(2)	118.2(6)
C(25)-C(24)	1.338(13)	C(12)-C(11)-C(16)	118.4(7)
C(25)-H(25)	0.93	C(12)-C(11)-P(1)	117.4(6)
C(34)-C(35)	1.365(15)	C(16)-C(11)-P(1)	123.7(6)
C(34)-H(34)	0.93	C(32)-C(31)-C(36)	118.3(8)
C(43)-H(43)	0.93	C(32)-C(31)-P(2)	122.7(7)
C(24)-H(24)	0.93	C(36)-C(31)-P(2)	118.9(7)
C(35)-H(35)	0.93	C(25)-C(26)-C(21)	120.0(8)
		C(25)-C(26)-H(26)	120
		C(21)-C(26)-H(26)	120
		C(31)-C(36)-C(35)	122.7(9)
		C(31)-C(36)-H(36)	118.6
		C(35)-C(36)-H(36)	118.6
		C(33)-C(32)-C(31)	121.3(9)
		C(33)-C(32)-H(32)	119.4
		C(31)-C(32)-H(32)	119.4
		C(21)-C(22)-C(23)	121.4(8)
		C(21)-C(22)-H(22)	119.3
		C(23)-C(22)-H(22)	119.3
		C(43)-C(42)-C(41)	121.2(8)
		C(43)-C(42)-H(42)	119.4
		C(41)-C(42)-H(42)	119.4
		C(16)-C(15)-C(14)	118.6(9)
		C(16)-C(15)-H(15)	120.7
		C(14)-C(15)-H(15)	120.7
		C(14)-C(13)-C(12)	118.4(9)
		C(14)-C(13)-H(13)	120.8
		C(12)-C(13)-H(13)	120.8
		C(32)-C(33)-C(34)	119.2(9)
		C(32)-C(33)-H(33)	120.4
		C(34)-C(33)-H(33)	120.4
		C(44)-C(45)-C(46)	118.8(9)
		C(44)-C(45)-H(45)	120.6
		C(46)-C(45)-H(45)	120.6

C(11)-C(12)-C(13)	120.8(8)
C(11)-C(12)-H(12)	119.6
C(13)-C(12)-H(12)	119.6
C(15)-C(16)-C(11)	121.2(9)
C(15)-C(16)-H(16)	119.4
C(11)-C(16)-H(16)	119.4
C(13)-C(14)-C(15)	122.4(8)
C(13)-C(14)-H(14)	118.8
C(15)-C(14)-H(14)	118.8
C(22)-C(23)-C(24)	117.9(9)
C(22)-C(23)-H(23)	121.1
C(24)-C(23)-H(23)	121.1
C(45)-C(44)-C(43)	119.9(8)
C(45)-C(44)-H(44)	120
C(43)-C(44)-H(44)	120
C(45)-C(46)-C(41)	121.6(8)
C(45)-C(46)-H(46)	119.2
C(41)-C(46)-H(46)	119.2
C(24)-C(25)-C(26)	119.8(9)
C(24)-C(25)-H(25)	120.1
C(26)-C(25)-H(25)	120.1
C(35)-C(34)-C(33)	121.2(8)
C(35)-C(34)-H(34)	119.4
C(33)-C(34)-H(34)	119.4
C(42)-C(43)-C(44)	121.1(8)
C(42)-C(43)-H(43)	119.4
C(44)-C(43)-H(43)	119.4
C(25)-C(24)-C(23)	121.7(9)
C(25)-C(24)-H(24)	119.2
C(23)-C(24)-H(24)	119.2
C(34)-C(35)-C(36)	117.2(9)
C(34)-C(35)-H(35)	121.4
C(36)-C(35)-H(35)	121.4

Table B12. Anisotropic displacement parameters ($A^2 \times 10^3$) for [$PdCl_2$(PNP-Dimprop)]. The anisotropic displacement factor exponent takes the form: -2 pi [h^2 a*^2 U11 + ... + 2 h k a* b* U12]

	U11	U22	U33	U23	U13	U12
Pd	28(1)	32(1)	43(1)	0(1)	-6(1)	2(1)
P(2)	35(1)	39(1)	46(1)	-2(1)	2(1)	2(1)
P(1)	39(1)	45(1)	44(1)	4(1)	-3(1)	0(1)
N(1)	48(4)	36(3)	44(3)	-2(2)	-7(3)	7(3)
C(1A)	42(4)	48(3)	113(7)	-11(4)	-39(4)	4(3)

C(2A)	42(4)	48(3)	113(7)	-11(4)	-39(4)	4(3)
C(3A)	63(6)	65(6)	126(9)	11(6)	-36(6)	8(5)
C(4A)	55(6)	64(5)	84(7)	-6(5)	-1(5)	-12(4)
C(5A)	31(4)	106(7)	60(5)	2(5)	-23(4)	-8(4)
C(1B)	42(4)	48(3)	113(7)	-11(4)	-39(4)	4(3)
C(2B)	42(4)	48(3)	113(7)	-11(4)	-39(4)	4(3)
C(3B)	63(6)	65(6)	126(9)	11(6)	-36(6)	8(5)
C(4B)	55(6)	64(5)	84(7)	-6(5)	-1(5)	-12(4)
C(5B)	31(4)	106(7)	60(5)	2(5)	-23(4)	-8(4)
C(21)	44(4)	49(4)	49(5)	-5(3)	8(4)	-6(3)
C(41)	39(4)	42(4)	47(4)	-6(3)	-2(3)	3(3)
C(11)	37(4)	46(4)	43(4)	6(3)	3(3)	3(3)
C(31)	54(5)	52(4)	48(5)	1(3)	-1(4)	-11(4)
C(26)	54(5)	54(4)	50(5)	-6(4)	-4(4)	10(4)
C(36)	70(6)	48(4)	62(6)	11(4)	-7(5)	-12(4)
C(32)	58(4)	83(4)	60(4)	14(3)	-3(3)	-25(3)
C(22)	62(5)	50(4)	47(5)	2(3)	-1(4)	11(4)
C(42)	66(6)	48(4)	55(5)	-1(4)	6(4)	2(4)
C(15)	67(6)	47(5)	96(8)	15(5)	0(6)	-11(4)
C(13)	63(4)	60(3)	61(4)	2(3)	9(3)	-6(3)
C(33)	58(4)	83(4)	60(4)	14(3)	-3(3)	-25(3)
C(45)	66(6)	72(6)	64(6)	-15(5)	9(5)	1(5)
C(12)	63(4)	60(3)	61(4)	2(3)	9(3)	-6(3)
C(16)	46(5)	54(5)	73(6)	-3(4)	6(4)	9(4)
C(14)	51(5)	72(6)	68(6)	17(5)	-6(5)	-21(4)
C(23)	68(7)	49(5)	102(9)	-4(5)	21(6)	-1(4)
C(44)	52(5)	59(5)	73(7)	-24(4)	-6(4)	7(4)
C(46)	60(5)	55(4)	56(5)	1(4)	1(4)	9(4)
C(25)	49(5)	79(6)	68(6)	-30(5)	2(4)	0(4)
C(34)	103(9)	83(7)	63(6)	20(5)	1(6)	-52(6)
C(43)	59(5)	39(4)	77(7)	-7(4)	-7(5)	5(4)
C(24)	65(6)	73(6)	81(7)	-26(5)	29(5)	-15(5)
C(35)	101(9)	48(5)	71(7)	-3(4)	-3(6)	-11(5)
Cl(2)	70(2)	72(2)	48(1)	2(1)	-14(1)	5(1)
Cl(1)	35(1)	73(2)	81(2)	2(1)	8(1)	4(1)

Table B13: Atomic coordinates (x 10^4) and equivalent isotropic displacement parameters ($Å^2$ x 10^3) for [$PdCl_2$(PNP-n-Prop)] U(eq) is defined as one third of the trace of the orthogonalize Uij tensor.

	X	Y	z	U(eq)
Pd(1)	5000	7734(1)	2500	43(1)
N(1)	5000	6002(6)	2500	90(2)
P(1)	6202(2)	6647(1)	2487(1)	43(1)

Cl(1)	6556(2)	8691(1)	2306(1)	67(1)
C(1A)	4450(50)	5290(30)	1840(30)	90(2)
C(3A)	5000	3680(20)	2500	90(2)
C(1B)	4990(50)	5100(30)	2380(20)	90(2)
C(3B)	4950(40)	3710(30)	2070(20)	90(2)
C(12)	8443(7)	6860(4)	3508(4)	56(2)
C(21)	7068(5)	6347(4)	1570(4)	45(1)
C(11)	7224(6)	6575(4)	3504(4)	51(2)
C(26)	7950(6)	5720(4)	1688(4)	56(2)
C(25)	8480(7)	5437(5)	953(5)	72(2)
C(22)	6769(5)	6668(5)	723(4)	54(2)
C(15)	7565(9)	6371(5)	5109(4)	76(2)
C(16)	6801(7)	6324(4)	4308(4)	59(2)
C(24)	8180(8)	5753(5)	119(5)	76(2)
C(13)	9193(8)	6887(5)	4298(5)	75(2)
C(23)	7337(7)	6357(5)	-4(4)	74(2)
C(14)	8775(9)	6648(5)	5081(5)	78(3)
C(2)	4804(9)	4673(6)	1877(7)	90(2)

Table B14. Bond lengths [Å] and angles [°] for [$PdCl_2$(PNP-n-Prop)].

Atoms	Bond length (Å)	Atoms	Bond angle (°)
Pd(1)-P(1)#1	2.2226(17)	P(1)#1-Pd(1)-P(1)	71.54(9)
Pd(1)-P(1)	2.2226(17)	P(1)#1-Pd(1)-Cl(1)	166.97(6)
Pd(1)-Cl(1)	2.3475(18)	P(1)-Pd(1)-Cl(1)	97.07(7)
Pd(1)-Cl(1)#1	2.3475(18)	P(1)#1-Pd(1)-Cl(1)#1	97.07(7)
N(1)-C(1B)	1.50(5)	P(1)-Pd(1)-Cl(1)#1	166.97(6)
N(1)-C(1B)#1	1.50(5)	Cl(1)-Pd(1)-Cl(1)#1	94.90(11)
N(1)-C(1A)	1.62(5)	C(1B)-N(1)-C(1B)#1	14(3)
N(1)-C(1A)#1	1.62(5)	C(1B)-N(1)-C(1A)	37(2)
N(1)-P(1)	1.683(7)	C(1B)#1-N(1)-C(1A)	49.0(17)
N(1)-P(1)#1	1.683(7)	C(1B)-N(1)-C(1A)#1	49.0(17)
P(1)-C(11)	1.797(6)	C(1B)#1-N(1)-C(1A)#1	37(2)
P(1)-C(21)	1.793(6)	C(1A)-N(1)-C(1A)#1	86(3)
P(1)-P(1)#1	2.598(4)	C(1B)-N(1)-P(1)	129(2)
C(1A)-C(1A)#1	2.20(7)	C(1B)#1-N(1)-P(1)	129(2)
C(1A)-C(2)#1	2.24(4)	C(1A)-N(1)-P(1)	135(2)
C(1A)-C(2)	1.08(5)	C(1A)#1-N(1)-P(1)	103.4(19)
C(3A)-C(2)#1	1.90(3)	C(1B)-N(1)-P(1)#1	129(2)
C(3A)-C(2)	1.90(3)	C(1B)#1-N(1)-P(1)#1	129(2)
C(1B)-C(1B)#1	0.36(7)	C(1A)-N(1)-P(1)#1	103.4(19)
C(1B)-C(2)	1.04(4)	C(1A)#1-N(1)-P(1)#1	135(2)
C(1B)-C(2)#1	1.32(4)	P(1)-N(1)-P(1)#1	101.1(6)
C(3B)-C(3B)#1	1.29(6)	N(1)-P(1)-C(11)	111.4(3)

C(3B)-C(2)	1.62(5)	N(1)-P(1)-C(21)	106.7(3)
C(12)-C(13)	1.369(9)	C(11)-P(1)-C(21)	107.5(3)
C(12)-C(11)	1.398(9)	N(1)-P(1)-Pd(1)	93.7(3)
C(12)-H(12)	0.93	C(11)-P(1)-Pd(1)	111.2(2)
C(21)-C(22)	1.381(8)	C(21)-P(1)-Pd(1)	125.2(2)
C(21)-C(26)	1.410(9)	N(1)-P(1)-P(1)#1	39.5(3)
C(11)-C(16)	1.381(8)	C(11)-P(1)-P(1)#1	121.8(2)
C(26)-C(25)	1.362(9)	C(21)-P(1)-P(1)#1	126.9(2)
C(26)-H(26)	0.93	Pd(1)-P(1)-P(1)#1	54.23(5)
C(25)-C(24)	1.360(10)	C(1A)#1-C(1A)-C(2)#1	28.2(12)
C(25)-H(25)	0.93	C(1A)#1-C(1A)-C(2)	78(2)
C(22)-C(23)	1.390(9)	C(2)#1-C(1A)-C(2)	55.8(19)
C(22)-H(22)	0.93	C(1A)#1-C(1A)-N(1)	47.2(16)
C(15)-C(16)	1.391(8)	C(2)#1-C(1A)-N(1)	74.6(15)
C(15)-C(14)	1.390(11)	C(2)-C(1A)-N(1)	123(3)
C(15)-H(15)	0.93	C(2)#1-C(3A)-C(2)	58.8(12)
C(16)-H(16)	0.93	C(1B)#1-C(1B)-C(2)	136(5)
C(24)-C(23)	1.355(11)	C(1B)#1-C(1B)-N(1)	83.0(14)
C(24)-H(24)	0.93	C(2)-C(1B)-N(1)	140(4)
C(13)-C(14)	1.346(11)	C(1B)#1-C(1B)-C(2)#1	33(3)
C(13)-H(13)	0.93	C(2)-C(1B)-C(2)#1	104(4)
C(23)-H(23)	0.93	N(1)-C(1B)-C(2)#1	116(3)
C(14)-H(14)	0.93	C(3B)#1-C(3B)-C(2)	99.8(13)
C(2)-C(1A)#1	2.24(4)	C(13)-C(12)-C(11)	120.0(7)
C(2)-C(1B)#1	1.32(4)	C(13)-C(12)-H(12)	119.9
C(2)-C(2)#1	1.865(19)	C(11)-C(12)-H(12)	120.1
		C(22)-C(21)-C(26)	119.9(6)
		C(22)-C(21)-P(1)	119.5(5)
		C(26)-C(21)-P(1)	120.2(5)
		C(16)-C(11)-C(12)	118.8(6)
		C(16)-C(11)-P(1)	121.6(6)
		C(12)-C(11)-P(1)	119.2(5)
		C(25)-C(26)-C(21)	118.8(7)
		C(25)-C(26)-H(26)	120.6
		C(21)-C(26)-H(26)	120.6
		C(24)-C(25)-C(26)	121.2(7)
		C(24)-C(25)-H(25)	119.3
		C(26)-C(25)-H(25)	119.5
		C(21)-C(22)-C(23)	119.0(7)
		C(21)-C(22)-H(22)	120.6
		C(23)-C(22)-H(22)	120.5
		C(16)-C(15)-C(14)	118.7(7)
		C(16)-C(15)-H(15)	120.6

C(14)-C(15)-H(15)	120.8
C(15)-C(16)-C(11)	120.7(7)
C(15)-C(16)-H(16)	119.7
C(11)-C(16)-H(16)	119.6
C(23)-C(24)-C(25)	120.7(7)
C(23)-C(24)-H(24)	119.6
C(25)-C(24)-H(24)	119.6
C(14)-C(13)-C(12)	121.0(8)
C(14)-C(13)-H(13)	119.5
C(12)-C(13)-H(13)	119.5
C(24)-C(23)-C(22)	120.4(7)
C(24)-C(23)-H(23)	119.8
C(22)-C(23)-H(23)	119.8
C(13)-C(14)-C(15)	120.8(7)
C(13)-C(14)-H(14)	119.6
C(15)-C(14)-H(14)	119.6
C(1B)-C(2)-C(1A)#1	18(3)
C(1B)-C(2)-C(1A)	55(3)
C(1A)#1-C(2)-C(1A)	73(3)
C(1B)-C(2)-C(3B)	123(3)
C(1A)#1-C(2)-C(3B)	106.0(15)
C(1A)-C(2)-C(3B)	163(4)
C(1B)-C(2)-C(1B)#1	11(3)
C(1A)#1-C(2)-C(1B)#1	12(3)
C(1A)-C(2)-C(1B)#1	64(2)
C(3B)-C(2)-C(1B)#1	112(2)
C(1B)-C(2)-C(2)#1	44(3)
C(1A)#1-C(2)-C(2)#1	28.7(12)
C(1A)-C(2)-C(2)#1	95(2)
C(3B)-C(2)-C(2)#1	79.5(11)
C(1B)#1-C(2)-C(2)#1	32.7(19)
C(1B)-C(2)-C(3A)	104(3)
C(1A)#1-C(2)-C(3A)	87.9(13)
C(1A)-C(2)-C(3A)	150(3)
C(3B)-C(2)-C(3A)	19.2(13)
C(1B)#1-C(2)-C(3A)	93(2)
C(2)#1-C(2)-C(3A)	60.6(6)

Table B15. Anisotropic displacement parameters (A^2 x 10^3) for [$PdCl_2$(PNP-n-Prop)]. The anisotropic displacement factor exponent takes the form: -2 pi [h^2 a*^2 U11 + ... + 2 h k a* b* U12]

	U11	U22	U33	U23	U13	U12
Pd(1)	51(1)	43(1)	34(1)	0	0(1)	0
N(1)	103(5)	70(4)	94(5)	0	-12(4)	0
P(1)	51(1)	39(1)	39(1)	0(1)	-1(1)	3(1)
Cl(1)	72(1)	62(1)	66(1)	0(1)	9(1)	-25(1)
C(1A)	103(5)	70(4)	94(5)	0	-12(4)	0
C(3A)	103(5)	70(4)	94(5)	0	-12(4)	0
C(1B)	103(5)	70(4)	94(5)	0	-12(4)	0
C(3B)	103(5)	70(4)	94(5)	0	-12(4)	0
C(12)	62(5)	49(4)	56(4)	-6(3)	-7(3)	1(3)
C(21)	43(3)	50(4)	41(3)	0(3)	4(3)	-3(3)
C(11)	68(5)	43(4)	41(3)	3(3)	-4(3)	16(3)
C(26)	59(4)	53(4)	57(4)	-12(3)	8(3)	-2(3)
C(25)	68(5)	58(5)	91(6)	-15(4)	23(4)	-6(4)
C(22)	26(3)	82(5)	57(4)	7(4)	14(3)	0(3)
C(15)	119(8)	62(5)	45(4)	4(4)	2(5)	33(5)
C(16)	64(4)	62(5)	51(4)	1(3)	0(3)	15(4)
C(24)	86(6)	77(6)	69(5)	-19(4)	30(4)	-20(5)
C(13)	70(5)	74(5)	75(5)	-14(5)	-24(4)	14(4)
C(23)	84(6)	90(6)	46(4)	3(4)	6(4)	-17(5)
C(14)	106(7)	75(6)	47(4)	-9(4)	-23(4)	26(5)
C(2)	103(5)	70(4)	94(5)	0	-12(4)	0

Table B13: Atomic coordinates (x 10^4) and equivalent isotropic displacement parameters ($Å^2$ x 10^3) for [$PdCl_2$(PNP-i-Pent]. U(eq) is defined as one third of the trace of the orthogonalize Uij tensor.

	X	Y	z	U(eq)
Pd(1)	8702(1)	2500	8865(1)	10(1)
N(1)	8255(3)	2500	12173(6)	13(1)
P(1)	8393(1)	1758(1)	10893(1)	11(1)
Cl(1)	8999(1)	1505(1)	7091(1)	20(1)
C(1A)	8063(6)	2500	13910(14)	55(2)
C(1B)	8063(6)	2500	13910(14)	55(2)
C(2)	7413(4)	2149(5)	14250(10)	55(2)
C(3A)	6809(8)	2500	13520(20)	92(2)
C(3B)	6809(8)	2500	13520(20)	92(2)
C(4)	6636(5)	1708(8)	14612(17)	92(2)
C(5)	6230(5)	2002(8)	13586(16)	92(2)
C(11)	8991(2)	1123(3)	11725(5)	13(1)
C(12)	9069(2)	395(3)	11043(6)	16(1)
C(13)	9563(2)	-83(3)	11577(6)	19(1)
C(14)	9989(2)	168(3)	12771(6)	20(1)
C(15)	9914(2)	890(3)	13440(6)	20(1)

C(16)	9421(2)	1368(3)	12930(6)	17(1)
C(21)	7674(2)	1187(3)	10586(5)	14(1)
C(22)	7251(3)	1380(3)	9322(6)	22(1)
C(23)	6700(3)	954(3)	9070(6)	25(1)
C(24)	6558(2)	338(3)	10042(6)	20(1)
C(25)	6974(3)	137(3)	11290(7)	24(1)
C(26)	7532(2)	566(3)	11568(6)	20(1)

Table B14. Bond lengths [Å] and angles [°] for [$PdCl_2$(PNP-i-Pent)].

Atoms	Bond length (Å)	Atoms	Bond angle (°)
Pd(1)-P(1)#1	2.2106(14)	P(1)#1-Pd(1)-P(1)	71.65(7)
Pd(1)-P(1)	2.2106(14)	P(1)#1-Pd(1)-Cl(1)	168.24(4)
Pd(1)-Cl(1)	2.3529(13)	P(1)-Pd(1)-Cl(1)	96.66(5)
Pd(1)-Cl(1)#1	2.3529(13)	P(1)#1-Pd(1)-Cl(1)#1	96.66(5)
N(1)-C(1A)	1.488(12)	P(1)-Pd(1)-Cl(1)#1	168.24(4)
N(1)-P(1)	1.696(4)	Cl(1)-Pd(1)-Cl(1)#1	95.00(7)
N(1)-P(1)#1	1.696(4)	C(1A)-N(1)-P(1)	130.27(14)
P(1)-C(11)	1.797(5)	C(1A)-N(1)-P(1)#1	130.27(14)
P(1)-C(21)	1.806(5)	P(1)-N(1)-P(1)#1	99.5(3)
P(1)-P(1)#1	2.588(3)	N(1)-P(1)-C(11)	110.4(2)
C(1A)-C(2)	1.503(14)	N(1)-P(1)-C(21)	111.7(2)
C(1A)-H(1A1)	0.97	C(11)-P(1)-C(21)	106.2(2)
C(1A)-H(1A2)	0.97	N(1)-P(1)-Pd(1)	94.30(15)
C(2)-C(3A)	1.515(17)	C(11)-P(1)-Pd(1)	116.95(15)
C(2)-H(2A)	0.97	C(21)-P(1)-Pd(1)	116.95(16)
C(2)-H(2B)	0.97	N(1)-P(1)-P(1)#1	40.27(14)
C(3A)-C(5)	1.480(16)	C(11)-P(1)-P(1)#1	128.09(16)
C(3A)-C(4)#1	1.690(17)	C(21)-P(1)-P(1)#1	123.48(15)
C(3A)-H(3A)	0.98	Pd(1)-P(1)-P(1)#1	54.18(4)
C(5)-H(5A)	0.96	N(1)-C(1A)-C(2)	114.7(9)
C(5)-H(5B)	0.96	N(1)-C(1A)-H(1A1)	108.6
C(5)-H(5C)	0.96	C(2)-C(1A)-H(1A1)	108.6
C(11)-C(12)	1.397(7)	N(1)-C(1A)-H(1A2)	108.6
C(11)-C(16)	1.401(6)	C(2)-C(1A)-H(1A2)	108.6
C(12)-C(13)	1.390(7)	H(1A1)-C(1A)-H(1A2)	107.6
C(12)-H(12)	0.93	C(1A)-C(2)-C(3A)	119.8(8)
C(13)-C(14)	1.392(7)	C(1A)-C(2)-H(2A)	107.4
C(13)-H(13)	0.93	C(3A)-C(2)-H(2A)	107.4
C(14)-C(15)	1.385(8)	C(1A)-C(2)-H(2B)	107.4
C(14)-H(14)	0.93	C(3A)-C(2)-H(2B)	107.4
C(15)-C(16)	1.381(7)	H(2A)-C(2)-H(2B)	106.9
C(15)-H(15)	0.93	C(5)-C(3A)-C(2)	114.3(8)
C(16)-H(16)	0.93	C(5)-C(3A)-C(4)#1	106.7(11)

C(21)-C(26)	1.385(7)	C(2)-C(3A)-C(4)#1	106.8(12)
C(21)-C(22)	1.403(7)	C(5)-C(3A)-H(3A)	109.6
C(22)-C(23)	1.377(7)	C(2)-C(3A)-H(3A)	109.6
C(22)-H(22)	0.93	C(4)#1-C(3A)-H(3A)	109.6
C(23)-C(24)	1.372(8)	C(3A)-C(5)-H(5A)	109.5
C(23)-H(23)	0.93	C(3A)-C(5)-H(5B)	109.5
C(24)-C(25)	1.387(7)	H(5A)-C(5)-H(5B)	109.5
C(24)-H(24)	0.93	C(3A)-C(5)-H(5C)	109.5
C(25)-C(26)	1.393(7)	H(5A)-C(5)-H(5C)	109.5
C(25)-H(25)	0.93	H(5B)-C(5)-H(5C)	109.5
C(26)-H(26)	0.93	C(12)-C(11)-C(16)	119.4(4)
		C(12)-C(11)-P(1)	119.0(4)
		C(16)-C(11)-P(1)	121.3(4)
		C(13)-C(12)-C(11)	120.0(5)
		C(13)-C(12)-H(12)	120
		C(11)-C(12)-H(12)	120
		C(12)-C(13)-C(14)	120.0(5)
		C(12)-C(13)-H(13)	120
		C(14)-C(13)-H(13)	120
		C(15)-C(14)-C(13)	119.9(5)
		C(15)-C(14)-H(14)	120
		C(13)-C(14)-H(14)	120
		C(16)-C(15)-C(14)	120.6(5)
		C(16)-C(15)-H(15)	119.7
		C(14)-C(15)-H(15)	119.7
		C(15)-C(16)-C(11)	120.0(5)
		C(15)-C(16)-H(16)	120
		C(11)-C(16)-H(16)	120
		C(26)-C(21)-C(22)	119.5(4)
		C(26)-C(21)-P(1)	121.6(4)
		C(22)-C(21)-P(1)	118.9(4)
		C(23)-C(22)-C(21)	119.9(5)
		C(23)-C(22)-H(22)	120.1
		C(21)-C(22)-H(22)	120.1
		C(24)-C(23)-C(22)	120.7(5)
		C(24)-C(23)-H(23)	119.6
		C(22)-C(23)-H(23)	119.6
		C(23)-C(24)-C(25)	120.1(5)
		C(23)-C(24)-H(24)	119.9
		C(25)-C(24)-H(24)	119.9
		C(24)-C(25)-C(26)	119.9(5)
		C(24)-C(25)-H(25)	120.1
		C(26)-C(25)-H(25)	120.1

C(21)-C(26)-C(25)	120.0(5)
C(21)-C(26)-H(26)	120
C(25)-C(26)-H(26)	120

Table B15. Anisotropic displacement parameters ($A^2 \times 10^3$) for [$PdCl_2$(PNP-n-Butyl)]. The anisotropic displacement factor exponent takes the form: -2 pi [h^2 a*^2 U11 + ... + 2 h k a* b* U12]

	U11	U22	U33	U23	U13	U12
Pd(1)	13(1)	9(1)	9(1)	0	-1(1)	0
N(1)	15(2)	10(3)	13(2)	0	-1(2)	0
P(1)	12(1)	10(1)	11(1)	1(1)	-2(1)	-1(1)
Cl(1)	31(1)	13(1)	15(1)	-3(1)	3(1)	2(1)
C(1A)	63(4)	53(4)	50(4)	0	13(3)	0
C(1B)	63(4)	53(4)	50(4)	0	13(3)	0
C(2)	63(4)	53(4)	50(4)	0	13(3)	0
C(3A)	57(4)	104(6)	115(6)	0	2(4)	0
C(3B)	57(4)	104(6)	115(6)	0	2(4)	0
C(4)	57(4)	104(6)	115(6)	0	2(4)	0
C(5)	57(4)	104(6)	115(6)	0	2(4)	0
C(11)	11(2)	15(2)	14(2)	5(2)	1(2)	0(2)
C(12)	18(2)	13(2)	16(2)	1(2)	3(2)	-1(2)
C(13)	24(2)	14(2)	19(2)	3(2)	6(2)	3(2)
C(14)	18(2)	23(3)	19(2)	7(2)	1(2)	9(2)
C(15)	17(2)	25(3)	20(2)	1(2)	-4(2)	0(2)
C(16)	19(2)	17(2)	15(2)	1(2)	-2(2)	0(2)
C(21)	14(2)	15(2)	13(2)	-1(2)	-1(2)	-1(2)
C(22)	28(3)	14(2)	23(2)	3(2)	-6(2)	-3(2)
C(23)	24(3)	28(3)	22(2)	-1(2)	-12(2)	-4(2)
C(24)	14(2)	22(3)	25(2)	-7(2)	2(2)	-5(2)
C(25)	20(2)	22(3)	31(3)	7(2)	1(2)	-6(2)
C(26)	19(2)	20(3)	22(2)	7(2)	-1(2)	-6(2)

Table B13: Atomic coordinates (x 10^4) and equivalent isotropic displacement parameters ($Å^2 \times 10^3$) for [$PdCl_2$(PNP-n-Butyl)] U(eq) is defined as one third of the trace of the orthogonalize Uij tensor.

	X	Y	z	U(eq)
Pd(1)	4634(1)	1381(1)	8089(1)	26(1)
Pd(2)	10193(1)	6541(1)	6897(1)	24(1)
N(1)	5236(11)	-366(8)	7302(6)	23(3)
N(2)	10147(11)	4545(9)	7559(7)	27(3)
P(1)	3901(4)	182(3)	7706(2)	25(1)
P(2)	6138(4)	384(3)	7517(2)	26(1)
P(3)	9106(3)	5363(3)	7074(2)	24(1)

P(4)	11240(4)	5205(3)	7553(2)	24(1)
Cl(1)	2772(4)	2108(3)	8656(2)	32(1)
Cl(2)	5668(4)	2559(3)	8419(2)	33(1)
Cl(3)	8743(3)	7719(3)	6203(2)	28(1)
Cl(4)	11629(4)	7589(3)	6792(2)	30(1)
C(1)	5576(14)	-1348(11)	7053(9)	29(2)
C(2)	4950(14)	-1480(11)	6367(9)	29(2)
C(3)	5370(14)	-2517(10)	6148(9)	29(2)
C(4)	4730(13)	-2698(11)	5451(9)	29(2)
C(5)	9946(16)	3664(11)	8103(9)	37(2)
C(6)	9735(16)	2781(12)	7753(10)	37(2)
C(7)	9134(15)	2003(12)	8293(9)	37(2)
C(8)	9794(15)	1555(12)	8947(9)	37(2)
C(11)	2853(14)	519(11)	6964(9)	29(2)
C(12)	1640(14)	416(11)	7132(9)	29(2)
C(13)	827(14)	783(10)	6553(9)	29(2)
C(14)	1242(14)	1182(11)	5821(9)	29(2)
C(15)	2428(14)	1259(11)	5692(9)	29(2)
C(16)	3223(14)	926(10)	6264(9)	29(2)
C(21)	3369(15)	-686(12)	8419(9)	33(2)
C(22)	3511(15)	-631(12)	9203(9)	33(2)
C(23)	3288(15)	-1359(11)	9761(9)	33(2)
C(24)	2889(14)	-2194(12)	9561(9)	33(2)
C(25)	2754(15)	-2259(12)	8809(9)	33(2)
C(26)	2970(15)	-1528(11)	8226(9)	33(2)
C(31)	7322(15)	-364(11)	8110(9)	33(2)
C(32)	8468(14)	-718(11)	7768(9)	33(2)
C(33)	9358(15)	-1301(11)	8232(9)	33(2)
C(34)	9156(15)	-1479(11)	8992(9)	33(2)
C(35)	7944(14)	-1135(11)	9328(10)	33(2)
C(36)	7044(15)	-571(11)	8885(9)	33(2)
C(41)	6862(14)	873(11)	6669(9)	28(2)
C(42)	7245(13)	1780(11)	6671(9)	28(2)
C(43)	7833(13)	2206(11)	6048(9)	28(2)
C(44)	8084(14)	1738(11)	5386(9)	28(2)
C(45)	7754(13)	824(11)	5370(9)	28(2)
C(46)	7171(13)	408(11)	6027(9)	28(2)
C(51)	8820(13)	4843(11)	6241(8)	25(2)
C(52)	7738(15)	5251(12)	5894(9)	32(4)
C(53)	7574(14)	4914(11)	5172(8)	25(2)
C(54)	8462(13)	4213(11)	4855(9)	25(2)
C(55)	9555(14)	3844(11)	5217(8)	25(2)
C(56)	9691(14)	4173(11)	5903(8)	25(2)

C(61)	7710(13)	5599(11)	7654(9)	27(2)
C(62)	7468(13)	6442(11)	8051(8)	27(2)
C(63)	6407(13)	6621(11)	8531(8)	27(2)
C(64)	5618(13)	5938(11)	8655(9)	27(2)
C(65)	5919(13)	5091(11)	8278(8)	27(2)
C(66)	6947(13)	4895(11)	7803(8)	27(2)
C(71)	11574(15)	5233(11)	8526(9)	30(2)
C(72)	12591(14)	4653(11)	8847(9)	30(2)
C(73)	12813(15)	4684(11)	9589(9)	30(2)
C(74)	11990(14)	5265(11)	10022(9)	30(2)
C(75)	10968(14)	5851(11)	9728(9)	30(2)
C(76)	10773(14)	5846(11)	8987(9)	30(2)
C(81)	12620(14)	4630(11)	7065(9)	29(2)
C(82)	12863(14)	3665(11)	6892(9)	29(2)
C(83)	13945(13)	3275(11)	6517(9)	29(2)
C(84)	14815(14)	3870(11)	6324(9)	29(2)
C(85)	14610(14)	4827(11)	6522(9)	29(2)
C(86)	13526(13)	5217(12)	6888(9)	29(2)

Table B14. Bond lengths [Å] and angles [°] for [$PdCl_2$(PNP-n-Butyl)].

Atoms	Bond length (Å)	Atoms	Bond angle (°)
Pd(1)-P(1)	2.205(4)	P(1)-Pd(1)-P(2)	71.25(15)
Pd(1)-P(2)	2.227(4)	P(1)-Pd(1)-Cl(1)	93.98(15)
Pd(1)-Cl(1)	2.345(4)	P(2)-Pd(1)-Cl(1)	165.10(15)
Pd(1)-Cl(2)#1	2.346(4)	P(1)-Pd(1)-Cl(2)#1	172.19(16)
Pd(1)-Cl(2)	2.346(4)	P(2)-Pd(1)-Cl(2)#1	100.94(15)
Pd(2)-P(3)	2.201(4)	Cl(1)-Pd(1)-Cl(2)#1	93.82(15)
Pd(2)-P(4)	2.223(4)	P(1)-Pd(1)-Cl(2)	172.19(16)
Pd(2)-Cl(4)#1	2.360(4)	P(2)-Pd(1)-Cl(2)	100.94(15)
Pd(2)-Cl(4)	2.360(4)	Cl(1)-Pd(1)-Cl(2)	93.82(15)
Pd(2)-Cl(3)	2.364(4)	Cl(2)#1-Pd(1)-Cl(2)	0.00(19)
N(1)-C(1)	1.457(17)	P(3)-Pd(2)-P(4)	71.49(15)
N(1)-P(2)	1.690(12)	P(3)-Pd(2)-Cl(4)#1	170.15(14)
N(1)-P(1)	1.690(13)	P(4)-Pd(2)-Cl(4)#1	98.78(15)
N(2)-C(5)	1.48(2)	P(3)-Pd(2)-Cl(4)	170.15(14)
N(2)-P(3)	1.668(13)	P(4)-Pd(2)-Cl(4)	98.78(15)
N(2)-P(4)	1.674(13)	Cl(4)#1-Pd(2)-Cl(4)	0.0(2)
P(1)-C(21)	1.765(16)	P(3)-Pd(2)-Cl(3)	95.09(15)
P(1)-C(11)	1.794(15)	P(4)-Pd(2)-Cl(3)	166.58(15)
P(1)-P(2)	2.581(6)	Cl(4)#1-Pd(2)-Cl(3)	94.62(14)
P(2)-C(41)	1.754(16)	Cl(4)-Pd(2)-Cl(3)	94.62(14)
P(2)-C(31)	1.833(15)	C(1)-N(1)-P(2)	129.0(10)
P(3)-C(61)	1.798(15)	C(1)-N(1)-P(1)	129.2(10)

P(3)-C(51)	1.804(15)	P(2)-N(1)-P(1)	99.6(6)
P(3)-P(4)	2.584(6)	C(5)-N(2)-P(3)	127.0(11)
P(4)-C(71)	1.798(15)	C(5)-N(2)-P(4)	127.5(10)
P(4)-C(81)	1.805(16)	P(3)-N(2)-P(4)	101.3(7)
Cl(2)-Cl(2)#1	0.000(8)	N(1)-P(1)-C(21)	108.8(7)
Cl(4)-Cl(4)#1	0.000(8)	N(1)-P(1)-C(11)	107.3(7)
C(1)-C(2)	1.504(19)	C(21)-P(1)-C(11)	109.0(8)
C(2)-C(3)	1.513(19)	N(1)-P(1)-Pd(1)	95.0(4)
C(3)-C(4)	1.554(19)	C(21)-P(1)-Pd(1)	117.6(6)
C(5)-C(6)	1.51(2)	C(11)-P(1)-Pd(1)	117.6(5)
C(6)-C(7)	1.55(2)	N(1)-P(1)-P(2)	40.2(4)
C(7)-C(8)	1.43(2)	C(21)-P(1)-P(2)	123.2(6)
C(11)-C(16)	1.35(2)	C(11)-P(1)-P(2)	124.0(6)
C(11)-C(12)	1.41(2)	Pd(1)-P(1)-P(2)	54.77(13)
C(12)-C(13)	1.41(2)	N(1)-P(2)-C(41)	109.3(7)
C(13)-C(14)	1.41(2)	N(1)-P(2)-C(31)	108.6(7)
C(14)-C(15)	1.36(2)	C(41)-P(2)-C(31)	107.2(8)
C(15)-C(16)	1.38(2)	N(1)-P(2)-Pd(1)	94.2(4)
C(21)-C(22)	1.42(2)	C(41)-P(2)-Pd(1)	118.3(5)
C(21)-C(26)	1.42(2)	C(31)-P(2)-Pd(1)	118.0(5)
C(22)-C(23)	1.35(2)	N(1)-P(2)-P(1)	40.2(4)
C(23)-C(24)	1.42(2)	C(41)-P(2)-P(1)	126.2(5)
C(24)-C(25)	1.37(2)	C(31)-P(2)-P(1)	123.1(6)
C(25)-C(26)	1.38(2)	Pd(1)-P(2)-P(1)	53.98(13)
C(31)-C(36)	1.38(2)	N(2)-P(3)-C(61)	110.6(7)
C(31)-C(32)	1.40(2)	N(2)-P(3)-C(51)	108.4(7)
C(32)-C(33)	1.41(2)	C(61)-P(3)-C(51)	108.3(7)
C(33)-C(34)	1.34(2)	N(2)-P(3)-Pd(2)	94.1(5)
C(34)-C(35)	1.46(2)	C(61)-P(3)-Pd(2)	116.5(5)
C(35)-C(36)	1.38(2)	C(51)-P(3)-Pd(2)	117.8(5)
C(41)-C(46)	1.36(2)	N(2)-P(3)-P(4)	39.4(4)
C(41)-C(42)	1.41(2)	C(61)-P(3)-P(4)	125.1(5)
C(42)-C(43)	1.35(2)	C(51)-P(3)-P(4)	123.6(5)
C(43)-C(44)	1.39(2)	Pd(2)-P(3)-P(4)	54.65(13)
C(44)-C(45)	1.39(2)	N(2)-P(4)-C(71)	108.9(7)
C(45)-C(46)	1.39(2)	N(2)-P(4)-C(81)	111.0(7)
C(51)-C(56)	1.37(2)	C(71)-P(4)-C(81)	107.0(7)
C(51)-C(52)	1.40(2)	N(2)-P(4)-Pd(2)	93.1(5)
C(52)-C(53)	1.45(2)	C(71)-P(4)-Pd(2)	120.3(5)
C(53)-C(54)	1.39(2)	C(81)-P(4)-Pd(2)	115.6(5)
C(54)-C(55)	1.41(2)	N(2)-P(4)-P(3)	39.3(4)
C(55)-C(56)	1.381(19)	C(71)-P(4)-P(3)	125.7(6)
C(61)-C(66)	1.41(2)	C(81)-P(4)-P(3)	124.1(5)

C(61)-C(62)	1.413(19)	Pd(2)-P(4)-P(3)	53.85(13)
C(62)-C(63)	1.40(2)	Cl(2)#1-Cl(2)-Pd(1)	0(10)
C(63)-C(64)	1.41(2)	Cl(4)#1-Cl(4)-Pd(2)	0(10)
C(64)-C(65)	1.397(19)	N(1)-C(1)-C(2)	114.6(12)
C(65)-C(66)	1.37(2)	C(1)-C(2)-C(3)	110.7(12)
C(71)-C(72)	1.38(2)	C(2)-C(3)-C(4)	112.8(12)
C(71)-C(76)	1.40(2)	N(2)-C(5)-C(6)	116.5(13)
C(72)-C(73)	1.363(19)	C(5)-C(6)-C(7)	116.6(14)
C(73)-C(74)	1.36(2)	C(8)-C(7)-C(6)	114.6(15)
C(74)-C(75)	1.37(2)	C(16)-C(11)-C(12)	120.6(15)
C(75)-C(76)	1.345(19)	C(16)-C(11)-P(1)	119.4(13)
C(81)-C(82)	1.38(2)	C(12)-C(11)-P(1)	119.8(12)
C(81)-C(86)	1.42(2)	C(11)-C(12)-C(13)	117.6(15)
C(82)-C(83)	1.38(2)	C(12)-C(13)-C(14)	120.6(15)
C(83)-C(84)	1.39(2)	C(15)-C(14)-C(13)	119.1(15)
C(84)-C(85)	1.39(2)	C(14)-C(15)-C(16)	120.5(16)
C(85)-C(86)	1.38(2)	C(11)-C(16)-C(15)	121.5(16)
		C(22)-C(21)-C(26)	118.6(14)
		C(22)-C(21)-P(1)	119.3(12)
		C(26)-C(21)-P(1)	121.4(12)
		C(23)-C(22)-C(21)	121.6(16)
		C(22)-C(23)-C(24)	119.3(16)
		C(25)-C(24)-C(23)	119.7(15)
		C(24)-C(25)-C(26)	122.5(16)
		C(25)-C(26)-C(21)	118.3(15)
		C(36)-C(31)-C(32)	122.0(14)
		C(36)-C(31)-P(2)	118.2(12)
		C(32)-C(31)-P(2)	119.8(12)
		C(31)-C(32)-C(33)	118.9(15)
		C(34)-C(33)-C(32)	121.4(16)
		C(33)-C(34)-C(35)	118.4(15)
		C(36)-C(35)-C(34)	121.4(16)
		C(31)-C(36)-C(35)	117.7(16)
		C(46)-C(41)-C(42)	117.1(15)
		C(46)-C(41)-P(2)	125.2(12)
		C(42)-C(41)-P(2)	117.4(12)
		C(43)-C(42)-C(41)	121.7(15)
		C(42)-C(43)-C(44)	119.9(15)
		C(45)-C(44)-C(43)	120.0(15)
		C(46)-C(45)-C(44)	118.1(14)
		C(41)-C(46)-C(45)	123.0(15)
		C(56)-C(51)-C(52)	120.9(14)
		C(56)-C(51)-P(3)	121.3(12)

C(52)-C(51)-P(3)	117.2(12)
C(51)-C(52)-C(53)	117.1(15)
C(54)-C(53)-C(52)	120.6(14)
C(53)-C(54)-C(55)	120.2(14)
C(56)-C(55)-C(54)	118.2(15)
C(51)-C(56)-C(55)	123.0(14)
C(66)-C(61)-C(62)	119.5(14)
C(66)-C(61)-P(3)	121.2(11)
C(62)-C(61)-P(3)	118.8(12)
C(63)-C(62)-C(61)	119.9(15)
C(62)-C(63)-C(64)	120.4(14)
C(65)-C(64)-C(63)	117.9(14)
C(66)-C(65)-C(64)	123.2(16)
C(65)-C(66)-C(61)	118.9(14)
C(72)-C(71)-C(76)	118.2(14)
C(72)-C(71)-P(4)	122.3(12)
C(76)-C(71)-P(4)	119.5(12)
C(73)-C(72)-C(71)	120.9(15)
C(74)-C(73)-C(72)	118.9(15)
C(73)-C(74)-C(75)	122.1(15)
C(76)-C(75)-C(74)	118.9(15)
C(75)-C(76)-C(71)	121.0(15)
C(82)-C(81)-C(86)	119.0(14)
C(82)-C(81)-P(4)	125.0(13)
C(86)-C(81)-P(4)	115.9(11)
C(81)-C(82)-C(83)	121.7(16)
C(82)-C(83)-C(84)	118.7(14)
C(85)-C(84)-C(83)	120.5(15)
C(86)-C(85)-C(84)	120.6(16)
C(85)-C(86)-C(81)	119.4(14)

Table B15. Anisotropic displacement parameters ($A^2 \times 10^3$) for [$PdCl_2$(PNP-n-Butyl)]. The anisotropic displacement factor exponent takes the form: -2 pi [h^2 a*^2 U11 + ... + 2 h k a* b* U12]

	U11	U22	U33	U23	U13	U12
Pd(1)	22(1)	18(1)	39(1)	-8(1)	-6(1)	-3(1)
Pd(2)	20(1)	19(1)	34(1)	-8(1)	-3(1)	-5(1)
N(1)	27(7)	23(6)	24(7)	-7(5)	4(6)	-15(6)
N(2)	20(7)	37(8)	29(8)	-6(6)	2(6)	-17(6)
P(1)	21(2)	19(2)	36(3)	-5(2)	-5(2)	-5(2)
P(2)	24(2)	19(2)	34(3)	-10(2)	-3(2)	-1(2)
P(3)	15(2)	21(2)	34(2)	-7(2)	0(2)	0(2)
P(4)	19(2)	17(2)	39(3)	-9(2)	-2(2)	-3(2)

Cl(1)	30(2)	27(2)	37(2)	-5(2)	1(2)	-1(2)
Cl(2)	32(2)	28(2)	43(3)	-10(2)	-4(2)	-13(2)
Cl(3)	23(2)	25(2)	35(2)	-6(2)	-4(2)	2(2)
Cl(4)	27(2)	28(2)	39(2)	-8(2)	-3(2)	-12(2)
C(1)	24(4)	22(4)	43(5)	-11(4)	-5(4)	-3(4)
C(2)	24(4)	22(4)	43(5)	-11(4)	-5(4)	-3(4)
C(3)	24(4)	22(4)	43(5)	-11(4)	-5(4)	-3(4)
C(4)	24(4)	22(4)	43(5)	-11(4)	-5(4)	-3(4)
C(5)	37(5)	29(5)	45(6)	-8(4)	0(4)	-3(4)
C(6)	37(5)	29(5)	45(6)	-8(4)	0(4)	-3(4)
C(7)	37(5)	29(5)	45(6)	-8(4)	0(4)	-3(4)
C(8)	37(5)	29(5)	45(6)	-8(4)	0(4)	-3(4)
C(11)	25(3)	20(3)	41(4)	-4(3)	-4(3)	-3(3)
C(12)	25(3)	20(3)	41(4)	-4(3)	-4(3)	-3(3)
C(13)	25(3)	20(3)	41(4)	-4(3)	-4(3)	-3(3)
C(14)	25(3)	20(3)	41(4)	-4(3)	-4(3)	-3(3)
C(15)	25(3)	20(3)	41(4)	-4(3)	-4(3)	-3(3)
C(16)	25(3)	20(3)	41(4)	-4(3)	-4(3)	-3(3)
C(21)	36(4)	28(4)	34(4)	3(3)	1(3)	-12(3)
C(22)	36(4)	28(4)	34(4)	3(3)	1(3)	-12(3)
C(23)	36(4)	28(4)	34(4)	3(3)	1(3)	-12(3)
C(24)	36(4)	28(4)	34(4)	3(3)	1(3)	-12(3)
C(25)	36(4)	28(4)	34(4)	3(3)	1(3)	-12(3)
C(26)	36(4)	28(4)	34(4)	3(3)	1(3)	-12(3)
C(31)	34(4)	24(4)	40(4)	-7(3)	-11(3)	1(3)
C(32)	34(4)	24(4)	40(4)	-7(3)	-11(3)	1(3)
C(33)	34(4)	24(4)	40(4)	-7(3)	-11(3)	1(3)
C(34)	34(4)	24(4)	40(4)	-7(3)	-11(3)	1(3)
C(35)	34(4)	24(4)	40(4)	-7(3)	-11(3)	1(3)
C(36)	34(4)	24(4)	40(4)	-7(3)	-11(3)	1(3)
C(41)	24(4)	23(3)	37(4)	-2(3)	0(3)	-9(3)
C(42)	24(4)	23(3)	37(4)	-2(3)	0(3)	-9(3)
C(43)	24(4)	23(3)	37(4)	-2(3)	0(3)	-9(3)
C(44)	24(4)	23(3)	37(4)	-2(3)	0(3)	-9(3)
C(45)	24(4)	23(3)	37(4)	-2(3)	0(3)	-9(3)
C(46)	24(4)	23(3)	37(4)	-2(3)	0(3)	-9(3)
C(51)	23(4)	28(4)	28(4)	-3(3)	-3(3)	-10(3)
C(53)	23(4)	28(4)	28(4)	-3(3)	-3(3)	-10(3)
C(54)	23(4)	28(4)	28(4)	-3(3)	-3(3)	-10(3)
C(55)	23(4)	28(4)	28(4)	-3(3)	-3(3)	-10(3)
C(56)	23(4)	28(4)	28(4)	-3(3)	-3(3)	-10(3)
C(61)	14(3)	36(4)	34(4)	-16(3)	-7(3)	1(3)
C(62)	14(3)	36(4)	34(4)	-16(3)	-7(3)	1(3)

C(63)	14(3)	36(4)	34(4)	-16(3)	-7(3)	1(3)
C(64)	14(3)	36(4)	34(4)	-16(3)	-7(3)	1(3)
C(65)	14(3)	36(4)	34(4)	-16(3)	-7(3)	1(3)
C(66)	14(3)	36(4)	34(4)	-16(3)	-7(3)	1(3)
C(71)	32(4)	27(3)	32(4)	-8(3)	-4(3)	-8(3)
C(72)	32(4)	27(3)	32(4)	-8(3)	-4(3)	-8(3)
C(73)	32(4)	27(3)	32(4)	-8(3)	-4(3)	-8(3)
C(74)	32(4)	27(3)	32(4)	-8(3)	-4(3)	-8(3)
C(75)	32(4)	27(3)	32(4)	-8(3)	-4(3)	-8(3)
C(76)	32(4)	27(3)	32(4)	-8(3)	-4(3)	-8(3)
C(81)	22(4)	29(4)	37(4)	-7(3)	-3(3)	-4(3)
C(82)	22(4)	29(4)	37(4)	-7(3)	-3(3)	-4(3)
C(83)	22(4)	29(4)	37(4)	-7(3)	-3(3)	-4(3)
C(84)	22(4)	29(4)	37(4)	-7(3)	-3(3)	-4(3)
C(85)	22(4)	29(4)	37(4)	-7(3)	-3(3)	-4(3)
C(86)	22(4)	29(4)	37(4)	-7(3)	-3(3)	-4(3)

Appendix C

Table C1: Atomic coordinates (x 10^4) and equivalent isotropic displacement parameters ($Å^2$ x 10^3) for $[NH_3\text{-n-Pent}][CrCl_4(PNP\text{-n-Pent})]\,2C_7H_8$ U(eq) is defined as one third of the trace of the orthogonalize Uij tensor.

	x	y	z	U(eq)
Cr(1)	6243(1)	2808(1)	6304(1)	14(1)
Cr(2)	3759(1)	2193(1)	8696(1)	15(1)
N(11)	7316(5)	3057(4)	5170(3)	14(2)
N(21)	2696(5)	1945(4)	9832(4)	17(2)
P(11)	7070(2)	3734(1)	5674(1)	15(1)
P(12)	6916(2)	2238(1)	5462(1)	14(1)
P(21)	3085(2)	2767(1)	9541(1)	14(1)
P(22)	2932(2)	1266(1)	9322(1)	16(1)
Cl(11)	5907(2)	3676(1)	7063(1)	19(1)
Cl(12)	7712(2)	2876(1)	7316(1)	18(1)
Cl(13)	5468(2)	1707(1)	6617(1)	19(1)
Cl(14)	4804(2)	2715(1)	5255(1)	19(1)
Cl(21)	4533(2)	3293(1)	8383(1)	18(1)
Cl(22)	2288(2)	2123(1)	7683(1)	20(1)
Cl(23)	4095(2)	1326(1)	7936(1)	20(1)
Cl(24)	5197(2)	2285(1)	9743(1)	19(1)
C(11)	7097(6)	2229(5)	8941(5)	23(2)
C(12)	7174(6)	1539(5)	8538(5)	27(2)
C(13)	8065(6)	1290(5)	9026(5)	28(2)
C(14)	8130(9)	576(6)	8631(6)	53(3)
C(15)	8287(9)	645(6)	7887(6)	61(4)
C(16)	2895(6)	2759(5)	6063(4)	23(2)
C(17)	2814(6)	3465(5)	6451(4)	23(2)
C(18)	1930(7)	3717(6)	5983(5)	36(3)
C(19)	1865(7)	4432(5)	6365(6)	45(3)
C(20)	1723(9)	4361(6)	7118(6)	57(4)
C(21)	2150(7)	1095(5)	4602(5)	25(2)
C(22)	1221(6)	1077(5)	4614(5)	28(2)
C(23)	979(6)	845(5)	5220(5)	33(2)
C(24)	1662(8)	644(5)	5826(6)	39(3)
C(25)	2584(8)	668(5)	5820(5)	40(3)
C(26)	2826(7)	892(5)	5222(5)	28(2)
C(27)	2404(7)	1334(5)	3935(5)	47(3)
C(31)	1473(7)	3241(5)	2293(7)	54(3)
C(32)	726(8)	2601(5)	1862(6)	40(3)
C(33)	311(8)	2485(7)	1068(6)	50(3)
C(34)	617(11)	3021(8)	672(8)	79(4)
C(35)	1324(9)	3651(8)	1057(7)	57(4)

C(36)	1781(9)	3796(6)	1868(8)	61(4)
C(37)	1899(8)	3347(7)	3158(7)	90(5)
C(41)	8561(7)	1757(6)	2735(5)	42(3)
C(42)	8251(8)	1221(6)	3155(7)	47(3)
C(43)	8660(9)	1329(6)	3922(7)	58(4)
C(44)	9390(7)	1986(6)	4343(5)	39(2)
C(45)	9702(8)	2522(6)	3943(6)	46(3)
C(46)	9272(7)	2402(6)	3140(6)	44(3)
C(47)	8092(7)	1629(5)	1873(5)	48(3)
C(51)	7845(7)	3899(5)	392(5)	30(2)
C(52)	8774(7)	3940(5)	379(5)	33(3)
C(53)	9005(7)	4161(5)	-234(5)	35(3)
C(54)	8334(7)	4347(5)	-837(5)	36(3)
C(55)	7390(6)	4316(5)	-831(5)	32(2)
C(56)	7156(7)	4101(5)	-218(5)	31(2)
C(57)	7579(7)	3682(6)	1057(5)	46(3)
C(101)	8051(5)	3198(5)	4800(5)	22(2)
C(102)	7758(6)	3533(5)	4070(4)	21(2)
C(103)	7015(6)	3004(5)	3363(4)	22(2)
C(104)	6658(7)	3385(5)	2668(4)	29(2)
C(105)	5948(7)	2834(6)	1947(5)	38(3)
C(111)	8246(6)	4460(4)	6195(4)	20(2)
C(112)	8748(7)	4881(5)	5798(6)	31(2)
C(113)	9643(6)	5411(5)	6198(6)	37(3)
C(114)	0021(7)	5536(5)	7003(6)	45(3)
C(115)	9518(8)	5135(6)	7388(6)	43(3)
C(116)	8634(7)	4590(5)	6993(5)	31(2)
C(121)	6380(6)	4237(5)	4989(5)	17(2)
C(122)	5693(6)	3855(5)	4260(5)	25(2)
C(123)	5142(6)	4231(6)	3745(5)	32(3)
C(124)	5245(7)	4971(6)	3949(6)	40(3)
C(125)	5895(7)	5354(6)	4663(6)	38(3)
C(126)	6460(7)	4979(5)	5177(5)	27(2)
C(131)	6119(6)	1511(4)	4643(4)	16(2)
C(132)	5245(6)	1071(5)	4677(4)	24(2)
C(133)	4642(7)	466(5)	4107(4)	29(2)
C(134)	4903(6)	286(5)	3492(5)	28(2)
C(135)	5759(7)	726(5)	3453(5)	27(2)
C(136)	6372(7)	1324(5)	4027(5)	23(2)
C(141)	8017(6)	1904(5)	5837(4)	14(1)
C(142)	8934(6)	2428(5)	6284(4)	20(2)
C(143)	9783(6)	2184(5)	6587(5)	21(2)
C(144)	9715(7)	1428(5)	6452(4)	24(2)

C(145)	8814(6)	905(5)	6038(5)	25(2)
C(146)	7962(6)	1140(5)	5722(4)	20(2)
C(201)	1936(6)	1802(5)	10187(4)	20(2)
C(202)	2233(6)	1452(5)	10913(5)	26(2)
C(203)	2986(6)	1996(5)	11623(5)	26(2)
C(204)	3334(7)	1608(5)	12316(5)	31(2)
C(205)	4033(7)	2156(6)	13031(5)	36(3)
C(211)	1983(6)	3087(5)	9157(5)	19(1)
C(212)	2029(6)	3835(5)	9273(4)	21(2)
C(213)	1184(7)	4075(5)	8968(5)	31(2)
C(214)	287(6)	3577(5)	8540(5)	26(2)
C(215)	223(6)	2818(5)	8426(4)	19(2)
C(216)	1067(6)	2584(5)	8722(4)	16(2)
C(221)	3899(6)	3505(5)	10350(4)	18(2)
C(222)	3629(6)	3670(5)	10963(4)	21(2)
C(223)	4231(7)	4273(5)	11547(5)	25(2)
C(224)	5093(7)	4698(5)	11525(5)	27(2)
C(225)	5358(6)	4544(5)	10914(5)	27(2)
C(226)	4775(6)	3936(5)	10335(5)	20(2)
C(231)	3629(6)	768(5)	10014(5)	19(2)
C(232)	3538(6)	8(5)	9815(5)	27(2)
C(233)	4111(7)	-353(6)	10346(6)	38(3)
C(234)	4765(7)	39(6)	11061(6)	39(3)
C(235)	4874(7)	795(5)	11258(5)	33(2)
C(236)	4304(6)	1155(5)	10723(4)	22(2)
C(241)	1766(6)	547(5)	8804(5)	24(2)
C(242)	1379(7)	401(5)	8002(5)	29(2)
C(243)	472(8)	-132(5)	7611(6)	46(3)
C(244)	-27(7)	-530(6)	8018(7)	47(3)
C(245)	359(7)	-416(6)	8801(6)	38(3)
C(246)	1264(6)	125(5)	9194(5)	25(2)
N(01)	3723(5)	2497(4)	6575(4)	23(2)
N(02)	6287(5)	2500(4)	8425(3)	18(2)

Table C2. Bond lengths [Å] and angles [°] for $[NH_3\text{-n-Pent}][CrCl_4(PNP\text{-n-Pent})]\,2C_7H_8$.

Atoms	Bond length (Å)	Atoms	Bond angle (°)
Cr(1)-Cl(14)	2.313(2)	Cl(14)-Cr(1)-Cl(12)	177.26(9)
Cr(1)-Cl(12)	2.315(2)	Cl(14)-Cr(1)-Cl(13)	90.18(9)
Cr(1)-Cl(13)	2.330(3)	Cl(12)-Cr(1)-Cl(13)	90.17(9)
Cr(1)-Cl(11)	2.341(2)	Cl(14)-Cr(1)-Cl(11)	92.69(9)
Cr(1)-P(12)	2.465(2)	Cl(12)-Cr(1)-Cl(11)	89.94(8)
Cr(1)-P(11)	2.497(3)	Cl(13)-Cr(1)-Cl(11)	99.01(9)

Cr(2)-Cl(24)	2.310(2)	Cl(14)-Cr(1)-P(12)	90.15(8)
Cr(2)-Cl(22)	2.318(2)	Cl(12)-Cr(1)-P(12)	87.11(8)
Cr(2)-Cl(21)	2.328(3)	Cl(13)-Cr(1)-P(12)	97.78(9)
Cr(2)-Cl(23)	2.342(2)	Cl(11)-Cr(1)-P(12)	162.96(10)
Cr(2)-P(21)	2.474(2)	Cl(14)-Cr(1)-P(11)	85.26(9)
Cr(2)-P(22)	2.492(3)	Cl(12)-Cr(1)-P(11)	93.66(9)
N(11)-C(101)	1.484(9)	Cl(13)-Cr(1)-P(11)	163.77(9)
N(11)-P(12)	1.704(7)	Cl(11)-Cr(1)-P(11)	96.76(9)
N(11)-P(11)	1.712(6)	P(12)-Cr(1)-P(11)	66.72(8)
N(21)-C(201)	1.497(9)	Cl(24)-Cr(2)-Cl(22)	177.33(9)
N(21)-P(21)	1.703(7)	Cl(24)-Cr(2)-Cl(21)	90.23(9)
N(21)-P(22)	1.711(7)	Cl(22)-Cr(2)-Cl(21)	90.22(9)
P(11)-C(121)	1.812(8)	Cl(24)-Cr(2)-Cl(23)	92.67(9)
P(11)-C(111)	1.836(8)	Cl(22)-Cr(2)-Cl(23)	89.86(9)
P(12)-C(131)	1.815(8)	Cl(21)-Cr(2)-Cl(23)	98.95(9)
P(12)-C(141)	1.822(8)	Cl(24)-Cr(2)-P(21)	90.18(8)
P(21)-C(211)	1.812(8)	Cl(22)-Cr(2)-P(21)	87.15(8)
P(21)-C(221)	1.820(8)	Cl(21)-Cr(2)-P(21)	97.70(9)
P(22)-C(231)	1.818(9)	Cl(23)-Cr(2)-P(21)	163.09(10)
P(22)-C(241)	1.821(9)	Cl(24)-Cr(2)-P(22)	85.35(9)
C(11)-N(02)	1.480(9)	Cl(22)-Cr(2)-P(22)	93.50(9)
C(11)-C(12)	1.496(11)	Cl(21)-Cr(2)-P(22)	163.89(9)
C(12)-C(13)	1.524(11)	Cl(23)-Cr(2)-P(22)	96.73(9)
C(13)-C(14)	1.520(13)	P(21)-Cr(2)-P(22)	66.88(8)
C(14)-C(15)	1.511(13)	C(101)-N(11)-P(12)	125.1(5)
C(16)-N(01)	1.487(9)	C(101)-N(11)-P(11)	125.2(6)
C(16)-C(17)	1.512(10)	P(12)-N(11)-P(11)	106.0(3)
C(17)-C(18)	1.508(11)	C(201)-N(21)-P(21)	124.1(5)
C(18)-C(19)	1.509(12)	C(201)-N(21)-P(22)	124.7(6)
C(19)-C(20)	1.519(13)	P(21)-N(21)-P(22)	106.6(4)
C(21)-C(22)	1.393(12)	N(11)-P(11)-C(121)	107.8(4)
C(21)-C(26)	1.391(12)	N(11)-P(11)-C(111)	107.4(3)
C(21)-C(27)	1.505(12)	C(121)-P(11)-C(111)	101.5(4)
C(22)-C(23)	1.382(12)	N(11)-P(11)-Cr(1)	92.9(3)
C(23)-C(24)	1.378(12)	C(121)-P(11)-Cr(1)	121.6(3)
C(24)-C(25)	1.376(13)	C(111)-P(11)-Cr(1)	123.7(3)
C(25)-C(26)	1.364(12)	N(11)-P(12)-C(131)	110.9(3)
C(31)-C(32)	1.389(13)	N(11)-P(12)-C(141)	104.4(4)
C(31)-C(36)	1.439(15)	C(131)-P(12)-C(141)	101.7(4)
C(31)-C(37)	1.505(15)	N(11)-P(12)-Cr(1)	94.2(2)
C(32)-C(33)	1.381(13)	C(131)-P(12)-Cr(1)	121.4(3)
C(33)-C(34)	1.375(16)	C(141)-P(12)-Cr(1)	122.6(2)
C(34)-C(35)	1.334(16)	N(21)-P(21)-C(211)	104.7(4)

C(35)-C(36)	1.412(15)	N(21)-P(21)-C(221)	112.1(4)
C(41)-C(46)	1.363(14)	C(211)-P(21)-C(221)	102.7(4)
C(41)-C(42)	1.410(14)	N(21)-P(21)-Cr(2)	93.6(2)
C(41)-C(47)	1.500(11)	C(211)-P(21)-Cr(2)	121.9(3)
C(42)-C(43)	1.334(14)	C(221)-P(21)-Cr(2)	120.5(3)
C(43)-C(44)	1.396(14)	N(21)-P(22)-C(231)	107.1(3)
C(44)-C(45)	1.384(14)	N(21)-P(22)-C(241)	107.9(3)
C(45)-C(46)	1.396(13)	C(231)-P(22)-C(241)	101.9(4)
C(51)-C(52)	1.385(12)	N(21)-P(22)-Cr(2)	92.8(3)
C(51)-C(56)	1.389(13)	C(231)-P(22)-Cr(2)	121.4(3)
C(51)-C(57)	1.497(12)	C(241)-P(22)-Cr(2)	123.7(3)
C(52)-C(53)	1.380(12)	N(02)-C(11)-C(12)	110.5(7)
C(53)-C(54)	1.354(13)	C(11)-C(12)-C(13)	111.7(7)
C(54)-C(55)	1.406(11)	C(14)-C(13)-C(12)	112.1(8)
C(55)-C(56)	1.380(12)	C(15)-C(14)-C(13)	114.7(9)
C(101)-C(102)	1.514(10)	N(01)-C(16)-C(17)	111.5(6)
C(102)-C(103)	1.498(11)	C(18)-C(17)-C(16)	113.6(7)
C(103)-C(104)	1.521(11)	C(17)-C(18)-C(19)	113.5(8)
C(104)-C(105)	1.518(11)	C(18)-C(19)-C(20)	113.4(8)
C(111)-C(116)	1.388(11)	C(22)-C(21)-C(26)	118.2(9)
C(111)-C(112)	1.394(12)	C(22)-C(21)-C(27)	120.2(9)
C(112)-C(113)	1.378(12)	C(26)-C(21)-C(27)	121.5(9)
C(113)-C(114)	1.400(13)	C(23)-C(22)-C(21)	120.3(9)
C(114)-C(115)	1.360(15)	C(24)-C(23)-C(22)	120.3(8)
C(115)-C(116)	1.381(13)	C(23)-C(24)-C(25)	119.6(9)
C(121)-C(126)	1.368(12)	C(26)-C(25)-C(24)	120.5(9)
C(121)-C(122)	1.407(11)	C(25)-C(26)-C(21)	121.1(9)
C(122)-C(123)	1.381(11)	C(32)-C(31)-C(36)	116.4(11)
C(123)-C(124)	1.362(13)	C(32)-C(31)-C(37)	120.8(11)
C(124)-C(125)	1.373(13)	C(36)-C(31)-C(37)	122.8(10)
C(125)-C(126)	1.388(12)	C(31)-C(32)-C(33)	122.6(10)
C(131)-C(136)	1.390(10)	C(34)-C(33)-C(32)	120.2(12)
C(131)-C(132)	1.399(11)	C(35)-C(34)-C(33)	119.7(14)
C(132)-C(133)	1.381(11)	C(34)-C(35)-C(36)	122.6(13)
C(133)-C(134)	1.394(11)	C(35)-C(36)-C(31)	118.5(11)
C(134)-C(135)	1.380(12)	C(46)-C(41)-C(42)	117.6(9)
C(135)-C(136)	1.381(12)	C(46)-C(41)-C(47)	121.6(10)
C(141)-C(146)	1.403(10)	C(42)-C(41)-C(47)	120.7(10)
C(141)-C(142)	1.411(11)	C(43)-C(42)-C(41)	121.4(11)
C(142)-C(143)	1.393(10)	C(42)-C(43)-C(44)	121.5(11)
C(143)-C(144)	1.385(12)	C(45)-C(44)-C(43)	118.1(9)
C(144)-C(145)	1.383(11)	C(44)-C(45)-C(46)	119.9(10)
C(145)-C(146)	1.391(10)	C(41)-C(46)-C(45)	121.5(11)

C(201)-C(202)	1.524(11)	C(52)-C(51)-C(56)	118.6(9)
C(202)-C(203)	1.517(11)	C(52)-C(51)-C(57)	122.3(9)
C(203)-C(204)	1.523(11)	C(56)-C(51)-C(57)	119.1(8)
C(204)-C(205)	1.504(12)	C(53)-C(52)-C(51)	120.9(9)
C(211)-C(212)	1.375(12)	C(54)-C(53)-C(52)	121.1(9)
C(211)-C(216)	1.389(11)	C(53)-C(54)-C(55)	118.9(8)
C(212)-C(213)	1.385(11)	C(56)-C(55)-C(54)	120.4(9)
C(213)-C(214)	1.365(12)	C(55)-C(56)-C(51)	120.2(9)
C(214)-C(215)	1.389(12)	N(11)-C(101)-C(102)	116.1(6)
C(215)-C(216)	1.375(10)	C(103)-C(102)-C(101)	115.8(7)
C(221)-C(226)	1.380(11)	C(102)-C(103)-C(104)	113.7(7)
C(221)-C(222)	1.392(10)	C(105)-C(104)-C(103)	112.8(8)
C(222)-C(223)	1.393(11)	C(116)-C(111)-C(112)	119.8(8)
C(223)-C(224)	1.364(12)	C(116)-C(111)-P(11)	119.4(7)
C(224)-C(225)	1.378(11)	C(112)-C(111)-P(11)	120.8(6)
C(225)-C(226)	1.390(11)	C(113)-C(112)-C(111)	120.1(9)
C(231)-C(236)	1.378(10)	C(112)-C(113)-C(114)	119.3(10)
C(231)-C(232)	1.399(11)	C(115)-C(114)-C(113)	120.5(9)
C(232)-C(233)	1.394(12)	C(114)-C(115)-C(116)	120.7(10)
C(233)-C(234)	1.380(13)	C(115)-C(116)-C(111)	119.6(10)
C(234)-C(235)	1.386(13)	C(126)-C(121)-C(122)	118.1(8)
C(235)-C(236)	1.395(11)	C(126)-C(121)-P(11)	121.7(7)
C(241)-C(246)	1.384(12)	C(122)-C(121)-P(11)	120.1(7)
C(241)-C(242)	1.396(11)	C(123)-C(122)-C(121)	120.2(9)
C(242)-C(243)	1.391(12)	C(124)-C(123)-C(122)	120.1(9)
C(243)-C(244)	1.385(14)	C(123)-C(124)-C(125)	120.8(9)
C(244)-C(245)	1.361(14)	C(124)-C(125)-C(126)	119.3(10)
C(245)-C(246)	1.397(12)	C(121)-C(126)-C(125)	121.5(9)
		C(136)-C(131)-C(132)	118.6(8)
		C(136)-C(131)-P(12)	124.0(7)
		C(132)-C(131)-P(12)	117.2(6)
		C(133)-C(132)-C(131)	120.7(8)
		C(132)-C(133)-C(134)	120.1(8)
		C(135)-C(134)-C(133)	119.3(8)
		C(136)-C(135)-C(134)	120.8(8)
		C(135)-C(136)-C(131)	120.5(9)
		C(146)-C(141)-C(142)	119.6(7)
		C(146)-C(141)-P(12)	121.6(6)
		C(142)-C(141)-P(12)	118.7(6)
		C(143)-C(142)-C(141)	119.7(8)
		C(144)-C(143)-C(142)	119.7(8)
		C(145)-C(144)-C(143)	121.3(8)
		C(144)-C(145)-C(146)	119.8(8)

C(145)-C(146)-C(141)	119.8(8)
N(21)-C(201)-C(202)	114.3(7)
C(203)-C(202)-C(201)	114.3(8)
C(202)-C(203)-C(204)	112.5(8)
C(205)-C(204)-C(203)	112.2(8)
C(212)-C(211)-C(216)	118.0(8)
C(212)-C(211)-P(21)	121.2(7)
C(216)-C(211)-P(21)	120.7(7)
C(211)-C(212)-C(213)	120.8(9)
C(214)-C(213)-C(212)	120.8(9)
C(213)-C(214)-C(215)	119.2(8)
C(216)-C(215)-C(214)	119.7(8)
C(215)-C(216)-C(211)	121.5(8)
C(226)-C(221)-C(222)	119.4(7)
C(226)-C(221)-P(21)	119.3(6)
C(222)-C(221)-P(21)	121.2(6)
C(221)-C(222)-C(223)	120.1(8)
C(224)-C(223)-C(222)	120.1(8)
C(223)-C(224)-C(225)	120.1(8)
C(224)-C(225)-C(226)	120.5(8)
C(221)-C(226)-C(225)	119.8(8)
C(236)-C(231)-C(232)	119.6(8)
C(236)-C(231)-P(22)	119.5(6)
C(232)-C(231)-P(22)	120.7(7)
C(231)-C(232)-C(233)	119.5(9)
C(234)-C(233)-C(232)	120.0(10)
C(233)-C(234)-C(235)	120.9(9)
C(234)-C(235)-C(236)	118.9(9)
C(231)-C(236)-C(235)	121.0(9)
C(246)-C(241)-C(242)	119.0(9)
C(246)-C(241)-P(22)	121.0(7)
C(242)-C(241)-P(22)	119.9(7)
C(241)-C(242)-C(243)	119.5(10)
C(244)-C(243)-C(242)	120.1(10)
C(245)-C(244)-C(243)	121.2(10)
C(244)-C(245)-C(246)	118.8(10)
C(241)-C(246)-C(245)	121.3(9)

APPENDIX C

Table C3. Anisotropic displacement parameters ($A^2 \times 10^3$) for $[NH_3\text{-n-Pent}][CrCl_4(PNP\text{-n-Pent})]\,2C_7H_8$. The anisotropic displacement factor exponent takes the form: -2 pi [h^2 a*^2 U11 + ... + 2 h k a* b* U12]

	U11	U22	U33	U23	U13	U12
Cr(1)	11(1)	15(1)	16(1)	5(1)	5(1)	3(1)
Cr(2)	12(1)	15(1)	17(1)	5(1)	5(1)	3(1)
N(11)	16(4)	11(4)	16(3)	2(3)	6(3)	3(3)
N(21)	13(4)	21(4)	22(4)	9(3)	10(3)	5(3)
P(11)	13(1)	13(1)	19(1)	4(1)	6(1)	3(1)
P(12)	14(1)	13(1)	14(1)	2(1)	4(1)	2(1)
P(21)	9(1)	15(1)	18(1)	6(1)	4(1)	3(1)
P(22)	13(1)	15(1)	19(1)	5(1)	5(1)	2(1)
Cl(11)	20(1)	18(1)	20(1)	3(1)	7(1)	7(1)
Cl(12)	13(1)	20(1)	18(1)	4(1)	3(1)	3(1)
Cl(13)	16(1)	17(1)	21(1)	5(1)	7(1)	2(1)
Cl(14)	12(1)	23(1)	19(1)	6(1)	4(1)	4(1)
Cl(21)	18(1)	16(1)	21(1)	7(1)	7(1)	3(1)
Cl(22)	15(1)	23(1)	19(1)	6(1)	3(1)	6(1)
Cl(23)	19(1)	20(1)	22(1)	5(1)	9(1)	7(1)
Cl(24)	14(1)	20(1)	20(1)	5(1)	4(1)	4(1)
C(11)	17(5)	32(6)	20(5)	6(4)	4(4)	9(5)
C(12)	19(5)	25(6)	37(5)	16(4)	10(4)	8(5)
C(13)	25(5)	31(6)	34(5)	10(5)	12(5)	15(5)
C(14)	71(8)	47(8)	55(7)	26(6)	28(6)	31(7)
C(15)	80(9)	48(9)	82(8)	9(7)	48(8)	41(8)
C(16)	20(5)	24(6)	20(5)	4(4)	4(4)	5(4)
C(17)	29(5)	19(5)	19(4)	0(4)	10(4)	3(4)
C(18)	35(6)	37(7)	37(6)	18(5)	6(5)	17(5)
C(19)	39(6)	30(6)	85(8)	22(5)	36(6)	20(5)
C(20)	72(9)	42(8)	75(9)	13(7)	42(8)	29(7)
C(21)	25(6)	18(6)	22(5)	-4(4)	7(5)	-6(5)
C(22)	16(5)	28(6)	32(5)	2(4)	7(4)	-3(4)
C(23)	21(5)	24(5)	56(6)	4(5)	14(5)	10(4)
C(24)	44(7)	17(5)	58(7)	4(5)	27(6)	4(5)
C(25)	64(7)	20(6)	22(5)	-1(4)	3(5)	7(5)
C(26)	17(5)	28(6)	32(6)	-6(4)	6(5)	-2(4)
C(27)	56(7)	42(7)	33(5)	-14(4)	26(5)	-13(5)
C(31)	42(6)	19(5)	112(9)	-15(5)	47(6)	5(5)
C(32)	60(7)	25(6)	55(6)	16(5)	39(6)	19(5)
C(33)	51(7)	42(8)	81(8)	14(6)	46(7)	22(6)
C(34)	06(11)	79(10)	116(10)	38(9)	91(9)	61(9)
C(35)	50(8)	65(10)	76(9)	17(7)	38(7)	26(7)
C(36)	55(7)	28(7)	122(11)	5(7)	60(8)	17(6)
C(37)	43(8)	76(10)	136(11)	-44(8)	30(8)	13(7)

C(41)	41(6)	54(7)	36(5)	11(5)	14(5)	22(6)
C(42)	29(6)	36(7)	76(7)	2(6)	22(6)	7(5)
C(43)	82(9)	33(6)	109(10)	28(7)	77(8)	35(6)
C(44)	47(6)	41(6)	35(5)	8(4)	13(4)	26(5)
C(45)	54(7)	39(7)	44(6)	4(5)	14(5)	17(6)
C(46)	30(6)	32(7)	74(8)	2(6)	27(6)	7(5)
C(47)	51(7)	42(6)	46(5)	5(4)	12(5)	14(5)
C(51)	25(5)	25(6)	33(6)	-6(4)	11(5)	-2(5)
C(52)	37(6)	24(6)	28(5)	-10(4)	-1(5)	15(5)
C(53)	34(6)	31(6)	43(6)	-7(5)	30(5)	-6(5)
C(54)	47(7)	39(7)	27(5)	9(4)	24(5)	4(6)
C(55)	22(5)	25(6)	42(6)	-4(4)	4(4)	10(4)
C(56)	21(5)	31(6)	34(6)	-5(5)	10(5)	-1(5)
C(57)	31(6)	71(8)	36(6)	19(5)	11(5)	12(5)
C(101)	7(4)	22(5)	41(5)	9(4)	13(4)	6(4)
C(102)	26(5)	23(5)	20(4)	15(4)	14(4)	8(4)
C(103)	23(5)	24(6)	18(4)	-1(4)	9(4)	2(4)
C(104)	40(6)	29(6)	20(5)	8(4)	12(5)	10(5)
C(105)	34(6)	48(7)	30(5)	2(5)	13(5)	9(6)
C(111)	20(4)	9(4)	20(4)	-3(3)	-1(4)	-3(4)
C(112)	31(5)	23(6)	48(6)	13(5)	26(5)	5(5)
C(113)	15(5)	18(6)	68(7)	1(5)	11(5)	-4(4)
C(114)	21(6)	19(6)	63(7)	-11(5)	-14(5)	-3(5)
C(115)	46(8)	30(7)	34(6)	-2(5)	-7(6)	13(6)
C(116)	37(6)	10(5)	35(6)	1(4)	3(5)	2(4)
C(121)	10(4)	22(6)	23(5)	11(4)	5(4)	7(4)
C(122)	27(6)	23(6)	28(5)	9(4)	15(5)	4(5)
C(123)	19(5)	51(8)	32(5)	29(5)	7(4)	19(5)
C(124)	37(7)	45(7)	59(7)	42(6)	25(6)	27(6)
C(125)	37(6)	25(6)	63(7)	24(6)	24(6)	15(5)
C(126)	19(5)	29(6)	32(5)	11(4)	9(4)	4(5)
C(131)	10(4)	8(4)	25(5)	11(3)	0(4)	-1(4)
C(132)	24(5)	29(6)	18(4)	4(4)	7(4)	4(5)
C(133)	28(5)	34(6)	23(4)	1(4)	11(4)	1(5)
C(134)	27(5)	12(5)	28(5)	4(4)	-5(4)	-3(4)
C(135)	36(6)	23(6)	14(4)	2(4)	0(4)	10(5)
C(136)	23(5)	23(6)	26(5)	9(4)	12(4)	9(5)
C(141)	14(1)	13(1)	14(1)	2(1)	4(1)	2(1)
C(142)	10(4)	16(5)	30(5)	5(4)	4(4)	2(4)
C(143)	13(5)	26(6)	22(5)	5(4)	3(4)	6(4)
C(144)	23(5)	25(6)	23(5)	2(4)	8(4)	9(5)
C(145)	9(4)	21(5)	45(5)	10(4)	5(4)	9(4)
C(146)	17(5)	12(5)	29(5)	2(4)	8(4)	6(4)

C(201)	29(5)	22(5)	9(4)	3(3)	8(4)	4(4)
C(202)	15(5)	27(6)	36(5)	1(4)	13(4)	1(4)
C(203)	20(5)	28(6)	38(5)	16(4)	17(5)	9(4)
C(204)	25(5)	35(7)	32(5)	9(5)	11(5)	7(5)
C(205)	30(6)	50(8)	23(5)	15(5)	6(5)	7(6)
C(211)	12(2)	25(3)	21(2)	7(2)	8(2)	4(2)
C(212)	12(5)	25(6)	20(5)	6(4)	1(4)	0(4)
C(213)	45(6)	18(5)	28(5)	-2(4)	15(5)	8(5)
C(214)	12(5)	34(6)	28(5)	7(4)	0(4)	14(5)
C(215)	11(5)	23(5)	15(4)	0(4)	-1(4)	2(4)
C(216)	17(5)	18(5)	13(4)	0(4)	6(4)	4(4)
C(221)	20(5)	18(5)	16(4)	-1(3)	7(4)	5(4)
C(222)	20(5)	14(5)	23(5)	2(4)	4(4)	-1(4)
C(223)	27(5)	27(6)	26(5)	7(4)	13(4)	9(5)
C(224)	30(6)	25(6)	21(5)	-5(4)	4(4)	10(5)
C(225)	14(5)	14(5)	41(6)	7(4)	1(4)	-6(4)
C(226)	14(5)	17(5)	26(5)	4(4)	7(4)	2(4)
C(231)	15(5)	14(5)	31(5)	10(4)	15(4)	0(4)
C(232)	26(5)	14(5)	53(6)	12(4)	25(5)	6(4)
C(233)	36(7)	23(6)	81(8)	31(6)	43(6)	18(5)
C(234)	27(6)	60(8)	45(7)	35(6)	20(5)	23(6)
C(235)	38(6)	40(6)	30(5)	14(4)	17(5)	15(5)
C(236)	16(5)	34(6)	21(5)	14(4)	5(4)	16(4)
C(241)	15(5)	24(6)	42(6)	15(4)	16(4)	12(4)
C(242)	26(6)	19(6)	28(5)	1(4)	-1(5)	1(5)
C(243)	42(7)	14(6)	45(7)	-4(5)	-18(6)	-1(5)
C(244)	15(5)	24(6)	89(9)	21(6)	3(6)	5(5)
C(245)	21(6)	27(6)	68(8)	11(6)	18(6)	3(5)
C(246)	14(5)	21(5)	28(5)	-6(4)	-1(4)	0(4)
N(01)	17(4)	23(5)	27(4)	7(3)	6(4)	5(4)
N(02)	18(4)	20(4)	17(4)	1(3)	8(3)	7(3)

Table C4: Atomic coordinates (x 10^4) and equivalent isotropic displacement parameters ($Å^2$ x 10^3) for $[NH_3\text{-n-Butyl}][CrCl_4(PNP\text{-n-Butyl})]\,2C_7H_8$.U(eq) is defined as one third of the trace of the orthogonalize Uij tensor.

	X	Y	z	U(eq)
Cr(1)	6810(1)	2637(1)	1555(1)	16(1)
Cr(2)	3293(1)	2540(1)	3404(1)	18(1)
P(12)	8091(1)	1723(1)	952(1)	18(1)
P(11)	7774(1)	3584(1)	1059(1)	17(1)
P(22)	2397(1)	1501(1)	3862(1)	19(1)
P(21)	2015(1)	3323(1)	4054(1)	19(1)
Cl(11)	5744(1)	3870(1)	1993(1)	22(1)
Cl(13)	6281(1)	1371(1)	1930(1)	22(1)

Cl(12)	7988(1)	2222(1)	2200(1)	20(1)
Cl(14)	5731(1)	3047(1)	870(1)	21(1)
Cl(23)	4377(1)	1337(1)	2956(1)	23(1)
Cl(22)	2122(1)	2983(1)	2751(1)	23(1)
Cl(21)	3797(1)	3833(1)	3051(1)	25(1)
Cl(24)	4402(1)	2125(1)	4077(1)	24(1)
C(51)	5930(5)	8918(5)	8997(2)	33(2)
C(56)	5994(5)	9091(4)	8454(2)	35(2)
C(55)	6900(5)	8924(5)	8201(3)	40(2)
C(54)	7752(5)	8589(5)	8484(3)	40(2)
C(53)	7693(5)	8402(5)	9019(3)	42(2)
C(52)	6794(5)	8553(5)	9283(3)	38(2)
C(57)	4895(6)	9152(6)	9285(3)	62(2)
C(31)	6885(5)	3013(5)	6367(3)	44(2)
C(36)	6961(5)	3789(5)	6554(3)	45(2)
C(35)	7807(6)	3661(5)	6823(3)	51(2)
C(34)	8580(6)	2779(6)	6909(3)	59(2)
C(33)	8489(6)	2003(6)	6723(3)	56(2)
C(32)	7635(6)	2116(5)	6450(3)	48(2)
C(37)	5962(6)	3135(6)	6056(3)	66(3)
C(41)	4649(5)	2508(5)	8490(3)	43(2)
C(42)	5405(5)	1662(5)	8414(3)	47(2)
C(43)	6217(6)	1690(6)	8088(3)	51(2)
C(44)	6298(6)	2538(6)	7841(3)	55(2)
C(45)	5538(6)	3392(6)	7918(3)	48(2)
C(46)	4718(6)	3381(5)	8249(3)	47(2)
C(47)	3730(6)	2468(6)	8835(3)	60(2)
C(21)	4132(5)	1670(5)	7230(3)	43(2)
C(23)	2830(5)	1343(5)	7783(3)	45(2)
C(24)	2258(6)	2311(5)	7707(3)	52(2)
C(25)	2638(6)	2957(5)	7392(3)	53(2)
C(26)	3572(6)	2646(5)	7154(3)	48(2)
C(27)	5165(6)	1318(6)	6946(4)	65(3)
C(12)	6083(5)	4377(5)	3389(3)	37(2)
C(16)	7213(7)	3576(7)	4211(4)	86(4)
C(15)	7834(8)	3732(6)	3768(4)	81(3)
C(14)	7838(11)	4053(12)	3253(6)	64(5)
C(11A)	6326(10)	4046(11)	3899(5)	73(6)
C(98)	5341(12)	4105(12)	4291(7)	56(4)
C(13)	6896(11)	4462(12)	2990(6)	68(6)
C(19)	7545(16)	4491(14)	2810(7)	76(7)
C(11B)	7082(7)	4182(8)	3367(5)	31(3)
C(17)	6229(10)	3641(10)	4325(5)	43(4)

C(18)	5654(11)	4077(8)	3887(4)	33(3)
C(231)	2950(4)	361(4)	4288(2)	22(1)
C(232)	2377(5)	-177(5)	4523(2)	32(2)
C(233)	2802(5)	-1033(5)	4860(3)	38(2)
C(234)	3808(5)	-1363(5)	4957(2)	35(2)
C(235)	4398(5)	-851(5)	4713(3)	37(2)
C(236)	3965(4)	13(4)	4377(2)	26(1)
C(211)	873(4)	4349(4)	3912(2)	22(1)
C(216)	666(5)	4831(5)	3397(3)	34(2)
C(215)	-211(5)	5607(5)	3294(3)	45(2)
C(214)	-905(5)	5907(5)	3692(3)	40(2)
C(213)	-712(4)	5432(5)	4203(3)	31(2)
C(212)	174(4)	4662(4)	4315(2)	25(1)
C(221)	2472(4)	3602(4)	4619(2)	21(1)
C(222)	2892(4)	2909(4)	5053(2)	23(1)
C(223)	3323(4)	3149(5)	5446(2)	29(2)
C(224)	3379(4)	4049(5)	5405(3)	34(2)
C(225)	2986(5)	4731(5)	4967(3)	36(2)
C(226)	2539(4)	4515(4)	4573(2)	24(1)
C(201)	818(5)	2259(5)	4575(3)	45(2)
C(202)	933(6)	2128(6)	5134(3)	51(2)
C(203)	-24(6)	2067(6)	5458(3)	63(3)
C(205)	-834(6)	2983(6)	5401(4)	67(3)
C(204)	-210(6)	1174(7)	5415(3)	72(3)
C(114)	9844(4)	4481(5)	1961(2)	31(2)
C(121)	7212(4)	4650(4)	586(2)	20(1)
C(115)	0121(4)	3534(5)	1879(2)	28(1)
C(116)	9508(4)	3259(4)	1603(2)	22(1)
C(131)	7699(4)	1370(4)	390(2)	21(1)
C(136)	7242(4)	2047(4)	-41(2)	20(1)
C(135)	6837(4)	1778(4)	-431(2)	25(1)
C(134)	6879(4)	836(5)	-396(2)	29(1)
C(133)	7332(5)	162(5)	33(3)	33(2)
C(132)	7738(4)	423(5)	423(2)	28(1)
C(141)	9144(4)	658(4)	1184(3)	27(1)
C(1)	3259(4)	3517(4)	1459(2)	27(1)
C(2)	2536(4)	4480(5)	1536(2)	31(2)
C(3)	2959(4)	5276(5)	1553(3)	32(2)
C(5)	3504(5)	5476(5)	1031(3)	46(2)
C(4)	2117(6)	6186(6)	1672(4)	62(2)
C(146)	9964(5)	271(5)	855(3)	42(2)
C(145)	0767(5)	-538(5)	1054(4)	62(3)
C(126)	7783(4)	5071(4)	233(2)	25(1)

C(144)	0734(6)	-979(5)	1568(4)	60(3)
C(143)	9905(6)	-628(5)	1884(3)	49(2)
C(22)	3768(5)	1025(5)	7541(3)	42(2)
C(142)	9122(5)	177(4)	1703(3)	32(2)
C(101)	9442(4)	2623(4)	450(2)	24(1)
C(102)	9454(4)	2600(5)	-138(2)	29(1)
C(103)	0490(5)	2537(5)	-397(3)	36(2)
C(104)	0654(7)	3485(7)	-397(3)	70(3)
C(105)	0588(5)	2299(5)	-946(3)	42(2)
C(8A)	7252(5)	-69(5)	3403(3)	35(2)
N(02A)	6161(3)	2147(3)	3078(2)	23(1)
C(6A)	6933(5)	1687(5)	3491(2)	32(2)
C(7A)	7604(10)	753(10)	3465(6)	39(3)
C(10A)	6653(10)	-275(10)	3933(6)	46(4)
C(9A)	8069(12)	-951(11)	3338(7)	58(5)
C(8B)	7252(5)	-69(5)	3403(3)	35(2)
N(02B)	6161(3)	2147(3)	3078(2)	23(1)
C(6B)	6933(5)	1687(5)	3491(2)	32(2)
C(7B)	7020(8)	683(9)	3722(4)	24(3)
C(9B)	8357(10)	-336(10)	3160(6)	40(4)
C(10B)	7143(11)	-992(10)	3678(5)	41(4)
C(242)	595(4)	1901(4)	3357(2)	24(1)
C(125)	7325(5)	5925(5)	-93(2)	30(2)
C(243)	15(4)	1747(5)	3012(2)	28(1)
C(244)	402(5)	970(5)	2736(3)	36(2)
C(245)	1375(5)	337(5)	2827(3)	35(2)
C(246)	1952(5)	472(5)	3191(3)	32(2)
C(124)	6298(4)	6388(4)	-70(2)	27(1)
C(123)	5730(4)	5978(4)	278(2)	28(1)
C(241)	1559(4)	1259(4)	3464(2)	22(1)
C(122)	6185(4)	5113(4)	607(2)	23(1)
C(111)	8613(4)	3935(4)	1396(2)	18(1)
C(112)	8356(4)	4883(4)	1477(2)	26(1)
C(113)	8950(5)	5160(5)	1761(2)	33(2)
N(11)	8497(3)	2659(3)	741(2)	20(1)
N(21)	1688(3)	2336(3)	4244(2)	22(1)
N(01)	3964(3)	3063(3)	1900(2)	23(1)

Table C5. Bond lengths [Å] and angles [°] for $[NH_3\text{-i-Pent}][CrCl_4(PNP\text{-i-Pent})]2C_7H_8$..

Atoms	Bond length (Å)	Atoms	Bond angle (°)
Cr(1)-Cl(14)	2.2974(17)	Cl(14)-Cr(1)-Cl(12)	175.89(6)
Cr(1)-Cl(12)	2.3150(17)	Cl(14)-Cr(1)-Cl(13)	91.43(6)
Cr(1)-Cl(13)	2.3269(17)	Cl(12)-Cr(1)-Cl(13)	91.11(6)
Cr(1)-Cl(11)	2.3306(16)	Cl(14)-Cr(1)-Cl(11)	92.12(6)
Cr(1)-P(11)	2.4626(17)	Cl(12)-Cr(1)-Cl(11)	90.59(6)
Cr(1)-P(12)	2.4697(16)	Cl(13)-Cr(1)-Cl(11)	100.51(6)
Cr(2)-Cl(24)	2.3034(17)	Cl(14)-Cr(1)-P(11)	91.23(6)
Cr(2)-Cl(22)	2.3164(17)	Cl(12)-Cr(1)-P(11)	85.40(6)
Cr(2)-Cl(23)	2.3242(16)	Cl(13)-Cr(1)-P(11)	163.03(6)
Cr(2)-Cl(21)	2.3282(18)	Cl(11)-Cr(1)-P(11)	96.14(6)
Cr(2)-P(22)	2.4572(18)	Cl(14)-Cr(1)-P(12)	86.17(6)
Cr(2)-P(21)	2.4804(17)	Cl(12)-Cr(1)-P(12)	90.34(6)
P(12)-N(11)	1.699(5)	Cl(13)-Cr(1)-P(12)	96.39(6)
P(12)-C(141)	1.813(6)	Cl(11)-Cr(1)-P(12)	163.05(6)
P(12)-C(131)	1.816(6)	P(11)-Cr(1)-P(12)	67.08(6)
P(11)-N(11)	1.699(5)	Cl(24)-Cr(2)-Cl(22)	177.57(6)
P(11)-C(121)	1.806(6)	Cl(24)-Cr(2)-Cl(23)	91.17(6)
P(11)-C(111)	1.809(5)	Cl(22)-Cr(2)-Cl(23)	91.04(6)
P(22)-N(21)	1.706(5)	Cl(24)-Cr(2)-Cl(21)	90.08(6)
P(22)-C(241)	1.810(6)	Cl(22)-Cr(2)-Cl(21)	90.51(6)
P(22)-C(231)	1.813(6)	Cl(23)-Cr(2)-Cl(21)	100.81(6)
P(21)-N(21)	1.695(5)	Cl(24)-Cr(2)-P(22)	92.72(6)
P(21)-C(221)	1.811(6)	Cl(22)-Cr(2)-P(22)	86.12(6)
P(21)-C(211)	1.813(6)	Cl(23)-Cr(2)-P(22)	93.61(6)
C(51)-C(56)	1.377(8)	Cl(21)-Cr(2)-P(22)	165.26(6)
C(51)-C(52)	1.381(8)	Cl(24)-Cr(2)-P(21)	85.50(6)
C(51)-C(57)	1.553(9)	Cl(22)-Cr(2)-P(21)	92.07(6)
C(56)-C(55)	1.363(8)	Cl(23)-Cr(2)-P(21)	159.80(7)
C(55)-C(54)	1.366(8)	Cl(21)-Cr(2)-P(21)	99.11(6)
C(54)-C(53)	1.355(8)	P(22)-Cr(2)-P(21)	66.72(6)
C(53)-C(52)	1.369(8)	N(11)-P(12)-C(141)	109.1(2)
C(31)-C(36)	1.376(8)	N(11)-P(12)-C(131)	109.5(2)
C(31)-C(32)	1.385(8)	C(141)-P(12)-C(131)	102.2(3)
C(31)-C(37)	1.545(9)	N(11)-P(12)-Cr(1)	92.99(16)
C(36)-C(35)	1.386(9)	C(141)-P(12)-Cr(1)	122.9(2)
C(35)-C(34)	1.385(9)	C(131)-P(12)-Cr(1)	119.14(18)
C(34)-C(33)	1.385(9)	N(11)-P(11)-C(121)	110.1(2)
C(33)-C(32)	1.407(9)	N(11)-P(11)-C(111)	106.7(2)
C(41)-C(42)	1.374(9)	C(121)-P(11)-C(111)	102.2(3)
C(41)-C(46)	1.385(9)	N(11)-P(11)-Cr(1)	93.26(16)
C(41)-C(47)	1.541(9)	C(121)-P(11)-Cr(1)	122.50(19)

C(42)-C(43)	1.387(9)	C(111)-P(11)-Cr(1)	120.61(18)
C(43)-C(44)	1.361(9)	N(21)-P(22)-C(241)	107.7(2)
C(44)-C(45)	1.387(9)	N(21)-P(22)-C(231)	108.5(3)
C(45)-C(46)	1.397(9)	C(241)-P(22)-C(231)	103.4(3)
C(21)-C(22)	1.370(8)	N(21)-P(22)-Cr(2)	93.90(17)
C(21)-C(26)	1.384(9)	C(241)-P(22)-Cr(2)	115.98(19)
C(21)-C(27)	1.550(9)	C(231)-P(22)-Cr(2)	125.83(19)
C(23)-C(24)	1.377(9)	N(21)-P(21)-C(221)	109.1(3)
C(23)-C(22)	1.388(9)	N(21)-P(21)-C(211)	107.2(2)
C(24)-C(25)	1.390(9)	C(221)-P(21)-C(211)	102.4(3)
C(25)-C(26)	1.381(9)	N(21)-P(21)-Cr(2)	93.38(16)
C(12)-C(11B)	1.356(10)	C(221)-P(21)-Cr(2)	116.41(18)
C(12)-C(11A)	1.348(12)	C(211)-P(21)-Cr(2)	126.8(2)
C(12)-C(13)	1.514(14)	C(56)-C(51)-C(52)	119.3(6)
C(12)-C(18)	1.446(12)	C(56)-C(51)-C(57)	120.3(6)
C(16)-C(15)	1.426(11)	C(52)-C(51)-C(57)	120.4(6)
C(16)-C(17)	1.391(13)	C(55)-C(56)-C(51)	120.4(6)
C(16)-C(11A)	1.447(12)	C(56)-C(55)-C(54)	120.2(7)
C(15)-C(14)	1.330(13)	C(53)-C(54)-C(55)	119.5(7)
C(15)-C(11B)	1.452(12)	C(54)-C(53)-C(52)	121.5(7)
C(14)-C(13)	1.440(14)	C(53)-C(52)-C(51)	119.0(6)
C(11A)-C(98)	1.651(14)	C(36)-C(31)-C(32)	120.8(7)
C(19)-C(11B)	1.593(14)	C(36)-C(31)-C(37)	120.2(7)
C(17)-C(18)	1.375(13)	C(32)-C(31)-C(37)	119.0(7)
C(231)-C(236)	1.385(8)	C(35)-C(36)-C(31)	118.9(7)
C(231)-C(232)	1.386(8)	C(36)-C(35)-C(34)	122.2(8)
C(232)-C(233)	1.384(9)	C(35)-C(34)-C(33)	118.2(8)
C(233)-C(234)	1.378(9)	C(34)-C(33)-C(32)	120.5(8)
C(234)-C(235)	1.384(9)	C(31)-C(32)-C(33)	119.4(7)
C(235)-C(236)	1.394(8)	C(42)-C(41)-C(46)	119.5(7)
C(211)-C(216)	1.395(8)	C(42)-C(41)-C(47)	119.4(7)
C(211)-C(212)	1.399(7)	C(46)-C(41)-C(47)	121.1(7)
C(216)-C(215)	1.381(8)	C(43)-C(42)-C(41)	119.8(7)
C(215)-C(214)	1.382(9)	C(44)-C(43)-C(42)	121.9(7)
C(214)-C(213)	1.381(9)	C(43)-C(44)-C(45)	118.5(8)
C(213)-C(212)	1.389(8)	C(44)-C(45)-C(46)	120.6(7)
C(221)-C(226)	1.394(8)	C(45)-C(46)-C(41)	119.7(7)
C(221)-C(222)	1.398(8)	C(22)-C(21)-C(26)	120.6(7)
C(222)-C(223)	1.388(8)	C(22)-C(21)-C(27)	120.7(6)
C(223)-C(224)	1.369(9)	C(26)-C(21)-C(27)	118.7(6)
C(224)-C(225)	1.390(9)	C(24)-C(23)-C(22)	119.9(7)
C(225)-C(226)	1.385(8)	C(23)-C(24)-C(25)	119.1(7)
C(201)-C(202)	1.432(10)	C(26)-C(25)-C(24)	121.3(7)

C(201)-N(21)	1.480(7)	C(25)-C(26)-C(21)	118.7(7)
C(202)-C(203)	1.570(10)	C(11B)-C(12)-C(11A)	78.1(9)
C(203)-C(205)	1.441(11)	C(11B)-C(12)-C(13)	40.5(7)
C(203)-C(204)	1.483(11)	C(11A)-C(12)-C(13)	118.6(9)
C(114)-C(115)	1.380(9)	C(11B)-C(12)-C(18)	117.2(9)
C(114)-C(113)	1.395(8)	C(11A)-C(12)-C(18)	39.7(7)
C(121)-C(122)	1.387(7)	C(13)-C(12)-C(18)	157.4(10)
C(121)-C(126)	1.396(7)	C(15)-C(16)-C(17)	139.6(10)
C(115)-C(116)	1.385(8)	C(15)-C(16)-C(11A)	91.3(9)
C(116)-C(111)	1.400(7)	C(17)-C(16)-C(11A)	49.1(8)
C(131)-C(132)	1.393(8)	C(16)-C(15)-C(14)	143.9(11)
C(131)-C(136)	1.395(8)	C(16)-C(15)-C(11B)	99.6(9)
C(136)-C(135)	1.382(8)	C(14)-C(15)-C(11B)	44.4(8)
C(135)-C(134)	1.381(8)	C(13)-C(14)-C(15)	118.1(13)
C(134)-C(133)	1.387(9)	C(12)-C(11A)-C(98)	112.5(11)
C(133)-C(132)	1.377(8)	C(12)-C(11A)-C(16)	138.8(12)
C(141)-C(146)	1.395(8)	C(98)-C(11A)-C(16)	108.5(11)
C(141)-C(142)	1.406(9)	C(14)-C(13)-C(12)	108.4(11)
C(1)-C(2)	1.481(8)	C(12)-C(11B)-C(15)	131.4(10)
C(1)-N(01)	1.487(7)	C(12)-C(11B)-C(19)	116.3(12)
C(2)-C(3)	1.532(9)	C(15)-C(11B)-C(19)	112.3(11)
C(3)-C(4)	1.522(9)	C(16)-C(17)-C(18)	110.4(12)
C(3)-C(5)	1.534(9)	C(17)-C(18)-C(12)	121.4(12)
C(146)-C(145)	1.395(10)	C(236)-C(231)-C(232)	119.2(6)
C(145)-C(144)	1.376(12)	C(236)-C(231)-P(22)	119.6(4)
C(126)-C(125)	1.378(8)	C(232)-C(231)-P(22)	121.2(4)
C(144)-C(143)	1.376(11)	C(233)-C(232)-C(231)	120.7(6)
C(143)-C(142)	1.364(9)	C(234)-C(233)-C(232)	119.8(6)
C(101)-N(11)	1.482(6)	C(233)-C(234)-C(235)	120.4(6)
C(101)-C(102)	1.516(8)	C(234)-C(235)-C(236)	119.6(6)
C(102)-C(103)	1.556(8)	C(231)-C(236)-C(235)	120.4(6)
C(103)-C(105)	1.496(9)	C(216)-C(211)-C(212)	118.7(5)
C(103)-C(104)	1.526(10)	C(216)-C(211)-P(21)	120.7(4)
C(8A)-C(9A)	1.443(15)	C(212)-C(211)-P(21)	120.6(5)
C(8A)-C(7A)	1.529(15)	C(215)-C(216)-C(211)	120.0(6)
C(8A)-C(10A)	1.595(15)	C(214)-C(215)-C(216)	121.2(6)
N(02A)-C(6A)	1.492(7)	C(213)-C(214)-C(215)	119.4(6)
C(6A)-C(7A)	1.397(14)	C(214)-C(213)-C(212)	120.2(6)
C(242)-C(243)	1.368(8)	C(213)-C(212)-C(211)	120.6(6)
C(242)-C(241)	1.392(8)	C(226)-C(221)-C(222)	119.2(5)
C(125)-C(124)	1.387(8)	C(226)-C(221)-P(21)	117.0(5)
C(243)-C(244)	1.387(9)	C(222)-C(221)-P(21)	123.0(4)
C(244)-C(245)	1.391(9)	C(223)-C(222)-C(221)	120.0(6)

C(245)-C(246)	1.387(8)	C(224)-C(223)-C(222)	120.8(6)
C(246)-C(241)	1.395(8)	C(223)-C(224)-C(225)	119.3(6)
C(124)-C(123)	1.377(8)	C(226)-C(225)-C(224)	121.0(6)
C(123)-C(122)	1.392(8)	C(225)-C(226)-C(221)	119.5(6)
C(111)-C(112)	1.385(8)	C(202)-C(201)-N(21)	115.8(7)
C(112)-C(113)	1.378(8)	C(201)-C(202)-C(203)	112.8(7)
		C(205)-C(203)-C(204)	120.0(8)
		C(205)-C(203)-C(202)	111.9(7)
		C(204)-C(203)-C(202)	112.1(7)
		C(115)-C(114)-C(113)	119.8(6)
		C(122)-C(121)-C(126)	118.9(5)
		C(122)-C(121)-P(11)	118.7(4)
		C(126)-C(121)-P(11)	122.1(4)
		C(114)-C(115)-C(116)	120.1(6)
		C(115)-C(116)-C(111)	120.7(6)
		C(132)-C(131)-C(136)	119.1(5)
		C(132)-C(131)-P(12)	118.7(5)
		C(136)-C(131)-P(12)	121.7(4)
		C(135)-C(136)-C(131)	120.4(5)
		C(136)-C(135)-C(134)	120.2(6)
		C(135)-C(134)-C(133)	119.6(6)
		C(132)-C(133)-C(134)	120.6(6)
		C(133)-C(132)-C(131)	120.1(6)
		C(146)-C(141)-C(142)	118.6(6)
		C(146)-C(141)-P(12)	121.9(5)
		C(142)-C(141)-P(12)	119.4(4)
		C(2)-C(1)-N(01)	112.9(5)
		C(1)-C(2)-C(3)	117.1(5)
		C(4)-C(3)-C(2)	109.5(5)
		C(4)-C(3)-C(5)	110.9(6)
		C(2)-C(3)-C(5)	111.0(6)
		C(145)-C(146)-C(141)	119.9(7)
		C(144)-C(145)-C(146)	120.1(7)
		C(125)-C(126)-C(121)	120.0(5)
		C(145)-C(144)-C(143)	120.0(7)
		C(142)-C(143)-C(144)	120.8(8)
		C(21)-C(22)-C(23)	120.4(7)
		C(143)-C(142)-C(141)	120.4(6)
		N(11)-C(101)-C(102)	116.0(5)
		C(101)-C(102)-C(103)	111.2(5)
		C(105)-C(103)-C(104)	110.7(6)
		C(105)-C(103)-C(102)	111.8(5)
		C(104)-C(103)-C(102)	109.5(6)

C(9A)-C(8A)-C(7A)	112.7(10)
C(9A)-C(8A)-C(10A)	107.8(10)
C(7A)-C(8A)-C(10A)	107.0(9)
C(7A)-C(6A)-N(02A)	118.7(8)
C(6A)-C(7A)-C(8A)	121.8(10)
C(243)-C(242)-C(241)	121.2(6)
C(126)-C(125)-C(124)	120.9(6)
C(242)-C(243)-C(244)	120.3(6)
C(243)-C(244)-C(245)	119.2(6)
C(246)-C(245)-C(244)	120.6(6)
C(245)-C(246)-C(241)	119.8(6)
C(123)-C(124)-C(125)	119.4(6)
C(124)-C(123)-C(122)	120.2(6)
C(242)-C(241)-C(246)	118.8(5)
C(242)-C(241)-P(22)	122.6(4)
C(246)-C(241)-P(22)	117.9(4)
C(121)-C(122)-C(123)	120.5(5)
C(112)-C(111)-C(116)	118.3(5)
C(112)-C(111)-P(11)	120.2(4)
C(116)-C(111)-P(11)	121.5(4)
C(113)-C(112)-C(111)	121.4(6)
C(112)-C(113)-C(114)	119.7(6)
C(101)-N(11)-P(12)	127.2(4)
C(101)-N(11)-P(11)	124.5(4)
P(12)-N(11)-P(11)	106.7(2)
C(201)-N(21)-P(21)	128.2(4)
C(201)-N(21)-P(22)	124.4(4)
P(21)-N(21)-P(22)	106.0(2)

Table C6. Anisotropic displacement parameters ($A^2 \times 10^3$) for $[NH_3\text{-i-Pent}][CrCl_4(PNP\text{-i-Pent})]\,2C_7H_8$.. The anisotropic displacement factor exponent takes the form: -2 pi [$h^2 a^{*2} U11 + ... + 2 h k a^* b^* U12$]

	U11	U22	U33	U23	U13	U12
Cr(1)	11(1)	17(1)	17(1)	-4(1)	-1(1)	-1(1)
Cr(2)	13(1)	21(1)	18(1)	-6(1)	-2(1)	-1(1)
P(12)	12(1)	19(1)	19(1)	-5(1)	-1(1)	-2(1)
P(11)	12(1)	18(1)	18(1)	-4(1)	-2(1)	-3(1)
P(22)	14(1)	21(1)	19(1)	-6(1)	-4(1)	-1(1)
P(21)	14(1)	20(1)	20(1)	-7(1)	-2(1)	-2(1)
Cl(11)	18(1)	21(1)	24(1)	-8(1)	2(1)	-2(1)
Cl(13)	19(1)	21(1)	24(1)	-4(1)	1(1)	-7(1)
Cl(12)	19(1)	22(1)	19(1)	-2(1)	-5(1)	-5(1)
Cl(14)	15(1)	24(1)	22(1)	-6(1)	-5(1)	-2(1)

Cl(23)	18(1)	23(1)	23(1)	-9(1)	1(1)	-1(1)
Cl(22)	18(1)	28(1)	20(1)	-3(1)	-5(1)	-4(1)
Cl(21)	24(1)	23(1)	27(1)	-7(1)	2(1)	-7(1)
Cl(24)	15(1)	28(1)	26(1)	-9(1)	-7(1)	1(1)
C(35)	63(5)	35(4)	53(5)	-7(4)	-1(4)	-16(4)
C(34)	56(5)	52(6)	63(6)	-4(5)	7(4)	-18(5)
C(33)	57(5)	36(5)	66(6)	-1(4)	10(5)	-13(4)
C(32)	65(5)	29(4)	47(5)	-5(4)	19(4)	-17(4)
C(37)	86(7)	70(6)	49(5)	-2(5)	-6(5)	-38(6)
C(41)	49(5)	42(5)	41(4)	-12(4)	-10(4)	-16(4)
C(42)	67(5)	35(4)	43(5)	-5(4)	-8(4)	-20(4)
C(43)	52(5)	45(5)	54(5)	-17(4)	0(4)	-11(4)
C(44)	60(5)	52(5)	57(5)	-13(4)	2(4)	-22(5)
C(45)	59(5)	43(5)	47(5)	-6(4)	-12(4)	-21(4)
C(46)	53(5)	29(4)	57(5)	-9(4)	-10(4)	-9(4)
C(47)	65(6)	63(6)	57(5)	-20(5)	13(5)	-26(5)
C(21)	50(5)	38(4)	43(4)	-7(4)	-13(4)	-15(4)
C(23)	58(5)	39(4)	37(4)	-4(4)	-6(4)	-17(4)
C(24)	56(5)	47(5)	47(5)	-16(4)	-1(4)	-6(4)
C(25)	70(6)	33(4)	46(5)	-12(4)	-12(4)	0(4)
C(26)	61(5)	36(4)	46(5)	-12(4)	-6(4)	-12(4)
C(27)	59(6)	47(5)	95(7)	-17(5)	5(5)	-23(5)
C(12)	44(4)	27(4)	38(4)	-8(3)	-12(3)	-8(3)
C(16)	60(6)	64(6)	137(10)	-74(7)	-37(7)	8(5)
C(15)	19(9)	53(6)	71(7)	-37(6)	-36(7)	-11(6)
C(14)	72(13)	59(12)	73(14)	-52(11)	1(11)	-18(11)
C(11A)	72(14)	28(10)	120(20)	-38(12)	-25(13)	0(10)
C(98)	57(11)	40(10)	71(13)	-4(9)	3(10)	-20(9)
C(13)	91(16)	33(10)	88(16)	-15(11)	-43(14)	-21(11)
C(19)	02(16)	68(13)	80(14	-51(11)	75(14)	-55(13)
C(11B)	16(6)	21(7)	65(11)	-27(7)	12(7)	-10(6)
C(17)	82(13)	24(8)	25(8)	-6(6)	-1(8)	-20(9)
C(18)	51(9)	12(6)	28(8)	-7(6)	-7(7)	2(7)
C(231)	25(3)	20(3)	21(3)	-6(2)	-5(2)	-4(3)
C(232)	25(3)	32(4)	37(4)	3(3)	-8(3)	-9(3)
C(233)	40(4)	31(4)	43(4)	4(3)	-6(3)	-15(3)
C(234)	50(4)	26(4)	26(4)	2(3)	-18(3)	-10(3)
C(235)	26(3)	39(4)	39(4)	-2(3)	-11(3)	-4(3)
C(236)	24(3)	25(3)	25(3)	-1(3)	-7(3)	-2(3)
C(211)	17(3)	22(3)	26(3)	-9(3)	-6(2)	-1(2)
C(216)	28(3)	31(4)	29(4)	-6(3)	2(3)	4(3)
C(215)	39(4)	39(4)	32(4)	-3(3)	-7(3)	16(3)
C(214)	30(4)	34(4)	38(4)	-9(3)	-5(3)	13(3)

C(213)	20(3)	34(4)	32(4)	-15(3)	-2(3)	4(3)
C(212)	22(3)	30(3)	20(3)	-7(3)	-5(2)	-1(3)
C(221)	12(3)	26(3)	24(3)	-14(3)	1(2)	-4(2)
C(222)	18(3)	25(3)	24(3)	-8(3)	0(2)	-4(3)
C(223)	22(3)	34(4)	27(3)	-5(3)	-8(3)	-2(3)
C(224)	24(3)	36(4)	41(4)	-18(3)	-9(3)	-5(3)
C(225)	30(4)	28(4)	54(5)	-15(3)	-9(3)	-11(3)
C(226)	22(3)	23(3)	26(3)	-4(3)	-3(2)	-4(3)
C(201)	56(5)	29(4)	46(5)	-18(3)	23(4)	-11(4)
C(202)	55(5)	43(5)	54(5)	0(4)	-8(4)	-19(4)
C(203)	65(6)	65(6)	56(5)	-7(5)	24(5)	-25(5)
C(205)	48(5)	67(6)	81(7)	-20(5)	40(5)	-21(5)
C(204)	78(6)	100(8)	81(6)	-59(6)	51(5)	-74(6)
C(114)	25(3)	42(4)	29(4)	-12(3)	-3(3)	-13(3)
C(121)	23(3)	19(3)	17(3)	-5(2)	-5(2)	-3(3)
C(115)	18(3)	35(4)	29(3)	-5(3)	-7(3)	-5(3)
C(116)	17(3)	22(3)	28(3)	-6(3)	-2(2)	-6(3)
C(131)	16(3)	24(3)	22(3)	-8(3)	3(2)	-6(2)
C(136)	18(3)	19(3)	25(3)	-10(3)	3(2)	-6(2)
C(135)	20(3)	30(4)	21(3)	-6(3)	4(2)	-5(3)
C(134)	25(3)	32(4)	33(4)	-19(3)	0(3)	-7(3)
C(133)	45(4)	23(3)	34(4)	-12(3)	-1(3)	-12(3)
C(132)	30(3)	25(3)	29(3)	-4(3)	0(3)	-9(3)
C(141)	15(3)	21(3)	42(4)	-12(3)	-2(3)	0(3)
C(1)	24(3)	29(4)	26(3)	-1(3)	-9(3)	-7(3)
C(2)	26(3)	35(4)	27(3)	-2(3)	-2(3)	-7(3)
C(3)	26(3)	28(4)	37(4)	-4(3)	-10(3)	-2(3)
C(5)	41(4)	37(4)	57(5)	9(4)	-2(4)	-17(4)
C(4)	47(5)	42(5)	83(7)	-26(5)	-15(4)	13(4)
C(146)	29(4)	28(4)	64(5)	-13(4)	12(3)	-4(3)
C(145)	21(4)	31(4)	125(9)	-23(5)	14(5)	2(3)
C(126)	21(3)	31(4)	25(3)	3(3)	-5(2)	-12(3)
C(144)	34(4)	26(4)	108(8)	-10(5)	-33(5)	9(4)
C(143)	55(5)	28(4)	57(5)	-13(4)	-25(4)	2(4)
C(22)	48(4)	27(4)	52(5)	-2(3)	-22(4)	-12(4)
C(142)	25(3)	25(3)	36(4)	-8(3)	-12(3)	5(3)
C(101)	19(3)	28(3)	26(3)	-8(3)	3(2)	-10(3)
C(102)	28(3)	40(4)	24(3)	-11(3)	3(3)	-17(3)
C(103)	30(4)	54(5)	31(4)	-8(3)	5(3)	-24(4)
C(104)	95(7)	106(8)	49(5)	-36(5)	38(5)	-82(7)
C(105)	33(4)	58(5)	39(4)	-16(4)	9(3)	-20(4)
C(8A)	40(4)	27(4)	35(4)	-3(3)	-9(3)	-6(3)
N(02A)	23(3)	25(3)	20(3)	-6(2)	0(2)	-7(2)

C(6A)	32(4)	35(4)	28(4)	4(3)	-14(3)	-11(3)
C(7A)	33(8)	32(8)	40(8)	6(7)	-10(7)	-1(7)
C(10A)	33(8)	33(8)	66(11)	-9(8)	-3(7)	-4(7)
C(9A)	54(10)	40(10)	61(11)	-19(9)	-13(9)	15(8)
C(8B)	40(4)	27(4)	35(4)	-3(3)	-9(3)	-6(3)
N(02B)	23(3)	25(3)	20(3)	-6(2)	0(2)	-7(2)
C(6B)	32(4)	35(4)	28(4)	4(3)	-14(3)	-11(3)
C(7B)	15(6)	34(8)	22(6)	-10(6)	0(5)	-6(5)
C(9B)	45(9)	32(8)	43(9)	-16(7)	21(7)	-15(7)
C(10B)	50(9)	45(9)	34(8)	-6(7)	-6(7)	-21(8)
C(242)	19(3)	26(3)	25(3)	-8(3)	-5(2)	-3(3)
C(125)	32(3)	36(4)	27(3)	2(3)	-3(3)	-20(3)
C(243)	22(3)	30(4)	30(4)	-5(3)	-5(3)	-4(3)
C(244)	40(4)	38(4)	35(4)	-7(3)	-16(3)	-16(3)
C(245)	34(4)	32(4)	37(4)	-10(3)	-10(3)	-7(3)
C(246)	24(3)	30(4)	39(4)	-11(3)	-8(3)	-3(3)
C(124)	35(4)	24(3)	22(3)	5(3)	-12(3)	-10(3)
C(123)	23(3)	25(3)	29(3)	-2(3)	-8(3)	-1(3)
C(241)	21(3)	21(3)	24(3)	-6(3)	-7(2)	-5(3)
C(122)	21(3)	21(3)	26(3)	-1(3)	-4(2)	-7(3)
C(111)	18(3)	18(3)	21(3)	-2(2)	-3(2)	-8(2)
N(11)	15(2)	20(3)	25(3)	-8(2)	4(2)	-5(2)
N(21)	18(2)	26(3)	21(3)	-8(2)	1(2)	-7(2)
N(01)	17(2)	29(3)	22(3)	-5(2)	-4(2)	-5(2)

Table C7: Atomic coordinates (x 10^4) and equivalent isotropic displacement parameters (A^2 x 10^3) for [NH_3-n-Butyl][$CrCl_4$(PNP-n-Butyl)]$2C_7H_8$. U(eq) is defined as one third of the trace of the orthogonalized Uij tensor.

	X	Y	z	U(eq)
Cr(1)	3273(1)	2954(1)	7143(1)	15(1)
Cr(2)	9118(1)	1892(1)	5310(1)	13(1)
Cr(3)	8338(1)	3254(1)	2250(1)	16(1)
Cr(4)	4183(1)	1861(1)	274(1)	14(1)
N(11)	4111(2)	1182(2)	6925(1)	18(1)
N(21)	8384(2)	3670(2)	5550(1)	15(1)
N(31)	9130(2)	1491(2)	2012(1)	16(1)
N(41)	3416(2)	3642(2)	467(1)	16(1)
P(31)	9388(1)	2029(1)	2376(1)	16(1)
P(32)	8361(1)	2135(1)	1795(1)	16(1)
Cl(31)	7372(1)	2932(1)	2738(1)	19(1)
Cl(32)	7339(1)	4248(1)	1965(1)	18(1)
Cl(33)	8619(1)	3974(1)	2778(1)	20(1)
Cl(34)	9303(1)	3492(1)	1733(1)	18(1)

P(11)	4327(1)	1747(1)	7296(1)	16(1)
P(12)	3392(1)	1822(1)	6673(1)	15(1)
P(21)	9137(1)	2996(1)	5761(1)	14(1)
P(22)	8087(1)	3144(1)	5193(1)	14(1)
Cl(11)	3481(1)	3679(1)	7693(1)	20(1)
Cl(12)	4231(1)	3273(1)	6654(1)	19(1)
Cl(13)	2300(1)	2564(1)	7583(1)	22(1)
Cl(14)	2262(1)	3928(1)	6860(1)	19(1)
Cl(21)	8177(1)	1641(1)	5835(1)	17(1)
Cl(22)	8825(1)	1161(1)	4791(1)	21(1)
Cl(23)	10147(1)	892(1)	5574(1)	17(1)
Cl(24)	10069(1)	2229(1)	4827(1)	19(1)
P(41)	4170(1)	3006(1)	697(1)	14(1)
P(42)	3130(1)	3072(1)	134(1)	14(1)
Cl(41)	3255(1)	1596(1)	810(1)	17(1)
Cl(42)	3893(1)	1093(1)	-230(1)	18(1)
Cl(43)	5100(1)	2206(1)	-242(1)	19(1)
Cl(44)	5230(1)	939(1)	554(1)	19(1)
C(01)	779(3)	4126(3)	9055(1)	29(1)
C(02)	900(3)	4627(3)	8666(1)	29(1)
C(03)	1338(3)	4121(3)	8271(1)	29(1)
C(04)	1544(3)	4593(3)	7899(2)	29(1)
C(05)	4079(3)	5281(3)	6772(1)	23(1)
C(06)	4088(3)	5303(3)	6289(1)	23(1)
C(07)	4849(3)	5424(3)	6051(2)	34(1)
C(08)	4895(3)	5366(3)	5562(2)	39(1)
C(09)	1189(3)	761(3)	4175(1)	26(1)
C(010)	1698(3)	259(2)	3797(1)	21(1)
C(011)	1870(3)	773(3)	3418(2)	30(1)
C(012)	2323(3)	292(3)	3018(2)	36(1)
C(013)	3113(4)	9098(4)	1543(2)	47(1)
C(014)	3254(4)	9336(4)	1073(2)	47(1)
C(015)	4031(4)	9499(4)	949(2)	47(1)
C(016)	4168(4)	9703(4)	488(2)	47(1)
C(017)	7631(3)	890(3)	9957(2)	34(1)
C(018)	7439(3)	199(3)	10026(2)	35(1)
C(019)	7889(3)	-496(3)	9807(2)	36(1)
C(020)	8555(4)	-510(4)	9514(2)	46(1)
C(021)	8764(4)	178(4)	9443(2)	46(2)
C(022)	8302(3)	873(3)	9660(2)	37(1)
C(023)	7135(3)	1636(4)	10198(2)	52(2)
C(024)	8467(3)	5954(3)	6630(2)	28(1)
C(025)	8237(4)	6726(3)	6480(2)	42(1)

C(026)	8691(5)	6932(3)	6125(2)	54(2)
C(027)	9376(4)	6380(4)	5921(2)	49(2)
C(028)	9595(3)	5630(3)	6069(2)	39(1)
C(029)	9147(3)	5419(3)	6418(2)	29(1)
C(030)	7988(4)	5716(4)	7020(2)	51(2)
C(031)	4136(3)	8167(3)	6375(2)	36(1)
C(032)	3317(3)	8607(3)	6419(2)	44(1)
C(033)	3058(4)	9260(4)	6179(2)	50(2)
C(034)	3590(4)	9506(3)	5884(2)	45(1)
C(035)	4388(4)	9084(3)	5829(2)	38(1)
C(036)	4656(3)	8418(3)	6069(2)	34(1)
C(037)	4426(4)	7471(3)	6651(2)	51(2)
C(038)	2956(3)	60(3)	4770(2)	38(1)
C(039)	2333(3)	480(3)	5080(2)	33(1)
C(040)	2076(3)	1300(3)	5098(2)	39(1)
C(041)	2435(4)	1721(4)	4805(2)	45(1)
C(042)	3064(4)	1299(4)	4491(2)	50(2)
C(043)	3308(4)	495(4)	4470(2)	46(2)
C(044)	3217(4)	-820(4)	4755(2)	53(2)
C(052)	9118(4)	8254(4)	1413(2)	53(1)
C(053)	8434(4)	8838(4)	1617(2)	53(1)
C(054)	8083(4)	9502(4)	1427(2)	53(1)
C(055)	8400(4)	9626(4)	1034(2)	53(1)
C(056)	9080(4)	9056(4)	795(2)	53(1)
C(057)	9405(4)	8350(4)	998(2)	53(1)
C(059)	9600(8)	7620(8)	1626(4)	53(1)
C(060)	166(3)	5864(4)	2499(2)	39(1)
C(061)	742(3)	5875(4)	2142(2)	41(1)
C(062)	1154(4)	5203(4)	1900(2)	43(1)
C(063)	997(4)	4493(4)	2006(2)	48(2)
C(064)	428(4)	4479(4)	2350(2)	48(2)
C(065)	21(3)	5159(4)	2596(2)	42(2)
C(066)	-271(4)	6595(4)	2765(2)	57(2)
C(067)	3930(3)	6215(3)	1189(2)	34(1)
C(068)	3511(4)	5908(4)	1527(2)	39(1)
C(069)	2715(4)	6300(4)	1679(2)	51(2)
C(070)	2312(4)	7001(4)	1502(2)	55(2)
C(071)	2727(4)	7311(4)	1170(2)	48(2)
C(072)	3515(4)	6920(3)	1016(2)	39(1)
C(073)	4777(4)	5790(4)	1019(2)	52(2)
C(101)	4321(3)	312(2)	6927(1)	20(1)
C(102)	5208(3)	-147(2)	6799(1)	22(1)
C(103)	5371(3)	-992(3)	6963(2)	29(1)

C(104)	6216(3)	-1517(3)	6823(2)	43(1)
C(111)	4316(3)	1251(2)	7811(1)	19(1)
C(112)	4914(3)	544(3)	7871(2)	23(1)
C(113)	4872(3)	163(3)	8266(2)	29(1)
C(114)	4268(3)	485(3)	8599(2)	34(1)
C(115)	3693(3)	1202(3)	8546(2)	38(1)
C(116)	3718(3)	1583(3)	8152(1)	29(1)
C(121)	5363(3)	1720(2)	7145(1)	19(1)
C(122)	5718(3)	1618(3)	6710(1)	23(1)
C(123)	6471(3)	1693(3)	6593(2)	25(1)
C(124)	6876(3)	1878(3)	6899(2)	31(1)
C(125)	6529(3)	1985(3)	7328(2)	33(1)
C(126)	5775(3)	1905(3)	7453(2)	26(1)
C(131)	3758(3)	1841(2)	6101(1)	19(1)
C(132)	3457(3)	2543(3)	5886(1)	23(1)
C(133)	3688(3)	2586(3)	5443(1)	26(1)
C(134)	4222(3)	1937(3)	5217(1)	29(1)
C(135)	4538(3)	1242(3)	5428(2)	33(1)
C(136)	4300(3)	1194(3)	5869(1)	28(1)
C(141)	2591(3)	1388(2)	6688(1)	20(1)
C(142)	2368(3)	1006(3)	7057(2)	26(1)
C(143)	1717(3)	732(3)	7087(2)	33(1)
C(144)	1263(3)	851(3)	6750(2)	41(1)
C(145)	1477(3)	1225(3)	6383(2)	36(1)
C(146)	2139(3)	1493(3)	6347(2)	26(1)
C(201)	8225(3)	4539(2)	5558(1)	18(1)
C(202)	7393(3)	5037(3)	5761(2)	25(1)
C(203)	7303(3)	5911(3)	5674(2)	37(1)
C(204)	6543(4)	6468(3)	5901(2)	55(2)
C(211)	9974(3)	3388(2)	5696(1)	18(1)
C(212)	10481(3)	3273(3)	6007(1)	23(1)
C(213)	11156(3)	3529(3)	5938(2)	31(1)
C(214)	11329(3)	3888(3)	5556(2)	35(1)
C(215)	10830(3)	4005(3)	5242(2)	30(1)
C(216)	10154(3)	3761(2)	5313(1)	21(1)
C(221)	8863(2)	2947(2)	6341(1)	17(1)
C(222)	8359(3)	3579(3)	6598(1)	23(1)
C(223)	8152(3)	3482(3)	7037(1)	27(1)
C(224)	8443(3)	2755(3)	7222(1)	25(1)
C(225)	8955(3)	2128(3)	6968(1)	27(1)
C(226)	9161(3)	2218(3)	6530(1)	21(1)
C(231)	7050(3)	3209(2)	5376(1)	18(1)
C(232)	6622(3)	3000(3)	5085(2)	24(1)

C(233)	5866(3)	2938(3)	5228(2)	31(1)
C(234)	5530(3)	3085(3)	5656(2)	30(1)
C(235)	5952(3)	3294(3)	5948(2)	26(1)
C(236)	6712(3)	3351(2)	5810(1)	21(1)
C(241)	8037(3)	3671(2)	4690(1)	17(1)
C(242)	8581(3)	3339(3)	4322(1)	26(1)
C(243)	8561(3)	3748(3)	3936(2)	35(1)
C(244)	8012(3)	4491(3)	3920(2)	33(1)
C(245)	7463(3)	4818(3)	4276(2)	29(1)
C(246)	7468(3)	4406(2)	4663(1)	22(1)
C(301)	9377(2)	618(2)	1967(1)	16(1)
C(302)	10232(4)	243(3)	1736(2)	46(2)
C(303)	10450(3)	-638(2)	1666(1)	16(1)
C(304)	10546(3)	-1072(2)	2082(1)	16(1)
C(311)	9418(3)	1511(2)	2883(1)	20(1)
C(312)	9986(3)	770(3)	2917(1)	21(1)
C(313)	9984(2)	377(2)	3304(1)	16(1)
C(314)	9438(3)	721(3)	3662(2)	30(1)
C(315)	8896(3)	1461(3)	3637(1)	29(1)
C(316)	8880(3)	1856(3)	3247(1)	23(1)
C(321)	10425(3)	1984(3)	2213(1)	23(1)
C(322)	10782(3)	1860(3)	1785(2)	33(1)
C(323)	11559(3)	1881(3)	1662(2)	46(2)
C(324)	11973(3)	2054(4)	1966(2)	53(2)
C(325)	11623(3)	2197(3)	2392(2)	45(2)
C(326)	10846(3)	2161(3)	2520(2)	30(1)
C(331)	8619(2)	2155(2)	1211(1)	18(1)
C(332)	8385(3)	2887(3)	1013(1)	20(1)
C(333)	8548(3)	2930(3)	567(1)	24(1)
C(334)	8956(3)	2253(3)	319(1)	28(1)
C(335)	9190(3)	1527(3)	512(2)	30(1)
C(336)	9014(3)	1479(3)	958(1)	26(1)
C(341)	7563(3)	1690(2)	1866(1)	19(1)
C(342)	7398(3)	1328(3)	2255(2)	26(1)
C(343)	6757(3)	1029(3)	2327(2)	34(1)
C(344)	6270(3)	1095(3)	2007(2)	35(1)
C(345)	6422(3)	1451(3)	1620(2)	32(1)
C(346)	7071(3)	1748(3)	1549(2)	23(1)
C(401)	3212(2)	4513(2)	472(1)	16(1)
C(402)	2341(3)	4967(2)	641(1)	19(1)
C(403)	2181(3)	5849(3)	576(2)	26(1)
C(404)	1321(3)	6340(3)	728(2)	37(1)
C(411)	4990(2)	3425(2)	626(1)	16(1)

C(412)	5480(3)	3359(3)	944(1)	22(1)
C(413)	6128(3)	3645(3)	877(2)	26(1)
C(414)	6303(3)	3991(3)	489(2)	26(1)
C(415)	5828(3)	4060(3)	166(1)	23(1)
C(416)	5176(3)	3777(2)	234(1)	19(1)
C(421)	3894(2)	3031(2)	1280(1)	16(1)
C(422)	3467(3)	3725(3)	1513(1)	24(1)
C(423)	3308(3)	3717(3)	1959(2)	27(1)
C(424)	3583(3)	3016(3)	2174(1)	26(1)
C(425)	4008(3)	2327(3)	1947(1)	26(1)
C(426)	4160(3)	2329(3)	1497(1)	20(1)
C(431)	2099(2)	3135(2)	326(1)	17(1)
C(432)	1657(3)	2909(3)	49(2)	25(1)
C(433)	894(3)	2865(3)	205(2)	32(1)
C(434)	570(3)	3052(3)	633(2)	33(1)
C(435)	998(3)	3277(3)	908(2)	27(1)
C(436)	1767(3)	3310(2)	758(1)	20(1)
C(441)	3104(3)	3511(2)	-395(1)	18(1)
C(442)	3549(3)	3061(3)	-754(1)	24(1)
C(443)	3546(3)	3391(3)	-1163(1)	26(1)
C(444)	3111(3)	4167(3)	-1214(1)	26(1)
C(445)	2650(3)	4618(3)	-859(1)	26(1)
C(446)	2631(3)	4288(3)	-452(1)	24(1)
N(5)	348(2)	4641(2)	9450(1)	29(1)
N(6)	3331(2)	5140(2)	7000(1)	21(1)
N(7)	923(2)	286(2)	4535(1)	19(1)
N(8)	2823(3)	9722(3)	1829(2)	47(1)
C(045)	4959(4)	4364(4)	2393(2)	53(1)
C(046)	4343(4)	4397(4)	2736(2)	53(1)
C(047)	3892(4)	5103(4)	2941(2)	53(1)
C(048)	4037(3)	5804(3)	2808(2)	37(1)
C(049)	4638(4)	5781(4)	2470(2)	53(1)
C(050)	5091(4)	5068(4)	2268(2)	53(1)
C(051)	5457(4)	3592(4)	2180(2)	53(1)

Table C8. Bond lengths [Å] and angles [°] for $[NH_3\text{-n-Butyl}][CrCl_4(PNP\text{-n-Butyl})]\,2C_7H_8$..

Atoms	Bond length (Å)	Atoms	Bond angle (°)
Cr(1)-Cl(12)	2.3044(11)	Cl(12)-Cr(1)-Cl(13)	174.72(5)
Cr(1)-Cl(13)	2.3072(12)	Cl(12)-Cr(1)-Cl(11)	92.21(4)
Cr(1)-Cl(11)	2.3131(12)	Cl(13)-Cr(1)-Cl(11)	93.06(4)
Cr(1)-Cl(14)	2.3353(11)	Cl(12)-Cr(1)-Cl(14)	90.19(4)
Cr(1)-P(11)	2.4579(12)	Cl(13)-Cr(1)-Cl(14)	89.17(4)

Cr(1)-P(12)	2.4607(12)	Cl(11)-Cr(1)-Cl(14)	99.86(4)
Cr(2)-Cl(21)	2.2972(11)	Cl(12)-Cr(1)-P(11)	87.81(4)
Cr(2)-Cl(24)	2.3009(11)	Cl(13)-Cr(1)-P(11)	91.62(4)
Cr(2)-Cl(22)	2.3171(12)	Cl(11)-Cr(1)-P(11)	93.37(4)
Cr(2)-Cl(23)	2.3505(11)	Cl(14)-Cr(1)-P(11)	166.69(5)
Cr(2)-P(21)	2.4578(12)	Cl(12)-Cr(1)-P(12)	89.16(4)
Cr(2)-P(22)	2.4607(12)	Cl(13)-Cr(1)-P(12)	85.79(4)
Cr(3)-Cl(34)	2.3013(11)	Cl(11)-Cr(1)-P(12)	160.18(4)
Cr(3)-Cl(31)	2.3154(11)	Cl(14)-Cr(1)-P(12)	99.92(4)
Cr(3)-Cl(33)	2.3178(12)	P(11)-Cr(1)-P(12)	66.91(4)
Cr(3)-Cl(32)	2.3438(11)	Cl(21)-Cr(2)-Cl(24)	174.76(5)
Cr(3)-P(31)	2.4525(12)	Cl(21)-Cr(2)-Cl(22)	92.47(4)
Cr(3)-P(32)	2.4617(13)	Cl(24)-Cr(2)-Cl(22)	92.65(4)
Cr(4)-Cl(41)	2.3124(11)	Cl(21)-Cr(2)-Cl(23)	90.76(4)
Cr(4)-Cl(43)	2.3235(11)	Cl(24)-Cr(2)-Cl(23)	89.46(4)
Cr(4)-Cl(42)	2.3245(12)	Cl(22)-Cr(2)-Cl(23)	99.30(4)
Cr(4)-Cl(44)	2.3266(11)	Cl(21)-Cr(2)-P(21)	89.07(4)
Cr(4)-P(41)	2.4500(12)	Cl(24)-Cr(2)-P(21)	85.72(4)
Cr(4)-P(42)	2.4511(12)	Cl(22)-Cr(2)-P(21)	162.60(4)
N(11)-C(101)	1.474(5)	Cl(23)-Cr(2)-P(21)	98.01(4)
N(11)-P(12)	1.700(3)	Cl(21)-Cr(2)-P(22)	86.88(4)
N(11)-P(11)	1.711(4)	Cl(24)-Cr(2)-P(22)	91.54(4)
N(21)-C(201)	1.482(5)	Cl(22)-Cr(2)-P(22)	95.90(4)
N(21)-P(21)	1.697(3)	Cl(23)-Cr(2)-P(22)	164.71(4)
N(21)-P(22)	1.715(3)	P(21)-Cr(2)-P(22)	66.87(4)
N(31)-C(301)	1.481(5)	Cl(34)-Cr(3)-Cl(31)	175.67(5)
N(31)-P(32)	1.700(3)	Cl(34)-Cr(3)-Cl(33)	92.81(4)
N(31)-P(31)	1.703(4)	Cl(31)-Cr(3)-Cl(33)	91.23(4)
N(41)-C(401)	1.476(5)	Cl(34)-Cr(3)-Cl(32)	90.27(4)
N(41)-P(41)	1.700(3)	Cl(31)-Cr(3)-Cl(32)	90.52(4)
N(41)-P(42)	1.704(4)	Cl(33)-Cr(3)-Cl(32)	100.31(4)
P(31)-C(321)	1.810(4)	Cl(34)-Cr(3)-P(31)	85.27(4)
P(31)-C(311)	1.811(4)	Cl(31)-Cr(3)-P(31)	92.90(4)
P(32)-C(341)	1.807(4)	Cl(33)-Cr(3)-P(31)	94.11(4)
P(32)-C(331)	1.818(4)	Cl(32)-Cr(3)-P(31)	165.10(5)
P(11)-C(121)	1.813(4)	Cl(34)-Cr(3)-P(32)	88.28(4)
P(11)-C(111)	1.817(4)	Cl(31)-Cr(3)-P(32)	87.40(4)
P(12)-C(141)	1.810(4)	Cl(33)-Cr(3)-P(32)	161.11(5)
P(12)-C(131)	1.813(4)	Cl(32)-Cr(3)-P(32)	98.54(4)
P(21)-C(211)	1.810(4)	P(31)-Cr(3)-P(32)	67.17(4)
P(21)-C(221)	1.813(4)	Cl(41)-Cr(4)-Cl(43)	176.23(5)
P(22)-C(231)	1.808(4)	Cl(41)-Cr(4)-Cl(42)	91.77(4)
P(22)-C(241)	1.807(4)	Cl(43)-Cr(4)-Cl(42)	91.52(4)

P(41)-C(411)	1.811(4)	Cl(41)-Cr(4)-Cl(44)	90.91(4)
P(41)-C(421)	1.814(4)	Cl(43)-Cr(4)-Cl(44)	90.22(4)
P(42)-C(431)	1.805(4)	Cl(42)-Cr(4)-Cl(44)	101.59(4)
P(42)-C(441)	1.810(4)	Cl(41)-Cr(4)-P(41)	89.95(4)
C(01)-C(02)	1.514(6)	Cl(43)-Cr(4)-P(41)	86.35(4)
C(01)-N(5)	1.513(6)	Cl(42)-Cr(4)-P(41)	161.43(4)
C(01)-H(01M)	0.97	Cl(44)-Cr(4)-P(41)	96.87(4)
C(01)-H(01N)	0.97	Cl(41)-Cr(4)-P(42)	87.56(4)
C(02)-C(03)	1.510(7)	Cl(43)-Cr(4)-P(42)	90.36(4)
C(02)-H(02A)	0.97	Cl(42)-Cr(4)-P(42)	94.49(4)
C(02)-H(02B)	0.97	Cl(44)-Cr(4)-P(42)	163.89(5)
C(03)-C(04)	1.483(6)	P(41)-Cr(4)-P(42)	67.10(4)
C(03)-H(03A)	0.97	C(101)-N(11)-P(12)	126.9(3)
C(03)-H(03B)	0.97	C(101)-N(11)-P(11)	125.3(3)
C(04)-H(04A)	0.96	P(12)-N(11)-P(11)	105.32(19)
C(04)-H(04B)	0.96	C(201)-N(21)-P(21)	125.6(3)
C(04)-H(04C)	0.96	C(201)-N(21)-P(22)	126.1(3)
C(05)-N(6)	1.497(5)	P(21)-N(21)-P(22)	105.19(18)
C(05)-C(06)	1.506(6)	C(301)-N(31)-P(32)	125.4(3)
C(05)-H(05A)	0.97	C(301)-N(31)-P(31)	127.1(3)
C(05)-H(05B)	0.97	P(32)-N(31)-P(31)	106.06(19)
C(06)-C(07)	1.512(6)	C(401)-N(41)-P(41)	125.6(3)
C(06)-H(06A)	0.97	C(401)-N(41)-P(42)	127.2(3)
C(06)-H(06B)	0.97	P(41)-N(41)-P(42)	105.46(19)
C(07)-C(08)	1.523(7)	N(31)-P(31)-C(321)	108.6(2)
C(07)-H(07A)	0.97	N(31)-P(31)-C(311)	108.23(18)
C(07)-H(07B)	0.97	C(321)-P(31)-C(311)	102.67(19)
C(08)-H(08A)	0.96	N(31)-P(31)-Cr(3)	93.49(12)
C(08)-H(08B)	0.96	C(321)-P(31)-Cr(3)	118.25(14)
C(08)-H(08C)	0.96	C(311)-P(31)-Cr(3)	124.24(15)
C(09)-C(010)	1.499(6)	N(31)-P(32)-C(341)	105.54(18)
C(09)-N(7)	1.497(5)	N(31)-P(32)-C(331)	110.26(18)
C(09)-H(09A)	0.97	C(341)-P(32)-C(331)	103.49(19)
C(09)-H(09B)	0.97	N(31)-P(32)-Cr(3)	93.25(13)
C(010)-C(011)	1.528(6)	C(341)-P(32)-Cr(3)	122.36(15)
C(010)-H(01A)	0.97	C(331)-P(32)-Cr(3)	120.22(14)
C(010)-H(01B)	0.97	N(11)-P(11)-C(121)	107.88(19)
C(011)-C(012)	1.505(7)	N(11)-P(11)-C(111)	108.10(18)
C(011)-H(01C)	0.97	C(121)-P(11)-C(111)	104.04(19)
C(011)-H(01D)	0.97	N(11)-P(11)-Cr(1)	93.65(12)
C(012)-H(01E)	0.96	C(121)-P(11)-Cr(1)	117.94(13)
C(012)-H(01F)	0.96	C(111)-P(11)-Cr(1)	123.58(15)
C(012)-H(01G)	0.96	N(11)-P(12)-C(141)	106.54(18)

C(013)-N(8)	1.361(7)	N(11)-P(12)-C(131)	109.86(19)
C(013)-C(014)	1.525(7)	C(141)-P(12)-C(131)	103.7(2)
C(013)-H(01Q)	0.97	N(11)-P(12)-Cr(1)	93.84(13)
C(013)-H(01R)	0.97	C(141)-P(12)-Cr(1)	122.07(15)
C(014)-C(015)	1.487(8)	C(131)-P(12)-Cr(1)	119.45(14)
C(014)-H(01O)	0.97	N(21)-P(21)-C(211)	106.52(18)
C(014)-H(01P)	0.97	N(21)-P(21)-C(221)	109.86(18)
C(015)-C(016)	1.480(7)	C(211)-P(21)-C(221)	104.87(19)
C(015)-H(01K)	0.97	N(21)-P(21)-Cr(2)	94.20(12)
C(015)-H(01L)	0.97	C(211)-P(21)-Cr(2)	122.18(14)
C(016)-H(01H)	0.96	C(221)-P(21)-Cr(2)	117.79(14)
C(016)-H(01I)	0.96	N(21)-P(22)-C(231)	108.34(18)
C(016)-H(01J)	0.96	N(21)-P(22)-C(241)	107.82(17)
C(017)-C(018)	1.376(7)	C(231)-P(22)-C(241)	102.92(19)
C(017)-C(022)	1.386(7)	N(21)-P(22)-Cr(2)	93.65(12)
C(017)-C(023)	1.496(8)	C(231)-P(22)-Cr(2)	117.50(13)
C(018)-C(019)	1.381(8)	C(241)-P(22)-Cr(2)	125.07(14)
C(018)-H(018)	0.93	N(41)-P(41)-C(411)	106.44(17)
C(019)-C(020)	1.375(8)	N(41)-P(41)-C(421)	110.00(18)
C(019)-H(019)	0.93	C(411)-P(41)-C(421)	102.82(18)
C(020)-C(021)	1.387(8)	N(41)-P(41)-Cr(4)	93.69(12)
C(020)-H(020)	0.93	C(411)-P(41)-Cr(4)	122.80(14)
C(021)-C(022)	1.381(8)	C(421)-P(41)-Cr(4)	119.71(13)
C(021)-H(021)	0.93	N(41)-P(42)-C(431)	108.20(19)
C(022)-H(022)	0.93	N(41)-P(42)-C(441)	108.91(18)
C(023)-H(02C)	0.96	C(431)-P(42)-C(441)	104.37(19)
C(023)-H(02D)	0.96	N(41)-P(42)-Cr(4)	93.54(12)
C(023)-H(02E)	0.96	C(431)-P(42)-Cr(4)	118.18(13)
C(024)-C(029)	1.372(7)	C(441)-P(42)-Cr(4)	122.24(15)
C(024)-C(025)	1.394(7)	C(02)-C(01)-N(5)	111.0(4)
C(024)-C(030)	1.505(7)	C(02)-C(01)-H(01M)	109.5
C(025)-C(026)	1.380(9)	N(5)-C(01)-H(01M)	109.4
C(025)-H(025)	0.93	C(02)-C(01)-H(01N)	109.4
C(026)-C(027)	1.381(9)	N(5)-C(01)-H(01N)	109.4
C(026)-H(026)	0.93	H(01M)-C(01)-H(01N)	108
C(027)-C(028)	1.357(8)	C(03)-C(02)-C(01)	111.6(4)
C(027)-H(027)	0.93	C(03)-C(02)-H(02A)	109.3
C(028)-C(029)	1.366(7)	C(01)-C(02)-H(02A)	109.3
C(028)-H(028)	0.93	C(03)-C(02)-H(02B)	109.3
C(029)-H(029)	0.93	C(01)-C(02)-H(02B)	109.3
C(030)-H(03C)	0.96	H(02A)-C(02)-H(02B)	108
C(030)-H(03D)	0.96	C(04)-C(03)-C(02)	112.6(4)
C(030)-H(03E)	0.96	C(04)-C(03)-H(03A)	109.1

C(031)-C(036)	1.391(7)	C(02)-C(03)-H(03A)	109.1
C(031)-C(032)	1.406(8)	C(04)-C(03)-H(03B)	109.1
C(031)-C(037)	1.488(8)	C(02)-C(03)-H(03B)	109.1
C(032)-C(033)	1.358(8)	H(03A)-C(03)-H(03B)	107.8
C(032)-H(032)	0.93	C(03)-C(04)-H(04A)	109.5
C(033)-C(034)	1.380(9)	C(03)-C(04)-H(04B)	109.5
C(033)-H(033)	0.93	H(04A)-C(04)-H(04B)	109.5
C(034)-C(035)	1.367(8)	C(03)-C(04)-H(04C)	109.5
C(034)-H(034)	0.93	H(04A)-C(04)-H(04C)	109.5
C(035)-C(036)	1.378(7)	H(04B)-C(04)-H(04C)	109.5
C(035)-H(035)	0.93	N(6)-C(05)-C(06)	111.2(4)
C(036)-H(036)	0.93	N(6)-C(05)-H(05A)	109.4
C(037)-H(03F)	0.96	C(06)-C(05)-H(05A)	109.4
C(037)-H(03G)	0.96	N(6)-C(05)-H(05B)	109.4
C(037)-H(03H)	0.96	C(06)-C(05)-H(05B)	109.4
C(038)-C(039)	1.386(7)	H(05A)-C(05)-H(05B)	108
C(038)-C(043)	1.395(8)	C(05)-C(06)-C(07)	112.1(4)
C(038)-C(044)	1.488(8)	C(05)-C(06)-H(06A)	109.2
C(039)-C(040)	1.387(8)	C(07)-C(06)-H(06A)	109.2
C(039)-H(039)	0.93	C(05)-C(06)-H(06B)	109.2
C(040)-C(041)	1.373(8)	C(07)-C(06)-H(06B)	109.2
C(040)-H(040)	0.93	H(06A)-C(06)-H(06B)	107.9
C(041)-C(042)	1.400(9)	C(06)-C(07)-C(08)	112.1(4)
C(041)-H(041)	0.93	C(06)-C(07)-H(07A)	109.2
C(042)-C(043)	1.360(9)	C(08)-C(07)-H(07A)	109.2
C(042)-H(042)	0.93	C(06)-C(07)-H(07B)	109.2
C(043)-H(043)	0.93	C(08)-C(07)-H(07B)	109.2
C(044)-H(04D)	0.96	H(07A)-C(07)-H(07B)	107.9
C(044)-H(04E)	0.96	C(07)-C(08)-H(08A)	109.5
C(044)-H(04F)	0.96	C(07)-C(08)-H(08B)	109.5
C(052)-C(057)	1.347(9)	H(08A)-C(08)-H(08B)	109.5
C(052)-C(059)	1.406(13)	C(07)-C(08)-H(08C)	109.5
C(052)-C(053)	1.408(9)	H(08A)-C(08)-H(08C)	109.5
C(053)-C(054)	1.323(9)	H(08B)-C(08)-H(08C)	109.5
C(053)-H(053)	0.93	C(010)-C(09)-N(7)	112.9(4)
C(054)-C(055)	1.314(9)	C(010)-C(09)-H(09A)	109
C(054)-H(054)	0.93	N(7)-C(09)-H(09A)	109
C(055)-C(056)	1.432(9)	C(010)-C(09)-H(09B)	109
C(055)-H(055)	0.93	N(7)-C(09)-H(09B)	109
C(056)-C(057)	1.387(9)	H(09A)-C(09)-H(09B)	107.8
C(056)-H(056)	0.93	C(09)-C(010)-C(011)	110.9(4)
C(057)-H(057)	0.93	C(09)-C(010)-H(01A)	109.5
C(059)-H(05C)	0.96	C(011)-C(010)-H(01A)	109.5

C(059)-H(05D)	0.96	C(09)-C(010)-H(01B)	109.5
C(059)-H(05E)	0.96	C(011)-C(010)-H(01B)	109.5
C(060)-C(065)	1.371(8)	H(01A)-C(010)-H(01B)	108.1
C(060)-C(061)	1.399(7)	C(012)-C(011)-C(010)	112.6(4)
C(060)-C(066)	1.492(8)	C(012)-C(011)-H(01C)	109
C(061)-C(062)	1.368(8)	C(010)-C(011)-H(01C)	109.1
C(061)-H(061)	0.93	C(012)-C(011)-H(01D)	109.1
C(062)-C(063)	1.395(8)	C(010)-C(011)-H(01D)	109.1
C(062)-H(062)	0.93	H(01C)-C(011)-H(01D)	107.8
C(063)-C(064)	1.366(9)	C(011)-C(012)-H(01E)	109.5
C(063)-H(063)	0.93	C(011)-C(012)-H(01F)	109.5
C(064)-C(065)	1.384(9)	H(01E)-C(012)-H(01F)	109.5
C(064)-H(064)	0.93	C(011)-C(012)-H(01G)	109.4
C(065)-H(065)	0.93	H(01E)-C(012)-H(01G)	109.5
C(066)-H(06A)	0.96	H(01F)-C(012)-H(01G)	109.5
C(066)-H(06B)	0.96	N(8)-C(013)-C(014)	113.9(5)
C(066)-H(06C)	0.96	N(8)-C(013)-H(01Q)	108.8
C(067)-C(072)	1.384(8)	C(014)-C(013)-H(01Q)	108.8
C(067)-C(068)	1.395(7)	N(8)-C(013)-H(01R)	108.8
C(067)-C(073)	1.479(8)	C(014)-C(013)-H(01R)	108.8
C(068)-C(069)	1.383(9)	H(01Q)-C(013)-H(01R)	107.7
C(068)-H(068)	0.93	C(015)-C(014)-C(013)	113.6(5)
C(069)-C(070)	1.378(9)	C(015)-C(014)-H(01O)	108.8
C(069)-H(069)	0.93	C(013)-C(014)-H(01O)	108.9
C(070)-C(071)	1.384(9)	C(015)-C(014)-H(01P)	108.9
C(070)-H(070)	0.93	C(013)-C(014)-H(01P)	108.9
C(071)-C(072)	1.371(8)	H(01O)-C(014)-H(01P)	107.7
C(071)-H(071)	0.93	C(016)-C(015)-C(014)	112.7(5)
C(072)-H(072)	0.93	C(016)-C(015)-H(01K)	109.1
C(073)-H(07A)	0.96	C(014)-C(015)-H(01K)	109.1
C(073)-H(07B)	0.96	C(016)-C(015)-H(01L)	109
C(073)-H(07C)	0.96	C(014)-C(015)-H(01L)	109.1
C(101)-C(102)	1.527(6)	H(01K)-C(015)-H(01L)	107.8
C(101)-H(10C)	0.97	C(015)-C(016)-H(01H)	109.5
C(101)-H(10D)	0.97	C(015)-C(016)-H(01I)	109.5
C(102)-C(103)	1.529(6)	H(01H)-C(016)-H(01I)	109.5
C(102)-H(10A)	0.97	C(015)-C(016)-H(01J)	109.5
C(102)-H(10B)	0.97	H(01H)-C(016)-H(01J)	109.5
C(103)-C(104)	1.505(7)	H(01I)-C(016)-H(01J)	109.5
C(103)-H(10E)	0.97	C(018)-C(017)-C(022)	118.2(5)
C(103)-H(10F)	0.97	C(018)-C(017)-C(023)	120.8(5)
C(104)-H(10G)	0.96	C(022)-C(017)-C(023)	121.0(5)
C(104)-H(10H)	0.96	C(017)-C(018)-C(019)	121.7(5)

C(104)-H(10I)	0.96	C(017)-C(018)-H(018)	119.2
C(111)-C(116)	1.382(6)	C(019)-C(018)-H(018)	119.2
C(111)-C(112)	1.399(6)	C(020)-C(019)-C(018)	119.8(5)
C(112)-C(113)	1.394(6)	C(020)-C(019)-H(019)	120.1
C(112)-H(112)	0.93	C(018)-C(019)-H(019)	120.1
C(113)-C(114)	1.370(7)	C(019)-C(020)-C(021)	119.3(5)
C(113)-H(113)	0.93	C(019)-C(020)-H(020)	120.3
C(114)-C(115)	1.387(7)	C(021)-C(020)-H(020)	120.3
C(114)-H(114)	0.93	C(022)-C(021)-C(020)	120.3(5)
C(115)-C(116)	1.392(6)	C(022)-C(021)-H(021)	119.9
C(115)-H(115)	0.93	C(020)-C(021)-H(021)	119.8
C(116)-H(116)	0.93	C(021)-C(022)-C(017)	120.6(5)
C(121)-C(126)	1.392(6)	C(021)-C(022)-H(022)	119.7
C(121)-C(122)	1.402(6)	C(017)-C(022)-H(022)	119.7
C(122)-C(123)	1.377(6)	C(017)-C(023)-H(02C)	109.5
C(122)-H(122)	0.93	C(017)-C(023)-H(02D)	109.5
C(123)-C(124)	1.381(7)	H(02C)-C(023)-H(02D)	109.5
C(123)-H(123)	0.93	C(017)-C(023)-H(02E)	109.5
C(124)-C(125)	1.380(7)	H(02C)-C(023)-H(02E)	109.5
C(124)-H(124)	0.93	H(02D)-C(023)-H(02E)	109.5
C(125)-C(126)	1.385(7)	C(029)-C(024)-C(025)	118.3(5)
C(125)-H(125)	0.93	C(029)-C(024)-C(030)	120.7(5)
C(126)-H(126)	0.93	C(025)-C(024)-C(030)	120.9(5)
C(131)-C(136)	1.386(6)	C(026)-C(025)-C(024)	119.8(5)
C(131)-C(132)	1.394(6)	C(026)-C(025)-H(025)	120.1
C(132)-C(133)	1.392(6)	C(024)-C(025)-H(025)	120.1
C(132)-H(132)	0.93	C(025)-C(026)-C(027)	120.3(5)
C(133)-C(134)	1.376(7)	C(025)-C(026)-H(026)	119.8
C(133)-H(133)	0.93	C(027)-C(026)-H(026)	119.8
C(134)-C(135)	1.383(7)	C(028)-C(027)-C(026)	119.5(5)
C(134)-H(134)	0.93	C(028)-C(027)-H(027)	120.2
C(135)-C(136)	1.390(6)	C(026)-C(027)-H(027)	120.3
C(135)-H(135)	0.93	C(027)-C(028)-C(029)	120.6(5)
C(136)-H(136)	0.93	C(027)-C(028)-H(028)	119.7
C(141)-C(142)	1.392(6)	C(029)-C(028)-H(028)	119.7
C(141)-C(146)	1.399(6)	C(028)-C(029)-C(024)	121.4(5)
C(142)-C(143)	1.375(7)	C(028)-C(029)-H(029)	119.3
C(142)-H(142)	0.93	C(024)-C(029)-H(029)	119.3
C(143)-C(144)	1.390(8)	C(024)-C(030)-H(03C)	109.5
C(143)-H(143)	0.93	C(024)-C(030)-H(03D)	109.5
C(144)-C(145)	1.375(8)	H(03C)-C(030)-H(03D)	109.5
C(144)-H(144)	0.93	C(024)-C(030)-H(03E)	109.5
C(145)-C(146)	1.387(7)	H(03C)-C(030)-H(03E)	109.5

C(145)-H(145)	0.93	H(03D)-C(030)-H(03E)	109.5
C(146)-H(146)	0.93	C(036)-C(031)-C(032)	117.0(5)
C(201)-C(202)	1.516(6)	C(036)-C(031)-C(037)	122.0(5)
C(201)-H(20A)	0.97	C(032)-C(031)-C(037)	121.0(5)
C(201)-H(20B)	0.97	C(033)-C(032)-C(031)	120.9(6)
C(202)-C(203)	1.532(6)	C(033)-C(032)-H(032)	119.5
C(202)-H(20C)	0.97	C(031)-C(032)-H(032)	119.5
C(202)-H(20D)	0.97	C(032)-C(033)-C(034)	120.9(6)
C(203)-C(204)	1.491(7)	C(032)-C(033)-H(033)	119.6
C(203)-H(20E)	0.97	C(034)-C(033)-H(033)	119.5
C(203)-H(20F)	0.97	C(035)-C(034)-C(033)	119.6(6)
C(204)-H(20G)	0.96	C(035)-C(034)-H(034)	120.2
C(204)-H(20H)	0.96	C(033)-C(034)-H(034)	120.2
C(204)-H(20I)	0.96	C(034)-C(035)-C(036)	120.0(5)
C(211)-C(212)	1.390(6)	C(034)-C(035)-H(035)	120
C(211)-C(216)	1.395(6)	C(036)-C(035)-H(035)	120
C(212)-C(213)	1.393(6)	C(035)-C(036)-C(031)	121.7(5)
C(212)-H(212)	0.93	C(035)-C(036)-H(036)	119.2
C(213)-C(214)	1.377(7)	C(031)-C(036)-H(036)	119.2
C(213)-H(213)	0.93	C(031)-C(037)-H(03F)	109.5
C(214)-C(215)	1.389(7)	C(031)-C(037)-H(03G)	109.5
C(214)-H(214)	0.93	H(03F)-C(037)-H(03G)	109.5
C(215)-C(216)	1.382(6)	C(031)-C(037)-H(03H)	109.5
C(215)-H(215)	0.93	H(03F)-C(037)-H(03H)	109.5
C(216)-H(216)	0.93	H(03G)-C(037)-H(03H)	109.5
C(221)-C(222)	1.385(6)	C(039)-C(038)-C(043)	117.5(5)
C(221)-C(226)	1.391(5)	C(039)-C(038)-C(044)	120.5(5)
C(222)-C(223)	1.387(6)	C(043)-C(038)-C(044)	122.0(6)
C(222)-H(222)	0.93	C(038)-C(039)-C(040)	121.6(5)
C(223)-C(224)	1.380(6)	C(038)-C(039)-H(039)	119.2
C(223)-H(223)	0.93	C(040)-C(039)-H(039)	119.2
C(224)-C(225)	1.380(7)	C(041)-C(040)-C(039)	120.3(6)
C(224)-H(224)	0.93	C(041)-C(040)-H(040)	119.9
C(225)-C(226)	1.381(6)	C(039)-C(040)-H(040)	119.8
C(225)-H(225)	0.93	C(040)-C(041)-C(042)	118.3(6)
C(226)-H(226)	0.93	C(040)-C(041)-H(041)	120.8
C(231)-C(232)	1.393(6)	C(042)-C(041)-H(041)	120.9
C(231)-C(236)	1.397(6)	C(043)-C(042)-C(041)	121.3(5)
C(232)-C(233)	1.385(6)	C(043)-C(042)-H(042)	119.4
C(232)-H(232)	0.93	C(041)-C(042)-H(042)	119.4
C(233)-C(234)	1.376(7)	C(042)-C(043)-C(038)	121.0(6)
C(233)-H(233)	0.93	C(042)-C(043)-H(043)	119.5
C(234)-C(235)	1.388(7)	C(038)-C(043)-H(043)	119.5

C(234)-H(234)	0.93	C(038)-C(044)-H(04D)	109.4
C(235)-C(236)	1.384(6)	C(038)-C(044)-H(04E)	109.5
C(235)-H(235)	0.93	H(04D)-C(044)-H(04E)	109.5
C(236)-H(236)	0.93	C(038)-C(044)-H(04F)	109.5
C(241)-C(246)	1.392(6)	H(04D)-C(044)-H(04F)	109.5
C(241)-C(242)	1.397(6)	H(04E)-C(044)-H(04F)	109.5
C(242)-C(243)	1.389(6)	C(057)-C(052)-C(059)	115.9(8)
C(242)-H(242)	0.93	C(057)-C(052)-C(053)	119.0(6)
C(243)-C(244)	1.383(7)	C(059)-C(052)-C(053)	124.5(8)
C(243)-H(243)	0.93	C(054)-C(053)-C(052)	122.8(7)
C(244)-C(245)	1.374(7)	C(054)-C(053)-H(053)	118.6
C(244)-H(244)	0.93	C(052)-C(053)-H(053)	118.7
C(245)-C(246)	1.395(6)	C(055)-C(054)-C(053)	118.3(7)
C(245)-H(245)	0.93	C(055)-C(054)-H(054)	120.8
C(246)-H(246)	0.93	C(053)-C(054)-H(054)	120.9
C(301)-C(302)	1.529(7)	C(054)-C(055)-C(056)	122.9(7)
C(301)-H(30A)	0.97	C(054)-C(055)-H(055)	118.5
C(301)-H(30B)	0.97	C(056)-C(055)-H(055)	118.6
C(302)-C(303)	1.506(7)	C(057)-C(056)-C(055)	117.0(6)
C(302)-H(30C)	0.97	C(057)-C(056)-H(056)	121.5
C(302)-H(30D)	0.97	C(055)-C(056)-H(056)	121.5
C(303)-C(304)	1.497(5)	C(052)-C(057)-C(056)	119.7(7)
C(303)-H(30E)	0.97	C(052)-C(057)-H(057)	120.1
C(303)-H(30F)	0.97	C(056)-C(057)-H(057)	120.2
C(304)-H(30G)	0.96	C(052)-C(059)-H(05C)	109.5
C(304)-H(30H)	0.96	C(052)-C(059)-H(05D)	109.4
C(304)-H(30I)	0.96	H(05C)-C(059)-H(05D)	109.5
C(311)-C(316)	1.388(6)	C(052)-C(059)-H(05E)	109.5
C(311)-C(312)	1.401(6)	H(05C)-C(059)-H(05E)	109.5
C(312)-C(313)	1.381(5)	H(05D)-C(059)-H(05E)	109.5
C(312)-H(312)	0.93	C(065)-C(060)-C(061)	117.8(6)
C(313)-C(314)	1.381(7)	C(065)-C(060)-C(066)	121.3(5)
C(313)-H(313)	0.93	C(061)-C(060)-C(066)	120.9(6)
C(314)-C(315)	1.376(7)	C(062)-C(061)-C(060)	121.2(6)
C(314)-H(314)	0.93	C(062)-C(061)-H(061)	119.4
C(315)-C(316)	1.391(6)	C(060)-C(061)-H(061)	119.4
C(315)-H(315)	0.93	C(061)-C(062)-C(063)	120.0(5)
C(316)-H(316)	0.93	C(061)-C(062)-H(062)	120
C(321)-C(322)	1.384(6)	C(063)-C(062)-H(062)	120
C(321)-C(326)	1.399(7)	C(064)-C(063)-C(062)	119.3(6)
C(322)-C(323)	1.384(7)	C(064)-C(063)-H(063)	120.4
C(322)-H(322)	0.93	C(062)-C(063)-H(063)	120.3
C(323)-C(324)	1.378(9)	C(063)-C(064)-C(065)	120.3(6)

C(323)-H(323)	0.93	C(063)-C(064)-H(064)	119.8
C(324)-C(325)	1.378(9)	C(065)-C(064)-H(064)	119.9
C(324)-H(324)	0.93	C(060)-C(065)-C(064)	121.4(5)
C(325)-C(326)	1.395(7)	C(060)-C(065)-H(065)	119.3
C(325)-H(325)	0.93	C(064)-C(065)-H(065)	119.3
C(326)-H(326)	0.93	C(060)-C(066)-H(06A)	109.5
C(331)-C(336)	1.388(6)	C(060)-C(066)-H(06B)	109.5
C(331)-C(332)	1.395(6)	H(06A)-C(066)-H(06B)	109.5
C(332)-C(333)	1.385(6)	C(060)-C(066)-H(06C)	109.5
C(332)-H(332)	0.93	H(06A)-C(066)-H(06C)	109.5
C(333)-C(334)	1.385(7)	H(06B)-C(066)-H(06C)	109.5
C(333)-H(333)	0.93	C(072)-C(067)-C(068)	117.2(5)
C(334)-C(335)	1.379(7)	C(072)-C(067)-C(073)	121.7(5)
C(334)-H(334)	0.93	C(068)-C(067)-C(073)	121.0(5)
C(335)-C(336)	1.387(6)	C(069)-C(068)-C(067)	120.8(6)
C(335)-H(335)	0.93	C(069)-C(068)-H(068)	119.6
C(336)-H(336)	0.93	C(067)-C(068)-H(068)	119.6
C(341)-C(342)	1.395(6)	C(070)-C(069)-C(068)	121.1(5)
C(341)-C(346)	1.398(6)	C(070)-C(069)-H(069)	119.5
C(342)-C(343)	1.384(7)	C(068)-C(069)-H(069)	119.4
C(342)-H(342)	0.93	C(069)-C(070)-C(071)	118.3(6)
C(343)-C(344)	1.394(7)	C(069)-C(070)-H(070)	120.8
C(343)-H(343)	0.93	C(071)-C(070)-H(070)	120.9
C(344)-C(345)	1.379(7)	C(072)-C(071)-C(070)	120.6(6)
C(344)-H(344)	0.93	C(072)-C(071)-H(071)	119.7
C(345)-C(346)	1.395(6)	C(070)-C(071)-H(071)	119.7
C(345)-H(345)	0.93	C(071)-C(072)-C(067)	121.9(5)
C(346)-H(346)	0.93	C(071)-C(072)-H(072)	119
C(401)-C(402)	1.524(6)	C(067)-C(072)-H(072)	119.1
C(401)-H(40A)	0.97	C(067)-C(073)-H(07A)	109.5
C(401)-H(40B)	0.97	C(067)-C(073)-H(07B)	109.5
C(402)-C(403)	1.519(6)	H(07A)-C(073)-H(07B)	109.5
C(402)-H(40C)	0.97	C(067)-C(073)-H(07C)	109.5
C(402)-H(40D)	0.97	H(07A)-C(073)-H(07C)	109.5
C(403)-C(404)	1.513(6)	H(07B)-C(073)-H(07C)	109.5
C(403)-H(40E)	0.97	N(11)-C(101)-C(102)	116.2(4)
C(403)-H(40F)	0.97	N(11)-C(101)-H(10C)	108.3
C(404)-H(40G)	0.96	C(102)-C(101)-H(10C)	108.2
C(404)-H(40H)	0.96	N(11)-C(101)-H(10D)	108.2
C(404)-H(40I)	0.96	C(102)-C(101)-H(10D)	108.2
C(411)-C(412)	1.394(6)	H(10C)-C(101)-H(10D)	107.4
C(411)-C(416)	1.401(5)	C(101)-C(102)-C(103)	109.5(4)
C(412)-C(413)	1.379(6)	C(101)-C(102)-H(10A)	109.8

C(412)-H(412)	0.93	C(103)-C(102)-H(10A)	109.8
C(413)-C(414)	1.383(6)	C(101)-C(102)-H(10B)	109.8
C(413)-H(413)	0.93	C(103)-C(102)-H(10B)	109.8
C(414)-C(415)	1.390(6)	H(10A)-C(102)-H(10B)	108.2
C(414)-H(414)	0.93	C(104)-C(103)-C(102)	113.9(4)
C(415)-C(416)	1.384(6)	C(104)-C(103)-H(10E)	108.8
C(415)-H(415)	0.93	C(102)-C(103)-H(10E)	108.8
C(416)-H(416)	0.93	C(104)-C(103)-H(10F)	108.8
C(421)-C(422)	1.388(6)	C(102)-C(103)-H(10F)	108.8
C(421)-C(426)	1.386(5)	H(10E)-C(103)-H(10F)	107.7
C(422)-C(423)	1.383(6)	C(103)-C(104)-H(10G)	109.5
C(422)-H(422)	0.93	C(103)-C(104)-H(10H)	109.5
C(423)-C(424)	1.385(6)	H(10G)-C(104)-H(10H)	109.5
C(423)-H(423)	0.93	C(103)-C(104)-H(10I)	109.5
C(424)-C(425)	1.373(7)	H(10G)-C(104)-H(10I)	109.5
C(424)-H(424)	0.93	H(10H)-C(104)-H(10I)	109.5
C(425)-C(426)	1.393(6)	C(116)-C(111)-C(112)	119.5(4)
C(425)-H(425)	0.93	C(116)-C(111)-P(11)	119.7(3)
C(426)-H(426)	0.93	C(112)-C(111)-P(11)	120.8(3)
C(431)-C(436)	1.391(6)	C(113)-C(112)-C(111)	119.4(5)
C(431)-C(432)	1.394(6)	C(113)-C(112)-H(112)	120.3
C(432)-C(433)	1.391(6)	C(111)-C(112)-H(112)	120.3
C(432)-H(432)	0.93	C(114)-C(113)-C(112)	120.8(5)
C(433)-C(434)	1.379(7)	C(114)-C(113)-H(113)	119.6
C(433)-H(433)	0.93	C(112)-C(113)-H(113)	119.6
C(434)-C(435)	1.371(7)	C(113)-C(114)-C(115)	119.9(4)
C(434)-H(434)	0.93	C(113)-C(114)-H(114)	120
C(435)-C(436)	1.391(6)	C(115)-C(114)-H(114)	120.1
C(435)-H(435)	0.93	C(114)-C(115)-C(116)	119.9(5)
C(436)-H(436)	0.93	C(114)-C(115)-H(115)	120
C(441)-C(442)	1.381(6)	C(116)-C(115)-H(115)	120
C(441)-C(446)	1.398(6)	C(111)-C(116)-C(115)	120.4(5)
C(442)-C(443)	1.393(5)	C(111)-C(116)-H(116)	119.8
C(442)-H(442)	0.93	C(115)-C(116)-H(116)	119.8
C(443)-C(444)	1.374(6)	C(126)-C(121)-C(122)	119.5(4)
C(443)-H(443)	0.93	C(126)-C(121)-P(11)	119.8(3)
C(444)-C(445)	1.382(7)	C(122)-C(121)-P(11)	120.1(3)
C(444)-H(444)	0.93	C(123)-C(122)-C(121)	119.6(4)
C(445)-C(446)	1.386(6)	C(123)-C(122)-H(122)	120.2
C(445)-H(445)	0.93	C(121)-C(122)-H(122)	120.2
C(446)-H(446)	0.93	C(122)-C(123)-C(124)	120.6(4)
N(5)-H(5A)	0.89	C(122)-C(123)-H(123)	119.7
N(5)-H(5B)	0.89	C(124)-C(123)-H(123)	119.7

N(5)-H(5C)	0.89	C(125)-C(124)-C(123)	120.2(4)
N(6)-H(6A)	0.89	C(125)-C(124)-H(124)	119.9
N(6)-H(6B)	0.89	C(123)-C(124)-H(124)	119.9
N(6)-H(6C)	0.89	C(124)-C(125)-C(126)	120.1(5)
N(7)-H(7A)	0.89	C(124)-C(125)-H(125)	119.9
N(7)-H(7B)	0.89	C(126)-C(125)-H(125)	119.9
N(7)-H(7C)	0.89	C(125)-C(126)-C(121)	119.9(5)
N(8)-H(8A)	0.89	C(125)-C(126)-H(126)	120
N(8)-H(8B)	0.89	C(121)-C(126)-H(126)	120
N(8)-H(8C)	0.89	C(136)-C(131)-C(132)	119.2(4)
C(045)-C(050)	1.380(9)	C(136)-C(131)-P(12)	123.5(3)
C(045)-C(046)	1.400(9)	C(132)-C(131)-P(12)	117.3(3)
C(045)-C(051)	1.494(9)	C(133)-C(132)-C(131)	120.1(4)
C(046)-C(047)	1.375(9)	C(133)-C(132)-H(132)	119.9
C(046)-H(046)	0.93	C(131)-C(132)-H(132)	119.9
C(047)-C(048)	1.390(8)	C(134)-C(133)-C(132)	120.0(4)
C(047)-H(047)	0.93	C(134)-C(133)-H(133)	120
C(048)-C(049)	1.377(8)	C(132)-C(133)-H(133)	120
C(048)-H(048)	0.93	C(133)-C(134)-C(135)	120.4(4)
C(049)-C(050)	1.383(9)	C(133)-C(134)-H(134)	119.8
C(049)-H(049)	0.93	C(135)-C(134)-H(134)	119.8
C(050)-H(050)	0.93	C(134)-C(135)-C(136)	119.7(5)
C(051)-H(05A)	0.96	C(134)-C(135)-H(135)	120.1
C(051)-H(05B)	0.96	C(136)-C(135)-H(135)	120.1
C(051)-H(05C)	0.96	C(135)-C(136)-C(131)	120.5(4)
		C(135)-C(136)-H(136)	119.8
		C(131)-C(136)-H(136)	119.8
		C(142)-C(141)-C(146)	119.0(4)
		C(142)-C(141)-P(12)	120.0(3)
		C(146)-C(141)-P(12)	120.8(3)
		C(143)-C(142)-C(141)	120.5(5)
		C(143)-C(142)-H(142)	119.7
		C(141)-C(142)-H(142)	119.7
		C(142)-C(143)-C(144)	120.1(5)
		C(142)-C(143)-H(143)	119.9
		C(144)-C(143)-H(143)	119.9
		C(145)-C(144)-C(143)	120.0(5)
		C(145)-C(144)-H(144)	120
		C(143)-C(144)-H(144)	120
		C(144)-C(145)-C(146)	120.3(5)
		C(144)-C(145)-H(145)	119.8
		C(146)-C(145)-H(145)	119.9
		C(145)-C(146)-C(141)	120.0(4)

C(145)-C(146)-H(146)	120
C(141)-C(146)-H(146)	120
N(21)-C(201)-C(202)	116.8(3)
N(21)-C(201)-H(20A)	108.1
C(202)-C(201)-H(20A)	108.1
N(21)-C(201)-H(20B)	108.1
C(202)-C(201)-H(20B)	108.1
H(20A)-C(201)-H(20B)	107.3
C(201)-C(202)-C(203)	108.8(4)
C(201)-C(202)-H(20C)	109.9
C(203)-C(202)-H(20C)	109.9
C(201)-C(202)-H(20D)	109.9
C(203)-C(202)-H(20D)	109.9
H(20C)-C(202)-H(20D)	108.3
C(204)-C(203)-C(202)	113.8(4)
C(204)-C(203)-H(20E)	108.8
C(202)-C(203)-H(20E)	108.8
C(204)-C(203)-H(20F)	108.8
C(202)-C(203)-H(20F)	108.8
H(20E)-C(203)-H(20F)	107.7
C(203)-C(204)-H(20G)	109.5
C(203)-C(204)-H(20H)	109.5
H(20G)-C(204)-H(20H)	109.5
C(203)-C(204)-H(20I)	109.5
H(20G)-C(204)-H(20I)	109.5
H(20H)-C(204)-H(20I)	109.5
C(212)-C(211)-C(216)	119.0(4)
C(212)-C(211)-P(21)	121.1(3)
C(216)-C(211)-P(21)	119.7(3)
C(211)-C(212)-C(213)	120.4(4)
C(211)-C(212)-H(212)	119.8
C(213)-C(212)-H(212)	119.8
C(214)-C(213)-C(212)	119.8(4)
C(214)-C(213)-H(213)	120.1
C(212)-C(213)-H(213)	120.1
C(213)-C(214)-C(215)	120.4(4)
C(213)-C(214)-H(214)	119.8
C(215)-C(214)-H(214)	119.8
C(216)-C(215)-C(214)	119.7(4)
C(216)-C(215)-H(215)	120.1
C(214)-C(215)-H(215)	120.1
C(215)-C(216)-C(211)	120.6(4)
C(215)-C(216)-H(216)	119.7

C(211)-C(216)-H(216)	119.7
C(222)-C(221)-C(226)	119.1(4)
C(222)-C(221)-P(21)	123.9(3)
C(226)-C(221)-P(21)	116.9(3)
C(221)-C(222)-C(223)	120.2(4)
C(221)-C(222)-H(222)	119.9
C(223)-C(222)-H(222)	119.9
C(224)-C(223)-C(222)	120.5(4)
C(224)-C(223)-H(223)	119.8
C(222)-C(223)-H(223)	119.8
C(223)-C(224)-C(225)	119.4(4)
C(223)-C(224)-H(224)	120.3
C(225)-C(224)-H(224)	120.3
C(224)-C(225)-C(226)	120.5(4)
C(224)-C(225)-H(225)	119.7
C(226)-C(225)-H(225)	119.8
C(225)-C(226)-C(221)	120.3(4)
C(225)-C(226)-H(226)	119.9
C(221)-C(226)-H(226)	119.9
C(232)-C(231)-C(236)	119.5(4)
C(232)-C(231)-P(22)	118.2(3)
C(236)-C(231)-P(22)	121.7(3)
C(233)-C(232)-C(231)	119.9(4)
C(233)-C(232)-H(232)	120.1
C(231)-C(232)-H(232)	120.1
C(234)-C(233)-C(232)	120.6(5)
C(234)-C(233)-H(233)	119.7
C(232)-C(233)-H(233)	119.7
C(233)-C(234)-C(235)	119.9(4)
C(233)-C(234)-H(234)	120
C(235)-C(234)-H(234)	120
C(236)-C(235)-C(234)	120.1(4)
C(236)-C(235)-H(235)	119.9
C(234)-C(235)-H(235)	119.9
C(235)-C(236)-C(231)	120.0(4)
C(235)-C(236)-H(236)	120
C(231)-C(236)-H(236)	120
C(246)-C(241)-C(242)	119.2(4)
C(246)-C(241)-P(22)	121.1(3)
C(242)-C(241)-P(22)	119.7(3)
C(243)-C(242)-C(241)	120.3(5)
C(243)-C(242)-H(242)	119.9
C(241)-C(242)-H(242)	119.9

C(244)-C(243)-C(242)	119.7(5)
C(244)-C(243)-H(243)	120.1
C(242)-C(243)-H(243)	120.1
C(245)-C(244)-C(243)	120.7(4)
C(245)-C(244)-H(244)	119.6
C(243)-C(244)-H(244)	119.7
C(244)-C(245)-C(246)	119.9(4)
C(244)-C(245)-H(245)	120
C(246)-C(245)-H(245)	120
C(241)-C(246)-C(245)	120.1(4)
C(241)-C(246)-H(246)	119.9
C(245)-C(246)-H(246)	119.9
N(31)-C(301)-C(302)	114.4(4)
N(31)-C(301)-H(30A)	108.7
C(302)-C(301)-H(30A)	108.7
N(31)-C(301)-H(30B)	108.6
C(302)-C(301)-H(30B)	108.7
H(30A)-C(301)-H(30B)	107.6
C(303)-C(302)-C(301)	113.4(5)
C(303)-C(302)-H(30C)	108.9
C(301)-C(302)-H(30C)	108.9
C(303)-C(302)-H(30D)	108.8
C(301)-C(302)-H(30D)	109
H(30C)-C(302)-H(30D)	107.8
C(304)-C(303)-C(302)	111.7(4)
C(304)-C(303)-H(30E)	109.2
C(302)-C(303)-H(30E)	109.1
C(304)-C(303)-H(30F)	109.4
C(302)-C(303)-H(30F)	109.5
H(30E)-C(303)-H(30F)	107.9
C(303)-C(304)-H(30G)	109.4
C(303)-C(304)-H(30H)	109.6
H(30G)-C(304)-H(30H)	109.5
C(303)-C(304)-H(30I)	109.4
H(30G)-C(304)-H(30I)	109.5
H(30H)-C(304)-H(30I)	109.5
C(316)-C(311)-C(312)	119.2(4)
C(316)-C(311)-P(31)	119.8(3)
C(312)-C(311)-P(31)	121.0(3)
C(313)-C(312)-C(311)	120.0(4)
C(313)-C(312)-H(312)	120
C(311)-C(312)-H(312)	120
C(312)-C(313)-C(314)	120.2(4)

C(312)-C(313)-H(313)	119.9
C(314)-C(313)-H(313)	119.9
C(315)-C(314)-C(313)	120.3(4)
C(315)-C(314)-H(314)	119.9
C(313)-C(314)-H(314)	119.8
C(314)-C(315)-C(316)	120.0(4)
C(314)-C(315)-H(315)	120
C(316)-C(315)-H(315)	120
C(311)-C(316)-C(315)	120.2(4)
C(311)-C(316)-H(316)	119.9
C(315)-C(316)-H(316)	119.9
C(322)-C(321)-C(326)	119.3(4)
C(322)-C(321)-P(31)	121.5(4)
C(326)-C(321)-P(31)	118.8(4)
C(321)-C(322)-C(323)	120.8(5)
C(321)-C(322)-H(322)	119.6
C(323)-C(322)-H(322)	119.6
C(324)-C(323)-C(322)	119.7(6)
C(324)-C(323)-H(323)	120.1
C(322)-C(323)-H(323)	120.1
C(323)-C(324)-C(325)	120.5(5)
C(323)-C(324)-H(324)	119.8
C(325)-C(324)-H(324)	119.7
C(324)-C(325)-C(326)	120.1(5)
C(324)-C(325)-H(325)	120
C(326)-C(325)-H(325)	119.9
C(321)-C(326)-C(325)	119.6(5)
C(321)-C(326)-H(326)	120.2
C(325)-C(326)-H(326)	120.2
C(336)-C(331)-C(332)	119.5(4)
C(336)-C(331)-P(32)	123.0(3)
C(332)-C(331)-P(32)	117.5(3)
C(333)-C(332)-C(331)	119.7(4)
C(333)-C(332)-H(332)	120.2
C(331)-C(332)-H(332)	120.2
C(334)-C(333)-C(332)	120.3(4)
C(334)-C(333)-H(333)	119.9
C(332)-C(333)-H(333)	119.8
C(335)-C(334)-C(333)	120.4(4)
C(335)-C(334)-H(334)	119.8
C(333)-C(334)-H(334)	119.8
C(334)-C(335)-C(336)	119.6(5)
C(334)-C(335)-H(335)	120.2

C(336)-C(335)-H(335)	120.2
C(331)-C(336)-C(335)	120.6(4)
C(331)-C(336)-H(336)	119.7
C(335)-C(336)-H(336)	119.7
C(342)-C(341)-C(346)	119.1(4)
C(342)-C(341)-P(32)	119.7(3)
C(346)-C(341)-P(32)	121.1(3)
C(343)-C(342)-C(341)	120.6(4)
C(343)-C(342)-H(342)	119.7
C(341)-C(342)-H(342)	119.7
C(342)-C(343)-C(344)	119.5(4)
C(342)-C(343)-H(343)	120.2
C(344)-C(343)-H(343)	120.2
C(345)-C(344)-C(343)	120.9(5)
C(345)-C(344)-H(344)	119.6
C(343)-C(344)-H(344)	119.5
C(344)-C(345)-C(346)	119.4(5)
C(344)-C(345)-H(345)	120.3
C(346)-C(345)-H(345)	120.3
C(345)-C(346)-C(341)	120.5(4)
C(345)-C(346)-H(346)	119.7
C(341)-C(346)-H(346)	119.7
N(41)-C(401)-C(402)	115.7(3)
N(41)-C(401)-H(40A)	108.4
C(402)-C(401)-H(40A)	108.4
N(41)-C(401)-H(40B)	108.4
C(402)-C(401)-H(40B)	108.4
H(40A)-C(401)-H(40B)	107.4
C(403)-C(402)-C(401)	110.6(3)
C(403)-C(402)-H(40C)	109.5
C(401)-C(402)-H(40C)	109.5
C(403)-C(402)-H(40D)	109.5
C(401)-C(402)-H(40D)	109.5
H(40C)-C(402)-H(40D)	108.1
C(404)-C(403)-C(402)	113.8(4)
C(404)-C(403)-H(40E)	108.8
C(402)-C(403)-H(40E)	108.8
C(404)-C(403)-H(40F)	108.8
C(402)-C(403)-H(40F)	108.8
H(40E)-C(403)-H(40F)	107.7
C(403)-C(404)-H(40G)	109.4
C(403)-C(404)-H(40H)	109.5
H(40G)-C(404)-H(40H)	109.5

C(403)-C(404)-H(40I)	109.5
H(40G)-C(404)-H(40I)	109.5
H(40H)-C(404)-H(40I)	109.5
C(412)-C(411)-C(416)	118.7(4)
C(412)-C(411)-P(41)	121.2(3)
C(416)-C(411)-P(41)	120.0(3)
C(413)-C(412)-C(411)	120.7(4)
C(413)-C(412)-H(412)	119.7
C(411)-C(412)-H(412)	119.6
C(412)-C(413)-C(414)	120.0(4)
C(412)-C(413)-H(413)	120
C(414)-C(413)-H(413)	120
C(413)-C(414)-C(415)	120.5(4)
C(413)-C(414)-H(414)	119.8
C(415)-C(414)-H(414)	119.8
C(416)-C(415)-C(414)	119.5(4)
C(416)-C(415)-H(415)	120.3
C(414)-C(415)-H(415)	120.3
C(415)-C(416)-C(411)	120.7(4)
C(415)-C(416)-H(416)	119.6
C(411)-C(416)-H(416)	119.7
C(422)-C(421)-C(426)	119.9(4)
C(422)-C(421)-P(41)	122.5(3)
C(426)-C(421)-P(41)	117.5(3)
C(423)-C(422)-C(421)	120.1(4)
C(423)-C(422)-H(422)	119.9
C(421)-C(422)-H(422)	120
C(422)-C(423)-C(424)	119.7(4)
C(422)-C(423)-H(423)	120.1
C(424)-C(423)-H(423)	120.1
C(425)-C(424)-C(423)	120.6(4)
C(425)-C(424)-H(424)	119.7
C(423)-C(424)-H(424)	119.7
C(424)-C(425)-C(426)	120.0(4)
C(424)-C(425)-H(425)	120
C(426)-C(425)-H(425)	120
C(421)-C(426)-C(425)	119.7(4)
C(421)-C(426)-H(426)	120.2
C(425)-C(426)-H(426)	120.1
C(436)-C(431)-C(432)	118.9(4)
C(436)-C(431)-P(42)	121.5(3)
C(432)-C(431)-P(42)	119.0(3)
C(433)-C(432)-C(431)	120.0(4)

C(433)-C(432)-H(432)	120
C(431)-C(432)-H(432)	120
C(434)-C(433)-C(432)	120.2(4)
C(434)-C(433)-H(433)	119.9
C(432)-C(433)-H(433)	119.9
C(435)-C(434)-C(433)	120.3(4)
C(435)-C(434)-H(434)	119.9
C(433)-C(434)-H(434)	119.9
C(434)-C(435)-C(436)	120.1(5)
C(434)-C(435)-H(435)	120
C(436)-C(435)-H(435)	119.9
C(435)-C(436)-C(431)	120.4(4)
C(435)-C(436)-H(436)	119.8
C(431)-C(436)-H(436)	119.8
C(442)-C(441)-C(446)	119.0(4)
C(442)-C(441)-P(42)	119.2(3)
C(446)-C(441)-P(42)	121.8(3)
C(441)-C(442)-C(443)	120.2(4)
C(441)-C(442)-H(442)	119.9
C(443)-C(442)-H(442)	119.9
C(444)-C(443)-C(442)	120.5(4)
C(444)-C(443)-H(443)	119.8
C(442)-C(443)-H(443)	119.7
C(443)-C(444)-C(445)	119.9(4)
C(443)-C(444)-H(444)	120
C(445)-C(444)-H(444)	120.1
C(444)-C(445)-C(446)	120.0(4)
C(444)-C(445)-H(445)	120
C(446)-C(445)-H(445)	120
C(445)-C(446)-C(441)	120.4(4)
C(445)-C(446)-H(446)	119.8
C(441)-C(446)-H(446)	119.8
C(01)-N(5)-H(5A)	109.5
C(01)-N(5)-H(5B)	109.5
H(5A)-N(5)-H(5B)	109.5
C(01)-N(5)-H(5C)	109.5
H(5A)-N(5)-H(5C)	109.5
H(5B)-N(5)-H(5C)	109.5
C(05)-N(6)-H(6A)	109.5
C(05)-N(6)-H(6B)	109.5
H(6A)-N(6)-H(6B)	109.5
C(05)-N(6)-H(6C)	109.5
H(6A)-N(6)-H(6C)	109.5

H(6B)-N(6)-H(6C)	109.5
C(09)-N(7)-H(7A)	109.5
C(09)-N(7)-H(7B)	109.5
H(7A)-N(7)-H(7B)	109.5
C(09)-N(7)-H(7C)	109.5
H(7A)-N(7)-H(7C)	109.5
H(7B)-N(7)-H(7C)	109.5
C(013)-N(8)-H(8A)	109.4
C(013)-N(8)-H(8B)	109.5
H(8A)-N(8)-H(8B)	109.5
C(013)-N(8)-H(8C)	109.5
H(8A)-N(8)-H(8C)	109.5
H(8B)-N(8)-H(8C)	109.5
C(050)-C(045)-C(046)	117.3(6)
C(050)-C(045)-C(051)	121.9(6)
C(046)-C(045)-C(051)	120.8(6)
C(047)-C(046)-C(045)	121.3(7)
C(047)-C(046)-H(046)	119.3
C(045)-C(046)-H(046)	119.4
C(046)-C(047)-C(048)	120.4(7)
C(046)-C(047)-H(047)	119.8
C(048)-C(047)-H(047)	119.8
C(049)-C(048)-C(047)	119.0(6)
C(049)-C(048)-H(048)	120.5
C(047)-C(048)-H(048)	120.5
C(048)-C(049)-C(050)	120.2(7)
C(048)-C(049)-H(049)	119.9
C(050)-C(049)-H(049)	119.9
C(049)-C(050)-C(045)	121.9(7)
C(049)-C(050)-H(050)	119.1
C(045)-C(050)-H(050)	119
C(045)-C(051)-H(05A)	109.4
C(045)-C(051)-H(05B)	109.5
H(05A)-C(051)-H(05B)	109.5
C(045)-C(051)-H(05C)	109.5
H(05A)-C(051)-H(05C)	109.5
H(05B)-C(051)-H(05C)	109.5

Table C9. Anisotropic displacement parameters ($A^2 \times 10^3$) for [NH_3-n-Butyl][$CrCl_4$(PNP-n-Butyl)] $2C_7H_8$. The anisotropic displacement factor exponent takes the form: -2 pi [$h^2 a^{*2} U11 + ... + 2 h k a^* b^* U12$]

	U11	U22	U33	U23	U13	U12
Cr(1)	16(1)	13(1)	14(1)	2(1)	-3(1)	-4(1)
Cr(2)	15(1)	12(1)	12(1)	2(1)	-2(1)	-4(1)
Cr(3)	15(1)	17(1)	16(1)	3(1)	-2(1)	-4(1)
Cr(4)	13(1)	14(1)	13(1)	2(1)	-1(1)	-5(1)
N(11)	20(2)	16(2)	19(2)	3(1)	-6(1)	-4(1)
N(21)	18(2)	14(2)	15(2)	4(1)	-5(1)	-5(1)
N(31)	15(1)	17(1)	16(1)	3(1)	-2(1)	-4(1)
N(41)	16(2)	17(2)	14(2)	3(1)	-4(1)	-5(1)
P(31)	15(1)	17(1)	16(1)	3(1)	-2(1)	-4(1)
P(32)	15(1)	17(1)	16(1)	3(1)	-2(1)	-4(1)
Cl(31)	16(1)	20(1)	20(1)	3(1)	2(1)	-7(1)
Cl(32)	16(1)	17(1)	20(1)	4(1)	-3(1)	-3(1)
Cl(33)	23(1)	22(1)	17(1)	2(1)	-4(1)	-9(1)
Cl(34)	15(1)	21(1)	18(1)	4(1)	0(1)	-7(1)
P(11)	17(1)	15(1)	16(1)	4(1)	-5(1)	-5(1)
P(12)	16(1)	15(1)	16(1)	2(1)	-5(1)	-5(1)
P(21)	14(1)	14(1)	13(1)	1(1)	-3(1)	-4(1)
P(22)	14(1)	15(1)	13(1)	3(1)	-3(1)	-5(1)
Cl(11)	25(1)	20(1)	16(1)	0(1)	-6(1)	-7(1)
Cl(12)	19(1)	18(1)	19(1)	3(1)	-1(1)	-7(1)
Cl(13)	21(1)	23(1)	20(1)	3(1)	0(1)	-8(1)
Cl(14)	18(1)	17(1)	21(1)	4(1)	-7(1)	-3(1)
Cl(21)	17(1)	17(1)	18(1)	4(1)	-1(1)	-7(1)
Cl(22)	31(1)	17(1)	16(1)	0(1)	-7(1)	-8(1)
Cl(23)	17(1)	15(1)	18(1)	2(1)	-4(1)	-3(1)
Cl(24)	20(1)	19(1)	18(1)	2(1)	2(1)	-6(1)
P(41)	13(1)	16(1)	14(1)	3(1)	-3(1)	-6(1)
P(42)	13(1)	17(1)	14(1)	4(1)	-3(1)	-6(1)
Cl(41)	16(1)	19(1)	17(1)	3(1)	1(1)	-8(1)
Cl(42)	20(1)	19(1)	17(1)	1(1)	-4(1)	-8(1)
Cl(43)	19(1)	20(1)	17(1)	2(1)	3(1)	-8(1)
Cl(44)	16(1)	19(1)	20(1)	4(1)	-4(1)	-3(1)
C(01)	30(1)	31(1)	24(1)	4(1)	2(1)	-7(1)
C(02)	30(1)	31(1)	24(1)	4(1)	2(1)	-7(1)
C(03)	30(1)	31(1)	24(1)	4(1)	2(1)	-7(1)
C(04)	30(1)	31(1)	24(1)	4(1)	2(1)	-7(1)
C(05)	20(2)	28(2)	22(2)	-2(2)	-1(2)	-10(2)
C(06)	23(2)	26(2)	20(2)	3(2)	-3(2)	-9(2)
C(07)	33(3)	42(3)	28(2)	-2(2)	5(2)	-18(2)
C(08)	37(3)	49(3)	25(2)	6(2)	2(2)	-8(3)

C(09)	32(3)	25(2)	20(2)	3(2)	0(2)	-12(2)
C(010)	26(2)	18(2)	21(2)	3(2)	-4(2)	-8(2)
C(011)	35(3)	27(2)	24(2)	5(2)	0(2)	-9(2)
C(012)	46(3)	29(3)	27(2)	4(2)	4(2)	-8(2)
C(013)	48(2)	53(2)	35(1)	10(1)	-1(1)	-12(1)
C(014)	48(2)	53(2)	35(1)	10(1)	-1(1)	-12(1)
C(015)	48(2)	53(2)	35(1)	10(1)	-1(1)	-12(1)
C(016)	48(2)	53(2)	35(1)	10(1)	-1(1)	-12(1)
C(017)	24(3)	47(3)	33(3)	-6(2)	-11(2)	-10(2)
C(018)	23(3)	57(4)	28(2)	-1(2)	-3(2)	-16(3)
C(019)	32(3)	41(3)	42(3)	7(2)	-9(2)	-20(2)
C(020)	43(4)	39(3)	53(4)	-12(3)	5(3)	-13(3)
C(021)	50(4)	55(4)	34(3)	-9(3)	11(3)	-24(3)
C(022)	44(3)	38(3)	34(3)	-2(2)	-8(2)	-15(3)
C(023)	28(3)	61(4)	65(4)	-24(3)	-9(3)	-8(3)
C(024)	27(3)	37(3)	23(2)	-5(2)	-1(2)	-13(2)
C(025)	46(4)	28(3)	45(3)	-5(2)	-12(3)	-1(2)
C(026)	94(6)	28(3)	50(4)	17(3)	-28(4)	-26(3)
C(027)	75(5)	57(4)	28(3)	3(3)	-2(3)	-44(4)
C(028)	38(3)	45(3)	33(3)	-7(2)	5(2)	-18(3)
C(029)	30(3)	28(2)	28(2)	-2(2)	-3(2)	-8(2)
C(030)	47(4)	79(5)	33(3)	-8(3)	8(3)	-33(4)
C(031)	35(3)	29(3)	42(3)	-9(2)	5(2)	-13(2)
C(032)	33(3)	40(3)	59(4)	-12(3)	4(3)	-17(3)
C(033)	31(3)	50(4)	66(4)	-9(3)	-9(3)	-7(3)
C(034)	57(4)	36(3)	45(3)	0(3)	-19(3)	-10(3)
C(035)	45(3)	37(3)	29(3)	-1(2)	1(2)	-10(3)
C(036)	29(3)	31(3)	38(3)	-3(2)	4(2)	-7(2)
C(037)	61(4)	30(3)	57(4)	5(3)	11(3)	-20(3)
C(038)	28(3)	46(3)	43(3)	0(3)	-11(2)	-14(2)
C(039)	26(3)	51(3)	26(2)	7(2)	-6(2)	-16(2)
C(040)	32(3)	50(3)	35(3)	-5(2)	-12(2)	-12(3)
C(041)	46(4)	53(4)	45(3)	3(3)	-14(3)	-23(3)
C(042)	53(4)	67(4)	43(3)	5(3)	-4(3)	-39(4)
C(043)	40(3)	70(4)	35(3)	-3(3)	3(3)	-28(3)
C(044)	40(4)	51(4)	70(4)	-5(3)	-18(3)	-13(3)
C(052)	48(1)	57(1)	52(1)	-7(1)	-16(1)	-7(1)
C(053)	48(1)	57(1)	52(1)	-7(1)	-16(1)	-7(1)
C(054)	48(1)	57(1)	52(1)	-7(1)	-16(1)	-7(1)
C(055)	48(1)	57(1)	52(1)	-7(1)	-16(1)	-7(1)
C(056)	48(1)	57(1)	52(1)	-7(1)	-16(1)	-7(1)
C(057)	48(1)	57(1)	52(1)	-7(1)	-16(1)	-7(1)
C(059)	48(1)	57(1)	52(1)	-7(1)	-16(1)	-7(1)

C(060)	29(3)	71(4)	23(2)	-3(2)	-6(2)	-24(3)
C(061)	38(3)	58(4)	32(3)	3(3)	1(2)	-27(3)
C(062)	46(4)	59(4)	28(3)	-1(3)	-2(2)	-22(3)
C(063)	47(4)	59(4)	45(3)	-8(3)	-20(3)	-22(3)
C(064)	36(3)	59(4)	61(4)	16(3)	-21(3)	-26(3)
C(065)	28(3)	80(4)	30(3)	13(3)	-11(2)	-32(3)
C(066)	34(3)	93(5)	47(4)	-30(4)	0(3)	-26(4)
C(067)	37(3)	39(3)	32(3)	-2(2)	-7(2)	-22(2)
C(068)	49(4)	50(3)	30(3)	7(2)	-11(2)	-28(3)
C(069)	51(4)	86(5)	27(3)	-2(3)	5(3)	-42(4)
C(070)	43(4)	81(5)	34(3)	-16(3)	4(3)	-13(4)
C(071)	54(4)	40(3)	45(3)	-4(3)	-10(3)	-8(3)
C(072)	47(4)	46(3)	31(3)	1(2)	-2(2)	-27(3)
C(073)	38(4)	67(4)	47(4)	-5(3)	-7(3)	-10(3)
C(101)	25(2)	15(2)	20(2)	2(2)	-5(2)	-6(2)
C(102)	22(2)	20(2)	23(2)	3(2)	-4(2)	-4(2)
C(103)	33(3)	20(2)	32(3)	3(2)	0(2)	-5(2)
C(104)	41(3)	30(3)	43(3)	9(2)	3(3)	3(2)
C(111)	22(2)	22(2)	16(2)	5(2)	-5(2)	-10(2)
C(112)	30(3)	19(2)	26(2)	6(2)	-13(2)	-10(2)
C(113)	49(3)	19(2)	29(2)	8(2)	-22(2)	-15(2)
C(114)	48(3)	43(3)	23(2)	17(2)	-18(2)	-27(3)
C(115)	38(3)	53(3)	22(2)	9(2)	-7(2)	-12(3)
C(116)	28(3)	36(3)	20(2)	10(2)	-8(2)	-7(2)
C(121)	17(2)	17(2)	24(2)	5(2)	-7(2)	-6(2)
C(122)	22(2)	22(2)	24(2)	6(2)	-6(2)	-5(2)
C(123)	20(2)	22(2)	32(2)	4(2)	0(2)	-5(2)
C(124)	19(2)	29(2)	46(3)	9(2)	-3(2)	-11(2)
C(125)	30(3)	32(3)	45(3)	6(2)	-17(2)	-16(2)
C(126)	25(3)	26(2)	29(2)	3(2)	-9(2)	-11(2)
C(131)	17(2)	21(2)	20(2)	0(2)	-7(2)	-6(2)
C(132)	27(2)	24(2)	18(2)	5(2)	-4(2)	-7(2)
C(133)	31(3)	30(2)	20(2)	8(2)	-6(2)	-11(2)
C(134)	30(3)	44(3)	15(2)	1(2)	-4(2)	-16(2)
C(135)	33(3)	36(3)	23(2)	-5(2)	-2(2)	-2(2)
C(136)	36(3)	25(2)	21(2)	1(2)	-5(2)	-6(2)
C(141)	20(2)	15(2)	26(2)	1(2)	-5(2)	-6(2)
C(142)	22(2)	24(2)	32(2)	2(2)	-2(2)	-8(2)
C(143)	32(3)	28(3)	43(3)	-3(2)	4(2)	-17(2)
C(144)	31(3)	39(3)	60(4)	-8(3)	-4(3)	-22(3)
C(145)	26(3)	41(3)	44(3)	-8(2)	-11(2)	-13(2)
C(146)	21(2)	29(2)	31(2)	-2(2)	-8(2)	-10(2)
C(202)	26(3)	20(2)	27(2)	-2(2)	-6(2)	-1(2)

C(203)	28(3)	22(2)	56(3)	-4(2)	-1(2)	-5(2)
C(204)	37(4)	25(3)	93(5)	-4(3)	2(3)	-2(2)
C(211)	18(2)	17(2)	21(2)	-4(2)	-2(2)	-8(2)
C(212)	19(2)	27(2)	25(2)	0(2)	-7(2)	-9(2)
C(213)	21(3)	41(3)	35(3)	-7(2)	-8(2)	-13(2)
C(214)	28(3)	42(3)	43(3)	-7(2)	-2(2)	-24(2)
C(215)	31(3)	32(3)	30(2)	1(2)	3(2)	-18(2)
C(216)	23(2)	20(2)	23(2)	-3(2)	-2(2)	-10(2)
C(222)	19(2)	27(2)	18(2)	1(2)	-4(2)	0(2)
C(223)	23(3)	31(2)	20(2)	-4(2)	0(2)	-1(2)
C(224)	29(3)	37(3)	12(2)	2(2)	-3(2)	-13(2)
C(225)	40(3)	24(2)	19(2)	6(2)	-10(2)	-12(2)
C(226)	28(3)	19(2)	17(2)	-1(2)	-5(2)	-6(2)
C(233)	26(3)	35(3)	37(3)	6(2)	-11(2)	-13(2)
C(234)	18(2)	35(3)	42(3)	13(2)	-5(2)	-14(2)
C(243)	36(3)	50(3)	22(2)	11(2)	-7(2)	-17(3)
C(244)	44(3)	44(3)	23(2)	20(2)	-16(2)	-29(3)
C(245)	41(3)	20(2)	34(3)	10(2)	-25(2)	-13(2)
C(246)	28(3)	17(2)	25(2)	3(2)	-13(2)	-6(2)
C(301)	15(1)	17(1)	16(1)	3(1)	-2(1)	-4(1)
C(302)	48(4)	35(3)	36(3)	-8(2)	-12(3)	18(3)
C(303)	15(1)	17(1)	16(1)	3(1)	-2(1)	-4(1)
C(304)	15(1)	17(1)	16(1)	3(1)	-2(1)	-4(1)
C(311)	22(2)	22(2)	16(2)	7(2)	-6(2)	-8(2)
C(312)	20(2)	21(2)	23(2)	1(2)	-7(2)	-6(2)
C(313)	15(1)	17(1)	16(1)	3(1)	-2(1)	-4(1)
C(314)	41(3)	34(3)	24(2)	16(2)	-16(2)	-19(2)
C(315)	32(3)	35(3)	15(2)	4(2)	-1(2)	-7(2)
C(316)	23(2)	23(2)	20(2)	3(2)	-5(2)	-5(2)
C(321)	13(2)	26(2)	27(2)	13(2)	-4(2)	-4(2)
C(322)	15(2)	43(3)	32(3)	15(2)	-2(2)	3(2)
C(323)	16(3)	52(3)	53(3)	25(3)	10(2)	3(2)
C(324)	18(3)	54(4)	83(5)	37(4)	-9(3)	-10(3)
C(325)	30(3)	44(3)	72(4)	24(3)	-28(3)	-20(3)
C(326)	29(3)	28(2)	39(3)	15(2)	-13(2)	-13(2)
C(331)	16(2)	21(2)	17(2)	0(2)	-3(2)	-6(2)
C(332)	16(2)	23(2)	21(2)	1(2)	-5(2)	-4(2)
C(333)	25(2)	30(2)	22(2)	7(2)	-7(2)	-12(2)
C(334)	25(3)	44(3)	18(2)	5(2)	-7(2)	-16(2)
C(335)	32(3)	31(3)	22(2)	-6(2)	-3(2)	-4(2)
C(336)	25(3)	28(2)	24(2)	1(2)	-6(2)	-7(2)
C(341)	20(2)	15(2)	22(2)	-1(2)	-2(2)	-5(2)
C(342)	36(3)	21(2)	26(2)	4(2)	-5(2)	-15(2)

C(343)	46(3)	33(3)	29(2)	-4(2)	2(2)	-26(3)
C(344)	33(3)	35(3)	44(3)	-5(2)	1(2)	-23(2)
C(345)	26(3)	37(3)	37(3)	-4(2)	-8(2)	-13(2)
C(346)	19(2)	22(2)	27(2)	1(2)	-4(2)	-6(2)
C(401)	19(2)	16(2)	16(2)	1(2)	-3(2)	-7(2)
C(402)	17(2)	23(2)	16(2)	2(2)	-3(2)	-4(2)
C(403)	20(2)	21(2)	32(2)	0(2)	0(2)	-2(2)
C(404)	29(3)	31(3)	39(3)	3(2)	3(2)	3(2)
C(411)	13(2)	15(2)	19(2)	2(2)	-2(2)	-5(2)
C(412)	21(2)	26(2)	21(2)	4(2)	-7(2)	-8(2)
C(413)	18(2)	37(3)	28(2)	1(2)	-8(2)	-13(2)
C(414)	16(2)	34(3)	31(2)	1(2)	-1(2)	-13(2)
C(415)	22(2)	25(2)	23(2)	1(2)	-1(2)	-10(2)
C(421)	15(2)	21(2)	15(2)	2(2)	-5(2)	-9(2)
C(422)	24(2)	27(2)	20(2)	3(2)	-5(2)	-7(2)
C(424)	29(3)	38(3)	12(2)	3(2)	-5(2)	-12(2)
C(425)	33(3)	30(2)	19(2)	7(2)	-7(2)	-14(2)
C(426)	24(2)	21(2)	17(2)	0(2)	-5(2)	-8(2)
C(431)	14(2)	14(2)	24(2)	4(2)	-4(2)	-4(2)
C(432)	22(2)	30(2)	26(2)	5(2)	-11(2)	-12(2)
C(433)	28(3)	42(3)	35(3)	7(2)	-14(2)	-21(2)
C(434)	16(2)	38(3)	46(3)	12(2)	-4(2)	-14(2)
C(435)	16(2)	28(2)	33(2)	7(2)	4(2)	-5(2)
C(436)	16(2)	23(2)	22(2)	5(2)	-4(2)	-8(2)
C(441)	20(2)	22(2)	13(2)	8(2)	-5(2)	-8(2)
C(442)	30(3)	23(2)	16(2)	5(2)	-4(2)	-5(2)
C(443)	34(3)	27(2)	14(2)	2(2)	-3(2)	-5(2)
C(444)	39(3)	30(2)	14(2)	7(2)	-8(2)	-14(2)
C(445)	36(3)	20(2)	26(2)	5(2)	-15(2)	-8(2)
C(446)	29(3)	21(2)	21(2)	0(2)	-9(2)	-7(2)
N(5)	30(1)	31(1)	24(1)	4(1)	2(1)	-7(1)
N(6)	22(2)	21(2)	20(2)	3(1)	-2(2)	-9(2)
N(7)	20(2)	19(2)	20(2)	-2(1)	0(1)	-9(2)
N(8)	48(2)	53(2)	35(1)	10(1)	-1(1)	-12(1)
C(045)	48(1)	57(1)	52(1)	-7(1)	-16(1)	-7(1)
C(046)	48(1)	57(1)	52(1)	-7(1)	-16(1)	-7(1)
C(047)	48(1)	57(1)	52(1)	-7(1)	-16(1)	-7(1)
C(048)	28(3)	36(3)	46(3)	0(2)	-12(2)	-4(2)
C(049)	48(1)	57(1)	52(1)	-7(1)	-16(1)	-7(1)
C(050)	48(1)	57(1)	52(1)	-7(1)	-16(1)	-7(1)
C(051)	48(1)	57(1)	52(1)	-7(1)	-16(1)	-7(1)

Appendix D

Appendix D lists the theoretically optimized compound names (see Chapters 7, 8 and 9) and the corresponding output file names which contain the computational results. These data files can be accessed in the folder Appendix D on the CD included.

D1. Non-coordinated PNP ligands

PNP-Ethyl isomer 9 (1*) – PNP-Ethyl.log

PNP-Dimprop isomer 11 (2*) – PNP-Dimprop.log

PNP-*i*-Pent isomer 11 (3*) – PNP-*i*-Pent.log

PNP-Cychex isomer 7 (4*) - PNP-Cychex.log

PNP-*n*-Pent isomer 10 (5*) - PNP-*n*-Pent.log

D2. [$PtCl_2$(PNP)] complexes

[$PtCl_2$(PNP-Ethyl)] structure (6*) - $PtCl_2$(PNP-Ethyl).log

[$PtCl_2$(PNP-*n*-Prop)] structure (7*) - $PtCl_2$(PNP-*n*-Prop).log

[$PtCl_2$(PNP-Dimprop)] (8*) - $PtCl_2$(PNP-Dimprop).log

[$PtCl_2$(PNP-*i*-Pent)] structure (9*) - $PtCl_2$(PNP-*i*-Pent).log

[$PtCl_2$(PNP-Cychex)] structure (10*) - $PtCl_2$(PNP-Cychex).log

D3. [$PdCl_2$(PNP)] complexes

[$PtCl_2$(PNP-*i*-Prop)] structure (11*) - $PtCl_2$(PNP-*i*-Prop).log

[$PdCl_2$(PNP-Dimprop)] structure (12*) - $PdCl_2$(PNP-Dimprop).log

[$PdCl_2$(PNP-*n*-Prop)] structure (13*) - $PdCl_2$(PNP-*n*-Prop).log

[$PdCl_2$(PNP-*i*-Pent)] structure (14*) - $PdCl_2$(PNP-*i*-Pent).log

[$PdCl_2$(PNP-*n*-Butyl)] structure (15*) - $PdCl_2$(PNP-*n*-Butyl).log

D4. [$CrCl_4$(PNP)]$^-$ complexes

[$CrCl_4$(PNP-*n*-Pent)]$^-$ (16*) - $CrCl_4$(PNP-*n*-Pent).log

[$CrCl_4$(PNP-*i*-Pent)]$^-$ (17*) - $CrCl_4$(PNP-*i*-Pent).log

[$CrCl_4$(PNP-*n*-Butyl)]$^-$ (18*) - $CrCl_4$(PNP-*n*-Butyl).log

Appendix E

Supplementary data for the substitution reactions between [$PtCl_2$(PNP-*i*-Pent)] and Br^-

Table E1: Temperature effect and [Br^-] dependence of the *pseudo* first order reaction (first reaction) between [$PtCl_2$(PNP-i-Pent)] and Br^- i.e. formation of [PtClBr(PNP-i-Pent)] in dichloroethane at 15, 25, 30 and 40 °C, [$PtCl_2$(PNP-i-Pent)] = 2.5 x 10^{-4} M) and [PPhCl] = 2.5 x 10^{-3} M at λ = 330 nm.

[Br^-]	k_{obs} (s^{-1}) 15 °C	k_{obs} (s^{-1}) 25 °C	k_{obs} (s^{-1}) 30 °C	k_{obs} (s^{-1}) 40 °C
0.0025	0.00252(1)	0.00519(3)	0.0076(1)	0.0183(9)
0.005	0.00316(1)	0.00731(3)	0.01073(9)	0.0207(5)
0.01	0.00463(3)	0.01037(8)	0.0162(3)	0.0287(4)
0.015	0.00625(2)	0.01333(6)	0.0190(9)	0.0370(6)
0.02	0.00772(3)	0.0165(1)	0.02398(2)	0.048(3)

Table E2: Temperature effect and [Br^-] dependence of the *pseudo* first order reaction (second reaction) between [$PtCl_2$(PNP-i-Pent)] and Br^- i.e. formation of [$PtBr_2$(PNP-i-Pent)] in dichloroethane at 30, 40, 50 and 60 °C, [$PtCl_2$(PNP-i-Pent)] = 2.5 x 10^{-4} M) and [PPhCl] = 2.5 x 10^{-3} M at λ = 330 nm.

[Br^-]	k_{obs} (x 10^{-3} s^{-1}) 30 °C	k_{obs} (x 10^{-3} s^{-1}) 40 °C	k_{obs} (x 10^{-3} s^{-1}) 50 °C	k_{obs} (x 10^{-3} s^{-1}) 60 °C
0.0025	0.0304(6)	0.1114(3)	0.262(4)	1.106(8)
0.005	0.031(1)	0.1141(3)	0.270(3)	1.10(5)
0.01	0.0291(1)	0.1365(3)	0.310(4)	1.124(4)
0.015	0.03671(8)	0.1448(4)	0.486(1)	1.270(5)
0.02	0.04472(7)	0.1579(3)	0.522(1)	1.317(6)

Table E3: The data for the spectophotometric determination (ΔAbs = Absorbance) of the equilibrium constants for the first reaction between [$PtCl_2$(PNP-i-Pent)] and Br^- i.e. formation of [PtClBr(PNP-i-Pent)] in dichloroethane at 15, 25, 30 and 40 °C, [$PtCl_2$(PNP-i-Pent)] = 2.5 x 10^{-4} M) and [PPhCl] = 2.5 x 10^{-3} M at λ = 330 nm.

[Br^-]	ΔAbs 15 °C	ΔAbs 25 °C	ΔAbs 30 °C	ΔAbs 40 °C
0.0025	0.070	0.050	0.050	0.035
0.005	0.105	0.070	0.062	0.048
0.01	0.140	0.100	0.090	0.058
0.015	0.150	0.120	0.105	0.060
0.02	0.160	0.130	0.110	0.067

APPENDIX E

Table E4: The data for the spectophotometric determination (ΔAbs = Absorbance) of the equilibrium constants for the second reaction between [$PtCl_2$(PNP-i-Pent)] and Br^- i.e. formation of [$PtBr_2$(PNP-i-Pent)] in dichloroethane at 30, 40, 50 and 60 ℃, [$PtCl_2$(PNP-i-Pent)] = 2.5 x 10^{-4} M) and [PPhCl] = 2.5 x 10^{-3} M at λ = 330 nm.

[Br^-]	ΔAbs 30 ℃	ΔAbs 40 ℃	ΔAbs 50 ℃	ΔAbs 60 ℃
0.0025	0.032	0.055	0.020	0.035
0.005	0.040	0.070	0.028	0.044
0.01	0.050	0.090	0.038	0.060
0.015	0.055	0.097	0.045	0.065
0.02	0.060	0.110	0.048	0.072

Table E5: Eyring plot data of the k_1 rate constant for the formation of [PtClBr(PNP-*i*-Pent)] in dichloroethane (see **Figure 11.10**).

1/T (x 10^{-3} K^{-1})	ln(k_{-1}/T)
3.472	-6.867
3.356	-6.1434
3.3003	-5.8191
3.19489	-5.2156

Table E6: Eyring plot data of the k_1 rate constant for the formation of [$PtBr_2$(PNP-i-Pent)] in dichloroethane (see **Figure 11.11**).

1/T (x 10^{-3} K^{-1})	ln(k_{-1}/T)
3.3003	-12.8446
3.19489	-11.6243
3.09587	-10.7685
3.003	-10.151

Rate laws and kinetic activation parameters

Rate constant

The rate of a reaction can be defined as the change in the concentration of a reactant or product per unit time. Denoted by the rate constant, *k*, that relates to the change of the reagent concentration per unit time. For a simple reaction, as given below:

$$A + B \xrightarrow{k} C \tag{E1}$$

The rate can be expressed by the equation:

$$Rate = \frac{-d[A]}{dt} = \frac{-d[B]}{dt} = \frac{d[C]}{dt} = k[A]^m[B]^n \tag{E2}$$

Where [] denotes concentration and the negative signs indicates the disappearance of A and B. The values m and n represent the order of the reaction with regard to the concentrations of A and B, the sum of m and n is equal to the total order of the reaction. The reaction order is the way in which the rate of the reaction will vary as the concentration of both of one of the reacting species is changed. The order of the reaction can be determined experimentally, but with a lot of difficulty. This is overcome by forcing the reaction to *pseudo*-first order conditions, where one of the species concentration stays constant by having the concentration of the second species much higher. With this the rate equation simplifies to:

$$\text{Rate} = k_{obs}[A]^m \tag{E3}$$

The pseudo-first order rate constant can now be given as

$$k_{obs} = k[B]^n \tag{E4}$$

By varying the concentration of B, as in the equation above, the rate constant, *k*, can be determined. If a second reaction occurs, the rate law is extended to (under *pseudo*-first order conditions):

$$\text{Rate} = k_1[A][B] + k_2[A] \tag{E5}$$

$$k_{obs} = k_1[B] + k_2 \tag{E6}$$

Intergration of the rate eauqtion:

$$\text{Rate} = \frac{-d[A]}{dt} = \frac{-d[B]}{dt} = \frac{d[C]}{dt} = k[A]^m[B]^n \tag{E7}$$

With boundaries of t = 0 and t, yields an expression on terms of C, where C denotes the concentration change of the reactants at time t and the initial time is obtained.

$$[C]_t = [C]_0 e^{k_{obs} t} \quad \text{(E8)}$$

$$\text{where } \frac{[C]_t}{[C]_0} = \frac{A_\infty - A_t}{A_\infty - A_0} \quad \text{(E9)}$$

Substitution of this equation into the Beer-Lambert law;

$$A = \varepsilon \cdot l \cdot C \quad \text{(E10)}$$

Where A = absorbance, ε = molar extinction coefficient, C = concentration and l = light path length. Gives the following equation:

$$A_t = A_\infty - (A_\infty - A_0) e^{k_{obs} t} \quad \text{(E11)}$$

Where A_t and A_∞ are the absorbance after time t and at the time of reaction completeness, respectively. A least-squares fit utilising absorbance vs. time data for a first order reaction, would yield k_{obs} for the reaction.

Spectophotometric determination of the equilibrium constant of the reaction.

Consider the following equilibrium reaction between complex (A) and a ligand (B):

$$MX + L \xrightarrow{K} ML + X$$

The equilibrium constant for the above-mentioned reaction is given by the following equation:

$$K = \frac{[ML][X]}{[MX][L]} \quad \text{(E12)}$$

Equation E13 can be applied for the observed absorbance (A_{obs}) according to Beer-Lambert law:

$$A_{obs} = \varepsilon_{MX}[MX] + \varepsilon_{ML}[ML] \quad \text{(E13)}$$

Where A_{obs} = observed absorbance, ε_{MX} = molar extinction coefficient of MX and ε_{ML} = molar extinction coefficient of ML.

Equation E14 can be applied for the total metal concentration according to the law of Gulberg and Waage (the law of conservation of mass).

$$[M]_t = [ML] + [MX] \quad \text{(E14)}$$

Where $[M]_t$ = total concentration of the absorbed M, [MX] = concentration of the MX complex, [ML] = concentration of the ML complex.

[MX] and [ML] can be defined respectively, as in Equation E15 and E16 by using Equation E12.

$$[MX] = \frac{[ML][X]}{K[L]} \tag{E15}$$

$$[ML] = \frac{K[MX][L]}{[X]} \tag{E16}$$

Separate substitution of Equation E15 and E16 in Equation E14 gives Equation E17 and E18 respectively.

$$[M]_t = \frac{[ML][X]}{K[L]} + [ML]$$

$$= [ML]\left(1 + \frac{[X]}{K[L]}\right)$$

$$[ML] = \frac{[M]_t}{1+\frac{[X]}{K[L]}} \tag{E17}$$

$$[M]_t = [MX] + \frac{K[MX][L]}{[X]}$$

$$= [MX](1 + \frac{K[L]}{[X]})$$

$$[MX] = \frac{[M]_t}{1+\frac{K[L]}{[X]}} \tag{E18}$$

In Equation E17 and E18, [MX] and [ML] are expressed in terms of experimental determined values. Similar substitution of the above-mentioned equations in Equation E13 will give the result in Equation E19.

$$A_{obs} = \frac{\varepsilon_{MX}[M]_t}{1+\frac{K[L]}{[X]}} + \frac{\varepsilon_{ML}[M]_t}{1+\frac{[X]}{K[L]}} \tag{E19}$$

For Equation E18 the following apply: if [L] = 0, then [ML] = 0 so that $A_{obs} = A_{MX} = \varepsilon_{MX}[M]_t$. If [L] >> $[M]_t$, then [MX] = 0 and $A_{MX} = \varepsilon_{ML}[M]_t$. Through substitution of the last mentioned absorbance in Equation E19 and further manipulation gives the results as in Equation E20.

$$A_{obs} = \frac{A_{MX}}{[X]+K[L]} + \frac{A_{ML}K[L]}{[X]+K[L]}$$

$$A_{obs} = \frac{A_{MX}+A_{ML}K[L]}{[X]+K[L]} \quad \text{(E20)}$$

Where A_M = absorbance at the beginning of the reaction and A_{ML} = absorbance when the reaction is finished.

Reaction half-life

The reaction half-life is the required time to convert 50% of the reactant, for first order reactions the half-life are determined by the equation:

$$t_{1/2} = \frac{\ln(2)}{k_{obs}} = \frac{0.6932}{k_{obs}} \quad \text{(E21)}$$

Activation enthalpy and entropy

The Transition State Theory states that an activated complex or transition state is in equilibrium with the reagents before the reaction occurs, and that the rate is given by the decomposition rate, k, of the activated complex to yield the products:

$$A + B \xleftrightarrow{K_c^{\neq}} (AB)^{\neq} \xrightarrow{k} prod. \quad \text{(E22)}$$

Where $K_c^{\neq}$ = equilibrium constant

The exponential form of the Eyering equation is given as:

$$k = \frac{k_B T}{h} e^{\left[\frac{\Delta S^{\neq}}{R} - \frac{\Delta H^{\neq}}{RT}\right]} \quad \text{(E23)}$$

That can be rewritten into a logarithmic form:

$$\ln\left(\frac{k}{T}\right) = \ln\left(\frac{k_B}{h}\right) + \left(\frac{\Delta S^{\neq}}{R}\right) - \left(\frac{\Delta H^{\neq}}{RT}\right) \quad \text{(E24)}$$

A graph of $\ln\left(\frac{k}{T}\right)$ versus $\frac{1}{T}$ will have a slope of $\frac{-\Delta H^{\neq}}{R}$, with $\Delta H^{\neq}$ = standard enthalpy change of activation and the Y-axis intercept $\frac{\Delta S^{\neq}}{R} + \ln\left(\frac{k_B}{h}\right)$, with $\Delta S^{\neq}$ = standard enthalpy change of activation.